Woodhead Publishing Series in Civil and Structural Engineering: Number 59

Science and Technology of Concrete Admixtures

Edited by

Pierre-Claude Aïtcin and Robert J Flatt

Knowing is not enough: we must apply.
Willing is not enough: we must do.
–Goethe



AMSTERDAM • BOSTON • CAMBRIDGE • HEIDELBERG
LONDON • NEW YORK • OXFORD • PARIS • SAN DIEGO
SAN FRANCISCO • SINGAPORE • SYDNEY • TOKYO
Woodhead Publishing is an imprint of Elsevier



Woodhead Publishing is an imprint of Elsevier
80 High Street, Sawston, Cambridge, CB22 3HJ, UK
225 Wyman Street, Waltham, MA 02451, USA
Langford Lane, Kidlington, OX5 1GB, UK

Copyright © 2016 Elsevier Ltd. All rights reserved.

No part of this publication may be reproduced or transmitted in any form or by any means, electronic or mechanical, including photocopying, recording, or any information storage and retrieval system, without permission in writing from the publisher. Details on how to seek permission, further information about the Publisher's permissions policies and our arrangements with organizations such as the Copyright Clearance Center and the Copyright Licensing Agency, can be found at our website: www.elsevier.com/permissions.

This book and the individual contributions contained in it are protected under copyright by the Publisher (other than as may be noted herein).

Notices
Knowledge and best practice in this field are constantly changing. As new research and experience broaden our understanding, changes in research methods, professional practices, or medical treatment may become necessary.

Practitioners and researchers must always rely on their own experience and knowledge in evaluating and using any information, methods, compounds, or experiments described herein. In using such information or methods they should be mindful of their own safety and the safety of others, including parties for whom they have a professional responsibility.

To the fullest extent of the law, neither the Publisher nor the authors, contributors, or editors, assume any liability for any injury and/or damage to persons or property as a matter of products liability, negligence or otherwise, or from any use or operation of any methods, products, instructions, or ideas contained in the material herein.

ISBN: 978-0-08-100693-1 (print)
ISBN: 978-0-08-100696-2 (online)

British Library Cataloguing-in-Publication Data
A catalogue record for this book is available from the British Library

Library of Congress Control Number: 2015952093

For information on all Woodhead Publishing publications visit our website at http://store.elsevier.com/



Related titles

Advances in Asphalt Materials
(ISBN 978-0-08-100269-8)

Acoustic Emission and Related Non-destructive Evaluation Techniques in the Fracture Mechanics of Concrete
(ISBN 978-1-78242-345-4)

Handbook of Alkali-activated Cements, Mortars and Concretes
(ISBN 978-1-78242-276-1)

Understanding the Rheology of Concrete
(ISBN 978-0-85709-028-7)

About the contributors

A. Yahia is Associate Professor in the Civil Engineering Department of the Université de Sherbooke.

A.B. Eberhardt is a research scientist with SIKA Technology AG in Zürich.

D. Marchon is a Ph.D. student of Professor R.J. Flatt at ETH Zürich.

G. Gelardi is a Ph.D. student of Professor R.J. Flatt at ETH Zürich.

B. Elsener is Titular Professor for Durability and Corrosion Materials in the Department of Civil, Environmental, and Geomatic Engineering of ETH Zürich.

P.-C. Aïtcin is Professor Emeritus in the Civil Engineering Department of the Université de Sherbooke.

P.-C. Nkinamubanzi is a research officer at the National Research Council of Canada in Ottawa.

M. Palacios is a postdoctoral researcher of Professor R.J. Flatt at ETH Zürich.

R. Gagné is Full Professor in the Civil Engineering Department of the Université de Sherbrooke.

R.J. Flatt is Full Professor for Physical Chemistry of Building Materials in the Department of Civil, Environmental, and Geomatic Engineering of ETH Zürich.

S. Mantellato is a Ph.D. student of Professor R.J. Flatt at ETH Zürich.

U. Angst is a postdoctoral researcher of Professor B. Elsener at ETH Zürich.

Part of the team



First row from the left to the right: Sara and Saverio, Marta, Giulia and Delphine. Second row from the left to the right: Richard, Pierre-Claude, Robert and Ammar. Are missing: Arnd, Bernhard, Pierre-Claver and Ueli.

Woodhead Publishing Series in Civil and Structural Engineering

1 **Finite element techniques in structural mechanics**
C. T. F. Ross
2 **Finite element programs in structural engineering and continuum mechanics**
C. T. F. Ross
3 **Macro-engineering**
F. P. Davidson, E. G. Frankl and C. L. Meador
4 **Macro-engineering and the earth**
U. W. Kitzinger and E. G. Frankel
5 **Strengthening of reinforced concrete structures**
Edited by L. C. Hollaway and M. Leeming
6 **Analysis of engineering structures**
B. Bedenik and C. B. Besant
7 **Mechanics of solids**
C. T. F. Ross
8 **Plasticity for engineers**
C. R. Calladine
9 **Elastic beams and frames**
J. D. Renton
10 **Introduction to structures**
W. R. Spillers
11 **Applied elasticity**
J. D. Renton
12 **Durability of engineering structures**
J. Bijen
13 **Advanced polymer composites for structural applications in construction**
Edited by L. C. Hollaway
14 **Corrosion in reinforced concrete structures**
Edited by H. Böhni
15 **The deformation and processing of structural materials**
Edited by Z. X. Guo
16 **Inspection and monitoring techniques for bridges and civil structures**
Edited by G. Fu
17 **Advanced civil infrastructure materials**
Edited by H. Wu
18 **Analysis and design of plated structures Volume 1: Stability**
Edited by E. Shanmugam and C. M. Wang
19 **Analysis and design of plated structures Volume 2: Dynamics**
Edited by E. Shanmugam and C. M. Wang

20 **Multiscale materials modelling**
Edited by Z. X. Guo
21 **Durability of concrete and cement composites**
Edited by C. L. Page and M. M. Page
22 **Durability of composites for civil structural applications**
Edited by V. M. Karbhari
23 **Design and optimization of metal structures**
J. Farkas and K. Jarmai
24 **Developments in the formulation and reinforcement of concrete**
Edited by S. Mindess
25 **Strengthening and rehabilitation of civil infrastructures using fibre-reinforced polymer (FRP) composites**
Edited by L. C. Hollaway and J. C. Teng
26 **Condition assessment of aged structures**
Edited by J. K. Paik and R. M. Melchers
27 **Sustainability of construction materials**
J. Khatib
28 **Structural dynamics of earthquake engineering**
S. Rajasekaran
29 **Geopolymers: Structures, processing, properties and industrial applications**
Edited by J. L. Provis and J. S. J. van Deventer
30 **Structural health monitoring of civil infrastructure systems**
Edited by V. M. Karbhari and F. Ansari
31 **Architectural glass to resist seismic and extreme climatic events**
Edited by R. A. Behr
32 **Failure, distress and repair of concrete structures**
Edited by N. Delatte
33 **Blast protection of civil infrastructures and vehicles using composites**
Edited by N. Uddin
34 **Non-destructive evaluation of reinforced concrete structures Volume 1: Deterioration processes**
Edited by C. Maierhofer, H.-W. Reinhardt and G. Dobmann
35 **Non-destructive evaluation of reinforced concrete structures Volume 2: Non-destructive testing methods**
Edited by C. Maierhofer, H.-W. Reinhardt and G. Dobmann
36 **Service life estimation and extension of civil engineering structures**
Edited by V. M. Karbhari and L. S. Lee
37 **Building decorative materials**
Edited by Y. Li and S. Ren
38 **Building materials in civil engineering**
Edited by H. Zhang
39 **Polymer modified bitumen**
Edited by T. McNally
40 **Understanding the rheology of concrete**
Edited by N. Roussel
41 **Toxicity of building materials**
Edited by F. Pacheco-Torgal, S. Jalali and A. Fucic
42 **Eco-efficient concrete**
Edited by F. Pacheco-Torgal, S. Jalali, J. Labrincha and V. M. John

43 **Nanotechnology in eco-efficient construction**
Edited by F. Pacheco-Torgal, M. V. Diamanti, A. Nazari and C. Goran-Granqvist
44 **Handbook of seismic risk analysis and management of civil infrastructure systems**
Edited by F. Tesfamariam and K. Goda
45 **Developments in fiber-reinforced polymer (FRP) composites for civil engineering**
Edited by N. Uddin
46 **Advanced fibre-reinforced polymer (FRP) composites for structural applications**
Edited by J. Bai
47 **Handbook of recycled concrete and demolition waste**
Edited by F. Pacheco-Torgal, V. W. Y. Tam, J. A. Labrincha, Y. Ding and J. de Brito
48 **Understanding the tensile properties of concrete**
Edited by J. Weerheijm
49 **Eco-efficient construction and building materials: Life cycle assessment (LCA), eco-labelling and case studies**
Edited by F. Pacheco-Torgal, L. F. Cabeza, J. Labrincha and A. de Magalhães
50 **Advanced composites in bridge construction and repair**
Edited by Y. J. Kim
51 **Rehabilitation of metallic civil infrastructure using fiber-reinforced polymer (FRP) composites**
Edited by V. Karbhari
52 **Rehabilitation of pipelines using fiber-reinforced polymer (FRP) composites**
Edited by V. Karbhari
53 **Transport properties of concrete: Measurement and applications**
P. A. Claisse
54 **Handbook of alkali-activated cements, mortars and concretes**
F. Pacheco-Torgal, J. A. Labrincha, C. Leonelli, A. Palomo and P. Chindaprasirt
55 **Eco-efficient masonry bricks and blocks: Design, properties and durability**
F. Pacheco-Torgal, P. B. Lourenço, J. A. Labrincha, S. Kumar and P. Chindaprasirt
56 **Advances in asphalt materials: Road and pavement construction**
Edited by S.-C. Huang and H. Di Benedetto
57 **Acoustic emission (AE) and related non-destructive evaluation (NDE) techniques in the fracture mechanics of concrete: Fundamentals and applications**
Edited by M. Ohtsu
58 **Nonconventional and vernacular construction materials: Characterisation, properties and applications**
Edited by K. A. Harries and B. Sharma
59 **Science and technology of concrete admixtures**
Edited by P.-C. Aïtcin and R. J. Flatt

Preface

During the last 40 years, concrete technology has made considerable progress—not due to some spectacular improvement in the properties of modern cements, but rather to the utilization of very efficient admixtures. For example, in the 1970s in the United States and Canada, concrete structures were typically built with concretes having a maximum compressive strength of 30 MPa and a slump of 100 mm. Today, 80–100 MPa concretes having a slump of 200 mm are used to build the lower portions of the columns of high-rise buildings (Aïtcin and Wilson, 2015). These concretes are pumped from the first floor to the very top (Aldred, 2010, Kwon et al., 2013a,b). Moreover, 40 MPa self-compacting concretes are being used for the prestressed floors in these high-rise buildings (Clark, 2014). Currently, 200 MPa ultra-high strength concretes are being used. Such achievements are the result of a massive research effort that has created a true science of concrete and a true science of admixtures.

It is the prime objective of this book to present the current state of the art of the science and technology of concrete admixtures. It is now possible to explain not only the fundamental mechanisms of the actions of the most important admixtures, but also to design specific new admixtures to improve particular properties of both fresh and hardened concretes. The time is long past when different industrial byproducts were selected by trial and error as concrete admixtures. Today, most concrete admixtures are synthetic chemicals designed to act specifically on some particular property of the fresh or hardened concrete.

At the end of the Second World War, the price of Portland cement was quite low because oil was not expensive. Thus, it was cheaper to increase concrete compressive strength by adding more cement to the mix rather than using concrete admixtures. This explains, at least partially, why the admixture industry was forced to use cheap industrial byproducts to produce and sell their admixtures.

Today, oil is no longer cheap and the price of Portland cement has increased dramatically. Thus, it is now possible for the admixture industry to base their admixture formulations on more sophisticated molecules synthesised specifically for the concrete industry. As a result, in some sophisticated concrete formulations, it now happens that the cost of the admixtures is greater than the cost of the cement—a situation unbelievable just a few years ago.

The development of a new science of admixtures has also resulted in a questioning of current acceptance standards for cement. For example, a given superplasticizer may perform differently from a rheological point of view with different Portland cements, although these cements comply with the same acceptance standards.

Expressions such as “cement/superplasticizer compatibility” or “robustness of cement/superplasticizer combinations” are often used to qualify these strange behaviors. It is now evident that the current acceptance standards for cement, which were developed for concretes of low strength having high water–cement ratios (w/c), are totally inadequate to optimize the characteristics of a cement that is to be used for the production of high-performance concrete having low w/c or water–binder ratios. It is a matter of sense to revise these acceptance standards because, in too many cases, they represent a serious obstacle to the progress of concrete technology.

Moreover, we are now more and more concerned by the environmental impact of civil engineering structures, which favors the use of low w/c concretes that require the use of superplasticizers. It is easy to show that a judicious use of concrete admixtures can result in a significant reduction of the carbon footprint of concrete structures. In some cases, this reduction may be greater than that resulting from the substitution of a certain percentage of Portland cement clinker by some supplementary cementitious material or filler.

To illustrate this point very simply, let us suppose that to support a given load L we decide to build two unreinforced concrete columns—one with a 25 MPa concrete and the other with a 75 MPa concrete, as shown in Figure 1.

As seen in Figure 1, the cross-sectional area of the 25 MPa column is three times as large as that of the 75 MPa column. Therefore, to support the same load L, it will be necessary to place three times more concrete and to use approximately three times more sand, three times as much coarse aggregate, and three times much water.

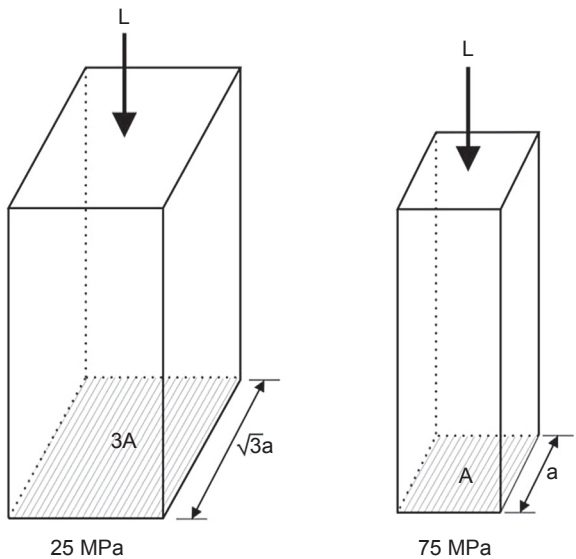


Figure 1 Comparison of the cross-section area and volume of two unreinforced concrete columns supporting the same load L built, respectively, with 25 and 75 MPa concretes.

Moreover, the dead weight of the 25 MPa column will be three times greater than the 75 MPa one.

To produce the 25 MPa concrete, let us suppose that it is necessary to use 300 kg of cement when using no admixture, and that to produce the 75 MPa concrete, it is necessary to use 450 kg of cement plus some liters of superplasticizer to reduce the w/c. Therefore, using only 1.5 times as much cement, we are able to obtain three times more strength. Thus, by constructing a 25 MPa column, we are using twice as much cement and three times as much water and aggregates to finally build a column of lower quality and durability that has a higher carbon footprint. Helene and Hartmann (2003) presented more detailed calculations in the case of the columns of a high-rise building built in Sao Paulo, Brazil. This is totally aberrant and unacceptable from both an economical and a sustainable development point of view. It is time to stop such a waste of money and material.

In the case of concrete elements working in flexure, such as floors and beams, the reduction of the carbon footprint is not as spectacular when using low w/c concrete, except if they are built using pre- or posttensioned concrete (Clark, 2014).

In the future, concretes will contain more admixtures, so it is very important to learn how to use them appropriately in the most efficient way possible to produce sustainable concretes perfectly fitted to their specific uses. This will increase concrete competitiveness and the construction of concrete structures having a lower carbon footprint.

P.-C. Aïtcin
Professeur Emeritus, Département de génie civil,
Université de Sherbrooke, QC, Canada

R.J. Flatt
Institute for Building Materials, ETH Zürich,
Zurich, Switzerland

References

Aïtcin, P.-C., Wilson, W., 2015. The Sky's the limit. Concrete International 37 (1), 53–58.

Aldred, J., 2010. Burj Khalifa – a new high for high-performance concrete. Proceedings of the ICE–Civil Engineering 163 (2), 66–73.

Clark, G., 2014. Challenges for concrete in Tall buildings. Structural Concrete (Accepted and Published Online) 15 (4), 448–453.

Helene, P., Hartmann, C., 2003. HPCC in Brazilian Office Tower. Concrete International 25 (12), 1–5.

Kwon, S.H., Jeong, J.H., Jo, S.H., Lee, S.H., 2013a. Prediction of concrete pumping: part I-development for analysis of lubricating layer. ACI Materials Journal 110 (6), 647–655.

Kwon, S.H., Jeong, J.H., Jo, S.H., Lee, S.H., 2013b. Prediction of concrete pumping: part II-analytical prediction and experimental verification. ACI Materials Journal 110 (6), 657–667.

Historical background of the development of concrete admixtures

P.-C. Aïtcin[1], *A.B. Eberhardt*[2]

[1] Université de Sherbrooke, QC, Canada, [2] Sika Technology AG, Zürich, Switzerland

Early developments

The idea of adding chemical compounds when making concrete is not new. Some Roman authors have reported that, several hundred years before Christ, Roman masons were adding blood or eggs to the lime and pozzolans when making concrete (Mindess et al., 2003; Mielenz, 1984). This idea of adding "exotic" products when making concrete lasted many years. According to Garrison (1991), in around 1230 Villard de Honnecourt, a cathedral builder, recommended the impregnation of the lime concrete of cisterns with linseed oil to make them more impervious.

Just before the Second World War, the beneficial effects of what we now call concrete admixtures were fortuitously discovered in the United States. There are two accounts to explain this discovery. The first one says that a faulty bearing of a grinding mill had been releasing some heavy oil, which resulted in the discovery of the beneficial effects of air-entraining agents (Mindess et al., 2003). In fact, more precisely, the discovery originates from the use of some American natural cements. The production of American natural cement dates back to 1818, after natural cement rock was discovered by Canvass White in Fayetteville, NY. This natural cement was known as Rosendale cement because it was produced in the Rosendale district in the state of New York in the middle of the nineteenth century (Eckel and Burchard, 1913). These cements were produced from marl limestone or argillaceous limestone, which were burnt between 800 and 1100 °C. Later, Portland cement production, with its faster hardening, put natural cement almost out of the market (Eckel and Burchard, 1913).

Salt scaling of concrete roads built with Portland cement became a major issue (Jackson, 1944) because they were not durable when facing freezing and thawing cycles in New York State. It was observed that Portland cement-based concrete started degrading after a few years, while structures made from natural Rosendale cement, such as the foundations of the Brooklyn Bridge and the Statue of Liberty (built around 1870) were still in perfect condition after decades of field exposure.

According to Holbrook (1941), an engineer named Bertrand H. Wait started experiments on blends of Portland cement and natural cements in 1933. He was able to make concretes with a scaling resistance against freezing and thawing in salt solution that was 12 times greater than that of concrete made of pure Portland cement. In 1934,

the first road was built using a blended cement containing about 85% of Portland cement and 15% of Rosendale natural cement. In 1937, this blend became the standard for highway construction in New York State and soon after in some other states (Holbrook, 1941; Jackson, 1944).

The reason for the greater resistance of these blended cements against freezing and thawing was not clear. It could have been a consequence of the natural cement itself or of the fact that one out of the two Rosendale cements that were used in the New York State contained a small amount of beef tallow as a grinding aid. This latter explanation was strengthened by the discovery that a Portland cement with a good service performance had been contaminated with some oil or grease from a leaking crusher bearing (Jackson, 1944). At the end of the 1930s, the Portland Cement Association initiated intensive studies on the effect of introducing small amounts of tallow, fish oil, and stearate resins as air-entraining agents.

The second story of the discovery (Dodson, 1990) says that the tenacity and perspicacity of a Department of Transportation (DOT) engineer in New York State led to the discovery of the beneficial effect of air-entraining agents. This engineer was in charge of the construction of one of the first three-lane concrete highways in New York State. To prevent accidents, he had the idea of coloring the concrete of the central lane in black so that the drivers realized that they were driving in the shared central lane.

The contractor added some black carbon to its concrete, but the DOT engineer was not satisfied by this first trial because the color of the concrete was not very uniform. Therefore, he asked the contractor to find a way to improve the dispersion of the black carbon within the concrete to end up with a more esthetic central lane. The concrete contractor asked his black carbon supplier if he had a special chemical product that could help the dispersion of black carbon particles in concrete. The supplier suggested a sodium salt of a polynaphthalene sulfonate dispersant that was already used in the painting industry to disperse black carbon particles in paints. After the addition of a small amount of this magic chemical product, the uniformity of the colored concrete was significantly improved and the New York DOT engineer was satisfied.

Some years (and winters) later, the same engineer observed that the black concrete was in much better condition than the concrete used in the other two pale lanes. He could have concluded that black carbon improved the freeze/thaw resistance of concrete. Fortunately for the sake of the concrete industry, this very conscientious engineer was not satisfied by such a direct and simplistic explanation, so he asked a friend to have a close look at a sample of the pale concrete and a sample of the black concrete to see if they were different.

Under a microscope, it was seen that the cement paste of the dark concrete contained very small air bubbles uniformly distributed within the concrete, while the pale concrete presented only the usual coarse and irregular entrapped air bubbles. Our engineer could have concluded that black carbon entrained air bubbles within a concrete, but he remembered that a dispersing agent was also added. Doing some experimental work on the concrete with and without the black carbon, as well as with and without the sodium salt of polynaphthalene sulfonate, he found that it was the dispersing agent that was responsible for the entrainment of the small air bubbles.

Sometimes, when this story is told, it is added that the contractor noticed that when he added the dispersing agent in the concrete, it became more workable and could be placed more easily.

This is how the beneficial dispersive properties of polysulfonates might have been discovered. Although this version could be perceived as a kind of fairy tale, the concrete industry could have its own anonymous Alexander Fleming to make such a fortuitous important discovery. The story does not tell if the initial objective of that tenacious DOT engineer was achieved—if there were less frontal collisions in the black lane. The first US patent on the use of polysulfonate as a cement dispersant was given to Tucker (1938).

Powers and his research team at the Portland Cement Association explained all the beneficial effects of these small air bubbles on the properties of fresh and hardened concrete, particularly its freezing and thawing behavior, at the end of the 1940s and the beginning of the 1950s (Powers, 1968). Thus, in North America and Japan, air-entraining agents are being systematically introduced in concrete, even in concrete that is not exposed frequently to freezing/thawing cycles.

The development of the science of admixtures

For a long time, admixture technology was closer to alchemy than to chemistry. The few companies involved in the admixture business were very secretive and jealously guarded their formulations. This is no longer the case, as there are some scientific books devoted to the science of admixtures (Dodson, 1990; Ramachandran, 1995; Ramachandran et al., 1998: Rixom and Mailvaganam, 1999). Moreover, several international conferences have been (and are still being) held on admixtures, such as the nine American Concrete Institute and Canada Center for Mineral and Energy Technology (ACI/CANMET) International Conferences on Superplasticizers; Ottawa (1978) ACI SP-72, Ottawa (1981) ACI SP-68; Ottawa (1989) ACI SP-119; Montreal (1994) ACI SP-148; Rome (1997) ACI SP-173; and Nice (2000) ACI SP-195. The seventh one was held in 2003 in Berlin, the eighth in Sorrento in Italy in 2006, the ninth in Seville in 2009, the tenth in Prague in 2012, and the twelfth in Ottawa in 2015.

Despite the recent knowledge and the increasing research done on the mechanisms of action of superplasticizers, there are still too many engineers who question the beneficial aspects of concrete admixtures and who believe that admixture salesmen are peddlers. There are even some engineers and cement producers who question the existence of the science of admixtures. Some engineers still believe that admixtures should be banned to avoid the compatibility problems that are so costly for contractors when they occur in the field. Others, on principle, believe that adding chemistry to cement is not a good thing, but do not seem to be bothered by the chemical reactions causing cement to harden. Would it not be better to continue to simply add a little water to favor cement particle dispersion?

Throughout this book, we will see that admixtures are essential components of modern concrete. The beneficial aspects of their use from a durability and sustainability point of view have made them essential components of concrete.

The use of admixtures

The use of admixtures varies greatly from one country to another. For example, in Japan and Canada, almost 100% of concrete contains at least a water reducer and an air-entraining agent. But, for example, in the United States and France, more than 50% of concrete contains admixtures, although this percentage is increasing constantly as the beneficial role of admixtures is understood. Indeed, the chemical system operating during cement hydration is becoming more and more complex due to the normal intrinsic complexity of Portland cement and hydraulic binders, as well as the complexity of the organic molecules used as admixtures that are active during the hydration process.

The use of synthetic molecules and polymers

In recent years, concrete technology has evolved rapidly—much faster than the standards of cement, concrete, and admixtures. Therefore, it is very important to close the gap between what is written in standards and what is known and done in practice. If such corrective action is not rapidly undertaken, artificial problems will slow down the evolution of concrete technology and impair the efficient use of Portland cement and hydraulic binders.

Modern admixtures are less frequently based on the use of industrial byproducts but rather on synthetic molecules or polymers specially produced for the concrete industry. Modern admixtures modify one or several properties of fresh and hardened concrete by correcting some of the technological weaknesses of Portland cement and hydraulic binders (Ramachandran et al., 1998). Their use is no longer a commercial issue—it is a matter of progress, science, durability, and sustainability.

An artificially complicated terminology

A great source of confusion in the field of admixtures comes from the fact that an artificially complicated terminology has been developed over the years, not only in the technical and commercial literature but also in the standards.

For example, in the 2001 edition of *Design of Concrete Mixtures* edited by the Canadian Cement Association (in metric units), in Chapter 7 that deals with admixtures, the following list of admixtures (in alphabetic order) is found (see Table 7.1): accelerators, air-detrainers, air-entraining admixtures, alkali-aggregate reactivity inhibitors, antiwashout admixtures, bonding admixtures, coloring admixtures, corrosion inhibitors, damp-proofing admixtures, foaming agents, fungicides, germicides, insecticides, gas formers, grouting admixtures, hydration control admixtures, permeability reducers, pumping aids, retarders, shrinkage reducers, superplasticizers, superplasticizers and retarders, water reducers, water reducers and accelerators, water reducers and retarders, water reducer–high range, and water reducer–mid range (Table 1).

Table 1 Concrete admixtures by classification

Desired effect	Material
Accelerate setting and early-strength development	Calcium chloride (ASTM D 98)
	Triethanolamine, sodium thiocyanate, calcium formate, calcium nitrite, calcium nitrate
Decrease air content	Tributyl phosphate, dibutyl phthalate, octyl alcohol, with insoluble esters of carbonic and boric acid, silicones
Improve durability in freeze/thaw, deicer, sulfate, and alkali-reactive environments, improve workability	Salts of wood resins (Vinsol resin), some synthetic detergents, salts of sulfonated lignin, salts of petroleum acids, salts of proteinaceous material, fatty and resinous acids and their salts, alkybenzene sulfonates, salts of sulfonated hydrocarbons
Reduce alkali-aggregate reactivity expansion	Barium salts, lithium nitrate, lithium carbonate, lithium hydroxide
Cohesive concrete for underwater placements	Cellulose, acrylic polymer
Increase bond strength, styrene copolymers	Polyvinyl chloride, polyvinyl acetate, acrylics, butadiene
Colored concrete	Modified carbon black, iron oxide, phthalocyanine, chromium oxide, titanium oxide, cobalt blue
Reduce steel corrosion activity in a chloride environment	Calcium nitrite, sodium nitrite, sodium benzoate, phosphates or fluosilicates, fluoaluminates
Retard moisture penetration into dry concrete	Soaps of calcium or ammonium stearate or oleate butyl stearate
	Petroleum products
Produce foamed concrete with low density	Cationic and anionic surfactants
	Hydrolyzed protein
Inhibit or control bacterial and fungal growth	Polyhalogenated phenols
	Dieldrin emulsions
	Copper compounds
Cause expansion before setting	Aluminum powder
Adjust grout properties for specific applications	See air-entraining admixtures, accelerators, retarders, water reducers
Suspend and reactivate cement hydration with stabilizer and activator	Carboxylic acids
	Phosphorus-containing organic acid salts

Continued

Table 1 Continued

Desired effect	Material
Decrease permeability	Latex
	Calcium stearate
Improve pumpability	Organic and synthetic polymers
	Organic flocculants
	Organic emulsions of paraffin, coal tar, asphalt, acrylic
	Bentonite and pyrogenic silica
	Hydrated lime (ASTM C 141)
Retard setting time	Lignin
	Borax
	Sugars
	Tartaric acid and salts
Increase flowability of concrete reduce water-cementing ratio	Sulfonated melamine formaldehyde condensates, sulfonated naphthalene formaldehyde condensates, lignosulfonate materials, polycarboxylates
Increase flowability with retarded set, reduce water-cementing materials ratio	See superplasticizers and also water reducers
Reduce water content at least 5%	Lignosulfonates, hydroxylated carboxylic acids, carbohydrates (also tend to retard set so accelerator is often added)
Reduce water content (minimum 5%) and accelerate set	See water reducer, type A (accelerator is added)
Reduce water content (minimum 12%)	See superplasticizers
Reduce water content (minimum 12%) and retard set	See superplasticizers and also water reducers
Reduce water content (between 6% and 12%) without retarding	Lignosulfonates, polycarboxylates

Reprinted with permission from the "Canadian Edition of Design and Control of Concrete Mixtures" Portland Cement Association.

The European terminology is as rich as the North American one. This rich terminology is also found in standards. For example, the ASTM C494 standard recognizes different types of water reducers identified by the letter A to G and the new European standards recognize nine different types of admixtures.

This complex terminology creates more confusion than clarification. It seems to be related to the fact that, for a long time, most concrete admixtures were made from industrial byproducts having more than one specific action on the properties of the fresh and hardened concrete. As it was too costly or sometimes impossible to beneficiate these byproducts, it was easier to create new subcategories of admixtures in the standards because of the complex nature of these byproducts and the different impurities that they contained.

Classification of admixtures

The terminology of admixtures could be easily simplified by looking at their physicochemical mechanisms of action rather than at their effects on the properties of fresh and hardened concrete (Dodson, 1990). Dodson classified admixtures into the following four categories according to their mechanism of action:

1. Dispersion of the cement in the aqueous phase of concrete
2. Alteration of the normal rate of hydration of cement, in particular the tricalcium silicate phase
3. Reaction with the byproducts of hydrating cement, such as alkalis and calcium hydroxide
4. No reaction with either the cement or its byproducts

Mindess et al. (2003) recognized that admixture terminology is complex and proposed a classification of concrete admixtures into four different categories:

1. Air-entraining agents (ASTM C260) that are added primarily to improve the frost resistance of concrete
2. Chemical admixtures (ASTM C494 and BS 5075) that are water-soluble compounds added primarily to control setting and early hardening of fresh concrete or to reduce its water requirements
3. Mineral admixtures that are finely divided solids added to concrete to improve its durability or to provide additional cementing properties (slags and pozzolans are important categories of mineral admixtures)
4. Miscellaneous admixtures, which include all those materials that do not come under one of the foregoing categories, many of which have been developed for specialized applications

In this book, as said in the Preface, we examine the principal mechanism of action of admixtures that modify the rheology of the fresh concrete and the properties of the hardened concrete. We develop the influence of the molecular structures and the action of most of these admixtures on each individual phase of Portland cement and on specific supplementary cementitious materials, although this information can be found in specialized books (Dodson, 1990; Ramachandran, 1995; Ramachandran et al., 1998; Rixom and Mailvaganam, 1999). This accumulated knowledge is very important to develop an efficient use of admixtures (dosage, sequence of introduction, duration of their effects, etc.).

The importance of cement particles dispersion

Experience shows that when the water–cement ratio is lower than 0.40, it is usually impossible to make a concrete having a slump greater than 100 mm when mixing only water and cement. However, experience also shows that when using a superplasticizer, it is possible to transform this concrete into a self-compacting concrete having a water–binder ratio lower than 0.35 that does not bleed or segregate in spite of its high workability.

How can such different behaviors be obtained when using the same cement in both cases? How can small amounts of organic molecules produce such a spectacular effect on the rheology of a cement paste and a concrete?

As seen in Chapter 3, the final grinding of clinker and gypsum to produce cement results in a fine powder with particles that are prompt to agglomerate. This agglomeration is inherent between all these phases, but it can also be increased because of the different surface potentials of the different phases present. It also takes place to a significant extent when cement particles come into contact with a liquid as polar as water (Kreijger, 1980; Chatterji, 1988; Dodson, 1990; Rixom and Mailvaganam, 1999; Flatt, 2001, 2004).

It is very easy to put in evidence the flocculation of cement particles by the following simple experiment:

- 50 g of cement are placed in three 1-L graduated cylinder (or a common plastic bottle); two of them are full of water. In the right graduated cylinder, 5 cm^3 of superplasticizer is added.
- A rubber tap is placed on the two graduate cylinders full of water. The graduated cylinders are shaken upside down 20 times in order to disperse as much as possible all of the cement particles (Figure 1).

Figure 2 shows the bottom of the two graduated cylinders almost 7 min after the beginning of the experiment.

Figure 2(a) shows the bottom of the left graduated cylinder that did not contain any superplasticizer 6.59 min after the beginning of the experience. At that time, all of the cement particles have settled at the bottom of the graduated cylinder, leaving almost clear water in the upper part of the graduated cylinder.

Figure 2(b) shows the bottom of the right graduated cylinder at 7.25 min. It is seen that only the coarser particles of the cement have settled at the bottom of the graduated cylinder and that a large fraction of particles (the finer ones) are still in suspension in the graduate cylinder.

Figure 3 shows the three graduated cylinders one day after the beginning of the experiment.

It is seen that in the left graduated cylinder, the water above the settled particles is clear and that the flocculated particles occupy a volume larger than the one of the dry cement on the graduated cylinder located at the center of Figure 3. On the right graduated cylinder, it is seen that almost all of the cement particles have settled at the bottom of the cylinder and that the water on top of them is not totally clear because there are a few of them still in suspension. Moreover, the water on top has also a pale brownish shade due to the dark brown color of the superplasticizer. It is also seen that the thickness

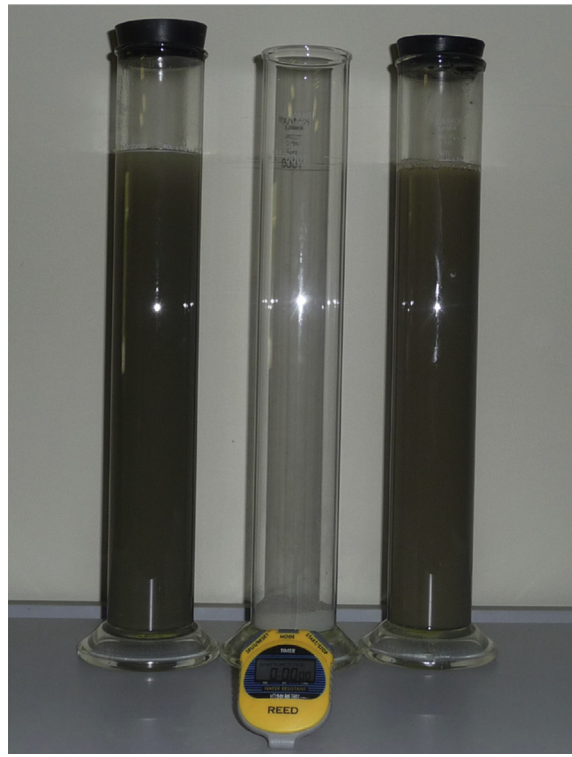


Figure 1 Sedimentation of cement particles with and without a superplasticizer at time $t = 0$. The suspension is then left to settle.

of the settled particles is smaller than the thickness of the uncompacted dry powder of the graduated cylinder located at the center of Figure 3.

Figure 4 presents a closer view of the bottom of the two graduated cylinders to compare the final volume of the cement particles at 24 h. The left graduated cylinder presents the flocculated cement particles that settled in pure water in the absence of a superplasticizer and the right one shows the cement particles that settled in the presence of a superplasticizer. The effect of the flocculation of the cement particles on their final volume is clearly observed in this figure.

From this very simple experiment, it can be concluded that some organic molecules strongly reduce or even destroy the flocculation tendency of cement particles, so that finally all the water introduced during concrete mixing can be efficiently used to improve the workability of concrete (Black et al., 1963; Dodson, 1990).

As discussed in Part 2 of this book, the interaction between cement particles and these organic molecules depends on the physicochemical characteristics of the cement and the architecture of the molecules of the dispersing agent used. In fact, the interaction mechanism can usually be deconstructed into two parts: a physical effect that is similar to the one produced when these molecules interact with a suspension of nonreactive (with

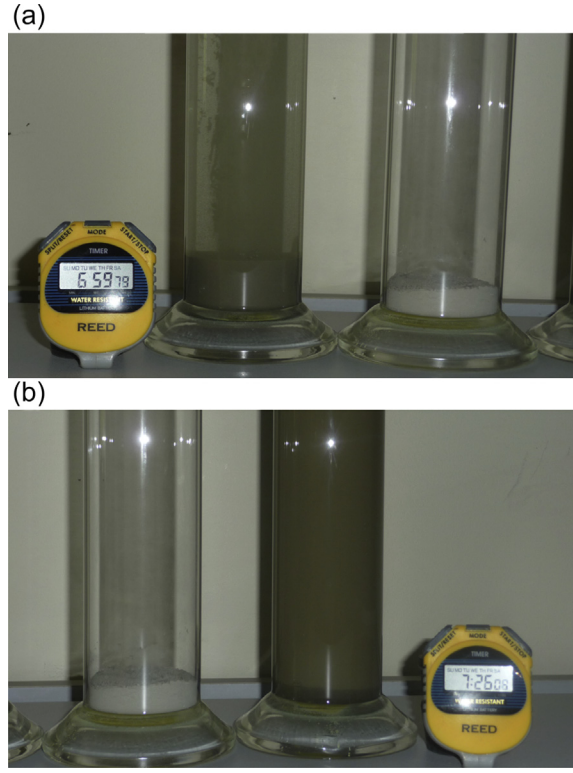


Figure 2 Bottom of the two graduated cylinders after about 7 min: without superplasticizer (left) and with superplasticizer (right). (a) 6.59 min, (b) 7.26 min.

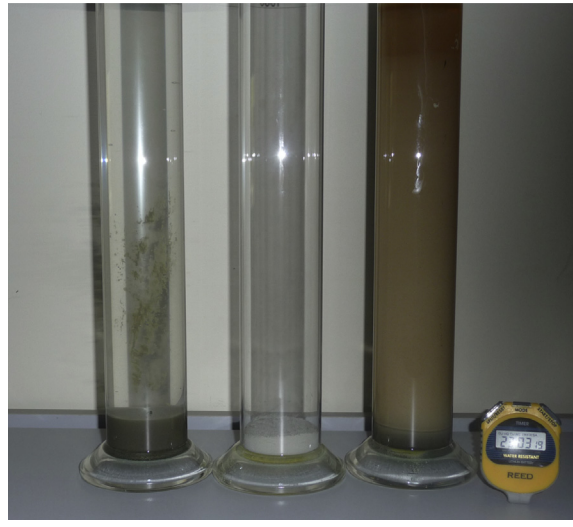


Figure 3 The graduated cylinders 24 h after the beginning of the experiment: without superplasticizer (left) and with superplasticizer (right).

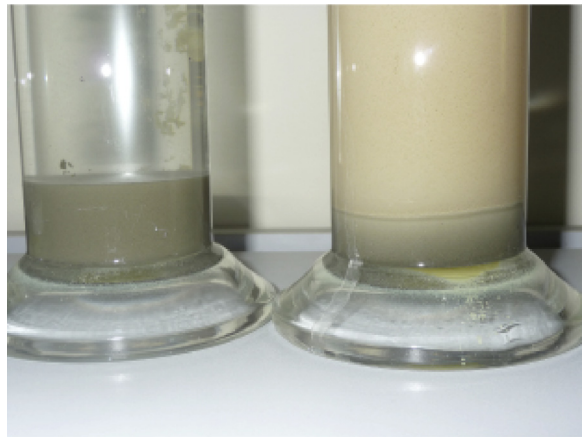


Figure 4 Close view of the bottom of the two graduated cylinders after 24 h: without superplasticizer (left) and with superplasticizer (right).

water) particles, such as TiO_2, Al_2O_3, $CaCO_3$, etc.; and a chemical effect that can be linked to the chemical reaction of these molecules with the most active sites of the anhydrous cement particles or with cement particles during their hydration. For example, the interaction of superplasticizers with hydrating aluminate phases may lead to loss of dispersion efficiency, either through formation of organo-aluminate compounds or of aluminate hydrates of higher specific surface than those produced otherwise.

References

Black, B., Rossington, D.R., Weinland, L.A., 1963. Adsorption of admixtures on Portland cement. Journal of the American Ceramic Society 46 (8), 395–399.

Chatterji, V.S., 1988. On the properties of freshly made Portland cement paste: part 2, sedimentation and strength of flocculation. Cement and Concrete Research 18, 615–620.

Dodson, V., 1990. Concrete Admixtures. Van Nostrand Reinhold, New York.

Eckel, E.C., Burchard, E.F., 1913. Portland Cement Materials and Industry in the United States. Department of the Interior, United States Geological Survey. Washington Government Printing Office, Bulletin 522.

Flatt, R.J., 2001. Dispersants in concrete. In: Hackley, V.A., Somasundran, P., Lewis, J.A. (Eds.), Polymers in Particulate Systems: Properties and Applications. Surfactant Science Series. Marcel Dekker Inc. (Chapter 9), pp. 247–294.

Flatt, R.J., 2004. Dispersion forces in cement suspensions. Cement and Concrete Research 34, 399–408.

Garrison, E., 1991. A History of Engineering. CRC Press, Boca Raton, Fla.

Holbrook, W., 1941. Natural cement comes back. Popular Sciences Monthly 139 (4), 118–120.

Jackson, F.H., 1944. And introduction and Questions to which Answers are Thought. Journal of the American Concrete Institute 15(6). In: Concretes containing Air-Entraining Agents-A Symposium, vol. 40. A part of the Proceedings of the American Concrete Institute, Detroit, pp. 509–515.

Kreijger, P.C., 1980. Plasticizeres and Dispersing Admixtures, Admixture Concret International Concrete. The Construction Press, London, UK, pp. 1–16.
Mielenz, R.C., 1984. History of chemical admixtures for concrete. Concrete International 6 (4), 40–53.
Mindess, S., Darwin, D., Young, J.F., 2003. Concrete. Prentice Hall, Englewood Cliffs, NJ, USA.
Powers, T.C., 1968. The Properties of Fresh Concrete. John Wiley and Sons, New York, 664 pp.
Ramachandran, V.S., 1995. Concrete Admixtures Handbook, second ed. Noyes Publications, Park Ridge, NJ, USA, 102–108.
Ramachandran, V.S., Malhotra, V.M., Jolicoeur, C., Spiratos, N., 1998. Superplasticizers. Properties and Applications in Concrete. Materials Technology Laboratory, CANMET, Ottawa, Canada.
Rixom, R., Mailvaganam, N., 1999. Chemical Admixtures for Concrete. E and FN Spon, London, UK.
Tucker, G.R., 1938. US Patent 201410589, Concrete and Hydraulic Cement, 5 pp.

Acknowledgments

The writing of this book on the *Science and the Technology of Concrete Admixtures* is the result of a team effort; therefore, our first acknowledgments are addressed to the two teams of the department of Civil Engineering of the Université de Sherbrooke and the Chair for Physical Chemistry of Building Materials in the department of Civil, Environmental, and Geomatic Engineering of the ETH Zürich (Swiss Federal Institute of Technology) that helped us in producing this book. None of us would have been able to write such a complete book that has roots in two different scientific fields—colloidal chemistry and Portland cement and concrete science—as well as in field applications. All of our collaborators had to fight to find hours in their overloaded schedules to find the necessary time to write a text that is easy to read but at the same time scientifically precise. For all of us, it has been a long work, quite often arduous but never painful, because our goal was to provide the best book we could.

I (Pierre-Claude Aïtcin) would like to particularly thank some of my former graduate students who are presently working in the industry—Nikola Petrov, Michel Lessard, Richard Morin, and Martin Vachon—for their judicious advice on the practical use of concrete admixtures in North America.

I would like also to mention the help received from Micheline Moranville, Sidney Mindess, and Adam Neville when I had some very technical questions to solve, had to edit my poor English writing, and needed to teach the team how to build a useful index. I would like also to thank my colleague Arezki Tagnit-Hamou and his assistant Irène Kelsey Lévesque for providing me with beautiful and instructive SEM pictures, as well as Patrick Paultre who provides me with the picture he has taken at the Museé des Civilisations Méditerranéennes (MUCEM) in Marseille.

As far as the production of the manuscript is concerned, I would like to thank William Wilson, a doctorate student at the Civil Engineering Department of Sherbrooke Université, who illustrated and improved my two-dimensional models explaining the crucial role of the w/c or w/b on concrete properties.

Finally, I would like to thank Regis Adeline and Armel Ract Madoux from Setec Batiment, who facilitated my introduction to the Louis Vuitton Foundation in order to obtain the necessary permission to reproduce some pictures of this outstanding building. I would like to thank Makoto Tonimura from Taiheyo Cement who introduced me to Osaka Gas. I would like also to thank Tomonari Niimura from Osaka Gas Company for the very useful information on the construction of the Senboku liquefied gas terminal, where one of the first major uses of self-compacting concrete occurred and for the authorization to incorporate in this book some pictures of this terminal.

Finally I would like to thank Robert Flatt for agreeing to participate in the writing of this book. I know that when starting a career as a professor, time is the most important and precious thing to deal with—and throughout the writing of this book you did not count it. Before writing this book, I had read some of your papers and listened to some of your presentations at various conferences. I knew that you were a brilliant young scientist, but after exchanging hundreds of email during the production of this book, I know you now as a friend that I can trust. Robert, not only was it a great pleasure to work with you, but you also helped me to make a dream come true: writing a comprehensive book on concrete admixtures.

I (Robert Flatt) would first like to thank the members of my research group for their fantastic team spirit, sense of humor, and strive for excellence. It is great to work with all of you. I would also in particular like to thank and congratulate Delphine, Giulia, and Sara—three PhD students working on admixtures who perfectly stood up to the challenge of contributing to this book. Sara greatly rejoiced, Giulia looked first absolutely terrified, while Delphine smiled and put on a look that said, "Sure, I can do that." You did do a fantastic job. I am very proud of you, but I also feel saddened realizing that you will be graduating soon and taking off to other horizons. I wish you all the best for continued success and happiness.

I would also like to thank Prof Bernhard Elsener, Dr Ueli Angst, my postdoc Dr Marta Palacios, and my former collaborator Dr Arnd B. Eberhardt from Sika Technology AG, who joined the team late in time and also produced excellent contributions. I know that this has come on top of a lot of other work, including family obligations. I also warmly thank my secretary, Ms Andrea Louys, for her crucial assistance in various administrative steps, in particular for collecting the reproduction rights for all figures reproduced from other works.

My special thanks also go to Pierre-Claude for inviting me to participate on this great adventure. Although I initially underevaluated the needed work, it has been a motivating and challenging experience. For me too, writing this book is a dream come true, but it was more on the horizon of a couple decades from now. Thanks for changing that so radically and thanks also for your trust, support, and friendship toward all of us.

Writing this book has indeed been very time consuming. In particular, it has taken a lot of time away from my family. I am sorry for this and thank my wife Inma for her incredible understanding, support, and immense patience, as well as my children Sophie and Léo for putting up with this endeavor.

We would like to thank all the journals and editing groups that allowed us to reproduce some important figures and tables already published by ourselves or our colleagues. We will not cite them in this note, but we have taken care to cite them in the different chapters where the work is used. We also are indebted to the American Concrete Institute and the Portland Cement Association for the permission granted to reproduce some parts of their technical documents.

Sherbrooke and Zurich
May 2015

Introduction

This book on concrete admixtures is neither the first one nor the last one. Concrete admixtures are becoming key components of modern concrete. Like some predecessors (Rixom and Mailvaganam, 1978; Kosmatka et al., 2002; Ramachandran, 1995), we could have decided to present the various admixtures presently on the market one after the other and actualize only the new scientific and technological knowledge acquired during recent years. Like Dodson (1990), we could have presented the admixtures in the following categories: the ones that disperse cement particles, the ones that modify the kinetics of hydration, the ones that react with one product of hydration, and the ones that have only a physical action on the properties of concrete. All of those books are interesting and useful, but we preferred to adopt a slightly different approach.

First, in Part 1, we start by presenting some basic knowledge on Portland cement and concrete, which will help the reader to understand the important role of admixtures in modifying the properties of the fresh and hardened concrete.

Then, in Part 2, we present some chemical and physical background to understand better what admixtures are chemically and through which mechanisms they modify the properties of the fresh and hardened concrete.

Thereafter, in Part 3, after presenting some general considerations of the principles governing the formulation of commercial admixtures, we present the technology of four categories of concrete admixtures:

- Admixtures that modify at the same time the properties of the fresh and hardened concrete
- Admixtures that modify the properties of the fresh concrete
- Admixtures that modify the properties of hardened concrete
- Admixtures that are used to water cure concrete

In Part 4, self-consolidating and ultra-high strength concrete, two special concretes where the use of admixtures is crucial, are presented.

In Part 5, we present our views of the future of the admixtures.

Finally, this book ends with three appendices not related specifically to admixtures but useful for developing an efficient use of admixtures.

Before entering into the theoretical and practical aspects of the use of admixtures, some introductory chapters are presented. One provides the vocabulary and the definitions used in this book in order to avoid any misunderstandings. One is a historical background of the development of concrete admixtures in order to better understand and focus on the progress realized in recent years in mastering the properties of the fresh and hardened concrete. We provide also a glossary to explain all the abbreviations used in this book.

In Part 1, Chapter 1 explains the physical meaning of the water–cement and water–binder ratios before explaining what exactly Portland cement is and how it hydrates. We opted for such an approach because we are convinced that the concept of the water–cement and water–binder ratios is the base of concrete technology. In fact, this ratio directly impacts the ultimate porosity and density of concrete, which as for other materials directly impacts mechanical and durability properties. Therefore, superplasticizers (which make it possible to produce concrete with lower water content without compromising workability) have opened the doors to radical improvements in concrete performance.

In Chapter 2, a hydration reaction is considered from two different points of view: first, from a physical point of view by insisting on the volumetric consequences of hydration reactions that are so important for understanding shrinkage; and second, from a chemical point of view in order to present the evolution of anhydrous cement particles into different chemical species with or without binding properties. A good knowledge of cement hydration is also essential to understand the behavior of Portland cement when it is blended with different supplementary cementitious materials and also to improve concrete durability towards aggressive environments.

Chapter 3 presents the basic principles governing the fabrication of Portland cement, focusing on its utilization to produce state-of-the-art concretes. The strengths and weaknesses of present cements are exposed to point out the technological challenges that the concrete industry has to face to minimize the carbon footprint of civil engineering constructions in order to remain competitive on a long-term basis.

In Chapter 4, the most important characteristics of the supplementary cementitious materials and fillers that are blended with ground clinker are exposed. Their use will increase substantially in the future in order to decrease the carbon footprint of concrete. When blending some filler with clinker, it is very important also to realize that it is not sufficient to substitute a certain volume of clinker by an equivalent volume of filler to decrease the carbon footprint of a concrete structure; it is also necessary at the same time to decrease the concrete's water–binder ratio in order to improve the long-term durability of concretes made with fillerized cements.

In Chapter 5, the important role played by water on the rheology of fresh concrete and the long-term durability of hardened concrete is emphasized. For a long time, water was the only ingredient whose dosage could be changed to modify concrete rheology, but presently several admixtures can be used to modify the rheology of the fresh concrete. As consequence of the mastering of the use of these new admixtures, it has been possible to pump concrete up to 600 m and very soon to 1000 m with a single pump. The behavior of water molecules in a porous system is presented also in order to explain how molecular forces can overcome gravity forces and explain the origin and development of the different forms of shrinkage that engineers have to take into consideration in their design.

In Chapter 6, the advantages of entraining air in concrete are presented. For too many engineers, entrained air is only introduced into concrete to make it freeze-thaw resistant in the presence or not of deicing salts. They do not realize, however, that entraining air bubbles in concrete may substantially improve its rheology and long-term durability. In Chapter 1, it was seen that concrete durability is essentially

linked to the water–cement (w/c) ratio rather than to the compressive strength of the concrete. An air-entrained concrete that has a lower compressive strength than a similar non-air-entrained concrete having the same workability, but a lower w/c, will be more durable. Finally, entrained air is commonly used in self-consolidating concretes to improve their rheology.

Chapter 7 presents the basic principles that are governing concrete rheology, which is of such great importance during the placing of concrete. Concrete competiveness is linked to the facility with which it can be handled, pumped, and placed because the cost of its placing has a direct impact on the final cost of concrete structures. Improving and controlling concrete pumpability is a key factor for the success of the concrete industry. Our focus lies on yield stress and superplasticizers. However, we also explain how other properties, such as plastic viscosity and thixotropy, may be modified by chemical admixtures.

Part 1 ends with Chapter 8, which is devoted to the mechanisms of cement hydration because, as we will see, chemical admixtures may interfere strongly positively, but also sometimes negatively, with the normal course of hydration.

Part 2 includes an important focus on superplasticizers because they are the most widely used type of chemical admixtures. However, as much as possible, a more generic approach to working mechanisms was adopted in order to lay a broader base for interpreting the action of admixtures on the basis of physics and chemistry.

In Chapter 9, we present an overview on the chemistry of organic admixtures. We have done so as these offer more flexibility in design and added value to chemists. The admixtures covered are Superplasticizers, Viscosity Modifiers, Shrinkage Reducing Admixtures, Air Entrainers and Retarders. The overview presented should set a basis to better understand the working mechanisms of these admixtures developed in the subsequent chapters.

Chapter 10 deals with the adsorption of admixtures at interfaces: both solid-liquid and liquid-vapor. This represents a major step in the working mechanisms of many admixtures. Superplasticizers must be adsorbed in order to exert their dispersing power, but retarders also involve adsorption to modify the dissolution of anhydrous phases or nucleation and/or growth of hydrates. Air entrainers and shrinkage reducing admixtures for their part must adsorb at liquid-vapor interfaces to be active. Therefore, we attempted to develop a comprehensive treatment of adsorption, covering both theoretical and experimental aspects.

Following this, in Chapter 11, the working mechanisms of superplasticizers are addressed. For this, we build upon material presented in the previous chapters. Additionally, we outline the nature of interparticle forces in cementitious systems, which are responsible for agglomeration. On this basis, we explain how chemical admixtures can reduce these attractive interparticle forces, reducing the degree of agglomeration, reducing yield stress, and improving workability. A specific section is devoted to polyacrylates, for which the consequences of molecular structure modifications are presented in a systematic way.

Because superplasticizers also tend to delay cement hydration, it appeared appropriate to discuss the reasons for this in Chapter 12. In our opinion, the retardation caused by this type of admixture will be of growing concern for cements having increasing levels

of clinker replacement. Indeed, to compensate for their lower early strength, one often resorts to water reduction, which requires an increased superplasticizer dosage. Unfortunately, this increases retardation and offsets (at least in part) the expected benefit. Because this subject still requires substantial research, we present a critical review of the main works on the subject. Additionally, we also cover the retardation of admixtures specifically used for this purpose, in particular sugars. There we attempt to summarize recent findings and point to possible interpretations in terms of working mechanisms.

Chapter 13 is then devoted to the working mechanisms of shrinkage-reducing admixtures of the different types of molecules used to control the development of autogenous shrinkage developed in concrete having a low w/c (<0.40) as well as in the development of drying shrinkage of concretes having a high w/c (>0.50).

Chapter 14 is devoted to explaining the basic principles involved in the corrosion of reinforcing steel bars and the different strategies that can be implemented to solve this problem.

Chapter 15 begins Part 3 of the book, where we address the question of formulating commercial products. Indeed, the majority of commercial admixtures are not composed of pure compounds. Therefore, a commercial admixture must balance many requirements. However, this reality is not clearly visible to most end users and very often is misperceived as "dark arts" in the academic community. This is why we present a brief overview on some aspects of formulation and a couple typical additions that may be found in commercial admixtures.

Thereafter, Part 3 continues by presenting the technology of admixtures that modify at the same time the properties of the fresh and hardened concrete. This category comprises the water reducers and superplasticizers, which are presented in Chapter 16. For us, water reducers are simply dispersants of cement particles that are less efficient than superplasticizers.

Chapter 17 is devoted to air-entraining agents that modify, at the same time, the rheology of fresh concrete as well as its strength and durability against freezing and thawing cycles in the presence or not of deicing salts.

In Chapters 18–21, we present admixtures that modify the properties of the fresh concrete. Chapter 18 concerns retarders and Chapter 19 is about accelerators. These two types of admixtures modify the kinetics of the hydration reaction. In one case, the hydration reaction is retarded; in the other, it is accelerated. Chapter 20 presents the use of viscosity-modifying admixtures, which are gaining a large acceptance in the concrete industry when producing self-consolidating concrete and pumping concrete or for underwater concreting. Finally, Chapter 21 concerns antifreeze admixtures. This type of admixture is currently used in Finland, Poland, Russia, and China but unfortunately not in North America. A successful experimental use in Canada is presented.

Next, the admixtures that modify the properties of hardened concrete are presented.

Chapter 22 deals with expansive agents that are used to counteract autogenous shrinkage. The expansion of the apparent volume of the concrete they produce can be adjusted to be almost equal to the reduction of its apparent volume resulting from the development of autogenous shrinkage. In Chapter 23, shrinkage modifiers are presented. By reducing the energy of the liquid-vapor interface (decreasing the surface tension in the menisci and the angle of contact of these menisci), they decrease the effects of the

different types of shrinkage that are developed in concrete. Finally, in Chapter 24, corrosion inhibitors are presented. In this chapter, the different mechanisms of corrosion are reviewed and different strategies to counteract this phenomenon are treated. These admixtures do not compensate for bad concrete practices, but their efficiency in controlling the corrosion of reinforcing increases with the quality of the concrete.

Chapter 25 is devoted to admixtures used to water-cure concrete; the appropriate use of curing membranes and evaporation retarders is explained. Too often, the top surface of high-performance concrete slabs or bridge decks is covered by a curing membrane as soon as they are finished so that this curing membrane prevents the later penetration of external water within the concrete to cure it properly. Low w/c concretes that do not contain enough water to fully hydrate all the cement particles they contain rapidly develop significant autogenous shrinkage. This shrinkage can result in an early severe cracking of the concrete surface when not properly water cured. One way to fight this uncontrolled development of autogenous shrinkage is to water-cure the concrete surface with an external source of water. Evaporation retarders that form a monomolecular film on the surface of the fresh concrete temporarily prevent the water contained in the concrete from evaporating—or at least strongly delay its evaporation. When the concrete is hard enough to support direct water curing with hoses, this film is washed away and the external water can penetrate into concrete.

In Part 4, two particular types of concrete are presented:

- self-consolidating concrete in Chapter 26
- ultra-high-strength concrete in Chapter 27

These particular concretes represent high-tech concretes. They are obtained through the use of well-dosed admixtures. Their use is growing rapidly because it increases concrete competitiveness in the construction industry.

In Part 5, the concluding chapter (Chapter 28) presents R.J. Flatt's views of the future of admixtures. Finally, the book ends with three appendices, which are not specifically linked to admixture technology but are very useful for learning how to use admixtures more efficiently:

- Appendix 1 provides useful formulae,
- Appendix 2 provides factorial design plans, and
- Appendix 3 discusses statistical control.

P.-C. Aïtcin and R.J. Flatt

References

Dodson, V., 1990. Concrete Admixtures. Van Nostrand Reinhold, New York, 211 p.

Kosmatka, S.H., Kerkhoff, B., Panarese, W.C., MacLeod, N.F., McGrath, R.J., 2002. Design and Control of Concrete Mixtures, 7th Canadian ed. Cement Association of Canada, Ottawa, Canada, 355p.

Ramachandran, V.S., 1995. Concrete Admixtures Handbook. Noyes Publications, Park Ridge, N.J., USA, 1153 p.

Rixom, R., Mailvaganam, N.P., 1978. Chemical Admixtures for Concrete. E and FN SPON, London, 437 p.

Terminology and definitions

Introduction

To take full advantage of a technical book, it is very important for the reader to know the exact significance of the technical terms used, which is why we include this appendix on terminology and definitions. The authors ask the reader to accept their choices. This does not imply that the proposed terminology and definitions in this book are better than any others; it is simply a matter of consistency and clarity. It has been decided to use the American Concrete Institute (ACI) terminology, although with some divergence from time to time. The corresponding European terminology and definitions are mentioned when they are quite different from those of the ACI.

Cement, cementitious materials, binders, fillers

ACI Standard 116 R contains 41 entries starting with the word "cement" to define some of the cements used in the concrete and asphalt industries, plus five additional entries containing the expression "Portland cement" (with an upper case P). There are no entries for *supplementary cementitious materials*, only for *cementitious* (having cementing properties) materials.

In accordance with the recommendation of ACI Committee 116, we use the expression "**blended cement**" to refer a cement containing various types of (hydraulic) powders mixed with ground clinker. We like this expression "blended cement" because it is simple: it clearly indicates that the cement is a mixture of fine materials. Of course, this "dilution" of Portland cement clinker with different supplementary cementitious materials or fillers is closely related to the necessity of decreasing the environmental impact of cement in terms of its CO_2 emissions.

However, we add a personal touch to this ACI terminology by also using in parallel the word "**binder**" when speaking of cements containing some finely divided materials that also react with water and the lime liberated by Portland cement hydration. We favor the use of this rather imprecise single word because its imprecision better reflects the diversity of the blends that are now being used all over the world and the even greater diversity that will be used in the future to make concrete more sustainable by minimizing the amount of Portland cement clinker contained in the cement.

We use the word "**clinker**" rather than "Portland cement clinker" because, for us, the word "clinker" automatically implies Portland cement. A clinker is the partially fused material produced in a cement kiln, which is ground to make Portland cement.

In this book, the word "**filler**" was used in a more restrictive way than that proposed by ACI. The word *filler* refers to a finely divided material that is either much less reactive than supplementary cementitious materials or not reactive at all. The fillers currently used in Portland cement primarily are pulverized limestone or silica. They are blended with Portland cement to improve its sustainability.

The expression "**CO_2 content of a binder**" represents the amount of CO_2 that was emitted during the extraction of the raw materials and their processing during the manufacture of the binder. For example, to produce 1 ton of clinker in a modern cement plant, it is necessary to emit about 0.8 ton of CO_2, half coming from the calcination of the limestone and most of the rest from the fuel necessary to reach partial fusion of the raw meal during the production of the clinker.

Binary, ternary, and quaternary cements (or binders)

These expressions will be used to designate certain blended cements. They indicate how many cementitous materials or fillers are included in the blend without indicating their nature or amount. For example, ternary cement can be composed of Portland cement, slag, and silica fume; Portland cement, fly ash, and silica fume; or Portland cement, slag, and fly ash, and so on. In more common usage, Portland cement refers as a combination of clinker and gypsum.

Cementitous material content

When a blended cement is composed of several cementitious materials, the content of each of these materials in the blend is always calculated as a percentage of the total mass of the blended cement. Therefore, a quaternary cement might be composed of 72% Portland cement, 15% slag, 10% fly ash, and 3% silica fume.

Specific surface area

The expression *specific surface area* refers to the total external surface of all of the particles contained in a unit mass of a material. As the specific surface area is always obtained through some indirect measurement, it is essential to specify by which method it has been determined, such as Blaine or BET (nitrogen adsorption). It is usually expressed in m^2/kg with no more than two significant digits. For example, the Blaine specific surface area of a typical Portland cement is 420 m^2/kg and the nitrogen (BET) specific surface area of a typical silica fume is 18,000 m^2/kg. Note that the Blaine and

BET techniques will give quite different values for the same material, and that there is no standard technique for converting from one value to the other.

Alite and belite

Alite and belite are used to refer to the impure forms of tricalcium silicate (C_3S) and dicalcium silicate (C_2S), as suggested by Thornborn in 1897 (Bogue, 1952).

Hemihydrate

We use the abbreviated expression hemihydrate to designate calcium sulfate hemihydrate ($CaSO_4 \cdot {}^1/_2H_2O$).

Water–cement, water–cementitious materials, water–binder ratios

We use the ACI notation for the water–cement ratio, using a dash to separate the word *water* from the word *cement*. In its abbreviated form, this ratio will be expressed as w/c (using the lower case w and c), but now with a slash to separate them. In this case "*w*" and "*c*" represent the mass of water and cement, respectively. The use of upper case *W* and *C* is used to express the *volumetric* water–cement ratio. These notations are opposite to the European usage. The water–cement ratio is the ratio of the mass of water, exclusive of that absorbed by the aggregates to the mass of cement in a concrete, mortar, grout, or cement paste mixture. It is stated as a decimal number and abbreviated as "*w/c*."

However, we do not use the expression "**net *w/c***" as used by ACI, where *w* represents the mass of the effective water used in the batch. We do not see the necessity of adding the qualification "net" because there is not a "gross" *w/c*: *w/c* is a unique number.

The definitions of the water–cementitious material ratio and water–binder ratio are obtained by substituting in the preceding definition the words *cementitious material* and *binder* for the word *cement*. Consequently, we use the abbreviated form *w/b* and occasionally *w/cm* to represent the water–binder and water–cementitious material ratios.

Saturated surface-dry state for an aggregate (SSD state)

This is an important concept for the design of concrete mixtures as well as for internal curing, which is treated in detail in Appendix A1. It refers to the condition of an aggregate particle or any other porous solid when all of its permeable voids are filled with water, but which does not have water on its exposed surfaces. SSD is the abbreviated

form that will be used. The SSD state represents the reference state of an aggregate when calculating or expressing the composition of concrete mixtures.

Water content, absorption, moisture content of an aggregate

We do not follow the ACI Committee 116 recommendations, instead using the following definitions:

The expression "(**total) water content**" is used instead of "moisture content" of an aggregate to represent the ratio of the mass of water contained in a given aggregate to its dry mass. The water content is expressed as a percentage, with **no more than 2 significant digits**.

The expression "**absorption of an aggregate**" is used instead of "absorbed moisture" to refer to the moisture that has entered a solid by absorption and that has physical properties not substantially different from ordinary water at the same temperature and pressure.

The expression "**moisture content of an aggregate**" is used instead of "free moisture" to refer to the moisture not absorbed by the aggregate and that has essentially the properties of pure water in bulk.

Specific gravity

Here, we (more or less) follow the ACI terminology.

Specific gravity is the ratio of the mass of a volume of a material at a stated temperature to the mass of the same volume of distilled water at the same temperature. It is a relative number, written always with no more than **2 digits after the decimal point**. Moreover, we use the expression "SSD specific gravity" for an SSD aggregate, not the recommended "bulk specific gravity" because the term "bulk" does not bring to mind the SSD state of the aggregate.

The term *specific gravity of a powder* is used rather the expression "absolute specific gravity" because we are uncomfortable using the qualification "absolute" before a relative number.

Moreover, for us, the theoretical specific gravity of Portland cement is not 3.15 or 3.16; it is instead 3.14—a number that is very easy to remember.

Superplasticizer dosage

We express the superplasticizer dosage as the percentage of active solids contained in its commercial solution relative to the mass of the binder used in a mixture. In some cases, we will indicate the number of liters of the commercial solution used to reach

this percentage. In Appendix A1, practical calculations to go from one form of the superplasticizer dosage to the other are presented.

Eutectic

In a phase diagram, a eutectic composition has a constant temperature of fusion/solidification, like a pure phase, in spite of the fact that it is not a pure phase.

P.-C. Aïtcin

Reference

Bogue, R.H., 1952. La chimie du ciment Portland. Eyrolles, Paris.

Glossary

δ_0 Solvent layer thickness (half the minimum separation distance between particle surfaces)
δ_P Adsorbed layer thickness of a polymer (regardless of its type)
δ_ζ Distance between particle surface charge location
θ Surface coverage (fraction of surface occupied by polymers)
σ Standard deviation
χ Ki parameter for polycarboxylate ether side chains
a_N Length of monomer in polycarboxylate ether backbone
a_P Length of monomer in polycarboxylate ether side chain
A Hamaker constant
ACI American Concrete Institute
AEA Air-entraining admixture
AFm General term for a family of caclium - aluminum layer double hydroxides, the most common of which is monosulfoaluminate hydrate, but that also includes hydrocalumite, carboaluminats and Friedel's salt
AFM Atomic force microscopy
ASR Alkali silica reaction
ASTM American Standard and Testing Material
BET Brunner, Emmer and Teller (determination of specific surface area)
BPR Béton de poudre réactive (Reactive Powder Concrete)
C/E Ratio of carboxylate groups to side chains in a polycarboxylate ether comb-copolymer
C_2S Bicalcium silicate, $2CaO \cdot SiO_2$
C_3A Tricalcium aluminate, $3CaO \cdot Al_2O_3$
C_3S Tricalcium silicate, $3CaO \cdot SiO_2$
C_4AF Tetracalcium ferroaluminate, $4CaO \cdot Al_2O_3 \cdot Fe_2O_3$
CAC Critical aggregation concentration
CE Cellulose ether
CH Portlandite, calcium hydroxide, $Ca(OH)_2$
Class C fly ash A fly ash containing at least 10% CaO
Class F fly ash A fly ash where $SiO_2 + Al_2O_3 + Fe_2O_3 > 70\%$
CMC Critical micelle concentration
C−S−H Hydrated calcium silicate
DEA Diethanol amine
DLVO Derjaguin, Landau, Verwey and Overbeck (theory of interparticle force additivitiy)
DOT Department of Transportation
DPG Dipropylene glycol
DPTB Dipropylene-*tert*-butyl ether
DS Degree of substitution
ECL Effective chain length

EO Ethylene oxide (monomer)
F_{ES} Electrostatic force between particles
F_{Ste} Steric hinderance force between particles
F_{VDW} Van der Waals force between particles
FA Fly ash
FBW Flexible backbone worm (most common polycarboxylate ether conformation)
FS Silica fume
G Interparticle force normalized to the particle radius
GPC Gel permeation chromatography
h Interparticle distance (from surface to surface)
HEC Hydroxyethyl cellulose
HEMC Hydroxyethyl methyl cellulose
HETCOR Heteronuclear correlation nuclear magnetic resonance
HLB Hydrophile–lipophile balance
HPC High-performance concrete
HPEG-MA ω-Hydroxy polyethylene glycol methacrylate macromonomer
HPG Hydroxypropyl guar
HPLC High-performance liquid chromatography
HPMC Hydroxypropyl methyl cellulose
κ^{-1} Debye length
k or k_B Boltzmann's constant
kT Thermal energy (product of *k* and *T*)
LAS Linear alkylbenzenesulfonate
LNG Liquefied natural gas
LOI Loss on ignition
LS Lignosulfonate (plasticizer)
MA Methacrylic acid
MS Molar substitution
Na_2O_{equi} Alkali equivalent $Na_2O+0{,}65\ K_2O$
n Number of side chains in a polycarboxylate ether comb-copolymer
N Number of backbone monomers per side chain in a polycarboxylate ether
NMR Nuclear magnetic resonance
OPC Ordinary Portland cement
P Number of monomers in a PCE side chain
PAA Polyacrylic acid
PCA Portland Cement Association
PCE Polycarboxylate ether
PCP Polycarboxylate polymer
PEG Polyethylene glycol (a PEO but shorter)
PEO Polyethylene oxide
PMS Polymelamine sulfonate (superplasticizer)
PNS Polynaphthalene sulfonate (superplasticizer)
PPO Polypropylene oxide
QC Quality control
RAC Adsorbed layer thickness for adsorbed polycarboxylate ether comb-copolymer
RPC Reactive powder concrete
SAP Superabsorbant polymers
SCC Self-compacting concrete
SCM Supplementary cementitious material

SEC Size exclusion chromatography
SEM Scanning electron microscope
SF Silica fume
SFA Surface force apparatus
SP Superplasticizer
SRA Shrinkage-reducing admixture
SSA Specific surface area
SSD Saturated surface dried
T Absolute temperature (in Kelvin)
TEA Triethanolamine
Three D model (3D) Three-dimensional model
TOC Total organic carbon (in solution)
Two D model (2D) Two-dimensional model
UHPC Ultra-high-performance concrete
UHSC Ultra-high-strength-concrete
V Coefficient of variation
VMA Viscosity-modifying admixture
w/b Massic water–binder ratio
W/B Volumetric water–binder ratio
w/c Massic water–cement ratio
W/C Volumetric water–cement ratio

The importance of the water–cement and water–binder ratios

1

P.-C. Aïtcin
Université de Sherbrooke, QC, Canada

1.1 Introduction

It may be surprising to start a book on the science and technology of concrete admixtures by a chapter devoted to the importance of the water–cement (w/c) and the water–binder (w/b) ratios, before even explaining what Portland cement is and how it reacts with water. We agree with Kosmatka (1991) that the w/c and w/b ratios are the most important characteristics of concrete; they govern its properties in the fresh and hardened states and also its durability. It is therefore fundamental to understand their profound significance in order to optimize the use of concrete with the help of admixtures and thus to maximize its economic value while minimizing at the same time its carbon footprint.

Despite what many cement chemists think, the most important parameters that control concrete compressive strength are not:

- the cement dosage expressed in kg/m^3
- the strength of the small cubes used to test the "cement compressive strength"
- the C_3S and C_3A content of the clinker
- the fineness of the cement, or
- the "gypsum" content.

In fact, the most important parameters have always been the w/c and w/b ratios, as was found in the nineteenth century by Féret (1892) for cement pastes and later on by Abrams, 1918 for concrete. As will be shown later, these ratios control the microstructure of the cement paste in both the fresh and hardened states, and consequently its rheology, mechanical properties, permeability, durability, and sustainability.

When batching concrete, each of its solid components is weighed; thus, it is common to express the w/c ratio as a mass ratio instead of a volumetric ratio. In this book, the symbols w/c and w/b will be used for the mass ratio, whereas W/C and W/B will be used for the volumetric ratios, according to American Concrete Institute (ACI) terminology. Note that the RILEM (*Rassemblement International des Laboratoires d'Essais sur les Matériaux*) terminology is the opposite.

It is always possible to transform the mass ratio into a volumetric one by taking into account the specific gravity of the cement. In this book, the theoretical specific gravity of Portland cement is taken as 3.14, which is an easy number to remember and a

Science and Technology of Concrete Admixtures. http://dx.doi.org/10.1016/B978-0-08-100693-1.00001-1
Copyright © 2016 Elsevier Ltd. All rights reserved.

number very close to that of an actual "pure" Portland cement. The specific gravity of a blended cement containing a filler or supplementary cementitious materials with specific gravities different from 3.14 will be usually less than 3.14. In this chapter, it will be shown that w/c and w/b ratios are more than simple abstract numbers with an inverse relationship to concrete compressive—they do have a physical meaning.

1.2 The hidden meaning of the w/c

Using a sophisticated three-dimensional model, Bentz and Aïtcin (2008) demonstrated that the w/c ratio is a number directly related to the average distance between cement particles within a cement paste after it is mixed with water just before it begins to hydrate. This distance between the cement and/or binder particles influences the hydration conditions and the microstructure of the hardened cement paste and, consequently, its mechanical properties and durability.

To illustrate this fundamental concept, we will instead use a very simple two-dimensional (2D) model to provide **a qualitative** explanation of the meaning of the w/c. Consider four **circular** cement particles having a radius a that are placed at the corners of a square with a side equal to $3a$, as represented in Figure 1.1. The minimum distance between these cement particles is their distance along the sides of the square: it is equal to a.

This arrangement of the cement particles can be represented by the unit cell shown in Figure 1.2.

Now calculate the W/C of this unit cell. The surface area of the unit cell is $3a \times 3a = 9a^2$. The surface of the cement particles is $4 \times {}^1/_4\,(3.14 \times a^2) = 3.14a^2$.

The mass of the cement particles in this unit cell is equal to 3.14 $(3.14 \times a^2)$ because our theoretical cement has a specific gravity of 3.14. Because the value of 3.14^2 is close to 10 (9.86 exactly), we can assume that the mass of cement in the

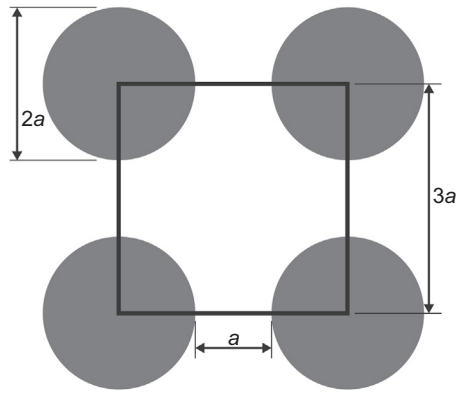


Figure 1.1 Schematic representation of the 2D model used to calculate the w/c and the distance between cement particles.
Courtesy of William Wilson.

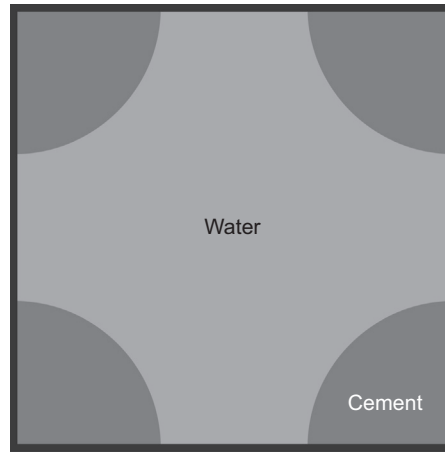


Figure 1.2 Unit cell corresponding to the previous arrangement of cement particles. Courtesy of William Wilson.

unit cell is equal to $10a^2$. The volume (and mass) of water contained in the unit cell is equal to $9a^2 - 3.14a^2 = 5.86a^2$. Therefore, the w/c (mass ratio) of this unit cell is $w/c = 5.86a^2/10a^2 = 0.586$, which can be rounded up to 0.60. This is the w/c of an ordinary concrete that has a compressive strength in the order of 25 MPa.

Now, as shown in Figure 1.3, let us place another cement particle having a radius a at the center of the unit cell, which diagonal is 4.24 long. In this case, the minimum distance between two cement particles along the diagonal is $^1/_2(4.24a - 4a) = 0.12a$.

A calculation similar to the previous case shows that the w/c of this new unit cell is now 0.14. This w/c is somewhat lower than that of an ultra high in strength concrete having a compressive strength of over 200 MPa (Richard and Cheyrezy, 1994).

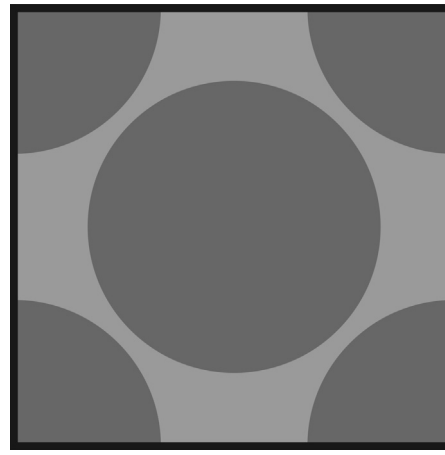


Figure 1.3 2D model of a more compact system. Courtesy of William Wilson.

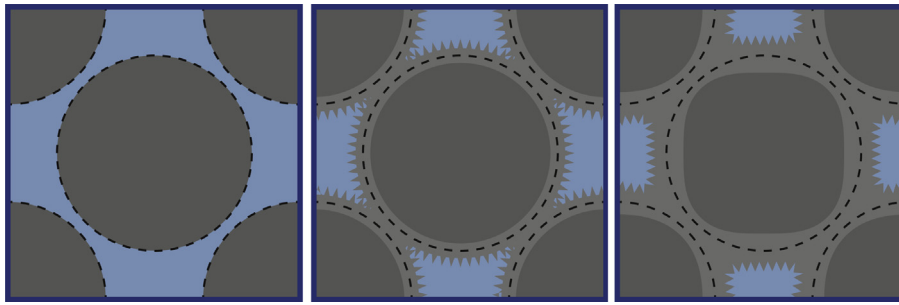


Figure 1.4 Hydration of cement particles in the previous system.
Courtesy of William Wilson.

Thus, by replacing the water in the center of the first unit cell by a cement particle, it is possible to decrease the following:

- The minimum distance between two cement particles to $0.12a$ instead of a (about an order of magnitude shorter)
- The w/c of the unit cell to 0.14 instead of 0.60 and to increase the compressive strength from 25 to 200 MPa

Moreover, in this second unit cell (Figure 1.4), it may be seen that the cement particles are so close to each other that the hydrates formed on the surface of one cement particle have only to grow a very short distance before reaching the hydrates growing on the surface of the adjacent cement particles (Granju and Maso, 1984; Granju and Grandet, 1989; Richardson, 2004).

The proximity of the cement particles in this unit cell results in the rapid development of very strong bonds and very low porosity. Therefore, in such an arrangement of cement particles, it is not necessary to use cements having high C_3A and C_3S contents and a high fineness in order to produce a rapid hardening of the cement paste. Moreover, it may also be seen that in such a unit cell, it is only necessary to form a very small amount of "glue" to obtain a high strength and it is not necessary for all of the cement particles be fully hydrated to obtain a high strength material. Finally, it will be seen later that in such a dense system, the unhydrated parts of the cement particles act as hard and rigid inclusions that serve to strengthen the resulting hydrated paste.

1.3 The water–cement and water–binder ratios in a cement paste made with a blended cement

To lower the carbon footprint of Portland cement, modern cements are increasingly becoming blended cements in which a certain amount of the ground clinker is replaced by a supplementary cementitious material or a filler (Kreijger, 1987; Mehta, 2000). Such a system can be characterized by its w/c and w/b ratios, which are different. In the first case, we are considering only the Portland cement contained in the system; in the second case, we are considering the amount of cement and supplementary

particles in the system. Using the same 2D model, we can show that knowing both numbers is very important to explain some of the physical and mechanical properties of a cement paste made with a blended cement.

1.3.1 Case of a blended cement containing a supplementary cementitious material

Let us go back to Figure 1.2 and replace one of the four cement particles with a circular particle of a supplementary cementitious material having the same diameter as the cement particles as shown in Figure 1.5. For this purpose, it is not necessary to know whether it is a slag or a fly ash particle, as long as it has the same radius of our theoretical circular cement particle. The substitution of one cement particle of the unit cell by a supplementary cementitious particle having the same diameter represents a volumetric substitution rate of 25%.

Now, the new unit cell can be characterized by two numbers, namely its w/c and w/b ratios. The w/b ratio of this new unit cell is the same as the w/c ratio of the unit cell shown in Figure 1.2, but its w/c ratio is greater because only three particles out of four are Portland cement particles. A simple calculation shows that now the w/c value of this unit cell is 0.78. The higher value of the w/c ratio is due to the fact that the Portland cement content of this unit cell has been diluted.

Because supplementary cementitious materials are initially less reactive than Portland cement particles, the *initial* strength of this blended cement will be lower than that of the pure Portland cement. The Portland cement particles adjacent to supplementary cementitious particles will have to develop their hydrates over a distance twice as long as in Figure 1.2 to reach the adjacent supplementary cement particle because the supplementary cementitious particle will not develop any hydrates

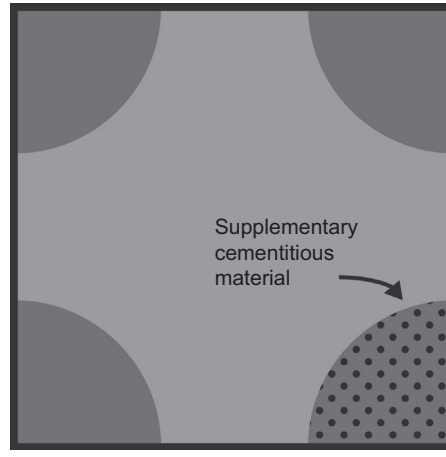


Figure 1.5 2D model of a blended cement containing 25% by volume of a supplementary cementitious material.
Courtesy of William Wilson.

on a short-term basis. Therefore, in the short term as far as compressive strength is concerned, the system is performing less well than the previous one.

Over the long term, when the supplementary cementitious particles will have reacted with the lime liberated by the hydration of the Portland cement particles, the system will be as strong as, or even stronger, than the one represented in Figure 1.2. However, to reach the same compressive strength, a **long water curing** period is a must. The compressive strength of a **well-cured** system containing supplementary cementitious materials will be greater than the equivalent pure Portland cement system. The lime crystals (portlandite) that are a byproduct of the hydration of the anhydrous calcium silicates that make up most of the Portland cement do not bring any strength to the hydrated cement paste in a pure Portland cement system. However, in a system with supplementary cementing materials, they are transformed into secondary calcium silicate hydrates that are the same as the "glue" developed in pure cement paste.

It is very important to note that the dilution of Portland cement results in a decrease in the short-term compressive strength of the concrete if the chemical composition of the clinker is not changed. However, in the long term, it results in equivalent (or even higher) strength.

The network of the capillary pores in this new system is characterized by its w/b ratio, which is much lower than the w/c ratio of the system. We will see later that the w/b ratio is a very important parameter when analyzing the different forms of shrinkage that develop in such a system.

Returning to Figure 1.2, let us introduce a particle of cementitious material having the same radius a as the cement particles in the center of the unit cell, as shown in Figure 1.6. In such a system, the substitution rate by volume of Portland cement is now 50%, double that of the previous one.

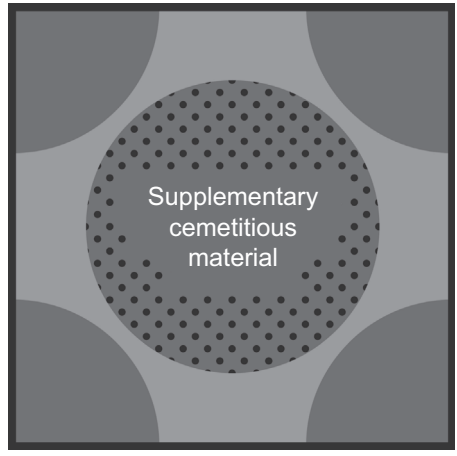


Figure 1.6 2D model of a unit cell containing a particle of supplementary cementitious material in the middle of the four cement particles.
Courtesy of William Wilson.

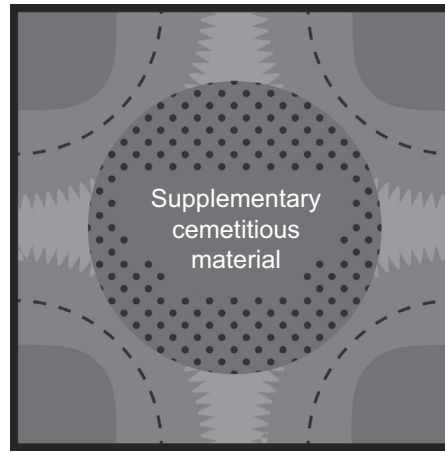


Figure 1.7 Hydration of the previous system.
Courtesy of William Wilson.

The w/b ratio of this new unit cell is 0.14 and its w/c ratio is 0.27. We can see in Figure 1.7 that as soon as the cement particles start to hydrate, the superficial hydrates will have to grow only a very short distance to surround this central supplementary cementitious particle and to create strong bonds.

This matrix will become even stronger when the supplementary cementitious particle starts to react with the lime liberated by the hydration of Portland cement particle, in spite of the fact that the volumetric rate of substitution of the Portland cement is now 50%. Therefore, both the early and the long-term compressive strength of blended cements do not essentially depend on the substitution rate of Portland cement, but rather on the w/b ratio of the system.

With superplasticizers, we are able to drastically decrease the w/b ratio of such systems that contain a large volume of supplementary cementitious materials. In the case of fly ash, Malhotra and Mehta (2008) refer to such concretes as *high-volume fly ash*. ACI (2014) published the "ACI 232.3R-14 Report on High-Volume Fly Ash Concrete for Structural Applications." High-volume fly ash concretes have been used in California in various civil engineering projects (Mehta and Manmohan, 2006).

Of course, high-volume slag concrete can be produced in the same way. It is important to note that in order to obtain an increase in the long-term strength, some water has to be available for hydrating the supplementary system on a long-term basis in such a system.

1.3.2 Case of a blended cement containing some filler

In our initial unit cell represented in Figure 1.2, let us replace one of the cement particles with a filler particle having the same diameter as the cement particles, as shown in Figure 1.8.

We now obtain a unit cell similar to that of Figure 1.5, with the difference being that one of the cement particles is replaced by a nonreactive limestone filler particle instead

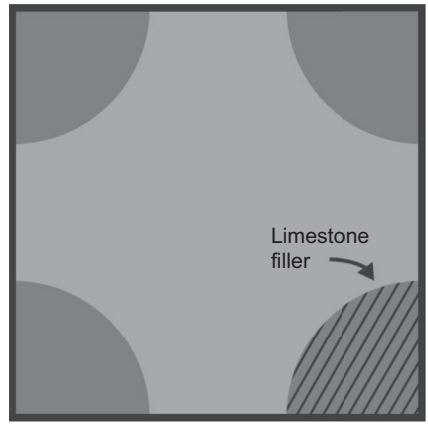


Figure 1.8 2D model of blended cement where one particle of filler has been substituted for one particle of cement.
Courtesy of William Wilson.

of a reactive supplementary cementitious material particle. The nonreactivity (or very low reactivity in the case of some limestone filler particles) of the substituted particle means that in this type of blended cement, Portland cement has been diluted. Consequently, on both a short-term and long-term basis, the system will underperform from a mechanical point of view.

To increase both the early and 28-day compressive strengths of their small cubes cast to test the strength of their cement, cement chemists usually modify the chemical composition of their clinker and the fineness of their blended cement to promote the formation of rapidly growing hydrates. This is not, in our opinion, a good approach when considering long-term concrete durability and sustainability.

When a filler particle is introduced among four cement particles, as shown in Figure 1.9, the system will be stronger than the previous one once the hydrates

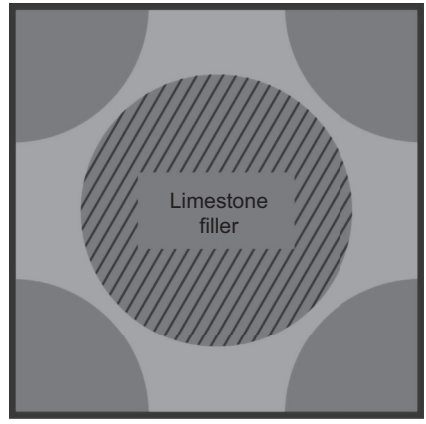


Figure 1.9 2D model representing a system in which a particle of filler has been placed at the center of the four cement particles.
Courtesy of William Wilson.

developed from the surfaces of the four cement particles reach the filler particle, in spite of the fact that the substitution rate is twice as high (50% instead of 25%).

In this system, the size of the capillaries in the hardened matrix is governed by the w/b ratio, which is very important from an autogenous shrinkage point of view.

Therefore, instead of changing the chemical composition of their clinkers, cement chemists should instead recommend to their customers that they decrease the w/b ratio of their concrete if they absolutely want to obtain with their blended cement the same **initial** compressive strength as with a "pure" Portland cement. This solution will be much better from both durability and sustainability points of view.

1.3.3 The relative importance of the w/c and w/b ratios

When part of the Portland cement has been substituted with a supplementary cementitious material or filler, this new cementing system can be characterized by two ratios: its w/c and w/b ratios. Which one of these two ratios is more useful in characterizing the system? The answer is both: the w/c ratio is not passé (Barton, 1989).

In the short term, the early mechanical properties are linked primarily to the w/c ratio, because the first hydrates that give the cement paste its strength are the ones that develop on the surface of the cement particles; supplementary cementitious materials and fillers are not as reactive as Portland cement particles, and their reactivity depends on their type. Very roughly, it can be assumed that silica fume begins to react significantly within the first 3 days, slag within the first 28 days, and fly ash within the first 56–91 days following the casting of concrete, and filler never.

However, the initial network of capillaries of the cement paste is generally governed by the w/b ratio and no longer by the w/c ratio. Therefore, the w/b ratio will determine the size of the menisci that form in the cement paste as a consequence of the chemical contraction that is observed when Portland cement hydrates in the absence of an external source of water, as will be seen in the following chapter.

In the long term, the w/b ratio also influences the compressive strength and durability of cement pastes made with blended cements containing supplementary cementitious materials.

1.4 How to lower the w/c and w/b ratios

Until recently, it was not possible to make 100-mm slump concretes with w/c or w/b ratios lower than 0.40 or 0.45 because the water reducers available in the market were not efficient enough to fully deflocculate the cement particles. As pointed out by Kreijger (1980), when cement particles come into contact with water molecules, they have a natural tendency to flocculate and to trap a certain amount of water inside the cement flocs. Because this water is then not available to provide workability to the concrete, it is necessary to increase the water dosage to increase the workability. However, increasing the water dosage means increasing the w/c or w/b ratio, and therefore decreasing concrete compressive strength and durability. As will be seen in Chapter 2, cement flocculation is due to the presence of positive and negative charges on the

surfaces of each cement particle because of the polyphasic nature of Portland cement clinker and of the electrical polarity of water molecules.

Once the very efficient dispersing properties of certain new synthetic molecules known as superplasticizers were discovered, it became possible simultaneously to decrease the w/c or w/b ratio, while increasing the slump of the concrete. With certain cements, it is possible to decrease the w/c or w/b ratio down to 0.25 and even in some cases to 0.20, while maintaining a slump of 200 mm long enough to place the concrete. These concretes do not contain enough water to fully hydrate all of their cement particles (Powers, 1968). However, we will see that it is not the full hydration of cement particles that is determining concrete compressive strength, but rather their closeness in the cement paste.

The compressive strength of the hydrated cement paste can increase so much when decreasing the w/c or w/b ratio that finally, in some cases, the rupture of the concrete starts within the coarse aggregates particles. Therefore, when decreasing the w/c or w/b ratios below 0.30, it is necessary to use coarse aggregates made from very strong natural rocks (granite, trap rock, basalt, or porphyry) to increase concrete compressive strength or even some artificial aggregates, such as calcined bauxite (Bache, 1981). However, even with such strong aggregates, it is difficult to obtain concrete compressive strengths greater than 150−180 MPa. To obtain Portland cement-based materials having compressive strength greater than 200 MPa, it is necessary to completely eliminate the coarse aggregates and make what Pierre Richard called *reactive powder concrete* (now referred to as *ultra-high strength concrete*; Richard and Cheyrezy, 1994). In such concretes, the coarsest sand and quartz particles have a maximum size of 0.2 mm, as will be shown in Chapter 27. By replacing the sand and quartz particles with iron powder, Pierre Richard was able to increase the compressive strength of its reactive powder concrete up to 800 MPa.

These impressive strengths were not obtained because we learned how to fully hydrate Portland cement particles, but rather because we have been able to lower the w/b ratio to around 0.20 so that the cementitious particles are very close to each other in these very dense fresh cement pastes.

1.5 Conclusion

The numerical values of the w/c and w/b ratios are directly related to the distance separating the particles in a cement paste when the hydration process starts. The lower the w/c or w/b ratio is, the stronger, more durable, and more sustainable the hydrated cement paste is.

Before the discovery of the very efficient properties of superplasticizers, when water reducers were essentially lignosulfonates (a byproduct of the pulp and paper industry), it was not possible to produce concrete having a 100-mm slump with a w/c or w/b ratio lower than 0.45 in the best circumstances. This is no longer the case. Currently, it is possible to produce concretes having a w/c or w/b ratio as low as 0.30, which are easier to place than a 0.45 w/c concrete having a slump of 100 mm in 1960.

As will we see in Chapter 2, this is in spite of the fact that in such concrete there is not enough water to fully hydrate all of the cement. Concrete compressive strength continues to increase as the w/c or w/b ratio decreases because concrete compressive strength depends on the proximity of the cement or the binder particles in the hardened matrix rather than on the amount of cement hydrates formed.

This ability of superplasticizers to lower almost at will the w/c or w/b ratio in modern concretes is the key factor that has resulted in the use of high-performance and self-consolidating concrete, with concrete even starting to displace steel in the construction of high-rise buildings (Aïtcin and Wilson, 2015).

References

Abrams, D.A., 1918. Design of Concrete Mixtures, Bulletin No1. Structural Materials Research Laboratory. Lewis Institute, Chicago, 20 pp.

ACI 232.3R-14, 2014. Report on High-volume Fly Ash Concrete for Structural Applications.

Aïtcin, P.-C., Wilson, W., 2015. The sky's the limit. Concrete International 37 (1), 53−58.

Bache, H.H., 1981. In: Densified Cement Ultra-fine Particle-based Materials, Second International Conference on Superplasticizers in Concrete, Ottawa, Canada, 10−12 June.

Barton, R.B., 1989. Water−cement ratio is passé. Concrete International 12 (11), 76−78.

Bentz, D., Aïtcin, P.-C., 2008. The hidden meaning of the water-to-cement ratio. Concrete International 30 (5), 51−54.

Féret, R., 1892. Sur la compacité des mortiers hydrauliques. Annales des Ponts et Chaussées IV, 5−161.

Granju, J.-L., Grandet, J., 1989. Relation between the hydration state and the compressive strength of hardened Portland cement pastes. Cement and Concrete Research 19 (4), 579.

Granju, J.-L., Maso, J.-C., 1984. Hardened Portland cement pastes. Modelisation of the microstructure and evolution laws of mechanical properties. Cement and Concrete Research 14 (3).

Kosmatka, S.H., 1991. In defense of the water−cement ratio. Concrete Construction 14 (9), 65−69.

Kreijger, P.C., 1980. Plasticizers and dispersing admixtures. In: Proceedings of the International Congress on Admixtures. The Construction Press, London, UK, 16−17 April, pp. 1−16.

Kreijger, P.C., 1987. Ecological properties of buildings materials. Materials and Structures 20, 248−254.

Malhotra, V.M., Mehta, P.K., 2008. High-performance Fly Ash Concrete, Supplementary Cementing Materials for Sustainable Development Inc., Ottawa, Canada, 142 pp.

Mehta, P.K., 2000. Concrete technology for sustainable development. An overview of essential elements. In: Gjorv, O., Sakai (Eds.), Concrete Technology for a Sustainable Development in the 21st Century. E and FN Spon, London, UK, pp. 83−94.

Mehta, P.K., Manmohan, R., 2006. Sustainable high performance concrete structures. Concrete International 28 (7), 32−42.

Powers, T.C., 1968. The Properties of Fresh Concrete. John Wiley & Sons, New York, 664 pp.

Richard, P., Cheyrezy, M., 1994. Reactive Powder Concrete with High Ductility and 200−800 MPa Compressive Strength. ACI Special Publication, 144, pp. 507−508.

Richardson, I.G., 2004. Tobermorite/jennite and tobermorite/calcium hydrate-based models for the structure of C-S-H: applicability to hardened pastes of tricalcium silicate, B-dicalcium silicate, Portland cement, and blends of Portland cement with blast-furnace, metakaolin, or silica fume. Cement and Concrete Research 34 (9), 1733−1777.

Phenomenology of cement hydration

2

P.-C. Aïtcin
Université de Sherbrooke, QC, Canada

2.1 Introduction

Portland cement hydration can be described in different ways. When Portland cement is hydrating,

- mechanical bonds are created,
- a certain amount of heat is liberated, and
- the absolute volume of the cement paste decreases.

The complex chemical reactions that are occurring during hydration of Portland cement are not discussed in this chapter. We present only the volumetric consequences that are very important for civil engineers. The mechanisms of cement hydration are discussed in Chapter 8 and the impact of chemical admixtures is presented in Chapter 12 (Marchon and Flatt, 2016a,b).

2.2 Le Chatelier's experiment

In 1904, Le Chatelier did the following very simple experiment: he filled two flasks (represented in Figure 2.1) with a cement paste up to the base of the necks. In the first flask (Figure 2.1(a)), the cement paste was covered with water up to a mark on the neck of the flask. In order to avoid any evaporation, Le Chatelier placed a cork presenting a hole at the top of the neck of the flask. The next morning, he observed that the level of water was well under the mark and continued to decrease slowly over the following days until it finally stabilized (Figure 2.1(b)). Moreover, after a while he observed that the base of the flask was cracked (Figure 2.1(c)). In the second flask (Figure 2.1(d)), where the cement paste was hydrating in air, he observed that after a while the volume of the hardened cement paste within the flask did not anymore occupy the entire volume of the base of the flask.

Le Chatelier concluded that a cement paste presents volumetric variations during its hydration and that these volumetric variations depend on the mode of curing of the cement paste. When a cement paste hydrates under water, its **absolute volume** decreases because some water penetrates in the cement paste. But later, the **apparent** volume of the cement paste increases so that the base of the flask is ruptured after a while. When a cement paste hydrates in air, its **apparent volume** decreases.

Science and Technology of Concrete Admixtures. http://dx.doi.org/10.1016/B978-0-08-100693-1.00002-3
Copyright © 2016 Elsevier Ltd. All rights reserved.

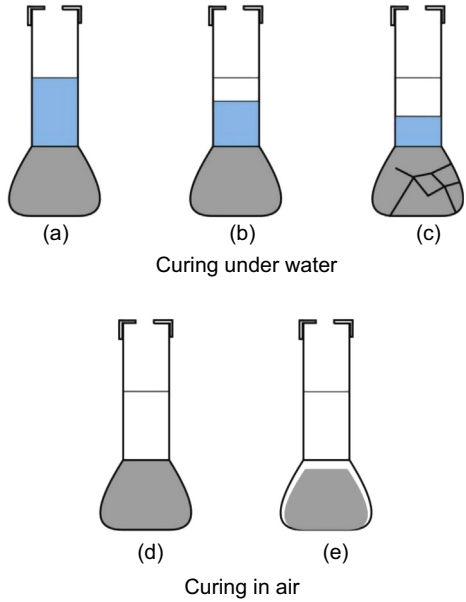


Figure 2.1 Schematic representation of the Le Chatelier's experiment.

Hydrated cement paste and concrete are not stable materials from a volumetric point of view. When they are cured under water, they **swell**; when they are cured in air, they shrink. But during hydration, whatever the mode of curing, the **absolute volume** of the cement paste experiences an 8% decrease. This contraction of the absolute volume is known as **chemical contraction** (or, in France, as *Le Chatelier's contraction*).

2.3 Powers' work on hydration

Powers and Brownyard (1948) and Powers (1968) studied the hydration reaction from a quantitative point of view. They found the following:

- To reach full hydration, a cement paste must have a water−cement ratio (w/c) at least equal to 0.42.
- Some water is reacting with the cement to form a "solid gel" responsible for the bonding properties of the hydrated cement paste.
- Some water is not reacting with the cement but is glued to the hydrated cement paste; Powers called this water the "gel water."

Despite all of the research that was done after Powers to refine our knowledge on the nature of the cement gel and the gel water (Richardson, 2004), Powers' model will be used in this chapter because it is simple and it is sufficient to explain the volumetric changes occurring during cement hydration.

Jensen and Hansen (2001) presented a very simple graphical representation of Powers' model for hydration (Figure 2.2). On the *x*-axis, they report the degree of

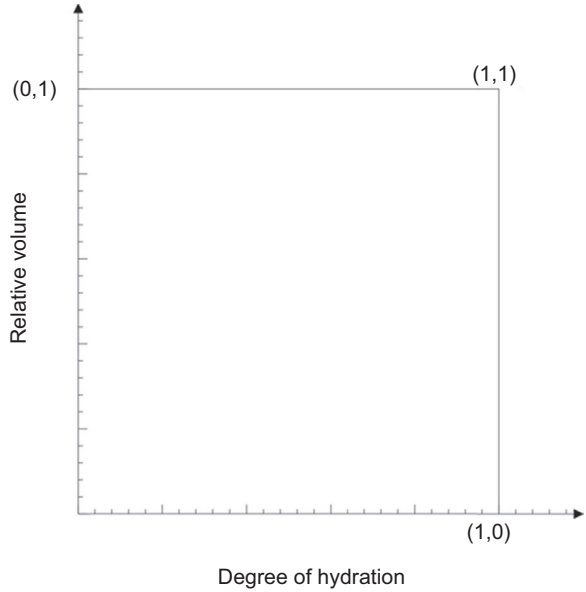


Figure 2.2 A system of coordinates to represent schematically Powers' work on hydration (Jensen and Hansen, 2001).
Courtesy of Ole Jensen.

hydration of the cement, that is, the fraction of the cement that has been hydrated. This fraction varies between 0 at the beginning of mixing and 1 when full hydration is reached. On the *y*-axis, the relative volume of the cement and water are expressed as a number. In this representation, the cement paste does not contain any entrapped air. This model will be used to represent the hydration of some pastes having a particular w/c ratio.

2.3.1 Hydration of a cement paste having a w/c ratio equal to 0.42

2.3.1.1 Hydration in a closed system

The hydration process occurring in a cement paste with a w/c ratio of 0.42 in a closed system appears in Figure 2.3.

In such a system, the cement paste does not have any possibility of exchange with its external environment. As hydration progresses, a certain amount of water is combined with Portland cement to form some solid gel and a second part is fixed as water gel. When full hydration is reached, there is no cement and water left in the system but only some solid gel, some water gel, and an 8% porosity filled with water vapor due to the chemical contraction of the absolute volume of the cement paste. During Portland cement hydration, the hydrated cement paste is becoming porous due to its chemical contraction so that some capillary water is drained by the very fine porosity created by the chemical contraction and menisci are appearing in the capillary pores. These menisci develop tensile stresses within the hydrated cement paste and therefore a contraction of its apparent volume when the bonds created by the first hydrates are

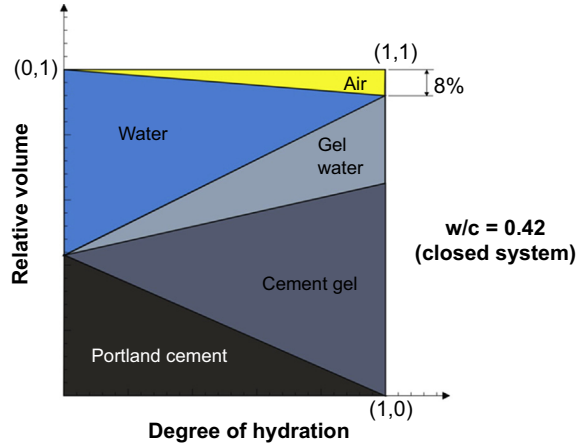


Figure 2.3 Schematic representation of the hydration of a 0.42 cement paste in a closed system. Courtesy of Ole Jensen.

strong enough to resist the tensile forces created by this chemical contraction. This contraction that occurs without any loss of water is called **autogenous shrinkage**.

This contraction of the apparent volume is not large when the menisci are appearing in large capillaries because these menisci generate weak tensile stresses. When full hydration is reached, there are no more menisci because all the capillary water has reacted with Portland cement.

2.3.1.2 Hydration under water

The hydration process for this same cement paste occurring under water is represented in Figure 2.4.

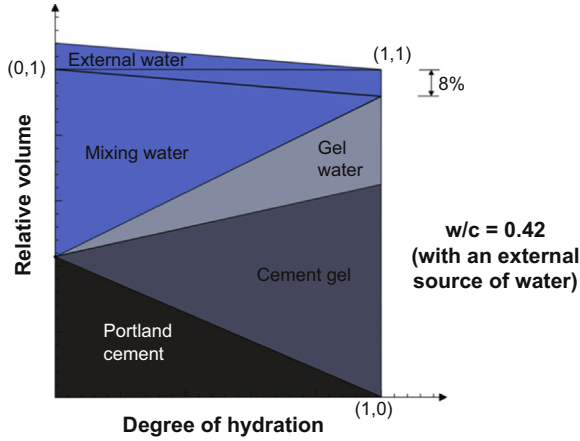


Figure 2.4 Schematic representation of the hydration of a 0.42 cement paste benefitting from an external source of water.
Courtesy of Ole Jensen.

As soon as the chemical contraction creates some porosity, this porosity is filled by the external source of water so that no menisci are appearing in the cement paste. Therefore, the apparent volume of the paste does not decrease. When final hydration is reached, the 8% porosity created by the chemical contraction is filled with water. In this particular case, the apparent volume of the paste did not change during the hydration process and the paste does not present any autogenous shrinkage.

Why not use the external water that has penetrated in the porosity created by the chemical contraction to hydrate an additional quantity of cement that would have been introduced within the cement paste before its mixing with water?

2.3.2 Hydration of a cement paste having a w/c ratio equal to 0.36 cured under water

Jensen and Hansen (2001) calculated that theoretically a paste having a w/c ratio of 0.36 cured under water would not contain any water at the end of the hydration process, as seen in Figure 2.5.

When full hydration is reached, the hydrated cement paste is a nonporous material composed of cement gel and gel water that has not developed any autogenous shrinkage.

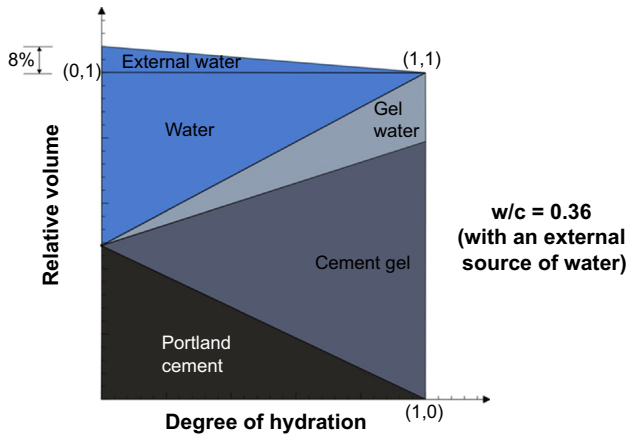


Figure 2.5 Schematic representation of the hydration of a cement paste having a w/c ratio equal to 0.36 benefitting from an external source of water.
Courtesy of Ole Jensen.

2.3.3 Hydration of a cement paste having a w/c ratio equal to 0.60 cured in a closed system

Such a system represented in Figure 2.6 contains more water than necessary to fully hydrate its cement particles so that at the end of the hydration process, the hydrated cement paste is composed of some solid gel, some water gel, the remaining capillary water, and the porosity created by the chemical contraction of the hydrated cement paste.

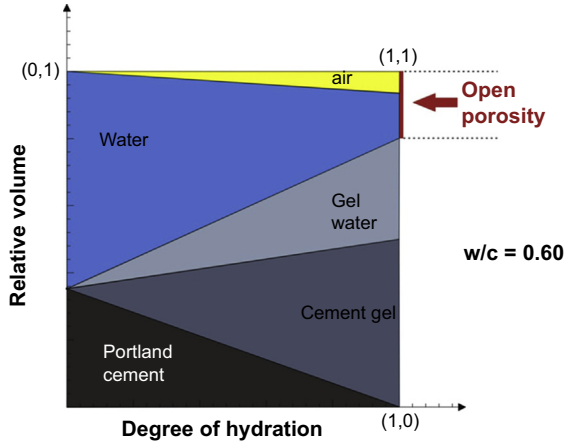


Figure 2.6 Schematic representation of the hydration of an air-cured 0.60 cement paste. Courtesy of Ole Jensen.

As this porosity is finer than the capillary porosity, it drains an equivalent volume of capillary water so that menisci appear in the larger capillaries. The tensile forces they generate are weak, so the resulting autogenous shrinkage is negligible.

At the end of the hydration process, the cement paste is composed of some solid gel, some gel water, some capillary water, and about 8% of the volume of the hydrated cement paste is filled with water vapor. The addition of the remaining capillary water and this capillary volume filled with water vapor constitute an open porosity by which aggressive agents can easily penetrate within the cement paste and attack it as well as the reinforcing steel in reinforced concrete.

If a 0.60 cement paste is cured under water, it does not present any autogenous shrinkage because no menisci are appearing within the cement paste. At the end of the hydration process, the capillary network is full of water. The external water that penetrates in the cement paste has only eliminated the autogenous shrinkage of the paste.

2.3.4 Hydration of a cement paste having a w/c ratio of 0.30

2.3.4.1 Hydration in a closed system

Hydration of a cement paste having a w/c ratio of 0.30 in a closed system is presented in Figure 2.7. It does not contain enough water to reach full hydration; therefore, hydration stops due to the lack of water.

At the end of the hydration process, the hardened cement paste is composed of unreacted Portland cement, some solid gel, and some gel water (Granju and Maso, 1984; Granju and Grandet, 1989). The unreacted cores of the cement particles can be considered as hard inclusions having very high compressive strength and an elastic modulus that have a strengthening effect on the strength of the hydrated cement paste. The inclusion of hard particles having a high compressive strength and elastic modulus is a current technique used in metallurgy to increase the

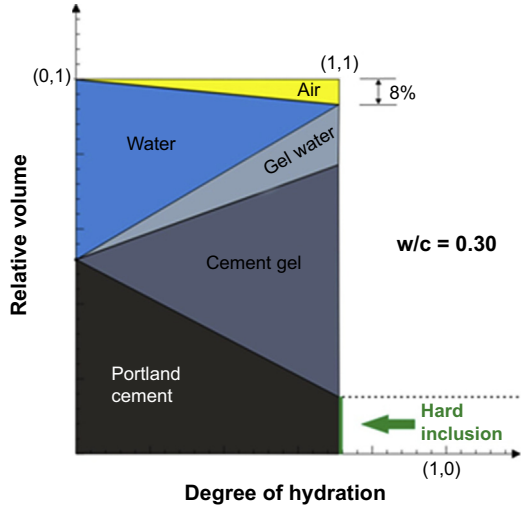


Figure 2.7 Schematic representation of the hydration of a 0.30 cement paste hydrating in a closed system.
Courtesy of Ole Jensen.

compressive strength and elastic modulus of some metals. This technique is known as strength hardening.

2.3.4.2 *Hydration under water*

This same cement paste hydrating under water, presented in Figure 2.8, does not contain enough water to reach full hydration; therefore, hydration stops due to the

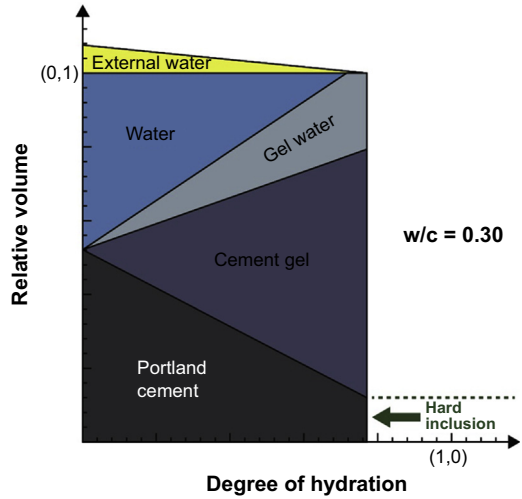


Figure 2.8 Hydration of a cement paste having a w/c ratio equal to 0.30 hydrating under water.
Courtesy of Ole Jensen.

lack of space. As the external water fills the porosity created by the chemical contraction as soon as hydration started, the paste does not develop any autogenous shrinkage during its hardening.

2.4 Curing low w/c ratio concretes

Because they ignore the very simple experiment by Le Chatelier, many engineers are convinced that autogenous shrinkage is only occurring in low w/c ratio concrete. This is not true: all concrete cured without an external source of water presents some autogenous shrinkage. Of course, the lower the w/c ratio is, the larger autogenous shrinkage is. On the contrary, as found by Le Chatelier, when a concrete is cured under water, it swells. This apparent volume increase could be the result of the pressure created by the growth of portlandite crystals, according to Vernet.

2.4.1 Different types of shrinkage

Concrete may develop three types of shrinkage:

- Plastic shrinkage
- Autogenous shrinkage
- Drying shrinkage

Carbonation shrinkage has been voluntarily excluded from this list. The so-called thermal shrinkage is also excluded, as it is not per se shrinkage but a normal volumetric contraction occurring in any material when it cools down.

All three forms of shrinkage have a common cause: the appearance of menisci in the capillary system of the hydrated cement paste. The appearance of menisci in concrete can be a result of the following:

- The evaporation of water from fresh concrete (**plastic shrinkage**)
- The chemical contraction occurring in a cement paste when it hydrates (**autogenous shrinkage**)
- The evaporation of some capillary water from the hardened cement paste (**drying shrinkage**)

However, when there is an external source of water that eliminates the apparition of menisci in the capillary system, these three types of shrinkage cannot develop because the capillary system of the cement paste is always full of water and does not present any menisci.

Therefore, in order to avoid the development of plastic and drying shrinkage, it is only necessary to keep that water from evaporating from the concrete. To avoid the appearance of autogenous shrinkage, it is only necessary to provide the hardening paste with an external source of water that fills the porosity created by the chemical contraction as soon as it develops. It is easier to write it than to do it in the field. To counteract the development of autogenous shrinkage, saturated lightweight aggregate (Klieger, 1957; Hoff and Elimov, 1995; Weber and Reinhart, 1997), or superabsorbent polymers (SAP) (Kovler and Jensen, 2005) have been proposed as an external source of water. An internal curing technique consists of including an additional volume of "hidden water" during concrete mixing.

2.4.2 Curing concrete according to its w/c ratio

Based on Powers' observation, it can be concluded that concrete must be cured differently according to its w/c ratio, as seen in Table 2.1.

Concretes having a w/c ratio greater than 0.42 contain more water than necessary to fully hydrate their cement particles so that they must be cured as follows: As soon as their surface is finished, they can be exposed to fogging until they are recovered with a curing membrane or until their surface is hard enough to receive and external water treatment with water hoses or be covered with wet geotextiles. If it is essential for the concrete surface to be protected from drying shrinkage, a sealant must be applied on it.

Concretes having a w/c ratio lower than 0.42 do not contain enough water to reach full hydration; therefore, very early severe plastic and autogenous shrinkage may occur if there is not an external source of water. Therefore, just after placing these concretes, they must be fogged until they are hard enough to support a direct external water curing. Alternatively, they can be covered for a few hours with an evaporation retarder, not a curing membrane, in order to avoid the development of plastic shrinkage until the surface is hard enough to receive a direct external water curing. The evaporation retarder is in fact a monomolecular layer of an aliphatic alcohol like the ones used in domestic swimming pools to avoid water evaporation. Even when a low w/c ratio concrete receives an internal curing treatment, it is very important to provide an external source of water to provide additional curing water to its surface because the surface will be exposed to the action of aggressive agents and it is important to make it as impervious as possible. Therefore, any means to reinforce the cover of concrete must be considered in order to improve the durability of the concrete structure.

When the w/c ratio is lower than 0.36, internal curing must be provided in order to lower as much as possible the risk of the development of an uncontrolled autogenous shrinkage.

In any case, whatever the w/c ratio of the concrete, it is very important to motivate contractors to cure concrete properly; this activity can be made lucrative by paying for it separately. It is only necessary to detail the recommended mode of curing and to ask for a unit price for each of the operations needed. However, it is always necessary to continue to hire inspectors to check that the contractors do what they are paid for.

Table 2.1 Concrete curing according to its w/c ratio

w/c ratio	Internal curing	Fogging	Curing	
Greater than 0.42	Not necessary	Not necessary	Curing membrane	
Lower than 0.42	No	Mandatory	Evaporation retarder	Water curing
	Yes		Curing membrane	

2.5 Conclusion

Portland cement hydration is a complex phenomenon that is well understood. It is very simple to explain the volumetric variations occurring during hydration according to the mode of curing using the representation by Jensen and Hansen. What is unfortunately ignored by many engineers is the origin of these volumetric variations and the different means that can be used to mitigate them. During its hydration in a closed system, cement paste develops a very fine porosity equal to 8% of the absolute volume of the cement and water that have been combined. When this cement paste does not receive any external water that could fill this porosity, menisci appear; these menisci create tensile forces and these tensile forces create autogenous shrinkage, whatever the w/c.

On the contrary, during its hydration, the hydrating cement paste can benefit from an external or internal source of water. This water will fill the porosity created by the chemical contraction menisci and tensile forces will not be created; thus, the concrete will not present any autogenous shrinkage. As was found by Le Chatelier, the apparent volume of the cement paste cured under water will swell.

According to Powers' work, a 0.36 w/c cement paste cured under water does not present any volumetric contraction and when full hydration is reached, this cement paste is a nonporous material composed of cement gel and gel water. When a concrete having a w/c ratio lower than 0.36 is cured under water, all the cement particles cannot hydrate due to lack of water and space; when it has been hydrated as a 0.36 w/c paste, it is observed that concrete compressive strength continue to increase as its w/c decreases. This phenomenon simply indicates that concrete compressive strength depends more on the proximity of the cement particles than on their full hydration. The unhydrated part of the cement particles are even acting as hard cores that are strengthening the hydrated cement paste.

As low w/c concretes are used increasingly, it will be necessary to learn how to cure them properly according to their w/c ratio. It is out of the question to apply a curing membrane on the surface of a concrete having a w/c ratio lower than 0.42 because this curing membrane will prevent the penetration of external water needed to fill the porosity created by the chemical contraction, except if in parallel an internal curing has been provided.

It is necessary to separately pay contractors to cure concrete in order to motivate them to do so. It will be important to explain to them in detail what they have to do, when they have to do it, and for how long.

I am absolutely convinced that if an internal curing has been provided for a low w/c concrete, it is **also imperative** to water cure its surface with an external source of water. The skin of a concrete has to be made as impervious as possible in order to protect the concrete and the reinforcing steel from the penetration of aggressive agents.

References

Granju, J.-L., Grandet, J., 1989. Relation between the hydration state and the compressive strength of hardened Portland cement pastes. Cement and Concrete Research 19 (4), 579–585.

Granju, J.-L., Maso, J.-C., 1984. Hardened Portland cement pastes, modelisation of the microstructure and evolution laws of mechanical properties II-compressive strength law. Cement and Concrete Research 14 (3), 303−310.

Hoff, G., Elimov, R., 1995. Concrete Production for the Hibernia Platform. Supplementary Papers, Second CANMET/ACI International Symposium on Advances in Concrete Technology, Las Vegas, pp. 717−739.

Jensen, O.M., Hansen, H.W., 2001. Water-entrained cement based materials: principles and theoretical background. Cement and Concrete Research 31 (4), 647−654.

Klieger, P., 1957. Early high-strength concrete for prestressing. In: Proceedings of the World Conference on Prestressed Concrete, San Francisco, pp. A5(1)−A5(14).

Kovler, K., Jensen, O.M., 2005. Novel technique for concrete curing. Concrete International 27 (9), 39−42.

Le Chatelier, H., 1904. Recherches expérimentales sur la constitutions des mortiers hydrauliques. Dunod, Paris.

Marchon, D., Flatt, R.J., 2016a. Mechanisms of cement hydration. In: Aïtcin, P.-C., Flatt, R.J. (Eds.), Science and Technology of Concrete Admixtures. Elevier (Chapter 8), pp. 129−146.

Marchon, D., Flatt, R.J., 2016b. Impact of chemical admixtures on cement hydration. In: Aïtcin, P.-C., Flatt, R.J. (Eds.), Science and Technology of Concrete Admixtures. Elevier (Chapter 12), pp. 279−304.

Powers, T.C., 1968. The Properties of Fresh Concrete. John Wiley & Sons, New York, 664 pp.

Powers, T.C., Brownyard, T.L., 1948. Studies of the Physical Properties of Hardened Portland Cement Paste. Reprint from the Journal of the American Concrete Institute. Portland Cement Association, Detroit, MI, USA. Bulletin 22.

Richardson, I.G., 2004. Tobermorite/jennite and tobermorite/calcium hydrate-based models for the structure of C-S-H: applicability to hardened pastes of tricalcium silicate, B-dicalcium silicate, Portland cement, and blends of Portland cement with blast-furnace, metakaolin, or silica fume. Cement and Concrete Research 34, 1733−1777.

Weber, S., Reinhart, H.W., 1997. A new generation of high performance concrete: concrete with autogenous curing. Advanced Cement Based Materials 6, 59−68.

Portland cement

3

P.-C. Aïtcin
Université de Sherbrooke, QC, Canada

3.1 Introduction

Portland cement is a complex product made from very simple and abundant materials: limestone and clay (or shale). Very precise proportions of these two basic materials have to be mixed with some additions to create a raw meal with a precise chemical composition; this will result in the production of clinker through the complex pyroprocessing presented in Figure 3.1. It is not always easy to maintain good operational conditions in the kiln for this pyroprocessing, and it requires some art from the cement producer. In this book, the word 'clinker' is used rather than the expression 'Portland cement clinker'.

The production cost of Portland cement is closely linked to the cost of the fuel used to create a kiln temperature sufficiently high to enable the different chemical reactions that transform the raw meal into clinker. Clinker comes out of the kiln as grey nodules, paler or darker according to the amount of iron it contains. When iron oxide content is lower than 1% the clinker is whitish, and the lower the iron oxide content, the whiter the cement produced.

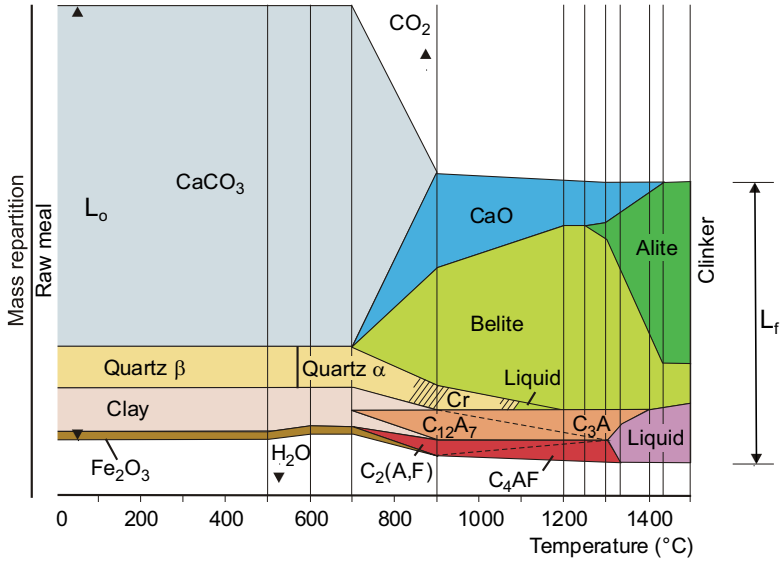


Figure 3.1 Transformation of raw meal into clinker.
With the permission of KHD Humboldt Wedag (Aïtcin, 2008).

Science and Technology of Concrete Admixtures. http://dx.doi.org/10.1016/B978-0-08-100693-1.00003-5
Copyright © 2016 Elsevier Ltd. All rights reserved.

During the 1980s, a beige clinker was produced when the clinker was quenched very rapidly after its passage through the burning zone. This clinker gave buff cement that was beautiful, but its production was hard on the refractory lining at the lower end of the kiln, so its fabrication was rapidly abandoned. Presently buff cements are obtained by adding brown pigments to white cement, but the buff cements thus obtained never match the visual aspect of cement made from a buff clinker.

As will be seen in this chapter, no two clinkers are identical, because no two raw feed materials are absolutely identical; even in the case of a cement plant running two similar kilns fed with the same raw meal, the clinker produced by these kilns is not absolutely identical because no two kilns are perfectly identical. Moreover, in a kiln it is not possible to maintain exactly the same pyroprocessing conditions all day long in the burning and quenching zones, so the clinker produced has a certain degree of variability. Usually, the clinker is temporarily stocked in a homogenization hall before being ground. This is the best way to produce Portland cement having almost constant properties that facilitates the production of concrete with predictable properties.

3.2 The mineral composition of Portland cement clinker

Usually, Portland cement raw meal is heated up to a temperature of about 1450 °C. The chemical composition of the raw feed is adjusted to obtain the formation of four minerals that react with water to create bonds:

- tricalcium silicate $SiO_2 \cdot 3CaO$ (Figure 3.2)
- dicalcium silicate $SiO_2 \cdot 2CaO$ (Figure 3.3)
- tricalcium aluminate $Al_2O_3 \cdot 3CaO$ (Figure 3.4)
- tetracalcicium ferroaluminate $4CaO \cdot Al_2O_3 \cdot Fe_2O_3$ (Figure 3.4(a)).

The first two minerals constitute the silicate phase of Portland cement, and the tricalcium aluminate and tetracalcium ferroaluminate its aluminous phase — also called the interstitial phase, because in the burning zone this part of the clinker reaches a more or less viscous state that bonds together the two silicate phases, as seen in Figure 3.4.

To simplify the writing of these four minerals, the following symbols taken from ceramic science will be used:

- S represents silica, SiO_2
- C represents lime, CaO
- A represents alumina, Al_2O_3
- F represents iron oxide, Fe_2O_3.

Using these pseudo-chemical notations, the four principal minerals can be written as:

- C_3S for $3CaO \cdot SiO_2$ (tricalcium silicate)
- C_2S for $2CaO \cdot SiO_2$ (dicalcium silicate)
- C_3A for $3CaO \cdot Al_2O_3$ (tricalcium aluminate)
- C_4AF for $4CaO \cdot Al_2O_3 \cdot Fe_2O_3$ (tetracalcium ferroaluminate).

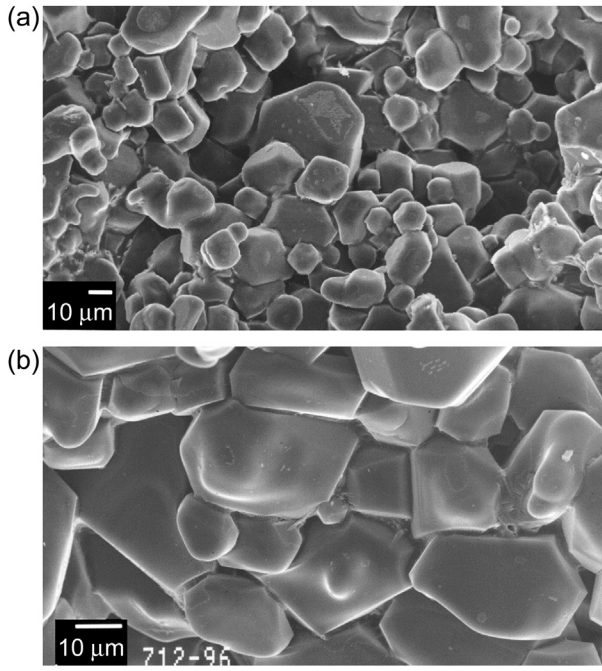


Figure 3.2 Tricalcium silicate crystals in two clinkers: (a) small crystals, smaller than 10 µm; (b) coarse crystals, coarser than 10 µm.
Courtesy of Arezki Tagnit-HAMOU (Aïtcin, 2008).

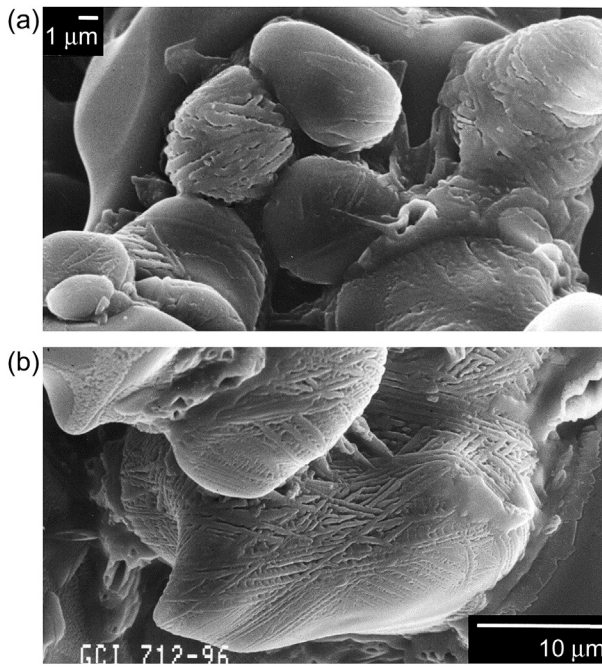


Figure 3.3 Dicalcium silicate crystals: (a) typical crystal; (b) detail of a dicalcium silicate crystal.
Courtesy of Arezki Tagnit-HAMOU (Aïtcin, 2008).

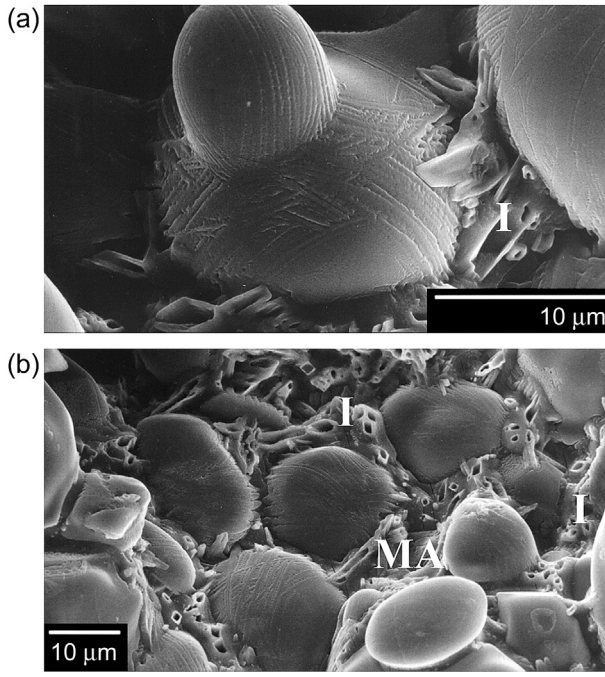


Figure 3.4 Interstitial phase (I) in two clinkers: (a) detailed view of clinker showing the interstitial phase (I) between two belite crystals and the tubular nature of tricalcic ferroaluminate crystals; (b) detailed view of clinker showing the interstitial phase (I) composed of well-crystallized tricalcium aluminate and tetracalcicium ferroaluminate in an amorphous phase (MA). Courtesy of Arezki Tagnit-HAMOU (Aïtcin, 2008).

The words ‘alite’ and ‘belite’, suggested by Thorborn in 1897 (Bogue, 1952), are still used to represent the impure forms of C_3S and C_2S found in Portland cement clinker. These impure forms are created because, during pyroprocessing in the burning zone, these minerals are contaminated by impurities contained in the raw meal and the fuel.

Some of these minerals can crystallize into different crystallographic forms depending on the presence or absence of impurities in their crystal structure. For example, pure C_3A crystallizes into a cubic shape: in this case it is a very reactive mineral, but at the same time it is easy to control its very rapid hydration. When a certain amount of alkalis are trapped in C_3A lattice, it crystallizes into the form of an orthorhombic or even monoclinic crystal. Depending on the amount of alkali it contains, it is less reactive than cubic C_3A but its reactivity is not so easy to control. Usually, in clinker C_3A crystallizes as a mixture of its cubic and orthorhombic forms (see Section Appendices of this chapter).

Portland cement clinker is ground with a certain amount of calcium sulphate, usually gypsum, to make Portland cement. The calcium sulphate found in Portland cement can be gypsum, anhydrite, hemihydrate, dehydrated hemihydrate, synthetic calcium

sulphate or a mixture of these different forms, depending of the purity and type of calcium sulphate used and the temperature reach in the ball mill during the final grinding of the cement (see Section Appendices of this chapter).

As can be seen, there are many reasons that make the production of two identical Portland cements fairly improbable.

3.3 The fabrication of clinker

The different steps that transform the raw meal into clinker in a modern kiln equipped with a precalcinator (Figure 3.5) will be described briefly.

The raw meal, ground to a fineness close to that of cement, passes first into a preheater composed of four or five cyclones, where it reaches a temperature of 700−800 °C using the hot kiln gases before they are released into the chimney. This temperature is not high enough to transform all the limestone into lime, so it is necessary to heat up the raw meal in a preheating unit called a precalcinator.

Before the development of this external part of the kiln, all the calcination occurred inside the kiln, and consequently the kilns were quite long; they were built with two or three separate supports. Now, with the introduction of preheaters and precalcinators, the kilns are very short and may have much larger diameters, so they can produce up to 10,000 tonnes of clinker per day (Bhatty et al., 2004).

After the quasi-total calcination of the limestone in the precalcinator, the raw meal enters the inclined kiln that is turning at a constant rate. As the raw meal moves towards the burning zone its temperature increases progressively to about 1450 °C, where C_3S, C_2S and the interstitial phase are developed according to the schematic representation presented in Figures 3.1 and 3.5. The burning zone is followed by a colder zone (1200 °C), where the clinker is quenched so that the hydraulic forms of C_3S and C_2S obtained at high temperature are stabilized. Looking at a $CaO-SiO_2$ phase diagram, it can be seen that if the clinker was cooled slowly it would be transformed into a material having no hydraulic properties (Aïtcin, 2008).

Figure 3.1 shows that alumina and iron oxides produce various minerals that have a liquefaction temperature much lower than that of the silicate phase. In the burning zone these compounds are found in a more or less viscous state that favours the transformation of C_2S into C_3S at a temperature much lower than the 2100 °C needed in the absence of Al_2O_3 and Fe_2O_3. This phase is called the interstitial phase, because it bounds the silicate phases of the clinker.

A very small amount of the raw meal passes through the burning zone without being transformed into clinker, which is why some clusters of lime can be observed from time to time, as well as belite nests each time a coarse quartz particle did not have enough time to react with lime in the burning zone to be transformed into C_3S.

The passage of the raw meal in the first part of the kiln must be short, to limit the size of the initial C_2S crystals. If the C_2S crystals are allowed to grow for too long, they become less prone to react with lime and transform into C_3S in the burning zone.

The nature of the atmosphere (oxidizing or reducing) of the kiln also influences the quality of the clinker. Finally, the rapidity of the quenching after the burning zone is

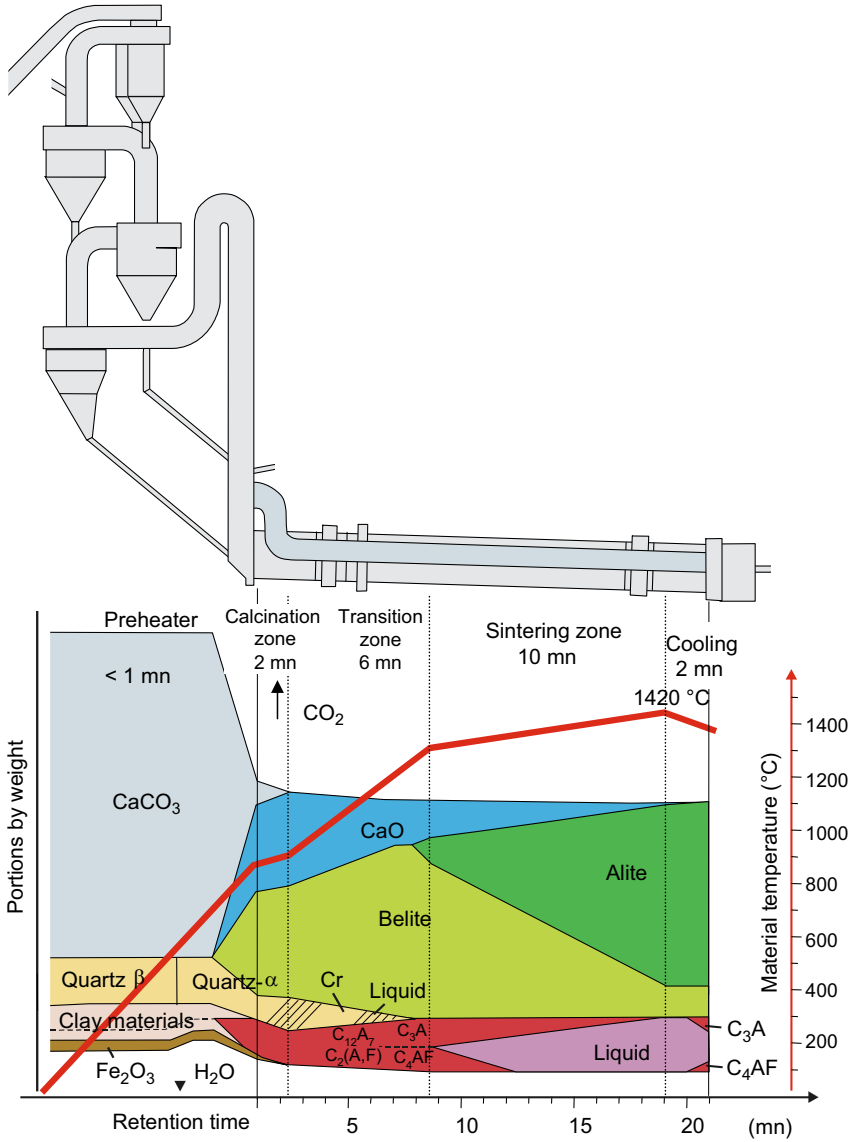


Figure 3.5 Formation of clinker in a short kiln equipped with a precalcinator. Courtesy of KHD Humboldt Wedag (Aïtcin, 2008).

very important, because it conditions the reactivity of the clinker: the faster the quenching, the more reactive the clinker.

The examination of clinker particles under an electron microscope reveals the presence of crystalline deposits on some C_2S and C_3S crystals and also in the interstitial phase; usually these deposits are alkali sulphates (Figure 3.6). In fact, the alkali

impurities contained in the raw meal are usually volatilized in the kiln and carried by the hot gases up the chimney, but a small quantity succeed in passing through the burning zone and are deposited in the clinker when it cools down in the quenching zone. Although present in small amounts, these alkalis may substantially affect the performance of chemical admixtures, in particular concerning competitive adsorption, as shown in Chapter 10 (Marchon et al., 2016).

Portland cement clinker is the fruit of complex chemical reactions which occur at the high temperature of 1450 °C and are very sensitive to the environment found at such a temperature. It is the art of the cement manufacturer that makes it possible to produce clinker that has constant characteristics all year round. Making clinker is not easy: it requires a good knowledge of the whole process and a skilled operator to anticipate or detect very rapidly any problems in the burning zone that require modification of certain kiln parameters until it returns to normal operation. More detailed explanations of clinker production can be found in Bhatty et al. (2004) and Aïtcin (2008), and in a recent review of various improvements made in clinker production from the engineering point of view (Chatterji, 2011).

3.4 Chemical composition of Portland cement

Table 3.1 presents the chemical analysis of a various commercial Portland cements. Their CaO, SiO_2, Al_2O_3, Fe_2O_3, etc. contents are given in terms of oxide content, as usually done in chemistry. Of course, these oxides do not exist separately as oxides in Portland cement, except perhaps for minute amounts of CaO and SiO_2. Rather, they are combined to form the different minerals that are found in Portland cement.

When looking at this chemical composition, it is seen that the CaO content of the different Portland cements is always high: 60−65% for grey cements, and close to 70% for white cement. The silica content (SiO_2) varies between 20% and 24%. In contrast, the Al_2O_3 and Fe_2O_3 contents are more variable. For example, the Fe_2O_3 content of white cement is always lower than 1%, while it is 5% for the Type 20M cement with a very low hydration heat and a dark colour. The higher the Fe_2O_3 content, the darker the colour of the cement.

Besides these principal oxides, the chemical analysis indicates the presence of other minor oxides. This does not mean that they do not have significant influence on the cement properties; the term minor indicates only that their percentage is not very high. For example, the alkali oxide content is usually calculated in terms of Na_2O equivalent that is equal to $Na_2O\% + 0.58\ K_2O\%$.

The chemical analysis also reveals four other components found in small percentages in Portland cement:

- magnesia MgO
- sulphates expressed as SO_3
- free lime, expressed as ‘free CaO’
- insolubles

and the loss on ignition is expressed as LOI.

Table 3.1 **Average chemical and Bogue compositions of some Portland cements**

Oxide	Cement type							
	CPA 32.5	**CPA 52.5**	**US type I without limestone filler**	**Canadian type 10 with limestone filler**	**Type 20M low hydration heat**	**US type V sulphate resisting**	**Low-alkali cement**	**White**
CaO	64.4	66.2	63.92	63.21	63.42	61.29	65.44	69.5
SiO_2	0	8	20.57	20.52	24.13	21.34	21.13	3
Al_2O_3	20.5	20.6	4.28	4.63	3.21	2.92	4.53	23.8
Fe_2O_3	5	6	1.84	2.85	5.15	4.13	3.67	4
MgO	5.21	5.55	2.79	2.38	1.80	4.15	0.95	4.65
K_2O	2.93	3.54	0.52	0.82	0.68	0.68	0.21	0.33
Na_2O	2.09	0.90	0.34	0.28	0.17	0.17	0.10	0.49
Na_2O equiv.	0.90	0.69	0.63	0.74	0.30	0.56	0.22	0.06
SO_3	0.20	0.30	3.44	3.20	0.84	4.29	2.65	0.03
L.O.I.	0.79	0.75	1.51	1.69	0.30	1.20	1.12	0.07

Free lime	1.60	2.40	0.77	0.87	0.40	–	0.92	1.06
Insolubles	–	–	0.18	0.64	–	–	0.16	1.60
	1.50	–						–
	–	–						–
Bogue composition								
C_3S	61	70	63	54	43	50	63	70
C_2S	13	6.1	12	18	37	24	13	20
C_3A	8.9	8.7	8.2	7.4	0	0.8	5.8	11.8
C_4AF	8.9	10.8	5.6	8.7	15	12.6	11.2	1.0
$C_3S + C_2S$	74	76	75	72	80	74	76	90
$C_3A + C_4AF$	17.8	19.5	13.8	16.1	15.0	13.4	17.0	12.8
Specific surface area m^2/kg	350	570	480	360	340	390	400	460

Based on the results of the chemical analysis and on more or less realistic hypothesis, Bogue (1952) proposed a series of calculations to determine the potential (theoretical) composition of a Portland cement in terms of C_3S, C_2S, C_3A and C_4AF. This mineral composition is also known as 'Bogue composition'. In general, it does not give the exact mineral composition of a clinker, unlike that obtained when counting the percentage of these mineral on a polished section of clinker under a microscope or by quantitative X-ray diffraction (XRD) analysis using Rietveld refinement, but usually the values are quite close.

When the C_3S and C_2S contents of the grey cements shown in Table 3.1 are added, it is found that the total varies slightly around a value of 75%. Only in two particular cements does it differ from this average value: in the case of white cement, it is higher; and in the Type 20M cement with very low hydration heat, it is lower.

If the C_3A and C_4AF contents of the grey cements are added, it is observed that these two minerals count for 15−16% of the total mass of the cement. Here, too, the two cements that had total C_3S and C_2S contents different from 75% have a C_3A and C_4AF content with a different sum from 15 to 16%: lower in the case of white cement, and higher in the case of Type 20M cement.

In Table 3.1 it is also seen that the Na_2O equiv. of the different Portland cements varies from 0.07% to 0.79%, which represents a variation of one order of magnitude. When this total is lower than 0.60%, the cement is said to be low-alkali cement.

The last line of Table 3.1 gives the specific surface area of the different cements to provide an idea of their fineness. Their Blaine fineness varies from 340 to 570 m^2/kg. It will be seen later how the value of the fineness influences concrete properties.

Why do the different cements presented in Table 3.1 have a silicate content of 75% and an interstitial phase of 15%?

This is because these proportions result in easy control of clinker production in a kiln. This balance between the silicate and interstitial phase contents provides optimal conditions for the transformation of the raw meal into clinker in the burning zone, and minimizes the risk of rings formation that may block the kiln in the burning zone.

When looking at Figure 3.1 it is seen that the iron and alumina act as fluxing agents; the iron having a stronger fluxing action. The optimal balance between the C_3A and C_4AF content is half and half (i.e. 8% of each). With such a balance it has been found that almost all of the C_2S is transformed into C_3S in the burning zone.

The more the C_3S, C_2S, C_3A and C_4AF contents depart from these average values, the more difficult it is to control the formation of clinker in the burning zone.

3.5 The grinding of Portland cement

As water always starts to react with the ionic species present at the surface of cement particles, the fineness of the cement particles plays a very important role in the development of cement hydration. The finer the cement, the more reactive it is. This is the reason why in pre-cast plants where concrete is poured very rapidly into the moulds, fine or very fine cements (450−500 m^2/kg) may be used without any problems, while

in ready-mix operations where the delivery time can be as long as 90 minutes, it is better to use coarser cements (350−400 m^2/kg). When making mass concrete, it is better to use an even coarser cement (300−350 m^2/kg).

3.5.1 Influence of the morphology of the cement particles

If the specific surface area plays an important role in determining the rheology of fresh concrete, the morphology of the cement particles is also important. Two clinkers may have a similar mineral composition but present very different reactivity, because during the grinding different minerals are exposed at the surface of the cement particles. To illustrate this point let us consider a few hypothetical cement particles presented in Figure 3.6 (Aïtcin and Mindess, 2011).

G_1, G_2 and G_3 cement particles contain the same proportions of silicate and interstitial phase, but particle G_1 will react initially as if it was exclusively composed of silicate because its interstitial phase is concentrated at the centre of the particle. In contrast, particle G_2 will behave initially as if it was composed exclusively of C_3A; and finally particle G_3 will present an intermediate behaviour. Particles G_4 and G_5 have the same silicate and interstitial phase content but will react differently: G_4 will be more reactive than G_5 because it contains twice as much C_3A than C_4AF. Because of the important impact of C_3A reactivity on the performance of chemical admixtures (see Chapters 10 and 16; Marchon et al., 2016; Nkinamubanzi et al., 2016) these changes in amounts of C_3A exposed initially to water can be expected to have important consequences.

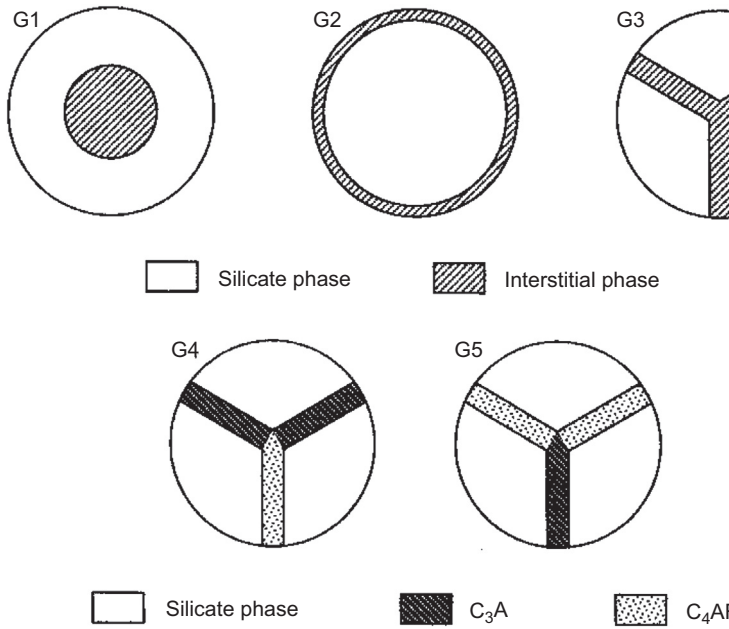


Figure 3.6 The importance of the morphology of cement particles.

3.5.2 Why is calcium sulphate added when grinding Portland cement?

In the absence of calcium sulphate, C_3A hydrates very rapidly in the form of hydrogarnets, so concrete loses its slump in a matter of minutes. In the concrete industry this type of accident is called 'flash set' – hopefully it does not happen frequently. If it occurs the only thing to do is fill the mixer with water as rapidly as possible to wash out the concrete; otherwise, it will be necessary to break the hardened mass of concrete with a hammer jack, which is a long and painful exercise.

The working mechanisms by which calcium sulphate passivates the reactivity of C_3A and its beneficial effect on C_3S hydration are explained in Chapter 8 (Marchon and Flatt, 2016a). For the time being we will only note that after water addition there is a rapid formation of **ettringite** and a **passivation** of the hydration of the C_3A, so there is no possibility of a flash-set situation developing if enough rapidly soluble calcium sulphates are available. Consequently, the cement paste keeps a sufficient workability until the concrete is poured.

In general, the amount of calcium sulphate added to the clinker is not sufficient to transform all the C_3A into ettringite. As explained in Chapter 8, after a few hours, when all the calcium sulphate is exhausted, ettringite is transformed into a calcium sulphoaluminate while releasing some calcium sulphate (Marchon and Flatt, 2016a). This new calcium sulphoaluminate is called monosulphoaluminate.

This transformation of the initial ettringite occurs when concrete has hardened form, so it is of little interest for contractors. But later, if for any reason some calcium sulphate penetrates into the hardened concrete, monosulphoaluminate may be transformed back into ettringite.

Another rheological problem related to calcium sulphate occurs from time to time: a false set. During the final grinding of the cement too much gypsum added to clinker is transformed into hemihydrate because the temperature in the grinding mill is too hot. When this hemihydrate gets into contact with mixing water it is transformed immediately into gypsum – a reaction that produces a stiffening of the cement paste. However, this initial loss of workability disappears when the clusters of gypsum crystals are broken by the action of the mixer, and some gypsum is consumed when reacting with the aluminate phase, so the concrete regains most of its initial workability.

Apart from these two accidental phenomena, C_3A hydration can cause serious rheological problems with some cements when making low w/c or w/b concretes where high dosages of superplasticizer have to be used. When the C_3A content is high and/or when the C_3A is very reactive, the initial rheology of some low w/c concrete deteriorates very rapidly so that in a matter of minutes these concretes lose their slump (see Chapter 16). In contrast, when the C_3A is low and not very reactive low w/c concretes lose their slump very slowly, so they can be poured easily (Aïtcin and Mindess, 2015).

Therefore, for those who are producing low w/c concretes, C_3A may be considered as poison. **When producing low w/c concretes or ultra-high-strength concretes, the lower the amount of C_3A, the easier is the control of concrete rheology**.

3.6 The hydration of Portland cement

This section presents only an overview of Portland cement hydration. A detailed chemical description of this hydration is given in Chapter 8 (Marchon and Flatt, 2016a). The impact of admixtures thereon is covered in Chapter 12 (Marchon and Flatt, 2016b).

The hydration of Portland cement and of its four main phases, C_3S, C_2S, C_3A and C_4AF, will be described only through their rate of heat evolution with time. Figure 3.7 presents the global rate of heat evolution of Portland cement during its hydration. The hydration of C_3S and C_3A is not simultaneous. The most important peak between phase III and IV corresponds to the main hydration of C_3S, while the shoulder in phase IV corresponds to the sulphate depletion point leading to a more massive hydration of C_3A. The hump in phase V is attributed to the conversion of AFt to AFm (see Chapter 8; Marchon and Flatt, 2016a). Therefore, the hydration of these two phases can be studied separately, but experience shows that there is a strong interaction between the two.

After a first liberation of heat corresponding to the dissolution of different ionic species and an initial hydration of C_3S and C_3A in Step I, there is a 'dormant period' corresponding to Step II during which chemical activity is much reduced. This dormant period precedes Steps III and IV, where C_3S and C_3A continue their hydration. Most C_2S and C_4AF hydrate essentially during Step V.

When C_3S and C_2S react with water they are transformed into calcium silicate hydrate and hydrated lime ($Ca(OH)_2$). The precise chemical composition and morphology of the calcium silicate hydrate vary, so it is written in the very vague formulation **C-S-H**. The crystalline form of hydrated lime found in hydrated cement paste is called **portlandite**. The hydration of C_3S liberates more portlandite than the hydration of C_2S, because C_3S is richer in lime than C_2S.

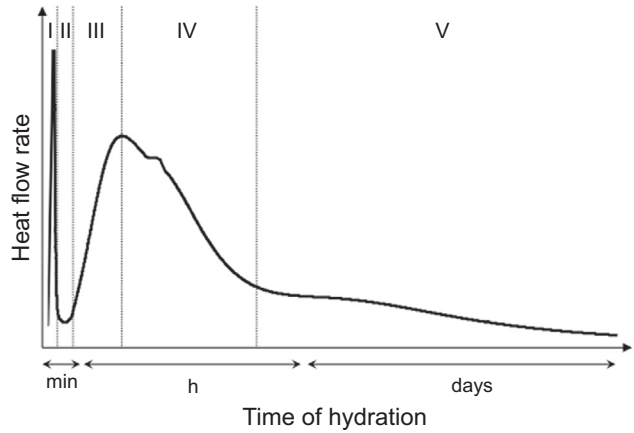


Figure 3.7 Schematic representation of the heat release and illustration of the different stages during the hydration of an ordinary Portland cement (Chapter 8; Marchon and Flatt, 2016a).

The hydration reaction of C_3S and C_2S can be represented schematically by the following equation:

$$(C_2S,\ C_3S) + \text{water} = \text{C-S-H} + \text{portlandite}.$$

In **the presence of calcium sulphate**, the interstitial phase ($C_3A + C_4AF$) is transformed into ettringite and monosulphoaluminate according to the following equation:

$$(C_3A,\ C_4AF) + \text{calcium sulphate} + \text{water} = \text{ettringite} + \text{monosulphoaluminate}.$$

Combining these two equations, the following equation is obtained:

$$(C_3S,\ C_2S,\ C_3A,\ C_4AF) + \text{calcium sulphate} + \text{water} = \text{C-S-H} + \text{portlandite} + \text{sulphoaluminates}.$$

It is easy to see all the crystals formed during hydration of cement or concrete under an electron microscope, especially in high w/c pastes, as seen in Figures 3.8–3.12.

The general aspect of the cement paste of a concrete with a very high water/cement ratio of 0.60:0.70 is shown in Figure 3.12, where the letters CH represent portlandite crystals and AG the aggregate.

Figure 3.12(b) and (c) shows the very porous structure of a cement paste with a high w/c ratio, particularly at the transition zone between the cement paste and the aggregate. Even in Figure 3.12(b) it is seen that some portlandite crystals present an epitaxial growth with the limestone aggregate.

But the morphology of the hydrated cement paste of low w/c concretes is completely different. It is no longer possible to see any beautiful hexagonal crystals of portlandite or fine needles of ettringite; rather, we see a compact mass of C-S-H that looks like an amorphous material, and a very few small clusters of badly crystallized portlandite (Figure 3.13). It is also evident that at the contact zone between the cement paste and the aggregate there is no loose transition zone, so the stresses present in the cement paste are directly transferred to the aggregate, and vice versa.

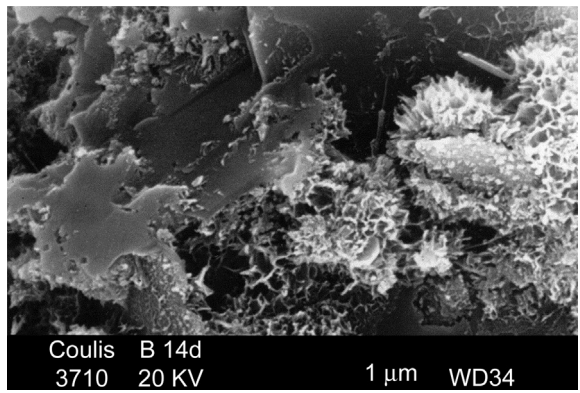


Figure 3.8 Calcium silicate hydrate (external product).
Courtesy of Arezki Tagnit-HAMOU.

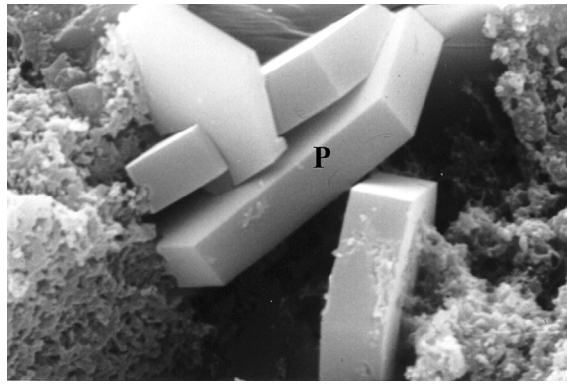


Figure 3.9 Portlandite crystals (P).
Courtesy of Arezki Tagnit-HAMOU.

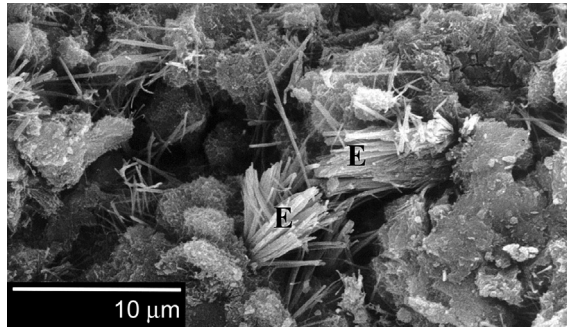


Figure 3.10 Ettringite crystals (E).
Courtesy of Arezki Tagnit-HAMOU.

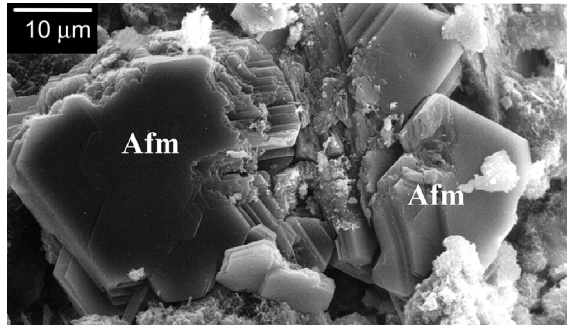


Figure 3.11 Hydrated tetracalciumaluminate crystals (Afm).
Courtesy of Arezki Tagnit-HAMOU.

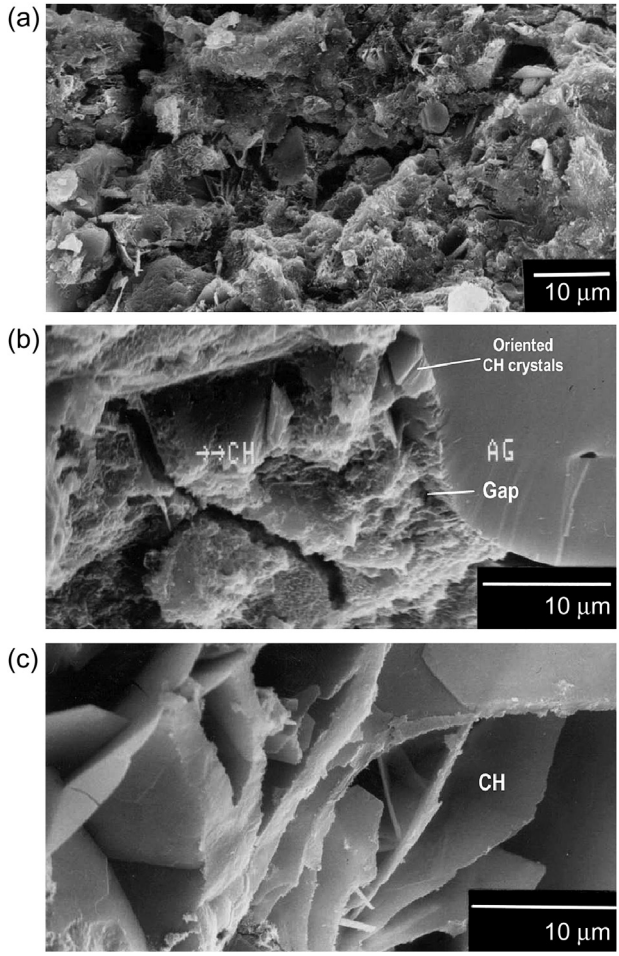


Figure 3.12 Microstructure of high w/c ratio concrete: (a) high porosity and heterogeneity of the matrix; (b) oriented crystal of portlandite (CH); (c) CH crystals.
Courtesy of Arezki Tagnit-HAMOU.

This difference in the morphology of cement pastes may be explained by various consequences of the difference in w/c. First, when the w/c is high there is a lot of water and space, so the growth of hydrates can proceed unhindered, leading to formation of large and beautiful crystals – referred to as the outer product of hydration as they form outside the boundaries of the initial cement particles (Richardson, 2004). In contrast, in low w/c paste hydrate growth is hindered much sooner and water availability becomes limited. Once water availability and space are particularly low, it can be argued that the hydration of cement further progresses via topochemical reactions rather than strict dissolution–precipitation.

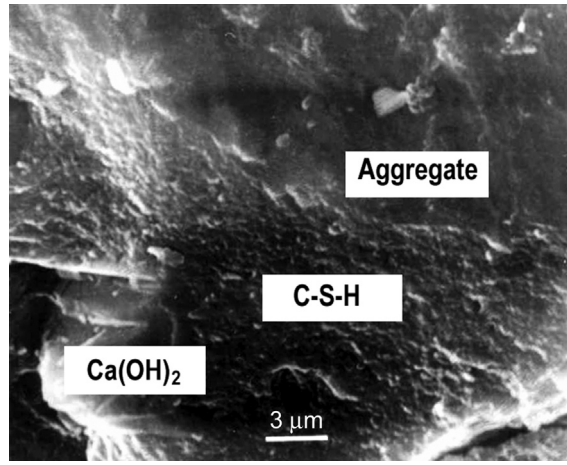


Figure 3.13 Hydrated cement paste of a very w/c concrete.
Courtesy of Arezki Tagnit-HAMOU.

3.7 Hydrated lime (portlandite)

Portland cement hydration results in the formation of a large amount of portlandite: 20−30% of the hydrated mass of cement according to the respective amounts of C_3S and C_2S in the clinker. In concretes having a high w/c, this portlandite appears in the form of large hexagonal crystals, as shown in Figure 3.12. These portlandite crystals have a marginal impact from a mechanical point of view, so they do not bring any strength to concrete. Moreover, in submerged concrete this lime can be leached out easily by diffusion, depending on the w/c ratio of the concrete and the purity of the water in which the concrete is submerged. Finally, the lime can be carbonated by CO_2 in the air. Its only advantage is that it maintains a high pH in the interstitial water and therefore protects reinforcing steel from carbonation-induced corrosion. But when the lime is fully carbonated by the CO_2 contained in air, this protection is lost.

The best way to make this lime beneficial from a mechanical, durability and sustainability point of view is to transform it into so-called secondary C-S-H by making it react with pozzolanic materials or slag, as it will be seen in Chapter 4 (Aïticin, 2016b).

Therefore, theoretically the hydration of a blended cement containing a pozzolanic material is:

$$\text{Clinker} + \text{pozzolan} + \text{gypsum} + \text{water} = \text{C-S-H} + \text{sulphoaluminates}.$$

Such blended cement also has the advantage of improving the sustainability of concrete structures by decreasing their carbon footprint.

3.8 Present acceptance standards for cements

These different aspects of cement hydration are presented to establish that it is almost impossible to produce two absolutely identical cements. It has thus been necessary to create a series of acceptance tests to maintain these variations within acceptable limits and produce cements having almost constant technological properties and concrete having predictable properties in both fresh and hardened states. Over time, a series of acceptance standards has been developed.

But after the great technological changes seen in concrete manufacture over the last 30 years, a question may be raised: are these standards, which have served the cement and concrete industry well for a long time, still valid? The answer is **no**.

The present acceptance standards were developed at a time when the concrete industry was producing concretes with high w/c greater than 0.50, and these are now considered as low-strength concretes. This is why the standards are based on the results of series of tests done on cement pastes or mortars having a w/c of about 0.50, where cement particles are not deflocculated at all. For a long time engineers and contractors were satisfied with such types of concrete, but this is no longer true: presently a significant (and profitable) part of the concrete market is composed of durable and sustainable concretes with a much lower w/c of between 0.30 and 0.40 (Aïtcin 2016a). Not only do these concretes have higher strength, but they also have longer durability and greater sustainability. Moreover, self-consolidating concretes that do not need any vibration to be poured are gaining a noticeable market share.

To satisfy the needs of these two growing and profitable market sectors, present acceptance standards for cement are totally inadequate, because the only rheological aspects they presently control are the initial flow and the initial setting time. New tests are needed to follow the rheology of cement pastes and mortars between zero and 90 minutes, the usual time for concrete delivery. Moreover, these tests have to be done on a deflocculated system with a w/c between 0.35 and 0.40.

3.9 Side-effects of hydration reaction

Hydration reactions transform the hydrated cement paste more or less rapidly into a hardened material that continues to gain strength with time as long as there is enough water to hydrate all the cement particles.

Portland cement hydration results in heat release that is a function of the mineral composition of the cement, and in that respect **it is important to repeat that it is not the amount of cement introduced into a mixer that determines the amount of heat released in a concrete, but the amount of cement that is actually hydrating when concrete has been poured into forms** (Cook et al., 1992).

Portland cement hydration also results in a **volumetric contraction** that is becoming very important from a technological point of view, because it may have dramatic consequences on the volumetric stability of concrete through the rapid development of **autogenous shrinkage**.

All concretes, whatever their w/c, develop some autogenous shrinkage because it is an ineluctable consequence of hydration reaction when this reaction occurs in a

closed system. However, when hydration reaction occurs in the presence of an external or internal source of water, a great part of this autogenous shrinkage can be annihilated, as will be seen in Chapter 5 (Aïtcin, 2016c).

Some researchers are promoting another technique to control autogenous shrinkage; it consists of introducing during mixing a small amount of an expansive chemical material that will compensate for the contraction of the apparent volume due to chemical contraction. Another solution is the use of a shrinkage-reducing admixture. The chemical nature of these admixtures is described in Chapter 10, and their behaviour in Chapter 22 (Marchon et al., 2016; Gagné, 2016).

3.10 Conclusion

Portland cement is a complex product obtained from unprocessed common natural materials: limestone and clay. Consequently, the characteristics of Portland cement clinker may vary from one cement plant to another. To limit the variations of the technological properties of Portland cement, acceptance standards have been developed, but presently these standards are not satisfactory for the whole concrete market. Low w/c cements are increasingly used; these concretes are made using large dosage of superplasticizers to disperse cement particles. It is therefore urgent for the cement industry to produce a clinker that will facilitate the production of the low w/c concretes that are more sustainable than normal-strength concretes. The production of the old Type I/II clinker must continue to satisfy the needs of this very profitable market, because now that we know how to increase concrete compressive strength, it is very important that we focus on how to improve the rheology of these concretes in order to transform concrete into a quasi-liquid material that can be poured without any problem.

Appendices

Appendix 1

Tricalcium aluminate

Why it is so important to discuss this particular mineral found in Portland cement when it usually represents only between 2% and 10% of its composition?

The reason is that, despite its relative low content in comparison to C_3S and C_2S, C_3A significantly influences the properties of the fresh and hardened concrete and the use of some admixtures.

In Portland cement C_3A may be found in different polymorphic forms. The structure of these various polymorphic forms of C_3A is well established (Regourd, 1978, 1982a,b; Moranville-Regourd and Boikova, 1993; Taylor, 1997; MacPhee and Lachowski, 1998).

Pure C_3A crystallizes in a cubic form. When pure cubic C_3A gets into contact with water, in the absence of any sulphate ions it reacts very rapidly and liberates a great amount of heat as it is transformed into hydrogarnet. In the presence of sulphate ions, C_3A is transformed into ettringite that temporarily blocks its hydration.

But in a cement kiln C_3A traps Na^+ ions very easily. This capture of Na^+ ions in the cubic structure generates distortions of the crystalline network, so that when Na_2O concentration becomes greater than 3.7% C_3A crystallizes in an orthorhombic form until its content is equal to 4.6%. Above this value it crystallizes in a monoclinic form (Regourd, 1982a,b). It is rare for the Na_2O content of C_3A of commercial clinkers to reach so high value, so this last crystallographic form is never found in commercial clinkers. Usually, in commercial clinkers, C_3A is found as a mixture of cubic and orthorhombic forms. The lower the Na_2O trapped in the C_3A network, the higher the amount of cubic C_3A and the more reactive is this C_3A. In contrast, the higher the Na_2O content of the clinker, the higher the amount of orthorhombic C_3A and the less reactive it is.

For cement chemists C_3A plays a very important and useful role − first during the fabrication of clinker, and second during the testing of the cement to see if it complies with acceptance standards.

As seen in Table 3.1, usually the interstitial phase ($C_3A + C_4AF$) represents 15−16% of the mass of the clinker. Moreover, an interstitial phase composed of an equal amount of C_3A and C_4AF (8%) represents the optimal conditions for clinker production. With such C_3A content it is not too difficult to adjust the calcium sulphate that must be added to control C_3A hydration and cement fineness to produce a cement complying with the acceptance standards and having maximum initial strength. **But it is no longer the initial compressive strength of small cubes with a high w/c that it is important to optimize, but rather the rheology of low w/c cement pastes**.

In contrast, for a concrete producer C_3A plays essentially a negative role from a rheological point of view, and to some extent from a durability one too. C_3A is the most reactive mineral of Portland cement and strongly influences its initial rheology despite the fact that its hydration is slowed down by the use of calcium sulphate. Calcium sulphate adsorption on C_3A stops its hydration temporarily. A high C_3A content can lead to excessive admixture consumption, as explained in Chapters 10 and 16, with negative impacts on rheology (Marchon et al., 2016; Nkinamubanzi et al., 2016), or a perturbation of the reactivity balance between aluminates, silicates and sulphates, as shown in Chapter 12, with the possible development of massive retardation (Marchon and Flatt, 2016b).

It is the variation of the C_3A content and its polymorphic forms as well as cement fineness that explain why admixture companies are recommending water reducer or superplasticizer dosages that can vary from one value to double that amount.

It is also the very high C_3A content of white cements that explains why these cements have a rheology that is particularly difficult to control when they are used with polysulphonate-based water reducers and superplasticizers.

The fineness of the cement is also a very important factor when trying to control concrete rheology, because as the clinker is ground finer more C_3A is exposed on the surface of cement particles.

Finally, the morphology of the cement particles also influences the rheological behaviour of a cement paste, as shown schematically in Figure 3.7.

Moreover, ettringite is not a stable mineral within concrete. For example, when the total calcium sulphate added to control the hydration of C_3A has been depleted, ettringite is transformed into monosulphoaluminate, while releasing some calcium sulphate

that will transform the remaining C_3A into monosulphoaluminate. If for any reason some SO_4^- ions later penetrate into hardened concrete, calcium monosulphoaluminate is transformed back into ettringite that crystallizes in the capillary system. These crystals of ettringite are referred to as secondary ettringite.

When pre-cast concrete elements are heated over 70 °C, or when concrete reaches this temperature during its hydration, ettringite is decomposed. When returning to ambient temperature, ettringite will crystallize again in a phenomenon called delayed ettringite formation, and this may result in severe cracking of concrete (Taylor et al., 2001; Flatt and Scherer, 2008).

Finally, when concrete specimens are submitted to freezing and thawing and have failed to pass the ASTM C 666 test, large clusters of ettringite crystals can be observed in the transition zone between aggregates and the cement paste, and even within some entrained air bubbles, as seen in Figure 3A.1.

For the concrete producer there is, however, one situation in which the C_3A content is beneficial: when concrete is exposed to chlorides rather than sulphates. The aluminates react to form Friedel salt, which strongly penalizes the propagation of chlorides in concrete and therefore extends its service life by slowing the initiation of chloride-induced corrosion.

Apart from this, the double role of C_3A – positive for the cement producer and negative for the concrete producer and the owner of the structure – deserves particular

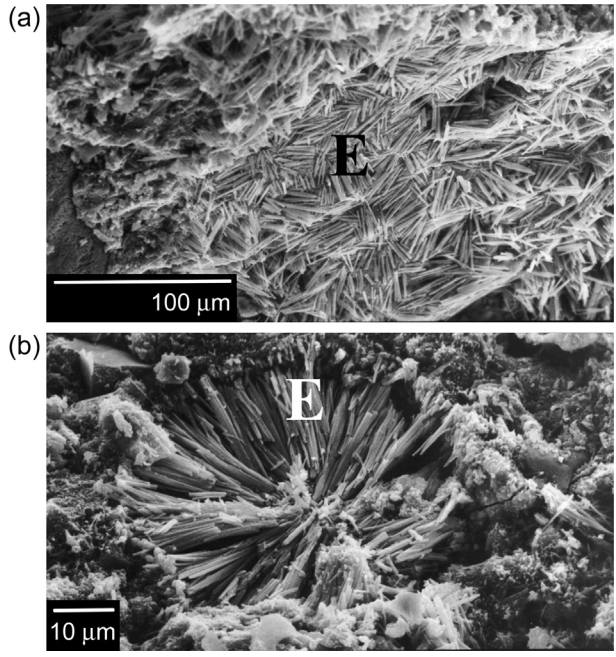


Figure 3A.1 Cluster of ettringite (E) crystals in some concretes: (a) ettringite in concretes destroyed by freezing and thawing cycles; (b) ettringite needles have almost filled an air-entrained bubble.
Photos taken by Guanshu Li (Aïtcin, 2008).

attention. If the long-term competitiveness of concrete is considered, to lower the carbon footprint of concrete structures the use of concretes with low w/c should be favoured. Therefore, it is imperative to find a satisfactory compromise between the preoccupations of cement producers and the needs of concrete producers wanting to facilitate the use of low w/c concretes and improve their durability.

It has been seen in this chapter that for economical reasons it is essential for Portland cement to contain some C_3A. But how much?

For cement producers, the answer is very simple: it is 8%, with 8% of C_4AF.

For the concrete producers, the answer is not so simple: it depends on the strength of the concrete and on the nature of the cement they are using (blended cement or Portland cement). When making an ordinary concrete with a high w/c and strength between 20 and 30 MPa, the optimum C_3A content is 8% because it gives good initial strength. When making high-performance concrete with a low w/c, a C_3A content of 6% results in relatively easy control of concrete rheology.

For an owner interested in the long-term durability of concrete structures, the answer is very simple: the lowest content possible.

For the author, the answer is as little as possible. The author is convinced that with a Type V clinker containing 5% of C_3A, it is possible to build all the concrete structures needed by the construction industry, using ordinary low-strength concretes as well as high-tech ones (Aïtcin, 2008). This type of clinker could be identified as an 'all-purpose clinker' rather than as an ASTM Type 5 clinker.

But more realistically, the good old Type I/II clinker containing 6−6.5% of C_3A that has served the US concrete industry so well for many years remains the best clinker for everybody. It would be a pity to stop the production of this clinker under the pretext that it does not provide a high early strength with blended cements. If high early strength is needed when using blended cements, it is only necessary to lower the w/b of the concrete, rather than to increase the C_3A and C_3S content of the clinker and the fineness of the cement, as shown in Chapter 1 (Aïtcin, 2016a).

It is not necessary to create a new type of clinker: let us rely on the Type I/II clinker to build easily, durable and sustainable concrete structures.

But taking into account the complication of the fabrication of cements with a low C_3A content, the author is convinced that it is imperative for **the cement industry to produce two types of clinkers**.

- One with a C_3A content of **no more than 8% (for durability reasons)**, to make high w/c concrete with either Portland cement or blended cements.
- One with **a C_3A content of about 6% (for rheological reasons)**, to make low w/c concretes using cement that may contain supplementary cementitious materials.

Appendix 2

Ettringite

It has been seen that the easiest way to control the rapid hydration of C_3A is to add calcium sulphate during the final grinding of cement. This calcium sulphate is usually added in the form of gypsum ($CaSO_4$, $2H_2O$), which is easily soluble in water, but during the final grinding a part of this gypsum can be transformed into hemihydrate

($CaSO_4$, $^1/_2H_2O$) due to an increase of the temperature within the ball mill, or even into totally dehydrated hemihydrate, improperly called anhydrite in the industry. As hemihydrate dissolves more rapidly in water than gypsum, it quickly releases SO_4^- ions that react rapidly with C_3A to form ettringite and also adsorb on the C_3A to passivate its reactivity.

It is not always pure gypsum that is added in the ball mill, because contaminated gypsums containing some anhydrite and calcium carbonate that are found on the borders of gypsum quarries are bought by cement companies because they are cheaper than pure gypsum. Pure gypsum is usually used for the fabrication of gypsum wall boards. Sometimes synthetic calcium sulphates ($CaSO_4$) are added in the ball mill instead of gypsum. Synthetic calcium sulphates are very often improperly called anhydrite in the industry. Anhydrite is the crystalline form of an unhydrated form of $CaSO_4$, whereas different synthetic calcium sulphates obtained from desulphurization processes are not crystalline at all, or at the best very poorly crystalline.

If from a chemical point of view all these materials are different forms of calcium sulphate, they do not have the same solubility rate in water; crystalline anhydrite being the less rapidly soluble, and totally dehydrated hemihydrate and synthetic calcium sulphate being the more rapidly soluble.

As it is important that SO_4^- ions are dissolved rapidly enough to react with C_3A in order to control its initial hydration, usually it is beneficial for a part of the gypsum added during the grinding to be transformed into hemihydrate. Moreover, the alkali sulphates of the clinker are more rapidly soluble than calcium sulphate, so they can provide the first SO_4^- ions that are dissolved in mixing water and avoid polynaphthalene sulfonate superplasticizer (PNS) and polymelamine sulphonate superplastizer (PMS) reacting with C_3A, particularly when superplasticizer dosage is high, as will be seen in Chapter 10 (Marchon et al., 2016).

The adjustment of the calcium sulphate content of cement is thus a very delicate operation that must take into account all these factors.

Because of calcium sulphate adsorption on C3A, the rheology of concrete evolves slowly during the induction (dormant) period, and the rheology of the cement paste of concrete evolves slowly, giving enough time to transport and pour concrete without too much loss of slump and workability. It is worth noting here that the ettringite formed in this stage can be viewed as a side product of the passivation rather than its cause, as is explained in Chapter 8 (Marchon and Flatt, 2016a). Thereafter cement paste starts to harden rapidly. Various hypotheses still exist concerning this change of hydration rate, and are also presented in Chapter 8 (Marchon and Flatt, 2016a).

The chemical composition of the unit cell of ettringite has long been a subject of controversy. Some books state that the unit cell of ettringite has 30 water molecules; in others it is 32 or 31. Some authors strongly criticized the suggestion of 31 water molecules, saying that a symmetrical molecule like ettringite could only contain a prime number of water molecules.

In fact, the number of water molecules strongly anchored on the hexagonal unit cell is 30, and there are two additional water molecules that are not so tightly anchored and can be detached easily (e.g. by mild drying and/or vacuum), as seen in Figure 3A.2. This explains the variation in the number of water molecules found by the different researchers.

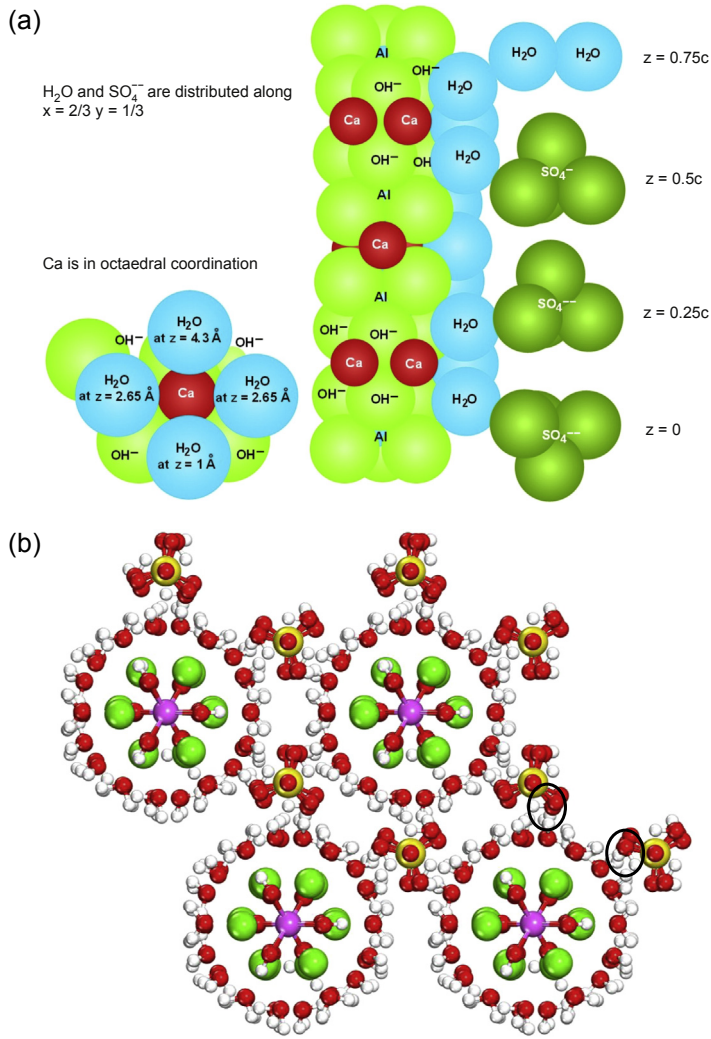


Figure 3A.2 Unit cells: (a) ettringite; (b) Trigonal crystal of ettringite. Courtesy of Mishra Ratan Kishore.

References

Aïtcin, P.-C., 2016a. The importance of the water−cement and water−binder ratios. In: Aïtcin, P.-C., Flatt, R.J. (Eds.), Science and Technology of Concrete Admixtures, Elsevier, (Chapter 1), pp. 3−14.

Aïtcin, P.-C, 2016b. Supplementary cementitious materials and blended cements. In: Aïtcin, P.-C., Flatt, R.J. (Eds.), Science and Technology of Concrete Admixtures, Elsevier (Chapter 4), pp. 53−74.

Aïtcin, P.-C., 2016c. Water and its role on concrete performance. In: Aïtcin, P.-C., Flatt, R.J. (Eds.), Science and Technology of Concrete Admixtures, Elsevier, (Chapter 5), pp. 75–86.
Aïtcin, P.-C., 2008. Binders for Durable and Sustainable Concrete. Taylor and Francis, London, UK.
Aïtcin, P.-C., Mindess, S., 2011. Sustainability of Concrete. Spon Press, London, UK.
Aïtcin, P.-C., Mindess, S., 2015. Back to the future. Concrete International 37 (5), 45–50.
Bhatty, J.I., Mac Gregor Miller, F., Kosmatka, S.H. (Eds.), 2004. Innovations in Portland Cement Manufacturing. Portland Cement Association, Skokie, Illinois, USA, 1404p.
Bogue, R.H., 1952. La chimie du ciment Portland. Eyrolles, Paris.
Chatterji, A.K., 2011. Chemistry and engineering of the clinkerisation process incremental advances and lack of breakthroughs. Cement and Concrete Research 41, 624–641.
Cook, W.D., Miao, B., Aïtcin, P.-C., Mitchell, D., 1992. Thermal stress in large high strength concrete columns. ACI Materials Journal 89 (1), 61–66.
Flatt, R.J., Scherer, G.W., 2008. Thermodynamics of crystallization stresses in DEF. Cement and Concrete Research 38, 325–336.
Gagné, R., 2016. Expansive agents. In: Aïtcin, P.-C., Flatt, R.J. (Eds.), Science and Technology of Concrete Admixtures, Elsevier (Chapter 22), pp. 441–456.
MacPhee, D.E., Lachowski, 1998. In: Hewlett, Peter, Arnold (Eds.), Cement Composition and Their Phase Relations, fourth ed., Lea's Chemistry of Cement and Concrete London, pp. 93–129.
Marchon, D., Flatt, R.J., 2016a. Mechanisms of cement hydration. In: Aïtcin, P.-C., Flatt, R.J. (Eds.), Science and Technology of Concrete Admixtures, Elsevier (Chapter 8), pp. 129–146.
Marchon, D., Flatt, R.J., 2016b. Impact of chemical admixtures on cement hydration. In: Aïtcin, P.-C., Flatt, R.J. (Eds.), Science and Technology of Concrete Admixtures, Elsevier, (Chapter 12), pp. 279–304.
Marchon, D., Mantellato, S., Eberhardt, A., Flatt, R.J., 2016. Adsorption of chemical admixtures. In: Aïtcin, P.-C., Flatt, R.J. (Eds.), Science and Technology of Concrete Admixtures. Elsevier, (Chapter 10), pp. 219–256.
Moranville-Regourd, M., Boikova, A.I., 1993. Chemistry, structure, properties and quality of clinker. In: Proceedings of the 9th International Congress on the Chemistry of Cement, New Delhi, vol. 1, pp. 407–414.
Nkinamubanzi, P.-C., Mantellato, S., Flatt, R.J., 2016. Superplasticizers in practice. In: Aïtcin, P.-C., Flatt, R.J. (Eds.), Science and Technology of Concrete Admixtures, Elsevier (Chapter 16), pp. 353–378.
Regourd, M., 1978. Cristallisation et réactivité de l'aluminate tricalcique dans les ciments Portland. II Cemento 3, 323–336.
Regourd, M., 1982a. Structure cristalline et caractérisation de l'aluminate tricalcique-Données récentes- Séminaire International sur les aluminates de calcium. Polytecnico de Torino, Italy, pp. 44–58.
Regourd, M., 1982b. In: J.Baron, Sauterey, R. (Eds.), L'hydratation du ciment Portland, Le Béton Hydraulique. Presses de l'École Nationale des Ponts et Chaussées, pp. 193–221.
Richardson, I.G., 2004. Tobermorite/jennite and tobermorite/calcium hydrate-based models for the structure of C-S-H: applicability to hardened pastes of tricalcium silicate, B-dicalcium silicate, Portland cement, and blends of Portland cement with blast-furnace, metakaolin, or silica fume. Cement and Concrete Research 34, 1733–1777.
Taylor, H.F.W., 1997. Cement Chemistry, second ed. Thomas Telford. 459p.
Taylor, H.F.W., Famy, C., Scrivener, K.L., 2001. Delayed ettringite formation. Cement and Concrete Research 31, 683–693.

Supplementary cementitious materials and blended cements

4

P.-C. Aïtcin
Université de Sherbrooke, QC, Canada

4.1 Introduction

The Phoenicians, Greeks, and Romans noticed that when certain natural materials were mixed with lime, they produced mortars and concrete that could harden under water. These products are known as natural pozzolans, named after the city of Puzzoli near Naples where the Romans extracted some particularly reactive volcanic ashes from Vesuvius.

We now know that natural pozzolans react with lime because they contain a certain amount of vitreous silica. Only volcanic ashes that have been cooled down very rapidly (quenched) react with lime, because their silica has not had enough time to crystallize and remains in a vitreous state. When volcanic ash cools down very slowly, there is enough time for the silica to form large crystals. As it does not contain any vitreous silica, this ash does not react with lime.

The use of pozzolanic materials was lost at the end of the Roman Empire, and it was not until the second half of the nineteenth century that the hydraulic properties of Portland cement were discovered.

Presently, the use of pozzolanic materials (Massazza, 1998) and what are called supplementary cementitious materials is becoming very important, because the sustainability of concrete structures is becoming a fundamental criterion. As will be seen in this chapter, the replacement of a certain mass of clinker by an equivalent mass of supplementary cementitious material or pozzolan is very important from a sustainability point of view because:

- it eliminates the emission of an equivalent mass of CO_2
- it results in the recycling of some industrial by-products
- it improves the durability of the hardened concrete because the pozzolanic reaction transforms hydrated lime that has no binding properties into secondary calcium silicate hydrate (C-S-H), the 'glue' of concrete.

Various artificial and natural pozzolans are used in different countries and their use will increase in the future. Of course, these pozzolanic materials react at different speeds and more or less completely according to their vitreous silica content and fineness and the amount of lime liberated during Portland cement hydration (Malhotra and Metha, 1996, 2012).

It is interesting to report the chemical composition of these materials in a ternary $SiO_2-CaO-Al_2O_3$ diagram to compare their composition to that of Portland cement (Figure 4.1).

Science and Technology of Concrete Admixtures. http://dx.doi.org/10.1016/B978-0-08-100693-1.00004-7
Copyright © 2016 Elsevier Ltd. All rights reserved.

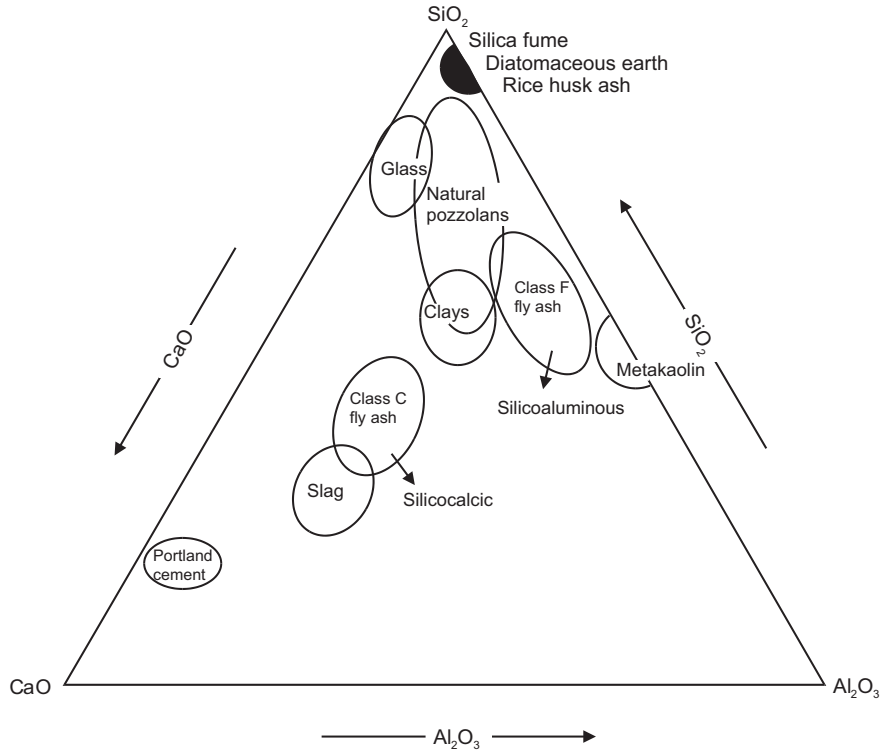


Figure 4.1 Chemical composition of the principal cementitious materials.

4.2 Crystallized and vitreous state

For a mineralogist, two types of materials exist: those with a crystalline structure (Figure 4.2b) and those that are amorphous or vitreous (Figure 4.2a). In a material with a crystalline structure, ions are arranged in a repetitive manner and form a crystal lattice that can be defined by an elementary cell called a unit cell. The spatial arrangement of the different ions is governed by their valence (number of shared electrons) and their respective diameters. For example, quartz one of the crystalline forms of silica (SiO_2) is built by assembling SiO_4 tetrahedrons having at their summit four large O^{2-} ions (1.32 nm in diameter) that surround a small Si^{4+} ion (0.39 nm).

These silica tetrahedrons can be arranged differently and form the large family of minerals called the silicates. When a monochromatic source of X-ray is projected on a crystallized mineral, a diffractogram presenting a certain number of peaks is obtained. Each peak corresponds to the refraction of the monochromatic X-ray on dense ionic plans, as can be seen in Figure 4.3(a) in the case of Portland cement.

A Portland cement diffractogram is in fact the addition of the characteristic peaks of each mineral found in Portland cement. ASTM tables give the characteristic peaks of pure mineral.

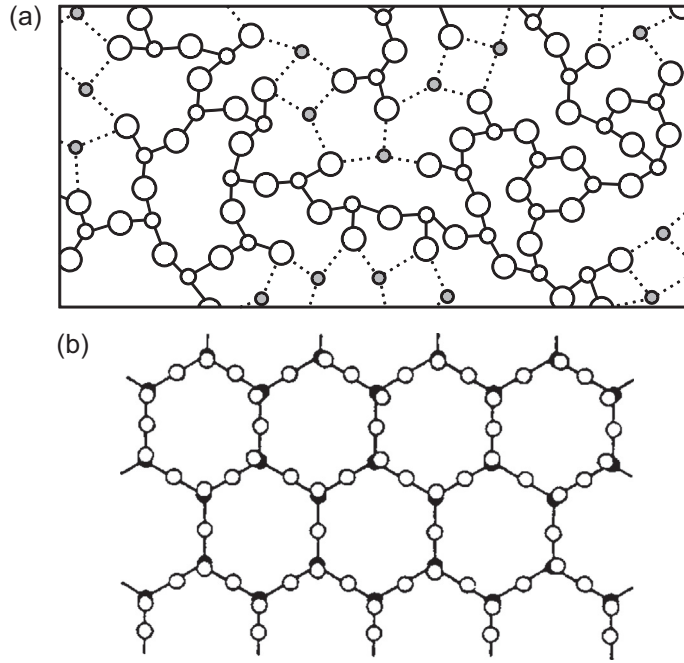


Figure 4.2 Comparison of the structure of a glass and a mineral. (a) Disorganized structure of a glass (2D). (b) Mineral (2D).

In a crystallized mineral, internal ions are in a stable equilibrium and are not very reactive. Those at the surface of the material which are not fully saturated from an electrical point of view are a little bit more reactive. In contrast, in a vitreous material, the different ions are not arranged systematically to form a regular network, but are more or less disorganized according to the severity of the quenching to which they were subjected when they were solidified. When amorphous materials are subjected to X-ray radiations, their diffractogram does not present a series of peaks but rather a kind of hump, more or less accentuated, as seen in Figure 4.4.

This hump indicates that on *a very short scale*, the ions have a more or less organized structure. The larger and flatter the hump, the more disorganized the structure of the glass and the greater the number of unsaturated valences. Thus, in a reactive medium, there are some ions that are active enough to react chemically to form new compounds. Moreover, the finer a vitreous material is, the more reactive it is, because its specific surface is greater, so it contains more unsaturated ions ready to react chemically.

Melted rocks containing a certain amount of silica are usually viscous so that when they are quenched, silica tetrahedrons have not enough time to become organized as a crystalline network so that the melted mineral solidifies in the form of a vitreous solid. On the contrary, if enough time is provided to the melted material as it cools down, it solidifies in the form of a crystalline material.

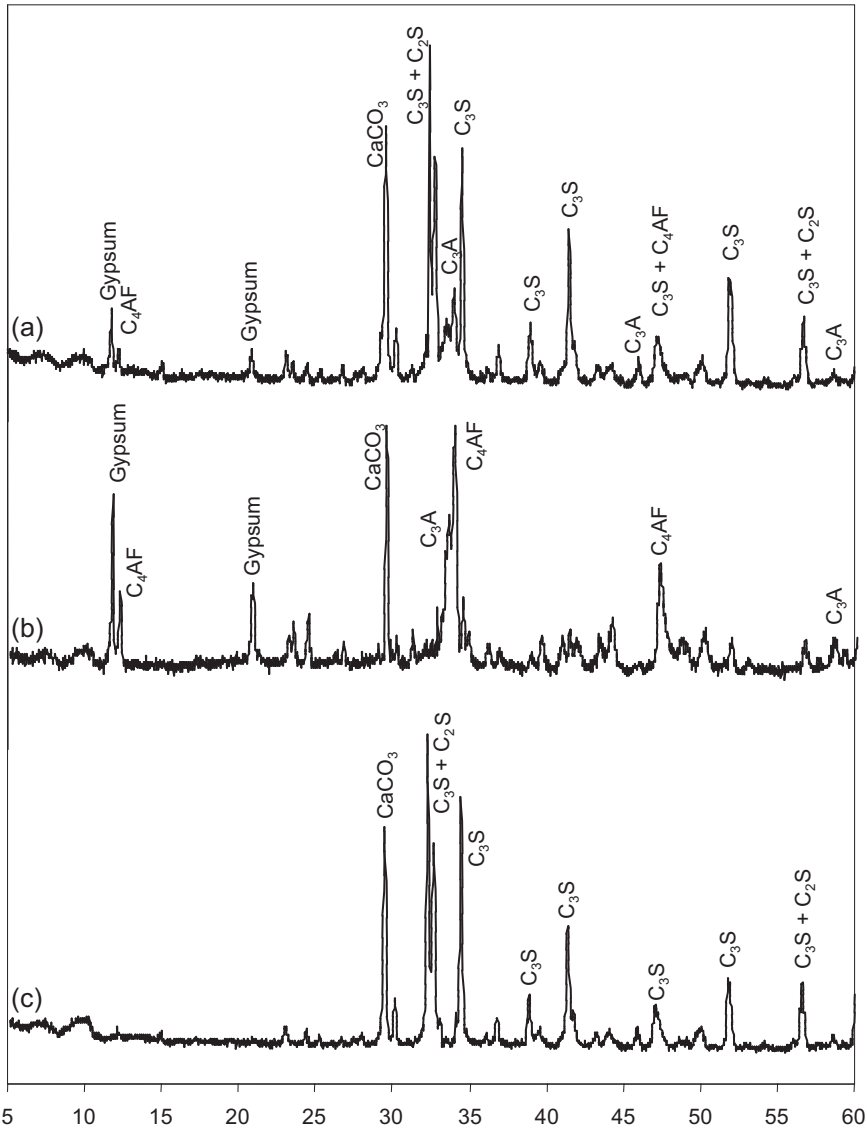


Figure 4.3 (a) X-ray diffractogram of a Portland cement. (b) X-ray diffractogram of the same cement after treatment with salicylic acid. (c) X-ray diffractogram of the same cement after a KOSH treatment: Calcium hydroxide/sucrose treatment.
Courtesy of Mladenka Saric Coric (Aïtcin, 2008).

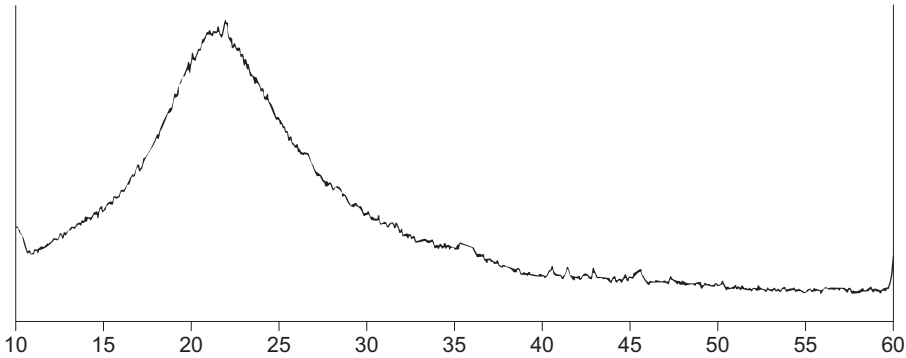


Figure 4.4 X-ray diffractogram of a vitreous slag.

4.3 Blast-furnace slag

Figure 4.5 presents schematically the principle of the fabrication of pig iron in a blast furnace.

The chemical process consists of reducing iron ore introduced in the form of iron oxide pellets at the top of the furnace by an appropriate amount of metallurgical

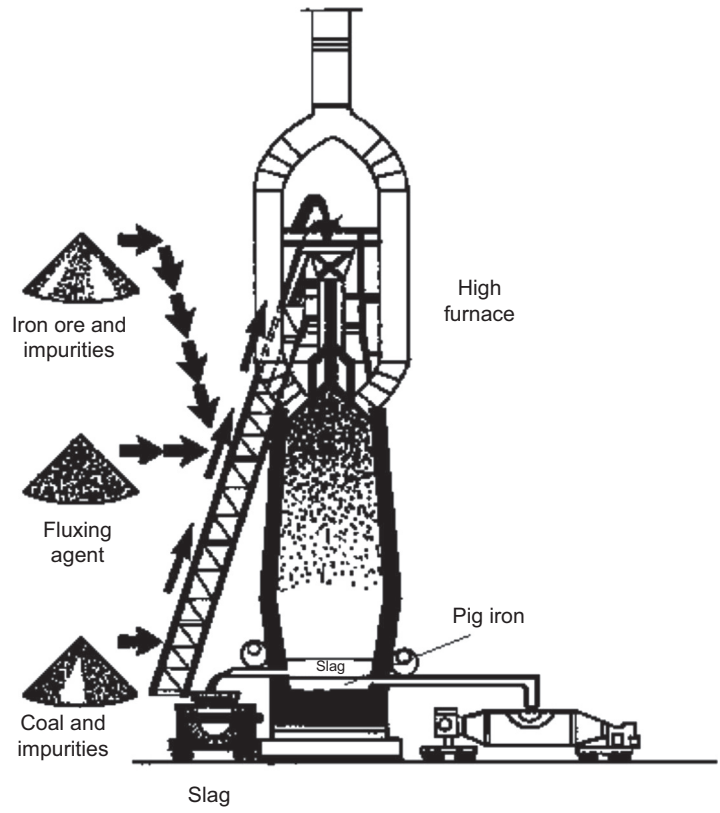


Figure 4.5 Schematic representation of a high furnace.
Aïtcin, P.C., 1998. High Performance Concrete, E and FN SPON.

coke. But the impurities contained in iron pellets and metallurgical coke also have to be melted to be eliminated. Usually, these impurities are composed of different silicates, carbonates, or aluminates. When looking at an SiO_2−CaO−Al_2O_3 phase diagram, it is seen that there are two particular points having a low melting temperature which composition are called eutectic compositions (Figure 4.6).

When slag has exactly one of the two chemical compositions, E_1 or E_2, it melts at a constant temperature lower than that of any other compositions. One composition melts at 1170 °C and the other at 1260 °C. To reduce the amount of metallurgical coke to be burned to reach fusion of the impurities, metallurgists adjust the composition of the impurities by adding a fluxing agent to match the composition of the eutectic mix melting at 1260 °C. The other eutectic, richer in silica, gives pig iron that contains too much silica. In the ternary diagram SiO_2−CaO−Al_2O_3, it is seen that this eutectic point is close to the one representative of Portland cement.

Therefore, the average chemical composition of all the slags produced worldwide is about 38% CaO, 42% SiO_2, and 20% Al_2O_3.

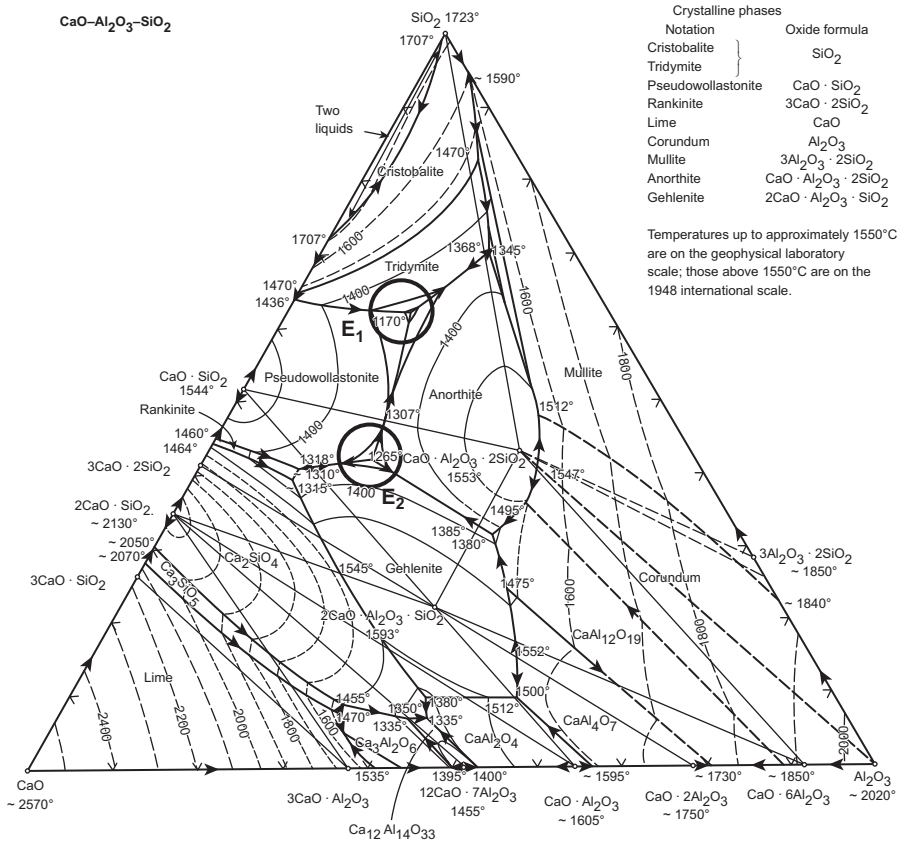


Figure 4.6 Position of the two eutectics with the lowest melting temperature in an SiO_2−CaO−Al_2O_3 phase diagram.

When the slag is tapped from the furnace and allowed to cool slowly, it crystallizes in the form of melilite, which is a solid solution of gehlenite ($2CaO \cdot Al_2O_3 \cdot SiO_2$) and ackermanite ($2MgO \cdot Al_2O_3 \cdot SiO_2$). In contrast, if the slag is rapidly quenched in cold water, it solidifies into the form of vitreous particles that after grinding react with the lime liberated by the hydration of the C_3S and C_2S in Portland cement.

Why do not all granulated slags have the same reactivity?

The reactivity of a granulated slag does not depend on its chemical composition, but rather on its degree of disorganization (degree of vitrification) (Figure 4.7).

The greater the disorganization, the more reactive the slag. The degree of disorganization is a function of the temperature of the liquid slag when it is quenched: the hotter the slag, the more vitreous and pale is the quenched slag. The colder the slag, the less reactive and darker are the granules. When a 'cold' slag has been quenched, it may contain some perfect crystals of melilite (Figure 4.8).

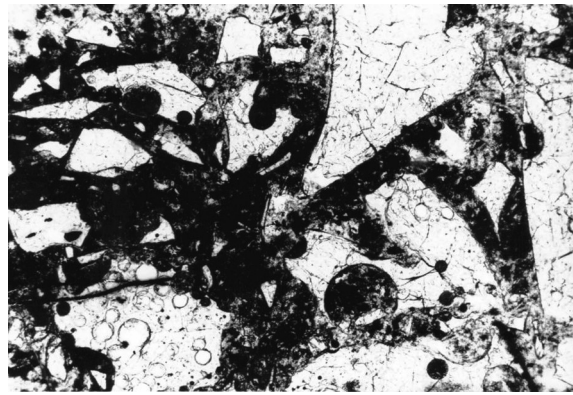


Figure 4.7 Granules in white, vitreous slag particles. Note the angular shape of the slag particles and their porosity. This hot slag was quenched at a high temperature, as can be seen by the fact that no crystals are visible in the vitreous particles.

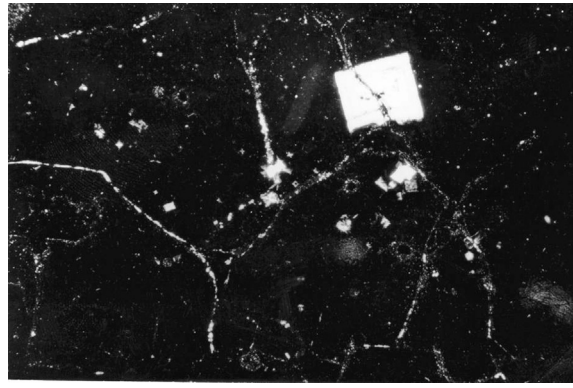


Figure 4.8 Melitite crystal in a slag particle after quenching. This slag was a cold slag quenched under a temperature of its liquidus.

In a blended cement, the reactivity of a slag depends also on its fineness. The finer the slag, the more reactive it is because it contains more disorganized superficial ions than a coarser slag (Nkinanubanzi and Aïtcin, 1999). As the slag is usually more difficult to grind than the clinker when trying to increase the fineness of a slag cement, in a blend it is the clinker part that is ground finer – the opposite of what should be obtained. This is why when making a blended cement containing slag, it is better to grind the clinker and slag separately and mix them afterwards.

4.4 Fly ashes

The impurities contained in coals or lignites burned in power plants melt when the pulverized coal passes through the flame in the combustion zone (Figure 4.9).

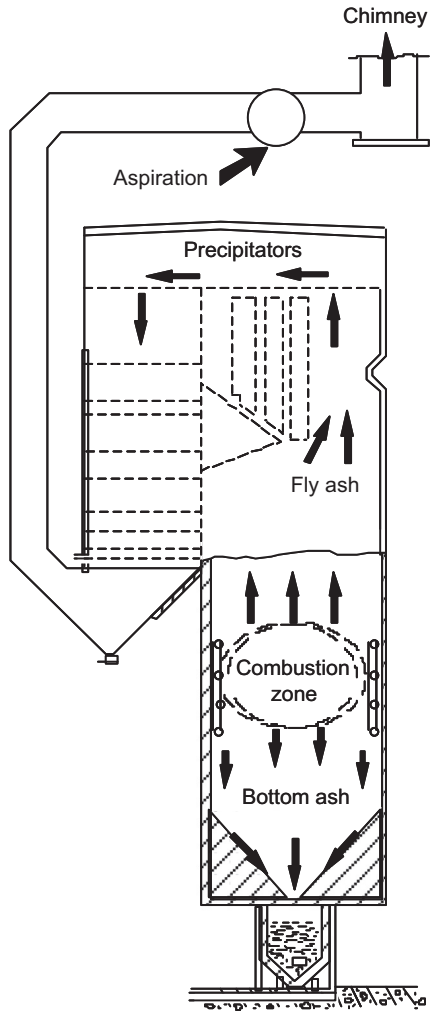


Figure 4.9 Schematic representation of the combustion zone in a power plant.

When these fine droplets leave the burning zone, they solidify in a spherical shape (to minimize their superficial energy) and are carried towards the de-dusting system with the combustion gases, as seen in Figures 4.10 and 4.11.

As these particles are usually rich in silica and are cooled quite rapidly as they leave the burning zone, they are quenched and do not have enough time to crystallize. Thus, the fly ashes collected in the de-dusting systems are vitreous and can react with the lime liberated during cement hydration.

Fly ashes can be considered as artificial pozzolans, and their chemical composition and vitreous state depend on the impurities contained in the coal or lignite burned in the power plant. In North America, fly ashes are classified in two categories: class F fly ashes that contain very little lime, and class C fly ashes that contain 10% lime. Some class C fly ashes are identified as sulfocalcic because they are also rich in sulfur.

Generally speaking, fly ashes have a grain size distribution that is close to that of Portland cement. They may contain a certain number of crystallized particles (rather

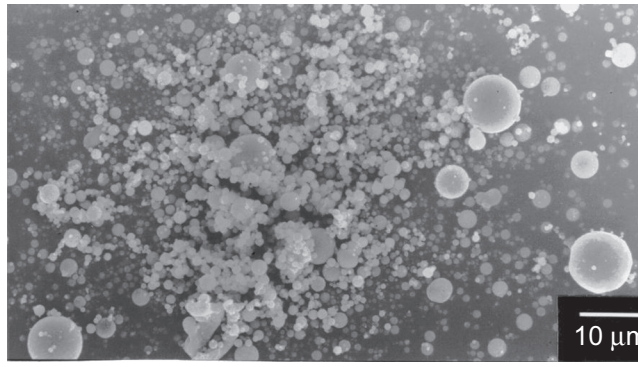


Figure 4.10 Spherical particles of fly ashes.

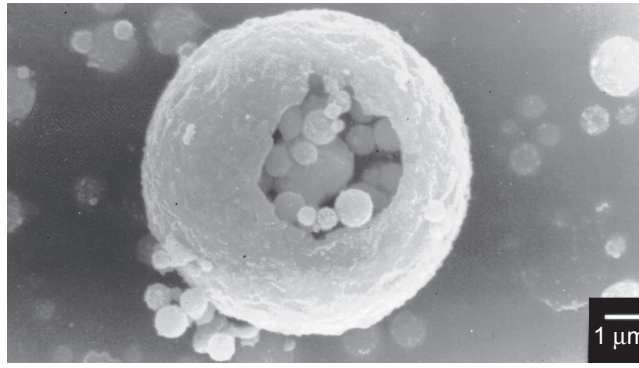


Figure 4.11 Plerosphere containing cenospheres in a fly ash.

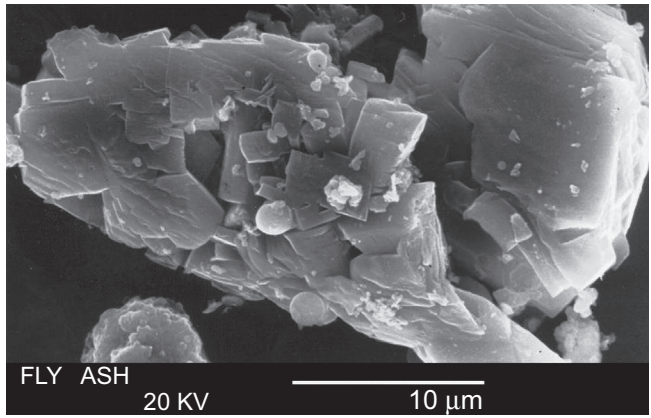


Figure 4.12 Coarse crystallized fly ash particle.
Courtesy of I. Kelsey-Lévesque.

coarse), corresponding to coarse impurities that pass so rapidly through the flame they do not have enough time to be fused. Fly ashes can also contain a certain percentage of unburned coal, and in some cases the particles are covered with soot. The presence of this unburned carbon and/or soot may cause serious problems when using admixtures, because the carbon and/or soot particles may preferentially absorb some admixture.

Several treatments can be implemented to improve the quality of fly ashes; for example, the passage of the fly ash through a cyclone easily eliminates its coarse particles, essentially the crystallized particles (Figure 4.12) and the coarse particles of unburned carbon. But the elimination of the soot that covers the fly ash particles is more problematic and costly.

When the effects of a particular type of fly ash on the properties of a concrete are studied, it is only possible to predict its specific action with greater or lesser accuracy. It is difficult to generalize one result obtained on a particular fly ash. For example, Claude Bédard (2005) studied an entirely crystallized fly ash that did not have any pozzolanic properties, but it was called fly ash because it was ash that had been collected in the de-dusting system of a power plant.

Malhotra and Mehta (2012) favor the use of concrete with a high fly ash content in order to lower the carbon footprint of sustainable concrete structures.

4.5 Silica fume

Silica fume collects in the de-dusting system of electric arc furnaces during the production of silicon, ferrosilicon, or zirconium (Figures 4.13a and 4.13b).

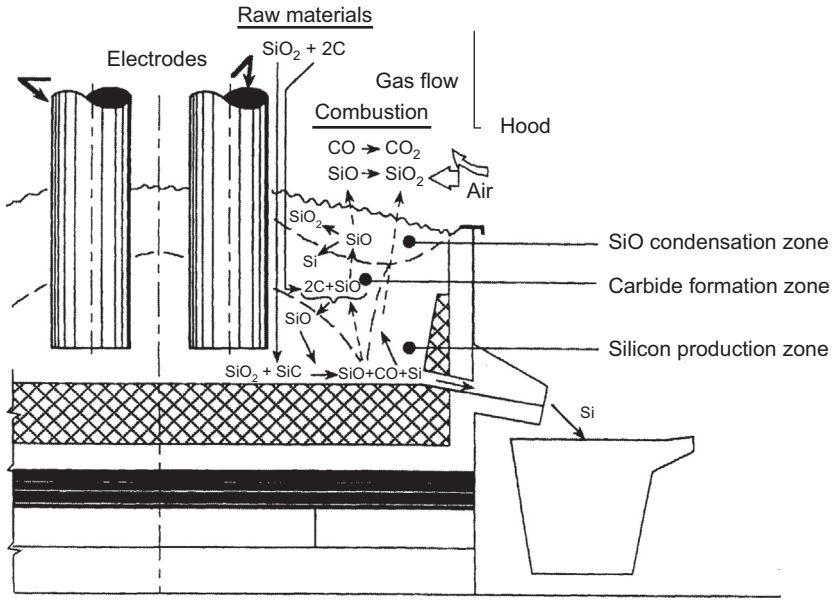


Figure 4.13a Schematic representation of an electric arc furnace that produces silica fume without a recovery system.

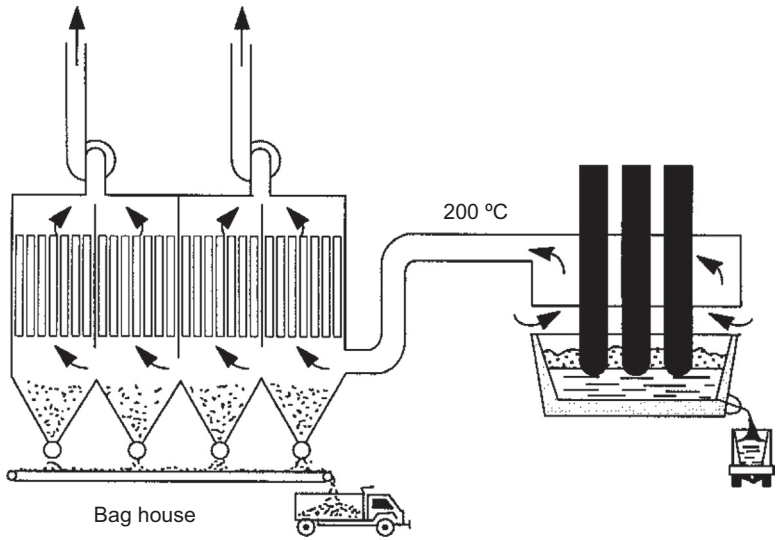


Figure 4.13b Collecting silica fume in the 'bag house' of an electric arc furnace equipped with a heat recovery system.

In the arc, SiO vapor is formed, but as soon as it leaves the electric arc and comes into contact with oxygen in the air, it is transformed into very fine spherical particles of SiO_2 (to minimize their superficial energy) that contain more than 85% of vitreous silica.

When the furnace is equipped with a heat recovery system, the silica fume particles collected in the de-dusting system are whitish, because they leave the furnace at a temperature of about 800 °C, which is sufficiently high to burn all the traces of carbon.

When the furnace is not equipped with a heat recovery system, the silica fume particles collected in the de-dusting system have a gray color, because they left the furnace at temperature lower than 200 °C after being mixed with fresh air to cool down the hot furnace gases, so they do not burn the de-dusting sacks used to collect them (Figure 4.13b).

Silica fume particles are vitreous due to their rapid quenching (Figure 4.14).

After reheating, the silica crystallizes as cristobalite. The hump found in the as-produced silica fume corresponds to the main pick of cristobalite, which indicates than in a silica fume particle, silica tetrahedrons are organized as in cristobalite α on a short-range distance.

The average diameter of amorphous silica particles is about to 0.1 μm (Figures 4.15). Silica fume particles are usually gray in color, darker or lighter according to their carbon and iron content.

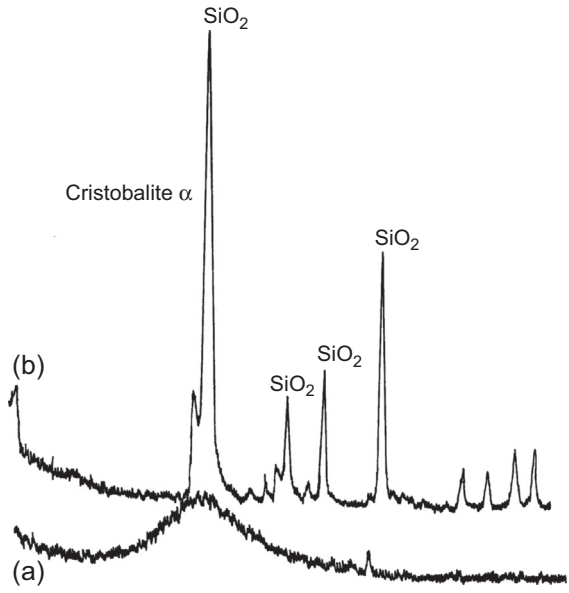


Figure 4.14 X-ray diffractogram of a silica fume particle: (a) as-produced, (b) after reheating at 1100 °C.

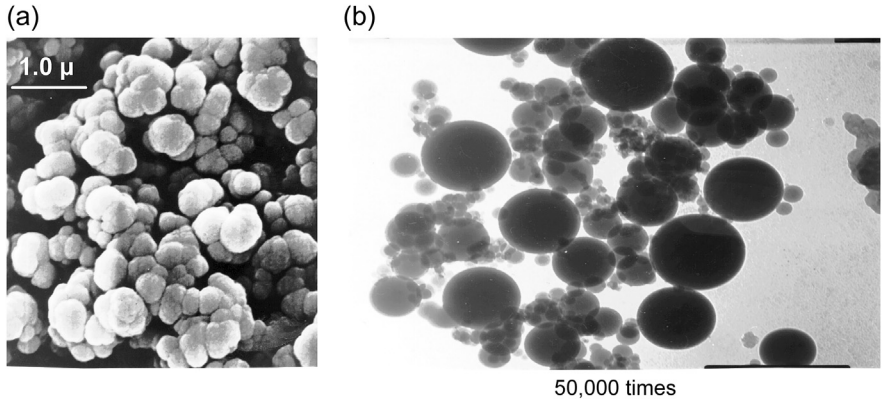


Figure 4.15 Silica fume as seen under an electronic microscope: (a) scanning electronic microscope − silica fume particles are naturally agglomerated in an as-produced silica fume. (b) Transmission electronic microscope − dispersed individual particles.

4.6 Calcined clays

Clays are silicates composed of different layers of ions bonded by OH^- ions. Pure kaolinite ($2SiO_2 \cdot Al_2O_3 \cdot 2H_2O$) is the clay used to make chinaware. It is an aluminosilicate composed of a layer of tetrahedral SiO_2 and octahedral $Al(OH)_3$ ions where the Al_3 ions are found at the center of the octahedrons. When kaolinite is heated between 450 and 750 °C, some water molecules leave the kaolinite layers and it is transformed in metakaolin, which presents a disorganized structure (Figure 4.16).

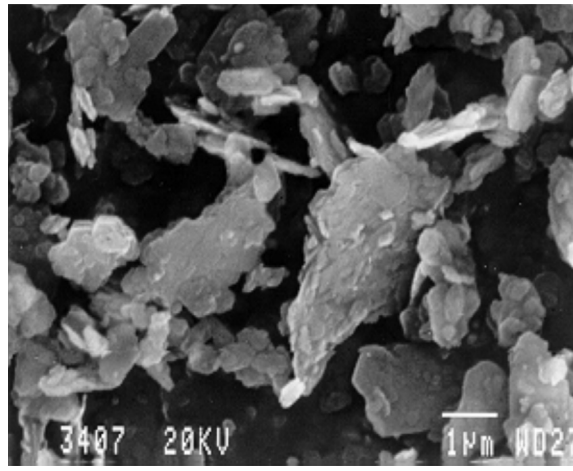


Figure 4.16 Metakaolin particles.

The Si_4^+ ions at the end of the tetrahedrons react with the lime liberated by the hydration of the C_3S and C_2S to form C-S-H.

The Phoenicians and Romans noticed that crushed pieces of fired bricks, tiles, or pottery gave strong mortars.

Kaolinite is essentially calcined to be used as artificial pozzolan – illites and montmorillonites are not of interest in civil engineering because they do not react with lime.

Large amounts of metakaolin were used in Brazil during the construction of the Itaïpu hydroelectric complex located at the border of Brazil and Argentina in order to lower the amount of cement that had to be transported by truck to this very remote place. Moreover, the use of metakaolin helped to decrease the temperature rise in the massive elements of the dam.

4.7 Natural pozzolans

In different countries, various natural pozzolans are blended with Portland cement. These natural pozzolans are essentially vitreous volcanic ashes rich in SiO_2 and may have different chemical compositions and present different degrees of vitrification. In Figure 4.17, the X-ray diffractogram of a natural pozzolan is compared to

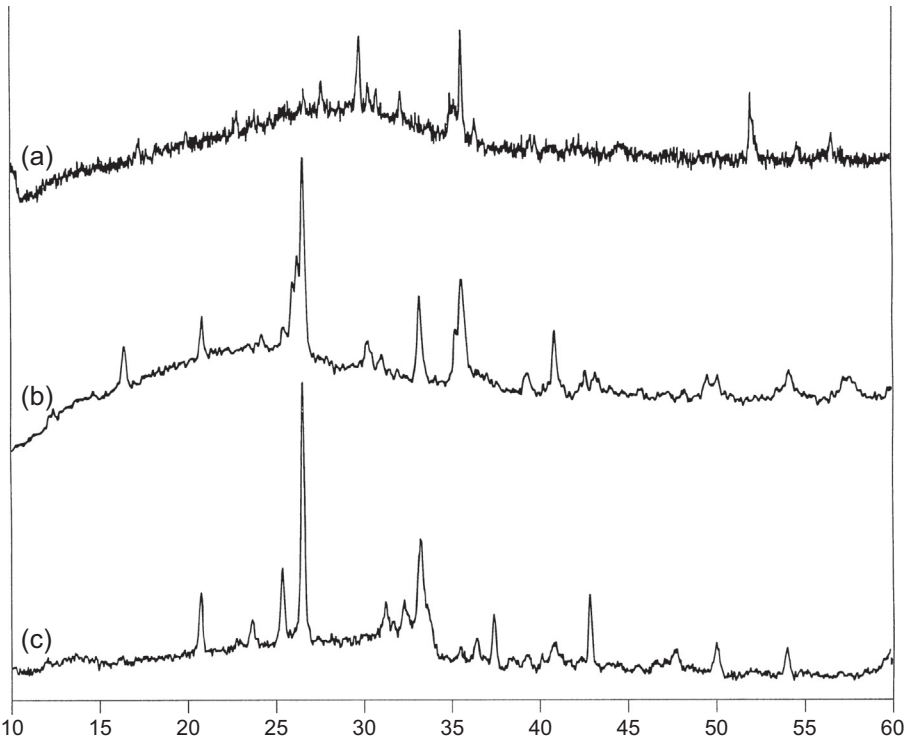


Figure 4.17 RX diffractogram of a natural pozzolan and two fly ashes. (a) Natural pozzolan, (b) Class F fly ash (Canada), and (c) Class C fly ash (USA).
Courtesy of Martin Cyr.

Table 4.1 Chemical composition of some pozzolanic materials (Bogue, 1952)

	SiO_2	Al_2O_3	Fe_2O_3	CaO	MgO	K_2O	Na_2O	SO_3	Loss on ignition
Santorin earth	63.2	13.2	4.9	4.0	2.1	2.6	3.9	0.7	4.9
Rhenan trass	55.2	16.4	4.6	2.6	1.3	5.0	4.3	0.1	10.1
Punice	72.3	13.3	1.4	0.7	0.4	5.4	1.6	tr.[c]	4.2
Calcined gaize	83.9	8.3	3.2	2.4	1.0	n.a.[b]	n.a.	0.7	0.4
Calcinated clay	58.2	18.4	9.3	3.3	3.9	3.1	0.8	1.1	1.6
Calcined shale	51.7	22.4	11.2	4.3	1.1	2.5	1.2	2.1	3.2
Blast-furnace slag[a]	33.9	13.1	1.7	45.3	2.0	n.a.	n.a.	tr.	n.a.

[a]Blast-furnace slag is no longer considered as a pozzolan.
[b]n.a., Not available.
[c]tr., Trace.

that of two fly ashes. It is seen that the hump is located almost at the same place in the three diagrams; this position corresponds to the main peaks of cristobalite, the stable form of crystallized silica at a high temperature.

Table 4.1 presents the chemical composition of various natural pozzolans.

4.8 Other supplementary cementitious materials

It is possible to find other natural or artificial materials that are rich in vitreous silica and can react with the lime liberated during Portland cement hydration. Examples are diatomaceous earths (Figure 4.18), perlite (Figure 4.19), rice husk ashes (Figure 4.20), and some hydrothermal vitreous silica. Presently, these vitreous silica are not used, because after grinding their particles present a particularly uninteresting morphology despite the fact that they are composed of vitreous silica, as seen in Figure 4.21. They are described in more details in *Binders for Durable and Sustainable Concrete* (Aïtcin, 2008).

4.9 Fillers

According to cement standards in several countries, it is possible to replace 15−35% of Portland cement clinker with a filler. A filler is normally a ground material with a grain size distribution similar to that of a Portland cement; it does not possess per se any binding properties, or in some cases may have very weak binding properties.

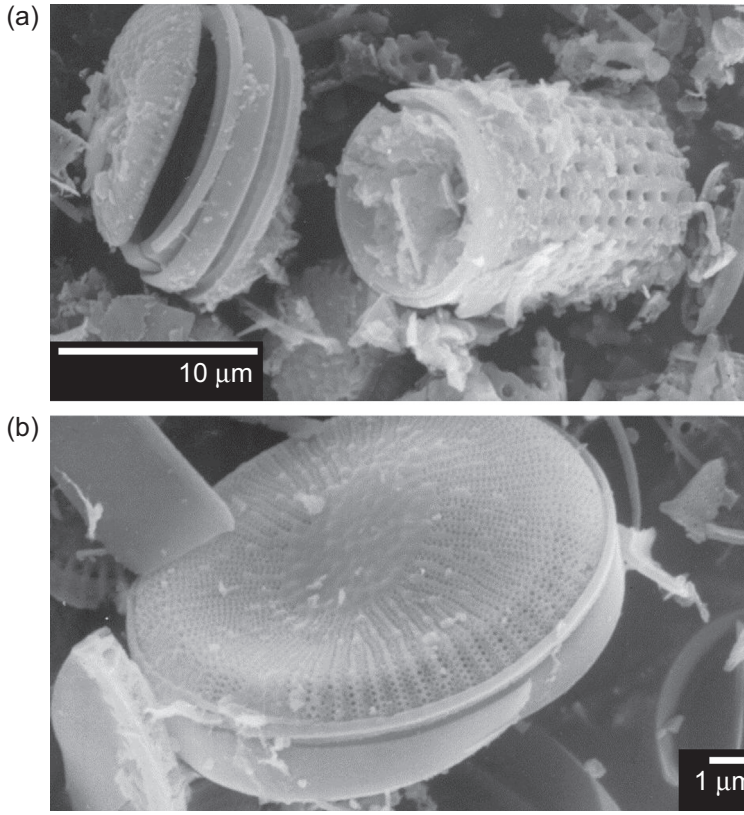


Figure 4.18 (a) Diatomaceous earth, (b) enlarged view.
Photos by I. Kelsey-Lévesque; Courtesy of Arezki Tagnit-HAMOU.

When the mineral composition of the clinker, its fineness, and its 'gypsum content' are modified, it is possible to obtain a blended cement that has almost the same 28-day compressive strength as an ordinary Portland cement and satisfactory durability when exposed to a mild climate. However, such cement must be used with a great caution in harsh, marine, and Nordic environments. It such cases, it is better to lower the w/c ratio of the concrete made with these blended cements to improve their short- and long-term strengths (Aïtcin et al., 2015).

The most common filler is limestone, obtained by pulverizing the limestone used to produce clinker. For a cement producer, it is inexpensive to produce and represents a very economical solution, because this part of the blended cement does not have to pass through the kiln. In some cases, silica fillers are used when they are available at a low cost.

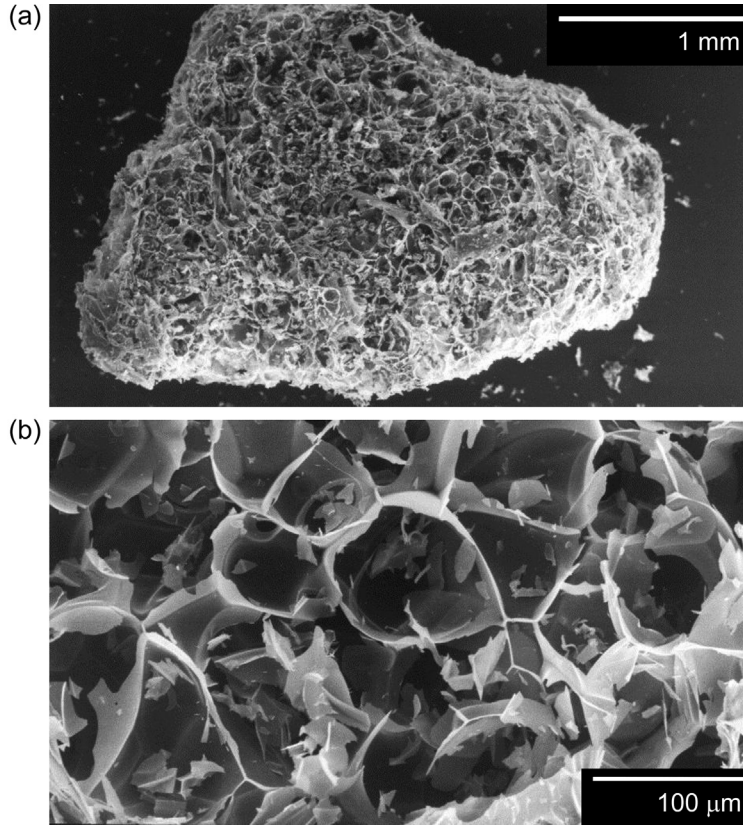


Figure 4.19 (a) Perlite, (b) enlarged view.
Photos by I. Kelsey-Lévesque; Courtesy of Arezki Tagnit-HAMOU.

4.10 Ground glass

Professor Arezki Tagnit-Hamou of the Université de Sherbrooke and his research team found that when unrecycled wine bottles are ground at different specific grain size distributions, they can be considered as a very interesting filler. For example, some of these glass powders have been used in the fabrication of an ultra-high-strength concrete (Soliman et al., 2014), as shown in Figure 4.22, to increase its strength and facilitate its pouring. Even in hardened cement paste, these glass particles can be considered as very hard and rigid inclusions that have a strengthening effect on the hydrated cement paste.

Moreover, ground glass gives a paler color to the surface of concrete, and thus reflects solar heat. The ambient temperature in a city street can be decreased by up

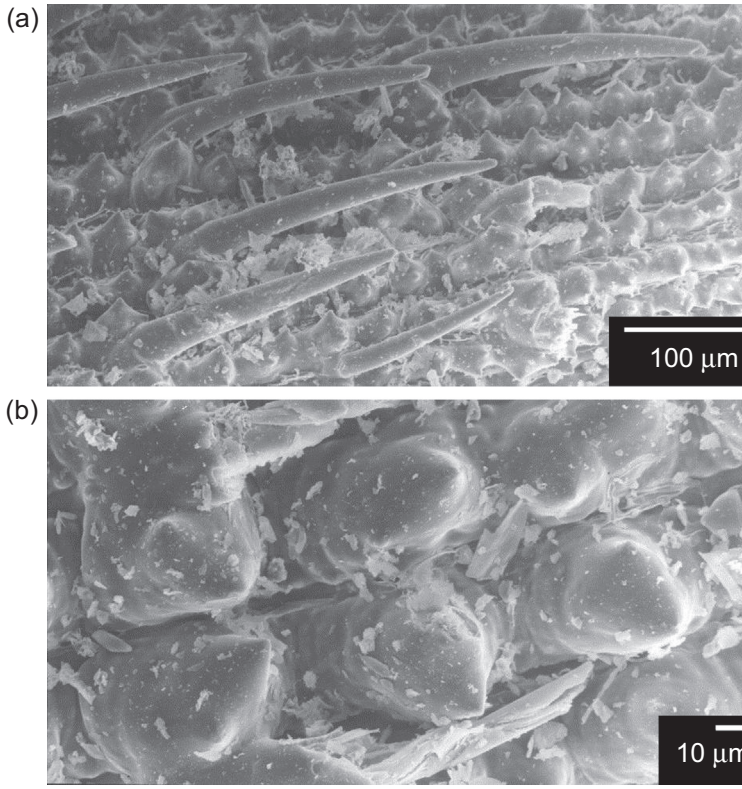


Figure 4.20 (a) Rice husk ash, (b) enlarged view.
Photos by I. Kelsey-Lévesque; Courtesy of Arezki Tagnit-HAMOU.

to 7 °C in some cases when its sidewalks are made with a concrete containing some glass powder. This is very economical for air conditioning of the buildings in the street.

4.11 Blended cements

Several supplementary cementitious materials are now blended with Portland cement clinker in order to produce more sustainable binders. The fabrication of such blended cements depends of course on the local availability of the supplementary materials. These blended cements can be identified as binary, ternary, and even quaternary binders without mentioning the nature of the different components of the blends. Binary cements may be slag cement, fly-ash cement, or silica fume cement. Ternary cements may contain slag and silica fume, or fly ash and silica fume. Finally, the use of quaternary cement containing slag, fly ash, and silica fume has been found to be very interesting due to the synergetic effect obtained when mixing slag and fly ash in low w/c concretes (Nkinamubanzi and Aïtcin, 1999).

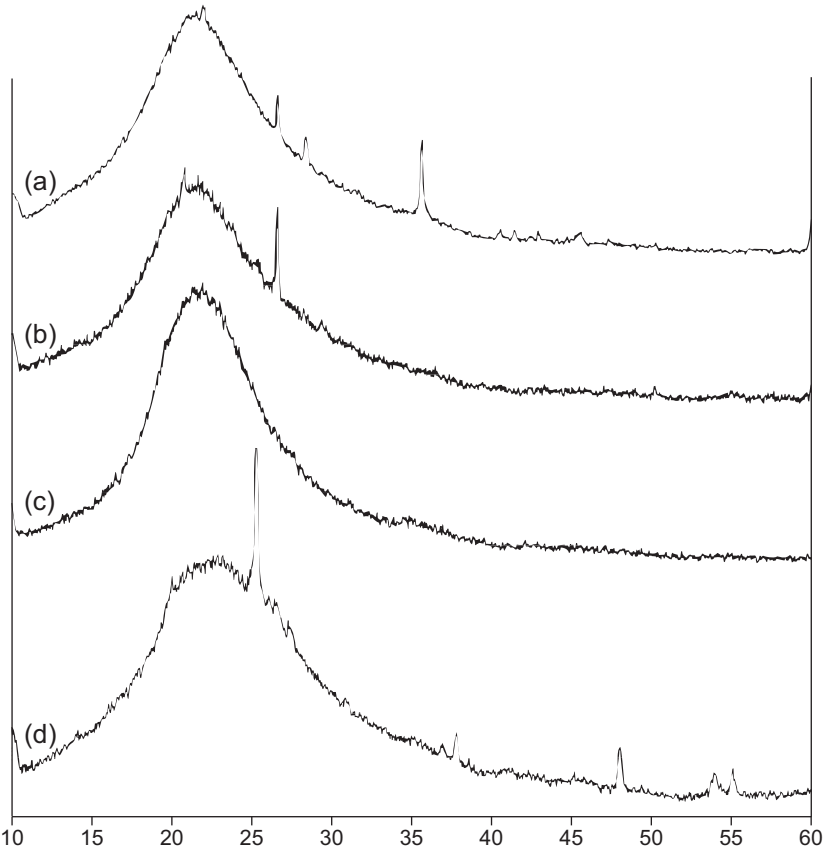


Figure 4.21 Typical diffractograms of various forms of amorphous silica used as supplementary cementitious materials: (a) silica fume, (b) rice husk ash, (c) diatomaceous earth, and (d) metakaolin.
Courtesy of I. Kelsey-Lévesque

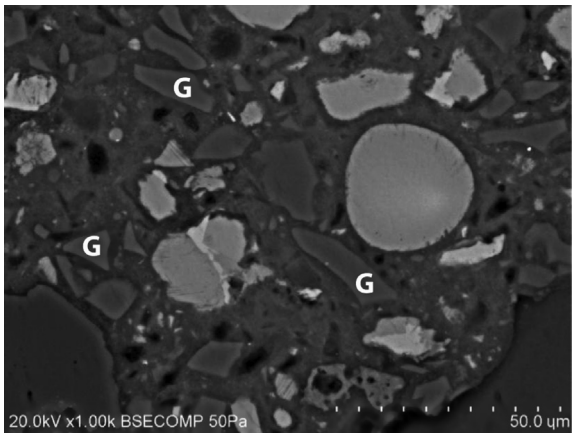


Figure 4.22 Cement paste of an ultra-high-strength concrete containing glass particles (G).
Courtesy of Professor Arezki Tagnit-HAMOU and Nancy Soliman.

Usually, in the short term (1−3 days), these blended cements do not have very high early strength except when their w/c ratio is lowered, as explained in Chapter 1 (Aïtcin, 2016) and by Aïtcin et al. (2015).

4.12 Conclusion

Today, several so-called cementitious materials or fillers are used to produce blended cements that are more environmentally sustainable than pure Portland cements. In fact, each time 1 kg of clinker is substituted by 1 kg of such material, 1 kg of CO_2 is not released in the atmosphere.

As these materials are less reactive than Portland cement when used in concrete with a high w/c ratio, the short-term compressive strength of the concrete is decreased. However, when the w/c ratio of the concrete is decreased, it can have greater short-term strength and better durability in the long term in mild environments. Thus, the development of blended cements should not be a pretext to modify the mineral composition, fineness, and gypsum content of cement to restore a short-term strength equivalent to that of pure Portland cement. As seen in Chapter 2, C_3A is a poison to concrete from a rheological and durability point of view (Aïtcin and Mindess, 2011, 2015).

Supplementary cementitious and filler particles do not react in the same way as cement particles when they are in contact with some admixtures. It could be simplistic to think that the admixture dosage can be decreased when a supplementary cementitious material is blended with clinker, because these particles are less reactive than those in a pure Portland cement. Every blended cement is unique, and its reactivity with admixture has to be tested in each particular case.

References

Aïtcin, P.-C., 2008. Binders for Durable and Sustainable Concrete. Taylor & Francis, London, UK.

Aïtcin, P.-C., 2016. The importance of the water−cement and water−binder ratios. In: Aïtcin, P.-C., Flatt, R.J. (Eds.), Science and Technology of Concrete Admixtures, Elsevier (Chapter 1) pp. 3−14.

Aïtcin, P.-C., Mindess, S., 2011. Sustainability of Concrete. Spon Press, London.

Aïtcin, P.-C., Mindess, S., 2015. Back to the Future. Concrete International 37 (5).

Aïtcin, P.-C., Mindess, S., Wilson, 2015. Increasing the compressive strength of blended cement. Concrete International 37 (x), xx.

Bédard, C., 2005. Superplasticizers−cement Interactions with Supplementary Cementitious Materials. Influence on the Rheology (Ph.D. thesis 1570). Université de Sherbrooke, Canada (in French).

Bogue, R.H., 1952. La chimie du ciment Portland. Eyrolles, Paris.

Malhotra, V.M., Mehta, P.K., 1996. Pozzolanic and Cementitious Materials. OPA, The Netherlands, Amsterdam.

Malhotra, V.M., Mehta, P.K., 2012. High-performance, High-volume Fly Ash Concrete for Building Durable and Sustainable Structures, fourth ed. Supplementary Cementing Materials for Sustainable Development Inc, Ottawa, Canada.

Massazza, F., 1998. Pozzolans and Pozzolanic Cements, Lea's Chemistry of Cement and Concrete. Arnold, London, UK, pp. 470−632.

Nkinamubanzi, P.-C., Aïtcin, P.-C., 1999. The Use of Slag in Cement and Concrete in a Sustainable Development Perspective, WABE International Symposium on Cement and Concrete. Montreal, Canada, pp. 85−110.

Soliman, N., Tagnit-Hamou, A., Aïtcin, P.-C., 2014. A New Generation of Ultra-high Performance Glass Concrete, Third All-Russian Conference on Concrete and Reinforced Concrete. Moscow, May 12−16, pp. 218−227.

Water and its role on concrete performance

5

P.-C. Aïtcin
Université de Sherbrooke, QC, Canada

5.1 Introduction

It was seen in Chapter 1 that the quantity of water used when making a concrete is as important as the quantity of cement, because water plays a very important physical and chemical role that conditions the properties of the fresh and hardened concrete (Aïtcin, 2016a). In fact, it is the ratio of the mass of the effective water and the mass of cement or binder used when making a concrete that determines, increasingly with the help of admixtures, the essential properties of the fresh and hardened concrete. As pointed out in Chapter 1, the great interest in the notion of w/c or w/b ratio is that it gives equal importance to the quantities of water and cement or binder used when making a concrete.

For too many people, water is only added in concrete to hydrate Portland cement and create bonds. The physical role of water during the batching and hardening of concrete is too often not well understood or ignored.

5.2 The crucial role of water in concrete

It is very important to calculate exactly the quantity of effective water that is present in a concrete batch. It is easy to know the amount of water introduced in the mixer through the water metre, but it is not as easy to calculate precisely all the different forms of 'hidden water' contained in the different materials introduced into the mixer.

For example, when wet sand is used to make a concrete, it is important to calculate the amount of extra water it brings into the mix. This quantity of water corresponds to the amount of water in excess of its saturated surface state (SSD). For example, when 800 kg of SSD sand are used to make a concrete, a variation of 2% of the total water content of the sand represents 16 L of water, which for an ordinary concrete represent about 10% of the amount of effective water needed to obtain the desired slump, strength and durability. This 10% variation in the quantity of water represents roughly a variation of 10% in the value of the w/c ratio, which significantly alters the strength and durability of the hardened concrete.

In this chapter, we are not interested in the chemical quality of the water that is used to make durable concrete; this information is available in reference books (e.g. Kosmatka et al., 2002). However, two very particular cases − the use of seawater

Science and Technology of Concrete Admixtures. http://dx.doi.org/10.1016/B978-0-08-100693-1.00005-9
Copyright © 2016 Elsevier Ltd. All rights reserved.

and of wastewater collected in ready-mix plants – are treated very briefly. Rather, attention is focused on the role of water in determining the properties of the fresh and hardened concrete, and the crucial role that water plays in the dimensional variation of the apparent volume of concrete.

In concrete's fresh state, the quantity of water introduced during mixing controls to a large extent:

- concrete rheology, with or without the help of admixtures
- the relative position of the cement particles when they start to hydrate
- the solubility of the different ionic species present in the binder
- the electrical and thermal conductivity of the concrete
- bleeding and segregation.

During the development of the hardening process, the quantity of water plays a key role in:

- the development of the hydration reaction of the four principal phases of Portland cement
- the physical, thermodynamic and volumetric consequences of hydration reaction on the properties of the concrete
- the development of autogenous shrinkage
- the evolution of the electrical and thermal conductibility of concrete.

In hardened concrete, water continues to participate to the hydration process of the four phases of Portland cement and of the various cementitious materials that are now commonly blended with cement.

Hydration reaction may stop for different reasons when:

- there are no more anhydrous cement particles to be hydrated – usually the case in concrete having a high w/c ratio greater than 0.42
- there is no more water available to hydrate the remaining anhydrous cement particles – this is the case in very low w/c concrete;
- there is no more space for accepting the hydrated product – this is the case for low w/c concrete
- the cement paste already developed is so dense that water cannot migrate easily to reach unhydrated cement particles that are still remaining in the paste – this is the case in some low w/c concretes.

In a hardened concrete, capillary water is the medium used by aggressive ions to penetrate concrete by percolation and osmotic pressure (differences in ionic concentrations). Some ions present in the interstitial solution of concrete can also be leached out by osmotic pressure.

As will be seen in the following, water also plays a key role in the development of different forms of shrinkage through the tensile forces that appear in the menisci developed in the porous system of the hydrated cement paste (hydrostatic pressure through capillary forces) and surface forces in the water films covering the walls of the emptying pores.

From a practical point of view, the major problem related to the use of water when making a concrete is that its beneficial action is inversely proportional to its ease of use.

For example, it is very easy to add more water in a mixer during batching or in the drum mixer of a truck when it arrives in the field, but in these cases it is essential to use

water with parsimony to avoid the alteration of the properties of the hardened concrete in terms of durability and sustainability. In contrast, when water can be used practically without limitation in the field to cure concrete, its use does not facilitate the task of contractors, who often perceive water curing as a nuisance unless they are specifically paid for doing it.

Finally, the lower the w/c ratio, the more difficult it is for curing water to penetrate within concrete to favour hydration of the cement present within the cover of the concrete. The skin of concrete is a very important part of the concrete, because it is the physical barrier that protects the reinforcing steel from rusting.

5.3 Influence of water on concrete rheology

The water introduced in a mixer participates, with the help of specific admixtures, in determining the rheological properties of concrete, as will be seen in Chapters 7 and 16 (Yahia et al., 2016; Nkinamubanzi et al., 2016). First water starts to wet the cement particles, creating cohesive forces between them and giving the mix what is usually called its workability – a kind of cohesiveness. These cohesive forces do not develop when the same amount of water is introduced in the same volume of limestone or silica filler with the same grain size distribution as the cement; the reasons for this are explained in Chapter 11 on working mechanisms of rheology modifiers (Gelardi and Flatt, 2016).

The cohesive forces created by the 'initial wetting' of the cement particles reduce considerably the risk of bleeding and segregation in a well-proportioned mixture. These cohesive forces are the result of the development of the first hydrates on the surface of the cement particles, the electrical forces created between cement particles, the very polar aqueous medium, and, very importantly, the difference in dielectric properties between cement and water (see Chapter 11, Gelardi and Flatt, 2016).

Filler and supplementary cementitious particles are not 'wet' by water like cement particles are, so when they are present in a substantial quantity in blended cement, the risk of bleeding and segregation is increased, unless if a viscosity modifier is added to the mix.

Usually the first cohesive bonds developed in a concrete at the beginning of hydration do not increase very rapidly, and concrete can be transported for about 90 min before its placing. However, if during transportation of the concrete to the field, these first bonds grow too fast and cause an unacceptable loss of workability, an adequate slump has to be restored to facilitate placing. In such a case, it is out of the question to restore workability by adding water (retempering), because any addition of water has a catastrophic effect on the concrete's compressive strength, durability and sustainability due to the resulting increase in the w/c ratio. The only way to restore concrete workability is to add an extra dosage of water reducer or superplasticizer.

When the weather is too hot and/or concrete temperature is too high, a retarder can be added during concrete mixing to slow down the hydration process of the C_3A and C_3S and decrease the slump loss.

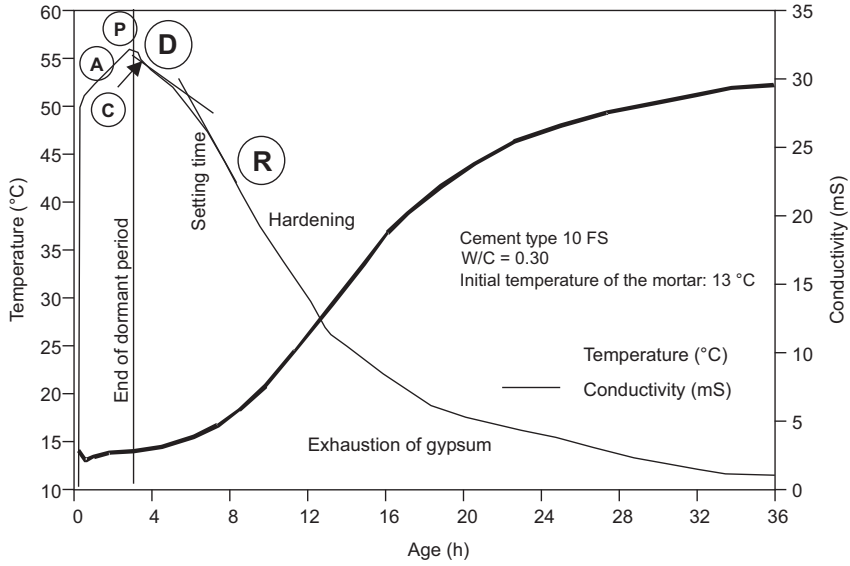


Figure 5.1 Electrical conductivity and heat release of a blended cement containing 8% silica fume (Aïtcin, 2008).

5.4 Water and cement hydration

Hydration reaction is described in general terms in Chapters 2 and 8 (Aïtcin, 2016b; Marchon and Flatt, 2016a) and in Chapter 12 in terms of the action of admixtures thereon (Marchon and Flatt, 2016b). In this section, some particular aspects of it are reviewed because of their technological importance.

First, the hydration reaction starts by the release of ions present at the surface of cement particles and the passage into solution of the different forms of sulphates that are present in the cement. The temperature of the cement paste increases slightly during this dissolution process, and the electrical conductivity of the paste increases rapidly. In a concrete, it is difficult to observe the increase in temperature because the aggregates act as a thermal sink, but it is easy to notice the increase in electrical conductivity of the concrete, as can be seen in Figure 5.1.

5.5 Water and shrinkage

5.5.1 General considerations

In Chapter 2, it was seen that concrete is not a stable material from a volumetric point of view: its apparent volume can change according to its curing conditions (Aïticn, 2016b). Usually, but not always, the apparent volume decreases: concrete shrinks.

Shrinkage is directly related to the displacement of water in the capillary network when concrete is only partially saturated. From a practical point of view, four types of shrinkage are observed.

- Plastic shrinkage appears on the surface of fresh concrete submitted to dry and windy conditions. Superficial water evaporates from the surface of the fresh concrete, provoking the appearance of cracks that are more or less large and deep according to the severity of the drying process and the presence or absence of bleeding water.
- Chemical shrinkage is developed in any concrete, whatever its w/c ratio is. This shrinkage is due to the chemical contraction of the absolute volume of the cement paste.
- Drying shrinkage occurs when water evaporates from hardened concrete submitted to a dry environment.
- Autogenous shrinkage is a special shrinkage that occurs in low w/c concrete and comes from the hydration of cement itself. The binding of water into solid hydrates leads to self-induced drying, which then initiates a process similar to drying shrinkage.

Essentially, all these forms of shrinkage derive from a loss of water from the fresh or hardened concrete. In the case of chemical shrinkage, the binding of water into hydrates leads to a volume loss in the course of the chemical reaction.

Drying of concrete, whether induced by environmental conditions or self-induced, leads to the build-up of capillary forces in the emptying pores of the hydrated cementitious matrix of the concrete and is also responsible for the volume reduction of hydrates themselves, as shown by Baquerizo et al. (2014). The first creates tensile stress pulling at the pore walls, causing contraction of the cementitious matrix, and the second leads to shrinkage of the solid skeleton itself (as in clay).

Because of the importance of capillary forces for volume stability of cementitious material, the concept of capillary forces is briefly explained. Water contained in the porous cementitious matrix of concrete will achieve long-term equilibrium with its surrounding environment. This means concrete stops losing water when the internal humidity of the partial saturated pore system equals that of the surroundings. To what extent the pore system empties depends on the total porosity and size distribution of pores and the humidity to which concrete is exposed.

Kelvin's Law states that water pressure in fully saturated concrete is assumed to be equal to atmospheric pressure, and depression in the residual water or pore solution of the partially saturated pore system depends only on relative humidity:

$$\Delta P = \frac{RT}{v_W} \ln(\mathrm{RH})$$

where

ΔP is the pressure gradient between the liquid and gas phases
R is the gas constant
T is the absolute temperature
RH is the relative humidity.

Laplace's Law teaches us that the smaller the menisci or the smaller the largest water-filled capillary, the greater the tensile forces:

$$\Delta P = \frac{2 \cdot \gamma \cdot \cos \theta}{r}$$

where

ΔP is the pressure gradient between the liquid and gas phases
γ is the surface tension of the liquid
θ is the contact angle between the liquid and the solid
r is the radius of a cylindrical capillary pore.

This explains the successive emptying of pores, starting with larger ones, forming menisci with tensile forces at the entrance of the largest remaining water-filled pores and leaving water films covering the pore walls of the emptied pores.

From these equations, one can see that depression in the pore water or capillary pressure increases with decreasing humidity, and the size of the largest water-filled pore decreases with humidity scaling:

$$\ln(\mathrm{RH}) \sim \frac{1}{r}$$

There is consensus in the scientific community that capillary pressure is the driving force for drying-induced shrinkage. However, exactly how these forces act on the cementitious material is still the subject of debate.

There are basically two current opinions on the mechanism of drying shrinkage. In the first, capillary forces are considered to act as hydrostatic pressure, causing the porous matrix to contract via tensile stress acting on the pore walls (Scherer, 1990; Granger et al., 1997a, 1997b; Coussy et al., 1998, 2004), and the second claims that disjoining pressure or surface forces in between the hydrates' surfaces would not only explain shrinkage of concrete, but also swelling upon resaturation (Badmann et al., 1981; Ferraris and Wittmann, 1987; Scherer, 1990; Beltzung and Wittmann, 2005; Setzer and Duckheim, 2006; Eberhardt, 2011). A more detailed discussion on shrinkage is given in Chapter 13, describing the working mechanism of shrinkage-reducing admixtures (Eberhardt and Flatt, 2016), and an overview of their chemical structures is given in Chapter 9 (Gelardi et al., 2016).

5.5.2 How to eliminate the risk of plastic shrinkage

As it is the evaporation of the water present at the top surface of concrete that is responsible for plastic shrinkage, the best way to eliminate it, whatever the w/c ratio of the concrete, is to saturate the air above the concrete surface with water vapour. This can be done easily using sprayers similar to those used in flower nurseries (Figure 5.2).

Another way is to spray an evaporation retarder or a curing membrane on the surface of the concrete as soon as its finishing has been completed.



Figure 5.2 Fogging to prevent plastic shrinkage.
Courtesy of Richard Morin.



Figure 5.3 Application of saturated geotextiles 24 h after casting.
Courtesy of Richard Morin.

When a concrete has a w/c ratio lower than 0.42, a curing membrane should never be applied on top of the concrete, because this concrete receives external water curing as soon as its surface is hard enough as shown in Figure 5.3. The application of a curing membrane will prevent this external curing of the top surface of the concrete that is essential to fight autogenous shrinkage. In this case, it is mandatory to use an evaporation retarder that will be washed away when direct external curing with a hose is applied.

5.5.3 How to mitigate autogenous shrinkage

Autogenous shrinkage is a consequence of volumetric contraction (Le Chatelier, 1904; Lynam, 1934; Davis, 1940) and is also due to the internal consumption of water occurring during cement hydration. In the absence of an external source of water (external to the paste) that could saturate the porous system of the hydrating cement paste, the very fine porosity created by this chemical contraction drains an equivalent volume of water from the coarse capillaries of the hydrating cement paste, so that menisci appear in

these large capillaries. As explained above, the emptying of the larger capillaries causes the internal humidity to drop (Lura et al., 2003; Jiang et al., 2005; Wyrzykowski et al., 2011), and this self-induced drying causes tensile stress and shrinkage, i.e. self-induced drying shrinkage.

As the hydration reaction goes on, more water is drained from increasingly finer capillaries, so the tensile stresses developed by the menisci are increasingly higher and can result in a significant contraction of the apparent volume. However, if during hydration an external source of water (external to the paste) fills the porosity created by the chemical contraction, the capillaries of the hydrated cement paste remain saturated and no tensile stresses are developed in the hydrating paste (Aïtcin, 1999). From a practical point of view, an external source of water (external to the concrete) or an internal one (internal to the concrete but external to the paste) has to be supplied to concrete.

5.5.4 How to provide an internal source of water

Various techniques have been proposed to provide an internal source of water. The basic idea consists of introducing during mixing a material that can temporarily stock a certain amount of water without affecting the water balance of the cement paste and then release it when necessary.

The use of saturated lightweight aggregates, either coarse or fine (Klieger, 1957; Bentz and Snyder, 1999; Weber and Reinhardt, 1997; Mather, 2001), or superabsorbent polymers (SAPs) has been proposed (Jensen and Hansen, 2001; Kowler and Jensen, 2005). A state-of-the-art report on the use of SAPs in cementitious material was published by Mechtcherine and Reinhardt (2012). Of course, it is essential that this internal water can be drained easily from these materials by the hydrating cement paste.

This technique represents a significant step forward in improving the durability and sustainability of concrete structures, particularly in the case of elements working essentially in flexure, because it eliminates the risk of cracking associated with the uncontrolled development of autogenous shrinkage when using low w/c concretes.

Coarse-saturated lightweight aggregates have been used successfully as an internal source of water, but as they absorb a lesser volume of water than an equivalent volume of fine lightweight aggregate, it is necessary to use a larger volume of them to stock an equivalent volume of water. Moreover, the substitution of a certain volume of normal coarse aggregate by an equivalent volume of a coarse lightweight aggregate may somewhat decrease the concrete's compressive strength and definitively elastic modulus.

The substitution of a certain volume of normal sand by the same volume of saturated lightweight sand is interesting due to the high porosity of the lightweight sand – this is usually greater than 10%, so 100 kg of lightweight sand can store 10 L of water, but it is important to check that the lightweight sand is composed of large pores that will easily release the water they contain.

Jensen and Hansen (2001) also suggested the use of SAPs as an internal source of water. These polymers are already used in diapers for babies. When they are introduced in a dry state in the mixer, they absorb a mass of water equal to 50–200 times their dry weight. In the case of concrete, where the mixing water becomes rapidly

saturated with many ionic species, the absorptive capacity of the SAP is limited to 50% rather than reaching 200%.

For both types of internal curing reservoirs, it is important to note that individual particles have to be homogeneously distributed so that water can migrate through the hydrating cementitious matrix and reach the drying zone in time (Henkensiefken et al., 2009). Basically, water supply can be seen as the same as entrained air void distribution. Also, water has to be distributed so that water migration into the reservoirs proceeds sufficiently fast.

Considering this, lightweight aggregates and SAPs have to be provided not only in sufficient quantities, but also with a sufficient fineness or particle size distribution.

5.5.5 How to eliminate drying shrinkage

Basically, drying-induced shrinkage could be eliminated simply by the elimination of drying.

If the development of drying shrinkage has to be eliminated, there is only one way to do so: it is necessary to seal all the superficial pores of concrete, so the capillary water can no longer leave the hardened concrete. A sealant or any impermeable film or layer can be applied on the surface of the concrete.

However, even with high-quality surface application, the sustainability of such an approach depends heavily on the durability of the sealant or protective layer.

5.6 Water and alkali/aggregate reaction

There is at least one point of agreement between all researchers studying alkali/aggregate reaction: in order to appear, this reaction needs water. Thus to stop the development of this reaction, theoretically it is only necessary to seal the concrete surface — but it is easier to write it than to do it efficiently in the field. The application of silane on the surface of concrete has been reported to stop the development of alkali/silica reaction (ASR). However, it is important to distinguish between cases of new construction, repair and attempts simply to mitigate ASR by applying such products. A priori, the effectiveness of surface treatments should decrease from the first to the third of these cases. In particular, in cases 2 and 3, structures already subjected to ASR probably already have enough water (deep) within. The author is therefore generally sceptical about the possibility of halting ASR durably in such structures, particularly massive ones, by surface treatments, but is also ready to change his mind in the light of clear evidence countering these expectations.

5.7 Use of some special waters

5.7.1 Seawater

Is it possible to use seawater to batch concrete? The answer to this frequently raised question is definitively ‘yes’ when there is no other choice. Seawater can be used to

make unreinforced concrete, but concrete compressive strength will decrease by about 20% in comparison to the same concrete made with pure water (Mindess et al., 2003).

5.7.2 Wastewaters from ready-mix operations

In many countries, concrete producers can no longer discharge their wastewater directly into the sewers; they have to recycle it or treat it, so it can be eliminated safely in the sewerage system.

The elimination of the solid particles present in these wastewaters is easy: it is only necessary to use centrifugation or a filter-press, or a special flocculent that will facilitate the rapid sedimentation of these particles. However, most of the time the water collected after this physical or chemical treatment contains many ionic species or organic matter coming from the admixtures used in previous batches. The use of this treated water as batching water can be problematic when making a high-tech concrete, because all these 'leftovers' of the previous batches can alter the action of the new admixtures that are used to produce the next concrete. Thus, in this case, only a limited volume of treated water can be substituted for pure water. In the case of low-grade concrete, treated wastewater can be used in greater quantity.

5.8 Conclusion

It is very important to control the volume of all the water that is used when batching concrete. A precise knowledge of this quantity of water is as important as the knowledge of the quantity of cement or binder that is used. In fac,t it is the w/c, the ratio of the mass of water to the mass of cement, that is the key factor controlling most of the properties of the fresh and hardened concrete, as well as its durability and sustainability.

For a long time, changing the water dosage was the only way to modify concrete rheology, but nowadays admixtures can be used for that purpose. Thus, the rheology of a modern concrete depends on a fine-tuned balance of water and these admixtures.

It is important to use water with parsimony during mixing, but in contrast it can be used abundantly in the field to water cure concrete. To be sure that concrete is properly cured in the field, it is only necessary to pay contractors separately to water cure, and specify what to do, how to do it, and when to stop. When these directives are given precisely, contractors become zealous because they can make a profit out of water curing.

Internal curing of low w/c concrete will be increasingly used for two reasons: it provides some water to enable the hydration of supplementary cementitious material and it mitigates the development of autogenous shrinkage in low w/c concrete. For example, it is common practice in Texas to use internal curing for highway pavements containing fly ash. It can be expected that the overall slower hydration of concrete made with blended cement necessitates the presence of an internal source of water to allow them to reach their full potential. This explains the specific benefit of internal curing in such concrete.

Finally, the concrete industry will have to learn how to make the best use of the wastewaters collected in ready-mix plants due to the increasingly severe restrictions concerning their elimination in municipal sewer systems.

References

Aïtcin, P.-C., 1999. Does concrete shrink or does it swell? Concrete International 21 (12), 77–80.

Aïtcin, P.-C., 2008. Binders for Durable and Sustainable Concrete. Taylor & Francis, London, UK.

Aïtcin, P.-C., 2016a. The importance of the water–cement and water–binder ratios. In: Aïtcin, P.-C., Flatt, R.J. (Eds.), Science and Technology of Concrete Admixtures. Elsevier (Chapter 1), pp. 3–14.

Aïtcin, P.-C., 2016b. Phenomenology of cement hydration. In: Aïtcin, P.-C., Flatt, R.J. (Eds.), Science and Technology of Concrete Admixtures. Elsevier (Chapter 2), pp. 15–26.

Badmann, R., Stockhausen, N., et al., 1981. The statistical thickness and the chemical potential of adsorbed water films. Journal of Colloid and Interface Science 82 (2), 534–542.

Baquerizo, L.G., Matschei, T., et al., 2014. Methods to determine hydration states of minerals and cement hydrates. Cement and Concrete Research 65, 85–95.

Beltzung, F., Wittmann, F.H., 2005. Role of disjoining pressure in cement based materials. Cement and Concrete Research 35 (12), 2364–2370.

Bentz, D.P., Snyder, K.A., 1999. Protected paste volume in concrete: extension to internal curing using saturated lightweight fine aggregates. Cement and Concrete Research 29, 1863–1867.

Coussy, O., Eymard, R., et al., 1998. Constitutive modeling of unsaturated drying deformable materials. Journal of Engineering Mechanics 124 (6), 658–667.

Coussy, O., Dangla, P., et al., 2004. The equivalent pore pressure and the swelling and shrinkage of cement-based materials. Materials and Structures 37 (1), 15–20.

Davis, R.E., 1940. A summary of the results of investigations having to do with volumetric changes in cements, mortars and concretes due to causes other than stress. Journal of the American Concrete Institute 1 (4), 407–443.

Eberhardt, A.B., 2011. On the Mechanisms of Shrinkage Reducing Admixtures in Self Consolidating Mortars and Concretes. Aachen, Shaker, ISBN 978-3-8440-0027-6.

Eberhardt, A.B., Flatt, R.J., 2016. Working mechanisms of shrinkage reducing admixtures. In: Aïtcin, P.-C., Flatt, R.J. (Eds.), Science and Technology of Concrete Admixtures. Elsevier (Chapter 13), pp. 305–320.

Ferraris, C.F., Wittmann, F.H., 1987. Shrinkage mechanisms of hardened cement paste. Cement and Concrete Research 17 (3), 453–464.

Gelardi, G., Flatt, R.J., 2016. Working mechanisms of water reducers and superplasticizers. In: Aïtcin, P.-C., Flatt, R.J. (Eds.), Science and Technology of Concrete Admixtures. Elsevier (Chapter 11), pp. 257–278.

Gelardi, G., Mantellato, S., Marchon, D., Palacios, M., Eberhardt, A.B., Flatt, R.J., 2016. Chemistry of chemical admixtures. In: Aïtcin, P.-C., Flatt, R.J. (Eds.), Science and Technology of Concrete Admixtures. Elsevier (Chapter 9), pp. 149–218.

Granger, L., Torrenti, J.M., Acker, P., 1997a. Thoughts about drying shrinkage: scale effects and modelling. Materials and Structures 30 (2), 96–105.

Granger, L., Torrenti, J.M., Acker, P., 1997b. Thoughts about drying shrinkage: experimental results and quantification of structural drying creep. Materials and Structures 30 (10), 588–598.

Henkensiefken, R., Bentz, D., et al., 2009. Volume change and cracking in internally cured mixtures made with saturated lightweight aggregate under sealed and unsealed conditions. Cement and Concrete Composites 31 (7), 427–437.

Jensen, O.M., Hansen, P.F., 2001. Water-entrained cement-based materials: I. Principles and theoretical background. Cement and Concrete Research 31 (4), 647–654.

Jiang, Z., Sun, Z., et al., 2005. Autogenous relative humidity change and autogenous shrinkage of high-performance cement pastes. Cement and Concrete Research 35 (8), 1539–1545.

Klieger, P., 1957. Early high-strength concrete for prestressing. In: Proceedings of the World Conference on Prestressed Concrete, San Francisco. A5(1) pp.

Kosmatka, S.H., Kerkoff, B., Panarese, W.C., McLeod, N.F., McGrath, R.J., 2002. Design and Control of Concrete Mixtures, EB 101, seventh ed. Cement Association of Canada, Ottawa, Canada, ISBN 0-89312-218-1. 368 pp.

Kovler, K., Jensen, O.M., 2005. Novel technique for concrete curing. ACI Concrete International 27 (9), 39–42.

Le Chatelier, H., 1904. Recherches Expérimentales Sur la Constitution des Mortiers Hydrauliques. Dunod, Paris.

Lura, P., Jensen, O.M., et al., 2003. Autogenous shrinkage in high-performance cement paste: an evaluation of basic mechanisms. Cement and Concrete Research 33 (2), 223–232.

Lynam, C.G., 1934. Growth and Movement in Portland Cement Concrete. Oxford University Press, London, pp. 25–45.

Marchon, D., Flatt, R.J., 2016a. Mechanisms of cement hydration. In: Aïtcin, P.-C., Flatt, R.J. (Eds.), Science and Technology of Concrete Admixtures. Elsevier (Chapter 8), pp. 129–146.

Marchon, D., Flatt, R.J., 2016b. Impact of chemical admixtures on cement hydration. In: Aïtcin, P.-C., Flatt, R.J. (Eds.), Science and Technology of Concrete Admixtures. Elsevier (Chapter 12), pp. 279–304.

Mather, B., January 2001. Self-curing Concrete, Why not? Concrete International 23 (1), 46–47.

Mechtcherine, V., Reinhardt, H.-W. (Eds.), 2012. Application of superabsorbent polymers (SAP) in concrete construction: state of the art report prepared by technical committee 225-SA, RILEM state-of-the-art reports, vol. 2. Springer, Dordrecht.

Mindess, S., Young, J.F., Darwin, D., 2003. Concrete, second ed. Prentice-Hall, Upper Saddle River, NJ. 644 pp.

Nkinamubanzi, P.-C., Mantellato, S., Flatt, R.J., 2016. Superplasticizers in practice. In: Aïtcin, P.-C., Flatt, R.J. (Eds.), Science and Technology of Concrete Admixtures. Elsevier (Chapter 16), pp. 353–378.

Setzer, M.J., Duckheim, C., 2006. The Solid–liquid Gel-system of Hardened Cement Paste, 2nd International RILEM Symposium on Advances in Concrete through Science and Engineering. RILEM Publications SARL, Quebec City, Canada.

Scherer, G.W., 1990. Theory of drying. Journal of the American Ceramic Society 73 (1), 3–14.

Weber, S., Reinhart, H.W., 1997. A new generation of high performance concrete: concrete with autogenous curing. Advanced Cement Based Materials (6), 59–68.

Wyrzykowski, M., Lura, P., et al., 2011. Modeling of internal curing in maturing mortar. Cement and Concrete Research 41 (12), 1349–1356.

Yahia, A., Mantellato, S., Flatt, R.J., 2016. Concrete rheology: A basis for understanding chemical admixtures. In: Aïtcin, P.-C., Flatt, R.J. (Eds.), Science and Technology of Concrete Admixtures. Elsevier (Chapter 7), pp. 97–128.

Entrained air in concrete: rheology and freezing resistance

6

P.-C. Aïtcin
Université de Sherbrooke, QC, Canada

6.1 Introduction

The discovery of the benefits obtained when a small percent of tiny air bubbles (diameters of 10−100 μm) form in both fresh and hardened concrete was accidental. It is well known that these air bubbles greatly improve the properties of hardened concrete, particularly its durability in severe winter conditions during freezing and thawing cycles. These small bubbles also drastically improve the rheology of the fresh concrete. For this reason, the Japanese systematically add 3−5% of entrained air in their concrete even though the resistance of concrete to freezing and thawing cycles is not a major problem in Japan, except in the northern part of Hokkaido Island.

6.2 Entrapped air and entrained air

When a non-air-entrained concrete is placed, large air bubbles always remain trapped in the hardened concrete after its vibration. These large bubbles have an irregular shape and are irregularly distributed within hardened concrete, which is referred to as "entrapped air." Usually, a concrete that has been vibrated carefully may contain 1 to 2% of entrapped air (10−20 L per m^3). The volume of entrapped air depends on the viscosity of the hydrated cement paste, the size of the coarse aggregate, the slump of the concrete, the intensity of vibration, and its duration. Each of these entrapped bubbles creates a point of weakness that decreases the mechanical properties of hardened concrete.

To obtain a network of very fine, well-dispersed air bubbles in the mortar of a concrete, it is necessary to use an air-entraining agent. An overview of the chemistry of these admixtures is given in Chapter 9 (Gelardi et al., 2016). It should be noted that the expression "air-entraining agent" may be confusing because this type of admixture does not entrain small spherical air bubbles by itself; rather, it stabilizes the air bubbles that are entrained in concrete during its mixing. This type of admixture should be rather called a "stabilizer of air." The working mechanisms of air-entraining agents are discussed in Chapters 10 and 17 (Marchon et al., 2016; Gagné, 2016).

As seen in Figure 6.1 in fresh concrete, this admixture is concentrated at the surface of the air bubbles, where it creates a thin film sufficiently strong to stabilize the bubbles in the form of a sphere. These bubbles are strong enough to resist destruction during mixing and they do not coalesce to form coarser bubbles.

Science and Technology of Concrete Admixtures. http://dx.doi.org/10.1016/B978-0-08-100693-1.00006-0
Copyright © 2016 Elsevier Ltd. All rights reserved.

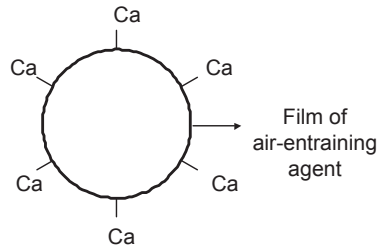


Figure 6.1 Air-entrained bubble (anionic type).

Therefore, the addition of an air-entraining agent stabilizes the air entrained during mixing in the form of millions of small air bubbles having an average diameter between 10 and 100 μm, which is the diameter range of the cement particles introduced in concrete.

In order to improve the resistance of concrete to freezing and thawing cycles, it is usually necessary to entrain 50−60 L of these fine bubbles. However, what is of the outmost importance is that these bubbles be homogeneously dispersed within concrete. This dispersion is characterized by what is called the **spacing factor** of the bubbles. It is evident that a big hole of 50−60 L filled with air at the center of 1 m^3 of concrete will not have any effect on the resistance of this block to freezing and thawing cycles.

6.3 Beneficial effects of entrained air

Unfortunately for many engineers, entrained air has only two effects on concrete: it protects against damage from freezing and thawing and decreases its compressive strength, so that if a concrete is not exposed to freezing and thawing it does not need entrained air that will weaken it. This is a totally false perception of the benefits that a few percent of entrained air brings to the properties of fresh and hardened concrete.

The benefits of entrained air include the following:

- An increase of the volume of the paste
- A fluidification of the cement paste
- An improvement of concrete rheology
- A decrease of the absorptivity and permeability of the hardened concrete
- The dissipation of the energy concentrated at the tip of fissures when, for any reason, hardened concrete starts to crack
- The presence of a free volume, which can receive deposits of expansive components (ettringite, silica gel) that can be formed in a concrete.

Of course, it is sure that a concrete that contains 50−60 L of air per cubic meter is not as strong as a concrete **having the same water−cement ratio (w/c)** that contains only 10−20 L of entrapped air. With such reasoning, it is forgotten that to reach the

same workability level an air-entrained concrete necessitates the use of less effective water. Less mixing water for a given mass of cement means a reduction of the w/c and consequently an improvement of concrete durability and sustainability. **The durability of a concrete depends more on its w/c than on its strength**. Even in low-strength concrete (20 MPa or less), an air-entrained concrete is slightly stronger than an equivalent non-air-entrained concrete made with the same amount of cement. In fact, due to their lubricating effect on the fresh concrete, air-entraining agents could be considered as water reducers.

6.3.1 The beneficial effect of entrained air on the workability of fresh concrete

As mentioned earlier, when 30−60 L of air are entrained in a fresh concrete, an equivalent volume of sand is eliminated and concrete becomes more "creamy." This modification of the composition of the paste improves the rheological properties of the fresh concrete, particularly its workability. The explanation behind this observation is that the small air bubbles are acting like the balls of a ball bearing within the paste. In fact, the explanation is more complex because entrained air modifies the viscosity of the paste and its cohesiveness at the same time.

Experience also shows that the presence of entrained air decreases significantly the risk of bleeding and segregation. This beneficial action of entrained air is also operating in the transition zone between the cement paste and the aggregates because internal bleeding is reduced for the same reasons. A small percent of entrained air improves the workability of concrete made with manufactured sand or sand produced from waste concrete that is composed of particles that have a shape and an absorption presenting a negative effect on concrete workability.

Entrained air can also be used to improve the workability of concretes made with very coarse sands. The author has added 8−10% of entrained air in a concrete made in the Canadian Arctic with a sand having a fineness modulus of 4.5, to concretes that were difficult to place. The resistance of freezing and thawing cycles was not a problem in this particular case because in the Arctic concrete is exposed to a rather dry environment comporting very few freezing and thawing cycles.

Finally, entrained air drastically improves the workability of low w/c or water−binder ratio (w/b) concretes that contain a high dosage of cement or binder (Aïtcin, 1998). It is very easy to demonstrate it when doing the following simple experiment:

- First, a non-air-entrained concrete having a w/c of 0.35 is used; it is seen that this concrete is cohesive and viscous and that it is difficult to shear it with a trowel.
- Second, a small amount of air-entraining agent is added to this concrete; it is seen quasi-instantaneously that the concrete becomes more workable, is less cohesive and viscous, and is easy to shear with a trowel.

This improvement of the workability of low w/c concrete has been used in many cases to facilitate concrete placing and pumping and improve the visual aspect of exposed surfaces. Entrained air is now an essential component of many self-consolidating concretes.

6.3.2 The beneficial action of entrained air against the propagation of cracks

When a crack develops in a cement paste, the greater part of its energy is concentrated at the tip of the propagating fissure. When the tip of this fissure meets an air bubble, its energy dissipates all over the surface of the bubble so that its progression may stop there.

6.3.3 The beneficial action of entrained air on the absorptivity and permeability of concrete

The effect of entrained air on concrete permeability is controversial. For example, Adam Neville (2011) thinks that entrained air reduces concrete permeability, while Kosmatka et al. (2002) are considering that it has no effect. The author is convinced that the presence of a network of noncommunicating air bubbles decreases the facility with which water can migrate through the capillary system. For the same reason, the absorptivity of an air-entrained concrete should be lower than that of a similar non-air-entrained concrete having the same w/c or w/b ratio.

6.3.4 Trapping expansive products

The 50−60 L of free space created by entrained air can be filled safely by expansive products. Very often, when observing concrete destroyed by the action of freezing and thawing cycles, it can be seen that several air bubbles are full of ettringite needles, as well as in the transition zone between the cement paste and the aggregates. The ions necessary to form the crystals of ettringite have been transported to the bubbles, where they found enough space to develop large crystals (Figure 6.2).

Raphaël et al. (1989) had the opportunity to observe under an electron microscope, concrete cores taken from seven dams built by Hydro Quebec with granitic aggregates presenting quartz crystals with ondulatory extinction under polarized light

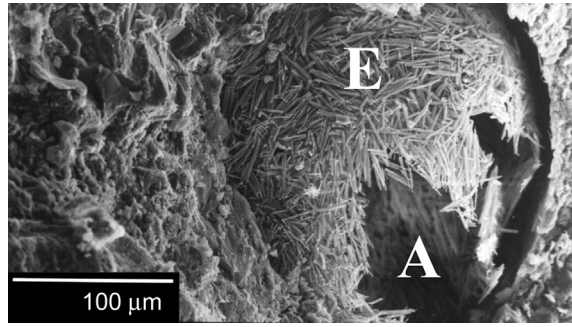


Figure 6.2 Ettringite needles formed in an air bubble of a concrete destroyed by freezing and thawing cycles.
Courtesy of Arezki Tagnit-Hamou (Aïtcin, 2008).

due to the internal stresses that have been developed in these crystals. This type of aggregate is known to be weakly reactive with the alkalis present in the cement paste. However, in the case of those seven dams, the entrained air bubbles and the transition zones were large enough to accommodate the deposition of the silica gel produced. Instead of destroying concrete, this reaction between the alkalis and the aggregates reinforced it; the compressive strength and elastic modulus of the tested concrete were far beyond their initial values. The permeability of these concretes was also very low.

On the contrary, in the case of three other dams built with very reactive aggregates, the presence of 50−60 L of air voids was not sufficient to protect these concretes from their destruction. The concretes of these three dams were severely damaged.

6.3.5 The beneficial effect of entrained air on the resistance to freezing and thawing cycles

In North America, the durability of concrete that faces freezing and thawing cycles is evaluated through the very severe ASTM C666 Standard Test Method. Two experimental procedures are proposed:

- Procedure A, consisting in freezing and thawing cycles under water (in France, this procedure is codified in the French standard NF P 18-424)
- Procedure B, where the freezing occurs in air (NF P 18-425 standard in France)

Generally, freezing and thawing tests are done according to procedure A, which is the more severe procedure. The temperature at the center of the concrete prisms has to pass from −15 to +15 °C in 6 h (from −18 to 9 °C in 4−6 h in France). In Canada, like in France, usually to be considered as freeze−thaw resistant, a concrete must withstand 300 cycles of freezing and thawing. Specimens are placed in a freezing cabinet after 2 weeks of water curing in Canada (4 weeks in France). Therefore, it is necessary to wait at least 75 days (13 weeks) to know if a concrete is freeze−thaw resistant. To shorten this testing period, a more rapid evaluation of the freezing and thawing resistance has been looked for. Based on Powers' work, it is the measurement of the **spacing factor of the bubble network** that permits a more rapid evaluation of the freezing and thawing resistance of concrete. The spacing factor is measured according to ASTM C 457-98 standard test method for microscopical determination of parameters of the air void system in hardened concrete.

In fact, the spacing factor corresponds to the average half distance between two air bubbles; it is the average distance that water has to travel before reaching an air bubble where it can freeze and take its expansion without creating disruptive forces within the cement paste. This spacing factor is obtained on a polish plaque measuring $100 \times 100\ mm^2$ in less than a week.

However, the Canadian A 231 standard accepts that, if the measured spacing factor is not satisfactory, the concrete can be tested according to ASTM C 666 Standard. If the concrete sustains successfully 300 or 500 freezing and thawing cycles, it can be considered as freeze−thaw resistant even if its spacing factor is not correct. When

using the ASTM C 666 test, it is assumed that the rapidity of the cycles may have the same destructive action as the accumulation of a greater number of milder freezing and thawing cycles in the field.

To evaluate the effect of the freeze–thaw cycles on the microstructure of the concrete, its ultrasonic resonance frequency is measured. A concrete is considered to be freeze–thaw resistant when, at the end of the cycling period, it still have a resonance frequency greater than 60% of its initial resonance frequency.

Two remarks must be made on the validity of this test:

- It is a very severe test.
- It is possible to destroy any type of concrete by increasing the number of cycles.

According to the present Canadian Standard A 23.1, the maximum value of the spacing factor for an ordinary concrete is 220 and 250 μm for a concrete having a low w/c. But as previously said, this standard permits one to submit concrete specimens to 300 freezing and thawing cycles if these two values cannot be met.

During the construction of the Confederation Bridge that links Prince Edward Island to the continent through a 13-km-long prefabricated concrete bridge, the Canadian Government was asking for a 100-year life cycle. Therefore, it was decided to submit concrete specimens to 500 cycles of freezing and thawing according to Procedure A of ASTM Standard C 666. As it was impossible to obtain after pumping a spacing factor of 220 μm that was required at that time for any type of concrete, it was necessary to undertake a research program to find the maximum value of the spacing factor for permitting concrete samples to withstand 500 cycles of freezing and thawing.

Five different concretes with spacing factors varying from 180 to 550 μm were made only by changing the dosage of the air-entraining agent. The result of this study showed that the maximum spacing factor allowing a satisfactory resistance to the 500 cycles was 350 μm. After reaching the 500 cycles, the specimens that were still in good condition were tested further until they failed. The last one that failed after 1950 cycles was the specimen having a spacing factor of 180 μm. The other specimens failed in the order of the decreasing values of their spacing factor. Of course, a low w/c concrete protected with a satisfactory network of entrained air is not protected forever against the action of freezing and thawing cycles. In nature, the harder rocks in mountains are destroyed by freezing and thawing.

The Canadian standards also specify the maximum value of the w/c that a concrete must have should be according to the class of exposition. It is too often forgotten that a low spacing factor is a necessary condition but not sufficient to make a concrete freeze–thaw resistant (Pigeon and Pleau, 1995; Aïtcin et al., 1998).

The dosage of an air-entraining agent has to be fine-tuned in the field to ensure that a satisfactory spacing factor is obtained. Keeping in mind that there are many types of mixers, the entrainment of air bubbles may vary from one sand to the other, the efficiency of the air-entraining agents to stabilize air bubbles vary from one commercial product to the other, the temperature of the concrete influences the formation of the network of entrained air bubbles, and the mode of placing can modify the initial characteristics of air-entrained system.

6.4 Effect of pumping on the air content and spacing factor

When an air-entrained concrete is pumped, usually two characteristics of the network of air bubbles are modified:

- The spacing factor is increased
- The total amount of air is decreased (except with some concretes made with certain polyacrylate superplasticizers)

This is why it is so important to measure the spacing factor of concrete at the end of the pumping line and not before. The increase of the spacing factor is usually linked to the coalescence of small air bubbles (several small air bubbles are joining to form coarser air bubbles) and to a lesser extent to the disparition of some coarse bubbles.

When pumping some concretes containing some polyacrylate superplasticizers, the total amount of entrained air, but not the spacing factor, may increase because only coarse bubbles are stabilized. Therefore, in order to obtain a good spacing factor at the end of the pumping line, it is important to use an air-entraining agent that stabilizes very fine air bubbles and to increase its dosage because small bubbles will coalesce during pumping.

The modification of the characteristics of the entrained air depends on many factors: the type of the pump used, the pressure applied, the amount of mixing water, the amount of binder and its composition, the type of air-entraining agent, and the type of other admixtures used when making concrete. A field test has to be done to fine-tune the right air-entraining admixture dosage. During this experiment, it will be possible to establish the air volume range at the end of mixing that will permit one to reach the right air bubble spacing in the concrete element after pumping.

During the construction of the Confederation Bridge, it was established that after its mixing, concrete should have at least an air content of 6% in order to have a spacing factor of less than 350 μm after its pumping. As the batching plant was producing only one type of concrete when the ice shields were built—a concrete having an average compressive strength of 93 MPa (to improve its resistance to abrasion)—it was not difficult to produce such a concrete, for which transportation time to the pump was less than 10 min.

6.5 Entraining air in blended cements

The effects of entrained air on concretes made with Portland cement are well documented, but the effect of the cementitious materials of blended cements on entrained air has not been studied so deeply. It seems that, in some cases, the addition of a supplementary cementitious material does not cause any problems. However, in some other cases, it can be difficult to stabilize a good network of entrained air. This is the case with some fly ashes that contain substantial amounts of unburned carbon (Hill and Sarkar, 1997; Baltrus and Lacount, 2001; Külaots and Hsu, 2003; Külaots and Hurt, 2004; Pedersen and Jensen, 2009). This carbon exists in two forms: usually as coarse unburned carbon particles or as a deposit of soot on the surface of fly ash particles

(Jolicoeur et al., 2009). Usually, it is easy to get rid of the coarse unburned particles of coal by passing the fly ash in a cyclone. It is rather difficult to get rid of the soot.

It seems that the air-entraining agent is preferentially absorbed by the carbon particles and the soot present in the fly ash so that it is no more available to stabilize the network of air bubbles. In such a case, it is necessary to double or triple the air-entraining dosage to stabilize a satisfying network of air bubbles in the concrete. However, in some cases, there is no other solution than changing the fly ash.

Another problem with some fly ashes comes from the variability of their carbon content. At night, some power plants are reducing their production of electricity so that the fly ash produced has a higher level of residual carbon as compared with the same power plant when producing at full capacity. In such a case, it is necessary to homogenize the fly ash or to use a cyclone to produce a fly ash having constant carbon content.

This is a very interesting research field but unfortunately it has not yet received all the attention it needs. It is hoped that with the increasing use of fly ash to decrease the carbon footprint of concrete structure, it will receive more attention.

6.6 Conclusion

The author is convinced that any concrete should contain some entrained air in order to improve its rheology, decrease the risks of bleeding and segregation, as well as improve the visual aspect of the surface of concrete elements. Only when concrete is submitted to freezing and thawing cycles should the spacing factor of the bubbles network be a concern.

Of course, when adding some air in an ordinary concrete its compressive strength decreases, as well as the amount of mixing water due to the lubrication action of the bubbles. Therefore, for a given workability, air-entrained concrete has a lower w/c than a corresponding non-air-entrained concrete, which means that it will be more durable. **It is important to repeat that it is not the compressive strength of a concrete that conditions its durability but rather its w/c**. Therefore, an air-entrained concrete made with the same cement dosage as a non-air-entrained concrete that has a lower compressive strength will be more durable.

To date, nothing better than a good network of entrained air bubbles having a small spacing factor has been found to make concrete freeze−thaw resistant in Canada, even in the case of low w/c concretes. When these freeze−thaw cycles are occurring in the presence of deicing salts, the specifications for the spacing factor are tougher than when the freezing and thawing cycles are occurring in the absence of deicing salts.

References

Aïtcin, P.C., 1998. High Performance Concrete. E and FN Spon, London, UK.

Aïtcin, P.C., Pigeon, M., Pleau, R., Gagné, R., 1998. Freezing and thawing durability of high-performance concrete. In: Concrete International Symposium on High-Performance Concrete and Reactive Powder Concrete, Sherbrooke, vol. 4, pp. 383−392.

Aïtcin, P.C., 2008. Binders for durable and sustainable concrete. ISBN:978-0-415-38588-6.
Baltrus, J.P., LaCount, R.B., 2001. Measurement of adsorption of air-entraining admixture on fly ash in concrete and cement. Cement and Concrete Research 31 (5), 819−824.
Gagné, R., 2016. Air entraining agents. In: Aïtcin, P.-C., Flatt, R.J. (Eds.), Science and Technology of Concrete Admixtures, Elsevier (Chapter 17), pp. 343−350.
Gelardi, G., Mantellato, S., Marchon, D., Palacios, M., Eberhardt, A.B., Flatt, R.J., 2016. Chemistry of chemical admixtures. In: Aïtcin, P.-C., Flatt, R.J. (Eds.), Science and Technology of Concrete Admixtures, Elsevier (Chapter 9), pp. 149−218.
Hill, R.L., Sarkar, S.L., 1997. An examination of fly ash carbon and its interactions with air entraining agent. Cement and Concrete Research 27 (2), 193−204.
Jolicoeur, C., Cong, T., Benoît, E., Hill, R., Zhang, Z., Pagé, M., 2009. Fly-ash carbon effects on concrete air entrainment: fundamental studies on their origin and chemical mitigation. In: World of Coal Ash (WOCA) Conference, May 4−7, Lexington, KY, USA, 23p. Available on: http://www.flyash.info/.
Kosmatka, S.H., Kerkoff, B., Panarase, W.C., Macleod, N.F., Machrath, J., 2002. Design and Control of Concrete Mixtures, Seven Canadian Edition, 356p. ISBN 0-89312-218-1.
Külaots, I., Hsu, A., 2003. Adsorption of surfactants on unburned carbon in fly ash and development of a standardized foam index test. Cement and Concrete Research 33 (12), 2091−2099.
Külaots, I., Hurt, R.H., 2004. Size distribution of unburned carbon in coal fly ash and its implications. Fuel 83 (2), 223−230.
Marchon, D., Mantellato, S., Eberhardt, A.B., Flatt, R.J., 2016. Adsorption of chemical admixtures. In: Aïtcin, P.-C., Flatt, R.J. (Eds.), Science and Technology of Concrete Admixtures, Elsevier (Chapter 10), pp. 219−256.
Neville, A.M., 2011. Properties of Concrete, fifth ed. Prentice Hall, Harlow, UK.
Pedersen, K.H., Jensen, A.D., 2009. The effect of combustion conditions in a full-scale low-NO_x coal fired unit on fly ash properties for its application in concrete mixtures. Fuel Processing Technology 90 (2), 180−185.
Pigeon, M., Pleau, R., 1995. Durability of Concrete in Cold Climates. E and FN SPON, NY, 244p.
Raphaël, S., Sarkar, S., Aïtcin, P.C., 1989. Alkali-aggregate reactivity − is it always harmful? In: Proceeding of the VIIIth International Conference on Alkali-aggregate Reaction, Kyoto, Japan, pp. 809−814.

Concrete rheology: a basis for understanding chemical admixtures

7

A. Yahia [1], *S. Mantellato* [2], *R.J. Flatt* [2]
[1]Université de Sherbrooke, Sherbrooke, QC, Canada; [2]Institute for Building Materials, ETH Zurich, Zurich, Switzerland

7.1 Introduction

This chapter presents an overview of the most important aspects of concrete rheology to serve as a basis for the other chapters which discuss chemical admixtures that modify rheological properties. Readers interested in a more detailed text about concrete rheology are referred to *Understanding the Rheology of Concrete* (Roussel, 2012a).

Concrete can be considered as a multiscale material in which solid particles (coarse aggregate) are suspended in a mortar matrix, while the mortar matrix can be viewed as a suspension of sand particles in a finer matrix (cement paste). Concrete can also be seen as a biphasic material, in which rigid sand and coarse aggregate particles are suspended in a cement paste matrix. No matter the chosen picture, in the context of this book it is important to mention that the action of chemical admixtures takes place at the paste level and that their effects are felt at the concrete level. However, in absolute terms we are interested in the rheological behaviour of concrete. This is why this chapter aims at defining the general rheological characteristics of concrete, although several of these cannot be directly impacted by chemical admixtures.

The rheology of concrete affects mixing, handling, transportation, pumping, casting, consolidation, finishing and surface quality after hardening. The facility with which concrete is processed is an extremely important aspect of its successful use in building economical structures presenting excellent long-term performance and durability, because the cost of the labour used to place concrete is quite significant.

For a long time the general term used to characterize the property of a concrete to be placed more or less easily was ‘workability’. However, in a more refined vision, three different ‘workability’ evaluations have been proposed (Table 7.1). The required level of workability of concrete depends on the application in which it is used. For example, high workability is required to cast concrete in heavily congested reinforced sections; on the other hand, zero-slump concretes are slip-formed in pavement construction.

Measurements of workability are essential to guarantee a good quality of concrete, and have been assessed for decades in various forms. Many of these assessments are, however, subject to operator judgement and/or of very limited applicability. The slump test (American Society for Testing Materials, ASTM C143/C143M-12, 2012) is the most used method to evaluate the workability of fresh concrete. It is a very simple

Science and Technology of Concrete Admixtures. http://dx.doi.org/10.1016/B978-0-08-100693-1.00007-2
Copyright © 2016 Elsevier Ltd. All rights reserved.

Table 7.1 Definition of workability based on different evaluations

Category	Output
Qualitative Fluidity Spread Stability Pumpability	Qualitative evaluation
Empirical evaluation Slump Slump flow V-funnel flow time Vebe	Quantitative evaluation
Fundamental Viscosity Yield stress Thixotropy	Fundamental rheological parameters

Tattersall and Banfill (1983).

test that simulates adequately the flow behaviour of concrete in a quasi-static (low-shear-rate) regime that directly relates to yield stress (Roussel, 2006a). However, it does not represent behaviours at higher rates, such as those reached during mixing and pumping. It is, for example, well known that two concrete mixtures can have the same slump but different flow behaviours (Tattersall and Banfill, 1983).

Most tests used in practice to qualify the rheological behaviour of concrete are of empirical origin, although many may also be related to real rheological properties (Roussel, 2012a). However, often a combination of at least two properties is needed to describe the rheological behaviour of concrete. This is becoming more important with the growing need to exploit the behaviour of fresh concrete better. In this context, different rheometers have been developed to measure the fundamental rheological properties of concrete.

7.2 Definition of rheology

Rheology is defined as the science of deformation and flow of matter under the influence of stresses (Tattersall and Banfill, 1983; Barnes, 2000). It is a science at the intersection of solid and fluid mechanics that is used in different industries — for example during the processing of medical, food and personal care products. Rheology deals more specifically with the relationship between shear stress, shear rate and time.

7.2.1 Shear laminar flow

To understand rheology better, it is important to consider the effect of a simple shear on a deformable material to define laminar shear flow, shear stress and shear rate. When a material is subjected to external forces, it is deformed depending on the stress

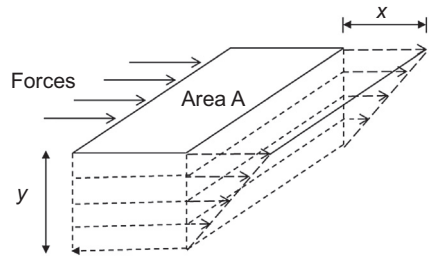


Figure 7.1 Schematic illustration of laminar shear flow.

distribution all over the material. A particular type of stress fields results in a laminar shear flow. For example, let us consider a liquid contained between two parallel plates at a distance y apart. The top plate slides in the x direction, while the bottom plate does not move. Material deformation occurs by the relative deformation (i.e. slipping) of the different layers without any transfer of material from one layer to the other. As can be seen in Figure 7.1, the velocity varies only in the y direction and not at all in the two directions perpendicular to y.

7.2.2 Shear stress

During a laminar flow, two layers move along each other. This relative displacement results in friction forces acting tangentially to the layers, and these are called shear forces (F). Let us consider two consecutive layers, 1 and 2, moving at parallel speeds, $\overrightarrow{\mathbf{V}_1}$ and $\overrightarrow{\mathbf{V}_2}$ (Figure 7.2). Assuming that layer 1 is moving faster than layer 2 (i.e. $\overrightarrow{\mathbf{V}_1} > \overrightarrow{\mathbf{V}_2}$), it is evident that layer 1 exerts on layer 2 a shear force that accelerates layer 2. Reciprocally, layer 2 exerts on layer 1 a shearing force that tends to slow down layer 1.

When reported to the unit areas (S) on which they are acting, these forces result in a physical quantity of great importance in rheology, namely shear stress. Shear stress (τ) is defined by the following relationship:

$$\tau = -\frac{F}{S} \tag{7.1}$$

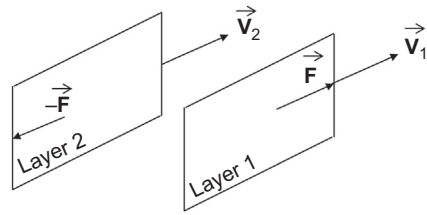


Figure 7.2 Relative movement between two successive layers.
Reproduced from Couarraze and Grossiord (2000) with authorization.

The shear stress τ is a force per unit area, and is expressed in Pascal in the International System of Units. It is a function defined at each point of the material, and varies from one layer to another. Due to symmetry, τ is usually considered constant at all points of the same layer (Couarraze and Grossiord, 2000; Tattersall and Banfill, 1983).

7.2.3 Shear rate

Let us consider the particular case of a laminar shear flow with a planar symmetry, as in the previous example where the material is sheared between two parallel planes, with one moving while the other is fixed to define the shear deformation.

Let us also consider particles that at time $t = 0$ belong to cross-sections located at distances x and $x + \mathrm{d}x$ from the fixed plane (Figure 7.3). At a later time t, the particles of the cross-sections located at x and $x + \mathrm{d}x$ have travelled the distances $u(x, t)$ and $u(x + \mathrm{d}x, t)$, respectively, where x is the location of the particle relative to the lower (fixed) plane. The shear deformation can be defined by the following relationship:

$$\gamma(x,t)\frac{u(x+\mathrm{d}x,t)-u(x,t)}{\mathrm{d}x} = \frac{\mathrm{d}u(x,t)}{\mathrm{d}x} \tag{7.2}$$

It is noted that the shear deformation does not depend on the displacement $u(x, t)$ itself, but on its variation when passing from one layer to another infinitely close layer. This relates to the shear rate $\dot{\gamma}$, which is the derivative with respect to time of the shear strain γ:

$$\dot{\gamma} = \frac{\mathrm{d}\gamma}{\mathrm{d}t} \tag{7.3}$$

The shear rate therefore has an inverse dimension of time and is expressed in s^{-1}.

7.2.4 Flow curve

The rheological behaviour of a material is described by the relationship between shear stress and shear rate, referred to as the flow curve, and this can be measured with

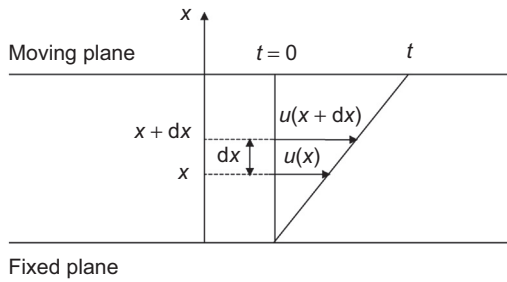


Figure 7.3 Definition of shear rate.
Reproduced Couarraze and Grossiord (2000) with authorization.

Table 7.2 Shear rates applied in various concrete processes

Flow pattern	Approximate maximum shear rate (s^{-1})
Mixing truck	10
Pumping	20–40
Casting	10
Tattersall two-point device, MKIII (Tattersall, 1991)	5
BML rheometer (Wallevik, 2003)	10

Roussel (2006b).

rheometers. Materials are subjected to various imposed shear rates (or shear stresses), and the resulting shear stresses (or shear rates) are measured.

In most concrete rheometers, shear stresses and shear rates are not directly imposed or measured. As most of the rheometers are based on concentric cylinders or parallel rotating plates, torque and angular velocities are usually measured. The torque and rotational velocity values can be transformed into shear stresses and shear rates (Murata, 1984; Wallevik, 2003; Yahia and Khayat, 2006; Wallevik and Ivar, 2011). The relevant rate of shear to be used for concrete should take into account the applications where concrete is processed. Examples of shear rates in different rheometers and processes are summarized in Table 7.2 (Roussel, 2006b).

The use of such rheological measurements reveals that, in the range of shear rates of interest, concrete behaves in general as a Bingham material (Tattersall and Banfill, 1983). This model is defined by two fundamental parameters, namely yield stress and plastic viscosity. In a Bingham material, the shear stresses vary linearly with shear rate beyond the threshold shear stress, defined as yield stress.

7.3 Different rheological behaviours

Several rheological models have been proposed to describe the flow curve of materials. These models are identified according to the macroscopic response of the material subjected to various shear rates. The most common models are shown in Figure 7.4.

7.3.1 Newtonian fluids

Newtonian fluids, such as water or oil, are characterized by a viscosity (i.e. the ratio between shear stress and shear rate) that is independent of shear rate. These fluids display a linear relation between shear stress and shear rate. The only parameter needed to describe the model is the slope of the shear stress–shear rate relationship

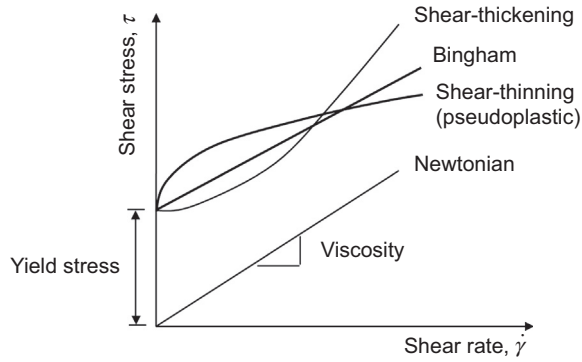


Figure 7.4 Illustration of different rheological behaviours – the cases of shear thinning and shear thickening shown include a yield stress, which is not necessarily always the case.

(Figure 7.4). By definition, this slope corresponds to the viscosity, η (Pa·s). Newtonian materials are characterized by a constant viscosity independent of shear rate. Newton's model is given by Eqn (7.4):

$$\tau = \eta\dot{\gamma} \tag{7.4}$$

7.3.2 Bingham fluid

The most commonly used rheological model to describe the flow behaviour of fresh cementitious materials is the Bingham model (Tattersall and Banfill, 1983; Tattersall, 1991; Wallevik and Níelsson, 2003). Unlike the Newtonian model, the Bingham curve does not pass through the origin, although above the yield stress τ_0 (Pa) the increment in shear stress is proportional to the increment in shear rate (Figure 7.5).

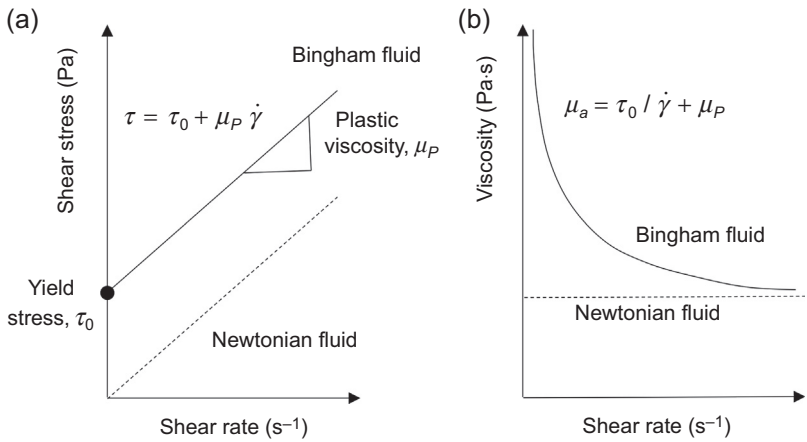


Figure 7.5 Schematic illustration of a Newtonian (discontinuous line) and a Bingham (continuous line) fluid. (a) Flow curve and (b) Viscosity curve.

The proportionality factor is called plastic viscosity μ_p (Pa·s), as illustrated in Figure 7.5. The Bingham model can be expressed as:

$$\tau = \tau_0 + \mu_p \dot{\gamma} \tag{7.5}$$

A modified form of the Bingham model has also been proposed to take into account the non-linearity sometimes observed with cement-based mixtures, especially at high shear rate (Yahia and Khayat, 2001; Khayat and Yahia, 1997):

$$\tau = \tau_0 + \mu_p \dot{\gamma} + c\dot{\gamma}^2 \tag{7.6}$$

where c is a constant in Pa·s^2.

Below the yield stress, the mixture does not flow and behaves as an elastic material.

A number of other materials apparently do not flow under gravity, and are thus referred to as yield stress materials. The statement that a material does not flow is of course associated with the time of observation. In suspensions such as cementitious materials, yield stress is a consequence of the attractive interparticle forces between cement grains and other fine particles that may or not be in the mix (Barnes, 1997; Roussel et al., 2012). An overview on these forces is given in Chapter 11 (Gelardi and Flatt, 2016). This yield stress is then amplified by the presence of inclusions such as sand and coarse aggregates (Mahaut et al., 2008; Yammine et al., 2008).

However, the existence of a yield stress has long been debated (Barnes and Walters, 1985; Yahia and Khayat, 2001; Moller et al., 2009), mainly because of the inherent difficulty in measuring it. Indeed, yield stress is determined by the extrapolation of the flow curve to zero shear rate. The accuracy in determining yield stress therefore mainly relies on the choice of the rheological models used to describe shear stress/shear rate flow curves, rheometer geometries (Lapasin et al., 1983; Nehdi and Rahman, 2004) and material behaviour (Roussel, 2012a). Among several models listed by Banfill (2006), the linear Bingham and the non-linear Herschel-Bulkley models are widely used to describe the rheological behaviour of cementitious systems.

Yield stress materials exhibit an elastic behaviour below the yield stress. Beyond this value they behave like a liquid and flow, but are shear thinning, as illustrated in Figure 7.5. It is widely accepted that cementitious suspensions, such as concrete, mortar and cement pastes, belong to this category of materials.

7.3.3 Shear-thinning and shear-thickening fluids with yield stress

Among the non-Newtonian fluids whose viscosity depends on shear rate or shear rate history, two different behaviours can be observed: shear thinning and shear thickening. Shear-thinning fluids are characterized by a decrease in the apparent viscosity when shear rate increases. An example is the application of vibration or pumping pressure that reduces the viscosity of concrete and enhances its flow performance. On the other hand, shear-thickening fluids correspond to materials for which the viscosity increases as the shear rate increases. The most commonly used model to

describe the rheological behaviour of these fluids is the Herschel-Bulkley model given in Eqn (7.7).

$$\tau = \tau_0 + K\dot{\gamma}^n \tag{7.7}$$

where K is the consistency factor (Pa·s), τ_0 is the yield stress in Pa, and n is the shear-thinning index (shear thinning if $n < 1$, shear thickening if $n > 1$). We note however that with $n > 1$, because of yield stress, the behavior will be shear thinning initially and then turn to shear thickening at higher shear rates.

7.4 Micromechanical behaviour of suspensions

The rheological behaviour of concrete is profoundly affected by the properties of the paste, and it is at this level that chemical admixtures act. Therefore, in the context of this book we devote a special section to the micromechanical behaviour of pastes (suspensions). This is influenced by various forces acting in the system, the most important of which can be summarized as follows:

- Hydrodynamic forces arise from the relative motion of particles to the surrounding fluid, but dominate for particles larger than ≈ 10 μm (Genovese et al., 2007);
- Colloidal forces exist between suspended particles and can be attractive or repulsive. Van-der-Waals, electrostatic and steric forces belong to this category, and are covered in Chapter 11 (Gelardi and Flatt, 2016);
- Brownian motion arises from thermal randomizing forces causing constant translational and rotational movements. However, this is of only secondary importance for the micrometre-size particles found in cementitious systems (see below);
- Inertial forces become important as shear rates increase. They can play a role in shear thickening of cementitious systems, even at relatively lower shear rates when the solids volume fraction is high;
- Gravitational forces cause segregation of the suspensions unless the particle size and density are balanced by adequate opposing forces (e.g. colloidal, browning or viscous).

We now discuss the behaviour of particle suspensions in relation to force balances, placing a particular focus on indicating in which cases it may be influenced by chemical admixtures.

7.4.1 Yield stress

The yield stress originates from the attractive interparticle forces at stake between particles in flocculated systems above the percolation threshold (ϕ_{perc}). Electrostatic forces are also present, but at high ionic strengths they are not sufficiently strong to prevent the particles from agglomerating (Israelachvili, 1990; Flatt, 1999). Hence, a flow is observed when the applied stress is sufficient to break down particle networks.

A detailed overview of interparticle forces and their relative importance in cementitious materials is presented in Chapter 11 (Gelardi and Flatt, 2016). In a broader context, Zhou et al. (1999, 2001) found that the yield stress increases when increasing the volume fraction and decreasing the particle size for spherical monodispersed alumina powders. They calculated that, without dispersant, the minimum distance between adjacent particles is about 2 nm, independent of the particle size.

Compared to conventional vibrated concrete, self-consolidating concrete, which is proportioned with a relatively higher volume of powders to lower friction between aggregates, has a relatively lower yield stress.

Establishing a quantitative relationship for all these parametric dependences is one of the challenges in proposing a model for yield stress. The yield stress model (Flatt and Bowen, 2006, 2007) deals with such challenges. It correctly accounts for interparticle forces, the volume fraction of solids, particle sizes and their distribution, and can also be extended to polydispersed powder mixes. It discriminates three main contributions affecting the yield stress (Eqn (7.8)). The first accounts for the powder characteristics as the particle size distribution (pre-factor m, particle average diameter d, and radius of curvature a^* among particles at contact points) and the Hamaker constant A_0. The second contribution is h the interparticle distance, on which superplasticizers play a major role. The third contribution accounts for the impact of volume fraction ϕ, which is affected by ϕ_m, the maximum packing fraction and the percolation threshold ϕ_{perc}:

$$\tau_0 \cong m\frac{A_0 a^*}{d^2 h^2}\,\frac{\phi^2\left(\phi-\phi_{\text{perc}}\right)}{\phi_m(\phi_m-\phi)} \tag{7.8}$$

The adsorption of superplasticizers on cement surfaces increases the average separation distance h, consequently reducing the maximum attractive interparticle forces, the yield stress and the degree of flocculation.

This average separation distance varies with the conformation and surface coverage achieved by adsorbed admixtures. Both of these relate to the molecular structure of admixtures in different ways. These relations and their impact on rheology are discussed in Chapter 11 (Gelardi and Flatt, 2016). The extent of adsorption also plays an important role and can be related to molecular structure (Marchon et al., 2013). The range of molecular structures of superplasticizers is covered in Chapter 9 (Gelardi et al., 2016), and their adsorption behaviour in Chapter 10 (Marchon et al., 2016).

7.4.2 Viscosity

Shear-thinning behaviour in superplasticized systems has been reported in literature (Asaga and Roy, 1980; Struble and Sun, 1995; Björnström and Chandra, 2003; Papo and Piani, 2004). To examine the origin of this phenomenon better, Hot et al. (2014) introduced the concept of residual viscosity. This isolates the hydrodynamic contribution from the yield stress by defining the residual viscosity in Eqn (7.9) as:

$$\mu_{\text{res}} = \left(\mu_{\text{app}} - \tau_0/\dot{\gamma}\right) \tag{7.9}$$

They confirmed that at low shear rates, viscous dissipation decreases with increasing polymer dosage. This occurs mainly in the interstitial fluid between cement particles, and its extent relates to the conformation of either adsorbed or non-adsorbed polymer, as discussed in Chapter 16 (Nkinamubanzi et al., 2016).

At higher shear rates cement suspensions become shear thickening (increase of apparent viscosity at high shear rates), often observed in the presence of superplasticizers (Roussel et al., 2010). This is mostly detrimental, since more energy is needed to increase the material flow rate, impacting mainly on mixing, pumping and extrusion

processes (see Table 7.2). The origin of this phenomenon is still debated. Two main theories are considered here.

The first theory states that the hydrodynamic viscous forces promoting the formation of hydro-clusters overcome Brownian motions, tending to distribute particles evenly in the fluid. This relation is expressed by the Peclet number defined as $\mathrm{Pe}_{\dot{\gamma}} = \eta_0 d^3 \dot{\gamma} / k_B T$, where η_0 is the viscosity of the suspending liquid, d the particle radius, k_B the Boltzmann constant and T the absolute temperature.

It is worth noting here that Brownian motions are negligible when compared to attractive forces of particles in the size range of 10-50 μm in flocculated systems (Roussel et al., 2010). In turn, this contribution becomes important when decreasing the particle size, and might compete with reduced colloidal forces (Neubauer et al., 1998). To examine this transition in cement pastes, Roussel et al. (2010) calculated that the critical shear rate at which shear thickening occurs should be in the order of 10^{-3} s^{-1}, far below realistic conditions. This theory seems to contradict results showing a decrease in the critical shear rate and an increase of shear-thickening intensity when the dosage of the polymer is increased (Feys et al., 2009; Hot et al., 2014).

The alternative theory proposes the dominance of particle inertia over the viscous contributions (Feys et al., 2009; Roussel et al., 2010). The critical shear rate decreases with increasing particle size, as implied by the Reynold number $\mathrm{Re} = \rho_0 d^2 \dot{\gamma} / \eta_0$, where ρ_0 is the density of the suspending fluid, η_0 the viscosity of the suspending liquid and d the particle radius.

Comparing results from the literature (Rosquoët et al., 2003; Lootens et al., 2003; Phan et al., 2006), the shear rate at which shear thickening occurs is observed to decrease with the increase of ϕ, where the gap between particles becomes smaller. Also, if one considers the residual viscosity discussed above, at a given volume fraction the intensity of the shear thickening is independent on the dosage of polymers, and seems to be promoted only by either collisions or sustained frictional contacts between particles under vigorous agitation (Hot et al., 2014).

This observation would tend to exclude a possible reduction in surface coverage at high shear rates, earlier proposed by Cyr et al. (2000). This reduction might occur if polymers cannot disentangle fast enough, so part of the polymer is pulled out of the surface, leading to higher interparticle forces. However, with increasing polymer dosage these sites would be very rapidly reoccupied. From this point of view, shear thickening should not directly depend on the nature of the superplasticizers, but appears more in highly dispersed systems because of lower volume fractions that can be accessed.

Additionally, it should be mentioned that shear thickening may take place progressively as the shear rate is increased (continuous shear thickening) or discontinuously (discontinuous shear thickening) (Fernandez, 2014). Recently, the transition between both modes has been related to a change in the lubrication regimes at particle contacts (Fernandez et al., 2013).

7.4.3 Thixotropy

Thixotropy is a phenomenon by which the structure of a fluid is broken down under shear and rebuilt at rest (Barnes, 1997; Roussel, 2006b; Roussel et al., 2012).

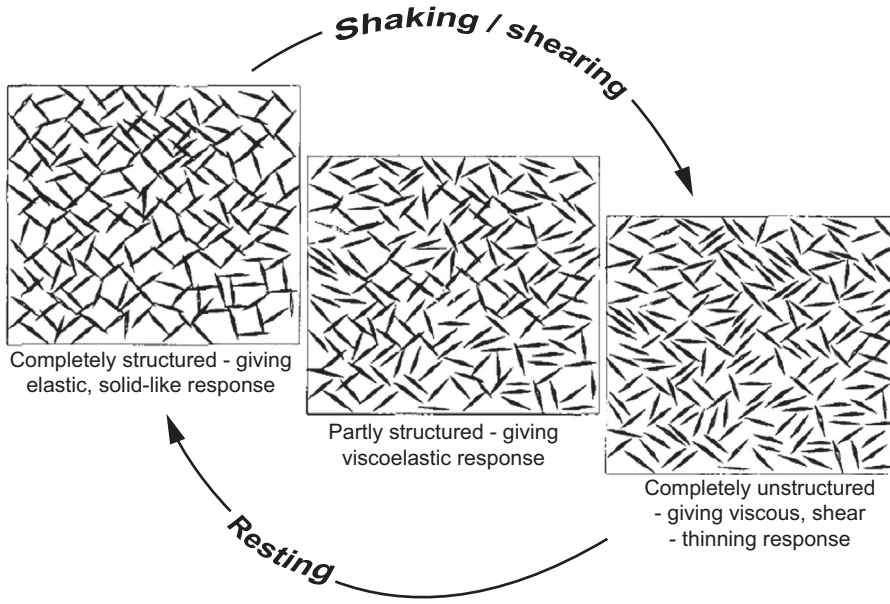


Figure 7.6 Breakdown and build-up of a 3D thixotropic structure. Reproduced from Barnes (1997) with authorization.

Thixotropy is therefore a reversible process, and a schematic representation of this can be seen in Figure 7.6.

A well-known thixotropic material is 'ketchup'. Stirring ketchup turns it from solid-like state to liquid-like state, and if left at rest it recovers its original viscosity. In particulate systems, the mechanism of thixotropy (i.e. deflocculation under shear and flocculation at rest) relies mainly on the interactions between suspended particles, as explained in Chapter 11 (Gelardi and Flatt, 2016).

In cementitious materials, thixotropy can be present in addition to irreversible structural breakdown. Thus, these materials can exhibit a combination of both reversible and irreversible structural breakdown, only the first of which is associated with thixotropy.

It is worth emphasizing that thixotropy is time-dependent. Immediately after mixing, cement particles are dispersed. At rest, cement particles flocculate due to the colloidal attractive forces, and form a percolated network of interacting particles. At a given shear rate, the viscosity evolves towards a steady-state value. A non-thixotropic shear-thinning fluid, in contrast, would (almost) immediately reach its steady-state viscosity in response to a change in shear rate.

Cementitious materials are rather complex, and lend themselves to easy mislabelling of their properties. Indeed, they combine both thixotropy and irreversible structural breakdown. The latter term was introduced by Tattersall and Banfill (1983) to emphasize the fact that cementitious materials exhibit shear-dependent behaviour. In particular, when exposed to high shear, as in a concrete mixer, they do not fully

recover their previous yield stress. However, the 'residual' yield stress is associated with a microstructure that can be broken down under shear and recovered at rest (or at lower shear rates), which corresponds to true thixotropic behaviour.

Furthermore, because of the ongoing chemical reactions, the yield stress increases over time. This contributes as an additional irreversible workability loss and the irreversible formation of additional hydrates that can contribute to the cohesion of the flocculated structure.

In summary, there are many factors that explain the time-dependent rheological properties of cementitious systems: irreversible structural breakdown, thixotropy and hydration. Chemical admixtures (including superplasticizers) can profoundly modify the time-dependent behaviour of cementitious systems, as explained in Chapter 12 (Marchon and Flatt, 2016b). They can affect any of these properties on the basis of their chemical nature, structure and dosage. To the best of our knowledge, this has not been systematically investigated, but we report later on some results concerning flow retention.

7.4.4 Concrete: A visco-elasto-plastic material

Concrete exhibits a visco-elasto-plastic behaviour, because it deforms elastically below the plastic yield stress and flows only once the yield stress is overcome. As explained above, in a majority of cases the most important parameter is yield stress, and this can be obtained from simple stoppage tests (Roussel, 2012b), as illustrated in Figure 7.7. Yield stress determines the ease of filling forms, and explains why construction was successful (enough) during the decades when only a slump test was used to characterize concrete rheology.

For some applications plastic viscosity is also important, but in many cases high accuracy is not needed and some simple tests may again be sufficient (Roussel, 2012a). If a more refined characterization of concrete rheology is needed, concrete rheometers may be used.

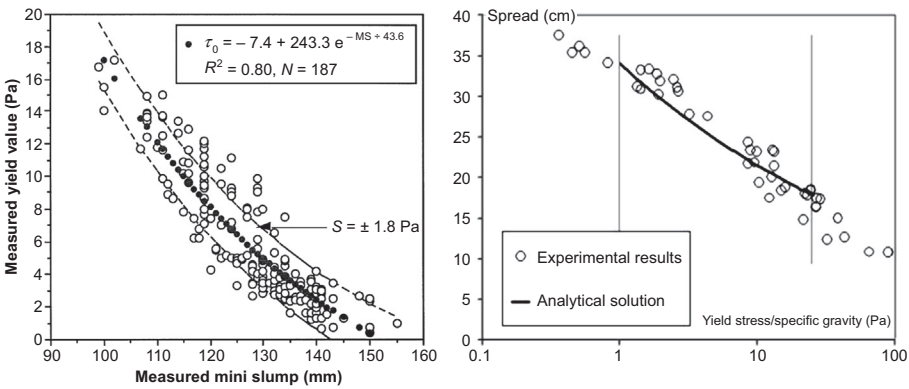


Figure 7.7 Relationship between slump and yield stress.
Reproduced from Khayat and Yahia (1998) (left) and Roussel (2007) (right) with authorization.

7.4.5 Bleeding and segregation

Bleeding is a form of segregation driven by gravitational forces that causes the consolidation of particles at the bottom and the migration of water to the surface. It has a major implication for the long-term permeability and strength of concrete, since this displacement implies a gradient of density that renders the matrix non-uniform.

Segregation is a more general term for the development of a non-uniform composition, but not necessarily with a migration of water upwards. It can be induced during flow by shear forces (Ovarlez, 2012), or at rest by gravity. The stability of aggregates in a paste can be expressed through a quantitative relation between aggregate size and yield stress of the paste (Roussel, 2006c). If aggregates are large enough to segregate, the extent to which they do so then depends on their volume fraction and maximum packing (Roussel, 2006c).

Both bleeding and segregation become more probable and ultimately more extensive as the superplasticizer efficiency and/or dosage is increased. This may, however, be countered by various adjustments to the mix design and/or the use of viscosity modifying admixtures (VMAs), described in Chapter 20 (Palacios and Flatt, 2016).

Bleeding is influenced by the size and volume fraction of the particles in the suspension, as well as their degree of flocculation. Above a critical concentration of superplasticizer, defined as saturation dosage, the attractive forces are so drastically reduced that the gravitational contribution becomes predominant (Perrot et al., 2012). Consequently, the rheological behaviour becomes essentially Newtonian and particles have a tendency to settle (Neubauer et al., 1998). For example, in the case of self-consolidating concrete, which is characterized by very low yield stress compared to conventional concrete, the stability of aggregates must be given some attention and ensured by changes in the mix design. When doing so, it is important to remember that segregation in concrete depends on the yield stress of its matrix, namely the mortar and not on the yield stress of the concrete itself (Roussel, 2006a).

Yield stress increases with the volume fraction of solids, and a critical volume fraction ϕ, above which bleeding does not occur, can be defined. In pastes, this is found to increase with the dosage of polymer (Flatt et al., 1998), but Perrot et al. (2012) showed that there is no direct correlation between yield stress and bleeding. Although both properties depend on interparticle forces, one does not result from the other. In particular, they do not have the same dependence on solid volume fraction. This implies that bleeding can be prevented by a combination of adjustments to the mix design, such as reducing water-to-cement ratio (w/c), increasing the content of fines or adjusting the superplasticizer type and/or dosage, without compromising the yield stress of the mix.

Furthermore, the use of VMAs can also reduce the bleeding rate (see Chapter 20) (Palacios and Flatt, 2016). While initially proposed to act by increasing the viscosity of the continuous phase (Khayat, 1998), there is now evidence that bridging flocculation (Brumaud, 2011; Brumaud et al., 2014) or dispersion forces may be at play (Palacios et al., 2012). The latter cases are supported by the observation of increases in yield stress and critical deformation when using VMAs (Brumaud, 2011; Brumaud et al., 2014). How superplasticizers and VMAs interact is a subject of ongoing research in which conflicting statements still remain to be elucidated.

7.5 Factors affecting concrete rheology

7.5.1 General considerations

The notion of the particulate nature of concrete distinguishes it from many other fluids, such as water and oil. Indeed, concrete is made of a wide variety of particles whose diameters vary from a few micrometres (cement and mineral admixtures) or even sub-micrometre (if silica fume is present) to several tens of millimetres (sand, coarse aggregate, fibres, etc.). Furthermore, the rheology of concrete changes with time, due to reversible physical phenomena (flocculation of its fine particles) and irreversible chemical reactions due to cement hydration described in Chapter 8 (Marchon and Flatt, 2016a).

In addition to mix design, concrete rheology is strongly influenced by the synergic effect of several parameters − these factors are briefly outlined below. The fundamental behaviour of cement pastes was dealt with in the previous section, so here we only address specific issues in the role of cement composition.

7.5.2 Effect of processing energy on concrete rheology

In every production step, fresh concretes are subject to changes and are deformed to different extents depending on the energy applied. The typical shear rate values corresponding to each step are given in Table 7.2 (Roussel, 2006b).

As already discussed, the fact that mixing intensity (or more generally the flow history) affects rheological properties (Tattersall and Banfill, 1983; Williams et al., 1999; Juilland et al., 2012) and hydration kinetics (Juilland et al., 2012; Oblak et al., 2013) of cementitious materials is well documented in the literature. This most probably occurs because changes in ion concentrations (or boundary layer thickness) can for example modify surface reaction rates, etch pit formation (Juilland et al., 2012) and polymer adsorption. Consequently, if rheological studies are to be downscaled from concrete to paste or upscaled from paste to concrete, it is important that the paste is exposed to the same mixing energy and/or flow history, otherwise its behaviour will not be the same. In particular, one must keep in mind that aggregates and sand, because they cannot be deformed, lead to some shear rate concentration and amplification in the paste located in the gap between these rigid grains. This is why sample preparation and pre-shear protocols are particularly important when studying cementitious systems.

7.5.3 Effect of solid concentration on viscosity and yield stress

The rheological behaviour of particulate systems depends strongly on the volume of particles. For Bingham fluids, this holds both for yield stress and plastic viscosity. Analytical expressions relating viscosity of dispersed suspensions to their volume fraction exist, but only hold at low volume fraction ($<12\%$) and are therefore not discussed here.

When the particle concentration is near the maximum ϕ_{max}, the viscosity of suspension can be estimated using the empirical Krieger-Dougherty model

(Krieger and Dougherty, 1959). This model takes into account the effect of the form of particles (Eqn (7.10)).

$$\mu(\phi) = \mu_0 \left(1 - \frac{\phi}{\phi_{\max}}\right)^{-\eta\phi_{\max}} \tag{7.10}$$

where

$\mu(\phi)$ is the (apparent) viscosity for a solid concentration of ϕ
μ_0 is the (apparent) viscosity of fluid
ϕ is the solid concentration, by volume
η is the intrinsic viscosity, which is a function of shape of particles (= 2.5 for spherical particles and between four and seven for cement particles (Struble and Sun, 1995)
$\phi_{\max}$ is the maximum solid concentration, by volume.

As can be seen in Figure 7.8, the viscosity increases with the volume fraction of solid particles, corresponding to lower w/c ratios. It also diverges to infinity as the maximum volume fraction is approached. This represents a strength of this model. Another is the fact that it recovers the correct analytical expression at the limit of low volume fractions. However, the behaviour in between these two limits is not necessarily well matched.

The yield stress of concrete increases with the decrease of w/c ratio, the fineness of the cement, the coarse aggregate content, etc. The most significant effect, however, comes from the flocculation of the paste, which results from attractive interparticle forces. The strength of the flocculated network increases with the number of particle contacts, and therefore decreases with particle size. This contribution to yield stress can only be changed by modifying the concentration of the solids. However, the strength of the individual interparticle forces can be reduced using a high-range water-reducer, as explained in Chapter 11 (Gelardi and Flatt, 2016).

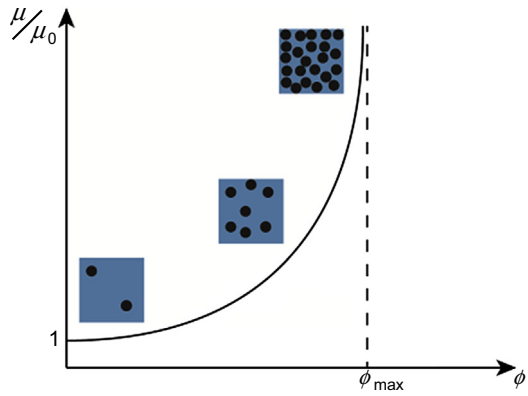


Figure 7.8 Relationship between solid concentration and relative viscosity. Reproduced from Roussel (2012a) with authorization.

7.5.4 Effect of paste/aggregate and mortar/aggregate ratio on the rheology of concrete

In much research the behaviour of concrete is studied using a two-phase approach in which the concrete is represented by a solid phase (aggregate) suspended in a cement paste. In this approach, the volume of the liquid phase can be divided into two parts as shown in Figure 7.9:

- the volume of paste necessary to fill the interparticle voids;
- the volume of paste in excess, which serves as a lubricating layer around the aggregates and facilitates the flow of concrete.

From this perspective, the rheological behaviour of concrete is influenced by the rheology of the paste as well as the thickness of excess paste.

The packing density of the granular skeleton is one of the most influential factors in the rheological parameters of concrete. Indeed, a well-graded skeleton leads to a higher thickness of excess paste, thus maximizing the beneficial lubricating effect of the paste. In the case of yield stress, Ferraris and de Larrard (1998) have shown that it is necessary to consider the impact of each of the granular classes on the threshold value through a model calculating the shear threshold. The results of this model show (via the coefficients a_i) that the impact of the fine particles is greater on the increase

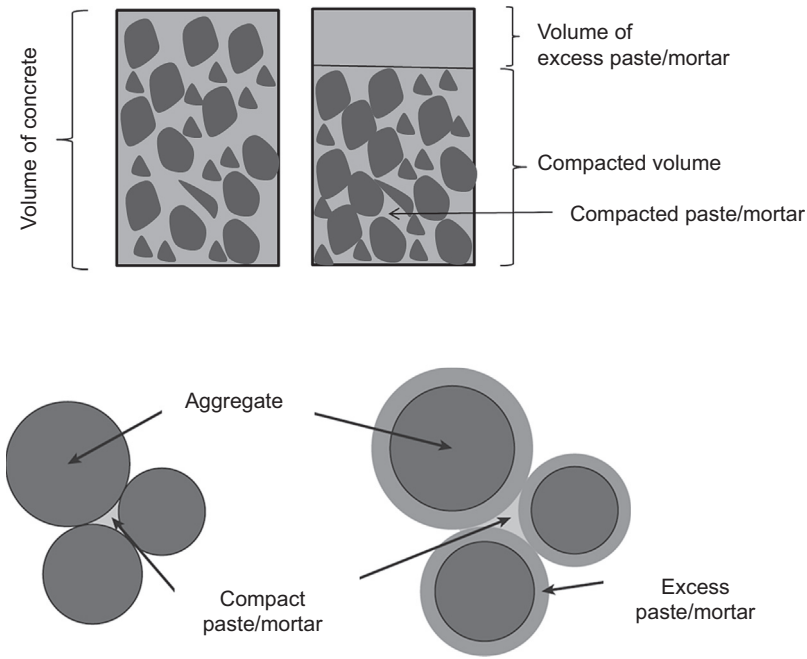


Figure 7.9 Excess paste/mortar approach. Compacted aggregates leave a certain porosity among each other that must be filled by paste. Additional paste serves to keep aggregates away from each other and facilitate flow (excess paste/mortar).
Adapted from Oh et al. (1999) with authorization.

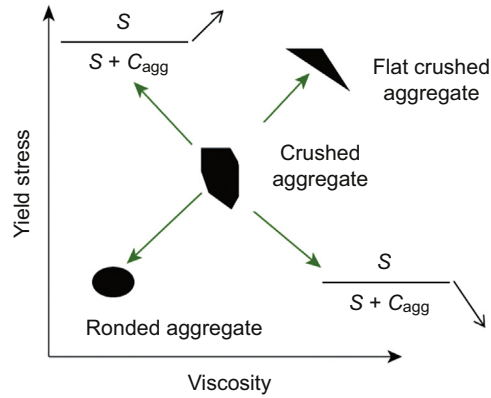


Figure 7.10 Effect of shape and aggregate content on the rheological diagram, S stands for Sand and Cagg for Coarse Aggregate.
Adapted from Wallevik and Wallevik (2011) with authorization.

in the yield stress than that of the larger particles. Some parameters that characterize aggregates and have a direct influence on the rheology of concrete are described in the following sections.

Crushed aggregates have a surface area greater than rolled aggregates, which results in a higher wettable surface. Furthermore, because of their shape and greater roughness, use of crushed aggregates results in higher internal friction than using rolled aggregates. The use of crushed aggregates therefore leads to a simultaneous increase of the yield stress and viscosity (Figure 7.10).

7.5.5 Effect of paste composition

Not only the volume but also the properties of the paste have an important impact on the rheology of concrete. The rheology of the paste is influenced by the cement type and its chemical composition, the w/c used, supplementary cementitious materials, temperature chemical admixtures and their interactions. The effect of these various mixture parameters on rheological parameters of the paste are shown schematically in Figure 7.11.

7.5.5.1 Effect of water content

The volume of water, usually expressed in terms of w/c or water-to-binder ratios, has a significant influence on both yield stress and plastic viscosity (Figure 7.12). Increased water content decreases both yield stress and plastic viscosity.

7.5.5.2 Effect of cement

The physical properties (size distribution and fineness) and chemical composition of the cement have a great influence on the rheology of concrete. In relation to admixture performance, the most important factors are type and amount of the C_3A phase,

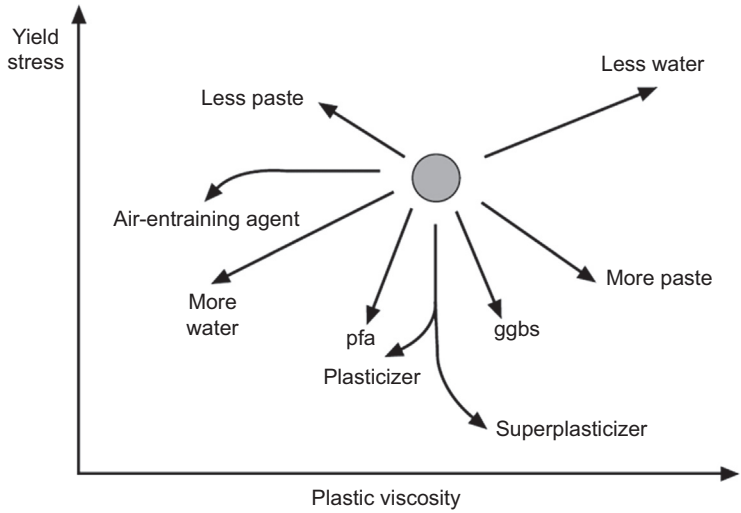


Figure 7.11 Influence of paste formulation parameters on the rheology of concrete. Reproduced from Newman and Choo (2003) with authorization.

calcium sulphate and soluble alkali. A more detailed account of the reasons for this is given in Chapter 16 (Nkinamubanzi et al., 2016).

7.5.5.3 Effect of mineral admixtures

A great variety of mineral admixtures can be used as replacement for cement in concrete to improve certain properties of concrete, as explained in Chapter 1 (Aïtcin, 2016a). As for any powder, their particle size distribution, specific gravity, morphology and interparticle forces are the major factors affecting their rheological behaviour.

Also, the change of the granular packing due to a variation of the concrete mix design should be taken into account. The choice of mineral admixtures should therefore be made by taking into account the mix design, the type and fineness of the cement and the packing density of the aggregates.

Partial replacement of cement with fly ash generally decreases both yield stress and plastic viscosity (Tattersall and Banfill, 1983). However, Kim et al. (2012) reported that, although replacing cement with fly ash in self-consolidating concrete reduces the yield stress, it may either increase or decrease viscosity, depending on the properties of the fly ash and its interaction with cement.

The effect of blast-furnace slag on rheology is generally much less apparent than that of fly ash. Tattersall (1991) reported that it is strongly dependent on the cement content and slag type.

As mentioned, silica fume can improve rheology when used at low replacement rates, but alters rheology at relatively higher contents. Due to the small size of its particles, a small volume of silica fume may enhance the powder particle size distribution. However, the use of silica fume should always be accompanied by the incorporation of a dispersant.

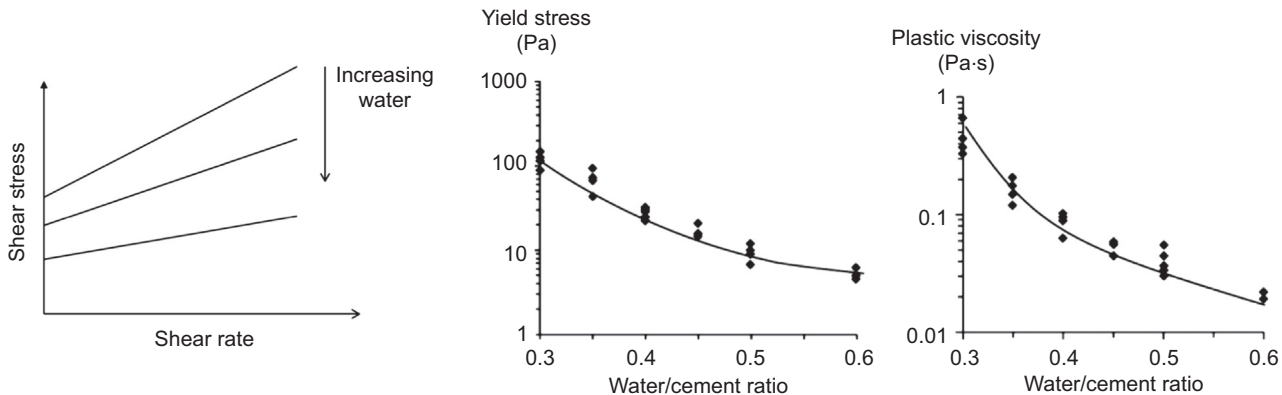


Figure 7.12 Influence of the volume of water on rheology.
Reproduced from Wallevik and Wallevik (2011) and Domone (2003) with authorization.

7.5.5.4 Clays

The presence of impurities, such as clay minerals, may alter concrete rheology or increase the water and admixture demands. This is discussed in more detail in Chapters 10 and 16 (Marchon et al., 2016; Nkinamubanzi et al., 2016).

7.5.6 Effect of air content on rheology of concrete

As mentioned in Chapter 6, the entrained air in concrete can be beneficial to the workability as well as to the stability of aggregates (Aïtcin, 2016b). However, exploiting the possibility of using entrained air most probably depends on the mix design and processing rates.

Recent work suggests that the deformability of entrained air under shear plays a crucial role (Hot, 2013). At low shear rates (and therefore low levels of stress), surface tension would prevent entrained air bubbles from deforming and they would behave as solid inclusions, apparently increasing the solid volume fraction. This clearly should increase the plastic viscosity. However, the effect on yield stress is less clear, as it would depend on the cohesion of the air bubbles in the paste microstructure, which is not known.

At higher shear rates (and therefore high levels of stresses), surface tension would not be able to prevent entrained air bubbles from deforming, and concentration of shear into these deformable air bubbles should reduce the plastic viscosity. This shear rate dependence of air is, a priori, an advantage for processing concrete because flow is easier, but segregation is hindered when concrete is at rest. Examples of practical situations in which this has been exploited are provided in Chapter 6 (Aïtcin, 2016b).

7.6 Thixotropy of concrete

As previously explained, thixotropy is defined as a continuous decrease of viscosity with time when flow is applied to a sample that has been previously at rest, and the subsequent recovery of viscosity when the flow is discontinued (Barnes, 1997).

The origin of thixotropy of cement paste was investigated by Roussel et al. (2012), and short-, medium- and long-term evolutions of fresh cement pastes were described. Hydrates start to nucleate at the pseudo-contact points between particles within the network, resulting in formation of bridges between cement particles. Basics of hydration processes are covered in Chapter 8 (Marchon and Flatt, 2016a), and the impact of chemicals admixtures on hydration is detailed in Chapter 12 (Marchon and Flatt, 2016b). In this section, we focus on explaining the consequences in terms of concrete processing, as well as providing an overview of methods that can be used to characterize thixotropic behaviour.

7.6.1 Consequences of thixotropy on concrete processing

Studies on thixotropy of concrete are gaining much attention in relation to the use of self-consolidating concrete (SCC), because it can have either positive or negative technological consequences (Roussel, 2006b; ACI 237 Committee Report, 2007).

For example, high thixotropy in SCC is useful to reduce the lateral pressure exerted by SCC on formwork. However, in the case of multilayer casting, relatively low thixotropy is preferable to allow good adhesion of a layer of concrete deposited on a previous layer in a discontinuous placement. In the case of high thixotropy, it is absolutely necessary to use vibrating needles to penetrate substantially into the previous layer to avoid the formation of a cold joint.

7.6.2 Experimental methods to quantify thixotropy

As mentioned earlier, the study of thixotropy of cement suspensions is complicated, as it originates from a combined effect of colloidal interactions and cement hydration, which are influenced by cement composition, fineness, grain size distribution and chemical and/or mineral admixtures. Thus, there is no broadly accepted method to measure thixotropy of cementitious materials, but rather a number of test protocols, some of which are discussed in the following subsections.

7.6.2.1 Hysteresis curves

Ish-Shalom and Greenberg (1960) used hysteresis measurements to characterize thixotropy of cement pastes. In such tests, the shear rate is increased from zero to some pre-defined maximum value and then decreased back to zero. When shear stress is plotted as a function of shear rate, the up (loading) and down (unloading) curves do not overlap in thixotropic materials, as illustrated in Figure 7.13.

The enclosed area between the up and down curves (i.e. hysteresis) provides a measure of the degree of thixotropy (Tattersall and Banfill, 1983). However, several researchers have criticized the use of this hysteresis loop. For example, it was shown that two suspensions of quite different thixotropic properties could give similar hysteresis loops (Banfill and Saunders, 1981). Also, Roussel (2006b) stated that flocculation and deflocculation cannot be separated. Consequently, the measured area (i.e. thixotropy index) can be the same for a mix displaying fast flocculation and fast deflocculation as for a mix displaying slow flocculation and slow deflocculation, although the two mixes will behave very differently in practice. Barnes (1997) also reported that hysteresis loop tests are not recommended because the evaluated thixotropy is a function of both shear rate and time.

7.6.2.2 Structural breakdown curves

Thixotropy of cement-based systems can be measured using the steady state or equilibrium approach. This involves measuring the variation of shear stress with time under a constant shear rate, as illustrated in Figure 7.14. The shear stress (τ_i) necessary to initiate flow at the shear rate is generally related to the initial suspension microstructure (Shaughnessy and Clark, 1988). On the other hand, the shear stress that decays with time towards an equilibrium shear stress (τ_e) corresponds to reaching a steady state between network breakdown and build-up that is independent of the shear history. The 'breakdown area' (A_b) determined at different shear rates between the initial and equilibrium shear stresses allows to quantify the energy per unit time and volume necessary to break down the initial structure until reaching equilibrium (steady) state.

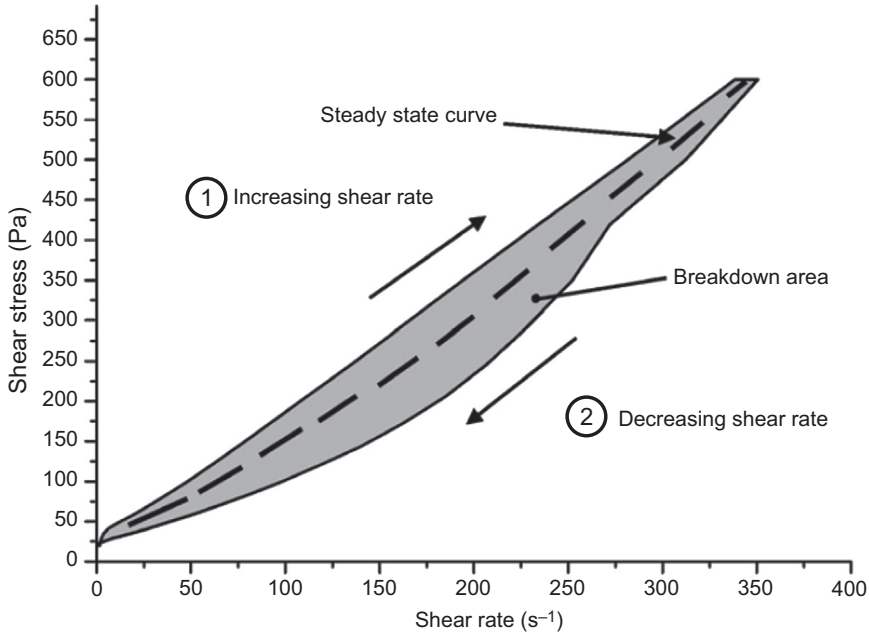


Figure 7.13 Example of thixotropic loop obtained with a cement paste submitted successively to increasing and decreasing shear rate ramps.
Reproduced from Roussel (2006b) with authorization.

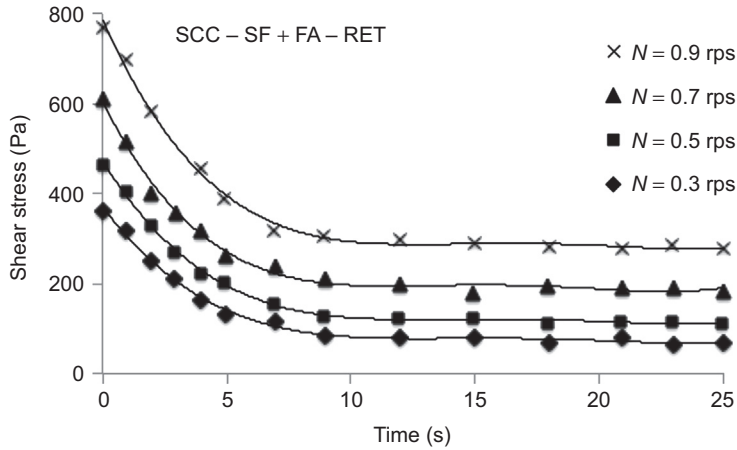


Figure 7.14 Structural breakdown curves at different rotational speeds (expressed in rps) for a ternary SCC system containing fly ash (FA), silica fume (SF), and set-retarding admixture (RET).
Adapted from Assaad et al. (2003) with authorization.

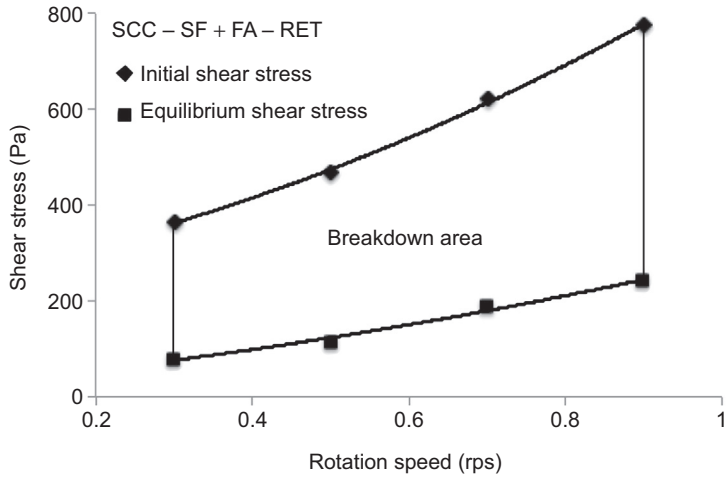


Figure 7.15 Calculation of the structural breakdown area for a ternary SCC system containing fly ash (FA), silica fume (SF), and set-retarding admixture (RET).
Adapted from Assaad et al. (2003) with authorization.

An example of such results is given in Figure 7.15 for SCC mixtures made with ternary cement containing silica fume (SF), fly ash (FA) and a set-retarding admixture (RET) (Assaad et al., 2003). The breakdown area (A_b) in Figure 7.15 can be calculated using Eqn (7.11):

$$A_b = \int_{0.3}^{0.9} (\tau_i(N) - \tau_e(N))\mathrm{d}N \tag{7.11}$$

where N is the applied shear rate (respectively rotation rate).

The value of A_b depends on the measuring procedure, including the time of rest before the test, the differences between the applied and recorded rotational speeds and the accuracy of the torque sensor. By fixing these experimental conditions, A_b provides a quantitative mean for comparing the thixotropy of different materials in a more rigorous way than thixotropy loops.

7.6.2.3 Structural build-up at rest

Another approach for measuring thixotropy involves the determination of the rate at which structural build-up takes place at rest. This can be done destructively many times on the same sample, giving it enough recovery time in between measurements. This procedure is not adequate for chemically reactive systems, which limits its applicability to cementitious systems. However, it is possible to prepare multiple samples and measure them at different times, which reduces the total time during which hydration can modify the system behaviour. Non-destructive methods may also be considered, and may include ultrasound spectroscopy and oscillation rheometry.

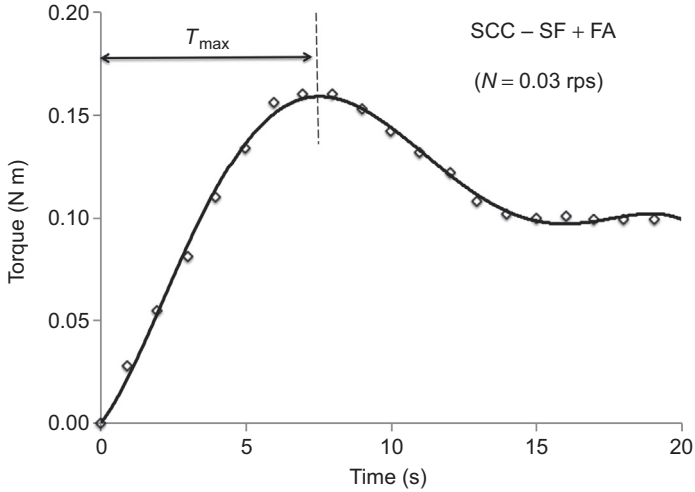


Figure 7.16 Typical torque−time profile for SCC submitted to a rotational speed of 0.03 rps. Adapted from Assaad et al. (2003) with authorization.

As static yield stress measurements are gaining interest in concrete research, we present a brief overview of the experimental approach. The measurement of static yield stress (also referred to as shear-growth yield stress) consists in subjecting the sample to stress at low and constant rotational speed. This allows the determination of the stress beyond which the sample starts flowing. As can be seen in Figure 7.16, data show a first linear elastic region domain, at the end of which yielding occurs when the torque (respectively the shear stress) reaches a maximum value. This corresponds to the beginning of microscopic destruction of the internal network due to the presence of bonds between flocculated particles. The torque, then, decreases to reach a plateau (equilibrium) value, representing the steady-state yield stress at the applied shear rate. The yielding torque is taken as a measure of yield stress. Plotting it as a function of resting time provides a fingerprint of thixotropic recovery at rest after shearing.

7.7 Conclusions

The main objective of this chapter was to give an overview of the most important factors that affect the rheology of concrete, providing insight into their physical origin. In the context of this book, it is essential to emphasize that the effect of admixtures takes place at the paste level, and propagates through length scales to be felt at the macroscopic level of concrete. Thus, properly conducted studies on paste can provide correct relative properties at the concrete level for different admixed concretes (Chapter 16, Nkinamubanzi et al., 2016). However, they cannot directly give the absolute rheological properties of concrete.

For this reason, in this chapter we have extended our coverage of concrete rheology beyond the strict impact of chemical admixtures. In particular, we highlighted the following.

- Most of the test methods existing to characterize workability of concrete are empirical. However, recent research makes it possible to extract real rheological parameters, although the full shear rate dependence cannot be (easily) obtained without a proper rheometer.
- Concrete behaves as a yield stress fluid, and the yield stress plays an essential role in many applications. Its viscosity and possible shear thickening must also be taken into account in a significant number of cases, particularly in formulations with low w/c ratios.
- Concrete exhibits a thixotropic behaviour. Depending on the rate of structural build-up, this must be taken into account (and possibly also exploited).

Over the past years much progress has been made in understanding concrete rheology from a practical and a fundamental point of view. Thanks to the remarkable progress that has been made in processing concrete, for example, pumping concrete up to 600 m in Dubai (Aïtcin and Wilson, 2015). More generally, SCC is increasingly used to build floors, slabs on the ground and bridge decks, because concrete pouring can be achieved without any external vibration and with higher productivity.

Terminology and definitions

This section provides the definition of the most important terms and expressions related to rheology.

Apparent viscosity (μ_{app})	is the ratio between the shear stress and corresponding shear rate. The apparent viscosity is a function of the shear rate.
Flow curve	is the graphical representation of the relationship between shear stress and shear rate.
Newtonian materials	correspond to materials in which a linear relationship exists between shear stress and shear rate. The coefficient of viscosity is the constant of proportionality between shear stress and shear rate.
Non-Newtonian materials	correspond to materials in which a non-linear relationship exists between shear stress and shear rate.
Plastic viscosity (μ_p)	corresponds to the coefficient of proportionality between an increment in shear stress and the corresponding increment in shear rate beyond the yield stress.
Rheology	is the science of the deformation and flow of matter.
Rheometer	is an instrument used to measure rheological properties.

Shear rate ($\dot{\gamma}$)	is the rate of change of the shear strain with time; also known as rate of shear strain.
Shear stress (τ)	is the component of a stress that causes successive parallel layers of a material to move relative to each other.
Shear thickening	corresponds to the behaviour of a material presenting an increase of its apparent viscosity when the shear rate increases.
Shear thinning (pseudoplastic behaviour)	corresponds to the behaviour of a material presenting a decrease in viscosity when shear rate increases.
Thixotropy	is a reversible time-dependent property of some materials; it consists of a continuous decrease of viscosity with time when flow is initiated, and the subsequent recovery of viscosity after a sufficient period of rest.
Yield stress (τ_0)	is the minimum shear stress that should be applied to initiate the flow of a material. Below the yield stress, a plastic material behaves as an ideal elastic solid (it does not flow).

Acknowledgements

Professor Ammar Yahia would like to thank his postdoctoral fellow Dr Paco Dierderich and PhD candidate Ahmed Mostafa for their help in preparing this chapter. Support for Sara Mantellato was provided by SNF Project No. 140615, titled 'Mastering flow loss of cementitious systems'. Finally, all authors would like to thank Dr Nicolas Roussel (IFSTARR) for helpful feedback on this text.

References

ACI 237, 2007. Self-consolidating Concrete (ACI 237R-07). American Concrete Institute, Farmington Hills, MI, 34 pp.

ASTM C143/C143M-12, 2012. Standard Test Method for Slump of Hydraulic-Cement Concrete. ASTM International, West Conshohocken, PA.

Aïtcin, P.-C., Willson, W., 2015. The Sky's the limit. Concrete International 37 (1), 53−58.

Aïtcin, P.-C., 2016a. The importance of the water−cement and water−binder ratios. In: Aïtcin, P.-C., Flatt, R.J. (Eds.), Science and Technology of Concrete Admixtures. Elsevier (Chapter 1), pp. 3−14.

Aïtcin, P.-C., 2016b. Entrained air in concrete: Rheology and freezing resistance. In: Aïtcin, P.-C., Flatt,, R.J. (Eds.), Science and Technology of Concrete Admixtures. Elsevier (Chapter 6), pp. 87−96.

Asaga, K., Roy, D.M., 1980. Rheological properties of cement mixes: IV. Effects of superplasticizers on viscosity and yield stress. Cement and Concrete Research 10, 287−295. http://dx.doi.org/10.1016/0008-8846(80)90085-X.

Assaad, J., Khayat, K.H., Mesbah, H., 2003. Assessment of thixotropy of flowable and self consolidating concrete. ACI Materials Journal 100 (2), 99−107.

Banfill, P.F.G., 2006. Rheology of fresh cement and concrete. Rheology Reviews 61−130.

Banfill, P.F.G., Saunders, D.C., 1981. On the viscometric examination of cement pastes. Cement and Concrete Research 11 (3), 363−370.

Barnes, H.A., 1997. Thixotropy—a review. Journal of Non-Newtonian Fluid Mechanics 70, 1−33. http://dx.doi.org/10.1016/S0377-0257(97)00004-9.

Barnes, H.A., 2000. A Handbook of Elementary Rheology. University of Wales, Institute of Non-Newtonian Fluid Mechanics.

Barnes, H.A., Walters, K., 1985. The yield stress myth? Rheologica Acta 24, 323−326. http://dx.doi.org/10.1007/BF01333960.

Björnström, J., Chandra, S., 2003. Effect of superplasticizers on the rheological properties of cements. Materials and Structures 36, 685−692. http://dx.doi.org/10.1007/BF02479503.

Brumaud, C., 2011. Origines Microscopiques Des Conséquences Rhéologiques de L'ajout D'éthers de Cellulose Dans Une Suspension Cimentaire (Ph.D. thesis). University Paris-Est. http://hal.archives-ouvertes.fr/docs/00/67/23/23/PDF/TH2011PEST1069_complete.pdf.

Brumaud, C., Baumann, R., Schmitz, M., Radler, M., Rousse, N., January 2014. Cellulose ethers and yield stress of cement pastes. Cement and Concrete Research 55, 14−21. http://dx.doi.org/10.1016/j.cemconres.2013.06.013.

Couarraze, G., Grossiord, J.L., 2000. Initiation to Rheology (available in French), third edn. Edition TEC & DOC. 300 p.

Cyr, M., Legrand, C., Mouret, M., 2000. Study of the shear thickening effect of superplasticizers on the rheological behaviour of cement pastes containing or not mineral additives. Cement and Concrete Research 30, 1477−1483. http://dx.doi.org/10.1016/S0008-8846(00)00330-6.

Domone, P.L., 2003. Fresh conrete. Advanced Concrete Technology 1, 3−29.

Fernandez, N., 2014. From Tribology to Rheology Impact of Interparticle Friction in the Shear Thickening of Non-Brownian Suspensions. ETH Zürich, Zürich.

Fernandez, N., Mani, R., Rinaldi, D., Kadau, D., Mosquet, M., Lombois-Burger, H., Cayer-Barrioz, J., Herrmann, H., Spencer, N., Isa, L., 2013. Microscopic mechanism for shear thickening of non-Brownian suspensions. Physical Review Letters 111 (10), 108301. http://dx.doi.org/10.1103/PhysRevLett.111.108301.

Ferraris, C.F., de Larrard, F., 1998. Testing and Modelling of Fresh Concrete Rheology. Report No. NISTIR 6094 (p. 61). Gaithersburg, USA.

Feys, D., Verhoeven, R., De Schutter, G., 2009. Why is fresh self-compacting concrete shear thickening? Cement and Concrete Research 39 (6), 510−523. http://dx.doi.org/10.1016/j.cemconres.2009.03.004.

Flatt, R.J., Houst, Y.F., Bowen, P., Hofmann, H., Widmer, Sulser, J.U., Mäder, U., Bürge, A., 1998. Effect of superplasticizers in highly alkaline model suspensions containing silica fume. In: Proc. 6th CANMET/ACI International Conference on Fly-Ash, Silica Fume, Slag and Natural Pozzolans in Concrete, 2, pp. 911−930.

Flatt, R.J., Bowen, P., 2006. Yodel: a yield stress model for suspensions. Journal of the American Ceramic Society 89 (4), 1244−1256. http://dx.doi.org/10.1111/j.1551-2916.2005.00888.x.

Flatt, R.J., Bowen, P., 2007. Yield stress of multimodal powder suspensions: an extension of the YODEL (Yield stress mODEL). Journal of the American Ceramic Society 90 (4), 1038−1044. http://dx.doi.org/10.1111/j.1551-2916.2007.01595.x.

Flatt, R.J., 1999. Interparticle forces in cement suspensions. PhD Thesis EPFL, no. 2040.

Gelardi, G., Flatt, R.J., 2016. Working mechanisms of water reducers and superplasticizers. In: Aïtcin, P.-C., Flatt, R.J. (Eds.), Science and Technology of Concrete Admixtures. Elsevier (Chapter 11), pp. 257−278.

Gelardi, G., Mantellato, S., Marchon, D., Palacios, M., Eberhardt, A.B., Flatt, R.J., 2016. Chemistry of chemical admixtures. In: Aïtcin, P.-C., Flatt, R.J. (Eds.), Science and Technology of Concrete Admixtures. Elsevier (Chapter 9), pp. 149–218.

Genovese, D.B., Lozano, J.E., Rao, M.A., 2007. The rheology of colloidal and noncolloidal food dispersions. Journal of Food Science 72 (2).

Hot, J., Bessaies-Bey, H., Brumaud, C., Duc, M., Castella, C., Roussel, N., 2014. Adsorbing polymers and viscosity of cement pastes. Cement and Concrete Research 63, 12–19. http://dx.doi.org/10.1016/j.cemconres.2014.04.005.

Hot, J., 2013. Influence of Super-plastisizer and Air-Entraining Agents on the Macroscopique Viscosityof Cement-Based Materials (Ph.D. dissertation) (in French). Université Paris-Est.

Ish-Shalom, M., Greenberg, S.A., 1960. The rheology of fresh Portland cement pastes. In: Proceedings of the 4th International Symposium on Chemistry of Cement, Washington, DC, pp. 731–748.

Israelachvili, J., 1990. Intermolecular and surface forces. Academic Press, London, England.

Juilland, P., Aditya Kumar, A., Gallucci, E., Flatt, R.J., Scrivener, K.L., 2012. Effect of mixing on the early hydration of alite and OPC systems. Cement and Concrete Research 42 (9), 1175–1188. http://dx.doi.org/10.1016/j.cemconres.2011.06.011.

Kim, J.H., Noemi, N., Shah, S.P., 2012. Effect of powder materials on the rheology and formwork pressure of self-consolidating concrete. Cement and Concrete Composites 34, 746–753.

Khayat, K.H., Yahia, A., 1997. Effect of welan gum high-range water reducer combinations on rheology of cement grout. ACI Materials Journal 94 (5), 365–372.

Khayat, K.H., 1998. Viscosity-enhancing admixtures for cement-based materials — An overview. Cement and Concrete Composites 20, 171–188. http://dx.doi.org/10.1016/S0958-9465(98)80006-1.

Khayat, K.H., Yahia, A., 1998. Simple field tests to characterize fluidity and washout resistance of structural cement grout. Cement, Concrete, and Aggregates 20 (1), 145–156.

Krieger, I.M., Dougherty, T.J., 1959. A mechanism for non-Newtonian flow in suspensions of rigid spheres. Journal of Rheology 3, 137.

Lapasin, R., Papo, A., Rajgelj, S., 1983. Flow behavior of fresh cement pastes. A comparison of different rheological instruments and techniques. Cement and Concrete Research 13, 349–356. http://dx.doi.org/10.1016/0008-8846(83)90034-0.

Lootens, D., Van Damme, H., Hébraud, P., 2003. Giant stress fluctuations at the jamming transition. Physical Review Letters 90 (17), 178301. http://dx.doi.org/10.1103/PhysRevLett.90.178301.

Mahaut, F., Mokeddem, S., Chateau, X., Roussel, N., Ovarlez, G., 2008. Effect of coarse particle volume fraction on the yield stress and thixotropy of cementitious materials. Cement and Concrete Research 38 (11), 1276–1285.

Marchon, D., Flatt, R.J., 2016a. Mechanisms of cement hydration. In: Aïtcin, P.-C., Flatt, R.J. (Eds.), Science and Technology of Concrete Admixtures. Elsevier (Chapter 8), pp. 129–146.

Marchon, D., Flatt, R.J., 2016b. Impact of Chemical Admixtures on Cement Hydration. In: Aïtcin, P.-C., Flatt, R.J. (Eds.), Science and Technology of Concrete Admixtures. Elsevier (Chapter 12), pp. 279–304.

Marchon, D., Sulser, U., Eberhardt, A.B., Flatt, R.J., 2013. Molecular design of comb-shaped polycarboxylate dispersants for environmentally friendly concrete. Soft Matter 9 (45), 10719–10728. http://dx.doi.org/10.1039/C3SM51030A.

Marchon, D., Mantellato, S., Eberhardt, A.B., Flatt, R.J., 2016. Adsorption of chemical admixtures. In: Aïtcin, P.-C., Flatt, R.J. (Eds.), Science and Technology of Concrete Admixtures. Elsevier (Chapter 10), pp. 219–256.

Moller, P., Fall, A., Chikkadi, V., Derks, D., Bonn, D., 2009. An attempt to categorize yield stress fluid behaviour. Philosophical Transactions of the Royal Society: Mathematical, Physical and Engineering Sciences 367, 5139−5155. http://dx.doi.org/10.1098/rsta.2009.0194.

Murata, J., 1984. Flow and deformation of fresh concrete. Material and Construction 17, 117−129. http://dx.doi.org/10.1007/BF02473663.

Nehdi, M., Rahman, M.-A., 2004. Estimating rheological properties of cement pastes using various rheological models for different test geometry, gap and surface friction. Cement and Concrete Research 34, 1993−2007. http://dx.doi.org/10.1016/j.cemconres.2004.02.020.

Neubauer, C., Yang, M.M., Jennings, H.M., 1998. Interparticle potential and sedimentation behavior of cement suspensions: effects of admixtures. Advanced Cement Based Materials 8 (1), 17−27. http://dx.doi.org/10.1016/S1065-7355(98)00005-4.

Newman, J., Choo, B.S., 2003. Advanced Concrete Technology 2: Concrete Properties, first ed. Butterworth-Heinemann. p. 352.

Nkinamubanzi, P.-C., Mantellato, S., Flatt, R.J., 2016. Superplasticizers in practice. In: Aïtcin, P.-C., Flatt, R.J. (Eds.), Science and Technology of Concrete Admixtures. Elsevier (Chapter 16), pp. 353−378.

Oblak, L., Pavnik, L., Lootens, D., 2013. From the concrete to the paste: a scaling of the chemistry (in French). Association française de génie Civil (AFGC), Paris, pp. 91−98. http://www.afgc.asso.fr/images/stories/visites/SCC2013/Proceedings/11-pages%2091-98.pdf.

Oh, S.G., Noguchi, T., Tomosawa, F., 1999. Towards mix design for rheology of self-compacting concrete. In: Proceedings of the 1st International RILEM Symposium on Self-Compacting Concrete, PRO7, pp. 361−372.

Ovarlez, G., 2012. 2-Introduction to the rheometry of complex suspensions. In: Roussel, N. (Ed.), Understanding the Rheology of Concrete. Woodhead Publishing Series in Civil and Structural Engineering. Woodhead Publishing, pp. 23−62. http://www.sciencedirect.com/science/article/pii/B9780857090287500029.

Palacios, M., Flatt, R.J., 2016. Working mechanism of viscosity-modifying admixtures. In: Aïtcin, P.-C., Flatt, R.J. (Eds.), Science and Technology of Concrete Admixtures. Elsevier (Chapter 20), pp. 415−432.

Palacios, M., Flatt, R.J., Puertas, F., Sanchez-Herencia, A., 2012. Compatibility between polycarboxylate and viscosity-modifying admixtures in cement pastes. In: Proceedings 10th CANMET/ACI International Conference on Superplasticizers and Other Chemical Admixtures in Concrete, Prague, ACI, SP-288, pp. 29−42.

Papo, A., Piani, L., 2004. Effect of various superplasticizers on the rheological properties of Portland cement pastes. Cement and Concrete Research 34, 2097−2101. http://dx.doi.org/10.1016/j.cemconres.2004.03.017.

Perrot, A., Lecompte, T., Khelifi, H., Brumaud, C., Hot, J., Roussel, N., 2012. Yield stress and bleeding of fresh cement pastes. Cement and Concrete Research 42 (7), 937−944. http://dx.doi.org/10.1016/j.cemconres.2012.03.015.

Phan, T.H., Chaouche, M., Moranville, M., 2006. Influence of organic admixtures on the rheological behaviour of cement pastes. Cement and Concrete Research 36 (10), 1807−1813. http://dx.doi.org/10.1016/j.cemconres.2006.05.028.

Rosquoët, F.A., Alexis, A., Khelidj, A., Phelipot, A., 2003. Experimental study of cement grout: rheological behavior and sedimentation. Cement and Concrete Research 33 (5), 713−722. http://dx.doi.org/10.1016/S0008-8846(02)01036-0.

Roussel, N., 2006a. Correlation between yield stress and slump: comparison between numerical simulations and concrete rheometers results. Materials and Structures 39, 501−509. http://dx.doi.org/10.1617/s11527-005-9035-2.

Roussel, N., 2006b. A thixotropy model for fresh fluid concretes: theory, validation and applications. Cement and Concrete Research 36, 1797−1806.

Roussel, N., 2006c. A theoretical frame to study stability of fresh concrete. Materials and Structures 39 (1), 81−91. http://dx.doi.org/10.1617/s11527-005-9036-1.

Roussel, N., 2007. The LCPC Box: a cheap and simple technique for yield stress measurements of SCC. Materials and Structures 40, 889−896. http://dx.doi.org/10.1617/s11527-007-923-4.

Roussel, N., 2012a. Understanding the Rheology of Concrete. Woodhead Publishing, Cambridge, UK.

Roussel, N., 2012b. 4-From industrial testing to rheological parameters for concrete. In: Roussel, N. (Ed.), Understanding the Rheology of Concrete. Woodhead Publishing Series in Civil and Structural Engineering. Woodhead Publishing, pp. 83−95. http://www.sciencedirect.com/science/article/pii/B9780857090287500042.

Roussel, N., Ovarlez, G., Garrault, S., Brumaud, C., 2012. The origins of thixotropy of fresh cement pastes. Cement and Concrete Research 42, 148−157. http://dx.doi.org/10.1016/j.cemconres.2011.09.004.

Roussel, N., Lemaître, A., Flatt, R.J., Coussot, P., 2010. Steady state flow of cement suspensions: a micromechanical state of the art. Cement and Concrete Research 40 (1), 77−84. http://dx.doi.org/10.1016/j.cemconres.2009.08.026.

Shaughnessy, R., Clark, P.E., 1988. The rheological behavior of fresh cement pastes. Cement and Concrete Research 18 (3), 327−341.

Struble, L., Sun, G.-K., 1995. Viscosity of Portland cement paste as a function of concentration. Advanced Cement Based Materials 2, 62−69. http://dx.doi.org/10.1016/1065-7355(95)90026-8.

Tattersall, G.H., 1991. Workability and Quality Control of Concrete. E&FN Spon, London, 262 pp.

Tattersall, G.H., Banfill, P.F.G., 1983. The Rheology of Fresh Concrete, Pitman Advanced Publishing Program.

Wallevik, O.H., Níelsson, I., 2003. Rheology - a Scientific Approach to Develop Self-Compacting Concrete. In: Wallevik, O., Níelsson, I. (Eds.), 3rd International RILEM Symposium on Self-Compacting Concrete. RILEM Publications, Reykjavik, Iceland, pp. 23−31.

Wallevik, O.H., Wallevik, J.E., 2011. Rheology as a tool in concrete science: the use of rheographs and workability boxes. Cement and Concrete Research 41 (12), 1279−1288. http://dx.doi.org/10.1016/j.cemconres.2011.01.009.

Wallevik, J.E., 2003. Rheology of Particle Suspensions; Fresh Concrete, Mortar and Cement Paste with Various Types of Lignosulfonates (Ph.D. thesis). The Norwegian University of Science and Technology, 411 pp.

Williams, D.A., Saak, A.W., Jennings, H.M., 1999. The influence of mixing on the rheology of fresh cement paste. Cement and Concrete Research 29 (9), 1491−1496. http://dx.doi.org/10.1016/S0008-8846(99)00124-6.

Yammine, J., Chaouche, M., Guerinet, M., Moranville, M., Roussel, N., 2008. From ordinary rheology concrete to self-compacting concrete: a transition between frictional and hydrodynamic interactions. Cement and Concrete Research 38 (7), 890−896.

Yahia, A., Khayat, K.H., 2001. Analytical models for estimating yield stress of high-performance pseudoplastic grout. Cement and Concrete Research 31 (5), 731−738.

Yahia, A., Khayat, K.H., September 2006. Modification of the concrete rheometer to determine rheological parameters of self-consolidating concrete − vane device. In: Marchand, J., et al. (Eds.), Proceeding of the 2nd International RILEM Symposium. Advances in Concrete through Science and Engineering, Québec, Canada, pp. 375−380.

Yahia, A., 2011. Shear-thickening behavior of high-performance cement grouts—influencing mix-design parameters. Cement and Concrete Research 41 (2), 230−235.

Zhou, Z., Scales, P.J., Boger, D.V., 2001. Chemical and physical control of the rheology of concentrated metal oxide suspensions. Chemical Engineering Science 56, 2901−2920. http://dx.doi.org/10.1016/S0009-2509(00)00473-5.

Zhou, Z., Solomon, M.J., Scales, P.J., Boger, D.V., 1999. The yield stress of concentrated flocculated suspensions of size distributed particles. Journal of Rheology (1978-Present) 43, 651−671. http://dx.doi.org/10.1122/1.551029.

Zingg, A., Holzer, L., Kaech, A., Winnefeld, F., Pakusch, J., Becker, S., Gauckler, L., 2008. The microstructure of dispersed and non-dispersed fresh cement pastes—new insight by cryo-microscopy. Cement and Concrete Research 38 (4), 522−529. http://dx.doi.org/10.1016/j.cemconres.2007.11.007.

Mechanisms of cement hydration

8

D. Marchon, R.J. Flatt
Institute for Building Materials, ETH Zürich, Zurich, Switzerland

8.1 Introduction

To better understand the influence of some concrete admixtures on the properties of the fresh and hardened concrete, it is important to have a good comprehension of the physical and chemical consequences of hydration. The physical consequences of cement hydration were discussed in Chapter 3 (Aïtcin, 2016). In this chapter, the chemical background knowledge of cement hydration is presented so that it will be easier to understand the modification of cement hydration when using concrete admixtures (Marchon and Flatt, 2016), as discussed in Chapter 12.

In Chapter 3, it was shown that ordinary Portland cement (OPC) is a material composed of four main phases, to which a small amount of calcium sulfate (formerly essentially gypsum but presently as a mixture of different forms of calcium sulfate) has been added (Aïtcin, 2016). These four main phases are: alite, an impure form of C_3S; belite, an impure form of C_2S; and an interstitial phase composed itself of two phases, namely tricalcium aluminate (C_3A) and tetracalcium aluminoferrite (C_4AF) that are more or less crystallized, depending essentially on the composition of the raw meal, the maximum temperature in the firing zone, and its final quenching after its passage in the firing zone. Depending on the type of final grinding, some gypsum can be partially dehydrated into calcium hemihydrate or even totally dehydrated to form a calcium sulfate, improperly called anhydrite in the industry.

OPC hydration involves processes of dissolution and precipitation in a complex chemical system, resulting in the formation of different hydrates. This leads to the setting and the hardening of the cement. The products of silicate hydration are a gel of calcium silicate hydrate (C−S−H) and a crystalline phase, calcium hydroxide, also called portlandite (CH). The hydration reactions between aluminates and calcium sulfate lead to the formation of two different families of phases that are called trisulfoaluminoferrite hydrates (AFt), in which the most important phase is ettringite, and monosulfoaluminoferrite hydrates (AFm), composed of positively charged platelets of calcium and aluminum on octahedral coordination with oxygen. The AFm phases differ among each other by their counter-ions intercalated between the platelets: sulfate (the phase is called monosulfoaluminate), hydroxide (hydrocalumite), carbonate (monocarboaluminate), carbonate and hydroxyl (hemicarboaluminate), and chloride (Friedel's salt).

Science and Technology of Concrete Admixtures. http://dx.doi.org/10.1016/B978-0-08-100693-1.00008-4
Copyright © 2016 Elsevier Ltd. All rights reserved.

8.2 Hydration of C_3A

As C_3A is the most reactive phase in cement, its role in (very) early hydration is important and concerns both mechanical properties as well as rheological performances. In the absence of sulfates, C_3A reacts quickly with water and leads to a rapid and unintended setting called "flash set." This is due to the precipitation on the clinker surface of irregular hexagonal platelets of calcium aluminate hydrates, C_4AH_{19} or C_4AH_{13} (depending on the water activity) and C_2AH_8; both of them convert finally into a cubic hydrogarnet, C_3AH_6 (Taylor, 1997; Corstanje et al., 1973; Breval, 1976).

To avoid this rapid setting and therefore to keep a needed period of workability before the setting, calcium sulfate is added to and co-ground with the clinker during production to control C_3A hydration. In the presence of sulfates (here gypsum), the hydration of C_3A leads to the precipitation of ettringite:

$$C_3A + 3C\$H_2 + 26H \rightarrow C_6A\$_3H_{32} \tag{8.1}$$

Depending on the degree of supersaturation, ettringite presents different morphologies. These can vary from short hexagonal prisms to long needles (Mehta, 1969; Meredith et al., 2004). Ettringite is stable as long as sulfates are still available in the system. Provided that ettringite is forming, the concentration of aluminum in the pore solution is kept at low levels, which has important implications on the hydration of C_3S, as discussed later.

Once the sulfate depletion point is reached, ettringite reacts with the remaining C_3A to form monosulfoaluminate:

$$2C_3A + C_6A\$_3H_{32} + 4H \rightarrow 3C_4A\$H_{12} \tag{8.2}$$

The hydration of C_3A in the presence of sulfates is exothermic and isothermal calorimetry allows following the process and dividing it into three main stages (Figure 8.1) (Minard et al., 2007; Minard, 2003).

The high heat release in stage I represents the dissolution of anhydrous phases and the rapid precipitation of ettringite. This reaction is quite short and directly followed by a deceleration, which is not yet fully understood. This could be due to either the formation of a protective membrane of ettringite or AFm phases (Taylor, 1997; Gaidis and Gartner, 1989; Collepardi et al., 1978; Brown et al., 1984; Gupta et al., 1973), but more likely to the adsorption of sulfates on active sites of C_3A, with the effect of slowing down its dissolution (Minard et al., 2007; Skalny and Tadros, 1977; Feldman and Ramachandran, 1966; Manzano et al., 2009). Both hypotheses are the subject of debate. In the case of the protective membrane, Scrivener and Pratt (1984) mentioned that the ettringite morphology in needles could not provide a dense barrier layer that would slow down in a sufficient way hydration of cement (Bullard et al., 2011). Furthermore, AFm precipitation has been observed in both systems with or without calcium sulfates (Quennoz, 2011; Scrivener and Nonat, 2011). The fact that only the system with sulfates shows a rapid deceleration is therefore in contradiction with the protective layer composed of AFm.

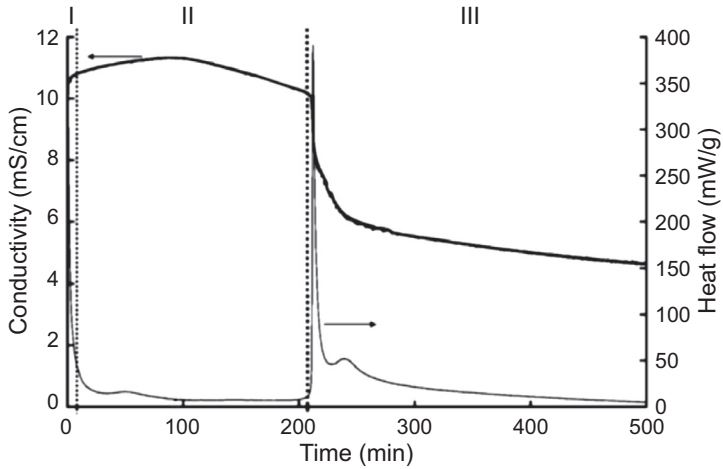


Figure 8.1 Heat release and conductivity measurements during hydration of C_3A with gypsum in saturated solution with respect to portlandite (L/S = 25).
Adapted from Minard et al. (2007) with authorization.

During stage II (Figure 8.1), although the heat release demonstrates that the reaction rate is low, a decrease in the conductivity in the middle of this stage (consequence of a consumption of sulfate and calcium ions) shows that ettringite is still forming (Minard, 2003).

Stage III starts when sulfate ions are no longer present in solution. At this point, a second sharp exothermic peak occurs, which is attributed to C_3A dissolution as well as to a faster precipitation of ettringite. During stage III, monosulfoaluminate precipitates from the reaction between ettringite and C_3A.

The source and the content of sulfates in the system have their importance, as they control the time of occurrence of the depletion point and therefore the length of stage II, the nature of the aluminate phases forming, as well as their morphology. For a low content of gypsum, an amorphous coating on C_3A particles has been observed and is attributed to an AFm type phase (Meredith et al., 2004). These reportedly form because normal hydration of aluminates cannot be totally prevented by a too low degree of sulfatation. In contrast, at high gypsum content, only ettringite formation has been reported (Hampson and Bailey, 1983). At intermediate gypsum content, at early age, normal precipitation of ettringite as well as formation of hydrocalumite (which converts slowly into a solid solution with monosulfoaluminate) have been observed (Minard et al., 2007; Scrivener and Pratt, 1984; Hampson and Bailey, 1983). However, when hemihydrate is used as sulfate carrier, the initial precipitation of hydroxy-AFm is not observed due to the higher solubility of hemihydrate, which releases sulfate ions faster (Pourchet et al., 2009).

8.3 Hydration of alite

Although C_3A is the most reactive phase, OPC hydration kinetics is dominated by alite hydration, as it is the main component of cement (50−70%).

8.3.1 Chemistry and stages of alite hydration

As stated, alite is a tricalcium silicate with impurities, such as aluminum, magnesium, iron, or sodium. Its hydration leads to the precipitation of C−S−H, an amorphous or poorly crystalline phase with variable stoichiometry, which is responsible for the strong development of the cement, and portlandite (CH), a crystalline phase:

$$C_3S + (3-x-n)\,H_2O \rightarrow C_x-S-H_n + (3-x)\,CH \tag{8.3}$$

Here, n represents the water to silicate ratio in C−S−H. The CaO to SiO_2 ratio varies between 1.2 and 2.1.

The hydration of alite can be divided into five to six periods, as described by Gartner et al. (2001) and shown in Figure 8.2. These stages are interpreted in relation to different rate-limiting mechanisms that are discussed in the following sections. Many of their aspects are still being debated and this does not make the task of understanding the impact of chemical admixtures on hydration easier. Therefore, we have attempted to summarize the main points of view present in the literature to provide a broader base for interpreting the retardation from chemical admixtures. In particular, we dedicate a special effort to the dissolution stage, which is of particular importance to chemical admixtures.

8.3.2 Stages 0 and I: initial dissolution

The first peak during stage 0 is due to the dissolution of alite, which is highly exothermic. This period lasts only a few minutes and is followed by a first deceleration in stage I and by a period of low reaction rates in stage II, which is called the induction

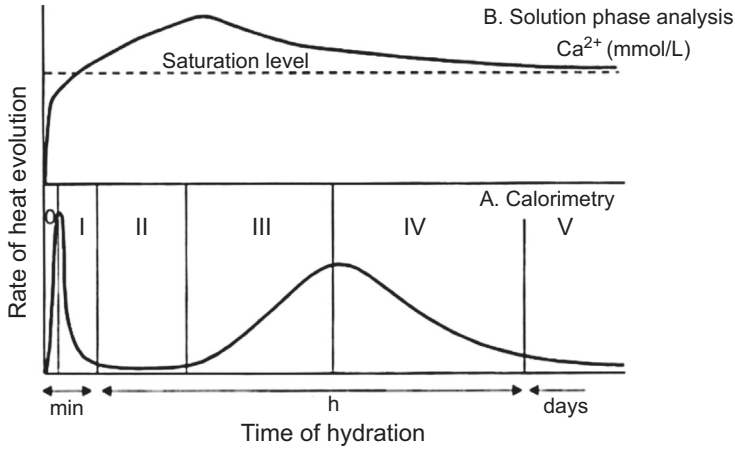


Figure 8.2 Illustration of the different stages of alite hydration following the Ca^{2+} concentration evolution and the associated heat release.
Adapted from Gartner et al. (2001).

period. The reasons for the first deceleration are not fully understood and various controversial hypotheses are discussed.

8.3.2.1 Protective membrane

The first hypothesis involves a protective membrane of hydrates on alite surface that prevents further dissolution and therefore slows down hydration reactions. This layer of metastable hydrates would either convert into a more permeable stable hydrate (Stein and Stevels, 1964; Kantro et al., 1962) or would break due to osmotic pressure, explaining the end of the induction period. By comparing solution concentrations of pore solutions, Gartner and Jennings (1987) proposed that a first metastable C−S−H with a higher solubility and protective properties precipitates on the C_3S surface. This metastable C−S−H would undergo a solid-state transformation into a more stable but permeable C−S−H with a lower solubility, causing the end of the induction period. Although nuclear magnetic resonance and X-ray photoelectron spectroscopy (XPS) measurements (Bellmann et al., 2010, 2012; Rodger et al., 1988) show the formation of an intermediate phase with different characteristics than the final C−S−H, no direct and visual evidence of such a continuous and impermeable layer has been observed.

8.3.2.2 Dissolution control

A theory based on crystal dissolution from geochemistry and applied on C_3S hydration has been used to explain the first deceleration and the induction period (Lasaga and Luttge, 2001; Juilland et al., 2010). This theory implies that the dissolution mechanisms depend on the solution concentrations and thus the degree of saturation. Three regimes of dissolution can be observed. At a very high undersaturation level, two-dimensional vacancy islands can nucleate on the surface with or without the help of impurities. This mechanism has a high activation energy barrier; as undersaturation decreases, it is not possible anymore to create etch pits on plain surfaces but on defects such as dislocations intersecting with the surface, which have an excess of energy. Close to equilibrium (at a low level of undersaturation), etch pit openings cannot be activated anymore, or at least only at a much lower frequency, and slow dissolution occurs by step retreat at pre-existing roughness. The rate of dissolution will therefore depend on the density of previously created etch pits. In support of this theory, it can be mentioned that an extensive pitting has been observed by Juilland et al. (2010) on alite surface in deionized water, whereas alite hydrated in saturated lime solution presents smoother surfaces. Additionally, calorimetric measurements performed on treated alite at 650 °C to remove defects on the surface have shown a quite long induction period.

Dissolution experiments performed by Nicoleau et al. (2013) on the C_3S dissolution rate in the function of undersaturation have shown similarities with the schematic representation of Juilland et al. (2010): dissolution kinetics of alite changes according to the solution concentration (Figure 8.3).

The change of dissolution mechanism from the creation of etch pits to the slow release of ions from preformed steps provides a satisfying explanation for the deceleration and the induction period, where the building up of calcium and silicate in solution

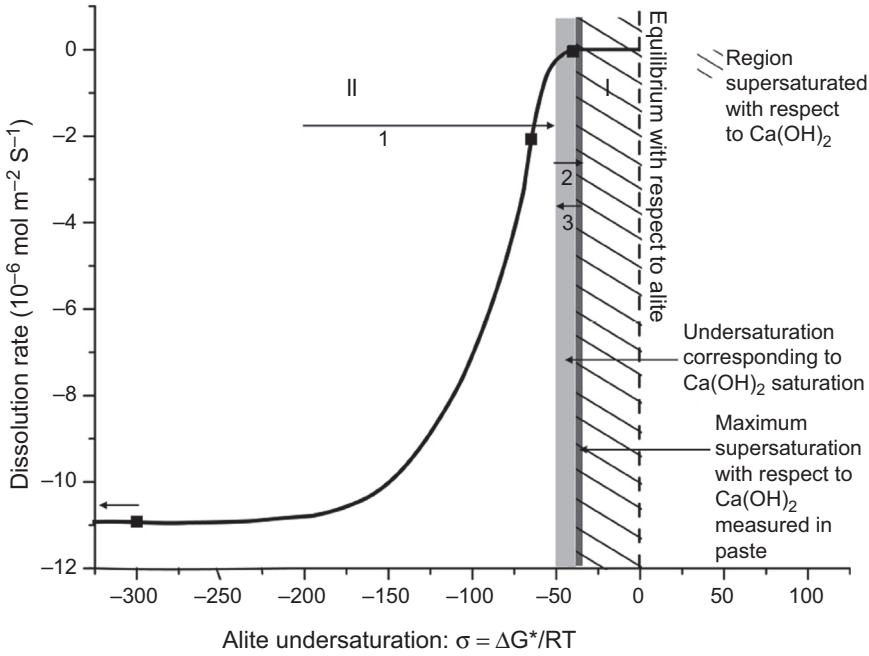


Figure 8.3 Schematic representation of the dissolution rate of alite as a function of undersaturation. Zone II represents the dissolution regimen controlled by etch pit formation and zone I is controlled by step retreat.
Reproduced from Juilland et al. (2010) with permission.

increases the saturation degree. Following this hypothesis, the onset of the acceleration period (i.e., the end of the induction period) would occur when reaching a high enough concentration for a critical event to occur, possibly the supersaturation needed to precipitate portlandite. Portlandite formation would increase the degree of undersaturation with respect to C−S−H, renew C_3S dissolution, and therefore offer a greater driving force for C−S−H precipitation (Bullard and Flatt, 2010; Young et al., 1977). However, limitations of the slow dissolution step hypothesis have been mentioned by Gartner (2011) because of a discrepancy between the effective solution concentration when the dissolution rate decreases and the theoretical values of C_3S solubility calculated from thermodynamics. But, as explained by Scrivener and Nonat (2011), this probably comes from the solubility of alite, determined by its bulk surface, which is different in its hydrolyzed state in water. More recently, it was proposed that dissolution kinetics alone are sufficient to explain hydration kinetics, provided its non-isotropic nature is taken into account (Nicoleau and Bertolim, 2015). In the same work it was also indicated that etch pits may be opened at a low frequency during the induction period with possibly important consequences on the overall hydration kinetics.

Physical parameters of the surface have a great importance regarding the dissolution process and kinetics. The most important ones are the particle size distribution and the specific surface area. The finer the cement powder, the higher is the specific surface and the higher is its reactivity. Other parameters include the density of defects

(MacInnis and Brantley, 1992), crystal orientation (Zhang and Lüttge, 2009), fracture surface, or damages coming from the grinding process (Mishra et al., in press).

8.3.3 Stage II: the induction period

For some authors, the induction period (stage II in Figure 8.2) corresponds to a latent time until a critical event as nucleation or polymerization of silicates takes place. The event would mark the end of the period of low chemical activity and the onset of the acceleration period. For others, the induction period is just the time in which a process of reducing rate (dissolution) is matched by a process of increasing rate (growth).

From this last perspective, the fast drop of silicate concentration already at the beginning of hydration proves that C−S−H nuclei form in the very first minutes after immersion in water and control the hydration kinetics (Garrault et al., 2005a,b; Garrault and Nonat, 2001; Thomas et al., 2009). During the induction period, C−S−H nuclei still form and, once they reach a certain critical size, start to grow, which represents the start of the acceleration period. The importance of the available surfaces provided initially by the nuclei for further growth has been shown in the study of Thomas et al. (2009), where stable C−S−H seeds added in hydrating C_3S accelerate notably the hydration by shifting the onset of the acceleration period to earlier times and increasing the slope of the main peak (Figure 8.4).

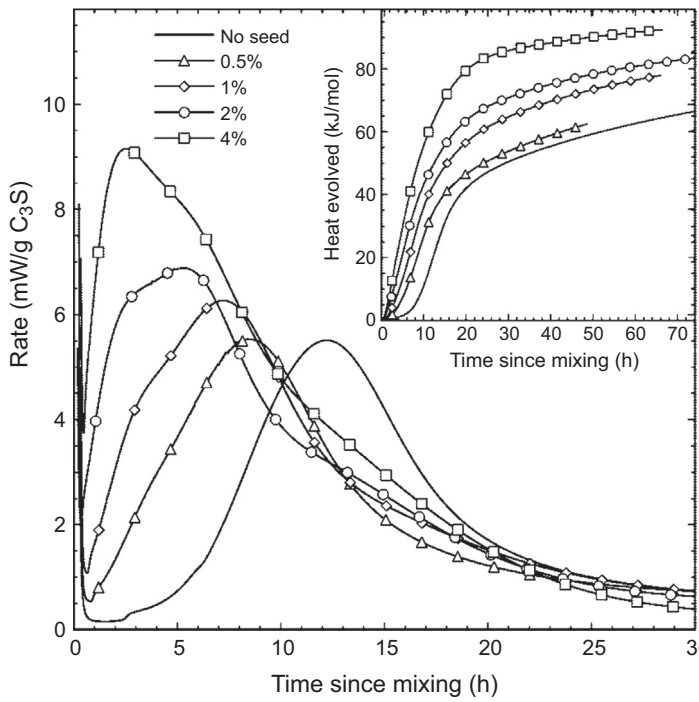


Figure 8.4 Impact of the addition of different dosages (% by weight of C_3S) of C−S−H seeds on hydration kinetics of C_3S.
Reproduced from Thomas et al. (2009) with permission.

This means that a certain amount of surface has to be reached to observe the significant precipitation of hydrates linked to the onset. This would imply that the induction and the acceleration periods are controlled by the nucleation and growth of hydrates, which is of course coupled with C_3S dissolution through ionic concentrations in the aqueous phase. Although this hypothesis can explain what is going on during the induction period and the start of the acceleration period, it does not explain the first rapid deceleration.

8.3.4 Stage III: the acceleration period

As seen above, during these first periods, concentrations of calcium and silicate increase until reaching a critical supersaturation level at which hydrates can nucleate and then grow. Stage III in Figure 8.2 represents the acceleration period, where the main peak of the heat release corresponds to a massive precipitation of C−S−H and CH responsible for setting and hardening. This is coupled with an increased dissolution of C_3S, which is mainly responsible for the heat release measured. It is generally agreed that in this period a heterogeneous nucleation and growth of hydrated controls the rate of hydration, which is assumed to be dependent on the C−S−H surface area (Gartner et al., 2001; Gartner and Gaidis, 1989; Zajac, 2007).

8.3.4.1 Structure of C−S−H

As mentioned above, C−S−H is poorly crystalline and is composed of sheets of calcium and oxygen surrounded by chains of tetrahedral silica, forming the main layers that are separated by water interlayers (Taylor, 1997). It is generally accepted that the C−S−H atomic structure is close to the ones of tobermorite and/or jennite—two crystalline phases that have a lower calcium-to-silicon ratio than C−S−H (Bonaccorsi et al., 2005, 2004; Richardson, 2004; Nonat, 2004). Nevertheless, the growth mechanism of C−S−H and its morphology are still a subject of much debate.

Two structural developments have been described: aggregation of nanoparticles (Jennings, 2000; Allen et al., 1987, 2007; Jennings et al., 2008) and large and defective sheets of silicate (Gartner, 1997; Gartner et al., 2000). In the first case, C−S−H particles would grow until reaching a maximum size of some nanometers. These nanoparticles would also provide new surfaces for further heterogeneous nucleation or agglomerate with other previously formed nanoparticles. This would explain the lack of long range order in C−S−H.

In the second case, Gartner (1997) assumed that the initially nucleated C−S−H particles have a tobermorite-like structure mostly consisting of only one layer, which grows as a two-dimensional product by the addition of silicate chains with regularly crystallized regions and others containing defects that present a certain curvature. A second sheet is assumed to nucleate on the perfect region of the first sheet. This second layer grows along the perfect region until reaching the curvature caused by the defects, where it separates and continues growing in an independent way. This process leads to well-organized nanocrystalline tobermorite-like structures surrounded by amorphous regions. This type of growth with branched nanoparticles might explain the cohesive characteristics of C−S−H as well as its lack of long range order.

Besides the uncertainty about the way C−S−H develops on a nanoscale, it also presents two types of more macroscopic morphology depending on where they develop. The first one is the outer product that develops from the boundary of the initial grain to wards the pore space and presents a fibrillar and directional morphology. The second one is the inner product, which forms in the volume originally filled by the anhydrous phase and presents a more compact and homogeneous morphology (Richardson, 1999, 2000; Bazzoni, 2014).

Concrete durability is dependent on the microstructure of the hydrated cement paste, and thus on the development and growth process of C−S−H. As mentioned earlier, Thomas et al. (2009) showed that the addition of C−S−H seeds not only increases the C_3S or cement hydration rate by providing more surface, but it also promotes hydrate precipitation in the capillary pore space, which is usually not possible in nonseeded systems (Figure 8.5). According to the authors, evidence of the occurrence of these two different processes can be observed on the calorimetric curves of Figure 8.4, where a shoulder appears before the main hydration peak of seeded systems and increases with the amount of added seeds. In the same study, scanning electron microscopy images performed on 28-days-old hydrated C_3S clearly show that the seeding provides a more uniform microstructure with a better distribution of C−S−H and less pores. This means that promoting a more homogeneous growth of hydrates impacts positively the microstructure by decreasing the capillary porosity. We can therefore expect that this should lead to better durability properties at equivalent

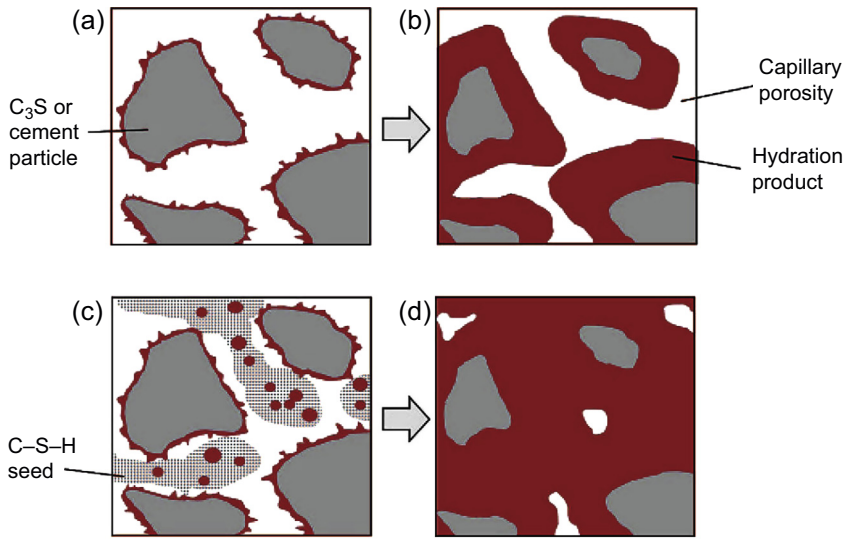


Figure 8.5 Schematic illustration of hydration process a few minutes (a) or several hours (b) after mixing a paste without seeding. The hydration product nucleates on the surface of the particles and grows toward the pore space. After some hours, the thickness of the hydration product limits further grows, which leads to a high volume of capillary porosity. With the seeding, hydration products precipitate on the surface of the particles and on C−S−H seeds after some minutes (c), which leads to less porosity after some hours (d).
Reproduced from Thomas et al. (2009) with permission.

mechanical strengths. Experimental investigation of this hypothesis would be an interesting subject to examine with important possible practical implications.

8.3.5 The deceleration period

Scanning transmission electron microscopy (STEM) images of early hydrated C_3S have confirmed that C−S−H grows as needles with a well-defined shape outside the grains (Bazzoni, 2014). The needles form on the C_3S surface until reaching a complete coverage that always corresponds to the maximum of the heat release, regardless of the impingement degree (and therefore the water content and the volume still free of hydrates). In the same study, to explain the deceleration of hydration leading to stage IV in Figure 8.2, Bazzoni proposed a transition from outer product to inner product growth. Instead of having new needles precipitating on previously formed ones, C−S−H would precipitate at the interface between anhydrous grains and the originally formed needles, leading to another slower growth mechanism.

This hypothesis shows a similarity with the model developed in Dijon (Garrault and Nonat, 2001; Garrault et al., 2005a,b), where the authors proposed that C−S−H precipitates and grows both parallel and perpendicular to the surface of the particles until full coverage is reached. At that point, the main hydration peak is reached and the model of Dijon assumes that C−S−H growth then only proceeds perpendicularly to the surface (outwards) on previously formed C−S−H. In this case, the lower rate of hydration is explained by a slower diffusion of ions through the hydrates. A transition to a diffusion regime because of denser hydrate layer has always been proposed for the deceleration but has never met all the conditions to explain the experimental observations.

Finally, the lower heat release of stage V corresponds to a limited transport process through the densifying microstructure.

8.4 Hydration of ordinary Portland cement

8.4.1 Stages of cement hydration

As already mentioned, Portland cement is composed mainly of silicates and a small amount of aluminates. Therefore, its heat release presents characteristics from the hydration of those anhydrous phases and can also be divided into five steps corresponding mainly to alite (or C_3S) hydration (Figure 8.6).

As for alite, the first exothermic peak in stage I is due to the wetting of the cement surface and to a fast dissolution of the anhydrous phases. Furthermore, in the very first minutes, ettringite precipitates due to the high reactivity of the aluminates and the availability of calcium sulfate. This sharp peak is followed by the sudden slowdown of the reaction and the induction period (stage II). As discussed earlier, the second main peak corresponds to the precipitation of the main products of the silicates hydration (stage III), with the increase in heat release mainly being due to the associated simultaneous increase in dissolution of C_3S. The reaction then slows down. This second deceleration can be seen in period 4. During this deceleration, a second peak occurs that represents the sulfate depletion point and, as explained earlier, corresponds to a faster precipitation of ettringite and a higher dissolution of C_3A. The last stage (V) is a period of low activity

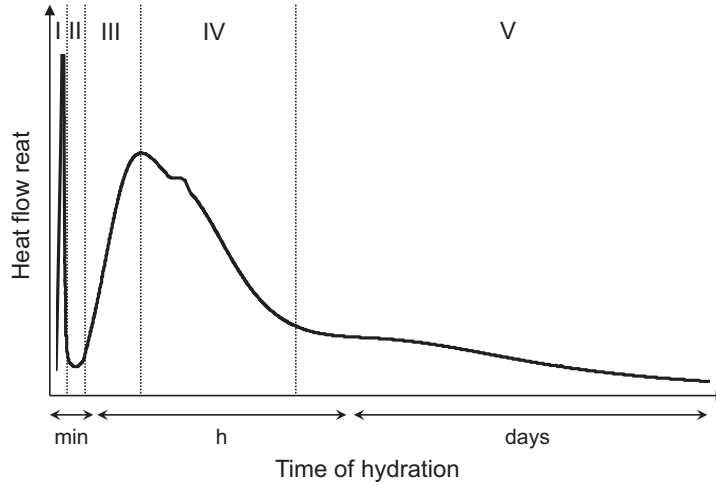


Figure 8.6 Schematic representation of the heat release and illustration of the different stages during the hydration of an ordinary Portland cement.

due to the slow diffusion of species in the hardened material and includes a third peak corresponding to the formation of AFm from the reaction between ettringite and C_3A.

8.4.2 *Silicate–aluminate–sulfate balance*

To understand all the mechanisms involved during cement hydration, studying the fundamental mechanisms with pure phases is a first step. However, it is also necessary to study the interaction between the different phases that might lead to other reactions or modify kinetics with respect to those observed in pure phase systems. Lerch (1946) and later Tenoutasse (1968) illustrated, in particular, the importance of the balance between the silicates, the aluminates, and the sulfates (Figure 8.7).

In a system with 80 wt% of pure C_3S and 20 wt% of C_3A, Tenoutasse showed that in the absence of sulfates, the aluminate hydration largely suppresses the silicate hydration. However, as gypsum is added, the extent of C_3S hydration also increases. This addition also delays the sulfate depletion point. At a certain dosage (about 4% in the case shown in Figure 8.7), there is an inversion of both peaks, so that the sulfate depletion point occurs right after the main silicate peak. From this dosage on, adding more sulfates further delays the sulfate depletion point but does not influence the silicate peak.

The explanation for this is thought to lie in the availability of aluminum ions in the pore solution. Several studies have indeed shown that they negatively impact C_3S hydration (Quennoz, 2011; Odler and Schüppstuhl, 1981; Quennoz and Scrivener, 2013; Begarin et al., 2011; Suraneni and Flatt, 2015). A longer induction period has been observed by Odler and Schüppstuhl (1981) after the addition of aluminum in the system. More recently, Minard (2003) and Quennoz (2011) observed that the extent of C_3S hydration can be decreased either by the addition of aluminum ions in the aqueous phase or by the release of ions from the dissolution of aluminum containing alite (Quennoz and Scrivener, 2013).

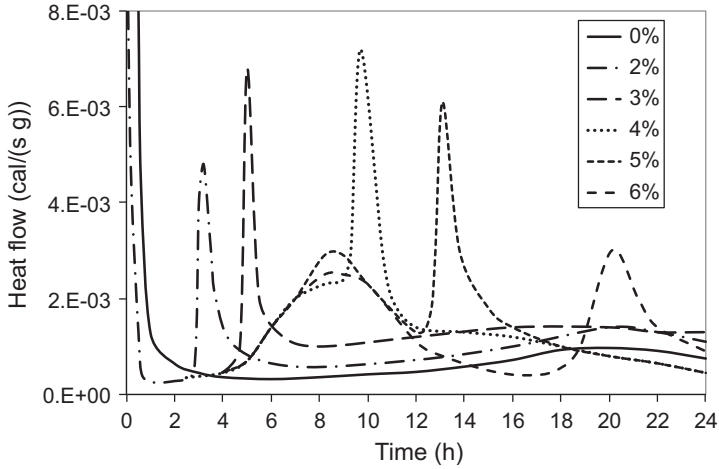


Figure 8.7 Isothermal calorimetry obtained on mixtures of 80% alite and 20% C_3A in the presence of variable amounts of gypsum (given in the insert).
Adapted from Tenoutasse (1968).

The addition of sulfates results in the consumption of free aluminum ions through the precipitation of ettringite. The low solubility of this mineral further contributes to reducing the concentration of aluminum ions in the aqueous phase, thereby preventing them from negatively affecting alite hydration. Here again, a number of open questions subsist. For example, the detailed mechanism through which aluminum affects alite hydration is still debated. One of the explanations proposed is that released aluminum ions precipitate as C−A−S−H particles, which cannot act as seeds for further C−S−H growth (Begarin et al., 2011).

Studies performed on silica-containing materials such as quartz or amorphous silicates showed that the adsorption of aluminum on their surface prevents their dissolution (Lewin, 1961; Bickmore et al., 2006; Iler, 1973; Chappex and Scrivener, 2012). Therefore, we must also consider that in cement it may be aluminum adsorption rather than C−A−S−H formation that is responsible for reduced dissolution. In fact, Nicoleau et al. (2014) showed that aluminate ions do not physically adsorb but covalently bind onto the surface of the silicate, which strongly inhibits C_3S dissolution. Although the condensation of these alumino-silicate species is favored at moderate alkaline conditions, which can be met only in the very first minutes of cement hydration, the authors mentioned that their stabilization is possible at higher pH thanks to the presence of calcium ions.

Most importantly, in the context of this book, the role of aluminum on cement hydration cannot be neglected. Moreover, its significance increases as more and more supplementary cementitious materials (which generally involve a high content of aluminum) are used in modern and more environment-friendly concrete. In Chapter 12, we discuss the consequences that admixtures can have on hydration if they perturb the aluminate−silicate−sulfate balance (Marchon and Flatt, 2016).

8.5 Conclusions

Although fundamental steps have been made in the comprehension of the different hydration mechanisms, important points are still subjects of debate. The main unresolved questions can be summarized as follows:

- Determining the rate-controlling steps for each period (this is a complex task because the different hydration processes cannot be easily isolated)
- Describing the growth mechanism and the exact structure of C−S−H
- Quantifying the impact of the balance between the silicates, sulfates, and aluminates (in particular, the exact role that aluminum plays during silicate hydration should be better defined, something that is highly relevant for many supplementary cementitious materials)

Another level of complexity is added with the use of different types of chemical admixtures that are known to disturb individually the overall hydration mechanism by interacting with these different aspects (see Chapter 12: Marchon and Flatt, 2016). This makes for modern concrete containing supplementary cementitious materials and chemical admixtures, a particularly complex system to master. It has therefore been a main objective of this chapter to present the mechanistic basis of cement hydration, which Chapter 12 will rely on to discuss mechanisms of retardation (Marchon and Flatt, 2016). We consider that this issue has become more important since low clinker concrete formulations tend to have limited early strength, so retardation will become increasingly less acceptable than it was in the past.

Acknowledgments

Support for Delphine Marchon was provided by Sika Technology Ag (Zürich, Switzerland).

References

Aïtcin, P.-C., 2016. Portland cement. In: Aïtcin, P.-C., Flatt, R.J. (Eds.), Science and Technology of Concrete Admixtures, Elsevier (Chapter 3), pp. 27−52.

Allen, A.J., Oberthur, R.C., Pearson, D., Schofield, P., Wilding, C.R., 1987. Development of the fine porosity and gel structure of hydrating cement systems. Philosophical Magazine Part B 56 (3), 263−288. http://dx.doi.org/10.1080/13642818708221317.

Allen, A.J., Thomas, J.J., Jennings, H.M., 2007. Composition and density of nanoscale calcium−silicate−hydrate in cement. Nature Materials 6 (4), 311−316. http://dx.doi.org/10.1038/nmat1871.

Bazzoni, A., 2014. Study of Early Hydration Mechanisms of Cement by Means of Electron Microscopy. EPFL, Lausanne.

Begarin, F., Garrault, S., Nonat, A., Nicoleau, L., 2011. Hydration of alite containing aluminium. Advances in Applied Ceramics 110 (3), 127−130. http://dx.doi.org/10.1179/1743676110Y.0000000007.

Bellmann, F., Damidot, D., Möser, B., Skibsted, J., 2010. Improved evidence for the existence of an intermediate phase during hydration of tricalcium silicate. Cement and Concrete Research 40 (6), 875−884. http://dx.doi.org/10.1016/j.cemconres.2010.02.007.

Bellmann, F., Sowoidnich, T., Ludwig, H.-M., Damidot, D., 2012. Analysis of the surface of tricalcium silicate during the induction period by X-ray photoelectron spectroscopy. Cement and Concrete Research 42 (9), 1189–1198. http://dx.doi.org/10.1016/j.cemconres.2012.05.011.

Bickmore, B.R., Nagy, K.L., Gray, A.K., Brinkerhoff, A.R., 2006. The effect of $Al(OH)_4^-$ on the dissolution rate of quartz. Geochimica et Cosmochimica Acta 70 (2), 290–305. http://dx.doi.org/10.1016/j.gca.2005.09.017.

Bonaccorsi, E., Merlino, S., Kampf, A.R., 2005. The crystal structure of tobermorite 14 Å (Plombierite), a C–S–H phase. Journal of the American Ceramic Society 88 (3), 505–512. http://dx.doi.org/10.1111/j.1551-2916.2005.00116.x.

Bonaccorsi, E., Merlino, S., Taylor, H.F.W., 2004. The crystal structure of jennite, $Ca_9Si_6O_{18}(OH)_6 \cdot 8H_2O$. Cement and Concrete Research 34 (9), 1481–1488.

Breval, E., 1976. C3A hydration. Cement and Concrete Research 6 (1), 129–137. http://dx.doi.org/10.1016/0008-8846(76)90057-0.

Brown, P.W., Liberman, L.O., Frohnsdorff, G., 1984. Kinetics of the early hydration of tricalcium aluminate in solutions containing calcium sulfate. Journal of the American Ceramic Society 67 (12), 793–795. http://dx.doi.org/10.1111/j.1151-2916.1984.tb19702.x.

Bullard, J.W., Flatt, R.J., 2010. New insights into the effect of calcium hydroxide precipitation on the kinetics of tricalcium silicate hydration. Journal of the American Ceramic Society 93 (7), 1894–1903. http://dx.doi.org/10.1111/j.1551-2916.2010.03656.x.

Bullard, J.W., Jennings, H.M., Livingston, R.A., Nonat, A., Scherer, G.W., Schweitzer, J.S., Scrivener, K.L., Thomas, J.J., 2011. Mechanisms of cement hydration. Cement and Concrete Research, Conferences Special: Cement Hydration Kinetics and Modeling, Quebec City, 2009 & CONMOD10, Lausanne, 2010, 41 (12), 1208–1223. http://dx.doi.org/10.1016/j.cemconres.2010.09.011.

Chappex, T., Scrivener, K.L., 2012. The influence of aluminium on the dissolution of amorphous silica and its relation to alkali silica reaction. Cement and Concrete Research 42 (12), 1645–1649. http://dx.doi.org/10.1016/j.cemconres.2012.09.009.

Collepardi, M., Baldini, G., Pauri, M., Corradi, M., 1978. Tricalcium aluminate hydration in the presence of lime, gypsum or sodium sulfate. Cement and Concrete Research 8 (5), 571–580. http://dx.doi.org/10.1016/0008-8846(78)90040-6.

Corstanje, W.A., Stein, H.N., Stevels, J.M., 1973. Hydration reactions in pastes $C_3S + C_3A + CaSO_4 \cdot 2aq + H_2O$ at 25°C.I. Cement and Concrete Research 3 (6), 791–806. http://dx.doi.org/10.1016/0008-8846(73)90012-4.

Feldman, R.F., Ramachandran, V.S., 1966. Character of hydration of $3CaO \cdot Al_2O_3$. Journal of the American Ceramic Society 49 (5), 268–273. http://dx.doi.org/10.1111/j.1151-2916.1966.tb13255.x.

Gaidis, J.M., Gartner, E.M., 1989. Hydration mechanism II. In: Skalny, J., Mindess, S. (Eds.), Materials Science of Concrete, vol. 2. American Ceramic Society, pp. 9–39.

Garrault, S., Behr, T., Nonat, A., 2005a. Formation of the C–S–H layer during early hydration of tricalcium silicate grains with different sizes. The Journal of Physical Chemistry B 110 (1), 270–275. http://dx.doi.org/10.1021/jp0547212.

Garrault, S., Finot, E., Lesniewska, E., Nonat, A., 2005b. Study of C–S–H growth on C_3S surface during its early hydration. Materials and Structures 38 (4), 435–442. http://dx.doi.org/10.1007/BF02482139.

Garrault, S., Nonat, A., 2001. Hydrated layer formation on tricalcium and dicalcium silicate surfaces: experimental study and numerical simulations. Langmuir 17 (26), 8131–8138. http://dx.doi.org/10.1021/la011201z.

Gartner, E.M., 1997. A proposed mechanism for the growth of C−S−H during the hydration of tricalcium silicate. Cement and Concrete Research 27 (5), 665−672. http://dx.doi.org/10.1016/S0008-8846(97)00049-5.

Gartner, E., 2011. Discussion of the paper 'dissolution theory applied to the induction period in alite hydration' by P. Juilland et al., Cement Concrete Research. 40 (2010), 831−844. Cement and Concrete Research 41 (5), 560−562. http://dx.doi.org/10.1016/j.cemconres.2011.01.019.

Gartner, E.M., Gaidis, J.M., 1989. Hydration mechanisms I. In: Materials Science of Concrete III, vol. 95.

Gartner, E.M., Jennings, H.M., 1987. Thermodynamics of calcium silicate hydrates and their solutions. Journal of the American Ceramic Society 70 (10), 743−749. http://dx.doi.org/10.1111/j.1151-2916.1987.tb04874.x.

Gartner, E.M., Kurtis, K.E., Monteiro, P.J.M., 2000. Proposed mechanism of C−S−H growth tested by soft X-ray microscopy. Cement and Concrete Research 30 (5), 817−822. http://dx.doi.org/10.1016/S0008-8846(00)00235-0.

Gartner, E.J., Young, J.F., Damidot, D.A., Jawed, I., 2001. Chapter 3: hydration of Portland cement. In: Bensted, J., Barnes, P. (Eds.), Structure and Performance of Cements, second ed.

Gupta, P.S., Chatterji, S., Jeffrey, W., 1973. Studies of the effect of different additives on the hydration of tricalcium aluminate: Part 5−a mechanicsm of retardation of C_3A hydration. Cement Technology 4, 146−149.

Hampson, C.J., Bailey, J.E., 1983. The microstructure of the hydration products of tri-calcium aluminate in the presence of gypsum. Journal of Materials Science 18 (2), 402−410. http://dx.doi.org/10.1007/BF00560628.

Iler, R.K., 1973. Effect of adsorbed alumina on the solubility of amorphous silica in water. Journal of Colloid and Interface Science, Kendall Award Symposium 163rd American Chemical Society Meeting 43 (2), 399−408. http://dx.doi.org/10.1016/0021-9797(73)90386-X.

Jennings, H.M., 2000. A model for the microstructure of calcium silicate hydrate in cement paste. Cement and Concrete Research 30 (1), 101−116. http://dx.doi.org/10.1016/S0008-8846(99)00209-4.

Jennings, H.M., Bullard, J.W., Thomas, J.J., Andrade, J.E., Chen, J.J., Scherer, G.W., 2008. Characterization and modeling of pores and surfaces in cement paste: correlations to processing and properties. Journal of Advanced Concrete Technology 6 (1), 5−29.

Juilland, P., Gallucci, E., Flatt, R., Scrivener, K., 2010. Dissolution theory applied to the induction period in alite hydration. Cement and Concrete Research 40 (6), 831−844. http://dx.doi.org/10.1016/j.cemconres.2010.01.012.

Kantro, D.L., Brunauer, S., Weise, C.H., 1962. Development of surface in the hydration of calcium silicates. II. Extension of investigations to earlier and later stages of hydration. The Journal of Physical Chemistry 66 (10), 1804−1809. http://dx.doi.org/10.1021/j100816a007.

Lasaga, A.C., Luttge, A., 2001. Variation of crystal dissolution rate based on a dissolution Stepwave model. Science 291 (5512), 2400−2404. http://dx.doi.org/10.1126/science.1058173.

Lerch, W., 1946. The influence of gypsum on the hydration and properties of Portland cement pastes. Proceedings of the American Society for Testing Materials 46.

Lewin, J.C., 1961. The dissolution of silica from diatom walls. Geochimica et Cosmochimica Acta 21 (3−4), 182−198. http://dx.doi.org/10.1016/S0016-7037(61)80054-9.

MacInnis, I.N., Brantley, S.L., 1992. The role of dislocations and surface morphology in calcite dissolution. Geochimica et Cosmochimica Acta 56 (3), 1113−1126. http://dx.doi.org/10.1016/0016-7037(92)90049-O.

Manzano, H., Dolado, J.S., Ayuela, A., 2009. Structural, mechanical, and reactivity properties of tricalcium aluminate using first-principles calculations. Journal of the American Ceramic Society 92 (4), 897–902. http://dx.doi.org/10.1111/j.1551-2916.2009.02963.x.

Marchon, D., Flatt, R.J., 2016. Impact of chemical admixtures on cement hydration. In: Aïtcin, P.-C., Flatt, R.J. (Eds.), Science and Technology of Concrete Admixtures, Elsevier (Chapter 12), pp. 279–304.

Mehta, P.K., 1969. Morphology of calcium sulfoaluminate hydrates. Journal of the American Ceramic Society 52 (9), 521–522. http://dx.doi.org/10.1111/j.1151-2916.1969.tb09215.x.

Meredith, P., Donald, A.M., Meller, N., Hall, C., 2004. Tricalcium aluminate hydration: microstructural observations by in-situ electron microscopy. Journal of Materials Science 39 (3), 997–1005. http://dx.doi.org/10.1023/B; JMSC.0000012933.74548.36.

Minard, H., 2003. Etude Intégrée Des Processus D'hydratation, de Coagulation, de Rigidification et de Prise Pour Un Système C_3S–C_3A–Sulfates–Alcalins. Université de Bourgogne, Dijon, France.

Minard, H., Garrault, S., Regnaud, L., Nonat, A., 2007. Mechanisms and parameters controlling the tricalcium aluminate reactivity in the presence of Gypsum. Cement and Concrete Research 37 (10), 1418–1426. http://dx.doi.org/10.1016/j.cemconres.2007.06.001.

Mishra, R.K., Geissbuhler, D., Carmona, H.A., Wittel, F.K., Sawley, M.L., Weibel, M., Gallucci, E., Herrmann, H.J., Heinz, H. Flatt, R.J., (in press). En route to multimodel scheme for clinker with chemical grinding aids. Advances in Applied Ceramics. http://dx.doi.org/10.1179/1743676115Y.0000000023.

Nicoleau, L., Bertolim, 2015. Analytical Model for the Alite (C_3S) Dissolution Topography, JACerS.

Nicoleau, L., Nonat, A., Perrey, D., May 2013. The di- and tricalcium silicate dissolutions. Cement and Concrete Research 47, 14–30. http://dx.doi.org/10.1016/j.cemconres.2013.01.017.

Nicoleau, L., Schreiner, E., Nonat, A., May 2014. Ion-specific effects influencing the dissolution of tricalcium silicate. Cement and Concrete Research 59, 118–138. http://dx.doi.org/10.1016/j.cemconres.2014.02.006.

Nonat, A., 2004. The structure and stoichiometry of C–S–H. Cement and Concrete Research 34 (9), 1521–1528. http://dx.doi.org/10.1016/j.cemconres.2004.04.035. H.F.W. Taylor Commemorative Issue.

Odler, I., Schüppstuhl, J., 1981. Early hydration of tricalcium silicate III. Control of the induction period. Cement and Concrete Research 11 (5–6), 765–774. http://dx.doi.org/10.1016/0008-8846(81)90035-1.

Pourchet, S., Regnaud, L., Perez, J.P., Nonat, A., 2009. Early C_3A hydration in the presence of different kinds of calcium sulfate. Cement and Concrete Research 39 (11), 989–996. http://dx.doi.org/10.1016/j.cemconres.2009.07.019.

Quennoz, A., 2011. Hydration of C_3A with Calcium Sulfate Alone and in the Presence of Calcium Silicate. EPFL, Lausanne.

Quennoz, A., Scrivener, K.L., February 2013. Interactions between alite and C_3A-Gypsum hydrations in model cements. Cement and Concrete Research 44, 46–54. http://dx.doi.org/10.1016/j.cemconres.2012.10.018.

Richardson, I.G., 1999. The nature of C–S–H in hardened cements. Cement and Concrete Research 29 (8), 1131–1147. http://dx.doi.org/10.1016/S0008-8846(99)00168-4.

Richardson, I.G., 2000. The nature of the hydration products in hardened cement pastes. Cement and Concrete Composites 22 (2), 97–113. http://dx.doi.org/10.1016/S0958-9465(99)00036-0.

Richardson, I.G., 2004. Tobermorite/jennite- and Tobermorite/calcium hydroxide-based models for the structure of C−S−H: applicability to hardened pastes of tricalcium silicate, B-dicalcium silicate, Portland cement, and blends of Portland cement with blast-furnace slag, Metakaolin, or silica fume. Cement and Concrete Research 34 (9), 1733−1777. H.F.W. Taylor Commemorative Issue. http://dx.doi.org/10.1016/j.cemconres.2004.05.034.

Rodger, S.A., Groves, G.W., Clayden, N.J., Dobson, C.M., 1988. Hydration of tricalcium silicate followed by 29Si NMR with cross-polarization. Journal of the American Ceramic Society 71 (2), 91−96. http://dx.doi.org/10.1111/j.1151-2916.1988.tb05823.x.

Scrivener, K.L., Nonat, A., 2011. Hydration of cementitious materials, present and future. Cement and Concrete Research 41 (7), 651−665. Special Issue: 13th International Congress on the Chemistry of Cement. http://dx.doi.org/10.1016/j.cemconres.2011.03.026.

Scrivener, K.L., Pratt, P.L., 1984. Microstructural studies of the hydration of C_3A and C_4AF independently and in cement paste. In: Proc. Br. Ceram. Soc., vol. 35.

Skalny, J., Tadros, M.E., 1977. Retardation of tricalcium aluminate hydration by sulfates. Journal of the American Ceramic Society 60 (3−4), 174−175. http://dx.doi.org/10.1111/j.1151-2916.1977.tb15503.x.

Stein, H.N., Stevels, J.M., 1964. Influence of silica on the hydration of $3CaO \cdot SiO_2$. Journal of Applied Chemistry 14 (8), 338−346. http://dx.doi.org/10.1002/jctb.5010140805.

Suraneni, P., Flatt, R.J., 2015. Use of micro-reactors to obtain new insights into the factors influencing tricalcium silicate dissolution. Cement and Concrete Research 78, 208−215. http://www.sciencedirect.com/science/article/pii/S0008884615002082.

Taylor, H.F.W., 1997. Cement Chemistry, second ed. Thomas Telford.

Tenoutasse, N., 1968. The hydration mechanism of C_3A and C_3S in the presence of calcium chloride and calcium sulfate. In: Proceedings of the 5th International Symposium on the Chemistry of Cement, No. II-118, pp. 372−378.

Thomas, J.J., Jennings, H.M., Chen, J.J., 2009. Influence of nucleation seeding on the hydration mechanisms of tricalcium silicate and cement. The Journal of Physical Chemistry C 113 (11), 4327−4334. http://dx.doi.org/10.1021/jp809811w.

Young, J.F., Tong, H.S., Berger, R.L., 1977. Compositions of solutions in contact with hydrating tricalcium silicate pastes. Journal of the American Ceramic Society 60 (5−6), 193−198. http://dx.doi.org/10.1111/j.1151-2916.1977.tb14104.x.

Zajac, M., 2007. Etude Des Relations Entre Vitesse D'hydratation, Texturation Des Hydrates et Résistance Mécanique Finale Des Pâtes et Micro-Mortiers de Ciment Portland. Dijon. http://www.theses.fr/2007DIJOS006.

Zhang, L., Lüttge, A., 2009. Morphological evolution of dissolving feldspar particles with anisotropic surface kinetics and implications for dissolution rate normalization and grain size dependence: a kinetic modeling study. Geochimica et Cosmochimica Acta 73 (22), 6757−6770. http://dx.doi.org/10.1016/j.gca.2009.08.010.

Chemistry of chemical admixtures

9

G. Gelardi[1], S. Mantellato[1], D. Marchon[1], M. Palacios[1], A.B. Eberhardt[2], R.J. Flatt[1]
[1]Institute for Building Materials, ETH Zürich, Zürich, Switzerland; [2]Sika Technology AG, Zürich, Switzerland

9.1 Introduction

Chemical admixtures are nowadays very important for concrete design, and are essential for the formulation of concrete with a low environmental impact (Flatt et al., 2012).

Chemical admixtures can modify the properties of fresh or hardened concrete or, in some cases, both. Superplasticizers and viscosity-modifying admixtures, discussed in more detail in Chapters 16 (Nkinamubanzi et al., 2016) and 20 (Palacios and Flatt, 2016) respectively, modify the rheological behaviour of fresh concrete. Retarders and accelerators modify cement hydration, with implications for concrete placing, and are discussed in Chapters 18 and 19 (Aïtcin, 2016b,c). Admixtures such as air entrainers and shrinkage reducers enhance durability; these are dealt with in Chapters 17 and 23 (Gagnè, 2016a,b).

Besides their main effect, many admixtures have secondary effects. For example, most compounds used as water reducers or high-range water reducers can cause some retardation of cement hydration, depending on factors such as dosage and molecular structure. In some circumstances these secondary effects can be beneficial, while in others they are undesired. The influence that chemical admixtures have on cement hydration (Marchon and Flatt, 2016a, Chapter 8) is dealt with in Chapter 12 (Marchon and Flatt, 2016b).

Many chemical admixtures are effective at low or very low dosages, and the reason for this is that they act at the interface, either solid−liquid (as for superplasticizers) or liquid−vapour (as for shrinkage-reducing and air-entraining admixtures). The adsorption of chemical admixtures at an interface is discussed in Chapter 10 (Marchon et al., 2016). The working mechanisms of admixtures are discussed in various chapters of this book, requiring in many cases a good knowledge of their chemical structure.

The main objective of this chapter is to regroup the information about molecular structure of chemical admixtures to make it easier to compare compounds among each other. It also serves as a source of chemical structures that may be consulted if this information is needed for any other chapters.

In preparing this chapter we decided to focus our presentation on organic chemical admixtures. This choice was guided by the fact that this is where the real added value of molecular structure comes into play in terms of design of new or modified chemical admixtures. It is therefore our hope that the chapter may serve not only as a general reference for people wanting to know about chemical admixtures, but also that it

Science and Technology of Concrete Admixtures. http://dx.doi.org/10.1016/B978-0-08-100693-1.00009-6
Copyright © 2016 Elsevier Ltd. All rights reserved.

may give chemists a comprehensive overview of molecular structures used in practice and inspire them to design new and/or improved compounds.

9.2 Water reducers and superplasticizers

9.2.1 Introduction

In this section the chemistry of the main types of superplasticizers (SPs), also called high-range water-reducing admixtures, is presented.

The first part is dedicated to natural polymers, which are rather plasticizers or mid-range water-reducing admixtures. The use of such dispersants dates back to the 1930s. Although the performance of natural polymers is limited compared to synthetic ones, it is worth mentioning them as they are still widely used in the concrete industry—mainly because of their low cost of production.

Next, synthetic linear polymers are described. This category includes some of the most commonly used SPs, such as polynaphthalene sulphonates (PNS), polymelamine sulphonates (PMS) and vinyl copolymers. The higher dispersing ability of these compounds qualifies them as true SPs or high-range water reducers (in contrast to lignosulphonates or other low- or mid-range water reducers). They were introduced during the 1960s and are generally referred to as electrostatic dispersants, although some show predominant steric effects. They made it possible to develop high-performance concrete as a reliable form now used in numerous structures. The practical use of SPs is dealt with in Chapter 16 (Nkinamubanzi et al., 2016).

Finally, the new generation of SPs, namely comb-shaped copolymers, is introduced. The development of comb-shaped SPs in the 1980s represented a breakthrough in concrete technology, as they allow use of a very low water/cement ratio (w/c of 0.20 or less) while keeping good workability. In this regard, one should in particular acknowledge that the formulation and large-scale use of self-compacting concrete (Okamura and Ouchi, 1999) have greatly benefited from the introduction of such admixtures. But these polymers have also found a place in ultra-high-strength concrete (Mitsui et al., 1994). Comb-shaped copolymers are steric admixtures, meaning that their dispersing ability is due to steric effects rather than electrostatic repulsion (even if, as mentioned previously, linear polymers often also work via steric hindrance, this terminology persists and it would be better to qualify comb-copolymer as "more effective" steric dispersants). The successful use of these SPs comes mainly from the possibility of tailoring their design, in terms of both chemical groups and molecular structure, to obtain SPs with different performance and applications (ready-mix concrete, pre-cast concrete, etc.).

9.2.2 Natural polymers

9.2.2.1 Lignosulphonates

Lignosulphonates (LSs) were the first dispersants added as water-reducing admixtures to concrete. LSs have been used since the 1930s as plasticizers and water reducers (Scripture, 1937) and ready-mix concrete represents their largest application.

LSs are obtained as by-products of bisulphite pulping of wood, which is used to separate pure cellulose fibres by dissolution of hemicellulose and lignin. Lignin is a natural and renewable biopolymer present in wood and is, after cellulose, the second most abundant organic molecule on Earth. The lignin content depends on the wood species: it is higher in softwood (27–37%) than in hardwood (16–29%). The production of extracted lignin amounts to 70 million tons per year: the majority is burnt for energy recovery and regeneration of pulping chemicals, and only 5% is used as a chemical product. Native lignin is water-insoluble, and presents a complex three-dimensional network built from randomly cross-linked monolignols, such as coumaryl, conyferil and synapyl alcohols.

The chemical process of sulphite pulping (delignification) involves the use of sulphite (SO_3^{2-}) or bisulphite (HSO_3^-) salts (typically sodium, magnesium, ammonium or calcium) at high temperatures (140–170 °C). During this process, lignin with a reduced molecular weight is formed because of the breaking of ester bonds that interconnect lignin units (fragmentation). At the same time the introduction of sulphonic groups on the aliphatic chains makes the lignin water-soluble (sulphonation). The insoluble cellulose fibres are separated from LSs by filtration. The resulting by-product, called 'spent liquor', contains poorly sulphonated lignins of different molecular size, inorganic salts, extracts from wood and pentose and hexose sugars coming from the acidic hydrolysis of the hemicellulose. LSs for concrete applications are further modified to achieve the desired properties.

Earlier presented as a spherical microgel unit, the structure of LSs has now been described as randomly branched polyelectrolyte macromolecules (Myrvold, 2008). The structure is formed by phenyl propane units connected in a non-regular manner by ether or C–C bonds, the latter between the aromatic rings. To optimize both water solubility and plasticizing effect, the degree of sulphonation is increased, typically up to 0.5–0.7 per phenyl propane unit, by sulphomethylation with sodium sulphite and formaldehyde. The sulphonate groups are distributed foremost on the surface of LS molecules.

LSs contain numerous functional groups, such as carboxylic acid, phenolic hydroxyl, cathechol, methoxyl, sulphonic acid and various combinations of these. The structure of a commercial LS is shown in Figure 9.1.

The solubility in water is influenced not only by the degree of sulphonation and polymerization, but also by the cation, usually sodium or calcium, used in the admixture production. Unlike calcium LSs, sodium LSs are generally more soluble, even at low temperatures (below −10 °C), preventing precipitation under cold conditions. Moreover, at constant concentration of counterion, the degree of ionization is higher in sodium LSs. However, calcium LSs are typically cheaper than sodium LSs, offsetting the cost of the extra dosage used to achieve a comparable dispersion.

Approximately 25% of the total solids in spent liquor is sugars, which can have a strong retarding effect on concrete setting time (see Marchon and Flatt, 2016b, Chapter 12). LSs can be purified and sugar content reduced by precipitation, alkaline heat treatment, ultrafiltration or amine extraction. However also sugar-free LSs show very pronounced retardation, so that the role of sugars is often stated as either secondary or complimentary. (Reknes and Gustafsson, 2000).

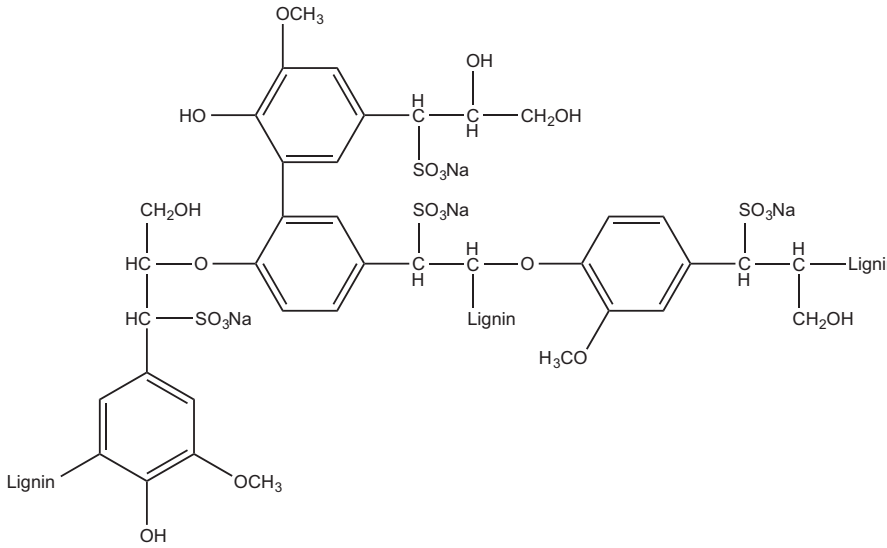


Figure 9.1 Chemical structure of a lignosulphonate.

The molecular weight of commercial LSs ranges from a few thousand to 150,000 Da, showing a much greater polydispersity than synthetic polymers. Ultrafiltration can be applied to narrow the molar mass distribution.

The degree of sulphonation increases with decreasing molecular weight, but it does not depend on the type of wood. Additionally, it was demonstrated that hardwood LSs have significantly lower molecular weights than softwood LSs (Fredheim et al., 2002).

The molecular weight of LSs and their fractions was typically characterized by size exclusion chromatography combined with either ultraviolet (UV) or multi-angle laser light-scattering detectors, but more techniques are available nowadays (Fredheim et al., 2002; Brudin and Schoenmakers, 2010). The study of LS adsorption on cement can be carried out by UV absorption at 280 nm prior to a calibration with the LS under investigation (Gustafsson and Reknes, 2000).

LSs as dispersants in concrete show a limited water reduction capability (8−10%), with an averaged dosage of about 0.1−0.3% by weight of cement. For this reason, although LS is the most used material for the formulation of water-reducing admixtures, it is hardly used in the design of high-performance concrete. To improve their water-reducing effect, many efforts and studies have been made to modify the structure of lignins and LSs. Oxidation, hydroxymethylation, sulphomethylation processes (Pang et al., 2008; Yu et al., 2013), graft copolymerization of LS with carbonyl aliphatics (Chen et al., 2011) and modification of lignin by the introduction of epoxylated polyethylene glycol (PEG) derivatives (Aso et al., 2013) seem to be effective in enhancing the hydrophilicity of LSs, promoting the dispersion of cement particles.

Tests with LSs with different molecular weights have shown that higher-molecular-weight fractions (>80 kDa) cause better plasticizing effects, enabling water reduction

of up to 20% with moderate retardation. Moreover, high-molecular-weight LSs also improve the workability retention (Reknes and Gustafsson, 2000; Reknes and Petersen, 2003).

In concrete, commercial LSs show a low content of entrapped air, of about 2%. This is basically the same as the 1−2% found in ordinary non-admixed concrete. More details are given in Chapter 6 (Aïtcin, 2016a). However, the air entrainment can rise to 8% in the presence of high-molecular-weight fractions (Reknes and Gustafsson, 2000; Ouyang et al., 2006).

LSs are among the cheapest concrete admixtures available on the market, costing about five times less than a commercial polycarboxylate-ether (PCE)-based polymer (Kaprielov et al., 2000). In 2005 the annual worldwide production of LSs was estimated at 1.8 million tons with a commercial value of about US$500 million (Will and Yokose, 2005). In 2007 up to 90% of total LS production was used in concrete constructions (Tejado et al., 2007).

9.2.2.2 Casein

Casein is a phosphoprotein found in bovine milk, and makes up to approximately 80% of the total milk protein. Casein is obtained by acid precipitation from milk, and is easily available in powder with high purity at a low cost.

The casein constituents, α, β, and κ-casein, exist in proportions of approximately 5:4:1 by weight. They differ in the amount of phosphate groups, which are linked to the amino acid serine through esterification. A proposed model for casein structure is shown in Figure 9.2.

Casein solubility is pH-dependent. In aqueous solution at neutral pH, casein is water-insoluble and forms spherical micelles with an average diameter of 150 nm. When dissolved in alkaline solution (pH 12−13), casein micelles dissociate to form

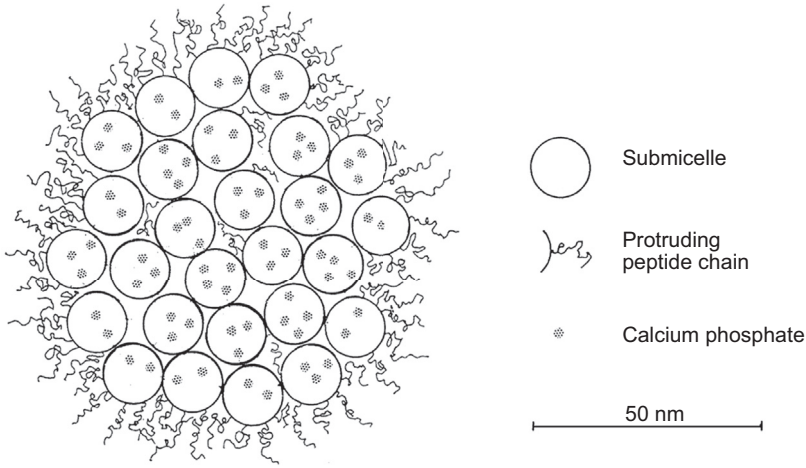


Figure 9.2 Model of a casein micelle (cross-section). Reproduced from Walstra (1999) with authorization.

negatively charged water-soluble submicelles of about 20 nm (Bian and Plank, 2012). Caseins possess high anionic charge density in alkaline media, because of the deprotonation of the amino acid residues.

Casein has been used as a dispersant and stiffening agent for a long time, but has only recently been developed for modern construction applications. When used with an appropriate cement composition, the casein reduces fluidity loss and has minimal effects on thickening time (Vijn, 2001). In self-levelling underlayments, the addition of casein provides good dispersing properties at dosages of 0.1−0.4% and shows a self-healing effect on the surface of the grout. Furthermore, it shows good compatibility with α-hydroxy carboxylic acid-based retarders, such as citric and tartaric acids (Plank and Winter, 2008).

Plank et al. (2008) and Winter et al. (2008) isolated the casein constituents and found that the α-casein has the highest negative net charge (−24 at pH 6.7) with respect to the other fractions, concluding that α-casein is the main fraction responsible for the dispersing effect, adsorbing on cement particles in large amounts. These results are supported by the fact that α-casein barely intercalates into layered double hydroxides. In this way, α-casein should be more available in solution than β-, and κ-caseins for cement dispersion (Yu et al., 2010). Furthermore, it has been observed that the unique self-healing property of casein derives from α-casein (Bian and Plank, 2013a). The plasticizing effect of caseins also depends on the content of κ-casein. A high proportion of κ-casein promotes the formation of submicelles smaller than 10 nm at alkaline pH, leading to an increased negatively charged surface in contact with the cement (Plank and Bian, 2010).

As observed for other biopolymers, casein-based water reducers show some disadvantages related to variability and storage. Indeed, the quality of casein varies depending on the species of animal, sampling season, manufacturing process, etc. Moreover, prolonged exposure to high temperatures (80−100 °C) during its production causes the denaturation of proteins, resulting in reduced plasticizing effectiveness (Bian and Plank, 2013b). A further limitation in using casein in cementitious systems is the unpleasant smell of ammonia due to the biodegradation of proteins under alkaline conditions and the proliferation of pH-tolerant moulds (Karlsson and Albertsson, 1990).

9.2.3 Linear synthetic polymers

9.2.3.1 Polynaphthalene sulphonates (PNS)

PNSs, also known as sulphonated naphthalene formaldehyde condensates (SNFC), were first developed in the 1930s and originally used in textile chemicals and the development of synthetic rubber. In the late 1960s PNSs were introduced into the concrete admixtures market in Japan as the first synthetized high-range water-reducing admixture, more commonly called superplasticizer.

The first step of PNS synthesis is the sulphonation of naphthalene with sulphuric acid, as shown in Figure 9.3(a).

Due to the symmetry of the naphthalene, the substitution of the hydrogen by the sulphonate can take place in two positions, α or β (Figure 9.4).

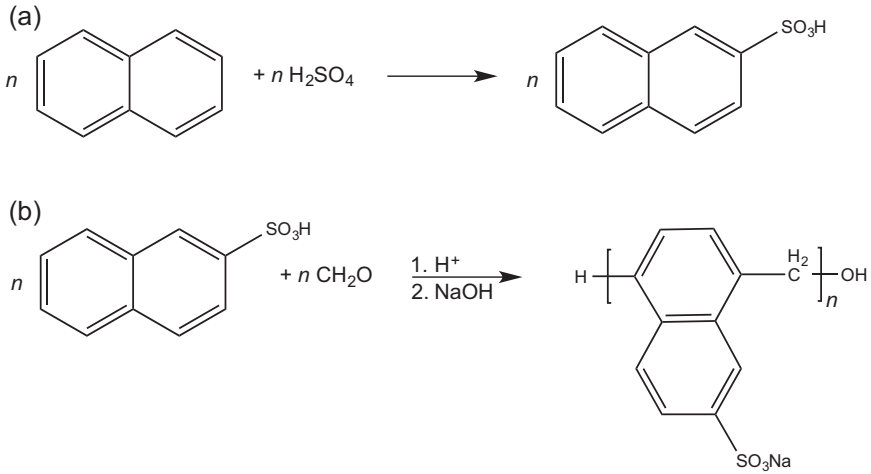


Figure 9.3 Synthetic route for preparation of PNSs. (a) Sulphonation of naphthalene with sulphuric acid and (b) polycondensation in the presence of formaldehyde.

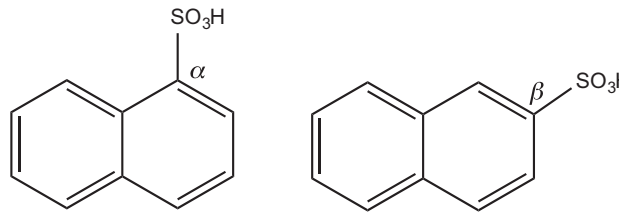


Figure 9.4 Chemical structure of naphthalene with a sulphonate group in α and β positions.

The α-substitution occurs mostly below a temperature of 100 °C, whereas at temperatures higher than 150 °C the β-isomer represents the most thermodynamicaly stable compound (Piotte, 1993). The quality and type of sulphonation are of great importance, as significant residual amounts of α-naphthalene sulphonic acid, naphthalene and sulphuric acid may influence the condensation of PNS. Furthermore, only PNSs polymerized with β-naphthalene sulphonic acid show the expected dispersing effect (Piotte, 1993). Aïtcin et al. (2001) mentioned that in a well-controlled synthesis of PNS, the sulphonation degree is about 90%. Furthermore, Piotte (1993) and Piotte et al. (1995) showed in a study of the quality of a non-purified batch of sulphonated naphthalene produced in typical conditions, as described in Hattori and Tanino (1963) and Miller (1985), that about 10% of the sulphonated functions were in position α.

The second step of PNS production (Figure 9.3(b)) is the condensation reaction of β-naphthalene sulphonic acid with formaldehyde, producing polymethylene naphthalene sulphonic acid. This polycondensation has been described as being similar to the reaction of phenol-formaldehyde resins (Piotte, 1993): first, after the protonation of its carbonyl function, the formaldehyde in its reactive form is added to the aromatic ring

by electrophilic addition. Then, after condensation, the methylol function of this new compound reacts with a second molecule of naphthalene and forms a methylene bridge between these two naphthalene molecules.

Once the desired degree of polymerization has been obtained (the molecular weight being time-dependent), the third and last step of PNS production consists of neutralizing the polymethylene naphthalene sulphonic acid with sodium hydroxide. When it is necessary to obtain a polymer free of alkalis, lime can be used, but filtration becomes mandatory to remove excess of lime and gypsum.

The conditions of reaction, such as the ratio between the reagents, the steric hindrance and the conformation changing during the polymerization, have a strong effect on the final structure of the PNS molecules and their molecular weight. The structure can be classified into three groups: linear, branched and cross-linked molecules. In a study of characterization of PNSs by ultrafiltration and high-performance liquid chromatography (HPLC), Piotte et al. (1995) showed that commercial products generally exhibit a high degree of polydispersity. They contain up to 10% of oligomers with a degree of polymerization between one and four, the monomers being the most abundant species. Some 20−30% of the polymers are linear molecules with a maximum degree of polymerization equal to 20 (which represents a molar mass of about 5000 g/mol) and a maximum population of around 10 (2500 g/mol). Finally, 35% of the polymers have a degree of polymerization between 20 and 40 (10,000 g/mol), and about 25% of species have a higher degree that can exceed 200 (50,000 g/mol), probably due to strong cross-linking. This indicates that commercial PNSs can contain a large amount of non-linear molecules with a more or less stiff three-dimensional conformation.

The structural composition of PNSs is an important factor in their dispersing properties. For example, the monomers and oligomers (degree of polymerization smaller than four) as well as the cross-linked molecules with a high molar mass do not disperse cement suspensions. PNS molecules show a dispersing ability when the degree of polymerization is between 5 and 80, with an optimum around 10 (Aïtcin et al., 2001). This optimum comes from the fact that at higher degrees of polymerization highly branched and, in the worst cases, cross-linked molecules cannot be completely avoided during the reaction, although the branching degree can be controlled by the amount of formaldehyde used in the condensation process (Miller, 1985). As the mode of action of these polymers involves adsorption on the solid particles, and thus the degree of particles coverage, these large molecules with high stiffness prevent a good covering of the particle surface and therefore lead to a low dispersing effect.

As seen above, characterization of the composition, structure and molar masses of PNSs is of great importance for determining and approaching the expected dispersing ability. As for other types of SPs, HPLC has shown its advantage in providing detailed profiles of the structural composition of commercial PNSs. Furthermore, the amount of molecules with a low degree of polymerization can be determined by UV spectroscopy (Piotte, 1993). These two methods can be applied to monitor the evolution of condensation reactions. Besides ultrafiltration to separate the polymeric fractions by molecular weight, selective precipitation allows the removal of oligomers with alcohols, as the solubility of the polymer changes with its polymerization degree and the type of alcohol.

The effect of PNSs on concrete fluidity has been intensively studied, as they were the most used SPs until the beginning of 2000. These studies include, for example, the effect of molar masse on adsorption and dispersing effect (Pieh, 1987; Pagé et al., 2000; Kim et al., 2000; Aïtcin et al., 2001), as discussed earlier, and the effect of the counterions on the performance of PNS in cement paste (Piotte, 1993), as well as their impact on hydration of cement phases (Singh et al., 1992; Uchikawa et al., 1992; Mollah et al., 2000). One of the great advantages of PNS is that their use does not alter the stability of the pore network in air-entrained concrete with freeze−thaw resistance, which explains their wide use in North America (Nkinamubanzi et al., 2016, Chapter 16). One of the most reported limitations of PNSs as concrete dispersants has been their incompatibility with low-alkali cement; but here PNSs containing a significant amount of residual sulphate can improve the situation.

9.2.3.2 Polymelamine sulphonates

The dispersing properties of another family of sulphonate-based SPs, called polymelamine sulphonates (PMSs) or sulphonated melamine formaldehyde condensates (SMFC), were discovered in the 1970s, and they are nowadays still widely used in the concrete industry.

As for PNSs, the synthesis of PMSs involves several steps. First, formaldehydes react with the amino groups of the melamine under alkaline conditions, leading to a methylolated melamine. Under the same alkaline conditions, sodium bisulphite is used to sulphonate one of the methylol groups (Figure 9.5).

Finally, polymerization by polycondensation is performed under acidic conditions. Increasing the pH to basic values stops the reaction.

As for PNSs, molecular weight distributions of PMSs are broad. Cunningham et al. (1989) measured by high-performance size exclusion chromatography a distribution between 1200 and 44,000 g/mol, with an average molecular weight of 7900 g/mol. Pojana et al. (2003) mentioned that a PMS exhibits a much higher average number of oligomeric units (around 50−60) with respect to a PNS (with its average number around 10). This would imply that PMSs can exhibit a more complex structure with possibly branched molecules.

As PNSs and PMSs are produced in the same way and were developed and used in the same period, there is a certain number of comparative studies on use, stability and toxicity of both admixtures. For example, they have the same water reduction or plasticizing ability, but cement pastes with a PMS show a higher slump loss. However, PMSs retard cement hydration less, which is why they are often preferred in the pre-cast industry (Flatt and Schober, 2012). It should be noted that the use of PMSs can be limited due to the probable presence in the solution of free formaldehydes, which have been listed since 1981 as a human carcinogen (Report on Carcinogens, 2011).

Another important aspect in toxicity is the impact on the environment when these SPs are used in concrete at construction sites (Redín et al., 1999; Ruckstuhl and Suter, 2003; Pojana et al., 2003). Ruckstuhl and Suter (2003) showed that oligomers of PNSs (up to a polymerization degree of four) were found in groundwater close to a tunnel

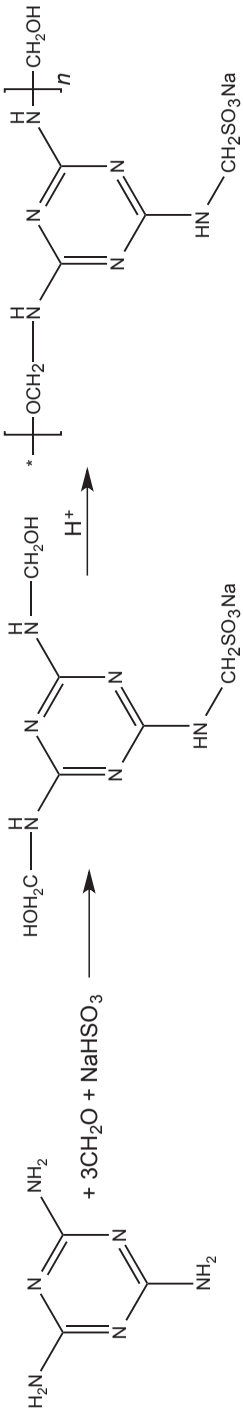


Figure 9.5 Sequence of reactions in the synthesis of polymelamine sulphonates.

being constructed in Switzerland. Similarly, Pojana et al. (2003) observed that released components of a PMS solution from leaching tests were composed only by shorter molecules. It seems that in both cases larger molecules that are strongly adsorbed on cement particles could not be washed out of the cement.

9.2.3.3 Phosphonate-terminated PEG brushes

Polyoxyethylene phosphonates or diphosphonates were developed at the beginning of the 1990s (Guicquero et al., 1999). These polymers are composed of one PEG chain with one or two phosphonate groups on one end (Figure 9.6).

The objective of developing such a molecule was to use a functional group with a higher affinity for cement surface than carboxylic or sulphonate groups. Indeed, phosphonates are known to have strong complexing ability for calcium, which means that they have a strong affinity for cement particles owing to the high calcium concentration in cement suspensions. The steric stabilization of these polymers then arises from the polyethylene glycol chain, which does not adsorb onto the surface and forms a layer on the particle surface from which other polymer-coated particles are expelled. The high adsorption and dispersion efficiency in $CaCO_3$ suspensions were shown by Mosquet et al. (1997) and Chevalier et al. (1997).

Polyoxyethylene phosphonates are polymerized in two steps, as shown in Figure 9.7.

First, the primary or secondary amino-terminated PEG is produced by anionic polymerization of ethylene oxide, initiated by potassium aminoalcoholates. The presence of the primary or secondary amine group at one end of the chain allows obtaining the mono- or diphosphonate end group, more specifically called the aminomethylenephosphonate group, by Moedritzer reaction with orthophosphorous acid and formaldehyde (Moedritzer and Irani, 1966).

The structure of the adsorbed polymer layer on particles consists of free end-anchored chains, and depends on the polymer molecular weight, solvent quality and the density of molecules adsorbed on the surface. Two regimes have been observed (Figure 9.8).

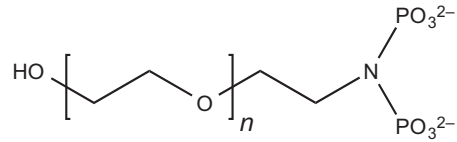


Figure 9.6 Chemical structure of a polyoxyethylene diphosphonate.

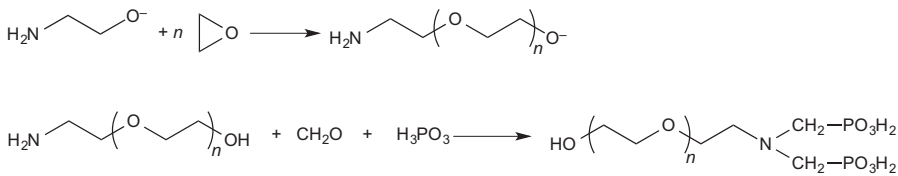


Figure 9.7 Scheme of the two-step synthesis of polyoxyethelene diphosphonate.

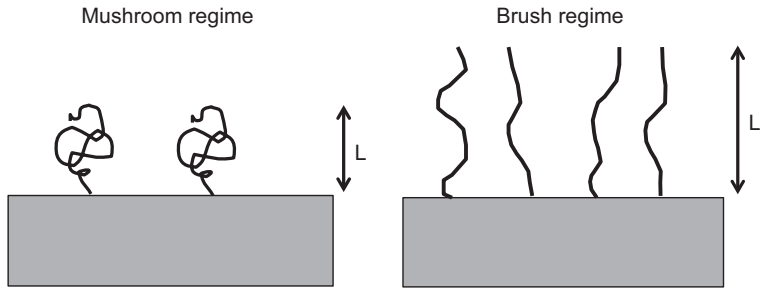


Figure 9.8 Schematic illustration of the change in conformation of end-anchored chains from a mushroom to a brush regime as a result of an increase in the density of surface occupancy.

At low coverage, adsorbed macromolecules are independent of each other and have an unperturbed coil conformation similar to that of non-functional PEG chains in bulk water. This is the 'mushroom' regime (Chevalier et al., 1997; Mosquet et al., 1997), where the thickness of the polymer layer, L, has been shown to be equal to the polymer radius of gyration. When the density of adsorbed polymers increases such that the adsorbed macromolecules cannot be considered as dilute and start to influence each other, a 'brush' regime is reached where the polymer chains stretch away radially from the surface, increasing the thickness of the adsorbed polymer layer and enhancing the steric repulsion.

Beside high dispersing ability, this type of SP has important advantages. They show an increased slump life (Guicquero et al., 1999) and a good resistance to soluble alkali sulphates due to their specific mode of adsorption and dispersion. Nevertheless, they induce strong retardation of hydration of C_3S, as Comparet et al. (2000) showed. This is discussed further in Chapter 12 dealing with the retardation of hydration by chemical admixtures (Marchon and Flatt, 2016b). Due to these properties, the phosphonates are particularly adapted to extreme conditions, such as hot weather, long slump requirement, long-distance pumping or oil-well cementing (Mosquet et al., 2003).

9.2.3.4 Vinyl copolymers

With the development of new concrete technologies, requirements for synthetic SPs with mixed functionality became more demanding to fulfil the expected performance. PNSs and PMSs already showed improved properties when polymerized with other chemical functionalities (Pagé et al., 2000; Shendy et al., 2002). However, the specific conditions of the condensation reactions limit the number and type of functional monomers, and thus the development of PNS- or PMS-based polymers with novel structures. Under these circumstances, a new type of linear polyacrylate-based polymers, first developed in the 1970s, found its place in the admixtures market in the 1980s and 1990s.

These polymers are produced by radical copolymerization, which allows greater possibilities in structural design due to the large number of monomers compatible with this type of reaction. For example, the monomers can bear sulphonate, carboxylate

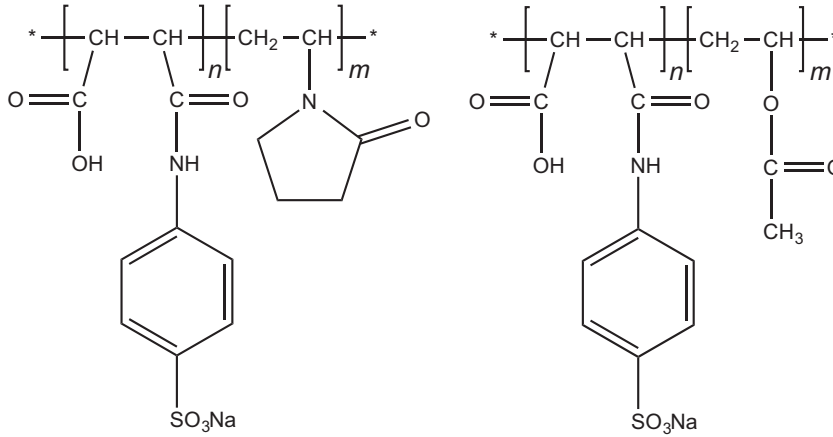


Figure 9.9 Chemical structure of two vinyl copolymers.

or phosphonate groups as anionic functional groups, as well as ether, amide or amine groups as bridging functions. This leads to a large variety of copolymers designed for specific applications and thus expected performance (Bradley and Szymanski, 1984; Jeknavorian et al., 1997; Bürge et al., 1994). Two examples are illustrated in Figure 9.9.

Unlike a PNS, which shows a molecular weight depending on reaction time, the molecular weight of these vinyl copolymers depends on the conditions of the radical polymerization, such as the quantity of initiator, the chain transfer agent and the type and reactivity of the monomers. In general, these molecules show a higher dispersing efficiency than PNSs and a significantly longer slump life (Mäder et al., 1999), but induce higher hydration retardation.

Vinyl copolymers represent the first step towards a new type of copolymers with side chains, called polycarboxylate ethers and developed later in the 1990s. These polymers, described below, mostly replaced vinyl copolymers in the 2000s as they showed a greater variety of structural design for better performance.

9.2.4 Comb-shaped copolymers

Comb-shaped copolymers are the last-generation SPs and were introduced in the mid-1980s (Tsubakimoto et al., 1984). This category includes many types of SPs exhibiting the same common comb-like structure.

The structure of comb-shaped SPs generally consists of a main chain, the so-called backbone, bearing carboxylic groups, to which non-ionic side chains made of polyethers are attached (Figure 9.10). These SPs are also called polycarboxylate ethers, polycarboxylate esters or polycarboxylates (PCEs).

The carboxylic groups, dissociated in water, confer a negative charge to the backbone. The negatively charged backbone is responsible for the adsorption of the SP onto the positively charged cement particles. The resulting charge of cement particles

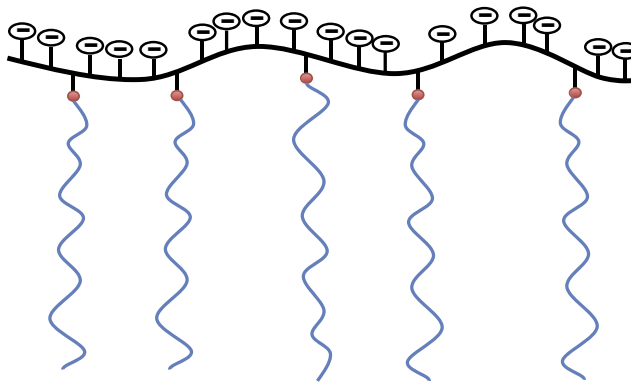


Figure 9.10 Schematic drawing of the comb-like structure of a PCE.

is lower compared to that induced by LSs, PNSs and PMSs. The dispersing ability of PCEs comes from the non-adsorbing side chains, which are responsible for the steric hindrance effect. While the adsorption depends strongly on the number of free carboxylic groups, the steric stabilization depends on the amount and length of the side chains of the adsorbed polymer (Flatt et al., 2009; Nawa et al., 2000). More precisely however, adsorption is affected by all structural parameters of the polymer, but to different extents (Marchon et al., 2013, 2016). More details about the dispersion mechanism of comb-shaped SPs are given in Chapter 11 (Gelardi and Flatt, 2016).

The key to the success of PCE SPs lies in the fact that they offer a broad range of possible molecular structures. Since the molecular structure greatly affects the performance of PCEs, tailoring their molecular structures enables the production of SPs with quite different properties that can be used in a broader range of applications.

The main factors determining the performance of polycarboxylates are:

- length of the backbone
- chemical nature of the backbone (acrylic, methacrylic, maleic, etc.)
- length of the side chains
- chemical nature of the side chains (PEG, polypropylene oxide, etc.)
- distribution of the side chains along the backbone (random, gradient)
- anionic charge density
- linkage between backbone functionalities and side chain (ester, ether, amide, etc.).

Two main synthetic approaches are used for producing PCEs. One is the free radical copolymerization of a monomer bearing carboxylic groups and a monomer bearing the side chain. This route is the most common, especially in industry, as it has a simpler experimental procedure and is cost-effective. Moreover, radical copolymerization is ideal for the incorporation of different kinds of monomer into the main chain. This procedure leads to a gradient distribution of the side chains along the backbone. It also gives rise to PCEs with a high degree of polydispersity, in terms of both statistical distribution of the monomers and size of the polymers. Since the reactivity of the two monomers can be different, PCEs synthesized by free radical copolymerization may

have a gradient distribution of side chains along the backbone. The typical polydispersity index (PDI) for such PCEs is between two and three.

The other approach is the polymer analogous esterification or amidation of a preformed backbone bearing carboxylic groups with monofunctional PEG. This procedure can lead to PCEs with a narrower distribution of structures and molecular weights, due to the fact that the length of the backbone is fixed, and also the side chains introduced this way are more uniformly distributed along the backbone.

A schematic representation of the two main synthetic routes is shown in Figure 9.11.

Recently, controlled radical polymerization techniques, such as reversible addition-fragmentation chain-transfer or RAFT polymerization, have been used for the production of methacrylic-based PCEs with a well-controlled structure (Rinaldi et al., 2009). These approaches should provide relatively monodisperse SPs that can serve as models for fundamental studies on the working mechanism of PCEs.

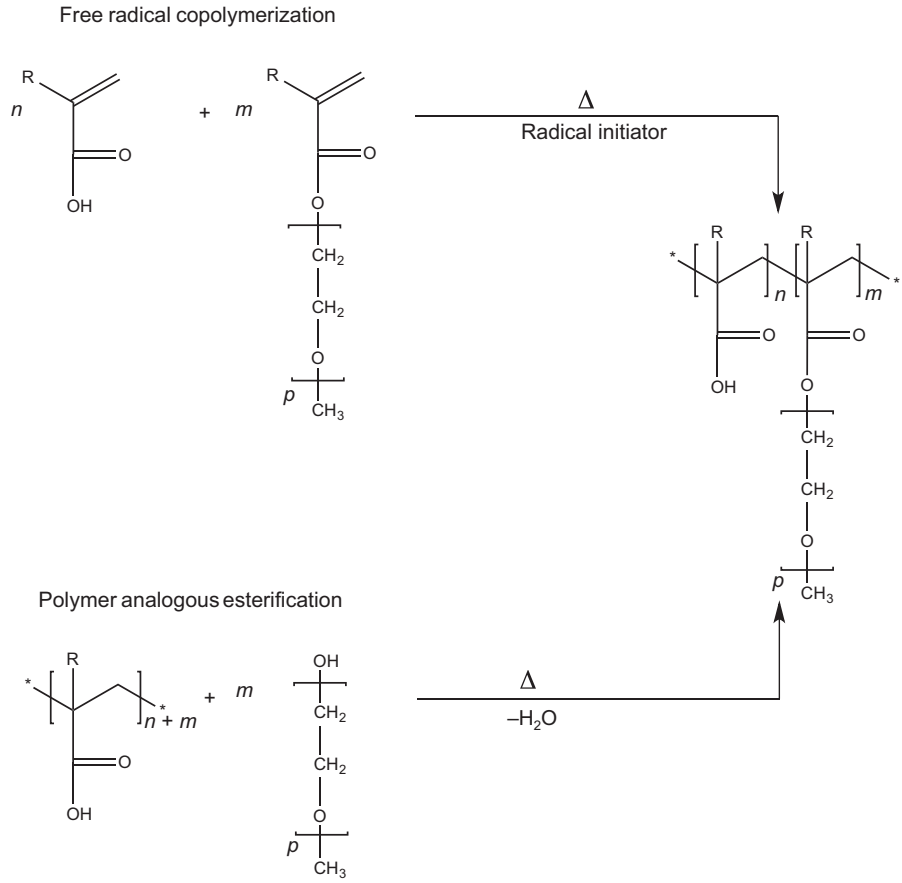


Figure 9.11 Schematic representation of the two main routes for synthesizing an acrylic or a methacrylic-based PCE (R = H, CH_3).

9.2.4.1 Chemical nature of the backbone

In acrylic-based copolymers the monomer unit of the backbone is acrylic acid, while the bond between these units and the side chains is an ester or amide bond (Figure 9.12).

The ester bond of acrylic-based as well as maleic-based SPs is prone to undergo hydrolysis in an alkaline medium, such as the aqueous phase of a cementitious system. The cleavage (detachment) of some of the side chains leads to an increase in the number of free carboxylic groups. Thus PCEs with higher charge density, and therefore adsorption ability, are formed over time. The change of adsorption ability can compensate for the flow loss of cement paste. Indeed, this feature has been exploited for the production of cement dispersants with improved slump-retention ability.

Cross-linked acrylic-based SPs show similar retention ability. A recent example of such dispersants is the PCE with a hyperbranched structure described by Miao et al. (2013). In this case the hydrolysis of the ester bond provides a continuous supply of SPs for adsorption on cement grains (Figure 9.13).

If methacrylic acid is used instead of acrylic acid, the resulting PCEs will be more stable towards hydrolysis of their side chains.

The hydrolysis of the ester bond can be overcome by substitution with more stable bonds. Amide, imide and ether bonds are examples, and are frequently introduced in the structure of PCEs for this purpose (Figure 9.14).

Allyl ether macromonomers are also frequently copolymerized with acrylic acid, maleic acid or maleic anhydride to produce PCEs. Compared to methacrylic-based PCEs, allyl ether-based SPs show generally a lower adsorption but better slump retention (Liu et al., 2013). Moreover, it has been demonstrated that they are more effective with silica fume (Schröfl et al., 2012). Plank and Sachsenhauser (2006) synthesized α-allyl-ω-methoxypolyethylene glycol-maleic anhydride copolymers with a well-defined primary structure of alternating monomer units. This was possible because

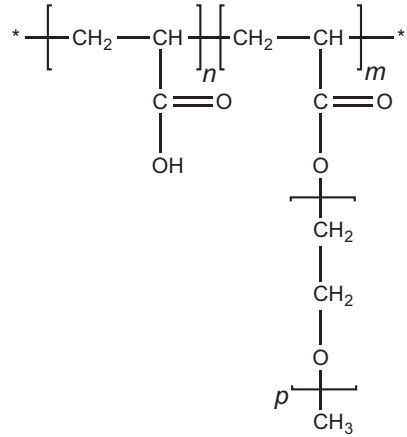


Figure 9.12 Structure of a PCE with an acrylic backbone and PEG side chains.

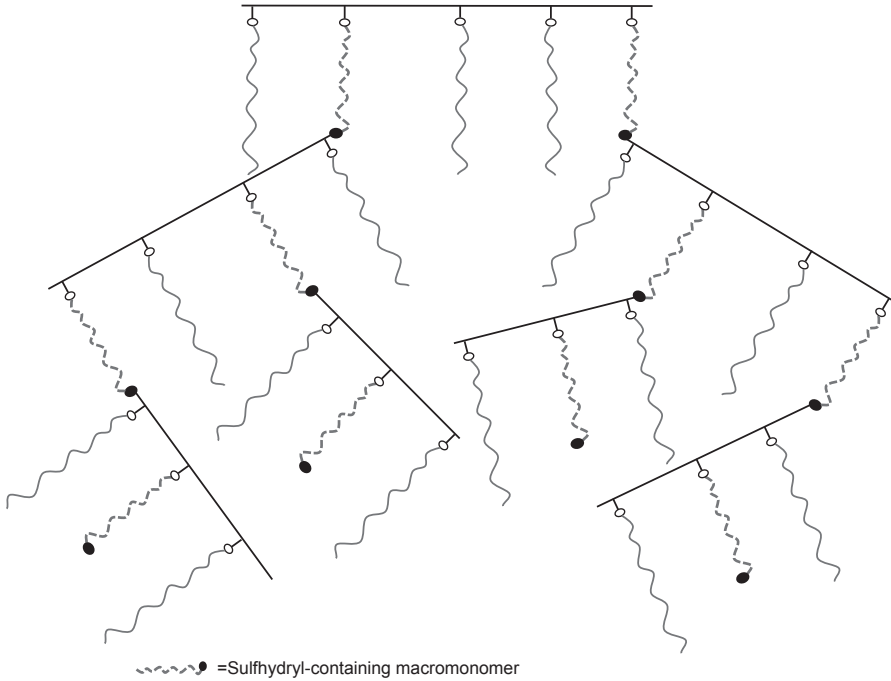


Figure 9.13 Possible structure of a hyperbranched PCE.
Adapted from Miao et al. (2013).

neither maleic anhydride nor allyl ether monomer undergoes homopolymerization. Isoprenyl oxypoly(ethylene glycol) macromonomers have been copolymerized with acrylic acid to produce PCEs with side chains connected by ether bonds (Yamamoto et al., 2004).

The type of monomer constituting the backbone of a PCE affects its performance as an SP. For instance, although the chemistry of the backbone of acrylic- and maleic-based SPs may look the same, such PCEs show different adsorption behaviour. This is due mainly to the additional chelating ability of the vicinal carboxylic groups of the maleic units. Methyl groups in α-position with respect to the carbonyl, as for meth-acrylic- and methallylic-based SPs, reduce the mobility of the main chain and can thus change the adsorption behaviour of the polymer. The flexibility of the backbone can be modified by the introduction of so-called spacer molecules, like for example styrene monomers (Figure 9.15).

The adjustment of the SP chemistry allows tailoring polymers with peculiar properties – for instance sulphate tolerance, as for allyl ether-based PCEs containing a five-membered lactone ring (Habbaba et al., 2013), or clay tolerance, as for terpolymers made of methacrylic acid-monoalkyl maleate-HBVE (Lei and Plank, 2014).

Recently, silyl functionalities were introduced in the methacrylate backbone of PCEs (Witt and Plank, 2012). The incorporation of such groups into the main chain of methacrylic-based SPs with a high grafting degree was found to increase the

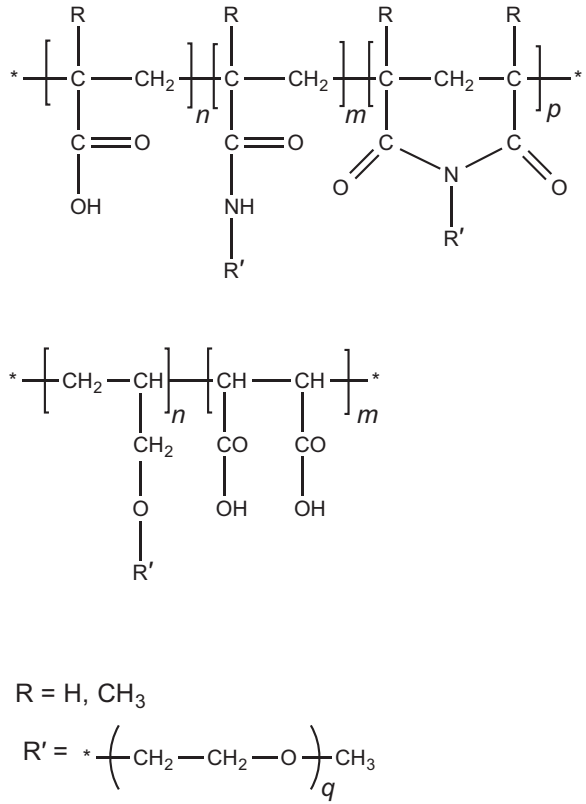


Figure 9.14 Chemical structure of PCEs with imide (top) and ether (bottom) bonds between the backbone and the side chains.

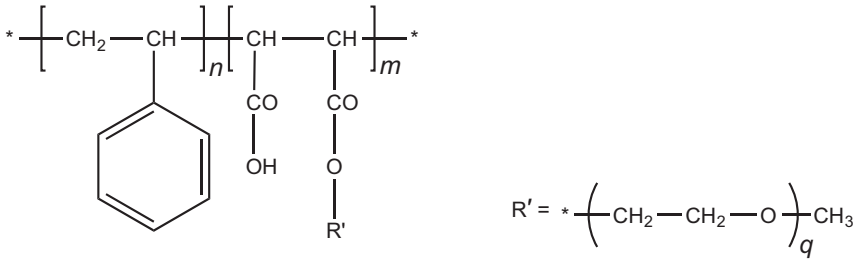


Figure 9.15 Structure of a comb-shaped copolymer made of styrene with a maleate bearing the side chain.

adsorption of such SPs. Fan et al. (2012) showed that incorporation of organosilane (trimethoxysilane) functionalities leads to SPs with high sulphate tolerance (Figure 9.16).

Methallyl sulphonic acid has been copolymerized in the acrylic backbone chain (Yamada et al., 2000).

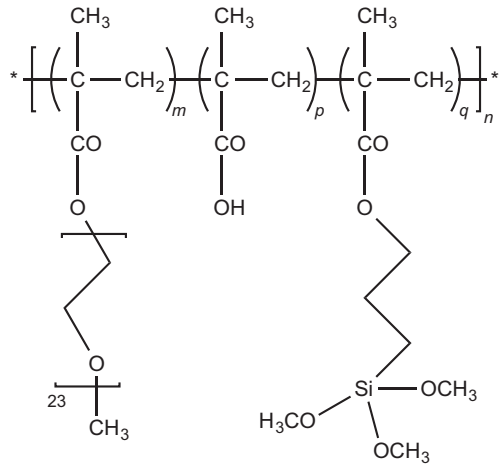


Figure 9.16 Structure of comb-shaped copolymers also carrying silyl functions. Adapted from Fan et al. (2012).

Amphoteric PCEs have been synthesized with the aim of improving the adsorption of the SP onto the negatively charged compounds, such as silica and calcium silicate hydrate, depending on the calcium concentration. These amphotheric PCEs were produced by polymerizing monomers bearing carboxylic groups with quaternary ammonium groups in the main chain, and showed significant performance benefits (Miao et al., 2011).

A new type of comb-shaped SPs is based on polyphosphonic acids. The structure is similar to that of PCEs, but the backbone is made of phosphonic groups (Bellotto and Zevnik, 2013). These SPs were found to be effective in self-consolidating concretes and more robust with regard to minor variations in the constituents of concrete. However, they have been reported to induce substantial retardation.

9.2.4.2 *Chemical nature of side chains*

Side chains used in the production of PCEs are usually made of PEG, also inaccurately called polyethylene oxide (PEO), with molar masses from 750 to 5000 g/mol. PEG with different masses, and therefore lengths, can be incorporated in the same polymer to balance the charge density.

PEG side chains confer high hydrophilicity to the PCE. The hydrophilic character of such PCEs can be reduced by using polypropylene oxide (PPO) side chains instead of PEG. They can also be copolymerized to produce mixed side chains of varying water solubility. PCEs with PPO side chains give a different performance; for instance, they were found to reduce air entrainment (Hirata et al., 2000).

PEG is usually introduced, in both polymer analogous esterification and synthesis of the macromonomer for radical copolymerization, as a monofunctional PEG. Its form is typically methoxy-PEG. The presence of PEG, a bifunctional molecule, during esterification would lead to cross-linking of polymer chains and formation of a

water-insoluble gel. However, PCEs with hydroxyl-terminated PEG side chains can be prepared by radical copolymerization of methacrylic acid and ω-hydroxy PEG methacrylate macromonomer (Plank et al., 2008). In terms of performance these PCEs behave similarly to methoxy-terminated PCEs.

The market for comb-shaped copolymers is dominated by PCEs with PEG or PEG/PPO as side chains. However, some attempts have been made to use other types of side chains. For instance, it has been demonstrated that PCEs with ethoxylated polyamides and PEG as side chains can be very effective as dispersants and allow use of a w/c ratio as low as 0.12 (Amaya et al., 2003).

9.2.4.3 Characterization of comb-shaped superplasticizers

Comb-shaped SPs, like polymers in general, are not monodisperse. PCEs are characterized by a high degree of polydispersity, as they can differ in the length of both backbone and side chains, as well as in the grafting degree. With respect to other SPs, PCEs are more complex than linear ones, such as PNSs or PMSs; but their polydispersity is limited compared to that of LSs.

The first step of the characterization of such complex polymers is the determination of their average properties. The anionic charge density of comb-shaped SPs can be easily determined by acid–base titration or titration with cationic polyelectrolytes, such as polydiallyldimethylammonium chloride (Plank and Sachsenhauser, 2009). The grafting degree of a comb-shaped acrylic-based SP, as well as the number average molecular weight of the PEG side chains, can be estimated by proton nuclear magnetic resonance (NMR). The ^{1}H-NMR spectrum of an acrylic-based PCE is shown in Figure 9.17.

Carbon-13 NMR has been shown to be a powerful tool to investigate the microstructure of these polymers, in particular in studying the repartition of the comonomers along the backbone (Borget et al., 2005). Moreover, the conformation in solution of comb-shaped SPs can be studied by static and dynamic light scattering, which provide average gyration and hydrodynamic radii, respectively. However, in many cases PCEs are on the lower end of the detection level, so these results must be treated with care.

Besides the determination of average properties, there is a need to consider the distributed properties. The role of the molar mass distribution of PCEs in adsorption behaviour has already been pointed out (Winnefeld et al., 2007). Furthermore, it has been shown that the distribution of the side chains along the backbone also plays an important role. For instance, for a same average grafting degree, polymers with a statistical and a gradient distribution of side chains do not show the same adsorption (Pourchet et al., 2012).

HPLC has been successfully used to distinguish between adsorption of different polymeric fractions (Flatt et al., 1998). However, understanding of the structure–activity relationships requires the use of more advanced techniques. Two-dimensional chromatography is a promising technique for this purpose (Adler et al., 2005).

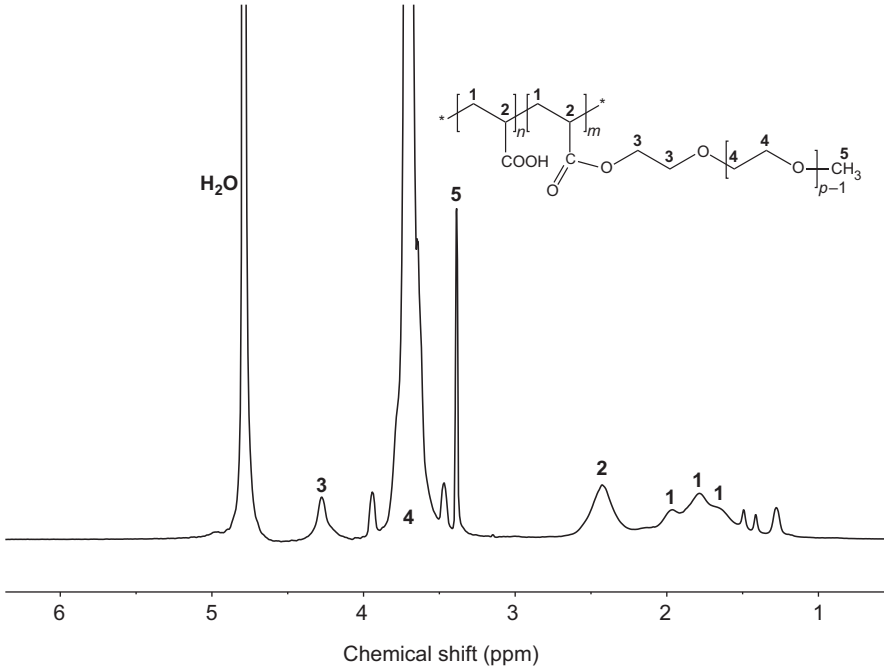


Figure 9.17 [1]H-NMR spectrum of a PCE made of an acrylic backbone and methoxy-PEG side chains.

9.2.4.4 Conformation of PCEs in solution

Conformation of comb-shaped copolymers in solution can be derived from the model by Gay and Raphaël (2001) for comb-shaped homopolymers in a good solvent. According to this model, comb-shaped homopolymers can be seen as an assemblage of n repeating units, each containing N monomers along the backbone and one side chain of P monomers (Figure 9.18).

Depending on the relative magnitude of these three structural parameters, the homopolymers can assume five different conformations (Figure 9.19). The possible conformations, shown in the phase diagram in Figure 9.19, are as follows.

1. Decorated chain (DC).
2. Flexible backbone worm (FBW).
3. Stretched backbone worm (SBW).
4. Stretched backbone star (SBS).
5. Flexible backbone star (FBS).

The PCEs used as dispersing agents most often belong to the FBW regime. This regime is typical of comb-shaped polymers whose side chains are short compared to the backbone. In this conformation, the comb-shaped homopolymer can be seen as a chain of cores, each having a radius of gyration R_C. Both the radius of gyration of

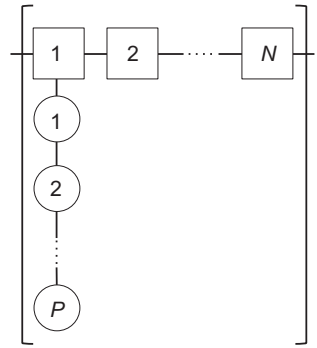


Figure 9.18 Schematic notation of the structure of a comb-shaped copolymer or homopolymer made of n repeat units each carrying one side chain made of P monomers and a backbone segment of N monomers.

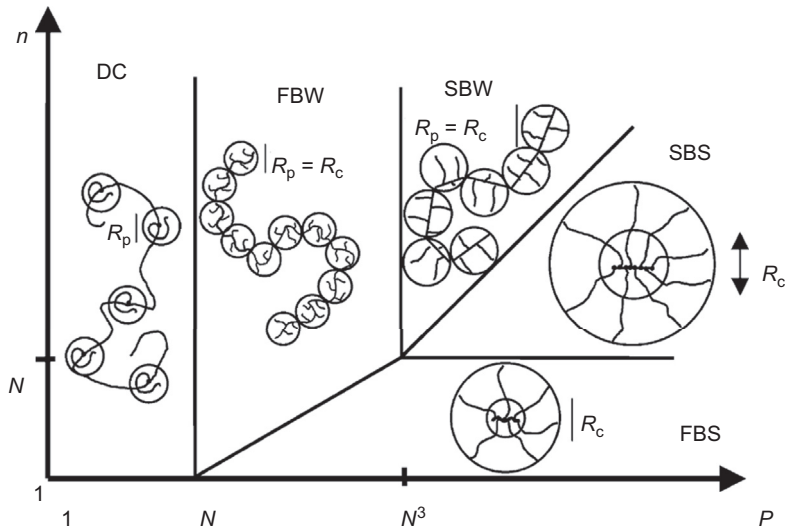


Figure 9.19 Phase diagram for comb-shaped homopolymers with the structure defined in Figure 9.18.
Reproduced from Gay and Raphaël (2001) with authorization.

the core and the overall chain follow a Flory scaling law. By minimizing the Flory free energy, the following expression for the overall radius of gyration of a comb-shaped homopolymer in the FBW conformation can be derived:

$$R = R_C\left(\frac{n}{n_C}\right)^{3/5} = (1-2\chi)^{1/5}aP^{2/5}N^{1/5}n^{3/5} \tag{9.1}$$

where

n_C = number of side chains per core
χ = Flory parameter
a = monomer size.

Flatt et al. (2009) extended this equation to comb-shaped copolymers having monomers of different size along the backbone and in the side chains. Equation (9.2) can be rewritten as:

$$R = \left(\left(\frac{a_N}{a_P} \right)^2 \frac{(1-2\chi)}{2} \right)^{1/5} a_P P^{2/5} N^{1/5} n^{3/5} \tag{9.2}$$

with a_N and a_P being the size of the backbone and side-chain monomers, respectively. For methacrylic backbones $a_N = 0.25$ nm, and for PEG side chains $a_P = 0.36$ nm and $\chi = 0.37$.

9.3 Retarders

9.3.1 Introduction

There are a very large number of compounds that may be used as retarders. Examples of these and their applications are given in Chapters 12 (Marchon and Flatt, 2016b) and 18 (Aïtcin, 2016b). Many retarders also have a water-reducing action, and many water reducers also have a retarding action on cement hydration − as stated by Collepardi (1996), who chose to treat retarders and water reducers together in a single chapter of a handbook of chemical admixtures. In this chapter we give only a very brief overview of the chemistry of retarders, and then focus more extensively on the case of sugars.

LSs (discussed earlier) may be considered as retarders that additionally have a decent water-reducing ability, or vice versa. Other compounds, such as hydroxycarboxylic acids or salts thereof, as well as carbohydrates lean more clearly towards the role of retarders that may additionally offer some (small) water-reducing ability.

Various inorganic salts are also known to retard cement hydration (see Aïtcin, 2016b, Chapter 18). However, as they are higher priced than organic alternatives, they are not used much in practice (Collepardi, 1996). This contrasts with LSs and sugar derivatives that can offer powerful retardation. For even longer retardation, phosphonates that have been described as superretarders may be considered (Ramachandran et al., 1993).

In this section we mainly examine the chemistry of sugars and their derivatives. Indeed, this is where a large range of controllable variations in chemistry can be achieved, giving a greater flexibility in design and a powerful tool for better understanding cement hydration. The information presented here constitutes a basis for Chapter 12, which discusses the retarding action of chemical admixtures on cement hydration (Marchon and Flatt, 2016b).

9.3.2 Carbohydrates

The terminology of carbohydrates comes from their average composition, which is analogous to a hydrate of carbon, $C_m(H_2O)_n$, where m and n can be different and m is typically equal to or larger than three. Carbohydrates offer a very large spectrum of structural variations, including, but not limited to, functionalization and polymerization. As a result, many criteria may be used to classify carbohydrates.

One criterion concerns the number of basic sugar units they contain. Only in a case where the units are identical, this does correspond to a degree of polymerization. This classification contains four groups: monosaccharides (e.g. glucose), disaccharides (e.g. sucrose), oligosaccharides (e.g. raffinose) and polysaccharides (e.g. starch).

9.3.2.1 Monosaccharides

Monosaccharides are the basic building groups for the higher-order saccharides (di, oligo and poly). Their general formula is $H{-}(CHOH)_x(C{=}O){-}(CHOH)_y{-}H$. If either x or y is zero they are aldehydes, otherwise they are ketones. Another characteristic is that all other carbon atoms carry a hydroxyl group.

Let us consider the open form of the monosaccharide D-glucose illustrated in the centre of Figure 9.20. It contains four chiral centres, and therefore is one compound of a family of 16 (2^4) stereoisomers. Additionally, it may self-react to form a six-member ring, leaving the hydroxyl closest to the oxygen in the ring either on the opposite or the same side of the $-CH_2OH$ group with respect to the ring plane (noted α and β, respectively) (Vollhardt and Schore, 2010). Figure 9.20 illustrates this, in addition to how both ring forms are in equilibrium with D-glucose and therefore also with each other. Resulting from these equilibria, D-glucose is found mainly in ring forms, with about 38% α-D-glucose and about 62% β-D-glucose (Robyt, 1998).

The stereochemistry of sugars plays a very important role in their chemical behaviour. In particular, in the cases we are interested in, it affects their ability to complex

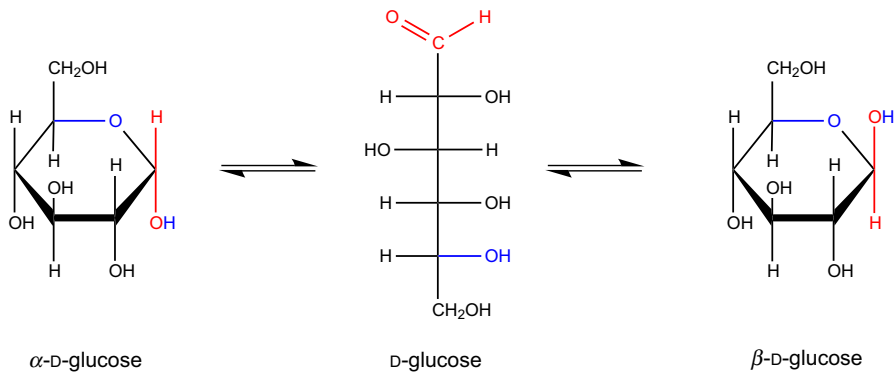


Figure 9.20 Schematic representation of the equilibrium between α- and β-D-glucose with an intermediate opened form.

metal cations in solution (Angyal, 1980; Pannetier et al., 2001), and can be expected to do so on surfaces for which such cations have an affinity. As explained in Chapter 12, complexation can be viewed as a necessary but not sufficient condition for retardation (Marchon and Flatt, 2016b).

The complexing ability of aldehyde sugars can be increased if they are partially oxidized to the corresponding carboxylic acids. Reducing sugars are subject to this, as they can suffer ring opening, forming an aldehyde group that can then be oxidized to an acid. Although this reaction is spontaneous, it is slow unless a catalyst is used. However, alkaline conditions such as those that prevail in cementitious systems can catalyse this process (de Bruijn et al., 1986, 1987a,b,c; Yang and Montgomery, 1996). This can lead to many different degradation products carrying carboxylate functions.

One must therefore consider that reducing sugars will be converted to salts of their corresponding acids, or even to smaller fragments (Thomas and Birchall, 1983; Smith et al., 2012). In contrast, non-reducing sugars such as sucrose, which is discussed below in the disaccharides section, are stable. This difference in behaviour has recently been evidenced in cementitious systems using NMR, showing explicitly that glucose degrades at 95 °C but sucrose does not (Smith et al., 2011, 2012). Earlier work also established by chromatography that sucrose is stable in alkaline solutions up to pH 13.5 at ambient temperature (Luke and Luke, 2000). From a structural point of view, reducing sugars are differentiated from non-reducing ones in that they have a free anomeric carbon (one that carries a hydroxyl group).

9.3.2.2 *Disaccharides*

Two monosaccharides can bond together in a reaction involving the elimination of water and the formation of a −C−O−C− bond between them. In polymer chemistry this is referred to as condensation, while in carbohydrate chemistry it would rather be called dehydration.

The bond between saccharides is part of a broader family of chemical bonds called glycosidic. They cover covalent bonds that link a chemical group to a saccharide, regardless of the nature of this chemical group (here another saccharide). If the formation of a glycosidic bond involves the hydroxyl on an anomeric carbon, then the associated ring is stabilized against ring opening. The formation of such bonds consequently influences the redox reactivity of sugars, including their stability in alkaline solutions, which is of particular interest for cementitious systems.

To illustrate this, let us consider two examples of disaccharide: maltose and sucrose (Figure 9.21). In both cases the aldehyde group of the left glucose ring is stabilized by the glycosidic bond. In maltose the right ring is not stabilized, as it has a free aldehyde, but in sucrose it is stabilized. This explains why maltose (and glucose) degrades in the alkaline aqueous phase of cementitious materials, but not sucrose (Thomas and Birchall, 1983; Smith et al., 2012).

It has also been found that sucrose can lose a proton in aqueous solutions above pH 11 without reacting further (Popov et al., 2006). Probable important implications

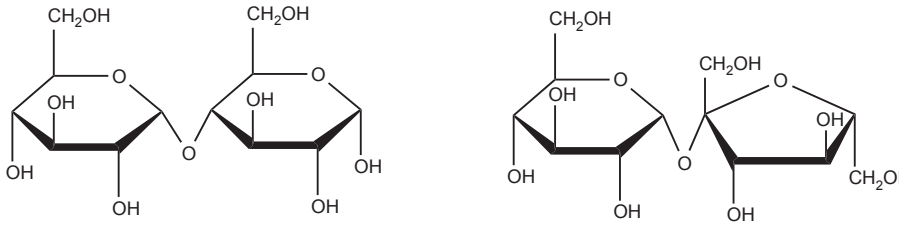


Figure 9.21 Illustration of two common disaccharides: left, maltose; right, sucrose.

of this in terms of complexation and cement hydration are discussed in Chapter 12 (Marchon and Flatt, 2016b).

9.3.2.3 Oligosaccharides

Oligosaccharides are molecules containing a small number of monosaccharides, typically from three to nine. With respect to cement chemistry, the case of raffinose is of particular interest as it acts as a very powerful retarder (Thomas and Birchall, 1983).

As can be seen in Figure 9.22, raffinose can be considered as a derivative of sucrose (Figure 9.21, right). It additionally has a α-D-galactose unit connected to the pendant $-CH_2OH$ of the glucose unit. As with sucrose, this sugar is non-reducing.

9.3.2.4 Polysaccharides

Polysaccharides are saccharides that have a higher number of monosaccharide units than oligosaccharides. They are very abundant components in natural products for energy storage (e.g. starch) or structural functions (e.g. cellulose). Their solubility decreases with molecular weight, which is further driven by an increasing number of intermolecular hydrogen bonds.

The most important use of polysaccharides in concrete technology is for viscosity-modifying admixtures, which are discussed in further detail below.

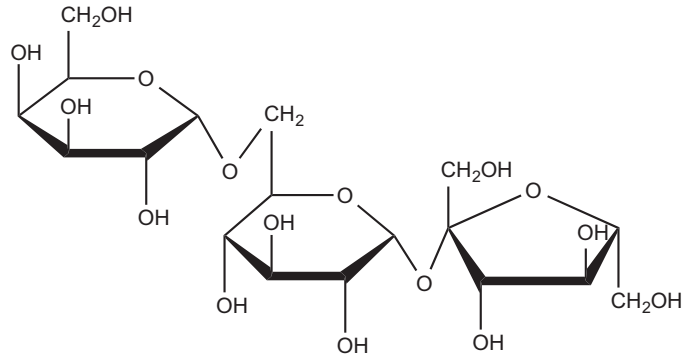


Figure 9.22 Chemical structure of raffinose.

9.4 Viscosity-modifying admixtures

9.4.1 Introduction

Viscosity-modifying admixtures (VMAs) are widely used to increase the stability, cohesion and robustness of self-compacting concrete, underwater concrete, shotcrete and cement grouts. These applications require highly fluid mixes to enable pouring but at the same time segregation and bleeding must be avoided. SPs are commonly used in these mixes to reach high flowability with low w/c ratio, while the use of VMAs increases stability. VMAs are also used to reduce the water loss of mortars due to evaporation or capillary suction when they are placed on a porous support (Cappellari et al., 2013; Khayat, 1998).

VMAs, specifically Xanthan gum, were introduced in the construction field in the 1960s (Plank, 2005), and since then their use has progressively increased. VMAs are also known as water-retaining or anti-washout admixtures. Most are hydrophilic, water-soluble organic polymers, although inorganic compounds such as nano-silica are also used as VMAs.

Table 9.1 shows a classification of the organic VMAs proposed by Kawai (1987) according to their nature. The most commonly used VMAs in cementitious systems are cellulose-ether derivatives and welan gum, although the use of starch has been progressively increasing in recent years. A more detailed explanation of the most relevant VMAs is given later in this chapter.

Table 9.1 Classification of VMAs

Natural polymers	Starch
	Welan gum
	Diutan gum
	Guar gum
	Xanthan gum
	Alginates
	Agar
Semi-synthetic polymers	Cellulose-ether derivatives
	Guar gum derivatives
	Modified starch
	Alginates derivatives
Synthetic polymers	Polyethylene oxide
	Polyvinyl alcohol, etc.

Adapted from Khayat and Mikanovic (2012).

9.4.2 Natural polymers

9.4.2.1 Welan gum and diutan gum

Welan gum and diutan gum are high-molecular-weight microbial polysaccharides produced by aerobic fermentation (Khayat and Mikanovic, 2012). They both belong to the sphingans group.

Welan gum is synthesized by the fermentation process of the *Alcaligenes* sp. ATCC 3155. It contains a tetrasaccharide backbone chain with L-mannose, L-rhamnose, D-glucose and D-glucuronic acid. The side chains contain a single unit of either L-mannose or L-rhamnose substituted in C3 of every 1,4-linked glucose molecule (Kaur et al., 2014). This polysaccharide has an approximate molecular weight of 10^6 g/mol.

Diutan gum has a similar structure to welan gum, but the side chains of the former consist of two units of L-rhamnose. In addition, diutan gum has a molecular weight up to three times higher than welan gum, of about $3-5 \times 10^6$ g/mol (Khayat and Mikanovic, 2012).

Figure 9.23 shows the structure of both polysaccharides. The presence of D-glucuronic acid in both gums gives them anionic charges and the ability to adsorb onto the surface of cement particles. Welan and diutan gum exhibit good rheological

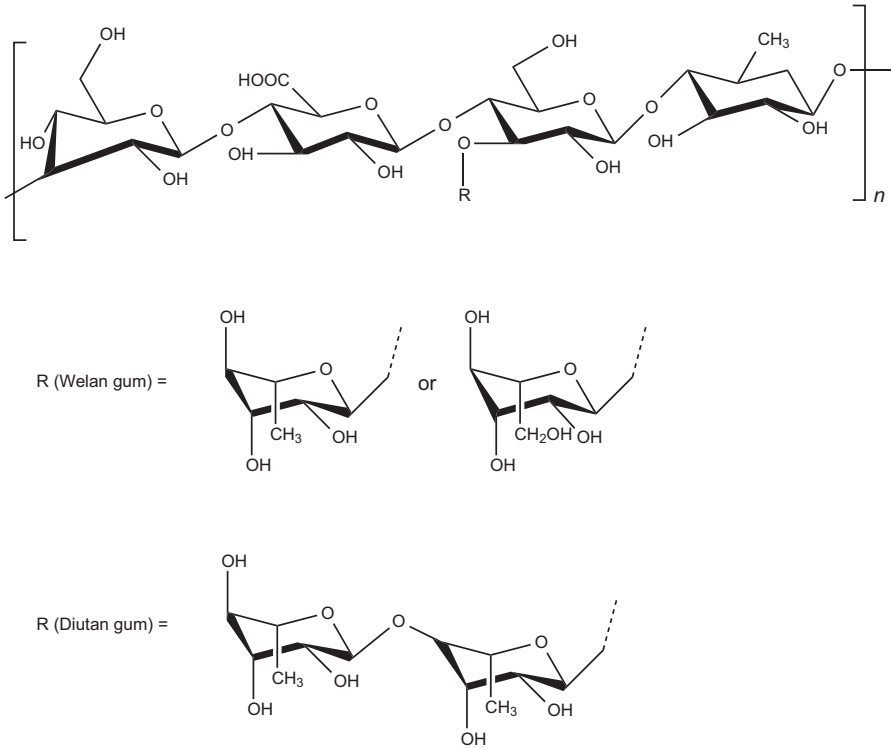


Figure 9.23 Chemical structure of welan gum and diutan gum.

properties and are stable at extreme temperature and pH. In aqueous solution, both gums adopt a double-helical conformation where the side chains screen the carboxylate groups of the backbone and prevent cross-linking by calcium ions. The shielding might be higher in the case of diutan gum due to its longer side chains compared to welan gum (Sonebi, 2006). This screening gives both gums high stability in media with high Ca^{2+} concentrations, as in cement pore solutions (Campana et al., 1990). With all these properties, welan and diutan gums are suitable VMAs for application in cementitious systems. However, their production is still rather expensive, so new and less costly synthesis methods need to be developed (Kaur et al., 2014).

9.4.3 Semi-synthetic polymers

9.4.3.1 Cellulose-ether derivatives

Cellulose-ether (CE) derivatives are the most widely used and effective water-retaining admixtures. It has been estimated that around 100,000 tons of cellulose derivatives are annually consumed by the construction industry (Plank, 2005), mainly for producing rendering mortars.

Cellulose is a uniform, linear glucose polymer and the most abundant of all natural substances (Khayat and Mikanovic, 2012). Cellulose consists of several hundreds to many thousands of β-1,4-linked D-glucose units, as shown in Figure 9.24. It is insoluble in water: to make it soluble, it is normally modified by attachment of small substituents in the hydroxyl groups of C2, C3 and C6.

In the case of CE derivatives, etherification occurs in alkaline conditions. The most widely used CE derivatives in building materials are hydroxypropyl methyl cellulose, hydroxyethyl methyl cellulose and hydroxyethyl cellulose (Figure 9.25). These admixtures have proved to be stable in the highly alkaline conditions of cementitious systems (Pourchez et al., 2006).

The behaviour of CE derivatives depends on its degree of substitution (DS), the nature of the substituent group and its structural parameters, such as molecular mass and amount of substitution groups (Brumaud et al., 2013). In general, the molecular weight is between 10^5 and 10^6 g/mol.

The DS is the number of substituted hydroxyl groups per glucose molecule, and ranges between zero and three. The solubility of cellulose derivatives will depend on the DS. Derivatives of cellulose with a DS lower than 0.1 are generally insoluble. Those with a DS between 0.2 and 0.5 are soluble in aqueous alkaline solutions. Cellulose derivatives with a DS between 1.2 and 2.4 are soluble in cold water (Richardson and Gorton, 2003; Brumaud, 2011; Khayat and Mikanovic, 2012). The substitution of hydroxyl groups in glucose molecules by chemical groups with additional free hydroxyl groups for further substitution is quantified by the molar substitution and has no theoretical upper limit.

9.4.3.2 Guar gum derivatives

Guar gum is a polysaccharide extracted from the seeds of *Cyamopsis tetragonolobus*. Its structure is based on a β-1,4-linked D-mannopyranose backbone with random

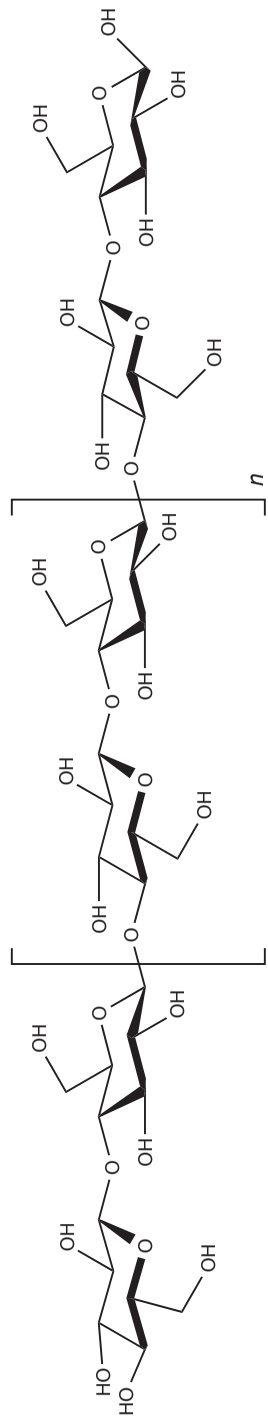


Figure 9.24 Chemical structure of cellulose.

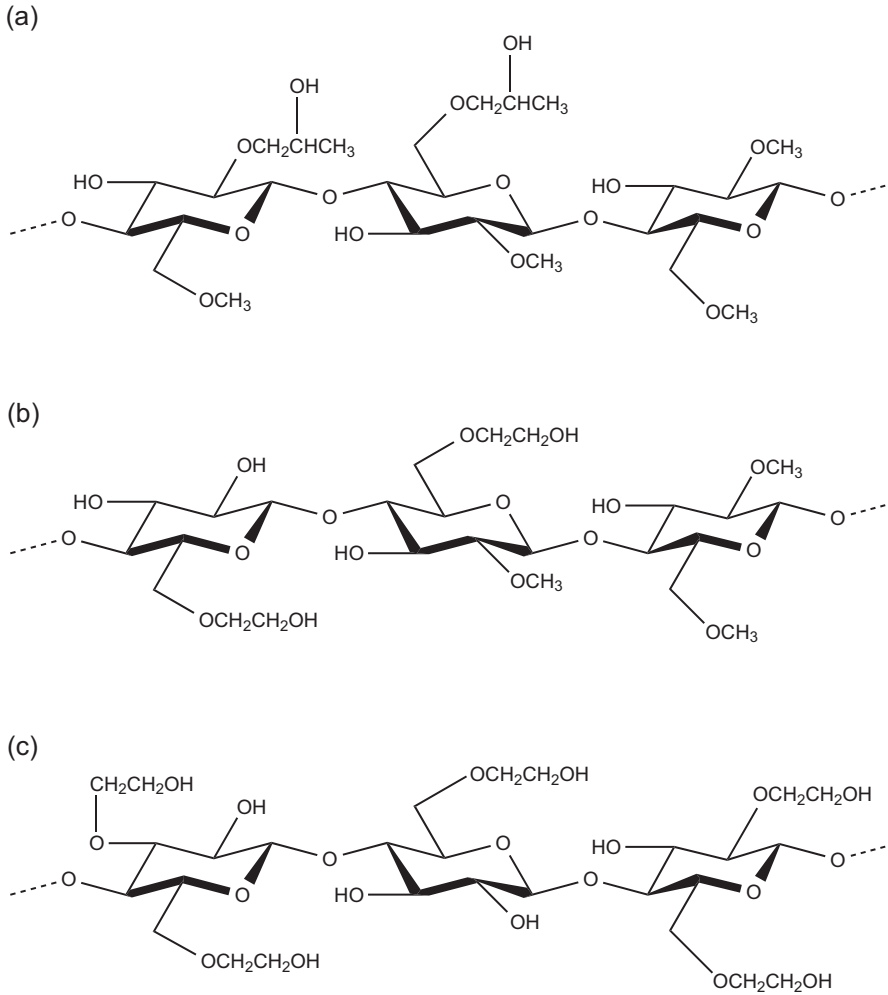


Figure 9.25 Chemical structure of cellulose ethers: (a) hydroxypropyl methyl cellulose; (b) hydroxyethyl methyl cellulose; (c) hydroxyethyl cellulose.

branch points of galactose via an α-1,6-linkage (Poinot et al., 2014) (Figure 9.26). Guar gum has a molecular weight in the order of 1×10^6 to 2×10^6 g/mol.

Guar gum is soluble in water, but its use causes problems such as solution clarity, alcohol solubility, uncontrolled rate of hydration, decrease of viscosity with time and microbial contamination susceptibility. To overcome this limitation, derivatives are produced (Iqbal and Hussain, 2013; Risica et al., 2005).

Hydroxypropylguar is the most commonly used derivative of guar gum (Figure 9.27). It is obtained from the guar gum by an irreversible nucleophilic substitution, using propylene oxide in the presence of an alkaline catalyst (Pourchez et al., 2006). It is highly soluble and shows high thermal stability. Functional

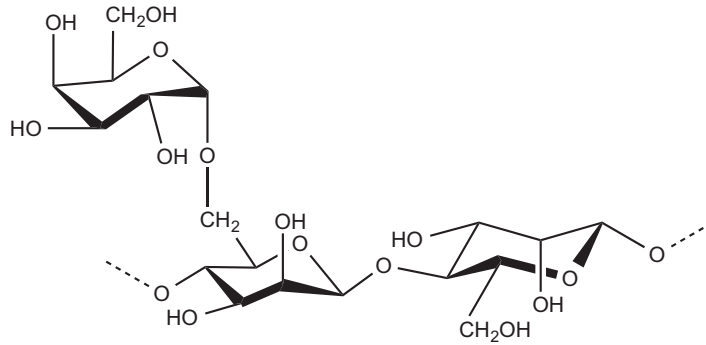


Figure 9.26 Chemical structure of guar gum.

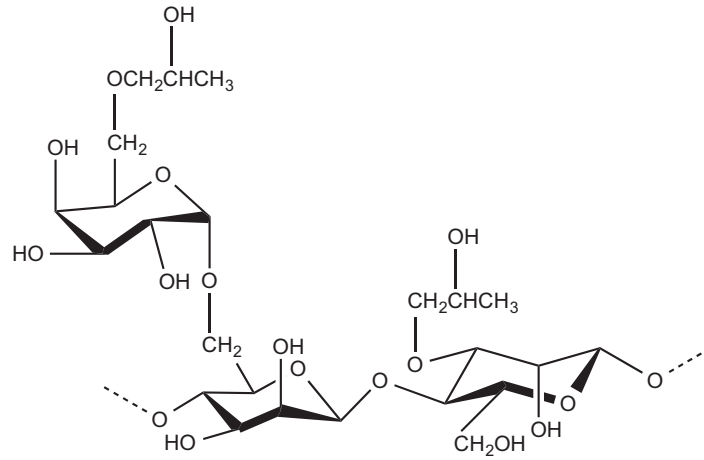


Figure 9.27 Chemical structure of hydroxypropylguar.

properties of hydroxypropylguar depend on its DS. As in the case of cellulose, the maximum DS is three, as three hydroxyl groups are available in each sugar unit for derivatization. As substituents are introduced in the molecule, additional hydroxyl groups can be also included for possible further derivatizations. The primary hydroxyl group at C6 is more susceptible to reacting than C2 and C3 (Brumaud et al., 2013).

9.4.3.3 Modified starch

After cellulose and hemicellulose, starch is the principal carbohydrate found in nature (Richardson and Gorton, 2003). Starch is a polysaccharide composed of two homopolymers of D-glucose: amylose and amylopectin (Figure 9.28). Amylose consists mainly of long linear chains of α-1,4-linked glucose, although a low degree of branching has

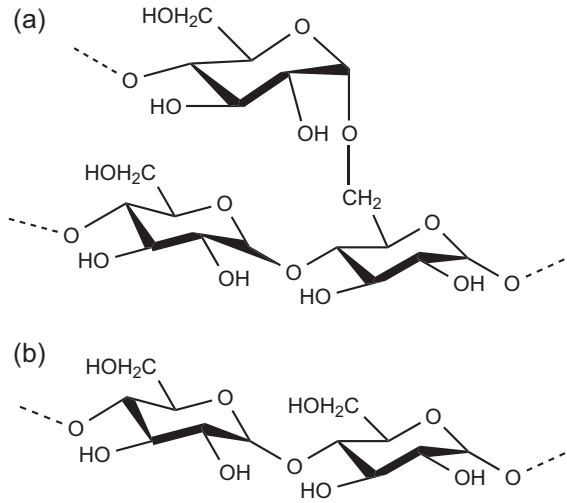


Figure 9.28 Chemical structures: (a) amylopectin and (b) amylose.

been identified. Amylopectin is a highly branched molecule (about once every 20 to 25 glucose units) with shorter α-1,4-linked glucose molecules and more frequent α-1,6 branches. The molecular weight of amylose is around 150,000−600,000 g/mol, while that of amylopectin is 10^7−10^9 g/mol. The percentage of amylose and amylopectin varies with the source of starch, ranging from 10% to 30% of amylose and 70−90% of amylopectin (Banks and Muir, 1980; Vollhardt and Schore, 2010). The main raw materials used for the extraction of starch are maize, potato, tapioca and wheat (Khayat, 1998).

Native starch is insoluble in cold water. For application in concrete, starches are normally modified through etherification or esterification to become soluble in cold water and stable at the high pH of cementitious systems. During etherification and esterification, hydroxyl groups of amylose and amylopectin are generally substituted (Khayat and Mikanovic, 2012). In construction, carboxymethyl and hydroxypropyl starch are the most used modified starches (Plank, 2005; Khayat and Mikanovic, 2012).

9.4.4 Synthetic polymers

9.4.4.1 Polyethylene oxide

PEO is a high-molecular-weight and non-ionic polymer. It is hydrophilic, linear and not cross-linked, and highly soluble in both aqueous and organic solvents.

Figure 9.29 shows the chemical structure of the repeating unit of ethylene oxide. This repeating unit contains a hydrophobic ethylene group and hydrophilic oxygen, which is also a hydrogen bond site (Zhang, 2011).

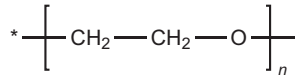


Figure 9.29 Structure of the repetitive unit in polyethylene glycol.

PEOs are synthesized by polymerization of ethylene oxide using a metallic catalyst. They are available in a very wide molecular weight range, from 200 to 7.0×10^6 g/mol, and the low-molecular-weight PEOs are called PEGs. They are completely soluble in cold and warm water.

9.4.4.2 Polyacrylamides

Polyacrylamides are a family of high molecular weight, water-soluble polymers. Anionic polyacrylamides (aPAMs) are used in the construction field as a thickener or flocculent. Their chemical structure is shown in Figure 9.30. APAMs are synthesized by free radical polymerization of acrylamide and acrylic acid salts or by partial hydrolysis of non-ionic polyacrylamide (Cheng 2004; Bessaies-Bey et al., 2015). Their molecular weight ranges from 10^3 to 20×10^6 g/mol.

APAMs can vary in molecular weight, structure (linear or branched) and charge density providing them different properties. At the high pH of cement pore solutions, aPMAs are susceptible to hydrolysis (Cheng 2004).

9.4.5 Inorganic powders

The stability of highly flowable concrete mix designs can be increased by the addition of high specific surface area inorganic powders such as colloidal silica, fine calcium carbonate, silica fume or fly ash. In addition, swelling powders such as bentonite can increase the water retention in cement mixes.

9.5 Air-entraining admixtures

9.5.1 Introduction

In this section the chemistry of air-entraining admixtures (AEAs), also called air entrainers, is presented. These molecules are surfactants, and understanding their

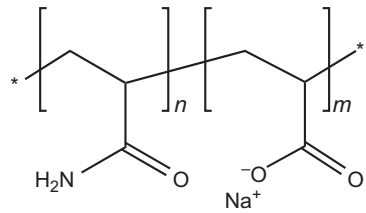


Figure 9.30 Structure of anionic polyacrylamide

working mechanisms therefore requires introducing some concepts about surfactant science. In particular, the parameter known as the hydrophile-lipophile balance (HLB), which gives an indication of the hydrophilic character of a surfactant, is introduced. While this concept has serious limitations, it is used in this chapter to show how this balance can be influenced through surfactant molecule architecture.

A first categorization of commercial AEAs dates back to 1954 (Torrans and Ivey, 1968), and distinguishes them into:

- salts of wood resins (pinewood stumps)
- synthetic detergents (petroleum fractions)
- salts of sulphonated lignin (paper pulp industry)
- salts of petroleum acids (petroleum refining)
- salts of proteinaceous materials (processing of animal hides)
- fatty and resinous acids and their salts (paper pulp and animal hide processing)
- salts of sulphonated hydrocarbons (petroleum refining).

The list indicates that the initial classification of AEAs was mainly based on the source of the raw materials and their treatment. A more recent screening conducted in the USA (Nagi et al., 2007) subdivided 41 commercially available AEAs into five categories based on infrared analysis:

- alpha olefin sulphonate (six admixtures)
- benzenesulphonate (four admixtures)
- resin/rosin and fatty acids (13 admixtures)
- vinsol resin (14 admixtures)
- combination (surfactants, urea, tall oil, and others).

Concrete Admixtures and the Environment; State-of-the-Art Report (2011), published by Deutsche Bauchemie, distinguishes two main categories: soaps made from natural resins (root resins, tall resins, gum resins and derivatives) and synthetic surfactants (alkyl polyglycol ethers, alkyl sulphates and alkyl sulphonates). The use of synthetic surfactants has increased due to a scarcity of natural sources, in particular wood resin/rosin. However, the classification of AEAs still contains terms relating to sources as well as types of synthetic surfactants in use.

There is abundant literature in which air entrainers are selected, named in one or another form and applied to concrete. However, few give a direct indication of the nature and properties of the surfactants or AEAs used.

In this section, a way to classify AEAs according to their surfactant nature is proposed. In doing this, we try to bridge a gap in surfactant science that has unfortunately grown since air entrainers have been introduced in concrete. First, a brief overview of the main characteristics of surfactants is provided.

9.5.2 General features of surfactants

9.5.2.1 Basic structural features

This subsection summarizes general features of surfactants, taken from Rosen (2004), that are of concern considering their use as AEAs for concrete.

Surfactants are surface-active amphiphilic molecules that consist of a hydrophobic 'tail', usually a long alkyl chain, and a hydrophilic 'head', ionic or polar. When a surfactant is in an aqueous environment, the tail tends to minimize its contact with the solvent. As a result, at the liquid−vapour interface a monolayer of surfactant molecules is formed, in which the tails are away from the solvent and oriented towards the air (non-polar). The presence of the hydrophilic group prevents the surfactant from being expelled completely from the solvent as a separate phase.

Based on the chemical nature of the hydrophilic head, surfactants can be distinguished into:

- anionic
- cationic
- amphoteric
- non-ionic.

Many changes can be brought to the hydrophobic portion of surfactants to tailor its properties. These modifications can include:

- Increasing the ***length of the hydrophobic chain***. This decreases solubility in water and increases solubility in oil or organic solvents; can cause a closer packing of molecules at the interface; increases the tendency to adsorb from solution at an interface or to self-associate into micelles; and increases precipitation from water by counterions in case of ionic surfactants.
- The introduction of ***branching or unsaturated bonds*** that increase solubility in water or organic solvents with respect to the corresponding linear or saturated ones; and decrease the tendency towards self-association into liquid crystal (a process that can reduce the surfactant availability and therefore performance).
- The presence of an ***aromatic nucleus*** will increase the adsorption of the surfactant onto the positively charged substrates, e.g. cement surfaces; and may cause looser packing at the liquid−vapour interface.

9.5.2.2 The concept of hydrophile-lipophile balance

The HLB was introduced by Griffin (1949) and indicates the emulsification behaviour of a surfactant. It quantitatively expresses the balance between the hydrophilic and lipophilic (hydrophobic) parts of the molecule. The larger the HLB, the more hydrophilic the surfactant.

The HLB value determines the most appropriate use for a given surfactant. Table 9.2 shows the main applications of surfactants with the corresponding HLB range.

Davies (1957) developed a cumulative concept in which the HLB value can be obtained from the individual contributions of the hydrophilic and hydrophobic portions of the molecule defined by group numbers (Table 9.3). While the first method used to calculate the HLB was strictly limited to non-ionic surfactants, Davies's method of individual group contributions broadened the applicability of the HLB concept to ionic surfactants.

The HLB of a surfactant calculated using group numbers according to Davies is:

$$\mathrm{HLB} = \sum_{k=0}^{n} (i_k \, \mathrm{GN}_k) \tag{9.3}$$

Table 9.2 Examples of surfactant applications with the corresponding most adapted HLB range and dispersability in water

HLB-range	Application	HLB range for dispersion in water
3–6	Water in oil emulsifier	<4 No dispersion
		3 < Poor dispersion < 6
7–9	Wetting agent	6 < Milky dispersion after vigorous agitation < 8
8–18	Oil in water emulsifier	8 < Stable milky dispersion <10;
		10 < Translucent to clear dispersion <12
		>13 Clear solution
13–15	Detergent	Clear solution
15–18	Solubilizer	Clear solution

Adapted from Tadros (2005).

where:

k: 0, …, n individual groups (hydrophilic and lipophilic)
i: quantity of group k
GN: group number according to Table 9.3.

Further development of this method includes the concept of effective chain length and leads to the values shown in Table 9.3 (Guo et al., 2006).

In Table 9.3 it can be seen that anionic head groups make a relatively high contribution to hydrophilicity (high group numbers). This contrasts with the individual contribution of an ethylene oxide (EO) group. Therefore to reach the same hydrophilicity as when using ionic groups, one must use very large head groups of non-ionic ethoxylated surfactants.

Tables 9.2 and 9.3 show that modifications of the molecular architecture of a surfactant, whether ionic or not, affect the HLB and the corresponding application range.

9.5.3 Sources for air-entraining admixtures

Traditional sources for AEAs are acids from wood resins and animal and vegetable fats and oils. The main compounds found in wood resins are abietic acid, pimaric acid (Figure 9.31) and their isomers, whereas natural fats and oils are sources of glycerides from which fatty acids can be derived by hydrolysis. Natural fatty acids are medium- to long-chain carboxylic acids with an even number of carbon atoms between 4 and 26 (Black, 1955). The structure of a saturated fatty acid is shown in Figure 9.32.

Another source of acids for AEAs is crude tall oil, a by-product of the Kraft process for paper manufacture. Among other compounds, it contains resin acids (see above) and fatty acids, mainly palmitic acid (C16, saturated), oleic acid (C18, unsaturated;

Table 9.3 HLB group numbers

Hydrophilic groups	Group number		Lipophilic groups	Group number	
	According to Davies	According to Guo et al.		According to Davies	According to Guo et al.
$-SO_4^-Na^+$	38.7	38.4	$-CH-$; $-CH_2-$; CH_3-; $=CH-$	−0.475	−0.475
$-COO^-K^+$	21.1	20.8	$-CF_2-$	–	−0.87
$-COO^-Na^+$	19.1	18.8	$-CF_3$	–	−0.87
$-SO_3Na^+$	–	10.7	Phenyl	–	−1.601
N (tertiary amine)	9.4	2.4	$-CH_2CH_2CH_2O-$ (PO)	−0.15	−0.15
Ester (free)	2.4	2.316	$-CH(CH_3)CH_2O-$	–	−0.15
−COOH	2.1	1.852	$-CH_2CH(CH_3)O-$	–	−0.15
−OH (free)	1.9	2.255	Sorbitan ring	–	−20.565
$-CH_2OH-$	–	0.724			
$-CH_2CH_2OH-$	–	0.479			
$-CH_2CH_2CH_2OH-$	–	0.382			
−O−	1.3	1.3			
$-CH_2CH_2O-$ (EO)	0.33	0.33			
$-CH_2CH_2OOC-$	–	3.557			
OH (sorbitan ring)	0.5	5.148			
Ester (sorbitan ring)	6.8	11.062			

From Davies (1957) and Guo et al. (2006).

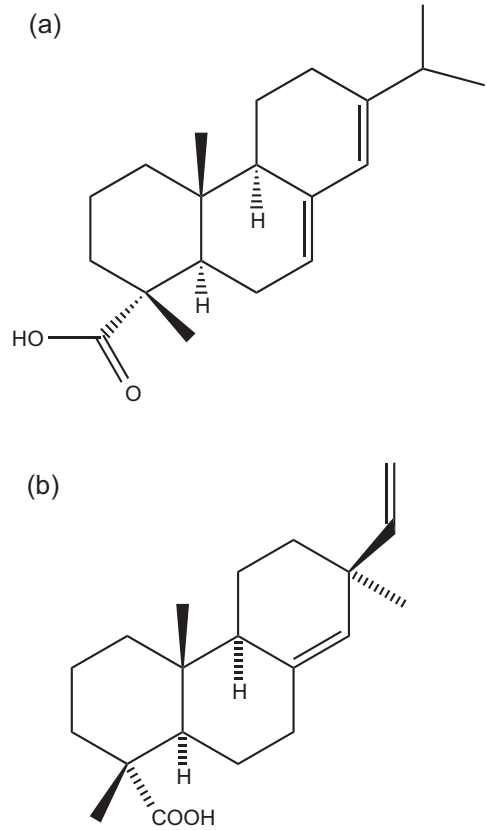


Figure 9.31 Chemical structures: (a) abietic acid and (b) pimaric acid.

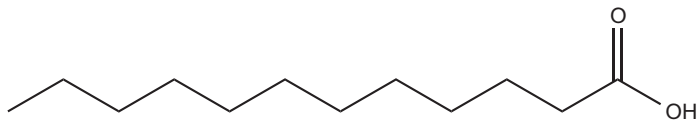


Figure 9.32 Chemical structure of lauric acid or dodecanoic (C12) acid.

one double bond; (9Z)-Octadec-9-enoic acid) and linoleic acid (C18, unsaturated; two double bonds; (9Z,12Z)-9,12-Octadecadienoic acid). Through further fractional distillation and reduction of the tall oil, fatty acids, mostly consisting of oleic acid (Figure 9.33), can be obtained.

Salts of petroleum acids are gained through alkaline extraction from crude oil containing naphtenic acids. Naphtenic acids are mostly mixtures of cyclopentyl and cyclohexyl carboxylic acids. An example of a naphtenic acid is shown in Figure 9.34.

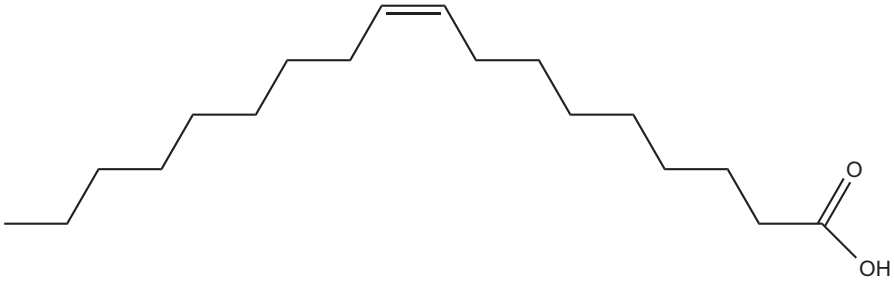


Figure 9.33 Chemical structure of oleic acid, or (9Z)-Octadec-9-enoic acid.

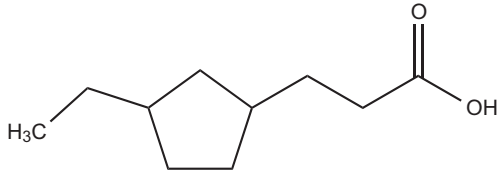


Figure 9.34 Chemical structure of a naphthenic acid.

9.5.4 Anionic surfactants

The hydrophilic portion of anionic surfactants has a negative charge. According to Tadros (2005), the most used head groups of anionic surfactants are carboxylates, sulphates, sulphonates and phosphates. Table 9.4 shows general formulae and characteristics for such anionic surfactants.

The presence of a negatively charged head renders the surfactant water-soluble, but is also responsible for its tendencies to adsorb onto cement particles and precipitate in

Table 9.4 Types of anionic surfactant and HLB group numbers

Surfactant type		Group and group number			
Head group	**Formula**	**Sodium head group**	**C12-alkyl**	**HLB**	**Application**
Carboxylates	$C_nH_{2n+1}COO^-X$	18.8	−5.7	20.1	Oil in water emulsifier
Sulphates	$C_nH_{2n+1}OSO_3^-X$	38.4		39.7	Wetting agent
Sulphonates	$C_nH_{2n+1}SO_3$ X	10.7		12.0	Oil in water emulsifier
Phosphates	$C_nH_{2n+1}OPO(OH)O^-X$	–		–	–

According to Guo et al. (2006).

cement pore solutions due to the presence of di- or trivalent cations. This has advantages and disadvantages.

Surfactants anchored or aggregated onto particle surfaces can catch and stabilize entrained air bubbles through hydrophobic interactions. However, early adsorption leads to some extent to a loss of active admixture and the consequent increase of the specific dosage needed for entrainment of a certain volume of air into concrete.

The same is true for surfactant precipitation in cement pore solutions. Indeed, while there is wide agreement in the scientific community that precipitation, or salting out, of anionic surfactants stabilizes air bubbles, it is also clear that early precipitation, prior to air bubble formation, results in an undesired loss of surfactant.

In general, one can consider that anionic surfactants from natural sources are rather robust admixtures that allow controllable adjustments of air content. However, this is at a rather high dosage compared to their synthetic competitors.

The influence of the hydrophobic group was summarized by Rosen (2004). In particular, it is stated that while the charged head of anionic surfactants used in cementitious material determines adsorption onto solids, changes in the length of the hydrophobic group increase adsorption efficiency from the aqueous solution.

Examples of anionic surfactants, whether from natural resources or synthetic, are given in the next subsections.

9.5.4.1 Carboxylic acid salts

From a categorization of commercial products in Torrans and Ivey (1968), carboxylic acid-based surfactants can be grouped as:

- salts of wood resins (abietic acid and pimaric acid)
- salts of petroleum acids (petroleum refining)
- fatty and resinous acids and their salts (paper pulp and animal hide processing).

According to Rosen (2004), such compounds are easily prepared by neutralization of the acids or saponification of triglycerides found in natural fats or vegetable oil. The surfactants obtained are soaps ($RCOO^{-}M^{+}$), and can be seen as a very early type of AEA. As previously stated, in cementitious systems they have the disadvantage of forming water-insoluble soaps with di- and trivalent metallic ions and are insolubilized readily by electrolytes.

However, experience teaches us that the advantage of such admixtures can be seen in their relative robustness and ease of controlling air entrainment. Furthermore, according to Mayer and Axmann (2006), this gives air void contents that are relatively independent of external conditions, such as agitation intensity and stirring time. Moreover, precipitation in the presence of Ca-ions of soaps prepared from wood resins is less significant than that of soaps obtained from other raw materials.

The issue of precipitation can be overcome by including additional SO_3H-groups in the oleoresin acid skeleton of anionic surfactants based on abietic acid (Mayer and Axmann, 2006). Another solution is to add lime soap-dispersing agents, i.e. sulphonates and sulphates (compatible anionic surfactants, discusssed later in this section) (Rosen, 2004).

One specific compound in anionic AEAs is based on the neutralization of resin acid and fatty acids using amines, in particular triethanolamine and diethanolamine,

a process well known to lead to surfactants (McCorkle and Brow, 1955). Through this process, quasi-synthetic soaps can be produced with the robustness of metal salts of anionic surfactants but better efficiency and less tendency to precipitate or be adsorbed on solid surfaces (Sychra and Steindl, 1998).

9.5.4.2 Sulphonic acid salts

In sulphonates, the sulphur atom is directly attached to the carbon atom of the alkyl group. This renders the molecule stable against hydrolysis, also in alkaline media, when compared with sulphates (described in the next subsection) (Tadros, 2005).

An example of such a surfactant used as an AEA is linear alkylbenzenesulphonate of the generic structure $RC_6H_4SO_3^-M^+$. The chain length of the alkyl portions is about 12 carbons in most cases. Linear alkylbenzenesulphonate is relatively cheap.

Regarding the hydrophilic head, salts with different cations have different characteristics. Calcium and magnesium salts are water-soluble, and therefore not affected by hard water. Sodium salts are sufficiently soluble in the presence of electrolytes for most uses.

A commercially available surfactant for AEAs is linear sodium dodecylbenzenesulphonate, shown in Figure 9.35.

Other surfactants, with HLB values ranging from about 11 to 14, are also used in commercial products:

- Sodium C10−16 benzenesulphonate
- Triethanolamine dodecylbenzenesulphonate.

α-Olefin sulphonates are produced by reacting a linear α-olefin with sulphur trioxide. This typically yields a mixture of alkene sulphonates (60−70%), hydroxyalkane sulphonates (~30%) and some disulphonates and other species (Tadros, 2005).

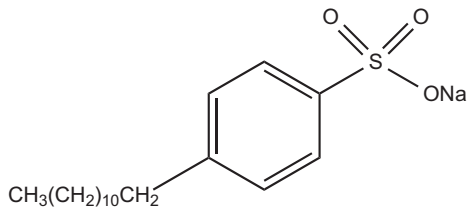


Figure 9.35 Chemical structure of sodium dodecylbenzenesulphonate.

1. 3,4 Olefin sulphonate:	$R-CH=CH(CH_2)_2SO_3^-$
2. 4-Hydroxy alkane sulphonate:	$R-CHOH-(CH_2)_3SO_3^-$
3. Disulphonate (sulphatosulphonate):	$R\text{-}CH_2\text{-}CH(OSO_3^-)\text{-}CH_2\text{-}SO_3^-$

Such surfactants are commercially available for concrete AEAs with C14 or C16 hydroxy alkane sulphonate (even numbered and C14−16 olefin sulphonate, respectively; $10 < HLB_{calculated} < 11$).

9.5.4.3 Sulphuric acid ester salts

Sulphates are synthetic anionic surfactants that are produced by reaction of an alcohol with sulphuric acid, and are therefore esters of sulphuric acid. Sulphates carrying alkali metals counterions show good solubility in water, but tend to be affected by the presence of electrolytes (Tadros, 2005). Ammonium alkyl sulphates can also be found.

Sulphates are usually prepared using alcohols with chain lengths ranging from dodecyl to hexadecyl (Rosen, 2004). The presence of a methyl branch in the hydrophobic group gives the surfactant a higher tolerance towards calcium ions in water.

An important sulphate surfactant is sodium dodecyl sulphate (or sodium lauryl sulphate), shown in Figure 9.36. It is extensively used for fundamental studies and in many industrial applications, as well as in air entrainers for concrete and gypsum. Sodium alkyl sulphates with chains of 8 and 10 carbons also have application in air entrainers.

Through modification of the hydrophobic group by introducing some EO units, better solubility and less sensitivity compared to straight alcohols are achieved, and the surfactant becomes more compatible with electrolytes in aqueous solution. These sulphates are then referred to as alcohol ether sulphates or sulphated polyoxyethylated straight-chain alcohols (Tadros, 2005). Commercial products mostly include C12 and EO units with a broad range of distribution in polyoxyethylated chain length (Rosen, 2004; Tadros, 2005). Recent products have a narrow range of chain lengths and contain fewer unreacted (non-ethoxylated) hydrophobic residues, making them more tolerant towards hard water (Rosen, 2004).

To the authors' knowledge, commercially available sodium alkyl ether sulphates for air entrainment of concrete include:

- sodium alkyl ether sulphate with two EO units and C12−14 chain
- sodium alkyl ether sulphate with three EO units and C12−15 chain.

Commercial ammonium alkyl ether sulphates can be found as:

- ammonium alkyl ether sulphate with 2.2 EO units and C8−10 chain
- ammonium alkyl ether sulphate with 2.5 EO units and C9−11 chain
- ammonium lauryl (C12) ether sulphate with three EO units.

It is important to note that in the above cases the HLB of the surfactant can be adjusted through modifications to both the hydrophilic head, via the salt type, and the hydrophobicity of the chain by the addition of certain number of EO units.

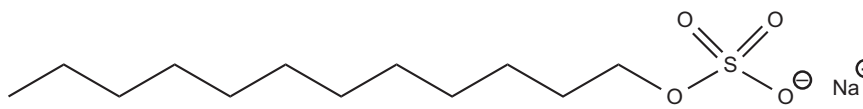


Figure 9.36 Chemical structure of sodium lauryl sulphate.

The advantages of alkyl ether sulphates over alkyl sulphates were summarized by Rosen (2004) as being:

- more water-soluble
- more electrolyte-resistant
- much better lime soap-dispersing agents
- foam is more resistant to water hardness and protein soil.

Of these four advantages, the second and the third are the most important for use as air entrainers in concrete.

9.5.4.4 Taurates

Surfactants of the group of taurates (taurides) are rather mild anionic surfactants. They show good compatibility with non-ionic and other anionic surfactants, and provide good stability against hydrolysis as well as good lime soap-dispersing power. Because of this, they find application in air entrainers as 'cosurfactants' to support the efficiency of the main active surfactant.

A general representation of taurates is shown in Figure 9.37, where R mostly comes from saturated C12−C18 fatty acids, oleic acid or coconut fatty acid. According to Rosen (2004), the solubility, foaming, detergency and dispersing powers of the *N*-methyl derivatives (Figure 9.37 with $R_1 = CH_3$) are similar to those of the corresponding fatty acid soaps, and are effective in hard and soft water.

Examples of commercially available products are sodium salts of oleic acid methyl taurate and coconut fatty acid methyl taurate.

9.5.5 Cationic surfactants

Cationic surfactants have a positively charged hydrophilic head; their advantage is their compatibility with non-ionic and amphoteric surfactants. They are mostly incompatible with ionic surfactants (Rosen, 2004; Tadros, 2005).

Ethoxylated amines are sometimes referred to as 'cationic' surfactants, but this is true only for low pH and low numbers of EO units. Considering the high pH of cement pore solution, their surfactant nature will be rather that of a 'non-ionic' compound (discussed later in this section).

Examples of pH-insensitive cationic surfactants are quaternary ammonium salts. On the quaternized amine group the electrical charge on the molecule is unaffected by pH changes, which means that the positive charge remains in acidic, neutral and alkaline media.

It is reported that using cationic surfactants can maintain the efficiency of air entrainers in the presence of clay contaminations in concrete (Hill et al., 2002).

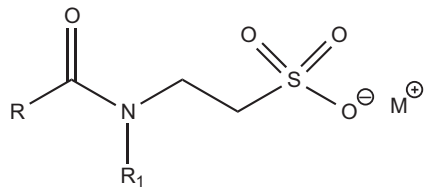


Figure 9.37 Chemical structure of an alkali metal salt of *n*-acyl-*n*-alkyl taurate.

In patents for AEAs one can find references to cationic surfactants. However, these compounds appear to be used as by-products or additions.

9.5.6 Amphoteric surfactants

The hydrophilic group of amphoteric surfactants bears both a negative and a positive charge, so the net charge of the molecule is zero. The main characteristic of amphoteric surfactants is that their behaviour depends on pH. For acidic solutions, the molecule acquires a positive charge and behaves like a cationic surfactant, whereas in alkaline solutions it becomes negatively charged and behaves like an anionic one. At their individual isoelectric point, the properties of amphoteric surfactants resemble those of non-ionic surfactants very closely (Tadros, 2005).

Examples of amphoteric surfactants used in air entrainers are betaines, amine oxides and amines. However, these compounds are mostly used as components in surfactant mixes of formulated products.

In patent literature on AEAs, betaines or their salts and derivates are found in combination with non-ionic surfactants, i.e. ethoxylated alcohols or alkylaryl polyether alcohol, polyoxyalkylene copolymer surfactants and others. This family of surfactants is used in AEAs compatible with shrinkage-reducing admixtures (SRAs) based on mixtures of non-ionic surfactants and cosolvents or hydrotropes. It can be speculated that the presence of cosolvents and hydrotropes increases the solubility of the AEA. The energy gain in stabilizing air bubbles is then reduced, but betaines probably compensate for that.

Betaine-type surfactants found in patent literature are derivatives of trimethylglycine (Figure 9.38(a)) with $R = CH_3$ (Bour and Childs, 1992; Kerkar and Dallaire, 1997; Kerkar et al., 2001; Budiansky et al., 2001a; Hill et al., 2002). Several types of betaine derivatives can be obtained by modifying the nature of both hydrophobic and hydrophilic portions of the surfactant. For example, the head group of an alkyl betaine can undergo sulphonation with formation of an alkyl sulphobetaine (Figure 9.38(b)). Other betaine-type surfactants are shown in Figure 9.38.

An example of a commercially available betaine is alkyl amidopropylsulphobetaine, for which, according to Bour and Childs (1992), the hydrophobic group can be decyl, cetyl, oleyl, lauryl and coco (C_{6-18} H_{13-37}) radicals.

To the authors' knowledge, commercial products can be found that include the following compounds:

- coco amidopropyl betaine
- coco amidopropyl hydroxy sulphobetaine.

A second important surfactant type of an amphoteric nature used in AEAs is the group of amine oxides which are sometimes referred to as cationic, but would be non-ionic according to Tadros (2005) and amphoteric according to Rosen (2004).

A commercial product designated for use in concrete air entrainment is coco alkyl dimethyl amine oxide (Figure 9.39). Coconut fatty acids have a distribution of alkyl chain lengths in the range of C8−C20. Commercial products listed as air entrainers are found to have more or less narrow ranges, such as C12−18, C12−16, C12−14 or even C14.

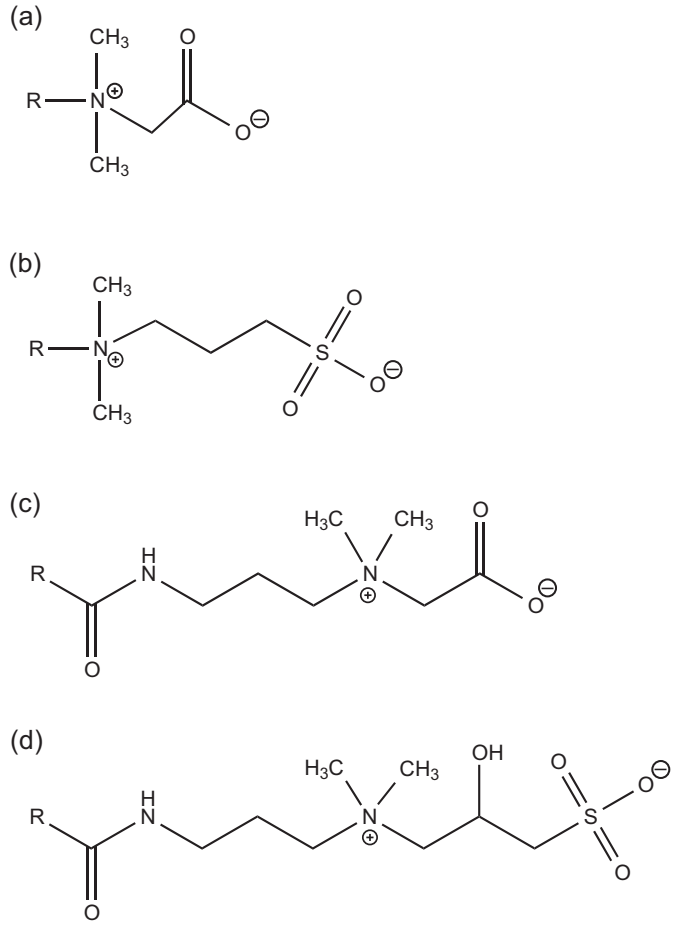


Figure 9.38 Chemical structure of betaine-type surfactants (with R = long hydrophobic chain): (a) alkyl betaine, (b) alkyl sulphobetaine, (c) alkyl amidopropyl betaine, (d) alkyl amidopropyl hydroxy sultaine.

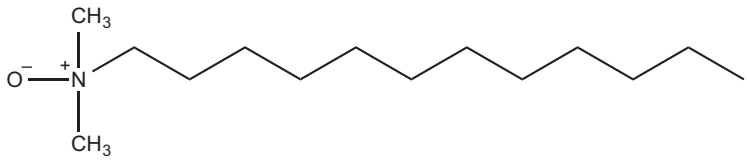


Figure 9.39 Chemical structure of a coco alkyl dimethyl amine oxide, where the alkyl chain has 12 carbon atoms.

To the authors' knowledge lauramine oxide and decyldimethylamine oxide are used in addition to the previously mentioned surfactants found in commercial products.

9.5.7 Non-ionic surfactants

Non-ionic surfactants are mostly based on EO, and are usually referred to as ethoxylated surfactants. Tadros (2005) distinguishes the following classes:

- alcohol ethoxylates
- alkyl phenol ethoxylates
- fatty acid ethoxylates
- monoalkaolamide ethoxylates
- sorbitan ester ethoxylates
- fatty amine ethoxylates
- ethylene oxide−propylene oxide copolymers (also known as polymeric surfactants).

There are also multihydroxy products, such as:

- glycol esters
- glycerol and polyglycerol esters
- glucosides and polyglucosides
- sucrose esters.

Considering their application in concrete, non-ionic surfactants have the advantage of good compatibility with all other types of surfactants. Because of their non-ionic nature these surfactants do not show strong adsorption onto charged surfaces. In terms of undesired loss of surfactant at the solid−liquid interface, this means that more surfactant remains available to saturate the liquid−vapour interface of the air bubbles created through mixing, and less surfactant is needed compared to their analogous ionic surfactants for a given air void surface to be created in concrete.

The main disadvantage of non-ionic surfactants is their inability to properly stabilize the air system they are creating, mitigating coalescence and bubble coarsening. In particular, unlike anionic surfactants, they cannot directly form salts with electrolytes of the cement pore solution at the liquid−vapour interface, while charged heads of ionic surfactants form a shell-like structure with increased rigidity through precipitation (for example lime soap).

This may be the reason why non-ionic surfactants are rarely used as a single compound in AEAs (Ziche and Schweizer, 1982) and are mostly found in mixtures with surfactants of different natures (Bour and Childs, 1992; Hill et al., 2002; Budiansky et al., 1999, 2001a,b; Wombacher et al., 2014; Berke et al., 2002). In this sense they can be considered as having mainly a supporting function in formulated admixtures, as discussed in Chapter 15 (Mantellato et al., 2016).

In this role of cosurfactants they increase the solubility of ionic surfactants and reduce the tendency of the ionic surfactant to adsorb at the solid−liquid interface. In the case of contamination with unburnt carbon in blended cements containing fly

ash, some non-ionic surfactants may serve as sacrifice material because they are good carbon dispersers.

Ethoxylated fatty acids and their amines are referred to as single-component air entrainers (Ziche and Schweizer, 1982). Their application is in cementitious material with rather high stiffness (plaster). Air entrainment in concrete for pavers is another field of application for non-ionic surfactants as a single component.

An example of a commercially available surfactant is coconut fatty amine with a number of EO units between 2 and 20.

In Berke et al. (2002) a triblock polyoxyalkylene copolymer surfactant has been claimed for use in AEAs. This has the general formula:

$$R_1O{-}(EO)_x{-}(PO)_y{-}(EO)_x{-}R_2$$

where,

R_1; R_2: C1−C7 alkyl group, C5−C6 cycloalkyl group or aryl group
x: 42−133
y: 21−68.

More preferred is:

$$HO{-}(EO)_x{-}(PO)_y{-}(EO)_x{-}H$$

with a molar mass between 8000 and 12,000 g/mol and an HLB between 20 and 30.

This polymeric surfactant is claimed to show good performance in concrete that contains a surfactant of the same nature used as an SRA.

In Budiansky et al. (1999, 2001a,b) a polymeric surfactant with explicit compatibility with an oxyalkylated SRA is introduced. In particular, the surfactant has a di-block structure:

$$R_1O{-}(EO)_m{-}(PO)_n{-}R_2$$

with preferences on:

R_1; R_2	H or CH_3
m; n	30−60

and a molar mass of $M > 2000$ g/mol. The SRA used in combination is dipropylene-tert-butyl ether (DPTB).

This preferred structure results in a range of $14.2 < \text{HLB} < 19.6$ and roughly between 3000 and 6000 g/mol.

In fact, formulators' experience shows that the compatibility issue between SRAs and AEAs is a real problem where a combination of an ethoxylated SRA with a common

air entrainer either consistently reduces air entrainment or requires disproportional high dosages. In Berke et al. (2002) this compatibility issue was solved using a polymeric non-ionic surfactant alone. However, the AEA of Budiansky et al. (1999, 2001a,b) contains not only a di-block polymeric surfactant but also a betaine-based surfactant.

Non-ionic polymeric surfactants have a major advantage with respect to other non-ionic surfactants, that is having a high degree of freedom for tailoring the overall size and HLB of the molecule, as well as the location of the hydrophilic/hydrophobic groups and their distribution.

A good example of this flexibility is provided by the above mentioned block copolymers. The triblock copolymer surfactant can be seen as an amphiphile containing two hydrophilic portions (EO units) and a hydrophobic group (propylene oxide-PO-units) between them, whereas the di-block polymeric surfactant has one hydrophilic block and one hydrophobic.

9.6 Shrinkage-reducing admixtures

9.6.1 Introduction

In this section the chemistry of SRAs is presented as an authorized excerpt of the authors' contribution to the subject (Eberhardt, 2011), with some additions.

First, an overview on general features of SRAs and their historical background is given. Like air entrainers, SRAs are mainly composed of surfactants, and basic information on this type of molecules was introduced in the section on AEAs. In this section we focus on non-ionic surfactants and/or hydrotropes that are more specifically used in SRAs. This serves to explain and distinguish the modes of action of both these admixture types on the basis of their molecular architecture.

The last section lists compounds present in commercially available SRAs, as well as compounds mentioned in patent literature.

9.6.2 History and working mechanism of SRAs

SRAs are composed of surfactants that decrease the surface tension of pore solution and of the water films that cover the solid surfaces exposed in the course of drying of cementitious porous material. They were introduced in a study by Sato et al. (1983), in which shrinkage reduction due to SRAs was suggested to come from reduced surface tension of the cement pore solution. There, the capillary force theory of drying shrinkage was explicitly referred to because of a more or less good correlation between shrinkage reduction, SRA dosage in cement paste and the dependence of surface tension on SRA concentration in its aqueous solutions.

Moreover, well before SRAs were introduced in 1983, Ostrikov et al. (1965) obtained similar results with shrinkage of cement paste subjected to solvent replacement prior to drying. This study focused on the mechanism of drying shrinkage rather than on shrinkage reduction of concrete; by coincidence, however, it revealed some very interesting results. Ostrikov et al. tried to eliminate capillary forces by osmotically

replacing the pore solution with several organic liquids with substantially lower surface tension. With hexane having a surface tension of about 25% of that of water ($\gamma_{hexane} \sim 18$ mN/m, $\gamma_{water} \sim 73$ mN/m), drying shrinkage deformation surprisingly was reduced to about 25%. At that point in time, however, it was not clear if this proportionality between the reduction of surface tension of the pore fluid and reduction of drying shrinkage deformation was of broader relevance.

It is possible to derive from thermodynamics how the reduction of the surface tension of the liquid−air interface (menisci and water films) leads to shrinkage reduction (Eberhardt, 2011). In particular, it can be shown that the reduction of surface tension coming from SRAs enables the cementitious matrix to reduce its free energy substantially, as it contains a large liquid−vapour interfacial area owing to its fine porosity. More specifically, this is done by increasing the portion of free energy used in the creation of the exposed liquid−air interfacial area, while at the same time reducing the free energy utilized in deformation. This mechanism is shown to be active as long as the surface tension can be maintained sufficiently low. The working mechanism of SRA is dicussed more in detail in Chapter 13 (Eberhardt and Flatt, 2016).

9.6.3 General features and overview of surfactants used in SRAs

Regarding the nature of SRAs, a patent search on materials used as SRAs was conducted by Eberhardt (2011). It revealed that two main groups of admixtures can be discriminated:

- SRAs containing one type of non-ionic surfactant or hydrotrope
- SRAs containing mixtures of non-ionic surfactants, cosolvents and hydrotropes.

In both cases there are similarities between SRAs and AEAs, as both contain amphiphilic compounds. However, SRAs distinguish themselves from AEAs in their mode of action. While AEA adsorption onto solids does in part support stabilization of air bubbles (anchoring), SRA surfactants are efficient only by adsorbing at the liquid−vapour interface.

Therefore, surfactants used in SRAs are non-ionic so they do not strongly adsorb onto the charged surfaces of cement or its hydrates. The adsorption of surfactants onto cement is discussed in more detail in Chapter 10 (Marchon et al., 2016). Moreover, non-ionic surfactants used in SRAs are generally less hydrophobic and smaller than surfactants used in air entrainers. This also comes from their different mode of action. In Table 9.5 the actual interfacial area or workspace of an AEA and an SRA is estimated using a standard concrete with 300 kg of Portland cement and an air volume of 50 L/m^3 entrained through 100 μm large spherical air bubbles.

One can see that the interface to be theoretically covered with surfactants is higher by a factor of 1000 to 2000 in the case of SRA. This is also the reason why AEAs are used at such low dosages (a few grams per kilo of binder), and why SRA dosages can be 1−2% per weight of binder. More importantly, this requires a significantly higher solubility of the non-ionic surfactants used as SRAs in the strong aqueous electrolyte cement solution.

The use of non-ionic cosolvents and hydrotropes results from the abovementioned need to solubilize non-ionic surfactants efficiently in cement pore solution. For this it is

Table 9.5 Considerations on interfacial area/workspace of an SRA compared to an AEA in 1 m^3 concrete

Workspace of air entrainer	**Interfacial area created by air bubbles**	
Assumptions		
Volume of air bubbles in 1 m^3 concrete	0.05	m^3
Assumed bubble diameter	100	μm
Bubble volume	5.2×10^{-13}	m^3
Number of bubbles	9.5×10^{10}	–
Bubble surface per 1 m^3 concrete	**3×10^3**	**m^2**
Workspace of SRA	**Area exposed during drying**	
Assumptions		
Surface of 1 cubic metre of fresh concrete (cube)	6	m^2
Cement hydrates content (300 kg cement) reacted	378	kg
Range-specific surface of cement hydrates (BET method)	8–150	m^2/g
Interface (l-v) exposed during drying of 1 m^3 concrete	**$3 \times 10^6 - 57 \times 10^6$**	**m^2**

necessary to close undesired miscibility gaps between the surfactant and the aqueous phase, and to reduce the surfactants' tendency to coprecipitation with electrolytes of the cement aqueous phase.

The previous section on AEAs introduced the HLB concept. Equation (9.3) can be used to calculate the HLB of non-ionic surfactants using the method of individual contributions (group numbers) of hydrophilic and hydrophobic portions or groups in the molecular structure of the surfactant. For mixtures of surfactants, as SRAs often are, an overall HLB of the mixture can be calculated by additivity, according to Tadros (2005), using this equation:

$$\mathrm{HLB} = \sum_{i=1}^{n} (x_i \mathrm{HLB}_i) \tag{9.4}$$

where,

i: integer, number of surfactants in the mixture
x_i: weight fraction of surfactant i
HLB_i: HLB of surfactant i.

In fact, several SRAs contain additional components like dispersing agents, accelerators and/or air entrainers, indicating that surfactants may influence hydration as well as the mechanical performance of the cementitious material.

Regarding mixtures of surfactants, it is explicitly pointed out that there is a synergistic effect that enhances drying shrinkage reduction (Wombacher et al., 2000, 2002, 2012; Gartner, 2008; Shawl and Kesling, 1995). This is because surfactants with different HLBs can serve each other as cosolvents. The cosolvent increases the surfactant solubility and reduces undesired phenomena such as surface aggregation (hydrates), salting out (coprecipitation with electrolytes from pore solutions) and self-aggregation (liquid crystals).

This is also true when surfactants of different admixture categories are combined in concrete, in particular in the case of air entrainers compatible with SRAs: the more soluble surfactants from an SRA (or the cosolvents and hydrotropes used therein) serve the AEA's rather large and less soluble surfactants as cosolvents, and can sometimes compromise the performance of the AEA. To maintain AEA performance a surfactant of a different nature − amphoteric, according to Berke et al. (2002), Budiansky et al. (1999, 2001a,b) and Kerkar and Dallaire (1997) − can be used to establish compatibility between the SRA and the AEA (see the previous section on AEAs).

It is important to note that the molecular design of several surfactants claimed as SRAs limits their applicability in mortar and concrete. Some materials turn out to be too expensive to be used in concrete. Other components have to be excluded because their low molecular weight causes issues regarding low saturation vapour pressure (highly explosive) and/or low flaming points (Wombacher et al., 2000, 2002, 2012; Gartner, 2008).

Several other important material characteristics concerning the use of surfactants in cementitious systems, as well as basic working mechanisms, can be derived from general knowledge on non-ionic surfactants, which is in part outlined in the previous section on the chemistry of air entrainers.

In the next section the chemistry of non-ionic surfactants used in commercial SRAs, as well as surfactants mentioned in patent literature on SRAs, is given.

9.6.4 Classes of compounds used in SRAs

This section covers the molecular architecture of non-ionic surfactants and hydrotropes used in SRAs.

The compounds used in SRAs can be classified as:

- monoalcohols
- glycols
- polyoxyalkylene glycol alkyl ethers
- polymeric surfactants.

Besides these compounds, others can be used as SRAs.

9.6.4.1 Monoalcohols

Monoalcohols are organic compounds characterized by the presence of a hydroxyl functional group, and can be represented by the generic chemical formula R−OH, where R is an alkyl radical (linear, branched or cyclic).

Umaki et al. (1993) claimed alcohols with a small number of carbon atoms, also called lower alcohols, to be efficient in shrinkage reduction. In particular, tert-butyl alcohol is considered to be the most efficient SRA.

The solubility of monoalcohols in water depends on the chemistry of the alkyl group. The C4−6 straight alcohols would have limited solubility in water, except tertiary butanol that shows complete miscibility in water. Compared to surfactants used in air entrainers, the HLB application range is rather of a wetting agent (HLB 7−9) than of an oil in water emulsifier (HLB 8−18).

Monoalcohols can be found in formulated SRAs in combination with polyoxyalkylene glycols, polyoxyalkylene glycol alkyl ethers or polymeric surfactants (Shawl and Kesling, 1995, 1997, 2001) (see below).

9.6.4.2 Glycols

The term glycols strictly refers to a class of alcohols that possess two hydroxyl functional groups attached to two adjacent carbon atoms. However, it can be used more generally as a synonym for diol.

Glycols of interest for SRAs are alkandiols (or alkylene glycol) and polyoxyalkylene glycols. The general chemical structure of alkandiols is given in Figure 9.40.

Schulze and Baumgartl (1989, 1993) claim that alkandiols with n between 5 and 10, in particular 2,2-dimethyl-1,3-propanediol (neopentyl glycol), shown in Figure 9.41, are good for reducing shrinkage. Lunkenheimer et al. (2004) classify this type of surface-active molecules as solvo-surfactants or hydrotropic detergents, because they combine properties of solvents and surfactants.

2,2-Dimethyl-1,3-propanediol has good solubility in water (830 g/L at 20 °C), and finds application as single-component SRA, but can also be used as a cosolvent in formulated SRAs containing non-ionic surfactants with lower HLB.

As an example of these multicomponent SRAs, alkane diols have been used in combination with a non-ionic fluorinated polyester (Gartner, 2008) capable of reducing the surface tension of water down to below 30 mN/m. The synergistic effect on enhancing shrinkage reduction by combining glycol and surfactant was explicitly pointed out.

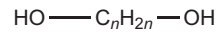


Figure 9.40 Chemical structure of alkane diols.

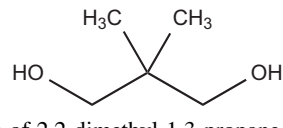


Figure 9.41 Chemical structure of 2,2-dimethyl-1,3-propanediol.

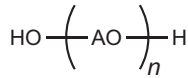


Figure 9.42 Chemical structure of polyoxyalkylene glycols.

The other class of compounds belonging to glycols are polyoxyalkylene glycols, whose chemical structure is shown in Figure 9.42. In the adopted notation, AO represents an oxyalkylene unit.

The number of oxyalkylene units in the molecule can vary, but it is small ($1 < n < 8$).

Berke and Dallaire (1997) claimed a cement admixture able to counteract drying shrinkage by use of alkylene glycol, that is 2-methyl 2,4 pentanediol, or polyoxyalkylene glycols, and maintain compressive strength of concrete using silica fume and a stabilizer as a second component.

The combination of glycols and polyoxyalkylene glycol alkyl ethers has been shown to have a synergistic effect on shrinkage reduction efficiency (Wombacher et al., 2000, 2002, 2012; Gartner, 2008).

9.6.4.3 *Polyoxyalkylene glycol alkyl ethers*

The general formula of polyoxyalkylene glycol alkyl ethers is shown in Figure 9.43.

The R group is a linear, branched or cyclic alkyl radical, and represents the hydrophobic tail of the surfactant. The hydrophilic head consists of the hydrated oxyalkylene chain (AO).

Polyoxyalkylene glycol alkyl ethers were claimed to be good SRAs by Sato et al. (1983). A reduction of drying shrinkage of up to 50% was derived theoretically using the capillary force shrinkage model and the reduction of surface tension. In 1985, a US patent (Goto et al., 1985) was granted to this group of authors.

According to patent literature, the alkyl radical R can vary, but it has a small number of carbon atoms ($C < 20$) and the alkylene group can be EO, PO or a block or random copolymer containing both, in the same proportions. The number of oxyalkylene units in the molecule (n) can be between 1 and 10 (Sato et al., 1983; Goto et al., 1985) or more (Sakuta et al., 1990, 1992, 1993).

It has been reported that cyclohexyl radicals are preferred for the shrinkage reduction effect, and that the random configuration of EO and PO units in the polar portion of the molecule is to be preferred for low foamability (Goto et al., 1985).

In commercial admixtures one representative of this class of compounds is dipropylene glycol tert-butyl ether (DPTB) (Figure 9.44), with an HLB of 7.05.

The HLB of 7.05 means that DPTB is a wetting agent (Table 9.2), and would be dispersed in water only by vigorous agitation. The relation between HLB and

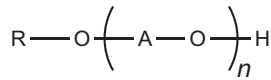


Figure 9.43 Chemical structure of polyoxyalkylene glycol alkyl ethers.

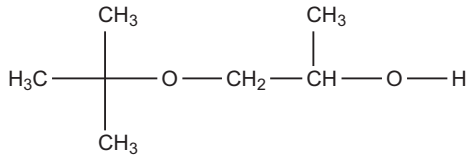


Figure 9.44 Chemical structure of dipropylene glycol tert-butyl ether.

solubility helps us to understand combinations of substances, as for example in the commercial SRA (Eberhardt, 2011). In that case the mix of compounds with very different HLBs (11.2 and 2.9) leads to a sufficient solubility that can be assessed on the basis of the average HLB value of this mix (10.1).

Multicomponent SRAs have been made that include polyoxyalkylene glycol alkyl ethers and other conventional cement admixtures, such as polycarboxylate-based SPs (Collepardi, 2006), naphthalene sulphonate formaldehyde condensate and melamine sulphonate formaldehyde condensate (Berke et al., 2000).

Because of the defoaming property of shrinkage-reducing compounds and to provide proper air entrainment for concrete, Berke et al. (1997) and Kerkar et al. (2000) combined a shrinkage-reducing compound based on polyoxyalkylene glycol alkyl ethers and an organic amine salt of tall oil fatty acid or an AEA, respectively.

9.6.4.4 *Polymeric surfactants*

Starting from 1988, Akimoto et al. (1988, 1990a, 1992) proposed a cement admixture efficient in shrinkage reduction obtained by copolymerization of a polyoxyalkylene derivative and maleic anhydride, a hydrolyzed product of the copolymer or a salt of the hydrolyzed product. Akimoto et al. (1990b) filed another US patent, claiming a dispersing compound with a component similar to the structure given in Figure 9.45.

In Figure 9.45, B is a residue carrying two to eight hydroxyl groups, and X and R are hydrocarbon chains of different length and chemistry. The number of oxyalkylene groups can vary from 1 to 1000. The indexes *l* and *n* are between 1 and 7, whereas *m* can be between 0 and 2.

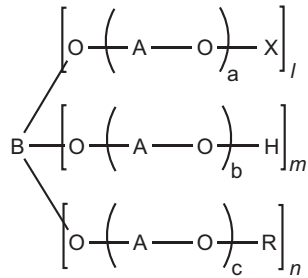


Figure 9.45 Chemical structure of a polymeric surfactant used in SRAs.
According to Akimoto et al. (1990b).

The polymer can be classified as a polymeric non-ionic surfactant. In comparison to monoalcohols and polyoxyalkylene glycols alkyl ethers, the surfactant can be rendered two- or three-headed. To prevent slump loss and provide drying shrinkage reduction, a copolymer that is to some extent soluble in water exhibits the best performance (Akimoto et al., 1990b).

As mentioned previously, the efficiency of some molecules as SRAs needs to be enhanced by the presence of a cosurfactant. This is probably for use of compounds with the general formula given in Figure 9.46, which are claimed for use in mixtures with other surfactants already known to be individually effective as SRAs (Shawl and Kesling, 2001).

In this molecule, the oxyalkylene groups have preferably two to four carbon atoms and R is either hydrogen or an alkyl group (C1−16). This surfactant can be classified as polyol ($n = 0$), or a two-headed and three-headed polymeric surfactant.

Starting in 1997, several patents were issued (Berke and Dallaire, 1997; Berke et al., 1997, 1998, 2000, 2001; Kerkar et al., 1997, 2000; Kerkar and Gilbert, 1997) claiming bi-component admixtures containing a shrinkage-reducing component A and a second component B, that is a dispersing admixture.

Berke et al. (2001) described a mixture of different SRAs (polyoxyalkylene glycols, polyoxyalkylene glycols alkyl ether, polyols) and a comb-shaped polymeric dispersant with free carboxylic acid groups and side chains containing oxyalkylene units. This molecule is shown in Figure 9.47, which basically is just a more generic expression of the structure shown in Figure 9.12. The claims in the mentioned patent indicate that the B group is a carboxylic acid ester, an amide, an alkylene ether or an ether

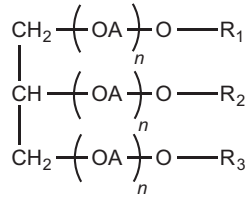


Figure 9.46 Chemical structure of a polymeric surfactant used in SRAs. Adapted from Shawl and Kesling (2001).

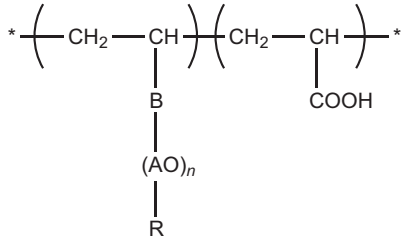


Figure 9.47 Chemical structure of a comb-shaped polymer dispersant used in SRAs (Berke et al., 2001).

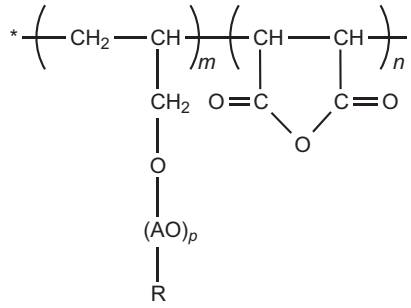


Figure 9.48 Chemical structure of a comb-shaped polymer dispersant used in SRAs (Kerkar and Gilbert, 1997).

group. The radical R can have from 1 to 10 carbon atoms, and the number of oxyalkylene units can vary from 25 to 100. A similar comb-shaped copolymer was proposed by Kerkar and Gilbert (1997) (Figure 9.48).

These structures are typical for comb-copolymer dispersants (see Section 9.2.4), but can also be classified as a polymeric macro-surfactant, in which the hydrophilic heads are formed by the grafted chains and the maleic unit serves as a hydrophobic 'head spacer'.

9.6.4.5 Other SRAs

Other SRAs include amino alcohols, whose chemical structure is shown in Figure 9.49. According to Abdelrazig et al. (1995), amino alcohols where the R groups are short linear or branched alkyl radicals or hydrogen atoms show good shrinkage-reducing properties.

The preferred amino alcohols are 2-amino-butanol and 2-amino-2-methyl-propanol. An estimate of the HLB of such compounds is complicated because of the pH dependence. In cement pore solution (pH > 12.5) the amine group is not protonated, and thus the surfactant will resemble a non-ionic nature. The hydrophilic main contribution comes from the free hydroxyl of the alcohol portion, and the HLB is about 8.

Amino alcohols have been used in formulation together with diols, glycols or alkyl ether glycols or neopentyl glycol (Wombacher et al., 2000, 2002, 2012). The chemical structure of the amino alcohol surfactant claimed is shown in Figure 9.50.

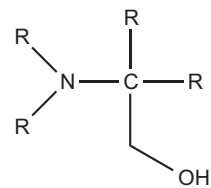


Figure 9.49 Chemical structure of an amino alcohol.

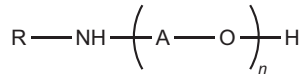


Figure 9.50 Chemical structure of an amino alcohol surfactant.

According to Wombacher et al. (2000, 2002, 2012), the radical R is a C1−6 alkyl group (linear, branched or cyclic) and the alkylene group is either an ethyl (C_2H_4) or a propyl (C_3H_6) group.

The structure of an amino alcohol surfactant is similar to that of polyoxyalkylene glycol alkyl ether, except that here the ether bond is substituted by a secondary amine group.

Shrinkage measurements on mortars modified by using different compositions of amino alcohols, glycols and/or alkyl ether glycols, alone and in combination, reveal a synergistic effect on the enhancement of shrinkage reduction. A similar phenomenon was shown by Shawl and Kesling (1995) for polyoxyalkylene glycol alkyl ethers and glycols or diols.

Abdelrazig et al. (1994, 1995) developed admixtures containing amides or formyl compounds whose general chemical structure is shown in Figure 9.51.

In Figure 9.51 R_1 is a C4−6 alkyl alcohol or alkanoyl radicals, X is either an oxygen atom or a secondary nitrogen group and R_2 is either a primary nitrogen group or a $-CH_2C-(O)-CH_3$ group if X is an oxygen atom.

According to Abdelrazig et al. (1994, 1995), the preferred SRAs are *n*-butyl urea (Figure 9.52(a)) and *n*-butyl acetoacetate (Figure 9.52(b)).

As for amino alcohols, the estimation of the HLB value of butyl urea is a delicate task because of the deprotonation of the amine group at its isoelectric point. Considering the high pH of cement pore solution, the hydrophilic contribution will mainly come from oxygen. For butyl acetoacetate the HLB is also hard to calculate because of missing group numbers. An estimate would be a range of HLB 7−9.

Engstrand and Sjogreen (2001) claimed a powdered SRA made of a cyclic acetal of a tri- or polyfunctional alcohol and amorphous silica, such as a silicic acid. For further

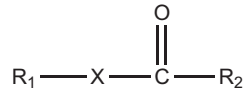


Figure 9.51 Chemical structure of amides or formyl compounds.

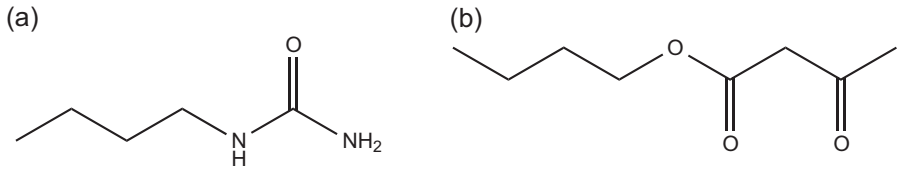


Figure 9.52 Chemical structures of (a) *n*-butyl urea and (b) *n*-butyl acetoacetate.

specification the acetal is a 1,3 dioxane of a trihydric alcohol, trimethylol-C1-8-alkane or trihydric alcoxylated alcohol.

9.7 Conclusions

Chemical admixtures include many types of compounds. In this chapter we have focussed on organic molecules, ranging from small organic compounds to large polymers with a certain polydispersity, of both natural origin and synthetic. The chapter provided an overview of the chemical characteristics of the different organic chemical admixtures.

We have done this because they offer the greatest possibility to chemists to modify properties and target improved performance by specific exploitation of structure—property relationships. This very important aspect of chemical admixtures is illustrated in more detail in the following chapters, where the working mechanisms of the chemical admixtures are discussed. Chapters 11 (Gelardi and Flatt, 2016), 13 (Eberhardt and Flatt, 2016) and 20 (Palacios and Flatt, 2016) deal respectively with the working mechanisms of dispersants, SRAs and VMAs, while Chapter 12 explains the impact that admixtures may have on cement hydration (Marchon and Flatt, 2016b).

Finally, it is important to recall that other aspects concerning the use of chemical admixtures, such as the cost of production, availability of raw materials and performance, are very important in practice and have also been mentioned in this chapter. Aspects relating to the formulation of commercial products are addressed separately in Chapter 15 (Mantellato et al., 2016).

Acknowledgements

Support for Giulia Gelardi and Sara Mantellato was provided by SNF Project No. 140615, titled ‘Mastering flow loss of cementitious systems’. Support for Delphine Marchon was provided by Sika Technology AG, Zürich, Switzerland.

References

Abdelrazig, B.E.I., Gartner, E.M., Myers, D.F., 1994. Low Shrinkage Cement Composition. US Patent 5326397, filed July 29, 1993 and issued July 5, 1994.

Abdelrazig, B.E.I., Scheiner, P.C., 1995. Low Shrinkage Cement Composition. US Patent 5389143, filed July 29, 1993 and issued February 14, 1995.

Adler, M., Rittig, F., Becker, S., Pasch, H., 2005. Multidimensional chromatographic and hyphenated techniques for hydrophilic copolymers, 1. Macromolecular Chemistry and Physics 206 (22), 2269−2277.

Aïtcin, P.-C., 2016a. Entrained air in concrete: Rheology and freezing resistance. In: Aïtcin, P.-C., Flatt, R.J. (Eds.), Science and Technology of Concrete Admixtures. Elsevier (Chapter 6), pp. 87−96.

Aïtcin, P.-C., 2016b. Retarders. In: Aïtcin, P.-C., Flatt, R.J. (Eds.), Science and Technology of Concrete Admixtures. Elsevier (Chapter 18), pp. 395−404.

Aïtcin, P.-C., 2016c. Accelerators. In: Aïtcin, P.-C., Flatt, R.J. (Eds.), Science and Technology of Concrete Admixtures. Elsevier (Chapter 19), pp. 405–414.

Aïtcin, P.-C., Jiang, S., Kim, B.-G., 2001. L'interaction ciment-superplastifiant. Cas Des Polysulfonates. Bulletin des laboratoires des ponts et chausses 233, 87–98.

Akimoto, S.-I., Honda, S., Yasukohchi, T., 1988. Additives for Cement. EP Patent 0291073 A2, filed May 13, 1988 and issued November 17, 1988.

Akimoto, S.-I., Honda, S., Yasukohchi, T., 1990a. Polyoxyalkylene Alkenyl Ether-Maleic Ester Copolymer and Use Thereof. EP Patent 0373621 A2, filed December 13, 1989 and issued June 20, 1990.

Akimoto, S.-I., Honda, S., Yasukohchi, T., 1990b. Additives for Cement. US Patent 4946904, filed May 13, 1988 and issued August 7, 1990.

Akimoto, S.-I., Honda, S., Yasukohchi, T., 1992. Additives for Cement. EP Patent 0291073 B1, filed May 13, 1988 and issued March 18, 1992.

Amaya, T., Ikeda, A., Imamura, J., Kobayashi, A., Saito, K., Danzinger, W.M., Tomoyose, T., 2003. Cement Dispersant and Concrete Composition Containing the Dispersant. EP Patent 1184353 A4, filed December 24, 1999 and issued August 13, 2003.

Angyal, S.J., 1980. Haworth Memorial Lecture. Sugar–cation complexes—structure and applications. Chemical Society Reviews 9 (4), 415–428.

Aso, T., Koda, K., Kubo, S., Yamada, T., Nakajima, I., Uraki, Y., 2013. Preparation of novel lignin-based cement dispersants from isolated lignins. Journal of Wood Chemistry and Technology 33 (4), 286–298.

Banks, W., Muir, D.D., 1980. Structure and chemistry of the starch granule. In: Preiss, J. (Ed.), The Biochemistry of Plants, 3. Academic Press, New York, pp. 321–369.

Bellotto, M., Zevnik, L., 2013. New poly-phosphonic superplasticizers particularly suited for the manufacture of high performance SCC. In: Rheology and Processing of Construction Materials – 7th RILEM International Conference on Self-compacting Concrete and 1st RILEM International Conference on Rheology and Processing of Construction Materials. RILEM Publications SARL, pp. 269–276.

Berke, N.S., Dallaire, M.P., 1997. Drying Shrinkage Cement Admixture. US Patent 5622558 filed September 18, 1995 and issued April 22, 1997.

Berke, N.S., Dallaire, M.P., Abelleira, A., 1997. Cement Admixture Capable of Inhibiting Drying Shrinkage and Method of Using Same. US Patent 5603760 A filed September 18, 1995 and issued February 18, 1997.

Berke, N.S., Dallaire, M.P., Kerkar, A.V., 1998. Shrinkage Reduction Cement Composition. EP Patent 0777635 A4, filed August 23, 1995 and issued December 2, 1998.

Berke, N.S., Dallaire, M.P., Kerkar, A.V., 2000. Cement Composition. EP Patent 0813507 B1, filed February 13, 1996 and issued May 17, 2000.

Berke, N.S., Dallaire, M.P., Gartner, E.M., Kerkar, A.V., Martin, T.J., 2001. Drying Shrinkage Cement Admixture. EP Patent 0851901 B1, filed August 13, 1996 and issued March 21, 2001.

Berke, N.S., Hicks, M.C., Malone, J.J., 2002. Air Entraining Admixture Compositions. US Patent 6358310 B1, filed June 14, 2001 and issued March 19, 2001.

Bessaies-Bey, H., Baumann, R., Schmitz, M., Radler, M., Roussel, N., 2015. Effect of Polyacrylamide on Rheology of Fresh Cement Pastes. Cement and Concrete Research 76 (October), 98–106. http://dx.doi.org/10.1016/j.cemconres.2015.05.012.

Bian, H., Plank, J., 2012. Re-association behavior of casein submicelles in highly alkaline environments. Zeitschrift Für Naturforschung B 67b, 621–630.

Bian, H., Plank, J., April 2013a. Fractionated and recombined casein superplasticizer in self-leveling underlayments. Advanced Materials Research 687, 443–448.

Bian, H., Plank, J., September 2013b. Effect of heat treatment on the dispersion performance of casein superplasticizer used in dry-mix mortar. Cement and Concrete Research 51, 1−5.

Black, H.C., 1955. Basic chemistry of fatty acids. In: Fatty Acids for Chemical Specialties, pp. 131−133.

Borget, P., Galmiche, L., Le Meins, J.-F., Lafuma, F., 2005. Microstructural characterisation and behaviour in different salt solutions of sodium polymethacrylate-g-PEO comb copolymers. Colloids and Surfaces A: Physicochemical and Engineering Aspects 260 (1−3), 173−182.

Bour, D.L., Childs, J.D., 1992. Foamed Well Cementing Compositions and Methods. US Patent 5133409 A, filed December 12, 1990 and issued July 28, 1992.

Bradley, G., Szymanski, C.D., 1984. Cementiferous Compositions. EP Patent 0097513 A1, filed June 20, 1983 and issued January 4, 1984.

Brudin, S., Schoenmakers, P., 2010. Analytical methodology for sulfonated lignins. Journal of Separation Science 33 (3), 439−452.

Brumaud, C., 2011. Origines microscopiques des conséquences rhéologiques de l'ajout d'éthers de cellulose dans une suspension cimentaire (Ph.D. thesis). Université Paris-Est.

Brumaud, C., Bessaies-Bey, H., Mohler, C., Baumann, R., Schmitz, M., Radler, M., Roussel, N., 2013. Cellulose ethers and water retention. Cement and Concrete Research 53, 176−184.

de Bruijn, J.M., Kieboom, A.P.G., van Bekkum, H., 1986. Alkaline degradation of monosaccharides III. Influence of reaction parameters upon the final product composition. Recueil Des Travaux Chimiques Des Pays-Bas 105 (6), 176−183.

de Bruijn, J.M., Kieboom, A.P.G., van Bekkum, H., 1987a. Alkaline degradation of monosaccharides V: kinetics of the alkaline isomerization and degradation of monosaccharides. Recueil Des Travaux Chimiques Des Pays-Bas 106 (2), 35−43.

de Bruijn, J.M., Kieboom, A.P.G., van Bekkum, H., 1987b. Alkaline degradation of monosaccharides Part VII. A mechanistic picture. Starch - Stärke 39 (1), 23−28.

de Bruijn, J.M., Touwslager, F., Kieboom, A.P.G., van Bekkum, H., 1987c. Alkaline degradation of monosaccharides Part VIII. A ^{13}C NMR spectroscopic study. Starch - Stärke 39 (2), 49−52.

Budiansky, N.D., Williams, B.S., Chun, B.-W., 1999. Air Entrainment with Polyoxyalkylene Copolymers for Concrete Treated with Oxyalkylene SRA. WO Patent 9965841 A1, filed June 14, 1999 and issued December 23, 1999.

Budiansky, N.D., Williams, B.S., Chun, B.-W., 2001a. Air Entrainment with Polyoxyalkylene Copolymers for Concrete Treated with Oxyalkylene SRA. EP Patent 1094994 A1, filed June 14, 1999 and issued May 2, 2001.

Budiansky, N.D., Williams, B.S., Chun, B.-W., 2001b. For Increasing Resistance of Hydraulic Cementitious Compositions, Such as Mortar, Masonry, and Concrete, to Frost Attack and Deterioration Due to Repeated Freezing and Thawing. US Patent 6277191 B1, filed June 14, 1999 and issued August 21, 2001.

Bürge, T.A., Schober, I., Huber, A., Widmer, J., Sulser, U., 1994. Water-Soluble Copolymers, a Process for Their Preparation and Their Use as Fluidizers in Suspensions of Solid Matter. EP Patent 0402563 B1, filed January 15, 1990 and issued August 10, 1994.

Campana, S., Andrade, C., Milas, M., Rinaudo, M., 1990. Polyelectrolyte and rheological studies on the polysaccharide welan. International Journal of Biological Macromolecules 12 (6), 379−384.

Cappellari, M., Daubresse, A., Chaouche, M., 2013. Influence of organic thickening admixtures on the rheological properties of mortars: relationship with water-retention. Construction and Building Materials, 25th Anniversary Session for ACI 228 − Building on the Past for the Future of NDT of Concrete 38, 950−961.

Chen, G., Gao, J., Chen, W., Song, S., Peng, Z., 2011. Method for Preparing Concrete Water Reducer by Grafting of Lignosulfonate with Carbonyl Aliphatics. US Patent 0124847 A1, filed May 4, 2008 and issued May 26, 2001.

Cheng, P., 2004. Chemical and Photolytic Degradation of Polyacrylamides Used in Potable Water Treatment (PhD, Thesis). University of South Florida.

Chevalier, Y., Brunel, S., Le Perchec, P., Mosquet, M., Guicquero, J.-P., 1997. Polyoxyethylene di-phosphonates as dispersing agents. In: Rosenholm, J.B., Lindman, B., Stenius, P. (Eds.), Trends in Colloid and Interface Science XI, Progress in Colloid & Polymer Science, 105, pp. 6–10.

Collepardi, M., 2006. Concrete Composition with Reduced Drying Shrinkage. EP Patent 1714949 A1, filed April 18, 2005 and issued October 25, 2006.

Collepardi, M., 1996. 6-Water Reducers/Retarders. In: Ramachandran, V.S. (Ed.), Concrete Admixtures Handbook, second ed. William Andrew Publishing, Park Ridge, NJ, pp. 286–409.

Comparet, C., Nonat, A., Pourchet, S., Guicquero, J.P., Gartner, E.M., Mosquet, M., 2000. Chemical Interaction of Di-phosphonate Terminated Monofunctional Polyoxyethylene Superplasticizer with Hydrating Tricalcium Silicate. In: ACI Special Publication, 195. American Concrete Institute, pp. 61–74.

Concrete Admixtures and the Environment; State-of-the-art Report, fifth ed., 2011. Deutsche Bauchemie e.V.

Cunningham, J.C., Dury, B.L., Gregory, T., 1989. Adsorption characteristics of sulphonated melamine formaldehyde condensates by high performance size exclusion chromatography. Cement and Concrete Research 19 (6), 919–928.

Davies, J.T., 1957. A quantitative kinetic theory of emulsion type: 1. Physical chemistry of the emulsifying agent. In: Gas/Liquid and Liquid/Liquid Interface (Proceedings of the International Congress of Surface Activity), pp. 426–438.

Eberhardt, A.B., 2011. On the Mechanisms of Shrinkage Reducing Admixtures in Self Consolidating Mortars and Concretes. Bauhaus Universität Weimar, 270.

Eberhardt, A.B., Flatt, R.J., 2016. Working mechanisms of shrinkage-reducing admixtures. In: Science and Technology of Concrete Admixtures. Aïtcin, P.-C., Flatt, R.J. (Eds.), Elsevier (Chapter 13), pp. 305–320.

Engstrand, J., Sjogreen, C.-A., 2001. Shrinkage-Reducing Agent for Cement Compositions. US Patent 6251180 B1, filed March 30, 1998 and issued June 26, 2001.

Fan, W., Stoffelbach, F., Rieger, J., Regnaud, L., Vichot, A., Bresson, B., Lequeux, N., 2012. A new class of organosilane-modified polycarboxylate superplasticizers with low sulfate sensitivity. Cement and Concrete Research 42 (1), 166–172.

Flatt, R.J., Houst, Y.F., Oesch, R., Bowen, P., Hofmann, H., Widmer, J., Sulser, U., Mäder, U., Bürge, T.A., 1998. Analysis of superplasticizers used in concrete. Analusis 26 (2), M28–M35.

Flatt, R.J., Schober, I., Raphael, E., Plassard, C., Lesniewska, E., 2009. Conformation of adsorbed comb copolymer dispersants. Langmuir 25 (2), 845–855.

Flatt, R.J., Schober, I., 2012. Superplasticizers and the rheology of concrete. In: Roussel, N. (Ed.), Understanding the Rheology of Concrete, Woodhead Publishing Series in Civil and Structural Engineering. Woodhead Publishing (Chapter 7), pp. 144–208.

Flatt, R.J., Roussel, N., Cheeseman, C.R., 2012. Concrete: an eco material that needs to be improved. Journal of the European Ceramic Society, Special Issue: ECerS XII, 12th Conference of the European Ceramic Society 32 (11), 2787–2798.

Fredheim, G.E., Braaten, S.M., Christensen, B.E., 2002. Molecular weight determination of lignosulfonates by size-exclusion chromatography and multi-angle laser light scattering. Journal of Chromatography A 942 (1−2), 191−199.

Gagnè, R., 2016a. Air entraining agents. In: Aïtcin, P.-C., Flatt, R.J. (Eds.), Science and Technology of Concrete Admixtures. Elsevier (Chapter 17), pp. 379−392.

Gagnè, R., 2016b. Shrinkage-reducing admixtures. In: Aïtcin, P.-C., Flatt, R.J. (Eds.), Science and Technology of Concrete Admixtures. Elsevier (Chapter 23), pp. 457−470.

Gartner, E., 2008. Cement Shrinkage Reducing Agent and Method for Obtaining Cement Based Articles Having Reduced Shrinkage. EP Patent 1914211 A1, filed October 10, 2006 and issued April 23, 2008.

Gay, C., Raphaël, E., 2001. Comb-like polymers inside nanoscale pores. Advances in Colloid and Interface Science 94 (1−3), 229−236.

Gelardi, G., Flatt, R.J., 2016. Working mechanisms of water reducers and superplasticizers. In: Aïtcin, P.-C., Flatt, R.J. (Eds.), Science and Technology of Concrete Admixtures. Elsevier (Chapter 11), pp. 257−278.

Goto, T.I., Narashino Sato, T., Kyoto Sakai, K., Motohiko II, U., 1985. Cement-Shrinkage-Reducing Agent and Cement Composition. US Patent 4547223 A, filed March 2, 1981 and issued October 15, 1985.

Griffin, W.C., 1949. Classification of surface active agents by HLB. Journal of the Society of Cosmetic Chemists 1 (5), 311−326.

Guicquero, J.-P., Mosquet, M., Chevalier, Y., Le Perchec, P., 1999. Thinners for Aqueous Suspensions of Mineral Particles and Hydraulic Binder Pastes. US Patent 5879445 A, filed October 11, 1993 and issued March 9, 1999.

Guo, X., Rong, Z., Ying, X., 2006. Calculation of hydrophile−lipophile balance for polyethoxylated surfactants by group contribution method. Journal of Colloid and Interface Science 298 (1), 441−450.

Gustafsson, J., Reknes, K., 2000. Adsorption and dispersing properties of lignosulfonates in model suspension and cement paste. In: 6th CANMET/ACI International Conference on Superplasticizers and Other Chemical Admixtures in Concrete, 195, pp. 196−210.

Habbaba, A., Lange, A., Plank, J., 2013. Synthesis and performance of a modified polycarboxylate dispersant for concrete possessing enhanced cement compatibility. Journal of Applied Polymer Science 129 (1), 346−353.

Hattori, K.-I., Tanino, Y., 1963. Separation and molecular weight determination of the fraction from the paper chromatography of the condensates of sodium β-naphthalene sulfonate and formaldehyde. The Journal of the Society of Chemical Industry, Japan 66 (1), 55−58.

Hill, C.L., Jeknavorian, A.A., Ou, C.-C., 2002. Air Management in Cementitious Mixtures Having Plasticizer and a Clay-Activity Modifying Agent. EP Patent 1259310 A1, filed February 15, 2001 and issued November 27, 2002.

Hirata, T., Kawakami, H., Nagare, K., Yuasa, T., 2000. Cement Additive. EP Patent 1041053 A1, filed March 9, 2000 and issued October 4, 2000.

Iqbal, D.N., Hussain, E.A., 2013. Green biopolymer guar gum and its derivatives. International Journal of Pharma and Bio Sciences 4 (3), 423−435.

Jeknavorian, A.A., Roberts, L.R., Jardine, L., Koyata, H., Darwin, D.C., 1997. Condensed polyacrylic acid-aminated polyether polymers as superplasticizers for concrete. In: 5th CANMET/ACI International Conference on Superplasticizers and Other Chemical Admixtures in Concrete, 173, pp. 55−82.

Kaprielov, S.S., Batrakov, V.G., Scheinfeld, A.B., 2000. Modified concretes of new generation-the reality and perspectives. Russian Journal of Concrete and Reinforced Concrete 14 (3), 1.

Karlsson, S., Albertsson, A.-C., 1990. The biodegradation of a biopolymeric additive in building materials. Materials and Structures 23 (5), 352−357.

Kaur, V., Bera, M.B., Panesar, P.S., Kumar, H., Kennedy, J.F., April 2014. Welan gum: microbial production, characterization, and applications. International Journal of Biological Macromolecules 65, 454−461.

Kawai, T., 1987. Non-dispersible underwater concrete using polymers. Marine concrete. In: International Congress on Polymers in Concrete. Chapter 11.5. Brighton, UK.

Kerkar, A.V., Dallaire, M.P., 1997. Cement Admixture Capable of Inhibiting Drying Shrinkage While Allowing Air Entrainment, Comprising Oxyalkylene Ether Adduct, Betaine. US Patent 5679150 A, filed August 16, 1996 and issued October 21, 1997.

Kerkar, A.V., Berke, N.S., Dallaire, M.P., 1997. Cement Composition. US Patent 5618344 A, filed November 6, 1995 and issued April 8, 1997.

Kerkar, A.V., Berke, N.S., Dallaire, M.P., 2000. Cement Composition. EP Patent 0813507 B1, filed February 13, 1996 and issued May 17, 2000.

Kerkar, A.V., Gilbert, B.S., 1997. Drying Shrinkage Cement Admixture. US Patent 5604273 A, filed September 18, 1995 and issued February 18, 1997.

Kerkar, A.V., Walloch, C.T., Hazrati, K., 2001. Masonry Blocks and Masonry Concrete Admixture for Improved Freeze-Thaw Durability. US Patent 6258161 B1, filed September 29, 1999 and issued July 10, 2001.

Khayat, K.H., 1998. Viscosity-enhancing admixtures for cement-based materials—an overview. Cement and Concrete Composites 20 (2−3), 171−188.

Khayat, K.H., Mikanovic, N., 2012. Viscosity-enhancing admixtures and the rheology of Concrete. In: Roussel, N. (Ed.), Understanding the Rheology of Concrete, Woodhead Publishing Series in Civil and Structural Engineering. Woodhead Publishing (Chapter 8), pp. 209−228.

Kim, B.-G., Jiang, S., Aïtcin, P.-C., 2000. Effect of sodium sulfate addition on properties of cement pastes containing different molecular weight PNS superplasticizers. In: 6th CANMET/ACI International Conference on Superplasticizers and Other Chemical Admixtures in Concrete, 195, pp. 485−504.

Lei, L., Plank, J., 2014. Synthesis and properties of a vinyl ether-based polycarboxylate superplasticizer for concrete possessing clay tolerance. Industrial & Engineering Chemistry Research 53 (3), 1048−1055.

Liu, M., Lei, J.-H., Du, X.-D., Huang, B., Chen, Li-na, 2013. Synthesis and properties of methacrylate-based and allylether-based polycarboxylate superplasticizer in cementitious system. Journal of Sustainable Cement-Based Materials 2 (3−4), 218−226.

Luke, G., Luke, K., 2000. Effect of sucrose on retardation of Portland cement. Advances in Cement Research 12 (1), 9−18.

Lunkenheimer, K., Schrödle, S., Kunz, W., 2004. Dowanol DPnB in water as an example of a solvo-surfactant system: adsorption and foam properties. Trends in Colloid and Interface Science XVII − Progress in Colloid and Polymer Science 126, 14−20.

Mäder, U., Kusterle, W., Grass, G., 1999. The rheological behaviour of cementitious materials with chemically different superplasticizers. In: International RILEM Conference on the Role of Admixtures in High Performance Concrete, 5, pp. 357−376.

Mantellato, S., Eberhardt, A.B., Flatt, R.J., 2016. Formulation of commercial products. In: Aïtcin, P.-C., Flatt, R.J. (Eds.), Science and Technology of Concrete Admixtures. Elsevier (Chapter 15), pp. 343−350.

Marchon, D., Sulser, U., Eberhardt, A.B., Flatt, R.J., 2013. Molecular design of comb-shaped polycarboxylate dispersants for environmentally friendly concrete. *Soft Matter*. http://dx.doi.org/10.1039/C3SM51030A.

Marchon, D., Flatt, R.J., 2016a. Mechanisms of cement hydration. In: Aïtcin, P.-C., Flatt, R.J. (Eds.), Science and Technology of Concrete Admixtures. Elsevier (Chapter 8), pp. 129−146.

Marchon, D., Flatt, R.J., 2016b. Impact of chemical admixtures on cement hydration. In: Aïtcin, P.-C., Flatt, R.J. (Eds.), Science and Technology of Concrete Admixtures. Elsevier (Chapter 12), pp. 279−304.

Marchon, D., Mantellato, S., Eberhardt, A.B., Flatt, R.J., 2016. Adsorption of chemical admixtures. In: Aïtcin, P.-C., Flatt, R.J. (Eds.), Science and Technology of Concrete Admixtures. Elsevier (Chapter 10), pp. 219−256.

Mayer, G., Axmann, H., 2006. Air-entraining Admixtures. EP Patent 1517869 B1, filed July 7, 2003 and issued October 25, 2006.

McCorkle, M.R., Brow, P.L.du, 1955. Nitrogen-containing derivates of the fatty acids. In: Fatty Acids for Chemical Specialties, pp. 138−141.

Miao, C., Qiao, M., Ran, Q., Liu, J., Zhou, D., Yang, Y., Mao, Y., 2013. Preparation Method of Hyperbranched Polycarboxylic Acid Type Copolymer Cement Dispersant. US Patent 0102749 A1, filed December 22, 2010 and issued April 25, 2013.

Miao, C., Ran, Q., Liu, J., Mao, Y., Shang, Y., Sha, J., 2011. New generation amphoteric comb-like copolymer superplasticizer and its properties. Polymers & Polymer Composites 19 (1), 1−8.

Miller, T.G., 1985. Characterization of neutralized β-naphthalenesulfonic acid and formaldehyde condensates. Journal of Chromatography A 347, 249−256.

Mitsui, K., Yonezawa, T., Kinoshita, M., Shimono, T., 1994. Application of a new superplasticizer for ultra high-strength concrete. In: 4th CANMET/ACI International Conference on Superplasticizers and Other Chemical Admixtures in Concrete, 148, pp. 27−46.

Moedritzer, K., Irani, R.R., 1966. The direct synthesis of α-aminomethylphosphonic acids. Mannich-Type reactions with orthophosphorous acid. The Journal of Organic Chemistry 31 (5), 1603−1607.

Mollah, M.Y.A., Adams, W.J., Schennach, R., Cocke, D.L., 2000. A review of cement−superplasticizer interactions and their models. Advances in Cement Research 12 (4), 153−161.

Mosquet, M., Chevalier, Y., Brunel, S., Pierre Guicquero, J., Le Perchec, P., 1997. Polyoxyethylene di-phosphonates as efficient dispersing polymers for aqueous suspensions. Journal of Applied Polymer Science 65 (12), 2545−2555.

Mosquet, M., Maitrasse, P., Guicquero, J.P., 2003. Ethoxylated di-phosphonate: an extreme molecule for extreme applications. In: 7th CANMET/ACI International Conference on Superplasticizers and Other Chemical Admixtures in Concrete, 217, pp. 161−176.

Myrvold, B.O., 2008. A new model for the structure of lignosulphonates: Part 1. Behaviour in dilute solutions. Industrial Crops and Products, 7th Forum of the International Lignin Institute "Bringing Lignin back to the Headlines" 27 (2), 214−219.

Nagi, M.A., Okamoto, P.A., Kozikowski, R.L., 2007. Evaluating Air-entraining Admixtures for Highway Concrete. National Cooperative Highway Research Program. Report 578.

Nawa, T., Ichiboji, H., Kinoshita, M., 2000. Influence of temperature on fluidity of cement paste containing superplasticizer with polyethylene oxide graft chains. In: 6th CANMET/ACI International Conference on Superplasticizers and Other Chemical Admixtures in Concrete, 195, pp. 181−194.

Nkinamubanzi, P.-C., Mantellato, S., Flatt, R.J., 2016. Superplasticizers in practice. In: Aïtcin, P.-C., Flatt, R.J. (Eds.), Science and Technology of Concrete Admixtures. Elsevier (Chapter 16), pp. 353−378.

Okamura, H., Ouchi, M., 1999. Self-compacting concrete. Development, present and future. In: First International RILEM Symposium on Self-Compacting Concrete, 7, pp. 3–14.

Ostrikov, M.S., Dibrov, G.D., Petrenko, T.P., 1965. Deforming effect of osmotically dehydrating liquid media. Kolloidnyi Zhurnal 27 (1), 82–86.

Ouyang, X., Qiu, X., Chen, P., July 2006. Physicochemical characterization of calcium lignosulfonate—a potentially useful water reducer. Colloids and Surfaces A: Physicochemical and Engineering Aspects 282–283, 489–497.

Pagé, M., Moldovan, A., Spiratos, N., 2000. Performance of novel naphthalene-based copolymer as superplasticizer for concrete. In: 6th CANMET/ACI International Conference on Superplasticizers and Other Chemical Admixtures in Concrete, 195, pp. 615–637.

Palacios, M., Flatt, R.J., 2016. Working mechanism of viscosity-modifying admixtures. In: Aïtcin, P.-C., Flatt, R.J. (Eds.), Science and Technology of Concrete Admixtures. Elsevier (Chapter 20), pp. 415–432.

Pang, Yu-X., Qiu, X.-Q., Yang, D.-J., Lou, H.-M., 2008. Influence of oxidation, hydroxymethylation and sulfomethylation on the physicochemical properties of calcium lignosulfonate. Colloids and Surfaces A: Physicochemical and Engineering Aspects 312 (2–3), 154–159.

Pannetier, N., Khoukh, A., François, J., 2001. Physico-chemical study of sucrose and calcium ions interactions in alkaline aqueous solutions. Macromolecular Symposia 166 (1), 203–208.

Pieh, S., 1987. Polymere Dispergiermittel I. Molmasse Und Dispergierwirkung Der Melamin-Und Naphthalin-Sulfonsäure-Formaldehyd-Polykondensate. Die Angewandte Makromolekulare Chemie 154 (1), 145–159.

Piotte, M., 1993. Caractérisation du poly(naphtalènesulfonate): influence de son contre-ion et de sa masse molaire sur son interaction avec le ciment (Ph.D. thesis). Université de Sherbrooke.

Piotte, M., Bossányi, F., Perreault, F., Jolicoeur, C., 1995. Characterization of poly (naphthalenesulfonate) salts by ion-pair chromatography and ultrafiltration. Journal of Chromatography A 704 (2), 377–385.

Plank, J., 2005. Applications of biopolymers in construction engineering. Biopolymers Online 10.

Plank, J., Bian, H., 2010. Method to assess the quality of casein used as superplasticizer in self-levelling compounds. Cement and Concrete Research 40 (5), 710–715.

Plank, J., Andres, P.R., Krause, I., Winter, C., 2008. Gram scale separation of casein proteins from whole casein on a Source 30Q anion-exchange resin column utilizing fast protein liquid chromatography (FPLC). Protein Expression and Purification 60 (2), 176–181.

Plank, J., Sachsenhauser, B., 2006. Impact of molecular structure on zeta potential and adsorbed conformation of α-Allyl-ω-methoxypolyethylene glycol − maleic anhydride superplasticizers. Journal of Advanced Concrete Technology 4 (2), 233–239.

Plank, J., Sachsenhauser, B., 2009. Experimental determination of the effective anionic charge density of polycarboxylate superplasticizers in cement pore solution. Cement and Concrete Research 39 (1), 1–5.

Plank, J., Pöllmann, K., Zouaoui, N., Andres, P.R., Schaefer, C., 2008. Synthesis and performance of methacrylic ester based polycarboxylate superplasticizers possessing hydroxy terminated poly(ethylene glycol) side chains. Cement and Concrete Research 38 (10), 1210–1216.

Plank, J., Winter, C., 2008. Competitive adsorption between superplasticizer and retarder molecules on mineral binder surface. Cement and Concrete Research 38 (5), 599–605.

Poinot, T., Govin, A., Grosseau, P., 2014. Influence of hydroxypropylguars on rheological behavior of cement-based mortars. Cement and Concrete Research 58 (April), 161–168.

Pojana, G., Carrer, C., Cammarata, F., Marcomini, A., Crescenzi, C., 2003. HPLC determination of sulphonated melamines-formaldehyde condensates (SMFC) and lignosulphonates (LS) in drinking and ground waters. International Journal of Environmental Analytical Chemistry 83 (1), 51–63.

Popov, K.I., Sultanova, N., Rönkkömäki, H., Hannu-Kuure, M., Jalonen, J., Lajunen, L.H.J., Bugaenko, I.F., Tuzhilkin, V.I., 2006. ^{13}C-NMR and electrospray ionization mass spectrometric study of sucrose aqueous solutions at high pH: NMR measurement of sucrose dissociation constant. Food Chemistry 96 (2), 248–253.

Pourchet, S., Liautaud, S., Rinaldi, D., Pochard, I., 2012. Effect of the repartition of the PEG side chains on the adsorption and dispersion behaviors of PCP in presence of sulfate. Cement and Concrete Research 42 (2), 431–439.

Pourchez, J., Govin, A., Grosseau, P., Guyonnet, R., Guilhot, B., Ruot, B., 2006. Alkaline stability of cellulose ethers and impact of their degradation products on cement hydration. Cement and Concrete Research 36 (7), 1252–1256.

Ramachandran, V.S., Lowery, M.S., Wise, T., Polomark, G.M., 1993. The role of phosphonates in the hydration of Portland cement. Materials and structures 26 (7), 425–432.

Redín, C., Lange, F.T., Brauch, H.-J., Eberle, S.H., 1999. Synthesis of sulfonated naphthalene-formaldehyde condensates and their trace-analytical determination in wastewater and river water. Acta Hydrochimica et Hydrobiologica 27 (3), 136–143.

Reknes, K., Gustafsson, J., 2000. Effect of modifications of lignosulfonate on adsorption on cement and fresh concrete properties. In: 6th CANMET/ACI International Conference on Superplasticizers and Other Chemical Admixtures in Concrete, 195, pp. 127–142.

Reknes, K., Petersen, B.G., 2003. Novel lignosulfonate with superplasticizer performance. In: 7th CANMET/ACI International Conference on Superplasticizers and Other Chemical Admixtures in Concrete, 217, pp. 285–299.

Report on Carcinogens, 2011. National Toxicology Program, twelfth ed. National Institute of Health. DIANE Publishing.

Richardson, S., Gorton, L., 2003. Characterisation of the substituent distribution in starch and cellulose derivatives. Analytica Chimica Acta 497 (1–2), 27–65.

Rinaldi, D., Hamaide, T., Graillat, C., D'Agosto, F., Spitz, R., Georges, S., Mosquet, M., Maitrasse, P., 2009. RAFT copolymerization of methacrylic acid and poly(ethylene glycol) methyl ether methacrylate in the presence of a hydrophobic chain transfer agent in organic solution and in water. Journal of Polymer Science Part A: Polymer Chemistry 47 (12), 3045–3055.

Risica, D., Dentini, M., Crescenzi, V., 2005. Guar gum methyl ethers. Part I. Synthesis and macromolecular characterization. Polymer 46 (26), 12247–12255.

Robyt, J.F., 1998. Transformations. In: Essentials of Carbohydrate Chemistry. Springer Advanced Texts in Chemistry. Springer, New York, pp. 48–75.

Rosen, M.J., 2004. Surfactants and Interfacial Phenomena, third ed. John Wiley & Sons, Inc.

Ruckstuhl, S., Suter, M.J.-F., 2003. Sorption and mass fluxes of sulfonated naphthalene formaldehyde condensates in aquifers. Journal of Contaminant Hydrology 67 (1–4), 1–12.

Sakuta, M., Saito, T., Yanagibashi, K., 1990. Durability Improving Agent for Cement-Hydraulic-Set Substances, Method of Improving Same, and Cement-Hydraulic-Set Substances Improved in Durability. US Patent 4975121, filed July 13, 1989 and issued December 4, 1990.

Sakuta, M., Saito, T., Yanagibashi, K., 1992. Durability Improving Agent for Cement-Hydraulic-Set Substances, Method of Improving Same, and Cement-Hydraulic-Set Substances Improved in Durability. US Patent 5174820 A, filed February 11, 1992 and issued December 29, 1992.

Sakuta, M., Saito, T., Yanagibashi, K., 1993. Durability Improving Agent for Cement-Hydraulic-Set Substances, Method of Improving Same, and Cement-Hydraulic-Set Substances Improved in Durability. EP Patent 0350904 B1, filed July 13, 1989 and issued March 31, 1993.

Sato, T., Goto, T., Sakai, K., 1983. Mechanism for reducing drying shrinkage of hardened cement by organic additives. Cement Association of Japan Review 52–54.

Schröfl, C., Gruber, M., Plank, J., 2012. Preferential adsorption of polycarboxylate superplasticizers on cement and silica fume in ultra-high performance concrete (UHPC). Cement and Concrete Research 42 (11), 1401–1408.

Schulze, J., Baumgartl, H., 1989. Mittel Zur Reduzierung Des Schwundmaßes von Zement. EP Patent 0308950 A1, filed September 23, 1998 and issued March 29, 1989.

Schulze, J., Baumgartl, H., 1993. Shrinkage-Reducing Agent for Cement. EP Patent 0308950 B1, filed September 23, 1998 and issued March 17, 1993.

Scripture Jr., E.W., 1937. Indurating Composition for Concrete. US Patent 2081643 A, filed February 5, 1937 and issued May 25, 1937.

Shawl, E.T., Kesling Jr., H.S., 1995. Cement Composition. US Patent 5413634 A, filed May 5, 1994 and issued May 9, 1995.

Shawl, E.T., Kesling Jr., H.S., 1997. Cement Composition. EP Patent 0637574 B1, filed August 3, 1994 and issued October 1, 1997.

Shawl, E.T., Kesling Jr., H.S., 2001. Cement Composition. EP Patent 0758309 B1, filed January 25, 1995 and issued June 13, 2001.

Shendy, S., Vickers, T., Lu, R., 2002. Polyether derivatives of β-naphthalene sulfonate polymer. Journal of Elastomers and Plastics 34 (1), 65–77.

Singh, N.B., Sarvahi, R., Singh, N.P., 1992. Effect of superplasticizers on the hydration of cement. Cement and Concrete Research 22 (5), 725–735.

Smith, B.J., Rawal, A., Funkhouser, G.P., Roberts, L.R., Gupta, V., Israelachvili, J.N., Chmelka, B.F., 2011. Origins of saccharide-dependent hydration at aluminate, silicate, and aluminosilicate surfaces. Proceedings of the National Academy of Sciences 108 (22), 8949–8954.

Smith, B.J., Roberts, L.R., Funkhouser, G.P., Gupta, V., Chmelka, B.F., 2012. Reactions and surface interactions of saccharides in cement slurries. Langmuir 28 (40), 14202–14217.

Sonebi, M., 2006. Rheological properties of grouts with viscosity modifying agents as diutan gum and welan gum incorporating pulverised fly ash. Cement and Concrete Research 36 (9), 1609–1618.

Sychra, M., Steindl, H., 1998. Air Entraining Agent for Concretes and Mortars. EP Patent 0752977 B1, filed March 30, 1995 and issued October 28, 1998.

Tadros, T.F., 2005. Applied Surfactants: Principles and Applications. Wiley-VCH Verlag GmbH & Co. KGaA, Weinheim.

Tejado, A., Peña, C., Labidi, J., Echeverria, J.M., Mondragon, I., 2007. Physico-chemical characterization of lignins from different sources for use in phenol–formaldehyde resin synthesis. Bioresource Technology 98 (8), 1655–1663.

Thomas, N.L., Birchall, J.D., 1983. The retarding action of sugars on cement hydration. Cement and Concrete Research 13 (6), 830–842.

Torrans, P.H., Ivey, D.L., 1968. Review of Literature on Air-entrained Concrete. Texas transportation institute; Texas A&M University.

Tsubakimoto, T., Hosoidi, M., Tahara, H., 1984. Copolymer and Method for Manufacture Thereof. EP Patent 0056627 B1, filed January 15, 1982 and issued October 3, 1984.

Uchikawa, H., Hanehara, S., Shirasaka, T., Sawaki, D., 1992. Effect of admixture on hydration of cement, adsorptive behavior of admixture and fluidity and setting of fresh cement paste. Cement and Concrete Research 22 (6), 1115−1129.

Umaki, Y., Tomita, R., Hondo, F., Okada, S., 1993. Cement Composition. US Patent 5181961 A, filed August 29, 1991 and issued January 26, 1993.

Vijn, J.P., 2001. Dispersant and Fluid Loss Control Additives for Well Cements, Well Cement Compositions and Methods. US Patent 6182758 B1, filed August 30, 1999 and issued February 6, 2001.

Vollhardt, K.P.C., Schore, N.E., 2010. Organic Chemistry: Structure and Function, sixth ed. W. H. Freeman.

Walstra, P., 1999. Casein sub-micelles: do they exist? International Dairy Journal 9 (3−6), 189−192.

Will, R.K., Yokose, K., 2005. Chemical Economics Handbook, Product Review: Lignosulfonates. Chemical Industry Newsletter, SRI Consulting.

Winnefeld, F., Becker, S., Pakusch, J., Götz, T., 2007. Effects of the molecular architecture of comb-shaped superplasticizers on their performance in cementitious systems. Cement and Concrete Composites 29 (4), 251−262.

Winter, C., Plank, J., Sieber, R., 2008. The efficiences of α-, β- and κ-casein fractions for plasticising cement-based self levelling grouts. In: Fentiman, C., Mangabhai, R., Scrivener, K. (Eds.), Calcium Aluminate Cements, pp. 543−556.

Witt, J., Plank, J., 2012. A novel type of PCE possessing silyl functionalities. In: 10th CANMET/ACI International Conference on Superplasticizers and Other Chemical Admixtures in Concrete, 288, pp. 1−14.

Wombacher, F., Bürge, C., Kurz, C., Schmutz, M., 2014. Air Void-Forming Material for Cementitious Systems. WO Patent 2014/060352 A1, filed October 14, 2013 and issued April 24, 2014.

Wombacher, F., Bürge, T.A., Mäder, U., 2000. Method for the Reduction of the Degree of Shrinkage of Hydraulic Binders. EP Patent 1024120 A1, filed January 26, 2000 and issued August 2, 2000.

Wombacher, F., Bürge, T.A., Mäder, U., 2002. Method for the Reduction of the Degree of Shrinkage of Hydraulic Binders. US Patent 0157578 A1, filed April 25, 2002 and issued October 31, 2002.

Wombacher, F., Bürge, T.A., Mäder, U., 2012. Method for the Reduction of the Degree of Shrinkage of Hydraulic Binders. EP Patent 1024120 B1, filed January 26, 2000 and issued March 7, 2012.

Yamada, K., Takahashi, T., Hanehara, S., Matsuhisa, M., 2000. Effects of the chemical structure on the properties of polycarboxylate-type superplasticizer. Cement and Concrete Research 30 (2), 197−207.

Yamamoto, M., Uno, T., Onda, Y., Tanaka, H., Yamashita, A., Hirata, T., Hirano, N., 2004. Copolymer for Cement Admixtures and Its Production Process and Use. US Patent 6727315 B2, filed June 1, 2002 and issued April 27, 2004.

Yang, B.Y., Montgomery, R., 1996. Alkaline degradation of glucose: effect of initial concentration of reactants. Carbohydrate Research 280 (1), 27−45.

Yu, B., Bian, H., Plank, J., 2010. Self-assembly and characterization of Ca−Al−LDH nanohybrids containing casein proteins as guest anions. Journal of Physics and Chemistry of Solids, 15th International Symposium on Intercalation Compounds − ISIC 15 May 10−15, 2009, Beijing 71 (4), 468−472.

Yu, G., Li, B., Wang, H., Liu, C., Mu, X., 2013. Preparation of concrete superplasticizer by oxidation-sulfomethylation of sodium lignosulfonate. BioResources 8 (1), 1055−1063.

Zhang, Q., 2011. Investigating Polymer Conformation in Poly (Ethylene Oxide) (PEO) Based Systems for Pharmaceutical Applications a Raman Spectroscopic Study of the Hydration Process (Master's thesis). Chalmers University of Technology.

Ziche, H., Schweizer, D.D., 1982. Mixtures of Mortar and Their Use. EP Patent 0054175 A1, filed October 30, 1981 and issued June 23, 1982.

Adsorption of chemical admixtures

10

D. Marchon[1], *S. Mantellato*[1], *A.B. Eberhardt*[2], *R.J. Flatt*[1]
[1]Institute for Building Materials, ETH Zürich, Zürich, Switzerland; [2]Sika Technology AG, Zürich, Switzerland

10.1 Introduction

The working mechanisms of numerous chemical admixtures involve the adsorption of water-soluble compounds at a solid−liquid interface. This is particularly the case for water reducers and high-range water reducers, to which most of this chapter is dedicated. Moreover, this process also concerns retarders. Additionally, adsorption of rather water-insoluble compounds and/or substances with a high affinity to surfaces is exploited in air-entraining and shrinkage-reducing admixtures, where surface active agents (surfactants) are used to specifically alter properties of the liquid−vapor interface of concrete. Despite having high affinity to liquid−air interfaces, these surfactants may, however, also adsorb onto the solid−liquid interface or self-associate into micelles or liquid crystals. This makes the description of surfactant adsorption a delicate task, as discussed in Section 10.4.3 for the solid−liquid interface and in Section 10.7 for the liquid−air interface.

If we consider a given dispersant, its impact on fluidity increases with dosage, provided that the admixture continues to adsorb on the surface of the solid particles to disperse (Section 10.2). In fact, it is especially the adsorbed fraction of the dispersant that is responsible for the effect on fluidity, as explained in Chapter 11 (Gelardi and Flatt, 2016). Depending on the admixture type and its dosage, there may or may not be an equilibrium established between the fraction of admixtures adsorbed and those remaining in solution. The nature of this relationship is most often reported in the form of adsorption isotherms, which are covered in Section 10.3.

In addition to the nature of the surface, this relation is profoundly affected by the chemical nature of the dispersant. Although it is difficult to establish general relationships owing to the variety of chemical compositions and structures available, we outline some general chemical features of dispersants that affect their adsorption in Section 10.4.

Molecules with a low affinity to the surface may desorb if the conditions are changed (Section 10.5). This may be by replacing the solution with water (Platel, 2005, 2009) or by modifying the ionic composition of the solution by increasing the sulfate or hydroxyl ions concentrations (Yamada et al., 2001; Marchon et al., 2013). Admixtures may therefore be subject to competitive adsorption, which can reduce their performance as discussed in Section 10.5.2.

Other factors that reduce the performance of admixtures can involve an apparent increase rather than reduction in adsorption (Section 10.6). Most of these are due to

Science and Technology of Concrete Admixtures. http://dx.doi.org/10.1016/B978-0-08-100693-1.00010-2
Copyright © 2016 Elsevier Ltd. All rights reserved.

artifacts linked to the standard way of solution depletion used to measure adsorption. Indeed, in this approach, adsorption is determined by measuring the difference between the amount of admixture added and its fraction remaining in solution after a given time. However, if admixtures are consumed by precipitation (Section 10.6.1) or intercalation (Section 10.6.2), their apparent adsorption increases. The amount of admixture adsorbed and acting as dispersant may either increase, remain equal, or even decrease. The latter situation happens if the admixtures are more effectively precipitated or intercalated, so that the surface coverage of particles to be dispersed decreases. A similar situation may occur if the admixtures modify the process of nucleation and growth of aluminates, causing an increase in the solid−liquid interfacial area (Section 10.6.3).

The above issues concerning the interpretation of adsorption data are tightly linked to experimental procedures. For this reason, we include at the end of this chapter an extensive section about experimental aspects (Section 10.8).

10.2 Adsorption and fluidity

10.2.1 Initial fluidity

The adsorption increases with polymer dosage until the surface of the solid particles is completely covered. At the same time, the fluidity increases and approaches a maximum level that is dictated by the adsorbed conformation of the polymer and the saturation of the surface (Yamada et al., 2000; Hanehara and Yamada, 2008) (Figure 10.1).

The polymer affinity for the surface has a critical effect on the amount of polymer that must be added before the surface is covered. For example, a polymer with a low affinity for the surface will have to be added in large amounts because a large fraction of it remains in solution rather than being adsorbed. This has led authors to define the so-called saturation dosage, above which a further addition of polymer does not affect much the fluidity.

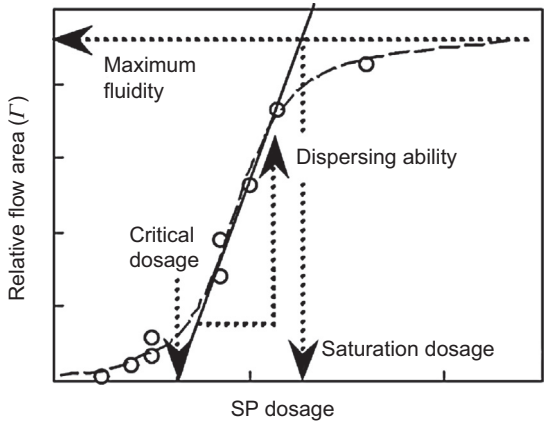


Figure 10.1 Critical and saturation dosages with respect to the dispersing ability. Adapted from Hanehara and Yamada (2008) with permission.

Another concept that is found in the literature with regard to polymer dosage is the critical dosage. This is defined as the dosage above which a dispersion effect is noticed. The results obtained from testing this dosage, however, are extremely dependent on the experimental conditions, such as the water−cement ratio (w/c) or volume fraction, the type of cement, and the type and the chemical structure of the polymer.

10.2.2 Fluidity retention

Vickers et al. demonstrated that the loss of fluidity depends on the amount of polymer remaining in solution (Vickers et al., 2005). This might be explained by considering that a reserve of polymer is available in solution to adsorb on newly formed hydrates (Flatt, 2004a,b). The question of why polymers that do not initially adsorb would adsorb later in time has two answers. The first is that if there is equilibrium between the solid particles surface and the solution, the distribution of polymers between both depends on the ratio of the surface area to the solution volume. Consequently, if more surface is created, at least one part of the nonadsorbed polymers will move onto the newly created surface, even if the original surface is not fully covered. The second reason is that during the initial 1−2 h of hydration, most of the hydrates formed are aluminates for which the polymers have a higher affinity, as seen above. Therefore, we could consider that aluminates may initially be at full surface coverage, but not silicates. As long as polymers are available in solution, they would extensively adsorb on the aluminates while remaining in equilibrium with partially covered silicate surfaces.

Apart from this, another general consideration is that the workability is lost much faster in systems reaching only partial surface coverage than that with a full surface coverage (Schober and Flatt, 2006). The explanation lies in the ability of adsorbed admixtures to modify the chemical kinetics of cement hydration and the associated creation of new surfaces that are detrimental to workability. It probably also includes the possibility that partially covered particles have to let polymers rearrange themselves on their surface, creating contact points having stronger cohesive forces.

10.3 Adsorption isotherms

10.3.1 Basic phenomenology of adsorption

Adsorption data are most often reported in terms of adsorption isotherms by plotting the amount of adsorbed polymers with respect to the amount remaining in solution. This procedure makes most sense if equilibrium is established between the surface and the solution. In what follows, we discuss basic characteristics of adsorption isotherms before discussing possible models for it in the next subsection.

Many theoretical approaches to adsorption isotherms predict that, at low surface and solution concentrations, the adsorbed amount should be proportional to the concentration in solution (Langmuir, 1918; Degennes, 1976; Bouchaud and Daoud, 1987; Fleer, 1993; Marchon et al., 2013). However, these approaches may differ substantially with respect to the extent of this linear zone.

The slope of this initial regime represents an adsorption equilibrium constant, K. It depends on the free energy of the adsorbate-solvent, adsorbate-surface of the adsorbent, and surface-solvent interactions. For polymers, the change in configurational entropy between solution and surface plays an important role. This depends on the molecular structure of the polymer. For linear chains various expressions have been proposed (Degennes, 1976; Bouchaud and Daoud, 1987; Fleer, 1993).

For compounds with sufficient affinity for the surface, increasing dosages mainly enriches the surface, while the concentration in solution remains dilute. Rising concentrations at the surface causes the adsorbed polymer to enter a semidilute regime in which the adsorbates start to have excluded volume interactions. In this situation, polymers reorganize themselves on the surface to minimize the system free energy. The extent of conformational change that they may undergo in this stage depends on the adsorption energy (high values allow more adsorption). The state of minimal energy corresponds to the so-called adsorption plateau, a regime in which the adsorbed amount becomes independent of the concentration in solution (Degennes, 1976; Bouchaud and Daoud, 1987).

For single-polymer chains, when the concentration in solution also reaches semidilute conditions, adsorption becomes less favorable and the adsorbed amounts decrease with increasing dosage. To the best of our knowledge, this situation is not relevant for most chemical admixtures and will therefore not be discussed further.

10.3.2 Simple adsorption isotherm models

In the previous section, we have indicated that, at low concentrations, adsorption includes a linear range in which the adsorbed amount and the solution concentrations are proportional to each other. Additionally, at higher solution concentrations, the adsorbed amount eventually reaches a plateau. These represent two basic features that any adsorption isotherm must capture.

For example, this is the case of the Langmuir adsorption isotherm (Langmuir, 1918) and explains the very popular use of this model. However, this does not guarantee that it adequately accounts for data in the intermediate regime. To better emphasize this, we present an alternative derivation of this relation and then an analogous one that is probably more adequate for polymers.

We begin by considering a chemical reaction in which an adsorbate A reacts reversibly with a free site S to form an occupied surface site SA:

$$S + A \leftrightharpoons SA \tag{10.1}$$

For this chemical reaction, we can write an equilibrium constant, K, as follows:

$$K = \frac{[SA]}{[S][A]} \tag{10.2}$$

where $[A]$ is the activity of the adsorbate in solution, $[S]$ is the activity of the free surface site, and $[SA]$ is the activity of the occupied surface site.

Considering an ideal mixing situation, $[S]$ and $[SA]$ may be represented by surface fractions. In absence of other substances, we have:

$$[SA] + [S] = 1 \tag{10.3}$$

The substitution of Eqn (10.3) into Eqn (10.2) leads to the first expression of the Langmuir isotherm:

$$[SA] = \frac{K\,[A]}{1 + K[A]} \tag{10.4}$$

This equation is generally transformed to account for the maximum adsorbed amount and is written as follows:

$$m_{SA} = \frac{m_{SA}^{\infty} K\, c_A}{1 + Kc_A} \tag{10.5}$$

where m_{SA} is the adsorbed mass, m_{SA}^{∞} is the adsorbed mass at the plateau, and c_A is the concentration in solution.

As explained in the previous section, the plateau for polymer adsorption depends on their ability to organize themselves in a compact way on the surface. This is affected by their adsorption energy. For linear chains, the adsorbed mass at the plateau m_{SA}^{∞} increases with the cubic root of the adsorption energy (Fleer, 1993). Although this dependence is much lower than for K, which varies as the exponential of adsorption energy, it is not negligible. Equation (10.5) is therefore somewhat misleading as it suggests that only K would depend on it. Reducing the adsorption energy should therefore affect the plateau, as discussed in Section 10.5.2.

However, there are other more important issues that one may consider before applying this equation to polymer adsorption. We present a simple modification of the above derivation, to illustrate one matter of concern.

We now consider a situation in which n sites S get occupied by one polymer P. Equations (10.1), (10.2), and (10.3) become

$$n\,S + P \leftrightharpoons S_nP \tag{10.6}$$

$$K = \frac{[S_nP]}{[S]^n[P]} \tag{10.7}$$

$$[S_nP] + [S] = 1 \tag{10.8}$$

Combining Eqns (10.7) and (10.8), we can write

$$[P] = \frac{[S_nP]}{K(1 - [S_nP])^n} \tag{10.9}$$

The important point here is that the relationship between amounts adsorbed and in solution depends on n. It can be shown that the equilibrium constant K, however, has an even stronger dependence on n. Consequently, the initial slope of the adsorption isotherm is initially much steeper, but would then curve over at larger concentrations in solution to reach the true adsorption plateau.

However, this model probably puts an overproportionate weight on the activity of the free sites. Indeed, for polymer adsorption, it may be more realistic to consider that on the surface covered by an adsorbed polymer, only a fraction of surface sites are occupied (Marchon et al., 2013). In such a situation, the free site activity may remain unity (or constant in case of competitive adsorption with small species) over a large range of concentrations (Degennes, 1976; Bouchaud and Daoud, 1987; Marchon et al., 2013). In this case, Eqn (10.2) may be rewritten as follows:

$$K \cong \frac{[SA]}{[A]} \tag{10.10}$$

In the next section, we examine experimental data for the adsorption of superplasticizers to determine the extent to which one or the other of these predictions may hold.

10.3.3 Linear zone of adsorption isotherms of superplasticizers

Studies on the adsorption of superplasticizers often show that the fraction of adsorbed polymer remains constant as dosage is increased. Moreover, this fraction can be quite different from unity over a large range of dosages (Perche et al., 2003). This large linear zone can be interpreted in two ways. First, it may be a result of polydispersity, with only one fraction of the polymers adsorbing strongly and the other barely adsorbing. Second, as explained in the previous section, it may be due to the fact that the free site activity remains roughly constant because the number of sites occupied in the surface covered by a polymer is small. In the latter case, the proportionality between adsorption and dosage is a result of the equilibrium expressed in Eqn (10.10).

To better identify situations in which adsorption is proportional to dosage, it can be helpful to also plot adsorption versus dosage. In this case, the same units should be used on both scales—for example, polymer mass with respect to solid (mass of surface). An example for lignosulfonates (LS) is illustrated in Figure 10.2. It clearly shows that the initial part of the adsorption is linear with dosage. A more careful analysis shows that the initial slopes are not at all identical and slightly lower than unity (0.82−0.98). This implies that, during this initial stage, only a fixed fraction of the polymer is adsorbed (82−98%), which most likely results from the polydispersity in size and/or molecular structure. On the same graph, it can also be observed that above this linear zone, some polymers are at their plateau, while others continue to adsorb gradually with increasing dosage.

A similar situation is shown in Figure 10.3 for various polycarboxylate ether (PCE) dispersants. In that case also, there is a distinct initial linear zone as a function of dosage. However, here the slopes are substantially lower and more differentiated (0.37−0.58). In this graph, it should be noted that the polymer PCP-3 does not reach a plateau. This is probably a result of precipitation, as discussed in Section 10.6.1.

The amount of polymer adsorbed at the end of the linear zone is far beyond what would be expected if a Langmuir-type isotherm were followed (true isotherms not

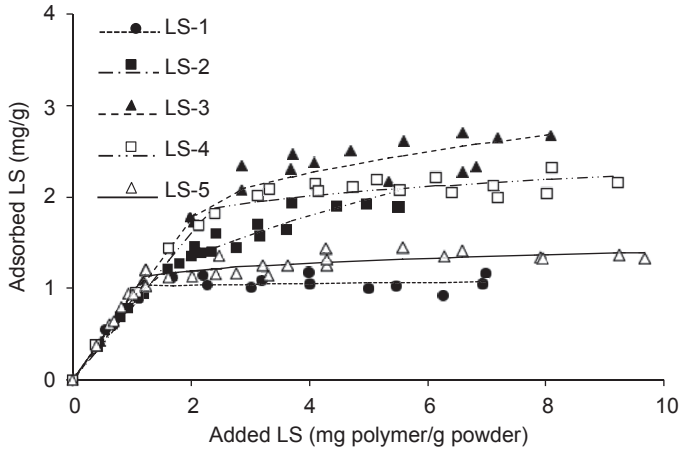


Figure 10.2 Adsorption data of different lignosulfonate polymers plotted as a function of the added polymer amount.
Adapted from Houst et al. (2008) with permission.

shown here). For LS, it could be argued that owing to the high fraction of polymers adsorbed, a relation of the form given in Eqn (10.9) may apply. A consequence of this would be that true equilibrium would be very difficult to reach at the plateau. However, we cannot exclude that Eqn (10.10) applies.

For PCEs, however, only a rather limited fraction of the polymer adsorbs in the linear regime. One possible reason for this could be polydispersity. Indeed, superplasticizers show typically a polydispersed structure, meaning that they contain many fractions of different molecular weights and/or structures. This can explain the discrimination that has been reported to take place during adsorption between these different fractions (Flatt et al., 1998; Winnefeld et al., 2007).

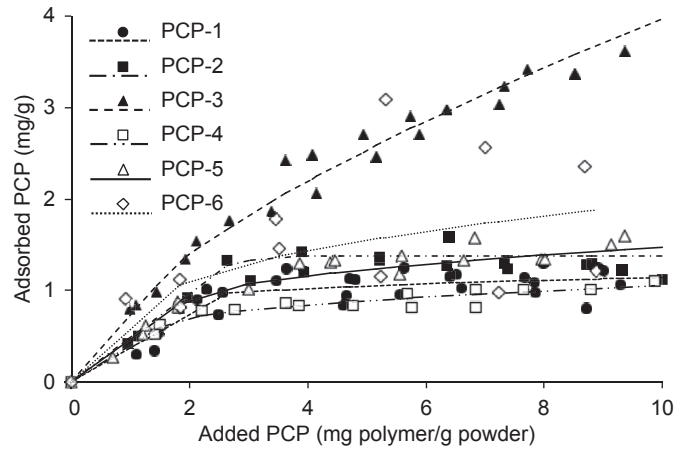


Figure 10.3 Adsorption data of different polycarboxylate polymers plotted as a function of the added polymer amount.
Adapted from Houst et al. (2008) with permission.

However, in the absence of polydispersity effects, we would infer that Eqn (10.9) does not apply. Rather, one would then conclude the existence of an extended linear zone resulting from a constant activity of the free sites, so that Eqn (10.10) applies. To distinguish between both situations, it would be necessary to compare adsorption data obtained in suspensions, of which the solid to liquid ratios would be varied. Platel (2005) has carried out such experiments, and his results support the reversibility of PCE adsorption above a certain adsorption threshold (see Section 10.5.1).

10.3.4 Specific issues in studying adsorption on cementitious systems

An important issue in measuring adsorption isotherms of polymers is to know whether true equilibrium has been reached. At high surface coverage, the rearrangement of polymers will take time, particularly if their adsorption energy is high. In cementitious systems, the problem is exacerbated by the fact that the surface area changes with time due to chemical reactions, so only limited contact times may be used.

Another issue in cementitious systems is that polymers are not expected to adsorb uniformly on the different phases present in cement. Indeed, several studies performed on pure cement clinker phases and hydration products showed that superplasticizers adsorb preferably on aluminate phases, which have a positively charged surface (ettringite has the highest affinity), than on silicates with a negatively charged surface (Yoshioka et al., 2002; Plank and Hirsch, 2007; Zingg et al., 2008). These studies show the importance of understanding the behavior of superplasticizers when facing each cement phase for controlling fluidity of cement paste and concrete.

10.4 Molecular structure and adsorption

10.4.1 General features

The energy balance controlling polymer adsorption is not trivial because of the entropy terms linked to conformation changes of the polymer between the solution and the surface. Consequently, analytical solutions are only available in a limited number of cases for which conformations can be well enough described, typically using scaling laws. This is the case for linear chains (Degennes, 1976; Bouchaud and Daoud, 1987; Fleer, 1993). Beyond these limited number of cases, molecular simulations are needed.

Having said this, it is nevertheless useful to outline the general principles underlying this complex process. For example, one can define a dimensionless adsorption energy parameter x_S (units of k_BT) for the free energy change associated with the adsorption of a polymer segment and the desorption of a solvent molecule. To be precise, by definition the free energy change for this exchange is $-k_BT\,x_S$, so that cases of favorable adsorption are characterized by positive values of x_S.

Polymer adsorption takes place if x_S is larger than a critical value x_{SC} (Fleer, 1993). This energy difference is needed to compensate for the entropy loss of the adsorbing polymer. Monomers have been found to have a lower value of x_{SC} than their corresponding segments in polymers, which has been explained by the reduced mobility of these segments

in the polymer chain (Cohen Stuart et al., 1984a). Therefore, monomers are not capable of desorbing a polymer.

However, low-molecular-weight compounds can act as displacers and desorb a polymer if their adsorption energy $x_{S(\text{displacer-solvent})}$ is sufficiently large (Cohen Stuart et al., 1984b). This leads to situations of competitive adsorption, which are more extensively discussed in Section 10.5.2.

Strictly speaking, the first-order analysis above should hold if the adsorbing segments dominate the loss of conformational entropy of the polymer. For such conditions, monomer adsorption would rather follow a Langmuir-type isotherm, while their polymer would have a behavior qualitatively described in Eqn (10.9).

However, the latter situation is clearly an oversimplified one. As mentioned in the previous section, superplasticizers exhibit a linear relationship between adsorption and solution concentration (or dosage). This may be simply due to polydispersity as previously mentioned (Flatt et al., 1998; Winnefeld et al., 2007). However, for PCEs, there are strong indications that this extended linear regime also involves an equilibrium so that Eqn (10.10) can be applied up to relatively high surface coverage, at least for the adsorbing fraction of the molecular structure distribution. The reasons for this are further developed at the end of the next section.

10.4.2 Adsorption of superplasticizers

Molecular mass plays an important role in superplasticizer adsorption, regardless of their molecular nature. Reports about this can be found for sulfonate naphtalene formaldehydes polycondensates (SNFCs) (Piotte, 1993), LSs (Reknes and Gustafsson, 2000; Reknes and Peterson, 2003), vinyl copolymers (Flatt et al., 1998), and PCEs (Peng et al., 2012; Magarotto et al., 2003; Winnefeld et al., 2007). Adjusting molecular mass is therefore a way to modify the performance of a superplasticizer. For derivatives of natural products, such as LSs, this may be done by ultrafiltration (Zhor, 2005; Zhor and Bremmer, 1997). For synthetic polymers, it can be done by modifying synthesis conditions, such as concentrations of monomers and chain transfer agents, as well as temperature and reaction time, among others. Additionally, as mentioned earlier, one should also consider that superplasticizers are polydispersed in size and structure so that a certain discrimination can take place during adsorption (Flatt et al., 1998; Winnefeld et al., 2007).

On the basis of the synthetic nature of PCEs, one can, in principle, change the chemistry of the backbone and its length, the amount of ionic groups with respect to the side chains, expressed as carboxylic−ester (C/E) ratio or grafting density, the length of the side chains, etc., depending on the performance desired (Chapter 9, Gelardi et al., 2016). All of these factors affect the adsorption, which in turn affects the rheological properties, as evidenced in numerous papers (Yamada et al., 2000; Winnefeld et al., 2007; Papo and Piani, 2004; Schober and Flatt, 2006; Peng et al., 2012; Kirby and Lewis, 2004; Li et al., 2005).

In Chapter 9 on the chemistry of PCEs (Gelardi et al., 2016), the conformation of a comb-shaped copolymer in solution—and more specifically, its radius of gyration (Eqn 9.2)—has been defined with the structural parameters P, N, and n (Figure 9.17) and the size of the different monomers in the backbone or in the side chains (Flatt et al., 2009a). As illustrated in Figure 10.4, a PCE is represented in solution as a chain of

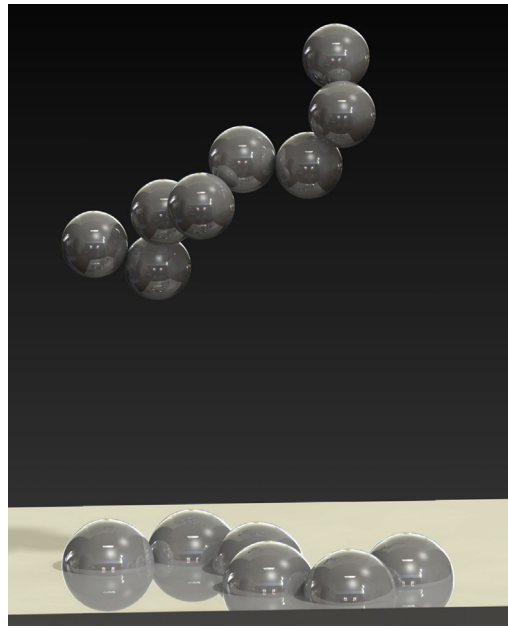


Figure 10.4 Schematic representation of a comb copolymer in solution (chain of spherical cores, each of radius RC) and one adsorbed on a mineral surface (chain of hemispheres, each of radius RAC).
Adapted with permission from Flatt et al. (2009a).

blobs (the size of which relates to the previously mentioned parameters). The conformation of such a comb-shaped copolymer adsorbed on a particle of cement can be derived in a similar way by using a chain of hemispheres on a surface (see also Figure 10.4). The radius of these hemispheres, R_{AC}, is defined as follows:

$$R_{AC} = \left(2\sqrt{2}(1-2\chi)\frac{a_P}{a_N}\right)^{1/5} a_P P^{7/10} N^{-1/10} \tag{10.11}$$

where a_N and a_P are the size of the monomers in the backbone and in the side chains, respectively; P the number of monomers in the side chain; and N the number of monomers in the backbone for one side chain. The surface S occupied by each molecule on a particle can be then calculated from:

$$S_A = \frac{\pi}{\sqrt{2}} a_N a_P \left(2\sqrt{2}(1-2\chi)\frac{a_P}{a_N}\right)^{2/5} P^{9/10} N^{3/10} n \tag{10.12}$$

The most important parameter during adsorption is the density of ionic groups in the backbone. Indeed, PCE adsorption increases with the density of ionic groups on the backbone (Yamada et al., 2000; Regnaud et al., 2006). Interestingly, independent studies from Regnaud et al. (2006) and Winnefeld et al. (2007) suggest that adsorption drops strongly below a C/E ratio of 2, regardless of the length of the side chains (Flatt and Schober, 2012).

The strong effect of the ionic charge can be understood to some extent using the first principle equilibrium constant proposed by Marchon et al. (2013). In that study, the authors considered that the charges are competing with other ions present on the surface that are present in much larger amounts. To support this approximation, we consider that, in the area occupied by a PCE, the density of functional groups is:

$$\sigma_A = \frac{n(N-1)}{S_A} \tag{10.13}$$

A first simple approximation for the charge density on the surface σ_S is to consider that there is one charge in an area given by the a_P*a_N. The ratio of charge densities between the surface and the adsorbing function of the polymer is then:

$$\frac{\sigma_S}{\sigma_A} = \frac{\frac{\pi}{\sqrt{2}}\left(2\sqrt{2}(1-2\chi)\frac{a_P}{a_N}\right)^{2/5} P^{9/10}N^{3/10}}{(N-1)} \tag{10.14}$$

This shows that the charge density ratio increases almost linearly with P. Its dependence on N is less trivial, but in first order would decrease with its -7/10 power (approximating $(N-1)$ to N). Higher values of N therefore decrease this ratio, which is expected because this directly increases the number of functional groups. Nevertheless, the dependence is not linear. In quantitative terms, we can consider polymethacrylate-based PCEs with polyethylene glycol (PEG) side chains, for which we have $a_P = 0.36$, $a_N = 0.25$ nm, and $\chi = 0.37$. Taking typical values of $P = 23$ and $N = 4$, we get a charge density ratio of about 20. Therefore, in the surface occupied by a typical PCE, we expect that only about 5% of the surface charges will be occupied by the functional groups. While this approximation depends a lot on our estimate of σ_S, the main conclusion should remain. In particular, it implies that the surface occupancy of charges does not need to be considered and leads to an adsorption isotherm of the form given in Eqn (10.10) (Marchon et al., 2013).

To estimate the adsorption equilibrium constant as a function of PCE molecular structure, Marchon et al. (2013) considered the balance between adsorption and desorption rates of functional groups. More specifically, they defined the rate constant for these processes respectively as k_A^a and k_A^d. For each of these constants, they proposed the following relationships to the structural parameters of the polymer:

$$k_A^a = \frac{n(N-1)z}{S_A}\frac{1}{n} = \frac{(N-1)z}{S_A} \tag{10.15}$$

$$k_A^d = \frac{S_A}{n(N-1)z} \tag{10.16}$$

where z is the number of charges carried by each monomer in the backbone and S_A is the surface occupied by the molecule proportional to $P^{9/10}N^{3/10}n$, as seen in Eqn (10.12).

The adsorption kinetic rate constant is proportional to $n(N\text{-}1)z/S_A$, which represents the surface charge density of the adsorbed molecule, and is inversely proportional

to the number of side chains n to take into account the steric hindrance induced by the side chains. The desorption rate constant is inversely proportional to the surface charge density.

Within the frame of these assumptions, the adsorption equilibrium constant is then obtained as the ratio between both constants:

$$K_A = \frac{k_A^a}{k_A^d} = \frac{z^2(N-1)^2}{nP^{9/5}N^{3/5}} \tag{10.17}$$

With this adsorption equilibrium constant, it is possible to link the structural parameter of a polymer with its adsorption ability.

10.4.3 Surfactant adsorption at the solid–liquid interface

In cementitious materials, surfactants are mostly wanted for their action at the liquid–vapor interface (e.g., air-entraining admixture (AEA), shrinkage-reducing admixture (SRA)). However, these same molecules may also adsorb at solid–liquid interfaces, which reduces their effectiveness for a given dosage. In this section, we discuss the latter process.

Surfactant adsorption at the solid–liquid interface is simpler than polymer adsorption. First, the conformation of adsorbed surfactants can be deduced from their amphipathic structure, the nature of the solvent, and the nature of the solid. Second, the adsorption is usually reversible, which allows a straightforward thermodynamic treatment of the problem (Tadros, 2005).

As for polymers, many factors influence surfactant adsorption onto the solid–liquid interface: molecular structure, such as the hydrophilic chain length (Partyka et al., 1984), pH (Denoyel and Rouquerol, 1991), temperature (Rosen, 2004; Tadros, 2005; Partyka et al., 1984), and dissolved salts (Denoyel and Rouquerol, 1991; Partyka et al., 1984; Nevskaia et al., 1998). The most significant differences in the adsorption mechanisms are between ionic and nonionic surfactants and their affinity for either hydrophilic or hydrophobic solid surfaces. Combinations of these different situations are discussed here because they cover situations of concern for the use either of SRAs or AEAs in concrete. In general, the adsorption of such admixtures at solid interfaces consumes admixtures that should be exerting their action elsewhere and is therefore something that one would rather want to avoid.

10.4.3.1 Adsorption of ionic surfactants

In concrete, adsorption of ionic surfactants may occur both on hydrophilic and hydrophobic surfaces. An example of the second case is for concrete containing fly ash that may itself contain carbonaceous particles. These are hydrophobic and have been reported to potentially adsorb AEAs (Chen et al., 2003; Külaots et al., 2004; Pedersen et al., 2010; Baltrus and LaCount, 2001; Hill et al., 1997; Külaots et al., 2003; Pedersen et al., 2009, 2008).

The adsorption of ionic surfactants is mainly governed by the hydrophobic interaction of the hydrophobic surfactant tail and the surface of the solid substrate. On hydrophilic surfaces, surfactant adsorption is governed by the charge of the surface and counter ions present in the electrolytes as well as hydrophobic interaction of their tails (Tadros, 2005). For highly charged surfaces, ion exchange and pairing as well as hydrophobic bonding mechanisms may occur (Rosen, 2004).

Basically, four regions in surfactant adsorption with specific features can be distinguished, which are summarized in Figure 10.5.

For low surfactant concentrations in Region 1, adsorption shows a gradual increase in which ions of the supporting electrolyte are exchanged by the ionic head group of the surfactants.

In Region 2, adsorption increases drastically and results in hydrophobic interactions between oncoming surfactants and those previously adsorbed. At a critical surfactant concentration, the hydrophobic interaction between surfactants leads to the formation of hemi-micelles at the interface. This occurs at the critical aggregation concentration (CAC), which is well below the critical micellation concentration (CMC).

In Region 3, adsorption decreases with increasing surfactant bulk concentration through increasing electrostatic repulsion between the reversed surface formed in Region 2 and the oncoming ionic heads of the surfactants.

Surface adsorption is completed near the CMC in Region 4.

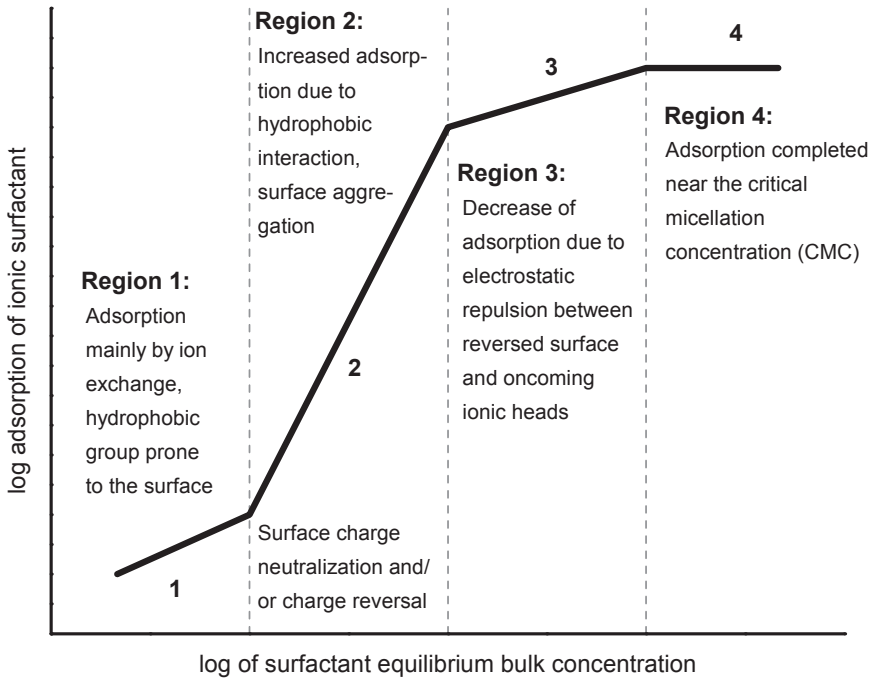


Figure 10.5 Illustration of various steps in surfactant adsorption.
Adapted from Rosen (2004).

10.4.3.2 Adsorption of nonionic surfactants

In this section, we deal with nonionic surfactants adsorption only on hydrophilic surfaces. The corresponding adsorption isotherms generally show a Langmuir-type behavior or two-stepped (L2) or even four-step (L4) Langmuir behavior with a plateau near the CMC. The different shapes of the adsorption isotherms are due to the adsorbate−adsorbate, adsorbate−adsorbent and adsorbate−solvent interactions (Rosen, 2004; Tadros, 2005; Denoyel and Rouquerol, 1991; Levitz, 2002; Narkiewicz-Michałek et al., 1992; Partyka et al., 1984; Narkis and Ben-David, 1985; Liu et al., 1992; Portet et al., 1997; Nevskaia et al., 1998; Kjellin et al., 2002; González-García et al., 2004; Paria and Khilar, 2004; Kharitonova et al., 2005; Chao et al., 2008). This is evidenced in various studies on the adsorption of nonionic surfactants onto several solids, such as precipitated silica (Denoyel and Rouquerol, 1991; Levitz, 2002; Narkiewicz-Michałek et al., 1992; Partyka et al., 1984), ground quartz (Denoyel and Rouquerol, 1991; Nevskaia et al., 1998; Kharitonova et al., 2005), pyrogenic silica (Denoyel and Rouquerol, 1991; Portet et al., 1997), soils (Liu et al., 1992; Chao et al., 2008), clay (Denoyel and Rouquerol, 1991; Narkis and Ben-David, 1985; Nevskaia et al., 1998; Chao et al., 2008), and activated carbon (Narkis and Ben-David, 1985; González-García et al., 2004).

With respect to cementitious materials, adsorption onto hydrophilic surfaces should be driven by hydrogen bonding of the polar moieties (hydrophilic heads) with the silanol groups (silica, amorphous quartz, etc.) and/or aluminol groups (clay). However, at the elevated pH of these systems, most of these groups are deprotonated (Nicoleau et al., 2014; Labbez et al., 2006) and not operational for hydrogen bonding (Merlin et al., 2005). Zhang et al. (2001) performed adsorption measurements on hydrating cement paste and showed no adsorption of some nonionic surfactants with low molecular weights in their system. Furthermore, Merlin et al. (2005) identified that adsorption of ethoxylated nonionic surfactants onto C-S-H lies at the detection limit ($\sim$1 μmol/$g_{C\text{-}S\text{-}H}$ or $\sim$0.01 μmol/m^2). However, it has to be noted that the nonionic surfactants used in the above studies have significantly different chemical natures than nonionic surfactants used in SRA (cf. Eberhardt (2011)).

At low bulk concentrations, the nonionic surfactant monomers are anchored to the surface. With increasing concentration, the surface coverage increases and the adsorption isotherms show a rather low slope. As for ionic surfactants, adsorption strongly increases above the CAC.

10.5 Dynamic exchanges between surface and solution

10.5.1 Reversibility of adsorption

The adsorption of admixtures at interfaces is a reversible process in which various admixtures will have different affinities for the surfaces. Moreover, just as adsorption depends on surface coverage, so does desorption. For example, if the aqueous phase of a suspension containing a large amount of admixtures both in solution and at the solid−liquid interface is replaced by pure water, part of the admixtures will desorb.

However, with lower amounts of admixtures in the systems, these will mainly be adsorbed at the surface; therefore, they will not or barely desorb if the solution is replaced by pure water. Such effects are well known and have also been measured with superplasticizers in cement suspensions (Platel, 2005, 2009).

The fundamental reason for this behavior is that adsorbed admixtures are not immobile on the surface. In particular, at high surface coverage, the equilibrium with the surface is dynamic. This was shown by Pefferkorn et al. (1985). They adsorbed labeled polymers on particles and subsequently replaced the continuous phase with a solution containing identical unlabeled polymers. By measuring the labeled polymers, they showed that radioactive decay is proportional both to the coverage by labeled polymers, Γ^*, and to the bulk concentration of unlabeled polymers, C_b. There is therefore a faster exchange of polymers when their concentration in solution is high and a much lower one otherwise. This explains why it is very difficult to completely desorb polymers by repeated washing with pure solvent (de Gennes, 1987). An interesting aspect of this result is also that at high polymer dosages, owing to polymer mobility, the system has the capacity to rearrange polymers at the surface and evolve toward a true equilibrium in full surface coverage. However, the kinetics of this process may be slow, even more so for polymers with a high affinity for the surface.

This finding emphasizes an important fact: adsorbed polymers are not irreversibly fixed. They can be replaced by similar polymers, but more generally also by other species. This brings us to the notion of competitive adsorption, which is dealt with in the next section.

10.5.2 Competitive adsorption

As explained in Chapter 16, one of the reasons for some cement−superplasticizer incompatibilities comes from soluble sulfates contained in the cement (Nkinamubanzi et al., 2016). More generally, the performance of superplasticizers can be perturbed by various ionic species, leading to a dramatic loss of the dispersive effect due to competitive adsorption. Hydroxides (Flatt et al., 1997; Marchon et al., 2013), sulfate ions (Yamada et al., 2001), citrates and tartrates (Plank and Winter, 2008), and other polymeric admixtures (Plank et al., 2007) are among the chemical species competing for the solid surface with superplasticizers and thus reducing their adsorption.

When dealing with competitive adsorption, it is important to consider that not only the initial slope K but also the plateau are affected by adsorption energy (see Section 10.3 and Flatt et al., 1997). Additionally, when extracting data from adsorption isotherms, the choice of the model will obviously affect the result.

Yamada et al. (2001) showed the competitive adsorption between PCEs and sulfates. By alternatively changing the concentration of sulfate ions in solution with the addition of $CaCl_2$ and Na_2SO_4, the authors showed the reversibility of the adsorption of at least part of the PCE polymer used (Figure 10.6, left) and its effect on the rheology (Figure 10.6, right).

Later, the correlation between the sulfate sensitivity and the structural parameters of the polymer was demonstrated on cement pastes with different PCEs (Zimmermann et al., 2009). By using a similar test to change sulfate content, the sulfate sensitivity of the PCEs was found to be proportional to P/N^2. With a theoretical approach, Flatt et al. (2009b) refined the dependence of the sensitivity with a molecular structure-dependent parameter called the sulfate sensitivity parameter (SSP), given by $P^{4/5}N^{3/5}(N-1)^{-2}$.

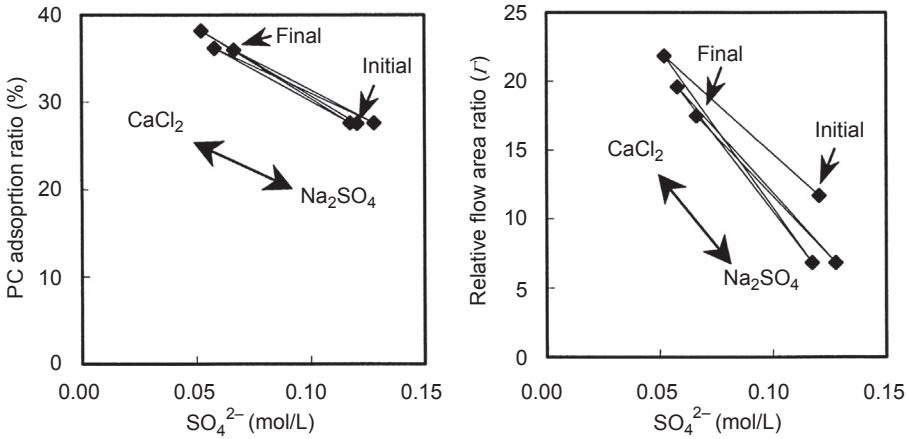


Figure 10.6 Illustration of the effect of sulfates on the performance of a PCE superplasticizer in cycles involving alternative additions of $CaCl_2$ and Na_2SO_4. Left: adsorbed PCE as a function of sulfate concentration in the aqueous phase. Right: relative flow area from paste flow tests as a function of sulfate concentration in the aqueous phase.
Reproduced from Yamada et al. (2001) with permission.

More recently, a study about alkaline activation of superplasticized blended cement focused on the sensitivity of PCEs to hydroxides (Marchon et al., 2013). By neutralizing the hydroxides with HCl, the authors were able to show that for PCEs with a methacrylate backbone, the loss of dispersive effect in an activated system with NaOH is not due to a possible loss of the side chains due to a hydrolysis of the ester functions linking them to the backbone, but to a competitive adsorption. Moreover, the sensitivity of PCEs to the presence of additional alkalis could be related to changes in the adsorption equilibrium constant given in Eqn (10.17). This criterion is particularly useful to easily determine the adsorption behavior of a molecular structure in extreme conditions, such as alkaline-activated systems, where strong incompatibilities between the PCE superplasticizers and the ionic species in solution have been observed. Recent works have also examined modifications to the PCE chemistry to reduced the sensitivity to sulfates, for example by introducing silane groups (Fan et al., 2012), changing the carboxylic backbone monomers (Dalas et al., 2015a,b) or the distribution of side chains on the backbone (Pourchet et al., 2012).

10.6 Consumption (ineffective adsorption)

10.6.1 Precipitation

With regard to the efficiency of dispersants, we are interested in molecules that are adsorbed and reduce the maximum attractive interparticle force (Chapter 11: Gelardi and Flatt, 2016). If admixtures precipitate with hydrates to form new organomineral phases, they will not be active as dispersants.

If such precipitation takes place on particle surfaces, it will create a layer of which the dielectric properties will contribute to the overall van der Waals forces. As a rule of thumb, the lower the density of this layer, the lower will be its contribution to the van der Waals force (Flatt, 2004b). However, unless it is several nanometers thick, one can expect a low-density layer to get compressed under the action of van der Waals forces between particles on which they have formed. They would do so until they cannot get more compressed, at which point the attraction between particles will result from a combination of the dielectric properties of both the layer and the particles. Such surface precipitates may therefore be beneficial in reducing the magnitude of the van der Waals force, but the extent to which they can do so is most likely limited. If precipitation occurs in the bulk solution, the impact on rheological properties should in general be low, unless a gel network were to be formed.

However, such precipitation reactions may have an important role on hydration kinetics. Indeed, the precipitation of admixtures on surfaces can most likely slow down diffusion, in particular if it takes place around high-energy sites (see Chapters 8 and 12: Marchon and Flatt, 2016a,b). Precipitation in the bulk of the solution might have an indirect effect. Indeed, it will deplete the solution from some ions and thereby increase the driving force for dissolution.

An indication of precipitation can be seen if adsorption measurements do not reach a plateau, even at very high dosages, as shown in Figure 10.3 with the PCE polymer PCP-3. This indicates that "normal" adsorption is not taking place. However, it does not indicate the nature of the compound forming or its location (solution or surface).

10.6.2 Organoaluminates

One type of precipitate that can form is an organoaluminate phase (Giraudeau et al., 2009; Fernon et al., 1997; Plank et al., 2006a,b). As explained in Chapter 8, a product of the hydration of aluminates is composed of positively charged platelets with counter ions intercalated between them (Marchon and Flatt, 2016a). An organoaluminate phase is a layered double hydroxide, between the layers of which polymers are intercalated, compensating only in part for the surface charge balanced otherwise by hydroxides (Giraudeau, 2009).

The conceptual model concerning the impact of the formation of this phase is that polymers would be trapped within it and incapable of dispersing cement particles (Flatt and Houst, 2001). Various observations were used to postulate the existence of such a process:

1. Delayed addition of superplasticizers generally leads to much better fluidity, even if this is only done less than a minute after water addition.
2. Atomic force microscopy measurements by Uchikawa et al. (1997) suggested the presence of a steric layer much larger than the polymer size (10−100 times). Their measurements therefore rather point to the formation of a gel on the clinker surfaces rather than simple steric hindrance from adsorbed polymers.
3. Addition of sulfates tends to reduce polymer adsorption, but it improves the fluidity for polymers that are sensitive to the addition time (Jiang et al., 1999).

Since then, the possibility of forming such phases has been demonstrated by different approaches. These involve reacting C_3A in water and in the presence of

PCEs (Plank et al., 2006a,b), precipitation by mixing a solution of sodium aluminate and polymer with a solution of calcium hydroxide (Giraudeau et al., 2009), and adding the polymer to a suspension of previously precipitated hydrocalumite (Giraudeau et al., 2009).

Thermal analysis, X-ray diffraction, nuclear magnetic resonance (NMR), and transmission electron microscopy (TEM) have all identified the formation of such phases in the absence of sulfates, confirming that layers of organoaluminates can indeed form (Giraudeau et al., 2009; Plank et al., 2010). An example for a polymethacrylate PCE is shown in Figure 10.7. In that case, the layer spacing is between 7 and 10 nm. The authors of that study found that small angle X-ray scattering gave small angle peaks that are also compatible with such distances. In fact, these would correspond to polymers adsorbed through their backbones and having coiled side chains, as explained in Chapters 9 and 11 (Gelardi et al., 2016; Gelardi and Flatt, 2016). Further evidence in support of the coiled conformation has been provided by NMR transfer of polarization measurements. Moreover, the layer spacing shows a scaling exponent with respect to the side chain length that is the same as that of coils.

The conclusion concerning the coiled conformation of the side chains and the relatively large interlayer spacing raises a serious question concerning the stability of such lamellar phases. Indeed, at such distances, it is difficult to understand which cohesion



Figure 10.7 TEM image of a poly(methacrylate-g-PEO)/hydrocalumite composite. Lines are drawn as guides for the eye. The interlayer spacing measured between those lines varies between 7 and 10 nm.
Reproduced from Giraudeau et al. (2009) with permission.

forces would hold the layers together as the polymers ought rather to be acting as steric dispersants. One possible explanation is that platelets are in fact dispersed and that a fraction of them align during sample preparation. This would be consistent with a coherence length determined from low-angle X-ray scattering, which suggest the average number of stacked layers only to be between three and four (Giraudeau, 2009).

Another important observation concerning this organo-aluminate phase is that it is destabilized in the presence of sulfates at the expense of either monosulfate or ettringite (Giraudeau et al., 2009; Plank et al., 2010). In the experiments of Giraudeau et al. (Giraudeau et al., 2009; Giraudeau, 2009), the conversion was shown to take place through a process of dissolution, nucleation, and growth. More importantly, an induction time before conversion was observed and its duration was dependent on the nature of the PCE. More ionic PCEs tend to lead to longer induction times.

Such observations point to the crucial role of sulfates in determining whether or not organoaluminates may form (Habbaba et al., 2014). The mixing process may also play a role in this phenomenon as it affects ion concentration at particle surfaces. Indeed, if organoaluminates are given a chance to form, they may remain stable beyond the mixing time and consequently affect rheological properties and their evolution. If they are immediately destabilized, they probably play an important role in the nucleation of ettringite, as discussed in the next section.

10.6.3 Change of specific surface

As explained by Yamada (2011), one may expect that the extent of dispersion that can be reached strongly depends on the specific surface of the system. This basic principle has far-reaching implications. One of them is methodological. It concerns mainly the sample preparation for BET measurements of hydrates, as explained in Section 10.8.6.

A second implication is that any replacement of a component with one having a higher specific surface will lead, in most cases, to a lower surface coverage (unless a large excess of polymer is used initially). The negative consequence of this reduction in surface coverage on yield stress is discussed in Chapter 11 (Gelardi and Flatt, 2016). Additionally, even if the surface coverage remained the same, the reduction in average particle size would also be detrimental to yield stress, as also explained in that chapter.

The case of organo-aluminates defined in the previous section can be understood from the perspective of an increase in specific surface. This surface would be internal if one has true intercalation and external otherwise. However, the result is the same.

A particularly interesting aspect of the case of organominerals is that their amount and surface results from hydration reactions. Such reactions can be modified by the presence of chemical admixtures, as explained in Chapter 12 (Marchon and Flatt, 2016b). For example, it is well known that the morphology of ettringite can be altered in the presence of superplasticizers (Rössler et al., 2007; Prince et al., 2002). At equivalent amounts of ettringite, the surface area of a given system is increased and the surface coverage is decreased. Consequently, the way in which admixtures affect early hydration reaction also affects their rheology. This may or may not also affect later

hydration, but there is no direct relationship. More specifically, for superplasticizers to disperse, they do not need to retard hydration. A more complete discussion on the effect of chemical admixtures on hydration is given in Chapter 12 (Marchon and Flatt, 2016b).

Finally, a last source of large surface areas in cementitious materials can be clay minerals, more specifically swelling clay minerals. In the latter case, both external and internal surfaces must be considered, as explained in the next section.

10.6.4 Adsorption on clay minerals

Superplasticizers—and in particular, "standard" PCEs—can also adsorb very extensively on swelling clay minerals. If such minerals are present in any component of a concrete mix (aggregate, sand, filler, etc.), a large portion of the superplasticizer will therefore be mobilized by the clays and will no more be available to disperse the other fine materials. This effect was first reported in a patent (filed in 1997) describing ways to counter the problem (Jardine et al., 2002) and then at a conference (Jeknavorian et al., 2003).

As stated by these authors and confirmed in a more recent study, the swelling clays (e.g., montmorillonite) are most critical, while nonswelling clays are much less problematic (e.g., kaolinite, muscovite, mica; Lei and Plank, 2014). Very importantly, this consumption by swelling clays predominantly affects PCE superplasticizers because PEG side chains can intercalate in between the layers of these minerals (Svensson and Hansen, 2010; Suter and Coveney, 2009). This effect gives an overproportionate increase of adsorption with respect to the specific surface of the clay mineral, in particular for swelling clays.

This crucial role of PEG is evidenced by the fact that the adsorption saturation plateau of PCEs with low carboxylate content closely matches the one of isolated PEG (Ng and Plank, 2012). However, the affinity of PCEs for clays is much higher than for isolated PEG because the initial slope of adsorption isotherms is higher (see Section 10.3). This has been attributed to electrostatic interactions playing a dominant role at low dosages (Ng and Plank, 2012). It is however worth also noting that differences in the entropic contribution to adsorption energy may also need to be considered in the comparison between PCEs and PEG.

The substantial role of PEG in the consumption of PCEs by clay minerals has led to different strategies to counter this effect (Jardine et al., 2002; Jeknavorian et al., 2003; Ng and Plank, 2012; Lei and Plank, 2012, 2013), which include the following:

- Changing the mixing sequence: for example, if possible, the swelling clay containing compound should be added after cement, water, and the superplasticizer are first mixed together, although this is not very practical (Jardine et al., 2002).
- Use of a sacrificial agent, such as as polyethylene oxide (PEO) (Jardine et al., 2002; Jeknavorian et al., 2003; Ng and Plank, 2012).
- Use of PEO-free PCEs (Lei and Plank, 2012, 2013, 2014).
- Various other solutions, such as multivalent cations, quaternary amines, etc. (Jardine et al., 2002).

10.7 Surfactant adsorption at the liquid–vapor interface

Basic principles about the adsorption of admixtures and specific issues concerning surfactants adsorption at liquid–solid interface were presented in Section 10.4. These notions can be as well applied to adsorption at liquid–vapor interface, which for specific surfactants, such as AEAs and SRAs, determines their efficiency. For AEAs, mainly mixtures of surfactants of various chemical natures can be found; in SRAs, mainly nonionic surfactants or hydrotropes as well as mixtures of nonionic surfactants with co-surfactants, solvo-surfactants, and hydrotropic compounds are used. Surfactants of both categories of admixtures are meant to mainly adsorb at the liquid–air interface. However, due to their chemical nature, they also adsorb onto the liquid–solid interface and may form aggregates through self-association. An overview on the chemical nature of these products is given in Chapter 9 (Gelardi et al., 2016). Some specific features for adsorption of this category of surfactants in cementitious environments have to be considered. This affects their selection to gain desired performance in concrete but is also important for choosing appropriate methods to measure their adsorption.

10.7.1 Driving force for adsorption of surfactants and micelle formation

In an aqueous environment, the hydrophobic moiety of the surfactant distorts the structure of the water by breaking hydrogen bonds between water molecules and causing a structuring of water in the vicinity of the hydrophobic group. This increases the free energy of the system and is the reason why the surfactant may be expelled from the bulk solution.

The driving force for surfactant adsorption in general is the reduction of free energy of interfaces or surfaces in a system. The free energy is minimized if surfactants adsorb at interfaces or surfaces in an oriented fashion so that contact with water is minimized. Complete removal of the surfactant molecule from the aqueous phase would require the complete dehydration of the hydrophilic group, which would be energetically unfavorable so that the hydrophilic group remains part of the aqueous phase. The amphipathic structure of surfactants determines in that way both the concentration of the surfactants at the surface or interface and their orientation, with the hydrophilic group directed to the solvent and the hydrophobic group directed away from the water (Rosen, 2004).

In the absence of a sufficient or suitable interfacial area and at a certain bulk concentration, surfactant molecules self-associate into micelles (CMC). As for adsorption onto interfaces, the driving force is the reduction of free energy by minimizing the contact of hydrophobic groups with water. This process is mainly entropy driven (Rosen, 2004; Tadros, 2005; Evans, 1988; Garnier, 2005; Molyneux et al., 1965; Wattebled, 2006) and the increase in entropy is explained in two ways (Rosen, 2004; Tadros, 2005).

- Water entropy gain due to hydrophobic bonding of hydrophobic segments in the oil-like core of micelles and release of previously structured water.
- Surfactant entropy gain due to increased degree of freedom of hydrophobic segments in the nonpolar core of micelles.

Moreover, for nonionic surfactants, it is reported that the number of monomers forming micelles is similar for aggregates formed in the bulk solution and aggregates formed at the solid–liquid interface. This implies that the free energy of surface aggregation is similar to the free energy of micellation (Denoyel and Rouquerol, 1991; Levitz, 2002; Narkiewicz-Michałek et al., 1992).

10.7.2 Surfactant adsorption at the liquid–air interface[1]

The adsorption of surfactants at the liquid–air interface reduces the surface tension of aqueous or aqueous electrolyte solutions. Hydrocarbon surfactants can reduce the surface tension down to about 30 mN/m and fluorocarbon surfactants to about 20 mN/m (Rosen, 2004; Tadros, 2005; Garnier, 2005).

Due to their amphipathic nature, surfactants adsorb at the liquid–air interface with the hydrophilic head pointed toward the water and the hydrophobic tail pointed toward the air. This adsorption behavior can be described with the Gibbs adsorption isotherm (Rosen, 2004; Tadros, 2005). As explained in Eberhardt (2011), by using Gibbs-Duhem equation, it is possible to derive a thermodynamic relationship between surface tension and the activity of the surfactant in the bulk:

$$\Gamma^{\sigma}_{1,2} = -\frac{1}{RT}\left(\frac{\mathrm{d}\gamma}{\mathrm{d}\ \ln a_2^L}\right) \tag{10.18}$$

where:

$\Gamma_{1,2}$ is the relative adsorption of the surfactant (2) with respect to water (1)
a_2^L is the activity of the surfactant in bulk solution equal to $C_2 f_2$ or $x_2 f_2$; C_2 being the concentration of surfactant in bulk solution; x_2 is the mole fraction of surfactant in bulk solution and f_2 is the activity coefficient
R is the gas constant; R = 8.31 J/(mol K) and
T is the temperature (K)

While activities and concentrations must be clearly distinguished, the derivative of the natural log of activity is much less affected by nonideality. Therefore, it is common to replace activity by concentration in the above expression:

$$\mathrm{d}\ \ln a_2 = \frac{\mathrm{d}a_2}{a_2} = \frac{C_2\mathrm{d}f_2 + f_2\mathrm{d}C_2}{f_2 C_2} \cong \frac{\mathrm{d}C_2}{C_2} \cong \mathrm{d}\ \ln C_2 \tag{10.19}$$

For aqueous solutions of surfactants, the plot of surface tension versus the bulk concentration of the surfactants generally follows the scheme given in Figure 10.8.

With increasing bulk concentration, more surfactant molecules adsorb at the liquid–air interface and decrease the surface tension of the aqueous solution. This enables the system to reduce its free energy. At a critical bulk concentration, Figure 10.8 shows a

[1] This section contains authorized excerpts of text and figures from Eberhardt (2011).

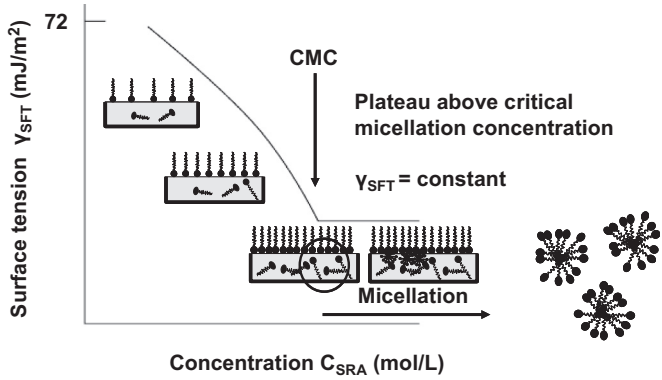


Figure 10.8 Surface tension of aqueous solutions of surfactants versus bulk concentration of surfactants.
Reprinted with permission from Eberhardt (2011).

sharp breaking point for the reduction of surface tension. Above this point, the surface tension virtually remains constant:

$$\left(\frac{\partial\gamma}{\partial \ln C_2}\right) = 0; \quad \text{for } C_2 > \text{CMC} \tag{10.20}$$

This breaking point is explained by an end of the surfactant enrichment at the liquid−air interface. Above that, there is a self-association of surfactant molecules to form micelles in the bulk. The surfactant bulk concentration at the break point therefore represents the CMC.

This introduction to surfactant adsorption provides a basis for the more detailed discussion of the working mechanisms of SRAs presented in Chapter 13 (Eberhardt and Flatt, 2016).

10.8 Experimental issues in measuring adsorption

As mentioned in the introduction, adsorption measurements are typically carried out by solution depletion. This involves preparing a suspension or paste with a known amount of admixture (Section 10.8.1), separating the aqueous phase from the suspension or paste (Section 10.8.2), stabilizing the solution against precipitation (Section 10.8.3), and measuring its admixture content (Section 10.8.4).

Multiplying the obtained concentration by the liquid volume yields the total amount of nonadsorbed admixture. This value can be deduced from the total initial amount of admixture to obtain the adsorbed amount. Various choices can be made to report such results. Considering dispersion efficiency, it would make sense to report results in terms of surface coverage. For this purpose, one would have to know how much admixture is adsorbed at full surface coverage. This may be higher than the amount adsorbed at the plateau, in particular in the presence of competing adsorbing species (Section 10.5.2) or if the equilibrium is not reached for kinetic reasons (Section 10.5.1).

One solution to this problem is to use as a reference a molecule for which one is confident can reach a true equilibrium plateau. However, rather than a mass ratio to express surface coverage, it would make more sense to calculate the occupied surfaces, which becomes necessary if the reference plateau value is taken with another molecule. For this, a model of the surface occupied by each molecule is needed. For PCEs, Eqn (10.12) could be used.

If such models are not available (or reliable enough), or if one does not have a good reference molecule to determine the plateau, then the next best expression of surface coverage is to report adsorption in the mass of adsorbed material with respect to the surface of solids. In this case, the surface coverage obtained relates to the real surface coverage by a numerical constant (the surface coverage by a unit mass of the adsorbed substance). A similar situation is reached if the plateau value of the considered admixture is used, although the numerical constants are different. In this case, the constant is not linked to the surface occupied by unit mass but to the real coverage that the considered substance can reach at the plateau. This unknown concerning surface coverage is problematic for calculating interparticle forces because of their nonlinear dependence on surface coverage, as discussed in Chapter 11 (Gelardi and Flatt, 2016).

As a last resort, one may simply choose to express adsorption with respect to the initial mass of solids. This provides the least physical insight, but it is the most straightforward choice. It can be seen as a pragmatic choice in the face of difficulties to determine true plateau values and/or to reliably measure the specific surface of hydrating cement suspensions (Section 10.8.6).

10.8.1 Suspension preparation

As explained in Sections 10.3 and 10.5, adsorption involves a reversible exchange of admixture between the solution and the surface. This tends to the establishment of a chemical equilibrium, of which the Langmuir isotherm can be used to conceptually consider some of the main aspects of the adsorption process. In particular, this equilibrium involves the amount of admixtures expressed with respect to the liquid volume and to the interfacial area. Consequently, changing any of these should result in a shift of the distribution of admixtures between the surface and the solution.

Therefore, it is advisable to measure adsorption on a suspension having the same liquid-to-solid ratio as the one on which rheological properties are being determined. This may pose problems in terms of liquid extraction from concentrated systems having low water contents. Technical solutions to this issue are discussed in the next section.

Beyond those technical solutions, one may simply measure adsorption at a different solid content and use the adsorption isotherm to recalculate adsorbed amounts at other solid contents. This requires using an adsorption isotherm that offers a reliable expression of the chemical equilibrium between the solution and the interface. An important step to ensure this is for the ionic compositions to be equal in both the concentrated and dilute suspensions. For cementitious systems or inert model representations thereof (inert powders with similar enough properties otherwise), this is particularly important with regard to the soluble alkalies. An initial measurement and adjustment of ionic compositions is therefore needed for this to be successful (Dalas et al., 2015a,b).

In cementitious systems, the initial high reactivity of the aluminates poses additional complications. Indeed, admixtures can modify the associated dissolution, nucleation, and/or crystal growth processes and thereby change the specific surface (Chapter 12: Marchon and Flatt, 2016b). How to best link this between diluted and concentrated systems is to the best of our knowledge still an unsolved problem. Consequently, two approaches may be considered.

First, one may measure systematically the specific surface of the paste of which one determines the adsorbed amount. Although this involves quite a lot of experimental effort, it circumvents the problem that the effect of admixtures on aluminates reactivity is dosage dependent. To illustrate this point, let us imagine the following conceptual example. We would use the same admixture at two different dosages. At the lowest dosage, the admixture would hypothetically not affect the aluminate phase hydration much, so that it would not substantially modify the specific surface. In contrast, at twice this dosage, the same admixture would strongly affect the aluminate hydration, increasing the specific surface as has been shown to occur with PCEs (Dalas et al. (2015b). Therefore, although the amounts of admixtures added are very different, the amounts of adsorbed admixtures per unit surface may be similar; thus, their impact on rheology may also be rather similar. This is, of course, just theoretical, but it serves to illustrate the important question concerning the surface created by the hydration of aluminate phases and how admixtures may affect it.

The second solution to the early high reactivity of some systems, such as aluminates, is to only add the admixture after initial reactions have substantially slowed down (Flatt et al., 1998; Hot et al., 2014; Perche, 2004; Hot, 2013). The considerable advantage of this approach is to eliminate a very complex problem. However, while this can be advantageous in practice, it is most often not easy or even not possible to implement. Consequently, although experimental research using this approach can provide useful insight into the working mechanism, it also eliminates the extremely important impact of aluminate hydration. Moreover, preparation of cement pastes without admixtures at low w/c can be problematic. In particular, for pastes to be adequately mixed, a minimum amount of water is needed, which is much higher than the normal water requirement of an admixed system. Consequently, there is an important risk for the differed admixture addition to induce segregation, at least at dosage relevant for low W/C mixes.

The issue of mixing and mixing energy is another concern when dealing with cementitious systems (Tattersall and Banfill, 1983; Williams et al., 1999; Juilland et al., 2012). Indeed, it is known that hydration kinetics (Juilland et al., 2012; Oblak et al., 2013) and rheological properties are strongly influenced by mixing. This is explained in Chapters 7, 12, and 16 (Yahia et al., 2016; Marchon and Flatt, 2016b; Nkinamubanzi et al., 2016). A possible solution to this issue is to use isothermal calorimetry as a fingerprint of the effect of mixing (Oblak et al., 2013). One would therefore adjust the mixing conditions in the dilute suspension (and possibly ionic composition), so that its heat evolution would be similar to that of the concentrated system. However, a detailed study of the reliability of this approach would be necessary.

Alternatively, one may consider diluting the concentrated system after a certain time, using a solution with the same ionic composition. This brings us back to the previously discussed case in which an adsorption isotherm must be used to convert

adsorption data in a dilute system to those of a concentrated one. The difference is that all the early reactivity of the system has taken place under identical conditions, so that the specific surfaces should be similar to the reference, although dependent on the initial admixture dosage.

The above considerations illustrate that many complications are hidden behind an apparent basic and trivial measurement. Being aware of these issues is important when one intends to give a physical interpretation to such data, in particular relating it to dispersion efficiency.

10.8.2 Separation of the liquid phase

Dilute suspensions are easily separated by centrifugation. It is then recommended to filter the supernatant, something conveniently done with filters that can be mounted on syringes. The filters must be resistant to high pH and must not leach organic compounds. Out of precaution, it is recommended to discard the first fraction of filtered solution.

At higher volume fractions of solids, pressure filtration is used. This is normally done by applying a lower pressure below the filter by connecting it to a vacuum. Alternatively, air pressure may be applied on top of the suspension. As filtration proceeds, the height of the particle bed on the filter increases. Additionally, the permeability of such particle beds decreases in well-dispersed systems. Both factors contribute to increasing the amount of time needed to filter a sample; this time may become problematic with respect to cement hydration, in particular aluminate reactivity in the early stages. It is therefore recommended to report typical filtration times in such experiments.

At higher volume fractions, approaches similar to filter pressing used in ceramic technology may be used (Gruber, 2010). This method is the most demanding approach. Additionally, as it is unclear whether polymer adsorption is pressure sensitive, results should be taken with care. The same holds for pressure filtration, although in that case the pressures applied are lower, which should reduce the risk of such a problem.

In all cases, it is important to determine whether an other organic substance is leached from the powders, such as by grinding aids. This is particularly important if adsorption is being determined by a method such as total organic carbon (TOC). Indeed, in this case the measurement does not distinguish these grinding aids from other chemical admixtures, in particular those deliberately added to the system. Therefore, each measurement must be corrected by deducing the value obtained on the blank, which is obtained from a sample prepared without adding any chemical admixture oneself. For high solid contents, this is not possible because of mixing limitations. Therefore, one must resort to measuring blanks on more dilute suspensions. Most preferably, this should to be done by adjusting their ionic composition to the one of the concentrated systems considered.

All the above procedures need the use of a filter at one stage. This may be a limiting factor if nano-hydrates are formed and stabilized, something that is more probable with chemical admixtures. Comparet (2004), for example, found that it was necessary to use filters with pore diameters as small as 0.1 μm to retain ettringite crystals formed in the presence of SNFCs. However, recent results (Lange and Plank, 2015, and Caruso et al., ETHZ, yet unpublished results) indicate that PCEs lead to ettringite particles and/or aluminum containing agglomerates of PCEs even smaller than 0.1 μm.

Using an ultracentrifuge, Sowoïdnich et al. (2012) demonstrated that much smaller particles can form in presence of PCEs. This result raises the question of what the effects

of admixtures adsorbed on nanoparticles are in terms of rheological behavior. To the best of our knowledge, this is an open question to which we suggest the following considerations. Presumably, the amount of particles passing the filter is relatively low. Additionally, they must be well-dispersed; otherwise, they would agglomerate and not go through the filter. This would suggest that neither those nanoparticles nor their adsorbed admixtures would greatly affect the rheological properties of the paste. Therefore, from a rheological point of view, it might be reasonable to consider them as nonadsorbed and to neglect the role of the nanoparticles on the created specific surface. From a chemical kinetic point of view, the situation would be different. Here again, this is an open subject to which no clear answers are yet available to the best of our knowledge.

10.8.3 Stabilization of the liquid phase after extraction

Aqueous phases extracted from cementitious systems at early ages tend to be supersaturated with respect to at least one hydrate. Given time, precipitates may therefore form, adsorb some of the admixtures, and perturb the admixture concentration measurement. Additionally, some admixtures are not stable at high pH, so neutralization is recommended (if techniques such as high performance liquid chromatography (HPCL), or size exclusion chromatography (SEC), also referred to a gel permeation chromatography (GPC), are to be used).

The above issues can be dealt with by neutralizing the suspension. Additionally, the same step would dissolve most nanohydrates, causing admixtures adsorbed thereon to be considered as nonadsorbed. However, with regard to the comments at the end of the previous section, this might not be critical when using adsorption data to interpret rheological behavior.

Depending on the analytical technique used, the acid to be used may vary. For HPLC and SEC or GPC, which separate organic molecules, acetic acid can be used (Flatt et al., 1998). For TOC, using an organic acid is not possible. Among inorganic acids, one should avoid those for which the associated base would precipitate with cations present in the extracted aqueous phase. As an example, sulfuric acid must be avoided because it could precipitate as gypsum with the calcium ions. Hydrochloric and nitric acids, in contrast, represent reasonable choices.

If one wants to mimic the aqueous phase of a pore solution, it is possible to make minor adjustments to avoid supersaturation with respect to specific minerals. For example, if an aqueous phase is supersaturated with respect to syngenite ($K_2Ca(SO_4)_2 \cdot H_2O$), it is possible to reconstitute the solution by replacing potassium with sodium ions (for an example of such a solution see for example Houst et al., 2008 or Kjeldsen et al., 2006).

10.8.4 Analysis of the liquid phase

Once the liquid phase has been extracted and stabilized, the admixture content must be measured. The most straightforward measurement for this is ultraviolet (UV) or visible (Vis) light absorption. A calibration curve must be set up using reference samples of known concentrations. It should be noted that UV/Vis spectrometry can only be applied to polymers that absorb light with the corresponding wavelengths, such as PNS, PMS, and LS.

For PCE polymers, other methods are to be considered. These include the measurement of the total organic carbon in solution (TOC). This method is also rather simple, but it does not offer any discrimination among organic compounds.

Evaporative light scattering is another technique that has been used to analyze PCEs in cementitious systems. For this method, the solution undergoes a flash evaporation and passes through a light source, which is then partially diffracted by the polymers. The change in light intensity at a given angle is related to the polymer dosage, which can be quantified provided a calibration curve is previously established.

UV/Vis and evaporative light scattering can easily be implemented as detectors on a chromatography systems, whether HPLC or GPC[2] (calibration curves are also needed). This coupling makes it possible to determine whether specific fractions of the molecular distribution are or are not adsorbed. For example, oligomers, residual monomers, and nongrafted side chains of PCEs typically do not adsorb and are detected in full amounts in chromatography measurements. The polymer peak(s) not only decrease due to adsorption but also change in shapes and/or relative intensities. This confirms the fact that all polymer fractions do not have the same affinity for the solid surface (Flatt et al., 1998; Winnefeld et al., 2007).

Concerning the separation by means of chromatography, it is important to emphasize that HPLC separates components on a chemical basis, while GPC does so on a physical basis (molecular size). In HPLC, the molecules with the greatest affinity for the chemistry or topography of the surfaces will come out last. For polymers, this affinity increases with molar mass, so that the largest polymers exit last.

In GPC, the largest molecules exit first. In this case, the solvent and columns should be chosen to prevent polymer adsorption. Under those conditions, smaller molecules that have a higher mobility will spend more time wandering through the porous network and exit last. GPC therefore offers a physical separation, based on size rather than on chemistry.

The GPC separation can be calibrated in different ways. One of them uses standards that do not have to be of the same molecular nature as the polymers analyzed. However, the resolution offered by GPC columns is not very high. In contrast, HPLC can offer a much higher resolution, but the nature of the peaks cannot be easily determined without additional case-by-case analytical efforts.

While GPC requires specific solvent compositions to be used and maintained constant, HPLC offers the possibility to change the eluent composition over time. This can provide a combination of high peak resolution and low total elution time (Flatt et al., 1998). Readers interested in more detail concerning chromatography, and in particular GPC, are referred to Striegel et al. (2009).

Finally, quite recently the use of Dynamic Light Scattering (DLS) of solutions has been proposed to quantify the amounts of admixtures remaining in solution (Bessaies-Bey,

[2] For water-soluble polymers analyzed in an aqueous mobile phase, it would be more appropriate to speak of Size Exclusion Chromatography (SEC) rather than Gel Permeation Chromatography (GPC). However, as the terminology of GPC is widespread, we also use it in the remainder of this text.

2015). This is of particular interest if different compounds of quite distinct sizes are being examined and cannot be differentiated by TOC.

10.8.5 Indirect measurement of adsorption using zeta potential

Zeta potential measurements are sometimes presented as a useful and efficient method of evaluation polymer adsorption (Houst et al., 2008; Nachbaur et al., 1998; Jolicoeur et al., 1994; Nkinamubanzi, 1994). Indeed, as adsorbing polymers generally change the surface charge, the zeta potential reflects adsorption. However, beyond this first-order relation, many limitations should be stated. First of all, sufficient charge changes must be detected. Second, adsorbing polymers can induce nontrivial modification to the double layer, in addition to shifting the position of the shear plane (Chapter 11, Gelardi and Flatt, 2016). Consequently, zeta potential does not (necessarily) vary linearly with the amount of adsorbed polymers. This implies that zeta potential titrations can be used to determine how much polymer must be added to reach full surface coverage (the point beyond which additional polymers do no change the zeta potential). However, this does not inform us about the amount of polymer adsorbed and is therefore of limited use in interpreting rheological results in terms of interparticle forces.

10.8.6 Measurement of the specific surface

The measurement of the specific surface area (SSA) of hydrated cement pastes is known to be delicate both on fresh (Yamada, 2011) and hydrated cement paste (Garci Juenger and Jennings, 2001; Odler, 2003; Thomas et al., 1999). This is due to the (partial) dehydration of hydrates in the drying process during the measurement, in particular the BET measurement. For pastes in the fresh state, this concerns aluminate hydrates, in particular ettringite (Yamada, 2011) but also gypsum (Mantellato et al., 2015).

For example, it was shown that gypsum dehydration can increase the BET-specific surface of anhydrous cements by 50%. This is because hemi-hydrate produced by thermal decomposition of gypsum presents a very high specific surface. Additionally, aluminate hydrates are also highly sensitive to temperature and relative humidity (Zhou et al., 2004), and it is suggested that drying at 60 °C is acceptable prior to BET measurements (Yamada, 2011). These conditions are in fact too harsh for gypsum, for which a temperature of 40 °C under a nitrogen flow during 16 h is recommended (Mantellato et al., 2015).

Because the contents of both ettringite and gypsum vary strongly while cementitious materials are in the fresh state, it is important to select appropriate drying conditions prior to BET measurements. To the best of our knowledge, the above conditions appear to be the most appropriate, but ongoing research is refining this question and further publications are under preparation by Mantellato et al., 2015. In any case, it is important for authors to explicitly report the conditions under which they prepare their samples when publishing specific surface data on cementitious materials.

10.9 Conclusions

The properties of most of concrete admixtures come from their ability to adsorb on cement particle surfaces, as observed for water reducers or retarders. Other admixtures, such as air-entraining or shrinkage-reducing admixtures, must adsorb on liquid−vapor interfaces to perform as expected. Adsorption efficiency of admixtures depends not only on their chemical composition, size, molecular structure, and dosage but also on the characteristics of the adsorbent surface and the composition of the liquid phase. These are important aspects regarding the fact that cement is a multicomponent system that differs from one producer to another one and may show strong variation between batches from the same plant. Furthermore, cement hydration processes in the early hours imply first the formation of new phases, which may lead to an undesired consumption of the admixtures, and secondly an evolving ionic activity in the pore solution that may as well influence the adsorption, as illustrated by the competitive adsorption between sulfates and PCE superplasticizers.

In practice, the determination of an adsorption isotherm allows one to compare the adsorption behavior of admixtures. The most common way to quantify the amount of adsorbed molecules in a cementitious system is the solution depletion method. However, this does not allow differentiating between molecules adsorbed and ones consumed in another process that may prevent them from working properly. Along with the fact that fitting the adsorption isotherm is not trivial, its interpretation becomes more complex.

Finally, adsorption is the fundamental phenomenon that controls efficiency of most concrete admixtures. Therefore, determining and modeling the exact connection between the molecular structure of the admixtures and their adsorption behavior on the different cement phases are important aspects that still need to be carefully addressed.

Acknowledgments

Support for Delphine Marchon was provided by Sika Technology AG (Zürich, Switzerland). Support for Sara Mantellato was provided by the SNF project (n. 140615) titled “Mastering flow loss of cementitious systems”.

References

Baltrus, J.P., LaCount, R.B., 2001. Measurement of adsorption of air-entraining admixture on fly ash in concrete and cement. Cement and Concrete Research 31 (5), 819−824. http://dx.doi.org/10.1016/S0008-8846(01)00494-X.

Bessaies-Bey, H., 2015. Polymères et propriétés rhéologiques d’une pâte de ciment : une approche physique générique. PhD Thesis Paris-Est.

Bouchaud, E., Daoud, M., 1987. Polymer adsorption − concentration effects. Journal De Physique 48 (11), 1991−2000. http://dx.doi.org/10.1051/jphys:0198700480110199100.

Chao, H.-P., Chang, Y.-T., Lee, J.-F., Lee, C.-K., Chen, I.-C., 2008. Selective adsorption and partitioning of nonionic surfactants onto solids via liquid chromatograph mass spectra analysis. Journal of Hazardous Materials 152 (1), 330−336. http://dx.doi.org/10.1016/j.jhazmat.2007.07.001.

Chen, X., Farber, M., Gao, Y., Kulaots, I., Suuberg, E.M., Hurt, R.H., 2003. Mechanisms of surfactant adsorption on non-polar, air-oxidized and ozone-treated carbon surfaces. Carbon 41 (8), 1489−1500. http://dx.doi.org/10.1016/S0008-6223(03)00053-8.

Cohen Stuart, M.A., Fleer, G.J., Scheutjens, J.M.H.M., 1984a. Displacement of polymers. II. Experiment. Determination of segmental adsorption energy of Poly(vinylpyrrolidone) on silica. Journal of Colloid and Interface Science 97 (2), 526−535. http://dx.doi.org/10.1016/0021-9797(84)90324-2.

Cohen Stuart, M.A., Fleer, G.J., Scheutjens, J.M.H.M., 1984b. Displacement of polymers. I. Theory. Segmental adsorption energy from polymer desorption in binary solvents. Journal of Colloid and Interface Science 97 (2), 515−525. http://dx.doi.org/10.1016/0021-9797(84)90323-0.

Comparet, C., 2004. Etude Des Interactions Entre Les Phases Modèles Représentatives D'un Ciment Portland et Des Superplastifiants Du Béton (Ph.D. thesis). University of Bourgogne, Dijon.

Dalas, F., Nonat, A., Pourchet, S., Mosquet, M., Rinaldi, D., Sabio, S., 2015a. Tailoring the anionic function and the side chains of comb-like superplasticizers to improve their adsorption. Cement and Concrete Research 67, 21−30. http://dx.doi.org/10.1016/j.cemconres.2014.07.024.

Dalas, et al., 2015b. Modification of the rate of formation and surface area of ettringite by polycarboxylate ether superplasticizers during early C3A−$CaSO_4$ hydration. Cement and Concreate Research. http://www.sciencedirect.com/science/article/pii/S000888461400249X.

Denoyel, R., Rouquerol, J., 1991. Thermodynamic (including microcalorimetry) study of the adsorption of nonionic and anionic surfactants onto silica, kaolin, and alumina. Journal of Colloid and Interface Science 143 (2), 555−572. http://dx.doi.org/10.1016/0021-9797(91)90287-I.

Eberhardt, A.B., 2011. On the Mechanisms of Shrinkage Reducing Admixtures in Self Consolidating Mortars and Concretes. Aachen, Shaker.

Eberhardt, A.B., Flatt, R.J., 2016. Working mechanisms of shrinkage reducing admixtures. In: Aïtcin, P.-C., Flatt, R.J. (Eds.), Science and Technology of Concrete Admixtures, Elsevier (Chapter 13), pp. 305−320.

Evans, D.F., 1988. Self-organization of amphiphiles. Langmuir 4 (1), 3−12. http://dx.doi.org/10.1021/la00079a002.

Fernon, V., Vichot, A., LeGoanvic, N., Columbet, P., Corazza, F., Costa, U., 1997. Interaction between Portland Cement Hydrates and Polynaphtalene Sulfonates. In: Proceedings of the 5th Canmet/ACI Int. Conf. Superplasticizers and Other Chemical admixtures in Concrete, SP 173-12. ACI, Rome, pp. 225−248.

Fan, et al., 2012. Cement and Concreate Research. http://www.sciencedirect.com/science/article/pii/S0008884611002511.

Flatt, R.J., 2004a. Towards a prediction of superplasticized concrete rheology. Materials and Structures 37 (5), 289−300. http://dx.doi.org/10.1007/BF02481674.

Flatt, R.J., 2004b. Dispersion forces in cement suspensions. Cement and Concreate Research. http://www.sciencedirect.com/science/article/pii/S0008884603002989.

Flatt, R.J., Houst, Y.F., Oesch, R., Bowen, P., Hofmann, H., Widmer, J., Sulser, U., Maeder, U., Burge, T.A., 1998. Analysis of superplasticizers used in concrete. Analusis 26 (2), M28−M35.

Flatt, R.J., Houst, Y.F., Bowen, P., Hofmann, H., Widmer, J., Sulser, U., Maeder, U., Burge, T.A., 1997. Interaction of superplasticizers with model powders in a highly alkaline medium. In: Proceedings of the 5th Canmet/ACI Int. Conf. Superplasticizers and Other Chemical Admixtures in Concrete, vol. 173. ACI, Rome, pp. 743−762. http://dx.doi.org/10.14359/6211. Special Publications.

Flatt, R.J., Houst, Y.F., 2001. A simplified view on chemical effects perturbing the action of superplasticizers. Cement and Concrete Research 31 (8), 1169−1176. http://dx.doi.org/10.1016/S0008-8846(01)00534-8.

Flatt, R.J., Schober, I., Raphael, E., Plassard, C., Lesniewska, E., 2009a. Conformation of adsorbed comb copolymer dispersants. Langmuir 25 (2), 845−855. http://dx.doi.org/10.1021/la801410e.

Flatt, R.J., Zimmermann, J., Hampel, C., Kurz, C., Schober, I., Frunz, L., Plassard, C., Lesniewska, E., 2009b. The role of adsorption energy in the sulfate-polycarboxylate competition. In: Proceedings of the 9th Canmet/ACI Int. Conf. Superplasticizers and Other Chemical Admixtures in Concrete, vol. 262. ACI, Sevilla, Spain, pp. 153−164. http://dx.doi.org/10.14359/51663229. Special Publications.

Flatt, R.J., Schober, I., 2012. Superplasticizers. In: Roussel, N. (Ed.), Understanding the rheology of concrete. Woodhead publishing, pp. 144−208.

Fleer, G., 1993. Polymers at Interfaces. Springer Science & Business Media.

de Gennes, P.G., 1976. Scaling theory of polymer adsorption. Journal De Physique 37 (12), 1445−1452. http://dx.doi.org/10.1051/jphys:0197600370120144500.

de Gennes, P.G., 1987. Polymers at an interface; a simplified view. Advances in Colloid and Interface Science 27 (3−4), 189−209. http://dx.doi.org/10.1016/0001-8686(87)85003-0.

Garci Juenger, M.C., Jennings, H.M., 2001. The use of nitrogen adsorption to assess the microstructure of cement paste. Cement and Concrete Research 31 (6), 883−892. http://dx.doi.org/10.1016/S0008-8846(01)00493-8.

Garnier, S., 2005. Novel Amphiphilic Diblock Copolymers by RAFT-Polymerisation, Their Self-organization and Surfactant Properties. Universität Potsdam, Potsdam.

Gelardi, G., Mantellato, S., Marchon, D., Palacios, M., Eberhardt, A.B., Flatt, R.J., 2016. Chemistry of chemical admixtures. In: Aïtcin, P.-C., Flatt, R.J. (Eds.), Science and Technology of Concrete Admixtures, Elsevier (Chapter 9), pp. 149−218.

Gelardi, G., Flatt, R.J., 2016. Working mechanisms of water reducers and superplasticizers. In: Aïtcin, P.-C., Flatt, R.J. (Eds.), Science and Technology of Concrete Admixtures, Elsevier (Chapter 11), pp. 257−278.

Giraudeau, C., 2009. Interactions Organo − Aluminates Dans Les Ciments. Intercalation de Polyméthacrylates-G-PEO Dans L'hydrocalumite (Ph.D. thesis). University Pierre et Marie Curie, Paris.

Giraudeau, C., d'Espinose de Lacaillerie, J.-B., Souguir, Z., Nonat, A., Flatt, R.J., 2009. Surface and intercalation chemistry of polycarboxylate copolymers in cementitious systems. Journal of the American Ceramic Society 92 (11), 2471−2488. http://dx.doi.org/10.1111/j.1551-2916.2009.03413.x.

González-García, C.M., González-Martín, M.L., González, J.F., Sabio, E., Ramiro, A., Gañán, J., 2004. Nonionic surfactants adsorption onto activated carbon. Influence of the polar chain length. Powder Technology 148 (1), 32−37. http://dx.doi.org/10.1016/j.powtec.2004.09.017.

Gruber, M., 2010. α-Allyl-ω-Methoxy-polyethylenglykol-comaleat- basierte Polycarboxylat-Fließmittel für ultra-hochfesten Beton (UHPC): Synthese, Eigenschaften, Wirkmechanismus und Funktionalisierung. TU Munich, Munich.

Habbaba, A., Dai, Z., Plank, J., 2014. Formation of organo-mineral phases at early addition of superplasticizers: the role of alkali sulfates and C3A content. Cement and Concrete Research 59, 112−117. http://dx.doi.org/10.1016/j.cemconres.2014.02.007.

Hanehara, S., Yamada, K., 2008. Rheology and early age properties of cement systems. In: Cement and Concrete Research, Special Issue—The 12th International Congress on the Chemistry of Cement. Montreal, Canada, July 8−13, 2007, vol. 38 (2), pp. 175−195. http://dx.doi.org/10.1016/j.cemconres.2007.09.006.

Hill, R.L., Sarkar, S.L., Rathbone, R.F., Hower, J.C., 1997. An examination of fly ash carbon and its interactions with air entraining agent. Cement and Concrete Research 27 (2), 193−204. http://dx.doi.org/10.1016/S0008-8846(97)00008-2.

Hot, J., 2013. Influence Des Polymères de Type Superplastifiants et Agents Entraineurs D'air Sur La Viscosité Macroscopique Des Matériaux Cimentaires. Université Paris-Est, Paris. http://tel.archives-ouvertes.fr/tel-00962408.

Hot, J., Bessaies-Bey, H., Brumaud, C., Duc, M., Castella, C., Roussel, N., 2014. Adsorbing polymers and viscosity of cement pastes. Cement and Concrete Research 63, 12−19. http://dx.doi.org/10.1016/j.cemconres.2014.04.005.

Houst, Y.F., Bowen, P., Perche, F., Kauppi, A., Borget, P., Galmiche, L., Le Meins, J.-F., et al., 2008. Design and function of novel superplasticizers for more durable high performance concrete (superplast project). Cement and Concrete Research 38 (10), 1197−1209. http://dx.doi.org/10.1016/j.cemconres.2008.04.007.

Jardine, L.A., Koyata, H., Folliard, K.J., Ou, C.-C., Jachimowicz, F., Chun, B.-W., Jeknavorian, A.A., Hill, C.L., 2002. Admixture and Method for Optimizing Addition of EO/PO Superplasticizer to Concrete Containing Smectite Clay-Containing Aggregates. http://www.google.es/patents/US6352952.

Jeknavorian, A.A., Jardine, L.A., Koyata, H., Folliard, K.J., 2003. Interaction of superplasticizers with Clay-Bearing aggregates. In: Proceedings of the 7th Canmet/ACI Int. Conf. Superplasticizers and Other Chemical Admixtures in Concrete, SP-216:1293−1316. ACI, Berlin.

Jiang, S.P., Kim, B.G., Aitcin, P.C., 1999. Importance of adequate soluble alkali content to ensure cement superplasticizer compatibility. Cement and Concrete Research 29 (1), 71−78. http://dx.doi.org/10.1016/S0008-8846(98)00179-3.

Jolicoeur, C., Nkinamubanzi, P.-C., Simard, M.A., Piotte, M., 1994. Progress in understanding the functional properties of superplasticizers in fresh Concrete. In: Proceedings of 4th Canmet/ACI Int. Conf. on Superplasticizers and Other Chemical Admixtures in Concrete, SP-148−4. ACI, Montreal, pp. 63−88.

Juilland, P., Kumar, A., Gallucci, E., Flatt, R.J., Scrivener, K.L., 2012. Effect of mixing on the early hydration of alite and OPC systems. Cement and Concrete Research 42 (9), 1175−1188. http://dx.doi.org/10.1016/j.cemconres.2011.06.011.

Kharitonova, T.V., Ivanova, N.I., Summ, B.D., 2005. Adsorption of cationic and nonionic surfactants on a SiO_2 surface from aqueous solutions: 1. Adsorption of dodecylpyridinium bromide and Triton X-100 from individual solutions. Colloid Journal 67 (2), 242−248. http://dx.doi.org/10.1007/s10595-005-0087-3.

Kirby, G.H., Lewis, J.A., 2004. Comb polymer architecture effects on the rheological property evolution of concentrated cement suspensions. Journal of the American Ceramic Society 87 (9), 1643−1652. http://dx.doi.org/10.1111/j.1551-2916.2004.01643.x.

Kjeldsen, A.M., Flatt, R.J., Bergström, L., 2006. Relating the molecular structure of comb-type superplasticizers to the compression rheology of MgO suspensions. Cement and Concrete Research 36 (7), 1231−1239. http://dx.doi.org/10.1016/j.cemconres.2006.03.019.

Kjellin, U.R.M., Claesson, P.M., Linse, P., 2002. Surface properties of tetra(ethylene oxide) dodecyl amide compared with poly(ethylene oxide) surfactants. 1. Effect of the headgroup on adsorption. Langmuir 18 (18), 6745−6753. http://dx.doi.org/10.1021/la025551c.

Külaots, I., Hsu, A., Hurt, R.H., Suuberg, E.M., 2003. Adsorption of surfactants on unburned carbon in fly ash and development of a standardized foam index test. Cement and Concrete Research 33 (12), 2091−2099. http://dx.doi.org/10.1016/S0008-8846(03)00232-1.

Külaots, I., Hurt, R.H., Suuberg, E.M., 2004. Size distribution of unburned carbon in coal fly ash and its implications. Fuel 83 (2), 223−230. http://dx.doi.org/10.1016/S0016-2361(03)00255-2.

Labbez, C., Jönsson, B., Pochard, I., Nonat, A., Cabane, B., 2006. Surface charge density and electrokinetic potential of highly charged minerals: experiments and Monte Carlo simulations on calcium silicate hydrate. The Journal of Physical Chemistry B 110 (18), 9219−9230. http://dx.doi.org/10.1021/jp057096+.

Langmuir, I., 1918. The adsorption of gases on plane surfaces of glass, mica and platinum. Journal of the American Chemical Society 40 (9), 1361−1403. http://dx.doi.org/10.1021/ja02242a004.

Lange, A., Plank, J., 2015. Formation of nano-sized ettringite crystals identified as root cause for cement incompatibility of PCE superplasticizers. In: Proceedings of the 5th International Symposium on Nanotechnology in Construction, Chicago.

Lei, L., Plank, J., 2012. A concept for a polycarboxylate superplasticizer possessing enhanced clay tolerance. Cement and Concrete Research 42 (10), 1299−1306. http://dx.doi.org/10.1016/j.cemconres.2012.07.001.

Lei, L., Plank, J., June 2014. A study on the impact of different clay minerals on the dispersing force of conventional and modified vinyl ether based polycarboxylate superplasticizers. Cement and Concrete Research 60, 1−10. http://dx.doi.org/10.1016/j.cemconres.2014.02.009.

Lei, L., Plank, J., 2013. Synthesis and properties of a vinyl ether-based polycarboxylate superplasticizer for concrete possessing clay tolerance. Industrial and Engineering Chemistry Research 53 (3), 1048−1055. http://dx.doi.org/10.1021/ie4035913.

Levitz, P.E., 2002. Non-ionic surfactants adsorption: structure and thermodynamics. Comptes Rendus Geoscience 334 (9), 665−673. http://dx.doi.org/10.1016/S1631-0713(02)01806-0.

Li, C.-Z., Feng, N.-Q., Li, Y.-D., Chen, R.-J., 2005. Effects of polyethlene oxide chains on the performance of polycarboxylate-type water-reducers. Cement and Concrete Research 35 (5), 867−873. http://dx.doi.org/10.1016/j.cemconres.2004.04.031.

Liu, Z., Edwards, D.A., Luthy, R.G., 1992. Sorption of non-ionic surfactants onto soil. Water Research 26 (10), 1337−1345. http://dx.doi.org/10.1016/0043-1354(92)90128-Q.

Magarotto, R., Torresan, I., Zeminian, N., 2003. Influence of the molecular weight of polycarboxylate ether superplasticizers on the rheological properties of fresh cement pastes, mortar and concrete. In: Proceedings 11th International Congress on the Chemistry of Cement, Durban/South Africa, vol. 2, pp. 514−526, 11-16 May 2003.

Mantellato, S., Palacios, M., Flatt, R.J., January 2015. Reliable specific surface area measurements on anhydrous cements. Cement and Concrete Research 67, 286−291. http://dx.doi.org/10.1016/j.cemconres.2014.10.009.

Marchon, D., Flatt, R.J., 2016a. Mechanisms of cement hydration. In: Aïtcin, P.-C., Flatt, R.J. (Eds.), Science and Technology of Concrete Admixtures, Elsevier (Chapter 8), pp. 129−146.

Marchon, D., Flatt, R.J., 2016b. Impact of chemical admixtures on cement hydration. In: Aïtcin, P.-C., Flatt, R.J. (Eds.), Science and Technology of Concrete Admixtures, Elsevier (Chapter 12), pp. 279−304.

Marchon, D., Sulser, U., Eberhardt, A.B., Flatt, R.J., 2013. Molecular design of comb-shaped polycarboxylate dispersants for environmentally friendly concrete. Soft Matter 9 (45), 10719−10728. http://dx.doi.org/10.1039/C3SM51030A.

Merlin, F., Guitouni, H., Mouhoubi, H., Mariot, S., Vallée, F., Van Damme, H., 2005. Adsorption and heterocoagulation of nonionic surfactants and latex particles on cement hydrates. Journal of Colloid and Interface Science 281 (1), 1−10. http://dx.doi.org/10.1016/j.jcis.2004.08.042.

Molyneux, P., Rhodes, C.T., Swarbrick, J., 1965. Thermodynamics of micellization of N-alkyl betaines. Transactions of the Faraday Society 61, 1043−1052. http://dx.doi.org/10.1039/TF9656101043.

Nachbaur, L., Nkinamubanzi, P.-C., Nonat, A., Mutin, J.-C., 1998. Electrokinetic properties which control the coagulation of silicate cement suspensions during early age hydration. Journal of Colloid and Interface Science 202 (2), 261–268. http://dx.doi.org/10.1006/jcis.1998.5445.

Narkiewicz-Michałek, J., Rudzinski, W., Keh, E., Partyka, S., 1992. A combined calorimetric—thermodynamic study of non-ionic surfactant adsorption from aqueous solutions onto silica surface. Colloids and Surfaces 62 (4), 273–288. http://dx.doi.org/10.1016/0166-6622(92)80053-5.

Narkis, N., Ben-David, B., 1985. Adsorption of non-ionic surfactants on activated carbon and mineral clay. Water Research 19 (7), 815–824. http://dx.doi.org/10.1016/0043-1354(85)90138-1.

Nevskaia, D.M., Guerrero-Ruiz, A., de D. López-González, J., 1998. Adsorption of polyoxyethylenic nonionic and anionic surfactants from aqueous solution: effects induced by the addition of NaCl and $CaCl_2$. Journal of Colloid and Interface Science 205 (1), 97–105. http://dx.doi.org/10.1006/jcis.1998.5617.

Ng, S., Plank, J., 2012. Interaction mechanisms between Na montmorillonite clay and MPEG-based polycarboxylate superplasticizers. Cement and Concrete Research 42 (6), 847–854. http://dx.doi.org/10.1016/j.cemconres.2012.03.005.

Nicoleau, L., Schreiner, E., Nonat, A., May 2014. Ion-specific effects influencing the dissolution of tricalcium silicate. Cement and Concrete Research 59, 118–138. http://dx.doi.org/10.1016/j.cemconres.2014.02.006.

Nkinamubanzi, P.-C., 1994. Influence des dispersants polymériques, superplastifiants, sur les suspensions concentrées et les pâtes de ciment [microforme] (Ph.D. thèse). Université de Sherbrooke.

Nkinamubanzi, P.-C., Mantellato, S., Flatt, R.J., 2016. Superplasticizers in practice. In: Aïtcin, P.-C., Flatt, R.J. (Eds.), Science and Technology of Concrete Admixtures, Elsevier (Chapter 16), pp. 353–378.

Oblak, L., Pavnik, L., Lootens, D., 2013. From the Concrete to the Paste: A Scaling of the Chemistry. Association française de génie Civil (AFGC), Paris, pp. 91–98. http://www.afgc.asso.fr/images/stories/visites/SCC2013/Proceedings/11-pages%2091-98.pdf.

Odler, I., 2003. The BET-specific surface area of hydrated Portland cement and related materials. Cement and Concrete Research 33 (12), 2049–2056. http://dx.doi.org/10.1016/S0008-8846(03)00225-4.

Papo, A., Piani, L., 2004. Effect of various superplasticizers on the rheological properties of Portland cement pastes. Cement and Concrete Research 34 (11), 2097–2101. http://dx.doi.org/10.1016/j.cemconres.2004.03.017.

Paria, S., Khilar, K.C., 2004. A review on experimental studies of surfactant adsorption at the hydrophilic solid–water interface. Advances in Colloid and Interface Science 110 (3), 75–95. http://dx.doi.org/10.1016/j.cis.2004.03.001.

Partyka, S., Zaini, S., Lindheimer, M., Brun, B., 1984. The adsorption of non-ionic surfactants on a silica gel. Colloids and Surfaces 12, 255–270. http://dx.doi.org/10.1016/0166-6622(84)80104-3.

Pedersen, K.H., Jensen, A.D., Berg, M., Olsen, L.H., Dam-Johansen, K., 2009. The effect of combustion conditions in a full-scale low-NO_x coal fired unit on fly ash properties for its application in concrete mixtures. Fuel Processing Technology 90 (2), 180–185. http://dx.doi.org/10.1016/j.fuproc.2008.08.012.

Pedersen, K.H., Jensen, A.D., Dam-Johansen, K., 2010. The effect of low-NO_x combustion on residual carbon in fly ash and its adsorption capacity for air entrainment admixtures in concrete. Combustion and Flame 157 (2), 208–216. http://dx.doi.org/10.1016/j.combustflame.2009.10.018.

Pedersen, K.H., Jensen, A.D., Skjøth-Rasmussen, M.S., Dam-Johansen, K., 2008. A review of the interference of carbon containing fly ash with air entrainment in concrete. Progress in Energy and Combustion Science 34 (2), 135−154. http://dx.doi.org/10.1016/j.pecs.2007.03.002.

Pefferkorn, E., Carroy, A., Varoqui, R., 1985. Dynamic behavior of flexible polymers at a solid/liquid interface. Journal of Polymer Science: Polymer Physics Edition 23 (10), 1997−2008. http://dx.doi.org/10.1002/pol.1985.180231002.

Peng, X., Yi, C., Qiu, X., Deng, Y., 2012. Effect of molecular weight of polycarboxylate-type superplasticizer on the rheological properties of cement pastes. Polymers and Polymer Composites 20 (8), 725−736.

Perche, F., Houst, Y.F., Bowen, P., Hofmann, H., 2003. Adsorption of lignosulfonates and polycarboxylates − depletion and electroacoustic methods. In: Proceedings 7th CANMET/ACI International Conference on Superplasticizers and Other Chemical Admixtures in Concrete (V.M. Malhotra), Berlin, Germany, 2003, Supplementary Papers, pp. 1−15.

Perche, F., 2004. Adsorption de Polycarboxylates et de Lignosulfonates Sur Poudre Modèle et Ciments (Ph.D. thesis), EPFL, Lausanne. http://dx.doi.org/10.5075/epfl-thesis-3041.

Piotte, M., 1993. Caractérisation du poly(naphtalènesulfonate) [microforme]: influence de son contre-ion et de sa masse molaire sur son interaction avec le ciment (Ph.D. thèse). Université de Sherbrooke.

Plank, J., Dai, Z., Andres, P.R., 2006a. Preparation and characterization of new Ca−Al−polycarboxylate layered double hydroxides. Materials Letters 60 (29−30), 3614−3617. http://dx.doi.org/10.1016/j.matlet.2006.03.070.

Plank, J., Keller, H., Andres, P.R., Dai, Z., 2006b. Novel organo-mineral phases obtained by intercalation of maleic anhydride−allyl ether copolymers into layered calcium aluminum hydrates. Inorganica Chimica Acta, Protagonist in Chemistry: Wolfgang Herrmann 359 (15), 4901−4908. http://dx.doi.org/10.1016/j.ica.2006.08.038.

Plank, J., Winter, C., 2008. Competitive adsorption between superplasticizer and retarder molecules on mineral binder surface. Cement and Concrete Research 38 (5), 599−605. http://dx.doi.org/10.1016/j.cemconres.2007.12.003.

Plank, J., Brandl, A., Lummer, N.R., 2007. Effect of different anchor groups on adsorption behavior and effectiveness of poly(N,N-dimethylacrylamide-co-Ca 2-acrylamido-2-methylpropanesulfonate) as cement fluid loss additive in presence of acetone−formaldehyde−sulfite dispersant. Journal of Applied Polymer Science 106 (6), 3889−3894. http://dx.doi.org/10.1002/app.26897.

Plank, J., Hirsch, C., 2007. Impact of zeta potential of early cement hydration phases on superplasticizer adsorption. Cement and Concrete Research 37 (4), 537−542. http://dx.doi.org/10.1016/j.cemconres.2007.01.007.

Plank, J., Zhimin, D., Keller, H., van Hössle, F., Seidl, W., 2010. Fundamental mechanisms for polycarboxylate intercalation into C3A hydrate phases and the role of sulfate present in cement. Cement and Concrete Research 40 (1), 45−57. http://dx.doi.org/10.1016/j.cemconres.2009.08.013.

Platel, D., 2009. Impact of polymer architecture on superplasticizer efficiency. In: Proceedings of the 9th Canmet/ACI Int. Conf. Superplasticizers and Other Chemical Admixtures in Concrete, vol. 262. ACI, Sevilla, Spain, pp. 381−394. http://dx.doi.org/10.14359/51663229. Special Publications.

Platel, D., 2005. Impact de L'architecture Macromoléculaire Des Polymères Sur Les Propriétés Physico-Chimiques Des Coulis de Ciment. (Ph.D. thesis) Université Pierre et Marie Curie - Paris VI. http://pastel.archives-ouvertes.fr/pastel-00001497.

Portet, F., Desbène, P.L., Treiner, C., 1997. Adsorption isotherms at a silica/water interface of the oligomers of polydispersed nonionic surfactants of the alkylpolyoxyethylated series. Journal of Colloid and Interface Science 194 (2), 379–391. http://dx.doi.org/10.1006/jcis.1997.5113.

Pourchet, et al., 2012. Cement and Concreate Research. http://www.sciencedirect.com/science/article/pii/S0008884611002961.

Prince, W., Edwards-Lajnef, M., Aïtcin, P.-C., 2002. Interaction between ettringite and a polynaphthalene sulfonate superplasticizer in a cementitious paste. Cement and Concrete Research 32 (1), 79–85. http://dx.doi.org/10.1016/S0008-8846(01)00632-9.

Regnaud, L., Nonat, A., Pourchet, S., Pellerin, B., Maitrasse, P., Perez, J.-P., Georges, S., 2006. Changes in cement paste and mortar fluidity after mixing induced by PCP: a parametric study. In: Proceedings of the 8th CANMET/ACI International Conference on Superplasticizers and Other Chemical Admixtures in Concrete., Sorrento, October 20–23, pp. 389–408. http://hal.archives-ouvertes.fr/hal-00453070.

Reknes, K., Gustafsson, J., 2000. Effect of modifications of lignosulfonate on adsorption on cement and fresh Concrete properties. In: Proceedings of the 6th CANMET/ACI International Conference on Superplasticizers and Other Chemical Admixtures in Concrete., Nice, ACI, SP-195, pp. 127–141.

Reknes, K., Peterson, B.G., 2003. Novel lignosulfonate with superplasticizer performance. In: Proceedings 7th CANMET/ACI International Conference on Superplasticizers and Other Chemical Admixtures in Concrete. ACI, Berlin. Supplementary Papers, pp. 285–299.

Rosen, M.J., 2004. Surfactants and Interfacial Phenomena, third ed. John Wiley & Sons, Inc.

Rössler, C., Möser, B., Stark, J., 2007. Influence of Superplasticizers on C3A Hydration and Ettringite Growth in Cement Paste. In: Proceedings of the 12th International Congress on the Chemistry of Cement, Montréal.

Schöber, I., Flatt, R.J., 2006. Optimizing polycaboxylate polymers. In: Proceedings 8th CANMET/ACI International Conference on Superplasticizers and Other Chemical Admixtures in Concrete, Sorrento, ACI, SP-239, pp. 169–184.

Sowoïdnich, T., Rössler, C., Ludwig, H.-M., Völkel, A., 2012. The formation of C-S-H phase in the aqueous phase of C3S pastes and the role of superplasticizers. Prague. In: Supplementary Papers of the 10th International Conference on Superplasticizers and Other Chemical Admixtures in Concrete, pp. 418–435.

Striegel, A., Yau, W.W., Kirkland, J.J., Bly, D.D., 2009. Modern Size-Exclusion Liquid Chromatography: Practice of Gel Permeation and Gel Filtration Chromatography. John Wiley & Sons.

Suter, J.L., Coveney, P.V., 2009. Computer simulation study of the materials properties of intercalated and exfoliated poly(ethylene)glycol clay nanocomposites. Soft Matter 5 (11), 2239–2251. http://dx.doi.org/10.1039/B822666K.

Svensson, P.D., Hansen, S., 2010. Intercalation of smectite with liquid ethylene glycol—Resolved in time and space by synchrotron X-ray diffraction. Applied Clay Science 48 (3), 358–367. http://dx.doi.org/10.1016/j.clay.2010.01.006.

Tadros, T.F., 2005. Applied Surfactants: Principles and Applications. Wiley-VCH Verlag GmbH & Co. KGaA, Weinheim.

Tattersall, G.H., Banfill, P.F.G., 1983. The Rheology of Fresh Concrete. Pitman Advanced Publishing Program.

Thomas, J.J., Jennings, H.M., Allen, A.J., 1999. The surface area of hardened cement paste as measured by various techniques. Concrete Science and Engineering 1, 45–64.

Uchikawa, H., Hanehara, S., Sawaki, D., 1997. The role of steric repulsive force in the dispersion of cement particles in fresh paste prepared with organic admixture. Cement and Concrete Research 27 (1), 37–50. http://dx.doi.org/10.1016/S0008-8846(96)00207-4.

Vickers Jr., T.M., Farrington, S.A., Bury, J.R., Brower, L.E., 2005. Influence of dispersant structure and mixing speed on concrete slump retention. Cement and Concrete Research 35 (10), 1882–1890. http://dx.doi.org/10.1016/j.cemconres.2005.04.013.

Wattebled, L., 2006. Oligomeric Surfactants as Novel Type of Amphiphiles: Structure – Property Relationships and Behaviour with Additives. Universität Potsdam, Potsdam.

Williams, D.A., Saak, A.W., Jennings, H.M., 1999. The influence of mixing on the rheology of fresh cement paste. Cement and Concrete Research 29 (9), 1491–1496. http://dx.doi.org/10.1016/S0008-8846(99)00124-6.

Winnefeld, F., Becker, S., Pakusch, J., Götz, T., 2007. Effects of the molecular architecture of comb-shaped superplasticizers on their performance in cementitious systems. Cement and Concrete Composites 29 (4), 251–262. http://dx.doi.org/10.1016/j.cemconcomp.2006.12.006.

Yahia, A., Mantellato, S., Flatt, R.J., 2016. Rheology of concrete. In: Aïtcin, P.-C., Flatt, R.J. (Eds.), Science and Technology of Concrete Admixtures, Elsevier (Chapter 7), pp. 97–128.

Yamada, K., Ogawa, S., Hanehara, S., 2001. Controlling of the adsorption and dispersing force of polycarboxylate-type superplasticizer by sulfate ion concentration in aqueous phase. Cement and Concrete Research 31 (3), 375–383. http://dx.doi.org/10.1016/S0008-8846(00)00503-2.

Yamada, K., 2011. Basics of analytical methods used for the investigation of interaction mechanism between cements and superplasticizers. Cement and Concrete Research 41 (7), 793–798. http://dx.doi.org/10.1016/j.cemconres.2011.03.007.

Yamada, K., Takahashi, T., Hanehara, S., Matsuhisa, M., 2000. Effects of the chemical structure on the properties of polycarboxylate-type superplasticizer. Cement and Concrete Research 30 (2), 197–207. http://dx.doi.org/10.1016/S0008-8846(99)00230-6.

Yoshioka, K., Tazawa, E., Kawai, K., Enohata, T., 2002. Adsorption characteristics of super-plasticizers on cement component minerals. Cement and Concrete Research 32 (10), 1507–1513. http://dx.doi.org/10.1016/S0008-8846(02)00782-2.

Zhang, T., Shang, S., Yin, F., Aishah, A., Salmiah, A., Ooi, T.L., 2001. Adsorptive behavior of surfactants on surface of Portland cement. Cement and Concrete Research 31 (7), 1009–1015. http://dx.doi.org/10.1016/S0008-8846(01)00511-7.

Zhor, J., 2005. Molecular Structure and Performance of Lignosulfonates in Water-Cement Systems (Ph.D. thesis). University of New Brunswick.

Zhor, J., Bremmer, T.W., 1997. Influence of lignosulphonate molecular weight fractions on the properties of fresh cement. In: Proceedings of the 5th Canmet/ACI Int. Conf. Super-plasticizers and Other Chemical Admixtures in Concrete, vol. 173. ACI, Rome, pp. 781–806. http://dx.doi.org/10.14359/6213. Special Publications.

Zhou, Q., Lachowski, E.E., Glasser, F.P., 2004. Metaettringite, a decomposition product of ettringite. Cement and Concrete Research 34 (4), 703–710. http://dx.doi.org/10.1016/j.cemconres.2003.10.027.

Zimmermann, J., Hampel, C., Kurz, C., Frunz, L., Flatt, R.J., 2009. Effect of polymer structure on the sulfate-polycarboxylate competition. In: Proceedings of the 9th Canmet/ACI Int. Conf. Superplasticizers and Other Chemical Admixtures in Concrete, vol. 262. ACI, Sevilla, Spain, pp. 165–176. http://dx.doi.org/10.14359/51663230. Special Publications.

Zingg, A., Winnefeld, F., Holzer, L., Pakusch, J., Becker, S., Gauckler, L., 2008. Adsorption of polyelectrolytes and its influence on the rheology, zeta potential, and microstructure of various cement and hydrate phases. Journal of Colloid and Interface Science 323 (2), 301–312. http://dx.doi.org/10.1016/j.jcis.2008.04.052.

Working mechanisms of water reducers and superplasticizers

11

G. Gelardi, R.J. Flatt
Institute for Building Materials, ETH Zürich, Zurich, Switzerland

11.1 Introduction

The yield stress of cement suspensions depends on the balance between attractive and repulsive interparticle forces on the one hand and shear forces on the other hand. If attractive forces dominate, the particles aggregate and suspensions will have a yield stress. If repulsive forces dominate, the dispersion is stable. The effect of superplasticizers on yield stress comes from introducing a repulsive interparticle force that reduces the overall attractive force between cement particles, and consequently the yield stress.

In this section, the nature of the interparticle forces in cement suspensions and how superplasticizers affect them are discussed.

11.2 Dispersion forces

Dispersion forces, also called van der Waals forces, 'arise because local fluctuations in the polarization within one particle induce, via the propagation of electromagnetic waves, a correlated response in the other' (Russel et al., 1992). For two particles made of the same isotropic matter, this interaction is always attractive. The range of interparticle dispersion forces is much larger than that of the individual dipoles. This is because in condensed media, the fluctuations of dipoles are correlated.

The first description of the dispersion forces was given by the microscopic theory, which is based on pairwise summation of interacting dipoles. The attractive potential due to dispersion forces between two spherical particles of radius a_1 and a_2 separated by a distance h was approximated by Hamaker (1937) by:

$$\Psi_{\mathrm{vdW}} = -AH_{(a_1,a_2,h)} \tag{11.1}$$

where A is the Hamaker constant and H a geometric factor. The Hamaker constant depends on the optical properties of particles and the intervening medium, whereas the geometric factor depends on the particle size and the separation distance, and can be written as:

$$H_{(a_1,a_2,h)} = \frac{1}{6}\left(\frac{2a_1a_2}{2(a_1+a_2)h+h^2} + \frac{2a_1a_2}{4a_1a_2+2(a_1+a_2)h+h^2} + Ln\left(\frac{2(a_1+a_2)h+h^2}{4a_1a_2+2(a_1+a_2)h+h^2}\right)\right) \tag{11.2}$$

Science and Technology of Concrete Admixtures. http://dx.doi.org/10.1016/B978-0-08-100693-1.00011-4
Copyright © 2016 Elsevier Ltd. All rights reserved.

The dispersion force is equal to the derivative with respect to separation distance of the interaction potential:

$$F_{\mathrm{vdW}} = -\frac{\partial \Psi_{\mathrm{vdW}}}{\partial h} = A\frac{\partial H_{(a_1,a_2,h)}}{\partial h} \tag{11.3}$$

If the radii of the spheres are substantially larger than the separation distance (a_1, $a_2 > h$), the expression for the van der Waals force can be simplified to:

$$F_{\mathrm{vdW}} \cong -A\frac{\overline{a}}{12h^2} \tag{11.4}$$

where $\overline{a}$ is the harmonic average radius:

$$\overline{a} = \frac{2a_1a_2}{a_1 + a_2} \tag{11.5}$$

In the microscopic theory, the Hamaker constant A is considered independent of the separation distance. However, beyond a certain distance (>5−10 nm) the dipoles of the particles may no longer be correlated, so the value of the Hamaker constant decreases with increasing separation distance because of this effect, known as retardation. Retardation of the Hamaker constant is taken into account in the continuum theory formulated by Lifshitz (1956). In cement suspensions the maximum attractive force, which is relevant for yield stress calculations, occurs at a very small separation. Even though this separation can be increased by the presence of adsorbed polymers, the values remain small. Hence for the size range of interest to cement suspension, the microscopic theory can be used to estimate the magnitude of the dispersion forces.

The Hamaker constant depends on the electrolyte concentration. The intervening electrolyte can reduce the attractive force by interacting with the fluctuating electromagnetic field. This screening effect can be taken into account by calculating a screened (retarded or non-retarded) Hamaker constant. More details on the dispersion forces in cement suspension can be found in Flatt (2004).

11.3 Electrostatic forces

Most solid surfaces in water are charged. This is because, due to its high dielectric permitivity, water is a good solvent for ions. Surface charge arises from the dissociation of surface groups and/or specific adsorption of ions or ionic polymers.

The distribution of ions at a charged interface is well described by the double-layer model of Goüy-Chapman that distinguishes between two zones, the Stern layer and the diffuse layer. The Stern, or inner, layer consists of counter-ions immobilized by the particles' surface (not influenced by Brownian motion). The diffuse, or outer, layer is made up of mobile ions, an excess of which with the same sign charge as the surface. The concentration of counterions is higher close to the surface than in the bulk solution. The ions in the diffuse layer show the opposite behaviour.

Within the limits of the continuum theory, ions in the double layer give rise to an electrical potential that decays exponentially with distance according to:

$$\Psi_{ES} = \Psi_0 e^{-\kappa x} \tag{11.6}$$

where Ψ_0 is the surface potential. The decay length, also called the Debye length, is given by κ^{-1} and is defined as:

$$\kappa^{-1} = \sqrt{\frac{\varepsilon\varepsilon_0 k_B T}{e^2 \sum_i c_i Z_i^2}} \tag{11.7}$$

where:

ε is the relative dielectric constant of the water
ε_0 is the permittivity of vacuum
k_B is the Boltzmann constant
T is the absolute temperature
e is the charge of an electron
c is the bulk concentration of the ith electrolyte of valence Z.

The Debye length is the thickness of the diffuse layer, and represents the distance between surfaces within which the repulsive potential is significant.

As two identically charged surfaces approach, their electrical double layers overlap, developing an excess ion concentration, particularly at mid-distance between both surfaces (Figure 11.1).

This results in an osmotic pressure that calls for a dilution of the ions between the surfaces by drawing water from the bulk. With more water in between particles, the surfaces have to move apart. Hence, electrostatic repulsive force does not require physical contact between objects.

The Debye length decreases with increasing ionic strength (Figure 11.2). At high salt concentration the screening of the surface charge by the ions in solution is more effective, and the range of the electrostatic repulsion is reduced. This is the case in cement suspensions, which have high ionic strength values of the order of magnitude of 100−200 mM (Yang et al., 1997). In cement suspensions, electrostatic repulsion is therefore only felt at a very short distance and in this range, the attractive van der Waals forces are predominant.

The evaluation of the magnitude of the electrostatic force in cement suspensions is complicated by the fact that such systems do not behave as an ideal system and ion activities cannot be approximated to concentrations. Flatt and Bowen (2003) found that the electrostatic force can be well described by the extended three-parameter Debye-Hückel approximation, valid up to 1 mol/L. In addition, attractive ion correlation forces can arise in cement suspensions. Indeed, divalent calcium ions can induce attraction between negatively charged surfaces of C−S−H. This effect may become important with time, because of the increasing number of C−S−H contact points as hydration proceeds (Pellenq et al., 1997; Lesko et al., 2001).

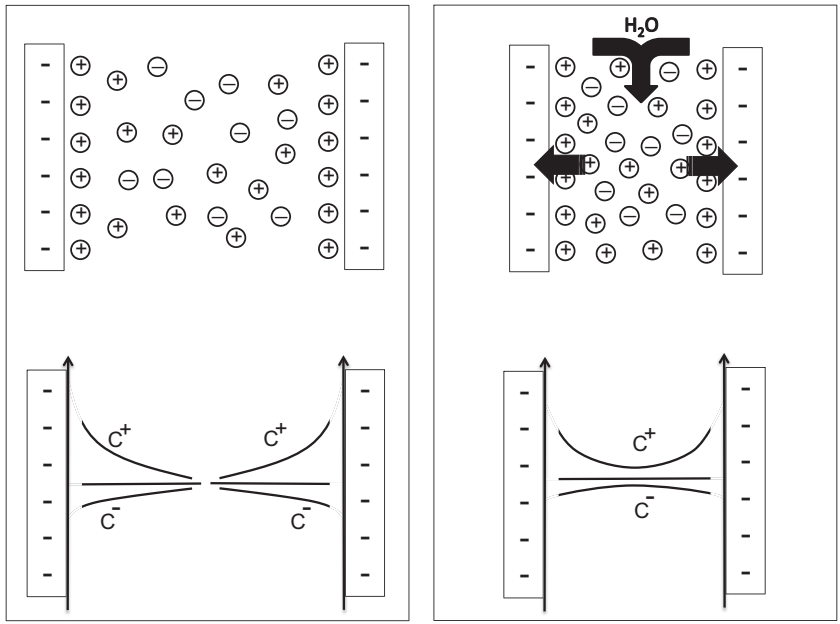


Figure 11.1 Schematic illustration of the underlying principle of electrostatic repulsion. As charged surfaces approach, their double layers overlap, creating an excess ion concentration that is greatest at the mid-plane. This causes an osmotic force that resists the approach of the charged surfaces. This force increases with decreasing ionic strength of the continuous phase.

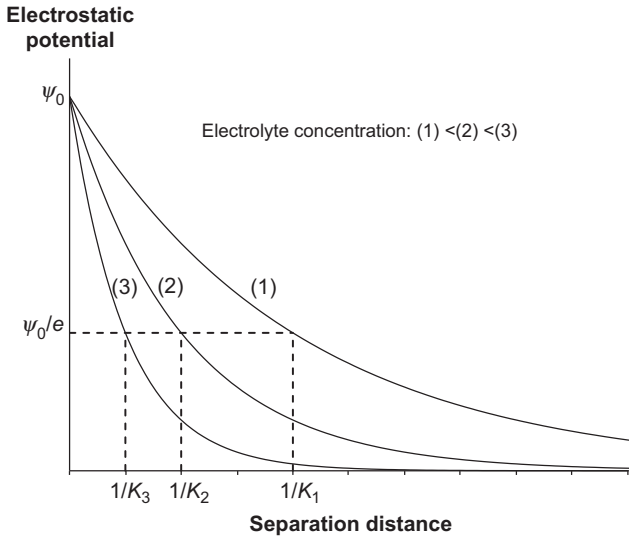


Figure 11.2 Variation in the electrostatic potential as a function of the distance from the surface of a colloidal particle and of the ionic strength (electrolyte concentration) of the continuous phase.

For a simple case of particles with identical surface potential and for which the continuum theory can be applied, the electrostatic repulsive force can be expressed by:

$$F_{ES} \cong -2\pi\varepsilon\varepsilon_0\bar{a}\psi_{ES}^2\frac{\kappa e^{-\kappa h}}{(1+e^{-\kappa h})} \tag{11.8}$$

Neither the surface potential nor the Stern potential can be directly measured. The experimentally determined potential is the zeta potential. This is the potential at the shear plane, which lies in the diffuse layer somewhat further from the surface than the Stern plane. Thus the use of zeta potential probably leads to an underevaluation of the electrostatic force (Figure 11.3).

The measurement of zeta potential shows some intrinsic limitations. One of the most common techniques to measure it is microelectrophoresis, but this method requires the use of very diluted suspensions that are not representative of cement pastes. In addition, particles larger than a few micrometres in diameter tend to settle, and only the fine particles are measured. Acoustophoresis allows the measurement of the zeta potential in concentrated suspension, but this technique shows some limitation, as reported by Flatt and Ferraris (2002).

The electrostatic potential of cement phases depends on their dissociation constants and amount of surface ionizable groups, which are mineral-specific. Since cement is a

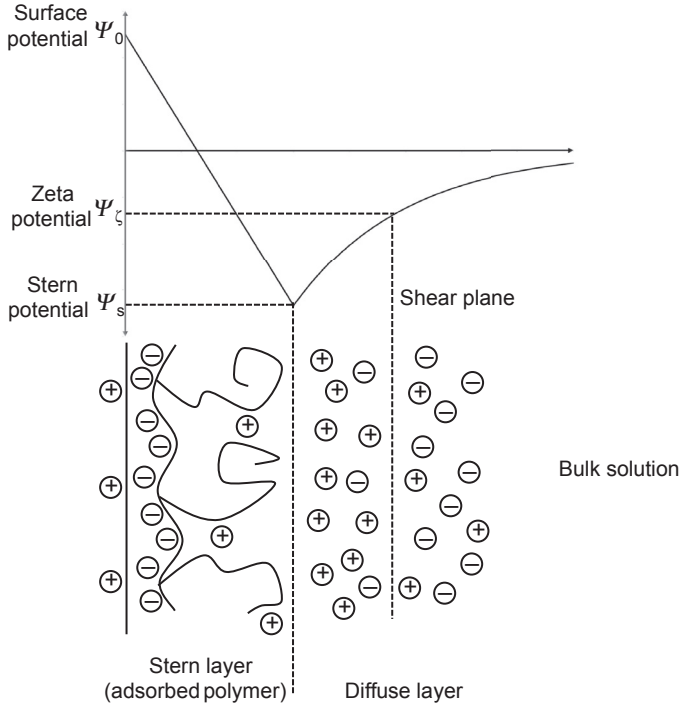


Figure 11.3 Schematic representation of how the presence of an adsorbed chemical admixture may change the potential away from a charged surface.
Adapted from Uchikawa et al. (1997).

multimineral powder, interacting surfaces may have different potentials, which would create an additional attractive force. This can be simply between positive and negatively charged surfaces. However, it can also be between surfaces with the same charge sign but different potentials (Russel et al., 1992). The probable existence of this additional attractive electrostatic force implies that any homogenization of the surface charge should reduce the overall interparticle attraction and thereby the yield stress. This could, for example, occur by adsorbing a zero-thickness film of charge-balancing molecules onto cement particles.

In the more realistic case of the adsorption of a molecule of finite size (Figure 11.3), in particular a polymer, the expression for the electrostatic force can be reformulated, integrating the adsorbed layer thickness L, leading to:

$$F_{ES} \cong -2\pi\varepsilon\varepsilon_0\bar{a}\psi^2\frac{\kappa e^{-\kappa(h-2L)}}{\left(1+e^{-\kappa(h-2L)}\right)} \tag{11.9}$$

Indeed, the potential one would use in such calculation would be a zeta potential, of which the plane of origin is located either at the outside of the adsorbed layer or even further away. Thus the relevant distance for the electrostatic force is $(h-2L)$. However, the distance relevant for the calculation of the dispersion forces remains that between the surfaces of the particles themselves, h.

11.4 DLVO theory

Derjaguin, Landau, Verwey and Overbeck developed a theory that explains the stability of aqueous dispersions in terms of a balance between the attractive van der Waals force and the repulsive electrostatic force (Derjaguin and Landau, 1993; Verwey et al., 1999). This is called DLVO theory after the initials of the authors. The basic hypothesis is that the forces (and potentials) between surfaces are additive and do not influence each other mutually.

Although it was originally formulated for the combination of van der Waals and electrostatic forces, the DLVO theory is often used in a broader sense, including other forces under the assumption of additivity of forces. An illustration of the DLVO summation of the attractive van der Waals potential and the repulsive electrostatic potential is shown in Figure 11.4.

Since the van der Waals and the electrostatic potential have different distance dependence, the total potential can show minima and maxima.

In the limit of zero separation, dispersion forces go to infinite values whereas electrostatic forces remain finite (see Eqns (11.4) and (11.8)). This means that at short separation distances, van der Waals attractive forces prevail. Under this condition, the total interaction energy is known as the primary minimum.

What happens beyond that depends on the balance of the van der Waals force and the electrostatic force, which in turn depends on the electrostatic potential and the ionic strength. The ionic strength is an expression of the effect of ions in solution on the

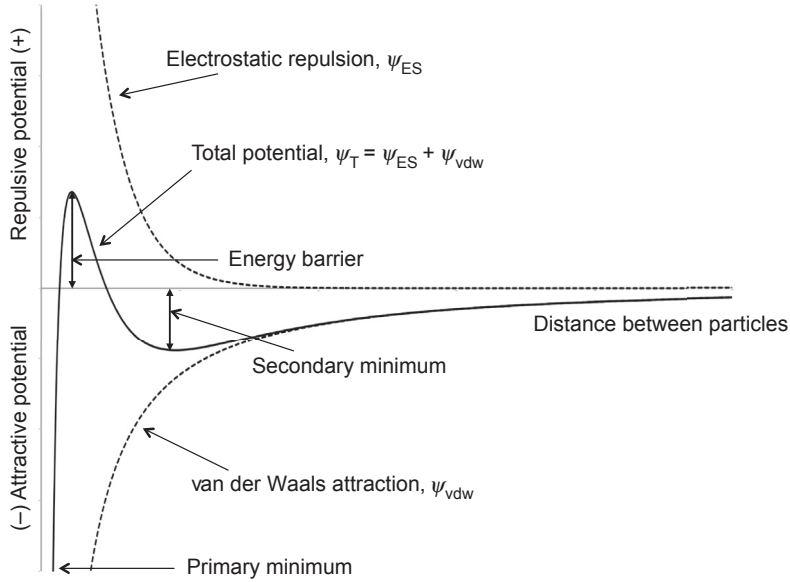


Figure 11.4 Illustration of interparticle potentials as a function of the distance from a charge surface. The positive potential corresponds to electrostatic repulsion, and the negative one to van der Waals attraction. In this specific case their summation leads to a primary minimum, a potential barrier and a secondary minimum.

electrostatic potential. Depending on the ionic strength, three main types of behaviours can be observed (Figure 11.5).

(A) At low ionic strengths, electrostatic repulsion is very long ranged and dominates the van der Waals forces. As the separation distance decreases, the repulsive force increases to a maximum. In terms of potentials, one talks about an energy barrier. The larger this energy barrier, the more stable the suspension. If the barrier is overcome, particles that come into a primary minimum stick together and are very hard to separate again. Otherwise, the system remains dispersed.

(B) As the ionic strength is increased, the range of the electrostatic repulsion is reduced. This leads to situations as depicted in curve B with a clear secondary minimum on plots of potential versus separation distance. This corresponds to a metastable equilibrium (a flocculated suspension) in which the system will rest unless it receives enough energy. This could lead to particle separation. Alternatively, if the energy is larger than the potential barrier, particles would come close together and agglomerate, remaining 'caught' in the primary minimum.

(C) At high ionic strength the energy barrier disappears and the interparticle potential only has a primary minimum.

For colloidal particles, stability is generally discussed in terms of the height of the potential barrier (case B). In particular, a multiple of the thermal energy kT, coming from Brownian motion, is considered necessary to have a dispersed, well flowing

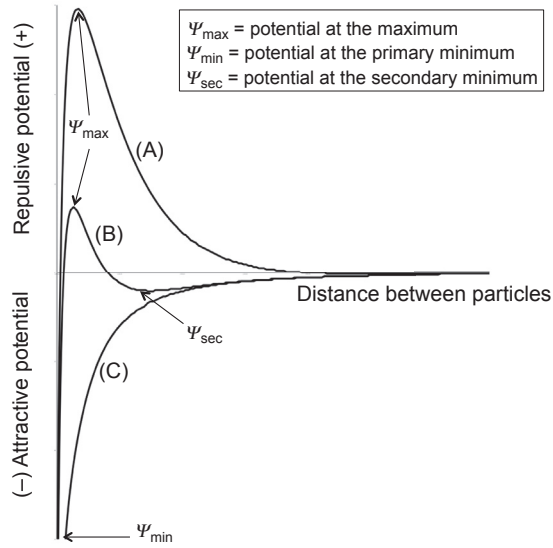


Figure 11.5 Illustration of various types of interparticle potentials. All cases show a primary minimum, as van der Waals attraction dominates over electrostatic at short separation distances. Depending on the surface charge and ionic concentration, one obtains in addition: (A) large energy barrier; (B) energy barrier and a secondary minimum; (C) no energy barrier. Adapted from Yang et al. (1997).

suspension. However, the interparticle potential of cement suspensions looks like that depicted in curve C. In that situation Brownian motion cannot provide the energy necessary to keep or move particles away from each other. Therefore, for cement particles it is rather shear forces than Brownian motion that provide the relevant criterion to decide on system's fate, a situation further enhanced by the fact that these particles are too large to be sensitive enough to Brownian motion. Thus for cement-type suspension the role of dispersion must be discussed in terms of attractive force (against which shear forces would act) rather than potential. We are therefore interested in knowing which force should be overcome to separate particles during flow, rather than determining whether a potential barrier is or is not large enough to prevent agglomeration.

In this chapter, the interparticle force of cementitious systems has been calculated using Hamaker 2 software (Aschauer et al., 2011), in which models derived for cement suspension were implemented.

Figure 11.6 shows the interparticle force normalized by the particle radius as a function of the separation distance for a system having a zeta potential equal to 5 mV, representative of a cement suspension (Plank and Winter, 2008; Plank and Sachsenhauser, 2006). The interparticle force is expressed in kT, where k is a Boltzmann constant and T is the temperature in Kelvin. For all the calculations in this chapter, the temperature is taken to be equal to 300 K.

The parameters used for the computation of the force are particle diameter 1 μm, specific gravity 3.15 and unscreened Hamaker constant 1.757×10^{-20} J (Flatt, 2004). The electrolyte composition of the cement pore solution of a paste having a w/c of 0.35 gives a Debye length of 0.67 nm (Flatt and Bowen, 2003).

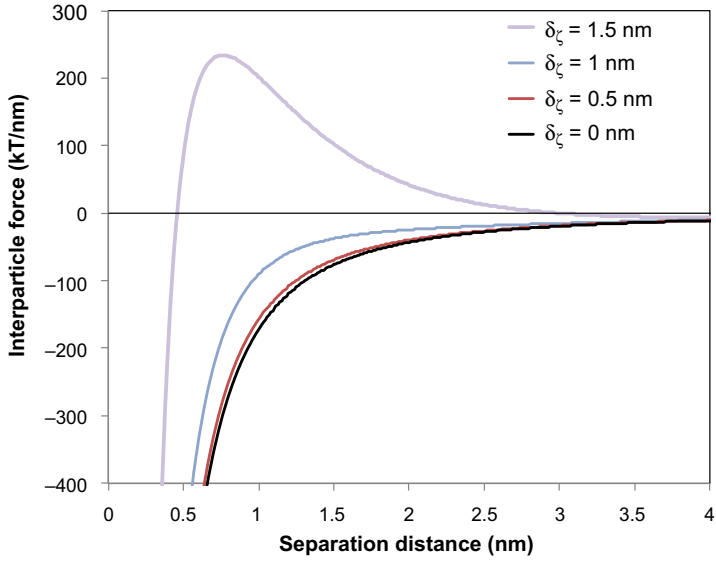


Figure 11.6 Normalized interparticle force as a function of separation distance, computed for cement particles with a diameter of 1 μm and specific gravity of 3.15. The zeta potential is 5 mV. The zeta potential plane is placed on the surface (0 nm), at 0.5, 1.0 and 1.5 nm from the surface.

Figure 11.6 shows the resulting force between cement particles using the above parameters and considering different positions for the electrostatic potential plane. Repulsion force has positive values, while attraction force has negative values. Results show that the distance at which the charge is located (δ_ζ) does not significantly change the interparticle force for reasonable values of δ_ζ.

However, the position of the charge plane becomes important for higher potentials, for example after the adsorption of a linear polyelectrolyte. This condition is represented in Figure 11.7. To illustrate this, let us consider first the case where the zeta potential plane is at the particle surface. Whatever the zeta potential is, if the charge is located directly on the cement surface, electrostatic repulsion is not effective. The maximum attractive force is dictated by van der Waals attraction, and decreases to infinity as the separation distance goes to zero.

In reality, however, the separation distance is not believed to decrease to zero, but rather a minimum separation distance between agglomerated particles can be defined (Zhou et al., 1999, 2001; Flatt and Bowen 2006, 2007). In the case of cement it is suggested that the minimum separation distance would be in the order of 1.6 nm, so one could assume a 'solvent' layer, δ_0, of about 0.8 nm cannot be removed from the particles (Perrot et al., 2012). From this perspective, we conclude that in pure cement the maximum attractive force would have to be calculated at a separation distance of 1.6 nm.

Let us now turn to situations in which the charge is located at a certain distance from the surface. Based on the above consideration of the solvent layer, we consider a value of 0.8 nm for δ_ζ. As shown in Figure 11.7, the electrostatic repulsion does become effective in such situations, with electrostatic potential values around or greater than 10 mV. Under these conditions, the distance at which the maximum attractive force is reached is higher than 2 δ_ζ.

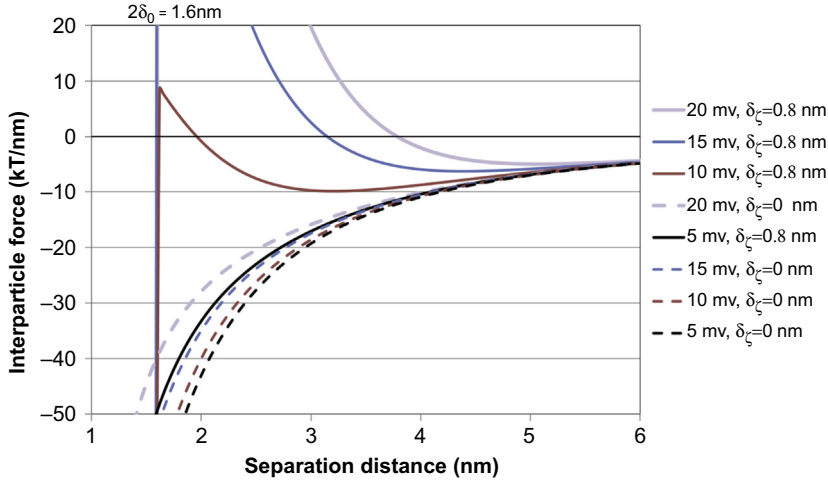


Figure 11.7 Normalized interparticle force as a function of separation distance for a system defined as in Figure 11.6. The dashed lines represent cases in which the charge is located at the surface of the particle.

This effect can fall into the category of electrosteric. The electrostatic repulsion plays an important role, but only because the charge plane is located at a certain distance from the particle surface. This distant location can be provided by a polymer. These results suggest that, if this is the case, the polymer itself would not additionally have to provide substantial steric hindrance if the charge is high enough.

Surface forces have been directly measured with an atomic force microscope (AFM). Using the so-called colloidal probe technique, it is possible to measure the forces between colloidal particles of few micrometres in a liquid. Pedersen and Bergström (1999) measured the interparticle forces between zirconia surfaces by AFM. Figure 11.8 shows (left) the effect of ionic strength on the magnitude of the repulsive force: as the ionic strength of the medium increases the repulsive force decreases, as predicted by the DLVO theory. At a very high ionic strength (I = 0.01 mol/L), as in Figure 11.8 (right), only attraction is measured. It is important to note that the ionic strength of cement pore solution is 10 times higher than this value.

11.5 Steric forces

Steric forces arise from the presence of polymers adsorbed onto particle surfaces. The most important steric force is repulsive and of entropic origin. Adsorbed polymers adopt a preferred conformation on the surface. When a polymer-coated particle approaches a second particle, polymer molecules have to distort from this preferred conformation, which results in a loss of conformational entropy. At the same time, the concentration of polymer segments between the particles increases with respect to the bulk solution, giving rise to an osmotic pressure that resists the particles approaching each other.

A repulsive steric force therefore develops as soon as the polymer layers start to overlap. This increases strongly upon further compression of the polymer layers, and diverges to infinite when maximum compression is reached.

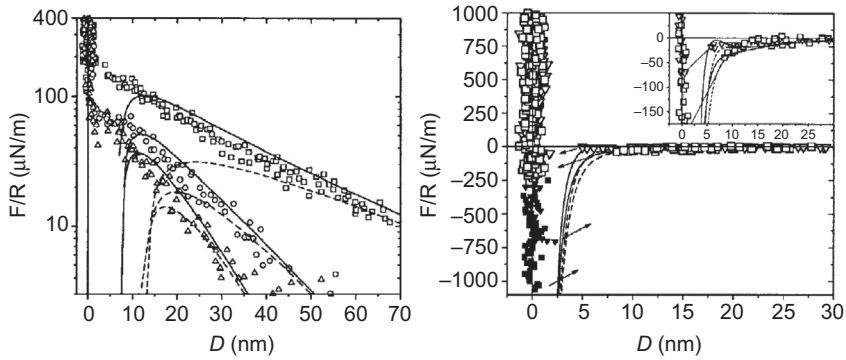


Figure 11.8 Illustration of colloidal probe measurements made between zirconia surfaces (sphere and plate). Forces are normalized with respect to the probe radius R. (Left) NaCl concentrations of 0.0001M (squares), 0.0005M (circles) and 0.001M (triangles). (Right) NaCl concentration of 0.01M; data show a jump into contact, revealing the strong attractive force that cannot be resisted by the tip cantilever stiffness.
Reproduced with authorization from Pedersen and Bergström (1999)

Various expressions have been proposed to describe steric repulsion. They all arise from considerations about the unfavourable entropy of mixing resulting from the overlap of adsorbed layers as particle separation distance decreases below twice the adsorbed layer thickness. The magnitude of this force depends on the adsorbed conformation, but also on the amount of adsorbed polymer or surface coverage and the nature of the solvent.

Assuming that superplasticizers (SPs) adsorb with a so-called mushroom-type adsorption morphology (where the density of polymer chains is highest not at the surface but some distance from it), the scaling theory developed by de Gennes (1987) can be used to calculate the steric force. The expression proposed for flat plates can be integrated for spheres using the Derjaguin approximation, giving the following expression:

$$F_{\mathrm{Ste}} = \overline{a}\frac{3\pi k_{\mathrm{B}}T}{5s^2}\left[\left(\frac{2L}{h}\right)^{5/3} - 1\right] \tag{11.10}$$

where s is the distance between the centres of two neighbouring mushrooms and L is the maximum length extending into the solvent.

Flatt et al. (2009) derived an expression for the steric force from AFM measurements under the assumption of a high surface coverage by adsorbed comb copolymers:

$$F = \beta\left(\frac{5}{2^{1/3}}R_{\mathrm{AC}}^{2/3} - \frac{1}{2}D^{-1/3}\left(3D + 4\left(2^{2/3}\right)R_{\mathrm{AC}}\left(\frac{R_{\mathrm{AC}}}{D}\right)^{2/3}\right)\right) \tag{11.11}$$

With

$$\beta = \frac{2\pi k_{\mathrm{B}}TR_{\mathrm{tip}}}{\alpha}P^{-29/30}N^{-13/30} \tag{11.12}$$

where R_{tip} is the radius of the AFM cantilever tip end, assumed to be hemispherical, and

$$\alpha = \pi 2^{-3/10} a_P^{5/3} a_N \left((1 - 2\chi) \frac{a_P}{a_N} \right)^{2/15} \tag{11.13}$$

R_{AC} is the adsorbed layer thickness of an adsorbed comb-shaped SP, given by:

$$R_{AC} = \left(2\sqrt{2}(1 - 2\chi) \frac{a_P}{a_N} \right)^{1/5} a_P P^{7/10} N^{-1/10} \tag{11.14}$$

For more information on these polymers, including their solution conformation and chemistry, as well as competitive adsorption, readers are referred respectively to chapter 9 and 10 (Gelardi et al. 2016; Marchon et al. 2016). In general, whatever the model used, it is found that the steric force balances the van der Waals force almost as soon as the overlap of the adsorbed layers begins. Consequently, the maximum attractive force between particles is more or less equal to the van der Waals force at a separation distance equal to twice the adsorbed layer thickness. However, this only strictly holds for systems with a high surface coverage. When the polymers do not cover surfaces, the situation becomes more complex. Average forces may be calculated on a statistical basis (Kjeldsen et al., 2006; Flatt and Schober, 2012) to extend the use of such calculations. However, this approach probably suffers from a bias in the particle contact statistics, as cohesive contacts are thermodynamically more favourable than dispersed ones (for large particles).

An additional complication at low surface coverage is that besides the repulsive steric force, attractive forces can arise. Indeed, bridging forces can arise when polymers adsorb onto two surfaces. The resulting bridging flocculation could explain attractions that are measured at large separation distances in AFM measurements, when, after an intimate approach, the surfaces are moved apart from one another. In practice this bridging could account for the much poorer performance, at low dosage, of traditional SPs with respect to PCEs that would not be expected to cause bridging.

Additionally, non-adsorbed polymers can give rise to depletion forces. If the gap between two particles is lower than the diameter of polymer molecules, a region of pure solvent is created. In the zone depleted of polymer an osmotic pressure arises, leading to an attractive force, as explained for viscosity modifying admixtures in Chapter 20 (Palacios and Flatt, 2016).

11.6 Effect of superplasticizers

Adsorption of SPs prevents cement particles from coming too close to each other. Keeping particles apart reduces the magnitude of the attractive van der Waals forces and consequently also the magnitude of the maximum attractive forces that have to be overcome for a suspension to flow.

11.6.1 Role of electrostatic repulsion

For cement suspensions without polymer additions, the zeta potential values reported are both negative and positive but always small (Nägele 1985, 1986; Uchikawa et al., 1997). SPs induce upon adsorption a negative zeta potential on cement particles, larger in magnitude than the initial potential of cement. Values of zeta potential between −30 mV and −50 mV have been reported for cement suspensions containing linear SPs (Ernsberger and France 1945; Daimon and Roy, 1979; Andersen et al., 1987). Most probably this is not only the result of the charges brought to the surface from polymer adsorption, but also the fact that some of these are located at the exterior of the adsorbed layer (Lewis et al., 2000). Because early-generation SPs increase the absolute value of zeta potential (more negative values), electrostatic stabilization has been considered for years the primary stabilization mechanism of SPs in cement suspensions. However, more recent measurements give maximum values of about 7.5 mV in white Portland cement (Lewis et al., 2000). As stated by Lewis et al. (2000), these lower zeta potential values reflect the fact that the measurements were carried out in a more concentrated solution than those used in previous studies. Indeed, zeta potential values upon adsorption of polynaphtalene sulfonates (PNS) onto white cement under dilute conditions, as well as onto γ-C_2S (inert powder), are much larger due to the lower concentration of Ca-ions in solution, as found by the same authors (Lewis et al., 2000).

11.6.2 Role of electrosteric repulsion

Figure 11.9 shows the interparticle force as a function of separation for cement particles onto which a linear polyelectrolyte, for example a PNS, is adsorbed. Based on the AFM study by Palacios et al. (2012), we consider the thickness of this layer, δ_P, to be 1.8 nm.

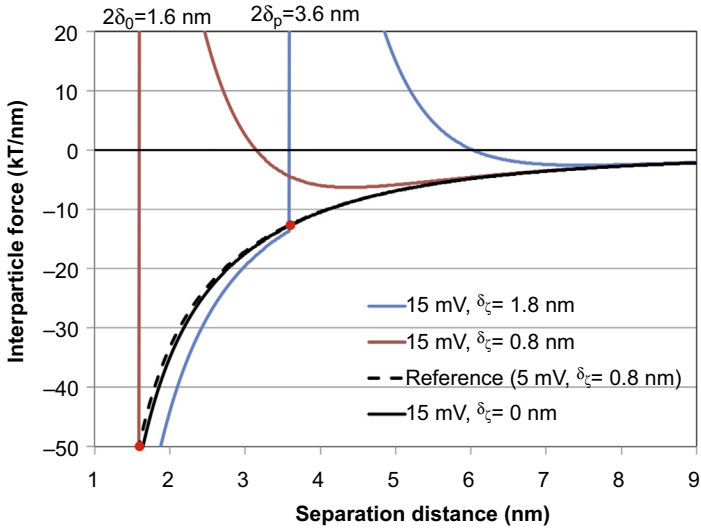


Figure 11.9 Normalized interparticle force as a function of separation distance for a system defined as in Figure 11.6 after adsorption of a linear polyelectrolyte whose layer thickness is 1.8 nm. The zeta potential induced upon adsorption is 15 mV.

The zeta potential after polymer addition is 15 mV. Results in Figure 11.9 again stress the importance of the distance at which the charge is located. In fact, if the charge is at the surface ($\delta\zeta = 0$ nm), any effect due to electrostatic stabilization can be neglected (see Figure 11.7). In contrast, if the charge is located at the outer boundary of the polymer adsorbed layer, the electrostatic force plays a role in the stabilization of the system.

In quantitative terms, we can state that the maximum attractive force is 50 kT/nm for bare cement and cement with PNS if its charge is located on the cement surface. This force drops to 13 kT/nm if the PNS acts as a perfect steric barrier making no electrostatic contribution. It further decreases to 6 kT/nm if the PNS charge is located within the PNS layer at 0.8 nm. Finally, if the charge is at the outside of the PNS layer, the force is only 3 kT/nm.

For the most realistic case of a zeta potential around 7.5 mV (Lewis et al., 2000), the interparticle force at different positions on the electrostatic potential plane is similar to that depicted in Figure 11.6 for bare cement. Thus the electrostatic force is important for the stabilization of the system only when the charge is located at a certain distance from the particle provided by the adsorbed polymer.

Unfortunately, it is not easy to determine which condition is most realistic. However, these examples clearly illustrate that stabilization by PNS should be referred to as electrosteric. It cannot be simply referred to as electrostatic, because in the absence of a shift of the plane of charge electrostatic repulsion would have no effect. It should also be noted that the presence of divalent ions, as mentioned in Section 11.3, may lead to more radical loss of dispersion efficiency than we calculate with the simple continuum model used in these calculations.

In a discussion of a paper by Daimon and Roy, Banfill (1979) stated that the adsorption of such linear SPs would lead to the formation of an adsorbed layer 40 nm thick, and suggested that steric hindrance could therefore be equally important as a dispersing mechanism.

11.6.3 Role of steric hindrance

With the introduction of comb-shaped copolymers, awareness of the importance of steric repulsion in the dispersion mechanism of SPs has grown (Uchikawa et al., 1997; Yoshioka et al., 1997; Flatt et al., 2001). In fact, polycarboxylate ethers (PCEs) were found to induce better dispersion despite a lower decrease of zeta potential with respect to linear SPs.

As previously mentioned, zeta potential measurements cannot be interpreted univocally, especially when PCEs are present. PCEs induce much smaller zeta potentials in cement particles because of their lower fraction of ionizable groups per molecule. In their assumed adsorbed conformation, these charges are located close to the particle surface, while the shear plane is extended towards the bulk solution due to the non-adsorbing side chains (Lewis et al., 2000) (Figure 11.3). The adsorbed layer thickness is in the order of 2.5 nm at least, while the Debye length κ^{-1} in cementitious systems is of the order of 0.7 nm (Flatt and Bowen, 2003). Bearing in mind the exponential decay of the surface potential, Eqn (11.6), the potential that could be measured outside a 2.5 nm layer would be only about 3% of the potential at the inner side of this layer, provided that is where the charge is localized.

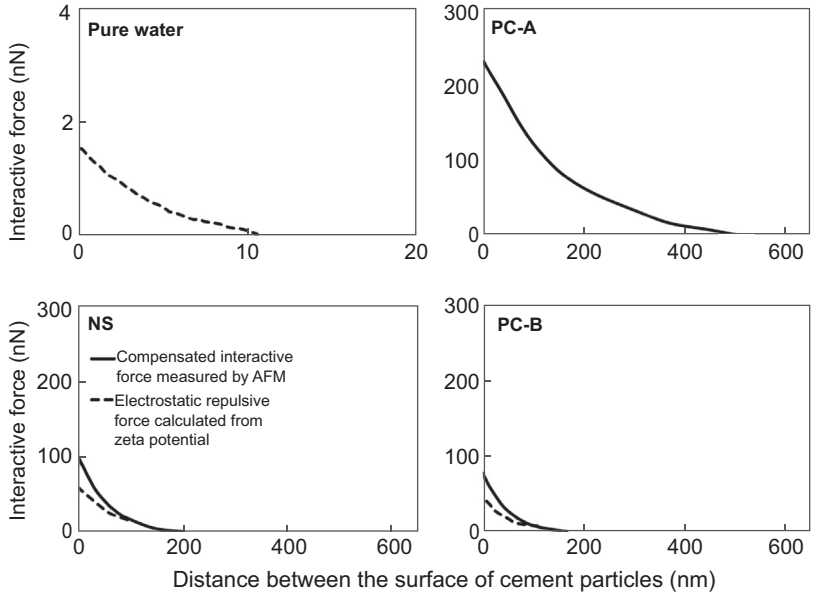


Figure 11.10 Illustration of the forces reported in the first study by atomic force microscopy on the dispersing effect of superplasticizers.
Reproduced with authorization from Uchikawa et al. (1997).

Uchikawa et al. (1997) stated that steric repulsive forces are responsible for the dispersion of cement particles. They used an AFM to measure the interactive force between clinker particles adsorbing polymers, and compared the results with the electrostatic force calculated from zeta potential. Results (see Figure 11.10) showed that steric forces are predominant when a comb-shaped copolymer is adsorbed on the clinker particle, while their contribution to the total repulsive force in the presence of a PNS or a linear polycarboxylate is 30% and 20%, respectively.

In the absence of SPs, the repulsion starts at a separation distance of about 10 nm. When an SP is added, the distance at which repulsion occurs increases. For a PNS (NS) or a linear polycarboxylate (PC-B), repulsion starts at around 90 nm. When a comb-shaped copolymer (PC-A) is adsorbed, the divergence starts at an even higher separation distance of about 500 nm. This separation distance is an order of magnitude higher than that expected, considering that the side-chain length of the comb-shaped copolymer used is reported to be approximately 20 nm. Possible reasons for the large distances measured have been suggested to arise from the formation of organo-aluminate compounds (Flatt and Houst, 2001). Thus while the measurements reported in Figure 11.10 have had the value of convincing the community of the existence and importance of steric hindrance, the results themselves most certainly involve a strong experimental artifact.

In terms of calculations, the total interparticle force can be determined by taking the sum of dispersion (F_{VdW}), electrostatic (F_{ES}) and steric forces (F_{Ste}). We have seen that all these forces depend linearly on the mean harmonic radius of spherical particles of

different sizes a_1 and a_2. Therefore, it is possible to introduce an interparticle force parameter $G_{(h)}$, given by:

$$G_{(h)} = (F_{\mathrm{vdW}} + F_{\mathrm{ES}} + F_{\mathrm{Ste}})/\overline{a} \tag{11.15}$$

11.6.4 Specific role of the PCE molecular structure

Because of the wide use of comb-copolymer dispersants and the flexibility in designing their molecular architecture (Gelardi et al., 2016), we devote a special section to examining how such changes affect the maximum attractive force. As PCEs only induce a low electrostatic charge, which is most likely located very close to the surface, we neglect any electrostatic contributions.

Figure 11.11 presents the cases of cement particles onto which PCEs with side-chain length of 1000 g/mol and 5000 g/mol would be adsorbed. The surface coverage is assumed to be 100%. Additionally, for each case three different grafting ratios are considered. These are the main parameters governing the steric hindrance by these polymers (Section 11.5). The examples illustrate that the side-chain length has a dominating effect. The grafting degree (C/E) has only a secondary and slightly detrimental effect on the interparticle force, but it has major importance in terms of adsorption, as noted in Chapter 10 (Marchon et al., 2016). Here we are considering situations in which enough polymers are present in the system to cover the surfaces of the particles fully.

From Figure 11.11 we note that the maximum attractive force is reached respectively for separation distances around 5.5 and 17 nm, which is very close to twice the layer thickness obtained with Eqn (11.14). This suggests that as soon as the layers start to overlap, the steric force overcomes the van der Waals attraction. In turn this would imply that the maximum attractive force could be evaluated by Eqn (11.4) using a separation distance of twice the layer thickness given in Eqn (11.14). A first test for this hypothesis is to plot the maximum attractive force determined in all the cases reported in Figure 11.11 versus the inverse square of the layer thickness R_{AC}. As shown in Figure 11.12, such data are well fitted by a linear regression passing through the origin. This demonstrates that the maximum attractive force does indeed

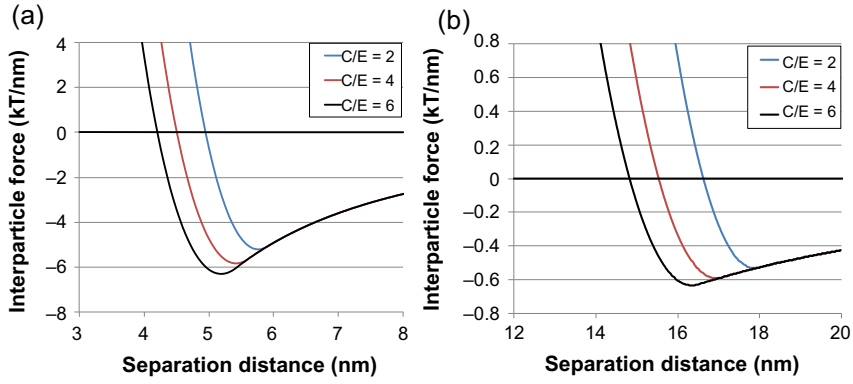


Figure 11.11 Interparticle force between cement particles with full coverage by PCEs having side-chains, respectively, of: (a) 1000 g/mol and (b) 5000 g/mol. In each case three carboxylate-to-ester (C/E) ratios are considered.

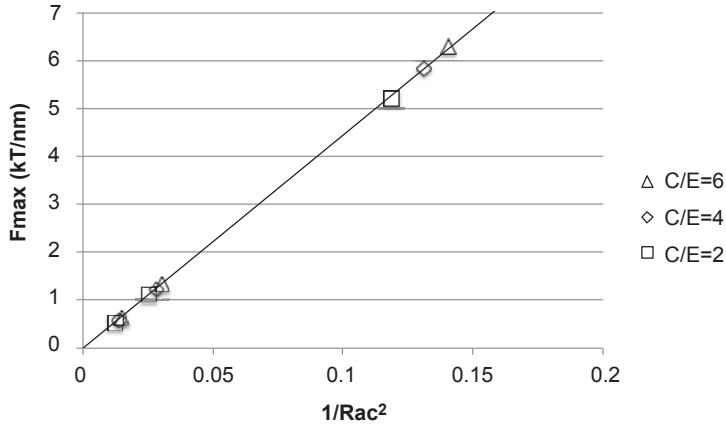


Figure 11.12 Maximum attractive interparticle force plotted versus the inverse square of the adsorbed layer thickness, R_{AC}. The three sets of points represent polymers with side chains of 1000, 3000 and 5000 g/mol with three different values of C/E. The straight line is a linear fit through the origin, demonstrating the scaling of the maximum attractive force with the inverse square of the layer thickness.

scale with the inverse second power of the layer thickness. The proportionality constant deviates, however, by about 40% from the one that would be derived from Eqn (11.4). This results from the various approximations leading to that equation. However, the scaling relation between force and layer thickness remains, which is very useful for comparing the dispersive power of PCEs at full surface coverage (Flatt and Schober, 2012; Kjeldsen et al., 2006).

The situation of incomplete surface coverage is more complex. As mentioned in Section 11.5, additional attractive forces can arise when the polymer does not completely cover the cement particle surface. The maximum attractive force at different surface coverage for a given PCE (side-chain molar mass = 1000 g/mol; C/E = 3) has been calculated with Hamaker 2 software (Aschauer et al., 2011). Results in Figure 11.13 (squares) show that the maximum attractive force remains more or less constant for surface coverage as low as 0.3. At surface coverage of 0.25 the potential barrier is in the order of few tens kT that corresponds to a metastable equilibrium: this situation is the same as that depicted in Figure 11.5 (curve B). At even lower surface coverage, the interparticle force jumps up and there is no effective stabilization due to the adsorbed polymers.

An average maximum attractive force can be calculated taking into account the statistical distribution of contact points between bare cement and polymer-coated particles (Kjeldsen et al., 2006):

$$F_{\max} \approx \left(\frac{\theta^2}{\delta_P^2} + 8\frac{\theta(1-\theta)}{(\delta_P + \delta_0)^2} + \frac{(1-\theta)^2}{\delta_0^2} \right) \tag{11.16}$$

where θ is the surface coverage, δ_P is the adsorbed layer thickness at full coverage and δ_0 is half the minimum separation distance between bare cement particles, taken equal to 0.8 nm (Perrot et al., 2012).

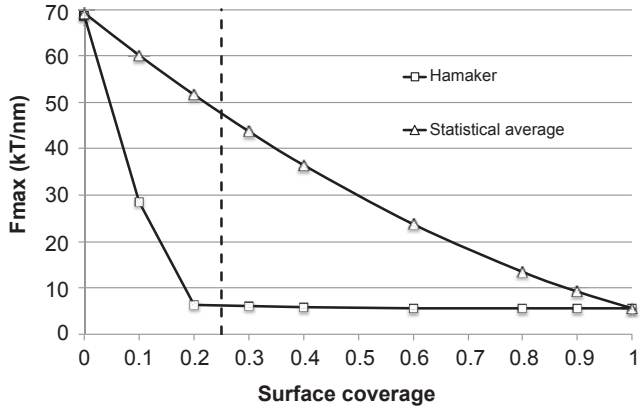


Figure 11.13 Maximum attractive force as a function of surface coverage for a PCE with structural parameters *P* and *N* equal to 23 and 4, respectively. The interparticle force is calculated by Hamaker 2.1 (squares) and by means of Eqn (11.16) (triangles).

An average layer thickness can be estimated from the values of the maximum attractive force calculated by Hamaker using Eqn (11.4). This average layer thickness is a function of the surface coverage, and is equal to δ_P and δ_0 for a surface coverage of one and zero, respectively. The maximum attractive force is calculated by using Eqn (11.16), and the average layer thickness at different surface coverage is shown in Figure 11.13.

Table 11.1 shows the contribution of the different interactions between contact points to the total maximum attractive force.

These data show that a statistical approach can be used for the calculation of the maximum attractive force at incomplete surface coverage up to a certain extent. When the interactions P−B and B−B become predominant over P−P, for $\theta \leq 0.6$, the maximum attractive force cannot be correctly evaluated. This means that the

Table 11.1 Contributions of the interaction between polymer-coated particles (P−P), polymer-coated and bare cement particles (P−B) and bare cement particles (B−B) to the maximum interparticle force at different surface coverage

Surface coverage	P−P	P−B	B−B
1.0	100%	0%	0%
0.8	26%	53%	21%
0.6	8%	45%	47%
0.4	2%	29%	68%
0.2	1%	21%	78%
0.1	0%	7%	93%
0.0	0%	0%	100%

scaling laws obtained for adsorbed polymers at full surface coverage can be extended to surface coverage as low as 0.6. To obtain consistent values of the maximum interparticle force, the equations describing the interactions between bare cement and polymer-coated particles need to be rederived.

11.7 Conclusions

Suspension stability can be expressed in terms of interparticle potential, and is controlled by the balance of attractive and repulsive terms. These notions can also be used in cementitious systems. In this case we do not compare an energy barrier to a multiple of thermal energy, but rather the maximum attractive force to the shear force between particles. More details about rheology of cement suspensions are given in Chapter 7 (Yahia et al., 2016).

A particularity of cement suspensions is their high ionic strength. This implies that it is very difficult to stabilize such systems by electrostatic repulsion. Cement research has a long history of attributing dispersion by early-generation SPs to electrostatic repulsion. The data presented in this chapter suggest that it is rather steric repulsion that must be considered at full surface coverage – the condition considered most favourable for these polymers, as explained in Chapter 16 (Nkinamubanzi et al., 2016).

PCE SPs are broadly accepted to act through steric hindrance. Here, however, another source of misinterpretation can be found in terms of the effectiveness of their molecular structure. Indeed, because these polymers are very effective, they are often used at lower dosages corresponding to incomplete surface coverage. Under those conditions the amount of adsorbed polymer plays a very important role, mostly overriding the molecular structure parameters determining layer thickness.

The conditions of incomplete surface coverage can in part be described by simplifications presented in this chapter. However, it has also been illustrated that these become unreliable at low surface coverage, so more advanced analysis of these situations seems to be needed.

Acknowledgements

We thank Dr Ulrich Johannes Aschauer (ETH Zurich) for implementing the model for comb-copolymer adsorption into the Hamaker software and for useful discussions.

Support for Giulia Gelardi was provided by SNF (Project No. 140615) titled ‘Mastering flow loss of cementitious systems’.

References

Andersen, P.J., Roy, D.M., Gaidis, J.M., 1987. The effects of adsorption of superplasticizers on the surface of cement. Cement and Concrete Research 17 (5), 805–813. http://dx.doi.org/10.1016/0008-8846(87)90043-3.

Aschauer, U., Burgos-Montes, O., Moreno, R., Bowen, P., 2011. Hamaker 2: a toolkit for the calculation of particle interactions and suspension stability and its application to mullite

synthesis by colloidal methods. Journal of Dispersion Science and Technology 32 (4), 470–479. http://dx.doi.org/10.1080/01932691003756738.

Banfill, P.F.G., 1979. Rheological properties of cement mixes – discussion. Cement and Concrete Research 9 (6), 795–796. http://dx.doi.org/10.1016/0008-8846(79)90075-9.

Daimon, M., Roy, D.M., 1979. Rheological properties of cement mixes: II. Zeta potential and preliminary viscosity studies. Cement and Concrete Research 9 (1), 103–109. http://dx.doi.org/10.1016/0008-8846(79)90100-5.

Derjaguin, B., Landau, L., 1993. Theory of the stability of strongly charged lyophobic sols and of the adhesion of strongly charged particles in solutions of electrolytes. Progress in Surface Science 43 (1–4), 30–59. http://dx.doi.org/10.1016/0079-6816(93)90013-L.

Ernsberger, F.M., France, W.G., 1945. Portland cement dispersion by adsorption of calcium lignosulfonate. Industrial and Engineering Chemistry 37 (6), 598–600. http://dx.doi.org/10.1021/ie50426a026.

Flatt, R.J., Ferraris, C.F., 2002. Acoustophoretic characterization of cement suspensions. Materials and Structures 35 (9), 541–549. http://dx.doi.org/10.1007/BF02483122.

Flatt, R.J., Houst, Y.F., Bowen, P., Hofmann, H., 2001. Electrosteric repulsion induced by superplasticizers between cement particles-an overlooked mechanism?. In: Malhotra, V.M. (Ed.), The Sixth Canmet/ACI Conference on Superplasticizers and Other Chemical Admixtures in Concrete, vol. 195, pp. 29–42.

Flatt, R., Schober, I., 2012. Superplasticizers and the rheology of concrete. In: Roussel, N. (Ed.), Understanding the Rheology of Concrete. Woodhead Publishing Series in Civil and Structural Engineering. Woodhead Publishing, pp. 144–208 (Chapter 7). http://www.sciencedirect.com/science/article/pii/B9780857090287500078.

Flatt, R.J., Bowen, P., 2003. Electrostatic repulsion between particles in cement suspensions: domain of validity of linearized Poisson–Boltzmann equation for nonideal electrolytes. Cement and Concrete Research 33 (6), 781–791. http://dx.doi.org/10.1016/S0008-8846(02)01059-1.

Flatt, R.J., Houst, Y.F., 2001. A simplified view on chemical effects perturbing the action of superplasticizers. Cement and Concrete Research 31 (8), 1169–1176. http://dx.doi.org/10.1016/S0008-8846(01)00534-8.

Flatt, R.J., 2004. Dispersion forces in cement suspensions. Cement and Concrete Research 34 (3), 399–408. http://dx.doi.org/10.1016/j.cemconres.2003.08.019.

Flatt, R.J., Bowen, P., 2006. Yodel: a yield stress model for suspensions. Journal of the American Ceramic Society 89 (4), 1244–1256. http://dx.doi.org/10.1111/j.1551-2916.2005.00888.x.

Flatt, R.J., Bowen, P., 2007. Yield stress of multimodal powder suspensions: an extension of the YODEL (Yield stress mODEL). Journal of the American Ceramic Society 90 (4), 1038–1044. http://dx.doi.org/10.1111/j.1551-2916.2007.01595.x.

Flatt, R.J., Schober, I., Raphael, E., Plassard, C., Lesniewska, E., 2009. Conformation of adsorbed comb copolymer dispersants. Langmuir 25 (2), 845–855. http://dx.doi.org/10.1021/la801410e.

de Gennes, P.G., 1987. Polymers at an interface; a simplified view. Advances in Colloid and Interface Science 27 (3–4), 189–209. http://dx.doi.org/10.1016/0001-8686(87)85003-0.

Gelardi, G., Mantellato, S., Marchon, D., Palacios, M., Eberhardt, A.B., Flatt, R.J., 2016. Chemistry of chemical admixtures. In: Science and Technology of Concrete Admixture (Chapter 9), pp. 149–218.

Hamaker, H.C., 1937. The London—van der Waals attraction between spherical particles. Physica 4 (10), 1058–1072. http://dx.doi.org/10.1016/S0031-8914(37)80203-7.

Kjeldsen, A.M., Flatt, R.J., Bergström, L., 2006. Relating the molecular structure of comb-type superplasticizers to the compression rheology of MgO suspensions. Cement and Concrete Research 36 (7), 1231–1239. http://dx.doi.org/10.1016/j.cemconres.2006.03.019.

Lesko, S., Lesniewska, E., Nonat, A., Mutin, J.C., Goudonnet, J.P., 2001. Investigation by atomic force microscopy of forces at the origin of cement cohesion. Ultramicroscopy 86 (1−2), 11−21. http://dx.doi.org/10.1016/S0304-3991(00)00091-7.

Lewis, J.A., Matsuyama, H., Kirby, G., Morissette, S., Young, J.F., 2000. Polyelectrolyte effects on the rheological properties of concentrated cement suspensions. Journal of the American Ceramic Society 83 (8), 1905−1913. http://dx.doi.org/10.1111/j.1151-2916.2000.tb01489.x.

Lifshitz, E.M., 1956. The theory of molecular attractive forces between solids. Soviet Physics JETP 2, 73−83.

Marchon, D., Mantellato, S., Eberhardt, A.B., Flatt, R.J., 2016. Adsorption of chemical admixtures. In: Aïtcin, P.-C., Flatt, R.J. (Eds.), Science and Technology of Concrete Admixtures, Elsevier (Chapter 10), pp. 219−256.

Nägele, E., 1985. The zeta-potential of cement. Cement and Concrete Research 15 (3), 453−462. http://dx.doi.org/10.1016/0008-8846(85)90118-8.

Nägele, E., 1986. The zeta-potential of cement: Part II: effect of pH-value. Cement and Concrete Research 16 (6), 853−863. http://dx.doi.org/10.1016/0008-8846(86)90008-6.

Nkinamubanzi, P.-C., Mantellato, S., Flatt, R.J., 2016. Superplasticizers in practice. In: Aïtcin, P.-C., Flatt, R.J. (Eds.), Science and Technology of Concrete Admixtures Elsevier (Chapter 16), pp. 353−378.

Palacios, M., Flatt, R.J., 2016. Working mechanism of viscosity-modifying admixtures. In: Aïtcin, P.-C., Flatt, R.J. (Eds.), Science and Technology of Concrete Admixtures, Elsevier (Chapter 20), pp. 415−432.

Palacios, M., Bowen, P., Kappl, M., Butt, H.J., Stuer, M., Pecharromán, C., Aschauer, U., Puertas, F., 2012. Repulsion forces of superplasticizers on ground granulated blast furnace slag in alkaline media, from AFM measurements to rheological properties. Materiales de Construcción 62 (308), 489−513. http://dx.doi.org/10.3989/mc.2012.01612.

Pedersen, H.G., Bergström, L., 1999. Forces measured between zirconia surfaces in poly(acrylic acid) solutions. Journal of the American Ceramic Society 82 (5), 1137−1145. http://dx.doi.org/10.1111/j.1151-2916.1999.tb01887.x.

Pellenq, R.J.-M., Caillol, J.M., Delville, A., 1997. Electrostatic attraction between two charged surfaces: a (N, V, T) Monte Carlo simulation. The Journal of Physical Chemistry B 101 (42), 8584−8594. http://dx.doi.org/10.1021/jp971273s.

Perrot, A., Lecompte, T., Khelifi, H., Brumaud, C., Hot, J., Roussel, N., 2012. Yield stress and bleeding of fresh cement pastes. Cement and Concrete Research 42 (7), 937−944. http://dx.doi.org/10.1016/j.cemconres.2012.03.015.

Plank, J., Winter, C., 2008. Competitive adsorption between superplasticizer and retarder molecules on mineral binder surface. Cement and Concrete Research 38 (5), 599−605. http://dx.doi.org/10.1016/j.cemconres.2007.12.003.

Plank, J., Sachsenhauser, B., 2006. Impact of molecular structure on zeta potential and adsorbed conformation of α-allyl-ω-methoxypolyethylene glycol − maleic anhydride superplasticizers. Journal of Advanced Concrete Technology 4 (2), 233−239.

Russel, W.B., Saville, D.A., Schowalter, W.R., 1992. Colloidal Dispersions. Cambridge University Press.

Uchikawa, H., Hanehara, S., Sawaki, D., 1997. The role of steric repulsive force in the dispersion of cement particles in fresh paste prepared with organic admixture. Cement and Concrete Research 27 (1), 37−50. http://dx.doi.org/10.1016/S0008-8846(96)00207-4.

Verwey, E.J.W., Overbeek, J.Th.G., Overbeek, J.T.G., 1999. Theory of the Stability of Lyophobic Colloids. Courier Dover Publications.

Yahia, A., Flatt, R.J., Mantellato, S., 2016. Concrete rheology: A basis for understanding chemical admixtures. In: Aïtcin, P-C., Flatt, R.J. (Eds.), Science and Technology of Concrete Admixtures Elsevier. (Chapter 7), pp. 97−128.

Yang, M., Neubauer, C.M., Jennings, H.M., 1997. Interparticle potential and sedimentation behavior of cement suspensions: review and results from paste. Advanced Cement Based Materials 5 (1), 1−7. http://dx.doi.org/10.1016/S1065-7355(97)90009-2.

Yoshioka, K., Sakai, E., Daimon, M., Kitahara, A., 1997. Role of steric hindrance in the performance of superplasticizers for concrete. Journal of the American Ceramic Society 80 (10), 2667−2671. http://dx.doi.org/10.1111/j.1151-2916.1997.tb03169.x.

Zhou, Z., Scales, P.J., Boger, D.V., 2001. Chemical and physical control of the rheology of concentrated metal oxide suspensions. Chemical Engineering Science NEPTIS 8, 56 (9), 2901−2920. http://dx.doi.org/10.1016/S0009-2509(00)00473-5.

Zhou, Z., Solomon, M.J., Scales, P.J., Boger, D.V., 1999. The yield stress of concentrated flocculated suspensions of size distributed particles. Journal of Rheology (1978-Present) 43 (3), 651−671. http://dx.doi.org/10.1122/1.551029.

Impact of chemical admixtures on cement hydration

12

D. Marchon, R.J. Flatt
Institute for Building Materials, ETH Zürich, Zurich, Switzerland

12.1 Introduction

Many chemical admixtures are known to retard cement hydration. In the case of retarders, this is an intentional effect. However, for many other admixtures, it is mostly an undesired side effect. Examples of the use of retarders as well as undesired retardation are given in Chapters 16 and 18 (Nkinamubanzi et al., 2016; Aïtcin, 2016b). The basics on cement hydration have been presented in Chapters 3 and 8 (Aïtcin, 2016a; Marchon and Flatt, 2016). We will in particular refer to the mechanisms of the hydration of different phases from Chapter 8 to discuss in this chapter the impact of chemical admixtures on hydration (Marchon and Flatt, 2016).

In the first part of this chapter, we deal in a general way with the mechanisms that affect hydration in order to encompass the behavior of most chemical admixtures (Section 12.2). However, most examples given are related to superplasticizers because this represents the main focus of this chapter. We have decided to do this because retardation is mostly an undesired effect with superplasticizers, and we believe that its consequences will be increasingly problematic in cements with reduced clinker contents. Also, because of the importance of polycarboxylate ether (PCE) superplasticizers (see Chapter 9: Gelardi et al., 2016) and the flexibility in their molecular design, we devote a special section to presenting information available in the literature concerning their impact on hydration (Section 12.3). Finally, sugars (and carbohydrates more generally) are detailed in the final section because they are the most used set retarders and important steps have been made in studying their impact on retardation. Additionally, they also offer a large variety of possible molecular structures and therefore design flexibility (see also Chapter 9: Gelardi et al., 2016).

In general, retardation by chemical admixtures depends not only on their dosage, chemical nature, molecular architecture, and the time of admixture addition (Figure 12.1), but also on the characteristics of the cement, such as its mineralogical composition, fineness, and sulfate availability. Additionally, as mentioned in Chapter 15 (Mantellato et al., 2016), commercial admixtures are often formulated products that can contain multiple components. For example, in addition to polymeric dispersants, commercial superplasticizers may also contain defoamers, accelerators, and viscosity-modifying admixtures, all of which can modify the extent of retardation.

In calorimetric measurements, retardation typically prolongs the induction period. However, the effect on hydration is not always only to delay the onset of the main hydration peak. For example, chemical admixtures can also change the

Science and Technology of Concrete Admixtures. http://dx.doi.org/10.1016/B978-0-08-100693-1.00012-6
Copyright © 2016 Elsevier Ltd. All rights reserved.

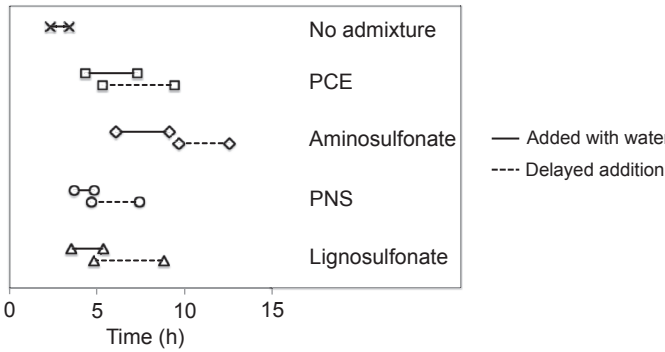


Figure 12.1 Illustration of the effect of addition time on setting times (initial and final) of normal Portland cement for different admixtures.
Adapted from Hanehara and Yamada (1999).

slope of the acceleration period, as well as the maximum heat release (i.e., the height of the main peak) and/or displace the sulfate depletion peak. Such changes can lead to a totally different calorimetric signature of the hydration process, as illustrated in Figure 12.2 for two different superplasticizers and in Figure 12.3 for different dosages of glucose used as set retarders for Portland cement. This implies that complex interactions between chemical admixtures and cement are taking place during hydration and that they can substantially modify the rates of the dissolution, nucleation and/or growth of various phases. These changes may also modify the nature of the step that is rate limiting for cement hydration, something addressed later in this chapter.

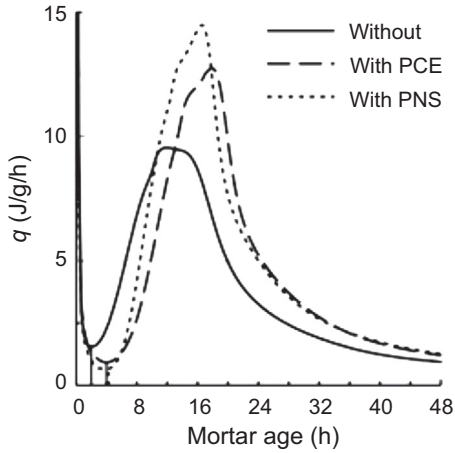


Figure 12.2 Example of isothermal calorimetry showing the effect of a PCE and polynaphtalene sulfonate (PNS) superplasticizer on a mortar with normal Portland cement. The difference in the shapes of the curve is particularly noted.
Reproduced from Robeyst et al. (2011) with permission.

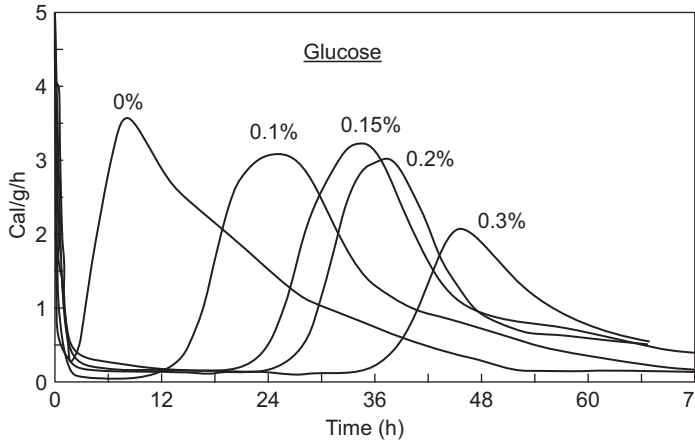


Figure 12.3 Effect of different dosages of glucose on the hydration of Portland cement. Reproduced from Ramachandran and Lowery (1992) with permission.

12.2 Mechanisms of retardation

The previous examples illustrate how a set of admixtures, differing in chemical nature and molecular structure, impact cement hydration in various ways. Although they are the subject of many studies, the mechanisms through which they modify hydration remain unclear (Cheung et al., 2011; Bishop and Barron, 2006). The different hypotheses that have been formulated to explain this include the following:

- Complexation of calcium ions
- Slowing down of dissolution of anhydrous phases
- Disrupting nucleation of hydrates
- Perturbation of the aluminate−silicate−sulfate balance

Each of these situations is discussed in a separate subsection.

12.2.1 Complexation of calcium ions in solution

Chemical admixtures interact with ionic species in solution (in particular calcium ion), and this may slow down the building up of the supersaturation needed for hydrates nucleation. It is well known that in a *clean* system (i.e., pure solution of polymers with generally one type of salt), organic admixtures can form complexes with ions in different ways, and that their stability depends on the nature of the chemical function, the metallic ion involved, as well as the environmental conditions (Smith et al., 2003).

In the case of PCE superplasticizers, a first mode of interaction, mentioned in several studies about interactions between polyoxyethylene and cations (Heeb et al., 2009; Tasaki, 1999; Masuda and Nakanishi, 2002), is similar to the ion complexation by crown ethers, where the cation is immobilized inside the polyether ring through ion−dipole interactions with ether oxygen atoms. The second type of possible complexation of PCEs has been mentioned by Plank and Sachsenhauser (2009).

In this case, the carboxylate functions of the backbone form a mono- or bidentate ligand with Ca ions, depending on the ionic charge density on the backbone.

Different studies show evidence of a formation of complexes between highly charged carboxylate polymers and Ca ions during either C_3S hydration (Comparet, 2004) or C−S−H nucleation (Picker, 2013). However, the amount of calcium mobilized by such complexes is limited by the low dosage of retarding molecules introduced in the system and the number of charges really involved in the complexing phenomenon. In addition, the complexation stability in solution of PCEs and other admixtures, such as phosphonates or sugars, which also present substantial chelating ability, are too low to significantly impact the calcium concentration and explain the cases of significant retardation (Comparet, 2004; Lothenbach et al., 2007; Richter and Winkler, 1987; Popov et al., 2009; Young, 1972). Furthermore, as Thomas and Birchall (1983) mentioned in the case of sugars (where, for example, the most retarding ones have the lowest binding ability), no direct correspondence has been found between the complexation ability and the retarding effect. Although relatively simple, this argument seems to provide a reasonable ground to disregard the role of calcium complexation on the retardation of cement hydration, at least until further evidence is brought to this debate.

12.2.2 Inhibition of the dissolution of anhydrous phases

Chemical admixtures may act on dissolution of anhydrous phases through adsorption, reducing the rate of ion release into solution. By electric conductivity measurements, Comparet (2004) observed that PCE superplasticizers delay the increase of conductivity coming from the dissolution of the anhydrous C_3S and the free growth of C−S−H. He concluded that PCEs strongly slow down C_3S dissolution with a probable additional effect on growth of hydrates, even blocking it for the polymers with the highest charge density. This is confirmed by Nicoleau (2004) and Pourchet et al. (2007), who showed that latexes composed of a core copolymer of styrene and butadiene with carboxylate groups on the surface slow down strongly the silicate dissolution after adsorption (Figure 12.4). This conclusion was reached on the basis of measuring the concentration of calcium and silicon by inductively coupled plasma optical emission spectrometry (ICP-OES) measurements during the dissolution of C_3S in a very diluted lime-saturated solution containing the latexes.

It is worth noting that, in both cases, the experiments were performed in lime-saturated and very diluted systems with a high admixture dosage, which are not representative of the real conditions in early-age hydration of cement paste. However, the results show clearly that carboxylate additives can strongly decrease the dissolution rate of C_3S as well as the primary C−S−H nucleation, which leads us to the next hypothesis. However, we must first also mention the fact that admixtures may slow down dissolution by hindering the opening of etch pits (Suraneni and Flatt, 2015b). Such a situation would probably shift the main hydration peak backwards, in a way compatible with retardation observed with PCEs. The possible impact of admixtures on the opening of etch pits has also been emphasized recently considering that a large fraction of etch pits may open during the course of hydration and that the frequency of their opening could be reduced by chemical admixtures (Nicoleau and Bertolim, 2015).

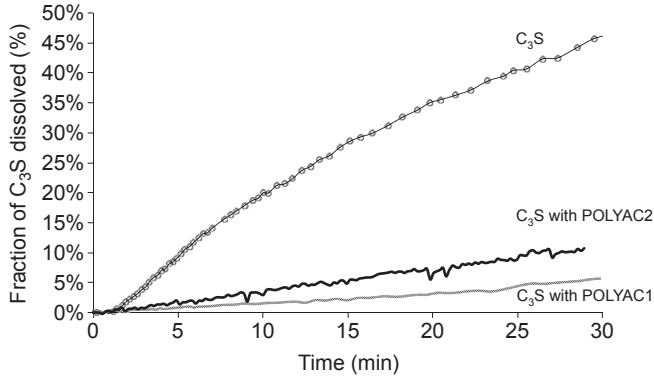


Figure 12.4 Dissolution of 1.5 mg of C_3S in 200 mL of 11 mmol/L lime-saturated solution in the presence of 0.4 g of two carboxylated latexes, POLYAC1 and POLYAC2. These latexes are composed of a core copolymer of styrene and butadiene with carboxylate groups on the surface. Adapted from Nicoleau (2004) with permission.

12.2.3 Inhibition of nucleation and/or growth of hydrates

Chemical admixtures can influence and modify nucleation and growth of minerals (Griffin et al., 1999; Fricke et al., 2006). In the case of C_3S and cement hydration, several studies have implied that chemical admixtures act on precipitation and growth of hydrates, interfering with them in various ways. These may include the poisoning of nuclei or the prevention of growth through adsorption onto nuclei or particles (Picker, 2013; Thomas and Birchall, 1983; Garci Juenger and Jennings, 2002), the alteration of dissolution kinetics due to the dispersive effect of superplasticizers (Ridi et al., 2003, 2012; Sowoidnich and Rössler, 2009), the blocking of the normally favored crystal growth directions, etc. To illustrate the first case, several studies (Thomas and Birchall, 1983; Garci Juenger and Jennings, 2002) have suggested that the retardation ability of sucrose comes from the poisoning of portlandite nucleation (this is further addressed in Section 12.4). If portlandite precipitation is suppressed, C_3S dissolution cannot be resumed, as the degree of saturation of the solution does not change, which does not allow C−S−H precipitation and leads to the prolongation of the induction period (Bullard and Flatt, 2010).

In the case of PCE superplasticizers, as a model system for studying the effect of such polymers on the precipitation of cement hydrates, several studies have dealt with the precipitation of $CaCO_3$ in the presence of linear and comb-shaped polycarboxylates (Rieger et al., 2000; Falini et al., 2007; Keller and Plank, 2013). In a first study, Rieger et al. (2000) showed that amorphous $CaCO_3$ precursors, which normally dissolve and recrystallize as calcite, are fixed in a network consisting of linear carboxylate chains bridged by Ca^{2+}, avoiding the dissolution of the precursors and their recrystallization. Falini et al. (2007) mentioned that carboxylate admixtures not only inhibit $CaCO_3$ precipitation in the case of high dosages but also modify the growth, size, and morphology of the crystals, depending on the length and density of the side chains. This has also been confirmed by Keller and Plank (2013), who mentioned that $CaCO_3$ nuclei are distributed along the polymer backbone through complexation of Ca ions by the

carboxylic groups. In this case, the authors concluded that, in the presence of PCEs, mesocrystals form via self-assembly of the PCE-stabilized initial calcite nanocrystals.

A similar mechanism occurring during C−S−H precipitation and involving the calcium ions could explain the delay of C_3S hydration. Indeed, it has been proposed that, during the first step of C−S−H nucleation, Ca ions trigger the oligomerization of the silicates and bridge these oligomers to form larger agglomerates (Picker, 2013). In the presence of PCEs, hydrate precursors could be adsorbed to negatively charged sites on the polymer via Ca^{2+} bridging and thus be stabilized against agglomeration, which would penalize C−S−H nucleation. This has been suggested by Picker (2013), who used calcium titration to study the effect of highly charged polyacrylate acid chains on the nucleation of C−S−H from a solution of Na_2SiO_3 and $CaCl_2$. His results show that, first, the polymer modifies the prenucleation slope (point 1 in Figure 12.5), indicating a change of interaction between the calcium and the silicate species. Then, the first nucleation point (point 2) is delayed and occurs at higher supersaturation. The primary particles are probably stabilized by the polymer but cannot assimilate all the additional Ca ions (point 3). Then, the calcium potential drops, indicating a secondary formation of C−S−H particles via a possible heterogeneous nucleation process on primary formed nuclei (point 4).

This last study offers useful insight into possible reasons for the retardation of cement hydration. However, it only targeted C−S−H precipitation in pure conditions and does not explain why, with a common dosage of PCEs (containing a concentration

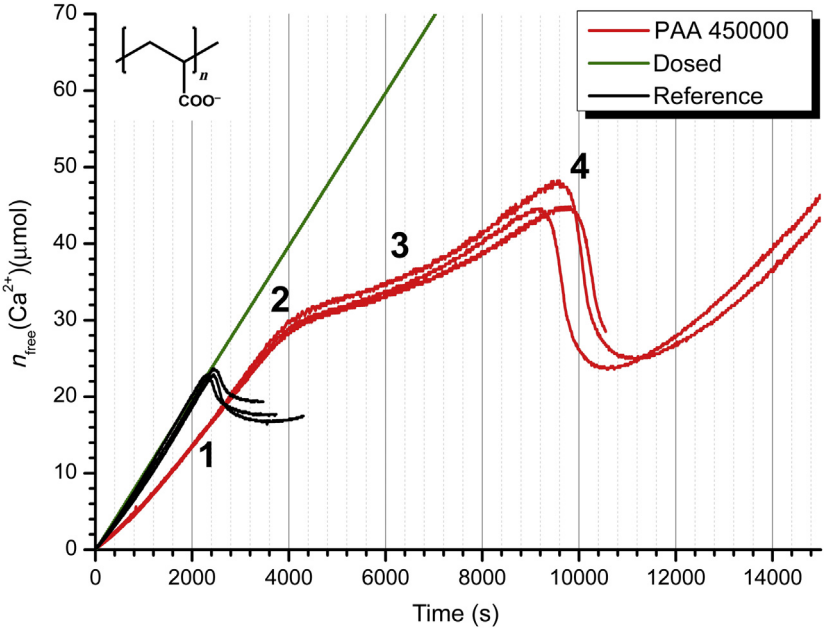


Figure 12.5 Evolution of free Ca^{2+} during addition of $CaCl_2$ solution into Na_2SiO_3 in absence (reference) and in presence of a highly charged polyacrylate (PAA 450000).
Reproduced from Picker (2013) with authorization.

of carboxylate groups much lower than in that study), the delay can increase up to hours, if not days, in superplasticized cement pastes where a part of the molecules can adsorb not only on C−S−H but also on other hydrates as well as anhydrous phases. In short, it is our opinion that the multicomponent nature of the cement cannot be neglected. This leads us to the last hypothesis concerning retardation.

12.2.4 Perturbation of the silicate−aluminate−sulfate balance

Superplasticizers can cause a drastic delay by perturbing the aluminate−silicate−sulfate balance. In contrast to most of the other mechanisms, this process is considered to be particularly difficult to predict (Cheung et al., 2011), which probably comes from an expected nonlinear dependence on the polymer dosage. It can also appear suddenly in cements having apparently similar compositions to others in which retardation is not problematic.

In our opinion, when it occurs, this mechanism of retardation is one of the most problematic because it can create a highly nonlinear and therefore nonpredictable increase in retardation. It is also one of the least well-studied and least well-understood processes. For this reason, we dedicate a certain effort in presenting the current state-of-the-art on the subject in order to expose the various mechanisms proposed to explain its occurrence.

As a basis for this mode of retardation, we can state that an additional level of complexity is added when the main cement phases, silicates, aluminates, and sulfates are taken into account simultaneously. This is not negligible in light of the fact that superplasticizer adsorption is not the same on all phases, as described in Chapter 10 (Marchon et al., 2016). Therefore, although studies performed on pure C_3S with superplasticizers are useful to understand their impact on fundamental mechanisms, data on the behavior of admixtures in systems containing silicates, aluminates, and sulfates are needed to better understand the massive retardation that can occasionally arise in such cases (Marchon et al., 2014). This requires studying the importance of the balance between silicates, aluminates, and sulfates, as explained in Chapter 8 and illustrated by the works of Lerch (1946) or Tenoutasse (1968). As for these works, studying the effect of superplasticizers on a cement model (Marchon et al., 2014) rather than on Portland cement allows one to separate the influence of important parameters that cannot be differentiated and controlled in normal Portland cement, such as the amount and type of alkalis and sulfate carriers.

Adding superplasticizers in such coupled chemical systems makes for a complex and challenging topic. Indeed, in addition to the noticeable delay of C_3S hydration, whose dependence with aluminates reactions has been discussed in Chapter 8 (Marchon and Flatt, 2016), water reducers and superplasticizers can modify the interaction between the aluminates and the sulfates. Evidence has shown that they disturb aluminates reaction by perturbing, for example, ettringite formation or the transition to monosulfoaluminate (Comparet, 2004; Young, 1972; Collepardi, 1996; Prince et al., 2003; Roncero et al., 2002; Chen and Struble, 2011; Prince et al., 2002). An important feature of many of these studies is that the C_3A hydration consumes a part of the added chemical admixture, for example either by increasing the specific surface or intercalating the admixtures in organomineral phases (see Chapter 10: Marchon et al., 2016).

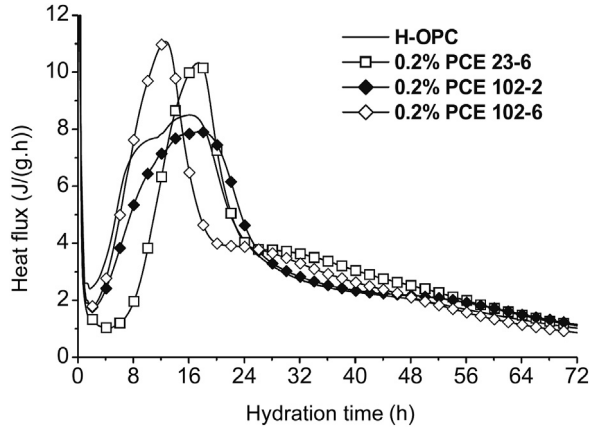


Figure 12.6 Isothermal calorimetry on cement paste containing different types of PCEs. The first number gives the number of ethylene oxide (EO) units in the side chains, while the second gives the grafting ratio.
Reproduced from Zingg et al. (2009) with permission.

The perturbation of the balance between the main phases during cement hydration illustrates itself by a change in the shape and the occurrence time of the so-called sulfate depletion peak. This can be observed for example in a study about the interaction of PCEs with cements containing different C_3A amounts (Zingg et al., 2009) where the strongest impact on the sulfate depletion peak occurs in the cement with the highest content of C_3A. In particular, as shown in the example of Figure 12.6, in the presence of the PCE with the highest charge density (PCE 23-6), it is no longer possible to distinguish between the main hydration peak and the sulfate depletion one.

This has also been observed in other studies (Lothenbach et al., 2007; Jansen et al., 2012; Winnefeld et al., 2009; Sandberg et al., 2007) where, in the presence of superplasticizers, the sulfate depletion peak seems to be shifted to earlier times with respect to silicate hydration. The merging of both peaks results in a narrower main peak and a change in the maximum of the heat release. This change in the heat release would imply that there is either a faster consumption of sulfates or a change in their availability. Indeed, as mentioned above, studies focused on the effect of superplasticizers on aluminate reactions in cement have shown that admixtures can affect ettringite precipitation (Comparet, 2004; Young, 1972; Collepardi, 1996; Prince et al., 2003; Roncero et al., 2002; Chen and Struble, 2011; Prince et al., 2002; Jansen et al., 2012; Rössler et al., 2007; Jiang et al., 2012) and consequently reactions involving sulfates. Various mechanisms have been proposed to explain this, as summarized below.

1. A first hypothesis would be that the adsorption of PCEs on the sulfate carriers hinders or slows down its dissolution (Rössler et al., 2007). The rate of sulfate supply can therefore no longer keep C_3A dissolution under control, creating a type of false set, which could also be called a "false" sulfate depletion point (the system behaves as if no more sulfates were available, while they are still present in their unreacted form).

2. A second explanation proposed is that the better dispersion of the anhydrous particles in the presence of PCEs enhances the dissolution of C_3A, leading to faster sulfate consumption (Jansen et al., 2012). An observation favoring this interpretation is that ettringite precipitation tends to be enhanced in the presence of PCEs (Jansen et al., 2012; Jiang et al., 2012).
3. However, the enhanced precipitation of ettringite mainly occurs in the first minutes of hydration, which leads us to the third hypothesis that PCEs would enhance ettringite nucleation (Comparet, 2004). This would provide a large surface area for growth, leading to a faster consumption of sulfates and thus to an earlier true sulfate depletion point. Although this increase of ettringite has been observed several times, the reasons for that are not well understood.

It should also be finally noted that any of the above mechanisms may result in a modification of ettringite morphology in the presence of PCEs. For example, the adsorption of molecules on ettringite may either hinder further growth or affect the growth rate of specific crystallographic planes (Rössler et al., 2007; Eusebio et al., 2011). Additionally, PCE adsorption on nuclei would change the saturation degree and consequently the nucleation rate of ettringite (Comparet, 2004). Beyond these rather general statements, there does not appear to be a clearer picture in the literature regarding the way in which PCEs modify the morphology of ettringite in relation to their dosage and/or molecular structure.

As mentioned above, the cases in which chemical admixtures cause a massive silicate retardation by perturbing the aluminate−silicate−sulfate balance are a very problematic situation, although not a very frequent one. This does not mean, however, that the interaction of chemical admixtures and the aluminate phases can be neglected. Indeed, it has been shown that the content of C_3A and alkalis in cement has an important effect on retardation in the presence of superplasticizers (Zingg et al., 2009; Winnefeld et al., 2007b; Regnaud et al., 2011). In these studies, the authors pointed out that the strong adsorption of PCEs on aluminates reduces the amount of PCEs that remain available to delay the C_3S hydration. This means that, for a given dosage, cements with a higher content of aluminates should suffer less retardation of the silicate peak. In this context, the challenge is to determine the proportion of polymers interacting with aluminates and in which way the molecular structure controls this. To the best of our knowledge, this remains an important challenge for research on the subject.

12.3 Retardation by superplasticizers

Comparative studies (Hanehara and Yamada, 1999; Robeyst and De Belie, 2009; Comparet, 2004; Wang et al., 2009) show that, at equal dosages, among all the superplasticizers, PCEs tend to be the most retarding (with the exception of lignosulfonates[1]). As explained above, this retardation is believed to originate from the adsorption of PCEs on one of the phases in the system (reactant or product).

[1] Lignosulfonates are rather to be considered as midrange water reducers. Taken alone, they can induce substantial retardation. This can be incremented by residual sugars. The effect of sugars on hydration will be addressed in Section 12.4. For a review on past literature relating to lignosulfonates and retardation, readers are referred to Collepardi (1996).

Qualitatively, we can expect that the same molecular structure features will affect adsorption on all these phases, although the extent of adsorption should differ. If this is the case, we can benefit from adsorption studies performed at an early age in the context of the study of the rheological performance of superplasticizers in relation to their molecular structure.

12.3.1 Role of the molecular architecture of PCE superplasticizers

As explained above, the extent of adsorption is one of the most important parameters for the dispersive effect of superplasticizers (see also Chapters 10 and 11 for more extensive treatment of this: Marchon et al., 2016; Gelardi and Flatt, 2016). In the case of PCEs, adsorption is mostly influenced by the length of the backbone and the side chains as well as by the grafting density (Marchon et al., 2013). Winnefeld et al. (2007b) showed that a higher charge density of the polymer (number of charges per unit mass) leads to a higher consumption of the polymer (i.e., better adsorption) and to a lower yield stress of the superplasticized cement paste (i.e., better dispersion), as shown in Figure 12.7. In the same study, the authors showed that the polymers that adsorb most extensively (those with the highest charge density)

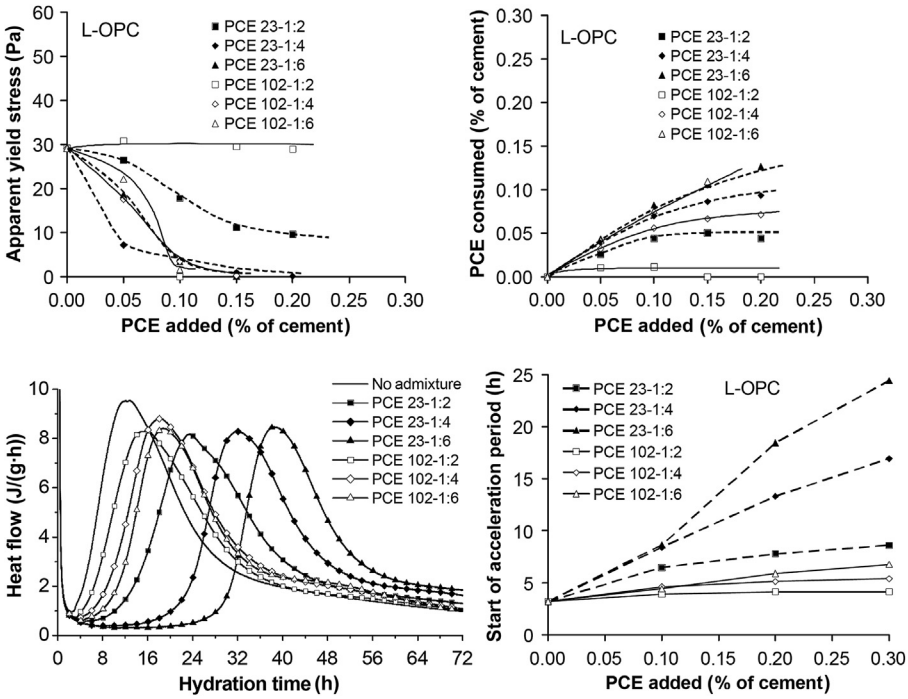


Figure 12.7 Impact of polymethacrylate molecular structure on yield stress (top left), adsorption (top right), isothermal calorimetry (bottom left), and start of the acceleration period (bottom right) of an ordinary Portland cement.
Reproduced from Winnefeld et al. (2007b) with permission.

induce the longest induction period and the latest start of the acceleration period (experiments performed with a 0.3% dosage of each polymer).

Concerning the relative influence of the length of the side chains and the grafting density, several studies (Comparet, 2004; Pourchet et al., 2007; Winnefeld et al., 2007a,b; Yamada et al., 2000) show that shorter side chains with a constant carboxylate to ether (*C/E*) ratio as well as an increasing *C/E* ratio with constant side chain length lead to an increase of the retarding effect. This is not surprising as, in both cases, the density of carboxylate functions by weight of polymer increases, leading to a more effective adsorption and probably longer retardation. In this regard, it would make sense to express the polymer dosage either as a function of the number of carboxylic groups introduced or of the concentration of carboxylate groups per molecule rather than a mass percentage of polymer with respect to cement (Kirby and Lewis, 2004; Moratti et al., 2011). However, adsorption is a complex process that depends on nontrivial combinations of molecular structure parameters so that single-variable explanations are rather unlikely to be successful. In contrast combinations thereof relating to, for example, adsorption energy may have a greater chance of success (Marchon et al., 2013).

12.3.2 Role of the chemical composition

Besides the molecular architecture of the PCEs, the nature of the monomers in the backbone and with/without the side chains is also important. For example, it has been observed that a polymer composed of backbones with methacrylate monomers without side chains shows the highest impact on cement hydration, as is expected from a polymer with the highest possible charge density (Winnefeld et al., 2007a; Middendorf and Singh, 2007).

However, Eusebio et al. (2011) showed that a backbone only composed of polyacrylate acid monomers does not influence the hydration of C_3S. It is tempting to explain this difference by the precipitation of a poorly soluble calcium salt of polyacrylic acid that would prevent this polymer from negatively impacting cement hydration. However, similar differences between acrylate- and methacrylate-based PCEs have also been reported for PCEs that are much more soluble than their pure backbones (Borget et al., 2005).

Regnaud et al. (2011) studied the hydration of Portland cements with different alkali and tricalcium aluminate contents in presence of different acrylate- and methacrylate-based PCEs. They reported that the delay caused by the methacrylate-based PCEs depends on the amount of initially adsorbed polymers, while the retardation caused by the acrylate-based PCEs depends on the amount of polymer remaining in the pore solution. They concluded that, in the first case, the adsorbed methacrylate-based PCEs act on the initial C_3S dissolution, while in the second case, the nonadsorbed acrylate-based PCEs act mainly on nucleation of C−S−H. However, they do observe differences in behavior between both polymers when the level of alkalis or the amount of C_3A is changed.

At this point in time, it is worth recalling that acrylate-based PCEs undergo a progressive cleavage of their side chains in alkaline media, while those of methacrylates are much more stable (see Chapter 9: Gelardi et al., 2016). While this can be beneficial

in terms of formulation to control the flow retention (see Chapter 15: Mantellato et al., 2016), it poses problems when studying the impact that the PCEs with an acrylic backbone have on hydration. Indeed, their ionic charge increases over time, which must certainly affect their adsorption and impact on hydration.

12.4 Retardation by sugars

12.4.1 Overview

Sugars are well known to be powerful retarders. However, there are substantial differences between them, with some even not retarding concrete hardening at all. This subject has intrigued researchers for decades and has been the object of many publications. Work on this subject prior to 1990 has been extensively summarized by Collepardi (1996).

Concerning early studies on the subject, we encourage readers to consult the milestone paper of Thomas and Birchall (1983) on the role of molecular structure of sugars on retardation and the very insightful review by Young (1972) on the subject. In this section, we summarize some important features in the light of recent developments on the subject. In particular, we attempt to give insight on the role of the molecular structure of sugars on the extent of retardation. While in this section we examine more the physico-chemical aspects, readers wanting to look up details on the chemical structure of sugars can consult the dedicated section in Chapter 9 (Gelardi et al., 2016).

12.4.2 General observations

It is often observed that many retarders delay the onset of the acceleration period. However, the rate in this period is then higher than the reference. This has led sugars and other products having the same effect to be referred to as "delayed accelerators" (Young, 1972; Milestone, 1979). Specifically for sugars, this has been reported for a wide range of aliphatic sugars (Zhang et al., 2010). However, as explained in the previous section, this is generally not observed with polycarboxylate-based superplasticizers, at least at low dosages.

It is also observed that long-term properties such as strength are not detrimentally affected by the addition of sugars (provided enough time is given for hydration to reach similar extents as the reference) (Zhang et al., 2010). Some reports mention minor strength increases, but we are not aware of studies dealing with durability. This may be a subject worth looking into, because sugars (and retarders in general) tend to promote growth from the bulk rather than from the surface of cement grains. As for seeding (see Chapter 8: Marchon and Flatt, 2016), this should in principle promote a more efficient closing of capillary pores.

Most comparative studies involving different sugars tend to conclude that sucrose is the most effective retarder (Thomas and Birchall, 1983; Zhang et al., 2010; Smith et al., 2012). Differences among sugars can be very substantial and the reasons for this are discussed below.

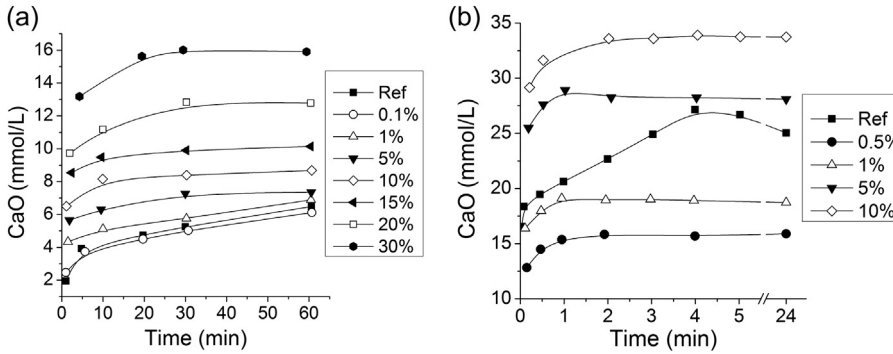


Figure 12.8 Evolution of the concentration of CaO in suspensions of C_3S with varying additions of sucrose. (a) One gram C_3S per liter of solution with 0%, 0.1%, 1%, 5%, 10%, 15%, 20%, and 30% sucrose. (b) Fifteen grams C_3S per liter of solution with 0%, 0.5%, 1%, 5%, and 10% sucrose.
Adapted from Andreeva et al. (1980).

Finally, concerning the effect of sugars on the aqueous phase composition, all publications report an increase in the aluminum and silicon concentrations (Thomas and Birchall, 1983; Luke and Luke, 2000). However, there is some discrepancy concerning calcium. Most papers report that it increases in the presence of sucrose (Thomas and Birchall, 1983; Luke and Luke, 2000), but Luke and Luke (2000) measured the opposite. Most likely, this results from different solid-to-liquid ratios (Luke and Luke, 2000 used pastes while most others used dilute suspensions). Indeed, as illustrated in Figure 12.8, dilute suspensions show a continuous increase in calcium concentration, both with time and with sucrose concentration (Figure 12.8(a)). In the more concentrated case (Figure 12.8(b)), the suspension without sucrose shows the expected calcium concentration peak corresponding to portlandite nucleation, with the maximum around 25 mM. In the presence of the lowest amounts of sucrose, this concentration is much lower, at about 15 mM—clearly below the saturation level of portlandite. This must indicate that dissolution is hindered. However, as the sucrose concentration is increased, the calcium concentration also increases, eventually surpassing that of the suspension without sucrose. As explained in Section 12.4.5.1, this probably results from changes in pH. The effect that sugars have on hydration is therefore dependent on the solid-to-liquid ratio, and care must be taken when doing a comparative study of the literature.

12.4.3 Role of molecular structure

Thomas and Birchall (1983) classified sugars studied in the literature for their retarding capacity into three different categories (Table 12.1). The molecular structures of the corresponding reducing and nonreducing sugars are given, respectively, in Figures 12.9 and 12.10.

Zhang et al. (2010) studied the retarding effect of various short linear saccharides covering various stereoisomers and chain lengths. The molecules used and the retardation

Table 12.1 Classification of the retarding capacity of carbohydrates as given by Thomas and Birchall (1983)

Nonretarding	Good retarders	Excellent retarders
α-Methyl glucoside[b] Thehalose[b]	Glucose[a] Maltose[a] Lactose[a] Cellobiose[a]	Sucrose[b] Raffinose[b]

[a]Reducing sugar.
[b]Nonreducing.

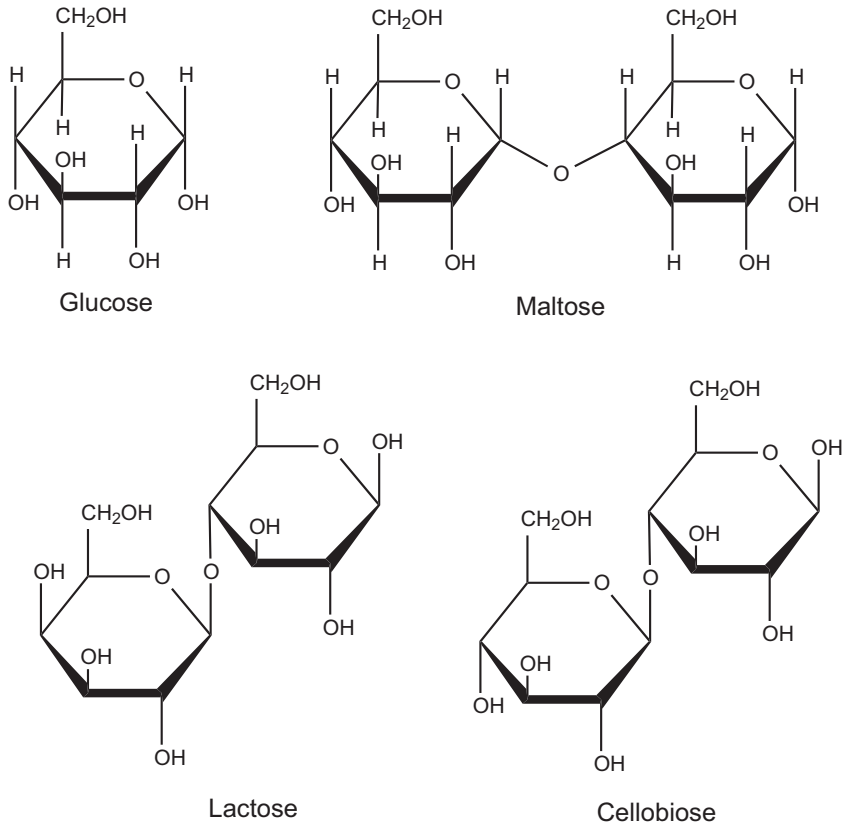


Figure 12.9 Molecular structure of the reducing sugars studied in Thomas and Birchall (1983).

times they obtained for different dosages are reported in Table 12.2. A graphical illustration of how the extent of reaction of C_3S is affected over time is given in Figure 12.11.

In terms of the impact of the molecular structure on retardation, it was concluded that aliphatic sugar alcohols, which contain threo-dihydroxy functionality, retard

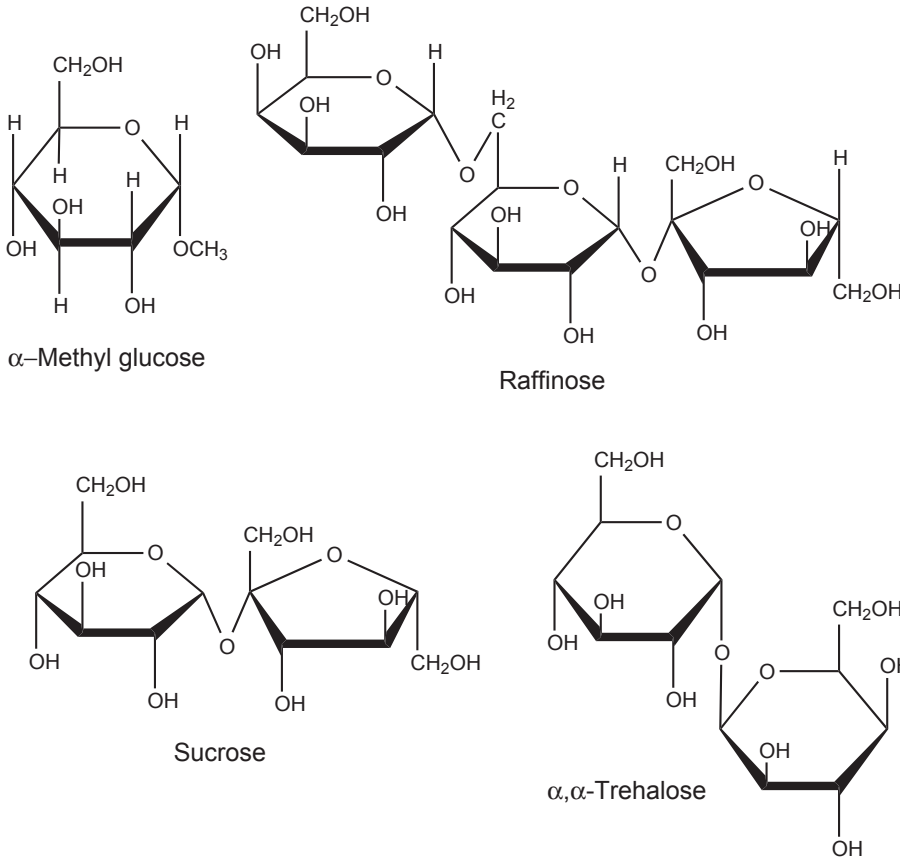


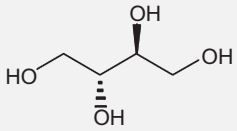
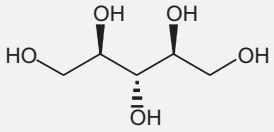
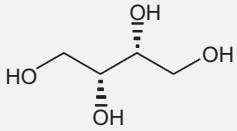
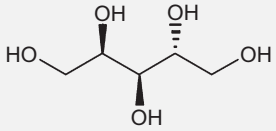
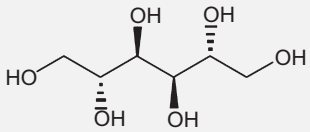
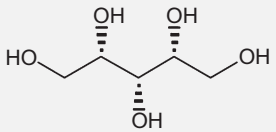
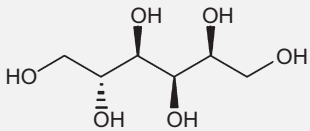
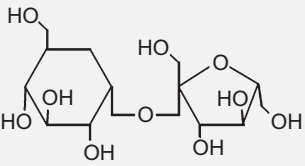
Figure 12.10 Molecular structure of the nonreducing sugars studied in Thomas and Birchall (1983).

setting of both C_3S and ordinary Portland cement (OPC) (Zhang et al., 2010). This refers to sugars for which neighboring hydroxyl groups on stereo-carbons are on the same side of the plane in a zigzag projection (type of projection used in Table 12.2). Such diastereoisomers are also referred to as having a *syn*-conformation. Zhang et al. (2010) concluded that the relative effectiveness of these aliphatic sugars increases with the number of threo−hydroxy pairs and, to a lesser extent, with the total number of hydroxy groups on the molecule.

12.4.4 The role of complexation and stability

In one form or another, researchers agree that complexation must play a role in retardation, whether in solution or at surfaces of hydrates or of anhydrous phases. However, complexation in solution does not follow the same ranking as retardation (Thomas and Birchall, 1983). For example, in Table 12.1, the nonreducing sugars sucrose (excellent

Table 12.2 Molecular structures and respective retardation obtained at selected dosages in Zhang et al. (2010). Experiments were conducted on C_3S paste at 21 ± 1 °C and a water to solids ratio of 0.6

	Additive	Concentration		Days to reach 40% hydration
		mol%	wt%	
Erythritol (0)[a]		–	–	0.3
		1.9	1.0	0.3[b]
Adonitol (0)		1.5	1.0	0.3[b]
Threitol (1)		2.0	1.1	<0.3[c]
		4.0	2.1	<0.3[c]
		6.0	3.2	1.5[c]
Arabitol (1)		2.0	1.3	1.5[c]
		4.0	2.7	Ca. 20
		6.0	4.0	>56
Mannitol (1)		1.3	1.0	2[c]
Xylitol (2)		0.50	0.33	<0.3
		1.0	0.67	2
		1.0	Ca. 10	
	1.5	2.0	1.3	Ca. 20
Sorbitol (2)		0.25	0.20	0.5[d]
		0.50	0.40	2[d]
		1.0	0.80	>56
Sucrose		0.025	0.037	2[d]
		0.10	0.15	>56

[a]Number of *threo* dihydroxy pairs on the sugar alcohol.
[b]Negligible effect over the entire curing period.
[c]80% degree of hydration reached by day 3. (The control attained 80% hydration by day 14.)
[d]80% hydration by day 7. C_3S, tricalcium silicate.
Reproduced with permission from Zhang et al. (2010).

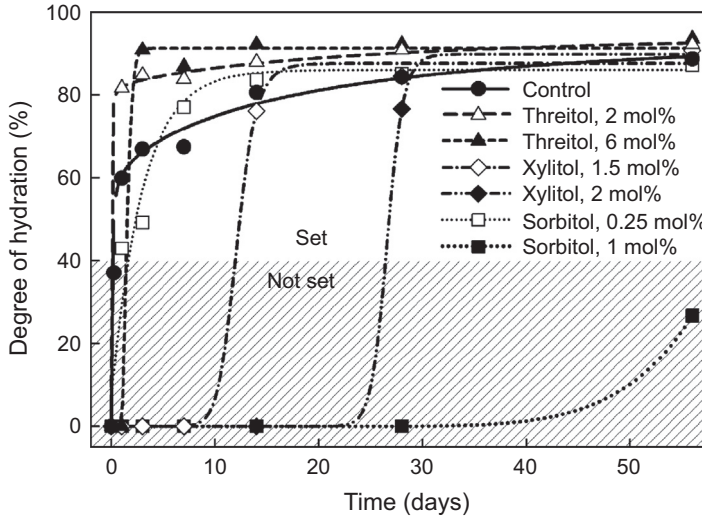


Figure 12.11 Representative effect of sugar alcohols on the degree of hydration and the final setting time of tricalcium silicate at 21 ± 1 °C.
Reproduced with permission from Zhang et al. (2010).

retarder) and α-methyl glucoside (nonretarding) have lower calcium binding capacity than glucose (average retarder).

The higher binding capacity of reducing sugars is explained by their chemical modification through extensive ring opening reactions and degradation at high pH (see Chapter 9: Gelardi et al., 2016; De Bruijn et al., 1986, 1987a,b; Smith et al., 2011, 2012). Using cement paste, C_3S, and a mixture of C_3A and gypsum, Smith et al. studied the effect of sucrose, glucose, and maltodextrin at 95 °C (Smith et al., 2011, 2012), motivated by applications to oil well cements. Such a high temperature modifies the stability of aluminate phases with respect to the ordinary processing conditions of concrete. Other expected changes include complexation and adsorption. Nevertheless, these studies propose very interesting results that offer new insights into the working mechanisms of cement retardation by sugars. In particular, it was reported that:

- Glucose degrades completely and sucrose does not.
- Degradation products of glucose adsorb on aluminate hydrates and probably also on silicates.
- Sucrose does not adsorb on aluminate hydrates but probably does on C_3A and on silicates.
- In the latter case, the adsorption appears to concern the surface of C_3S, probably on hydroxylated sites.

The stability of sucrose even under these drastic conditions motivates us to consider mainly the effect of this molecule in what follows.

At high pH, ^{13}C and ^{29}Si nuclear magnetic resonance (NMR) indicate that sucrose does not form complexes with silicates (Thomas and Birchall, 1983). However, it undergoes a change in chemical shift in ^{13}C NMR measurements above pH 10.5 (first observation at pH 12) and so does raffinose (Thomas and Birchall, 1983). This is consistent with a more recent and detailed investigation by Popov et al. (2006), who

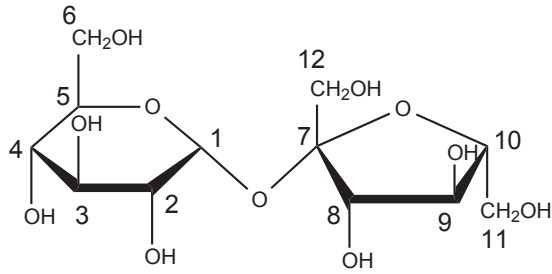


Figure 12.12 Molecular structure of sucrose with carbon numbering used in Popov et al. (2006).

found that above pH 11, the proton from the alcohol group on the C8 carbon (Figure 12.12) is deprotonated. More specifically, this is on the five-membered ring that is common to both sucrose and raffinose. This deprotonation at high pH probably makes these two sugars good complexing agents, despite the absence of any chemical degradation. It probably also allows them to adsorb more strongly on mineral phases than the smaller molecular weight degradation products of, for example, glucose (Smith et al., 2011, 2012).

12.4.5 The role of adsorption

12.4.5.1 Adsorption on portlandite

Based on their results, Thomas and Birchall (Thomas and Birchall, 1983) proposed that the reducing sugars form bidentate complexes that cannot poison the growth of portlandite and/or C−S−H, while monodentate complexes formed by sucrose and raffinose with calcium can.

Concerning portlandite, these conclusions are consistent with a more recent study showing extensive adsorption of sucrose on this mineral (Reiter et al., 2015). In the same study, it is also shown that adding portlandite to a cement paste retarded with sucrose reduces retardation, as shown in Figure 12.13. More interestingly, the reduced retardation varies linearly with the amount of added portlandite and is completely canceled at a dosage corresponding to its saturation plateau by sucrose. This suggests that the sucrose has a higher affinity for portlandite than for the other phase(s) on which it is initially adsorbed and from which it causes retardation. The transfer of sucrose from one phase to another must take place through solution. Sucrose present in solution would adsorb onto portlandite, causing a decrease in concentration of sucrose in solution. In response to this, sucrose would desorb from C_3S (or other) in an attempt to re-establish chemical equilibrium in terms of adsorption (see Chapter 10: Marchon et al., 2016). The rate of this coupled process benefits from the fact that the initial concentration of sucrose in solution is not extremely low. This suggests that sucrose may interfere with the growth of portlandite. It is compatible with observation that sucrose can cause elongated portlandite crystals to form (modified morphology) (Zhang et al., 2010).

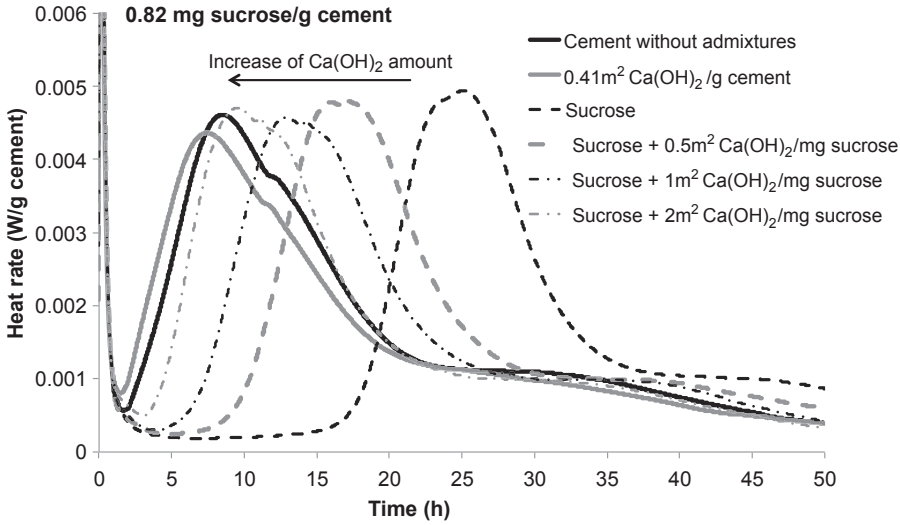


Figure 12.13 Rate of heat released for cement pastes containing 0.82 mg of sucrose per gram of cement and different dosages of $Ca(OH)_2$.
Adapted from Reiter et al. (2015).

However, having an impact on growth is one thing and poisoning nucleation is another. If portlandite is present, even in a modified morphology, its ion activity product in solution is probably not much higher than normal saturation. Therefore, it is unlikely that the conditions for the "shut off" mechanism are met (Bullard and Flatt, 2010) as they require an increase in the ion activity product of portlandite to develop. This conclusion is further supported by Luke and Luke (2000) who measured calcium concentrations in sucrose containing cement pastes that are lower than portlandite saturation in neat cement paste.

12.4.5.2 Adsorption on calcium silicates

It was mentioned that the retardation from sucrose could be reduced or even canceled by the addition of portlandite. A similar result was obtained by Thomas et al. (2009), who added well-dispersed C−S−H seeds. The most general interpretation of this observation is that, as for portlandite, the added C−S−H offers a surface onto which sucrose can adsorb, displacing it from the surface on which it is initially active. This may be C−S−H (of which the growth is blocked) or the surface of C_3S (hydroxylated or not).

The possibility of sucrose to adsorb on C_3S surfaces is indirectly supported by a study of the dissolution kinetics of alite using a microreactor (Suraneni and Flatt, 2015a). In that case, the addition of sucrose to a pH 13 solution of KOH completely blocks dissolution, while the addition to pure water does not. This suggests the possibility for sucrose to adsorb at high pH, perhaps in multiple layers. In fact, this has been shown to happen on mica at pH 12.7, using the surface force apparatus (SFA) (Smith et al., 2011).

It is also interesting to note that the possibility of blocking dissolution at high pH probably explains the effect of the solid-to-liquid ratio on retardation by sucrose (Figure 12.8). Indeed, at high dilution, the pH will rise much less (also observed in the study by Andreeva et al. (1980), although not reported in Figure 12.8). The lower pH would lead to a decrease in sucrose adsorption and thus prevent the formation of a passivation layer having a negative impact on dissolution. However, sufficiently high pH values may be reached with a higher ratio of solids to liquids. This also requires limiting the amounts of sucrose, as its acidity would negatively affect the pH. Consequently, we can qualitatively explain the different behavior in Figure 12.8(a) and (b) on the basis of pH changes. Sucrose does, however, appear to adsorb also at low solid fractions (Ivanova et al., 1980). Nevertheless, we expect that this occurs in a way that is not detrimental to dissolution.

12.4.5.3 Adsorption on calcium aluminates

Using advanced NMR techniques, Smith et al. found that sucrose does not adsorb on aluminate hydrates (Smith et al., 2011, 2012). This conclusion has been reached by 2D $^{27}Al\{^{1}H\}$ HETCOR and $^{13}C\{^{1}H\}$ HETCOR NMR measurements shown for Portland cement. Based on the absence of any correlation between protons from calcium aluminate hydrates and ^{13}C MAS spectrum of sucrose, they indicate that sucrose is not in close vicinity to the surface of calcium aluminate hydrates. They concluded that sucrose must adsorb on C_3A, hindering its dissolution (Smith et al., 2011).

Because of the low natural abundance of ^{29}Si, Smith et al. (2011) could not perform analogous measurements for the silicate phases. They could nevertheless establish that at the time of measurement, no C−S−H had formed (absence of Q^1 and Q^2 signals). However, since they measured sucrose adsorption, they concluded that it must occur on the surface of C_3S and/or portlandite and that this must be where it exerts its retarding action.

As previously mentioned, the unusual conditions of this study must be kept in mind (95 °C and 1% dosage, which is very high for sucrose). Nevertheless, these experiments offer very important insight into the possible working mechanisms of retarders and illustrate how modern tools can provide new insights into a very old problem.

12.4.6 Other issues

In summary, the impact of sugars on cement hydration is far from trivial. We have pointed out that adsorption onto the surface of tricalcium silicate likely appears to account for the main effect of sucrose. However, this seems to be strongly dependent on pH, so that changes in alkali concentration, for example due to dilution, may therefore have an important impact.

Some sugars degrade in alkaline conditions and may lose adsorbing capacity as well as selectivity. Substances that would adsorb both on aluminates and silicates may a priori be less retarding because of their consumption by aluminate phases. However, in this context, there is a possibility that the aluminate−silicate balance may be upset, which would introduce yet another mode of retardation (Cheung et al., 2011; Meyer and Perenchio, 1979).

Finally, we should comment that the adsorption of sucrose on C_3S discussed in this chapter is to be distinguished from a gel-like calcium aluminum hydrate reported in Luke and Luke (2000). Indeed, such a product is:

- Not compatible with the NMR measurements (Smith et al., 2011, 2012)
- Not compatible with the layer thickness measured by atomic force microscopy
- Not possible in pure C_3S, which is also retarded by sucrose

12.5 Conclusions

The retardation of cement hydration due to admixtures is a complex problem of a coupled system. Although this has been the subject of many studies involving all the types of superplasticizers, important aspects have not been carefully addressed and are still not fully understood:

- *The exact mechanism through which adsorbed molecules can delay the hydration*. Three fundamental hypotheses have been described in this chapter: complexation with Ca ions, decreased rate of dissolution, and perturbation of nucleation and growth. Although evidence (from studies generally performed on pure phases) exists for most of these hypotheses, questions subsist about their relative importance and possible interactions. Resolving such issues is of course dependent on the general understanding of cement hydration basics, which also account for a number of remaining open questions (see Chapter 8: Marchon and Flatt, 2016).
- *The destabilization of the silicate−aluminate−sulfate balance*. It is clear that admixtures affect aluminates hydration, which in consequence disturbs silicate hydration. However, the way they act is not yet fully understood. To address this issue, more information about the different adsorption behaviors of admixtures on aluminates or silicates are needed, as well as the role of the resulting change of specific surface of aluminate hydrates. Indeed, superplasticizers are becoming indispensable in numerous applications, many of which will increasingly suffer from limited early strength in systems using highly blended cements. Therefore, understanding the relationship between molecular structure and retardation is an important subject where fundamental insights can be used to design products with a great market potential.

Acknowledgment

Support for Delphine Marchon was provided by Sika Technology AG (Zürich, Switzerland).

References

Aïtcin, P.-C., 2016a. Portland cement. In: Aïtcin, P.-C., Flatt, R.J. (Eds.), Science and Technology of Concrete Admixtures. Elsevier (Chapter 3), pp. 27−52.

Aïtcin, P.-C., 2016b. Retarders. In: Aïtcin, P.-C., Flatt, R.J. (Eds.), Science and Technology of Concrete Admixtures. Elsevier (Chapter 18), pp. 395−404.

Andreeva, E.P., Ivanova, E.V., Stukalova, N.P., 1980. Mechanism of the effect of sucrose on the hydration of beta-dicalcium and tricalcium silicates in dilute suspensions. Colloid Journal of the USSR 42 (1), 1−7.

Bishop, M., Barron, A.R., 2006. Cement hydration inhibition with sucrose, tartaric acid, and lignosulfonate: analytical and spectroscopic study. Industrial & Engineering Chemistry Research 45 (21), 7042−7049. http://dx.doi.org/10.1021/ie060806t.

Borget, P., Galmiche, L., Meins, J-F.Le, Lafuma, F., 2005. Microstructural characterisation and behaviour in different salt solutions of sodium polymethacrylate-g-PEO comb copolymers. Colloids and Surfaces A: Physicochemical and Engineering Aspects 260 (1−3), 173−182. http://dx.doi.org/10.1016/j.colsurfa.2005.03.008.

Bullard, J.W., Flatt, R.J., 2010. New insights into the effect of calcium hydroxide precipitation on the kinetics of tricalcium silicate hydration. Journal of the American Ceramic Society 93 (7), 1894−1903. http://dx.doi.org/10.1111/j.1551-2916.2010.03656.x.

Chen, C.T., Struble, L.J., 2011. Cement−dispersant incompatibility due to ettringite bridging. Journal of the American Ceramic Society 94 (1), 200−208. http://dx.doi.org/10.1111/j.1551-2916.2010.04030.x.

Cheung, J., Jeknavorian, A., Roberts, L., Silva, D., 2011. Impact of admixtures on the hydration kinetics of Portland cement. Cement and Concrete Research, 41 (12), 1289−1309. http://dx.doi.org/10.1016/j.cemconres.2011.03.005.

Collepardi, M.M., 1996. Water reducers/retarders. In: Ramachandran, V.S. (Ed.), Concrete Admixtures Handbook, second ed. William Andrew Publishing, Park Ridge, NJ, pp. 286−409 (Chapter 6). http://www.sciencedirect.com/science/article/pii/B9780815513735500106.

Comparet, C., 2004. Etude Des Interactions Entre Les Phases Modèles Representatives D'un Ciment Portland et Des Superplastifiants Du Béton. Université de Bourgogne, Dijon, France.

De Bruijn, J.M., Kieboom, A.P.G., van Bekkum, H., 1986. Alkaline degradation of monosaccharides III. Influence of reaction parameters upon the final product composition. Recueil Des Travaux Chimiques Des Pays-Bas 105 (6), 176−183. http://dx.doi.org/10.1002/recl.19861050603.

De Bruijn, J.M., Kieboom, A.P.G., van Bekkum, H., 1987a. Alkaline degradation of monosaccharides V: kinetics of the alkaline isomerization and degradation of monosaccharides. Recueil Des Travaux Chimiques Des Pays-Bas 106 (2), 35−43. http://dx.doi.org/10.1002/recl.19871060201.

De Bruijn, J.M., Touwslager, F., Kieboom, A.P.G., van Bekkum, H., 1987b. Alkaline degradation of monosaccharides Part VIII. A13C NMR spectroscopic study. Starch − Stärke 39 (2), 49−52. http://dx.doi.org/10.1002/star.19870390206.

Eusebio, L., Goisis, M., Manganelli, G., Gronchi, P., 2011. Structural Effect of the Comb-Polymer on the Hydration of C3S Phase. In: Proceedings of the 13th International Conference of Cement Chemistry, Madrid, Spain.

Falini, G., Manara, S., Fermani, S., Roveri, N., Goisis, M., Manganelli, G., Cassar, L., 2007. Polymeric admixtures effects on calcium carbonate crystallization: relevance to cement industries and biomineralization. CrystEngComm 9 (12), 1162. http://dx.doi.org/10.1039/b707492a.

Fricke, M., Volkmer, D., Krill, C.E., Kellermann, M., Hirsch, A., 2006. Vaterite polymorph switching controlled by surface charge density of an amphiphilic dendron-calix[4]arene. Crystal Growth & Design 6 (5), 1120−1123. http://dx.doi.org/10.1021/cg050534h.

Garci Juenger, M.C., Jennings, H.M., 2002. New insights into the effects of sugar on the hydration and microstructure of cement pastes. Cement and Concrete Research 32 (3), 393−399. http://dx.doi.org/10.1016/S0008-8846(01)00689-5.

Gelardi, G., Mantellato, S., Marchon, D., Palacios, M., Eberhardt, A.B., Flatt, R.J., 2016. Chemistry of chemical admixtures. In: Aïtcin, P.-C., Flatt, R.J. (Eds.), Science and Technology of Concrete Admixtures. Elsevier (Chapter 9), pp. 149−218.

Gelardi, G., Flatt, R.J., 2016. Working mechanisms of water reducers and superplasticizers. In: Aïtcin, P.-C., Flatt, R.J. (Eds.), Science and Technology of Concrete Admixtures. Elsevier (Chapter 11), pp. 257–278.

Griffin, J.L.W., Coveney, P.V., Whiting, A., Davey, R., 1999. Design and synthesis of macrocyclic ligands for specific interaction with crystalline ettringite and demonstration of a viable mechanism for the setting of cement. Journal of the Chemical Society, Perkin Transactions 2 (10), 1973–1981. http://dx.doi.org/10.1039/a902760b.

Hanehara, S., Yamada, K., 1999. Interaction between cement and chemical admixture from the point of cement hydration, absorption behaviour of admixture, and paste rheology. Cement and Concrete Research 29 (8), 1159–1165. http://dx.doi.org/10.1016/S0008-8846(99)00004-6.

Heeb, R., Lee, S., Venkataraman, N.V., Spencer, N.D., 2009. Influence of salt on the aqueous lubrication properties of end-grafted, ethylene glycol-based self-assembled monolayers. ACS Applied Materials & Interfaces 1 (5), 1105–1112. http://dx.doi.org/10.1021/am900062h.

Ivanova, E., Andreeva, E., Stukalova, N., 1980. Adsorption interactions in hydration of individual binders in carbohydrate solutions. Colloid Journal of the USSR 42 (1), 35–39.

Jansen, D., Neubauer, J., Goetz-Neunhoeffer, F., Haerzschel, R., Hergeth, W.-D., 2012. Change in reaction kinetics of a Portland cement caused by a superplasticizer – calculation of heat flow curves from XRD data. Cement and Concrete Research 42 (2), 327–332. http://dx.doi.org/10.1016/j.cemconres.2011.10.005.

Jiang, Y., Zhang, S., Damidot, D., 2012. Ettringite and monosulfoaluminate in polycarboxylate type admixture dispersed fresh cement paste. Advanced Science Letters 5 (2), 663–666. http://dx.doi.org/10.1166/asl.2012.1798.

Keller, H., Plank, J., December 2013. Mineralisation of $CaCO_3$ in the presence of polycarboxylate comb polymers. Cement and Concrete Research 54, 1–11. http://dx.doi.org/10.1016/j.cemconres.2013.06.017.

Kirby, G.H., Lewis, J.A., 2004. Comb polymer architecture effects on the rheological property evolution of concentrated cement suspensions. Journal of the American Ceramic Society 87 (9), 1643–1652. http://dx.doi.org/10.1111/j.1551-2916.2004.01643.x.

Lerch, W., 1946. The influence of gypsum on the hydration and properties of Portland cement pastes. In: Proceedings of the American Society for Testing Materials, vol. 46.

Lothenbach, B., Winnefeld, F., Figi, R., 2007. The Influence of Superplasticizers on the Hydration of Portland Cement. In: Proceedings of the 12th International Congress on the Chemistry of Cement, Montréal.

Luke, G., Luke, K., 2000. Effect of sucrose on retardation of Portland cement. Advances in Cement Research 12 (1), 9–18. http://dx.doi.org/10.1680/adcr.2000.12.1.9.

Mantellato, S., Eberhardt, A.B., Flatt, R.J., 2016. Formulation of commercial products. In: Aïtcin, P.-C., Flatt, R.J. (Eds.), Science and Technology of Concrete Admixtures. Elsevier (Chapter 15), pp. 343–350.

Marchon, D., Juilland, P., Jachiet, M., Flatt, R.J., 2014. Impact of Polycarboxylate Superplasticizers on Polyphased Clinker Hydration. In: Proceedings of the 34th Annual Cement and Concrete Science Conference, pp. 79–82. Sheffield, England.

Marchon, D., Sulser, U., Eberhardt, A.B., Flatt, R.J., 2013. Molecular design of comb-shaped polycarboxylate dispersants for environmentally friendly concrete. Soft Matter 9 (45), 10719. http://dx.doi.org/10.1039/c3sm51030a.

Marchon, D., Flatt, R.J., 2016. Mechanisms of cement hydration. In: Aïtcin, P.-C., Flatt, R.J. (Eds.), Science and Technology of Concrete Admixtures. Elsevier (Chapter 8), pp. 129–146.

Marchon, D., Mantellato, S., Eberhardt, A.B., Flatt, R.J., 2016. Adsorption of chemical admixtures. In: Aïtcin, P.-C., Flatt, R.J. (Eds.), Science and Technology of Concrete Admixtures. Elsevier (Chapter 10), pp. 219–256.

Masuda, Y., Nakanishi, T., 2002. Ion-specific swelling behavior of poly(ethylene oxide) gel and the correlation to the intrinsic viscosity of the polymer in salt solutions. Colloid and Polymer Science 280 (6), 547–553. http://dx.doi.org/10.1007/s00396-002-0651-x.

Meyer, L.M., Perenchio, W.F., 1979. Theory of concrete slump loss as related to the use of chemical admixtures. Concrete International 1 (1), 36–43.

Middendorf, B., Singh, N.B., 2007. Poly (Methacrylic Acid) Sodium Salt Interaction with Hydrating Portland Cement. In: Proceedings of the 12th International Congress on the Chemistry of Cement, Montréal.

Milestone, N.B., 1979. Hydration of tricalcium silicate in the presence of lignosulfonates, glucose, and sodium gluconate. Journal of the American Ceramic Society 62 (7–8), 321–324. http://dx.doi.org/10.1111/j.1151-2916.1979.tb19068.x.

Moratti, F., Magarotto, R., Mantellato, S., 2011. Influence of Polycarboxylate Side Chains Length on Cement Hydration and Strengths Development. In: Proceedings of the 13th International Conference of Cement Chemistry, Madrid, Spain.

Nicoleau, L., 2004. Interactions Physico-Chimiques Entre Le Latex et Les Phases Minérales Constituant Le Ciment Au Cours de L'hydratation. Université de Bourgogne, Dijon, France.

Nicoleau, L., Bertolim, M.A., 2015. Analytical Model for the Alite (C3S) Dissolution Topography. Journal of the American Ceramic Society. n/a–n/a. http://dx.doi.org/10.1111/jace.13647.

Nkinamubanzi, P.-C., Mantellato, S., Flatt, R.J., 2016. Superplasticizers in practice. In: Aïtcin, P.-C., Flatt, R.J. (Eds.), Science and Technology of Concrete Admixtures. Elsevier (Chapter 16), pp. 353–378.

Picker, A., 2013. Influence of Polymers on Nucleation and Assembly of Calcium Silicate Hydrates. (Ph.D. thesis) Universität Konstanz, Konstanz.

Plank, J., Sachsenhauser, B., 2009. Experimental determination of the effective anionic charge density of polycarboxylate superplasticizers in cement pore solution. Cement and Concrete Research 39 (1), 1–5. http://dx.doi.org/10.1016/j.cemconres.2008.09.001.

Popov, K.I., Sultanova, N., Rönkkömäki, H., Hannu-Kuure, M., Jalonen, J., Lajunen, L.H.J., Bugaenko, I.F., Tuzhilkin, V.I., 2006. 13C NMR and electrospray ionization mass spectrometric study of sucrose aqueous solutions at high pH: NMR measurement of sucrose dissociation constant. Food Chemistry 96 (2), 248–253. http://dx.doi.org/10.1016/j.foodchem.2005.02.025.

Popov, K., Rönkkömäki, H., Lajunen, L.H.J., 2009. Critical evaluation of stability constants of phosphonic acids (IUPAC technical report). Pure and Applied Chemistry 73 (10), 1641–1677. http://dx.doi.org/10.1351/pac200173101641.

Pourchet, S., Comparet, C., Nicoleau, L., Nonat, A., 2007. Influence of PC Superplasticizers on Tricalcium Silicate Hydration. In: Proceedings of the 12th International Congress on the Chemistry of Cement, Montréal.

Prince, W., Edwards-Lajnef, M., Aïtcin, P.-C., 2002. Interaction between ettringite and a polynaphthalene sulfonate superplasticizer in a cementitious paste. Cement and Concrete Research 32 (1), 79–85. http://dx.doi.org/10.1016/S0008-8846(01)00632-9.

Prince, W., Espagne, M., Aïtcin, P.-C., 2003. Ettringite formation: a crucial step in cement superplasticizer compatibility. Cement and Concrete Research 33 (5), 635–641. http://dx.doi.org/10.1016/S0008-8846(02)01042-6.

Ramachandran, V.S., Lowery, M.S., January 1992. Conduction calorimetric investigation of the effect of retarders on the hydration of Portland cement. Thermochimica Acta 195, 373–387. http://dx.doi.org/10.1016/0040-6031(92)80081-7.

Regnaud, L., Rossino, C., Alfani, R., Vichot, A., 2011. Effect of Comb Type Superplasticizers on Hydration Kinetics of Industrial Portland Cements. In: Proceedings of the 13th International Conference of Cement Chemistry, Madrid, Spain.

Reiter, L., Palacios, M., Wanger, T., Flatt, R.J., 2015. Putting concret to sleep and waking it up with chemical admixtures. In: Proceedings of the 11th Canmet/ACI Int. Conf. Superplasticizers and Other Chemical Admixtures in Concrete. ACI, Ottawa.

Richter, F., Winkler, E.W., 1987. Das Calciumbindevermögen. Tenside Detergents 24 (4), 213–216.

Ridi, F., Dei, L., Fratini, E., Chen, S.-H., Baglioni, P., 2003. Hydration kinetics of tri-calcium silicate in the presence of superplasticizers. The Journal of Physical Chemistry B 107 (4), 1056–1061. http://dx.doi.org/10.1021/jp027346b.

Ridi, F., Fratini, E., Luciani, P., Winnefeld, F., Baglioni, P., 2012. Tricalcium silicate hydration reaction in the presence of comb-shaped superplasticizers: boundary nucleation and growth model applied to polymer-modified pastes. The Journal of Physical Chemistry C 116 (20), 10887–10895. http://dx.doi.org/10.1021/jp209156n.

Rieger, J., Thieme, J., Schmidt, C., 2000. Study of precipitation reactions by X-ray microscopy: $CaCO_3$ precipitation and the effect of polycarboxylates. Langmuir 16 (22), 8300–8305. http://dx.doi.org/10.1021/la0004193.

Robeyst, N., De Belie, N., 2009. Effect of Superplasticizers on Hydration and Setting Behavior of Cements. 9th Canmet/ACI Int. Conf. Superplasticizers and Other Chemical Admixtures in Concrete, ACI, Sevilla, Spain, pp. 61–73.

Robeyst, N., De Schutter, G., Grosse, C., De Belie, N., 2011. Monitoring the effect of admixtures on early-age concrete behaviour by ultrasonic, calorimetric, strength and rheometer measurements. Magazine of Concrete Research 63 (10), 707–721.

Roncero, J., Valls, S., Gettu, R., 2002. Study of the influence of superplasticizers on the hydration of cement paste using nuclear magnetic resonance and X-ray diffraction techniques. Cement and Concrete Research 32 (1), 103–108. http://dx.doi.org/10.1016/S0008-8846(01)00636-6.

Rössler, C., Möser, B., Stark, J., 2007. Influence of Superplasticizers on C3A Hydration and Ettringite Growth in Cement Paste. In: Proceedings of the 12th International Congress on the Chemistry of Cement, Montréal.

Sandberg, P., Porteneuve, C., Serafin, F., Boomer, J., Loconte, N., Gupta, V., Dragovic, B., Doncaster, F., Alioto, L., Vogt, T., 2007. Effect of Admixture on Cement Hydration Kinetics by Synchrotron XRD and Isothermal Calorimetry. In: Proceedings of the 12th International Congress on the Chemistry of Cement, Montréal.

Smith, B.J., Rawal, A., Funkhouser, G.P., Roberts, L.R., Gupta, V., Israelachvili, J.N., Chmelka, B.F., 2011. Origins of saccharide-dependent hydration at aluminate, silicate, and aluminosilicate surfaces. Proceedings of the National Academy of Sciences 108 (22), 8949–8954. http://dx.doi.org/10.1073/pnas.1104526108.

Smith, B.J., Roberts, L.R., Funkhouser, G.P., Gupta, V., Chmelka, B.F., 2012. Reactions and surface interactions of saccharides in cement slurries. Langmuir 28 (40), 14202–14217. http://dx.doi.org/10.1021/la3015157.

Smith, R.M., Martell, A.E., Motekaitis, R.J., 2003. NIST Critically Selected Stability Constants of Metal Complexes Database. NIST Standard Reference Database 46.

Sowoidnich, T., Rössler, C., 2009. The Influence of Superplasticizers on the Dissolution of C3S. In: Proceedings of the 9th Canmet/ACI Int. Conf. Superplasticizers and Other Chemical Admixtures in Concrete, Sevilla, Spain, vol. 262, pp. 335–346.

Suraneni, P., Flatt, R.J., 2015a. Micro-reactors to study alite hydration. Journal of the American Ceramic Society 98 (5), 1634−1641.

Suraneni, P., Flatt, R.J., 2015b. Use of micro-reactors to obtain new insights into the factors influencing tricalcium silicate dissolution. Cement and Concreate Research. http://dx.doi.org/10.1016/j.cemconres.2015.07.011.

Tasaki, K., 1999. Poly(oxyethylene)−cation interactions in aqueous solution: a molecular dynamics study. Computational and Theoretical Polymer Science 9 (3−4), 271−284. http://dx.doi.org/10.1016/S1089-3156(99)00015-X.

Tenoutasse, N., 1968. The hydration mechanism of C3A and C3S in the presence of calcium chloride and calcium sulfate. In: Proceedings of the 5th International Symposium on the Chemistry of Cement, No. II-118, pp. 372−378.

Thomas, J.J., Jennings, H.M., Chen, J.J., 2009. Influence of nucleation seeding on the hydration mechanisms of tricalcium silicate and cement. The Journal of Physical Chemistry C 113 (11), 4327−4334. http://dx.doi.org/10.1021/jp809811w.

Thomas, N.L., Birchall, J.D., 1983. The retarding action of sugars on cement hydration. Cement and Concrete Research 13 (6), 830−842. http://dx.doi.org/10.1016/0008-8846(83)90084-4.

Wang, Z.-M., Zhao, L., Tian, N., 2009. The Initial Hydration Behaviors of Cement Pastes with Different Types of Superplasticizers, 9th Canmet/ACI Int. Conf. Superplasticizers and Other Chemical Admixtures in Concrete, Sevilla, Spain, pp. 267−278.

Winnefeld, F., Becker, S., Pakusch, J., Götz, T., 2007a. Effects of the molecular architecture of comb-shaped superplasticizers on their performance in cementitious systems. Cement and Concrete Composites 29 (4), 251−262. http://dx.doi.org/10.1016/j.cemconcomp.2006.12.006.

Winnefeld, F., Zingg, A., Holzer, L., Figi, R., Pakusch, J., Becker, S., 2007b. Interaction of Polycarboxylate-Based Superplasticizers and Cements: Influence of Polymer Structure and C3A-Content of Cement. In: Proceedings of the 12th International Congress on the Chemistry of Cement, Montréal.

Winnefeld, F., Zingg, A., Holzer, L., Pakusch, J., Becker, S., 2009. The Ettringite − Superplasticizer Interaction and Its Impact on the Ettringite Distribution in Cement Suspensions. In: Supplementary Papers. 9th Canmet/ACI Int. Conf. Superplasticizers and Other Chemical Admixtures in Concrete. Sevilla, Spain.

Yamada, K., Takahashi, T., Hanehara, S., Matsuhisa, M., 2000. Effects of the chemical structure on the properties of polycarboxylate-type superplasticizer. Cement and Concrete Research 30 (2), 197−207. http://dx.doi.org/10.1016/S0008-8846(99)00230-6.

Young, J.F., 1972. A review of the mechanisms of set-retardation in Portland cement pastes containing organic admixtures. Cement and Concrete Research 2 (4), 415−433. http://dx.doi.org/10.1016/0008-8846(72)90057-9.

Zhang, L., Catalan, L.J.J., Balec, R.J., Larsen, A.C., Esmaeili, H.H., Kinrade, S.D., 2010. Effects of saccharide set retarders on the hydration of ordinary Portland cement and pure tricalcium silicate. Journal of the American Ceramic Society 93 (1), 279−287. http://dx.doi.org/10.1111/j.1551-2916.2009.03378.x.

Zingg, A., Winnefeld, F., Holzer, L., Pakusch, J., Becker, S., Figi, R., Gauckler, L., 2009. Interaction of polycarboxylate-based superplasticizers with cements containing different C3A amounts. Cement and Concrete Composites 31 (3), 153−162. http://dx.doi.org/10.1016/j.cemconcomp.2009.01.005.

Working mechanisms of shrinkage-reducing admixtures

13

A.B. Eberhardt[1], R.J. Flatt[2]
[1]Sika Technology, Zürich, Switzerland; [2]Institute for Building Materials, ETH Zürich, Zurich, Switzerland

13.1 Introduction

In this chapter, we examine the working mechanism through which shrinkage-reducing admixtures (SRAs) reduce the shrinkage of cementitious materials. The chemical structures of these compounds are reviewed in Chapter 9 (Gelardi et al., 2016). While our presentation refers to the case of drying shrinkage, the main principles can be transferred to situations of autogenous shrinkage and the main conclusions about mechanisms remain unchanged. In Chapter 23, the application of SRAs will be discussed by presenting various cases from practice where SRAs have been used to control either autogenous shrinkage or drying shrinkage (Gagné, 2016).

Another form of shrinkage is plastic shrinkage that develops before concrete starts to develop substantial strength. In this case, the strategies to mitigate are largely based on avoiding undesired water loss through various curing measures, many of which are described in chapter 5 (Aïtcin, 2016). However, in this case also SRAs can be useful and were found to provide an additional aid to reduce plastic shrinkage (Engstrand, 1997; Holt, 1999, 2000; Holt and Leivo, 2004; Bentz, Geiker et al., 2001; Lura et al., 2007; Mora-Ruacho et al., 2009; Sant et al., 2010; Saliba et al., 2011; Oliveira et al., 2015) and cracking of concrete (Bentz et al., 2001; Mora et al., 2003; Lura et al., 2007; Leemann et al., 2014). Moreover in cases where water curing is imperfect or simply not conducted, SRAs may be particularly useful as they are included in the mix and not dependent on workmanship involved in placing the concrete.

For the case of plastic shrinkage reduction, accounting for the action of SRAs is more straightforward to explain, being much more directly related to changes in interfacial energy. For this reason the focus of this chapter is laid on the slightly more complex and less well-described question of the impact of SRAs on drying shrinkage.

As we have seen in Chapter 10, SRAs are surfactants that are characterized by their ability to reduce the surface tension of the pore solution (Marchon et al., 2016). This alone, however, is not sufficient to achieve good shrinkage reduction because the admixture must remain in the liquid−vapor interface. For example, polycarboxylate ether (PCE) superplasticizers are also effective at reducing surface tension, but because they preferably adsorb on cement particles, their impact on drying shrinkage is only minor.

In contrast to other admixtures, the dosages of SRAs are relatively high on the order of 10 times higher than for superplasticizers, except for [ultra]high performance

Science and Technology of Concrete Admixtures. http://dx.doi.org/10.1016/B978-0-08-100693-1.00013-8
Copyright © 2016 Elsevier Ltd. All rights reserved.

concrete. We will see in this chapter that this higher dosage has to do with the fact that the interfacial area at which they must act increases radically in the course of drying. This comes from the fact that cementitious materials have large internal surface areas ($3-60\ km^2/m^3$ in concrete; compare to Table 23.1). When covered only by liquid films, this is a very large interfacial area where the SRAs must remain active. This large interfacial area is identified as a fundamental limitation of the ultimate efficiency of SRAs at low relative humidity and helps determine the limits of the efficiency of such products.

Because SRAs must be used in high concentrations and because their molecular structure requires a hydrophobic part (Chapter 9; Gelardi et al., 2016), some of them can exhibit a limited solubility. Some commercial formulations deal with this issue by introducing co-surfactants, as explained in Chapter 15 (Mantellato et al., 2016). The solubility issue can also manifest itself by the formation of micelles (Chapter 10; Marchon et al., 2016). If this takes place at low surface tensions, it is not a problem. Indeed, as the interfacial area is created, SRAs will be consumed from micelles to maintain the interfacial concentration constant (see Figure 10.8). However, the adsorption onto solid surfaces is a limiting factor and is discussed more extensively at the end of this chapter.

Understanding the effect of SRAs requires a proper description of the process of drying and/or autogenous shrinkage. These are complex processes; readers interested in a review of the topic may consult Scherer (2015). In this chapter, we present the basic aspects of drying shrinkage that are needed to discuss the main effects of SRAs from a mechanistic point of view. For this, we have found that the disjoining pressure theory provides the most useful insight and is therefore the one that is most discussed here, although capillary pressure is also briefly outlined.

13.2 Basic principles of the shrinkage of cementitious systems

The first attempts to relate drying and shrinkage of porous materials to standard thermodynamics go back to Bangham's work on charcoal (Bangham and Fakhoury, 1930; Bangham et al., 1932; Bangham, 1934, 1937). Later, Powers (1968) published "Thermodynamics of Volume Change and Creep," suggesting a combined action of surface free energy, disjoining pressure, and capillary pressure within the porous cementitious material, all derived from standard thermodynamics.

Later, Setzer (1973) proposed a thermodynamic approach for calculating pore space distributions using water vapor sorption isotherms, providing the basis for modeling the drying of a porous material. Building on this and using Bangham's approach, a relationship was established between the changes of surface free energy and deformation of drying of cement paste, mainly for the humidity range below 50% relative humidity, RH (Setzer and Wittmann, 1974; Hansen, 1987). Ferraris and Wittmann (1987) concluded that, in such a low humidity range, Bangham's law describes hygral length change, while above it (even starting at 40%) it is disjoining pressure that should be considered. Similar conclusions have also been reached in more recent studies (Beltzung and Wittmann, 2005; Setzer and Duckheim, 2006; Duckheim, 2008).

Drying shrinkage models for cementitious material often refer to the concept of capillary pressure in the pore fluid as driving force for deformation (Mackenzie, 1950; Granger et al., 1997; Bentz et al., 1998). A thermodynamic framework for drying of cementitious material was developed by Coussy et al. (1998, 2004), along with the concept of average pore pressure.

However, most models and approaches for predicting drying shrinkage do not properly account for surface tension effects of the liquid−vapor interface. Indeed, they do not consider that the creation of interfacial area during drying has an energy cost. In doing so, they neglect a key factor that determines how cementitious materials minimize their free energy, and more specifically how they distribute interfacial and deformation energy (i.e., shrinkage).

We will see that this plays an important role in explaining the working mechanism of SRAs because of their impact on surface tension. Because of this, it is worth recalling that in the literature two main theories can be found about how surface tension impacts shrinkage: capillary pressure and disjoining pressure. Both of these are explained in the following sections, after which we develop a general thermodynamic framework for shrinkage reduction by SRAs. This serves as a basis for the discussion on working mechanisms developed in the next section.

13.2.1 Capillary pressure theory

The pressure difference ΔP_C between a vapor phase at pressure P_V and a liquid at pressure P_L, is given by:

$$\Delta P_C = P_L - P_V = \kappa_{LV}\gamma_{LV} \tag{13.1}$$

where κ_{LV} is the curvature of the liquid−vapor interface and γ_{LV} is the interfacial energy (or surface tension).

Such a pressure can develop in capillaries during drying, which is why it is referred to as capillary pressure. If the liquid wets the pores, then the menisci formed lead to a negative value of κ_{LV}, implying that the pressure in the liquid is lower than the atmospheric pressure. As a result, if the solid skeleton is also at atmospheric pressure, there is a force imbalance, causing the solid to shrink and the pores to become smaller (Scherer, 1990).

The capillary pressure has been successfully applied to explain the drying shrinkage of materials with pores larger than about 10 nm (Scherer, 2015; Hua et al., 1995). An example is cementitious materials in their plastic state (Lura, 2003; Lura et al., 2003). However, later in the course of hydration, the pores of cementitious materials reduce to only a couple nanometers and this theory can no more be applied. It also generally fails below 40−50% RH (Coussy, 2004a,b; Coussy et al., 2004). For this, it is necessary to consider the disjoining pressure theory.

13.2.2 Disjoining force theory

In the literature on drying and shrinkage of hydrated cement paste, one can find serious doubts on the importance of capillary pressure and disjoining pressure is often

presented to be the dominating mechanism (Wittmann, 1973; Badmann et al., 1981; Ferraris and Wittmann, 1987; Setzer, 1991; Beltzung and Wittmann, 2005; Setzer and Duckheim, 2006).

The concept of *disjoining pressure*, which has been redefined by Setzer and Duckheim (2006), can describe drying shrinkage for the whole range of humidity, even in materials with a very fine porosity. It considers that pores are formed between hydrates that are separated by a distance h from each other. When this separation distance is small, surface forces such as van der Waals or electrostatic ones can be felt across the gap (see Chapter 11; Gelardi and Flatt, 2016). The disjoining pressure theory argues that, in the presence of water, repulsive forces exist that resist the van der Waals attraction. More importantly, the disjoining pressure theory proposes that by removing water, the overall force balance between opposing surfaces becomes attractive, causing the solid body to contract. This effect should be particularly important in small pores and is proposed to be the main driving force for drying shrinkage of well-hydrated cementitious materials.

However, the exact nature of this force is not further specified. For small separation distances and in a concentrated electrolyte, it could be hydration forces, which would be consistent with the existence of the minimum distance, which is estimated to be on the order of 1−2 nm, as mentioned in Chapter 11 (Gelardi and Flatt, 2016). However, water must also be able to modify attractive forces in pores that are not fully saturated, which cannot be explained by hydration forces. Rather, it is probable that the presence of water layers reduces the magnitude of the van der Waals attraction or introduces surface charge dissociation and corresponding electrostatic repulsion. Because the way in which water changes the force balance is not exactly known, it is not surprising that the exact form of the disjoining pressure is not known either.

In the context of this chapter, the most important aspect is that, from the disjoining pressure point of view, the following phenomena must be taken into account to explain drying shrinkage:

1. As water is removed, the thickness of the liquid films on the pore walls is reduced (Badmann et al., 1981; Bentz et al., 1998).
2. As a result, the net interfacial force balance becomes attractive and surfaces approach each other until a new point of equilibrium is reached (Wittmann, 1973; Badmann et al., 1981; Ferraris and Wittmann, 1987; Setzer, 1991; Beltzung and Wittmann, 2005; Setzer and Duckheim, 2006).
3. The corresponding displacement depends on the material rigidity (Nielsen, 1973; Granger et al., 1997; Bentz et al., 1998; Coussy et al., 1998, 2004; Coussy, 2004a,b; Setzer and Duckheim, 2006). Therefore, a plastic material may shrink while remaining water saturated (Eberhardt, 2011). In contrast, a rigid one would see its large pores empty and liquid films being formed, thus creating solid−liquid interfacial area within its porous network.
4. This shrinkage mechanism mostly affects pores small enough for interfacial forces of opposing pore walls to interact (Horn, 1990; Scherer, 1990; Grabbe and Horn, 1993).

This view on how shrinkage develops in cementitious materials has proved to be very useful in accounting for the impact of SRAs. We therefore use it to explain their working mechanism. First, however, we establish the general thermodynamic framework needed to do this in the next section.

13.2.3 A thermodynamic framework of shrinkage

Let us consider a drying cementitious material as an open pore system exchanging water with its environment. From a thermodynamic point of view, we consider that drying takes place as a succession of steps involving first the removal of an incremental amount of water, followed by a return to equilibrium. The incremental removal of water changes the Helmholtz free energy of the system and it is in this new condition that a new equilibrium is sought. This involves a redistribution of the total available Helmholtz free energy between its two contributions: deformation energy and interfacial energy (Eberhardt, 2011). At each relative humidity, the energy balance for the available Helmholtz free energy can therefore be written as:

$$\psi_{tot} = \psi_{def} + \psi_{int} \tag{13.2}$$

where ψ_{def} is the energy associated with the deformation of the solid and ψ_{int} is the interfacial energy associated with water loss.

Moreover, at each relative humidity, equilibrium is achieved by minimizing this energy, so that:

$$d\psi_{tot} = d\psi_{def} + d\psi_{int} = 0 \tag{13.3}$$

In other words, the change of energy at the interfaces should be equal and opposite to the change of deformation energy. In what follows, we describe successively the steps leading to a formal description of each of these terms.

13.2.3.1 Deformation energy

The differential form of the deformation energy is:

$$d\psi_{def.} = p_{disj.}dh + hdp_{disj.} \tag{13.4}$$

where h is the average distance between solid surfaces and $p_{disj.}$ is the disjoining pressure.

For an elastic solid, using macroscopic material properties, we get:

$$\psi_{def.} = \frac{K}{2}\int d^2\varepsilon \tag{13.5}$$

where K is the bulk modulus and ε is the volumetric shrinkage strain.

Note that in the literature on of drying cement paste, authors usually focus on the elastic properties and linear elastic approaches are applied, distinguishing the modulus of the porous body and modulus of the material forming the solid skeleton (Bentz et al., 1998; Coussy et al., 1998, 2004; Coussy, 2004a,b).

Independent of the methodology used, shrinkage strains and bulk modulus are related to the first term of the energy balance in Eqn (13.2). This gives access to the differential form and can be used to express $d\psi_{def.}$ in terms of measurable amounts in addition to dp.

For this, we further express the pressure difference as a function of relative humidity using the following assumptions:

1. The chemical potential of water in the liquid and the vapor phases only depend on pressure (temperature being fixed).
2. The liquid and the vapor phases are at equilibrium so the Clausius−Clapeyron relation can be used to describe the pressure difference between both phases. Together with Kelvin's law, this pressure difference can be written as a function of RH, which leads to:

$$\Delta p = \frac{RT}{v_{m,w}} \cdot \ln(\mathrm{RH}) \tag{13.6}$$

where R is the ideal gas constant, T is the absolute temperature, $v_{m,w}$ is the molar volume of the component, and RH is the relative humidity.

13.2.3.2 Interfacial energy

The differential change of the interfacial energy ψ_{int} can be expressed as a function of the interfacial area a and of the surface tension γ of the liquid−vapor interface:

$$\mathrm{d}\psi_{\mathrm{int}} = \gamma\, \mathrm{d}a + a\, \mathrm{d}\gamma \tag{13.7}$$

For a cementitious material without SRAs, γ does not vary in the course of drying, so the second term can be neglected. In the initial stages of hydration, γ would also be constant because of the presence of micelles (see Chapter 10, Figure 10.7), but its value would be lower. Consequently, the main difference between systems withandwithout SRAs initially comes from first term in Eqn (13.7) involving the following:

1. Absolute differences in tension
2. Differences in the extent of liquid−vapor interfacial area created

13.2.3.3 Variation in the total Helmholtz free energy

The Helmholtz free energy is calculated incrementally at each step of the desorption isotherm, starting at 100% RH where this energy is zero. For each step, some water is removed and its amount is determined from experimental desorption isotherms. The energy change linked to this water removal is obtained by the product of the incremental water loss and of the chemical potential of water at the relative humidity of the step in question. While we formally describe this process for drying shrinkage, a similar approach can be applied to self-desiccation. Indeed, rather than removing water from the system, it is getting fixed in hydrates. The problem has the added complication that the volume of solids increases, but on the other hand it suffers less from the possible presence of gradients in the samples.

With the above procedure, we obtain the total Helmholtz free energy as a function of RH, as illustrated in Figure 13.1. Moreover, a similar procedure can provide the cumulated deformation energy using Eqn (13.5), as also shown in Figure 13.1.

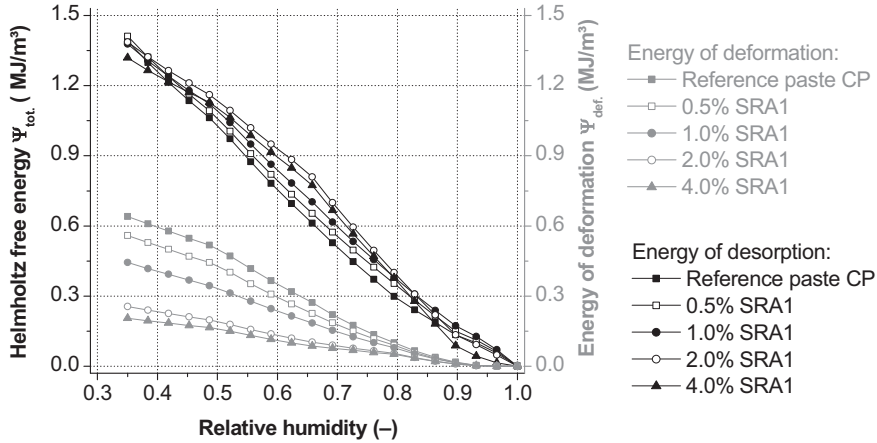


Figure 13.1 Computed changes of Helmholtz and deformation energy for cement paste containing an SRA.
Reproduced from Eberhardt (2011) with authorization.

13.3 Impact of SRAs on drying shrinkage

In the previous section, we explained the different theories concerning the driving force for shrinkage of cementitious materials. We elaborated on the implications of the disjoining pressure (role of interfaces) to develop a thermodynamic framework for considering shrinkage and its possible modification by SRAs. In this section, we elaborate on a mechanistic insight into the working mechanisms of SRAs. First, however, we begin by presenting a brief overview of the main macroscopic effects of SRAs. This mainly serves the purpose of determining the input parameters needed in the thermodynamic framework.

13.3.1 Macroscopic changes

13.3.1.1 Pore saturation

When a rigid porous body dries, the volume of water lost is not compensated by a volumetric shrinkage. The pores are emptied and on their walls a liquid films remains. This corresponds to the creation of liquid−vapor interfaces. These can become extremely large for materials having a fine porosity as cementitious materials. As illustrated in Eqn (13.7), this creation of interfacial energy plays an important role in the interfacial energy term of the Helmholtz free energy.

The quantification of its importance, however, is not trivial and requires a reliable (enough) representation of the porous structure. For this, we use here the pragmatic approach proposed by Eberhardt (2011), namely the NormCube. This consists of an artificial rigid porous network, of which the geometry is adjusted to match the desorption isotherm of a cement paste without SRA. With this representative porous structure, it is then possible to consider how the drying is changed in the presence of

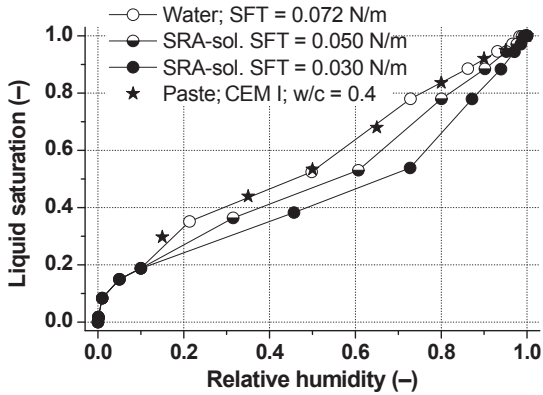


Figure 13.2 Influence of surface tension (SFT) on water vapor sorption as a function of relative humidity.
Reproduced from Eberhardt (2011) with permission.

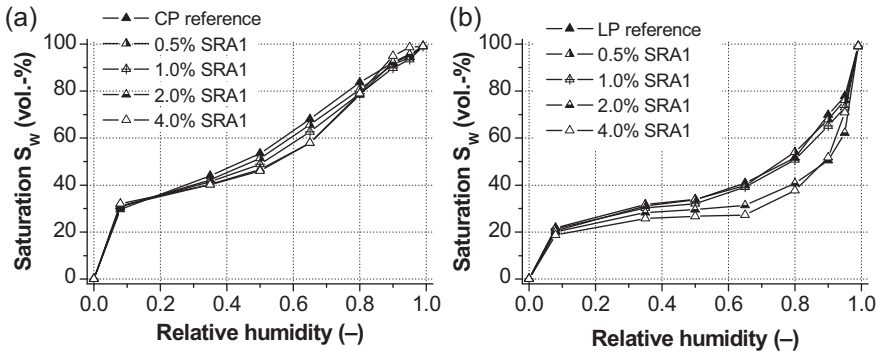


Figure 13.3 Saturation isotherms of pastes with SRA1: (a) cement paste (CP), w/b = 0.4; (b) lime stone composite binder (LP), w/b = 0.4.
Reproduced from Eberhardt (2011) with permission.

SRAs using a corresponding desorption isotherm. More specifically, it is possible to show that admixtures facilitate the creation of liquid−vapor interfaces.

This explains that SRAs reduce the liquid saturation at most for intermediate values of RH. Figure 13.2 shows that this depends on surface tension (modeled using Norm-Cube). Figure 13.3 shows a similar result (measurements) for cement pastes containing no or different dosages of SRAs. Rather than giving precise surface tensions, the different curves in Figure 13.3 represent different SRA dosages, where increasing dosages should be understood to give lower surface tensions.

13.3.1.2 Creation of internal surface in the course of drying

Concerning the efficiency of SRAs, it is important to recognize that in cementitious materials, the liquid−vapor interface increases in the course of drying as a liquid

film develops on the walls of the emptying pores. According to Eberhardt (2011), the ratio of pore water volume to exposed liquid−air interfacial area is in the range of 3.3×10^{-2} m for water-saturated concrete and less than 10^{-8} m for dried-out hydrated cement paste. This has been evaluated using the NormCube, through which the development of surface created can be quantified for the respective drying steps. Adjustment of the NormCube geometry to a measured sorption isotherm of a cement paste, as presented in Figure 13.2, provides the absolute increase of an internal surface in the course of drying.

With this, it is possible to show how the SRA concentration at the liquid−vapor interface decreases as a function of RH. In particular, it becomes obvious that at low RH, this concentration drops radically because of the tremendous increase in surface area (compare to Table 23.1). Consequently, the surface tension increases and the benefits of SRA are lost. This explains (in part) that incremental shrinkage below a certain RH is similar in samples with or without such admixtures (Eberhardt, 2011).

To illustrate the importance of this effect, the dependence of surface tension on changes of the interfacial area has been calculated (Eberhardt, 2011). The results displayed in Figure 13.4 show that surface tension increases drastically as more and more liquid−air interface is created (i.e., decreasing v/a ratio). To counter this, the only real solution is to increase the SRA dosage, as also shown in Figure 13.4.

However, it should be noted that as the SRA dosage is increased, micelles eventually form (above the critical micelle concentration [CMC]). This explains the lower plateau of surface tensions for high v/a (~25 mN/m) in Figure 13.4. Although micelles do not affect the surface tension, they can be important because they can provide surfactants as the interfacial area increases in the course of drying. In this sense, micelles act as a *surface tension buffer*.

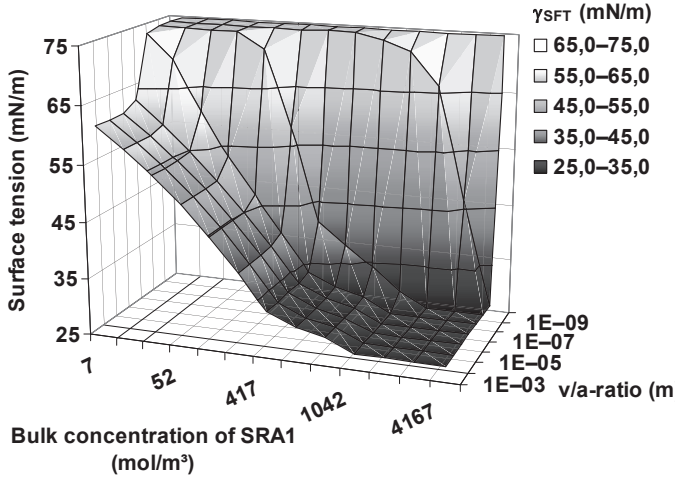


Figure 13.4 Impact of volume of remaining pore solution/interfacial area (v/a) ratio on surface activity of the SRA1.
Reproduced with permission from Eberhardt (2011).

This explains that SRAs are typically dosed in high amounts that might exceed the CMC. The downside to this solution is that surface aggregation may occur and permanently prevent a portion of SRA from being active (see last section of this chapter). This negative effect can be partially dealt with in terms of formulation by including co-surfactants, as explained in Chapter 15 (Mantellato et al., 2016).

In summary, considering that the surface tension of the liquid−vapor interface depends on the number of surfactant molecules adsorbed makes it necessary to consider not only bulk concentration but also the interfacial area. This is key to understanding how SRAs impact the drying of cementitious material.

13.3.1.3 Shrinkage strain

As previously mentioned, the deformation energy can be determined from the shrinkage strain for elastic solid using Eqn (13.5). This possibility is used to determine the elastic energy variation in the course of drying for different SRA dosages. The results in Figure 13.1 were therefore obtained from shrinkage strain data measured at different relative humidities, as given in Figure 13.5.

Figure 13.5 shows more specifically that the shrinkage reduction of SRAs develops above 50% RH. Below that, the shrinkage increase with decreasing humidity is the same regardless of the presence of SRAs. Our interpretation of this is that the liquid−vapor interfacial area is then so large that SRAs are too dilute (in the interface) to notably reduce the interfacial tension. Such conclusions are also supported by the NormCube analysis presented in the previous section.

13.3.2 Working mechanism of shrinkage reduction

Using the approach described in Section 13.2.2.3.3, we calculated the variation of the total Helmholtz free energy ψ_{tot} and of the deformation energy ψ_{def} as a function of

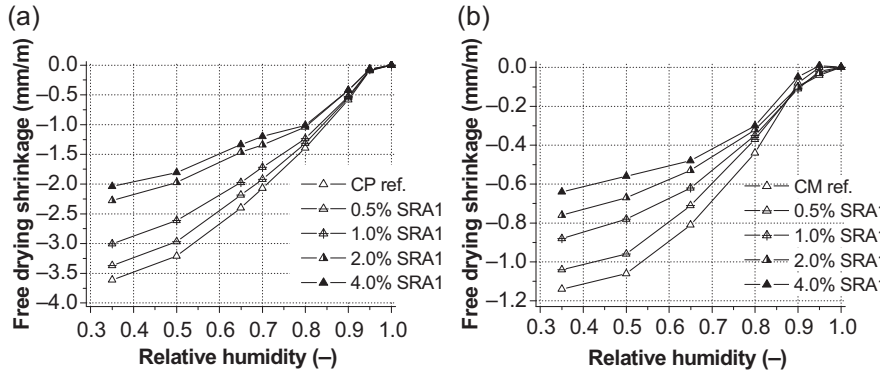


Figure 13.5 Shrinkage isotherms of paste and mortar containing similar OPC and different dosages of SRA. (a) Cement paste with/without SRA1. (b) Mortar with and without SRA1. SRA1: commercially available SRA used and analyzed in Eberhardt (2011). Reproduced from Eberhardt (2011) with permission.

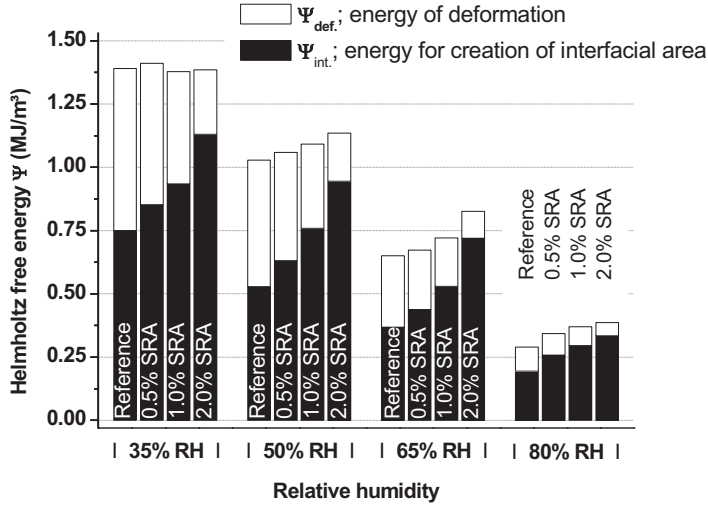


Figure 13.6 Total Helmholtz free energy, deformation energy, and energy utilized at interfaces for cement paste without SRA and with different dosages of SRA1 at different relative humidities.
Reproduced from Eberhardt (2011) with permission.

relative humidity. The example shown in Figure 13.1 indicates that the total energy does not change much depending on the presence of SRAs. However, there is a substantial change in the deformation energy. The interfacial energy, which is the difference between these two, therefore also varies a lot, as illustrated in Figure 13.6 for selected relative humidities.

For assessing the effect of SRAs, a more convenient representation consists of normalizing these energies by the total. Figure 13.7 shows that the fraction of interfacial energy increases with SRA dosage. This leaves less energy available for deformation and the direct consequence is that shrinkage is reduced. The other interesting feature in Figure 13.7 is that the fraction of energy used for deformation decreases with SRA dosage in a way that is more or less independent of relative humidity.

13.4 Dosage response of SRA on drying shrinkage

In this section, we illustrate a specific case of surfactant adsorption concerning an SRA. In particular, we examine how much of the dosed SRA is found in solution. In this case, the SRA is composed of nonionic surfactant and glycol co-solvent (Eberhardt, 2011). Figure 13.8 shows the bulk concentration of this SRA in pore solutions extracted cement between 10 min and 28 days. Values are reported versus the amount of SRA introduced (theoretical concentration "without losses").

The water content in these samples has also been measured so that the SRA concentration can be recalculated in the remaining liquid phase at each stage of

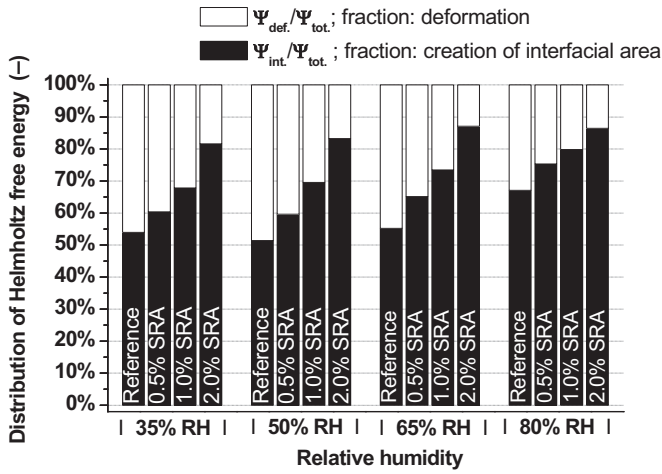


Figure 13.7 Energy fractions for deformation energy and energy utilized at interfaces for cement paste (CP) without SRA and with different dosages of SRA1 at different relative humidities.
Reproduced from Eberhardt (2011) with permission.

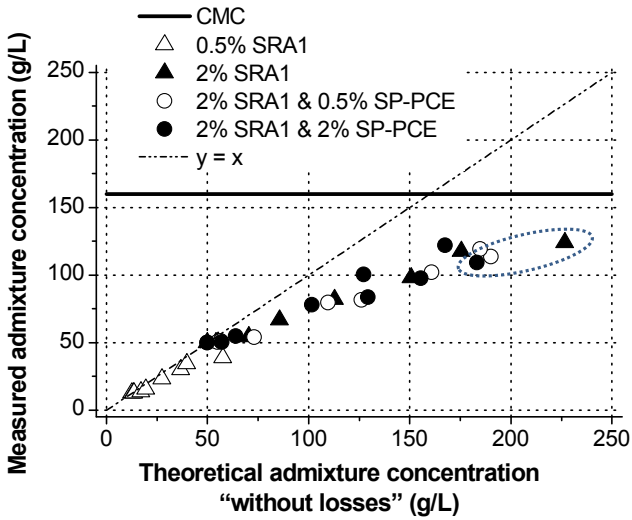


Figure 13.8 Admixture losses for SRA containing cement pastes with different dosages at different hydration stages.
Reproduced with permission from Eberhardt (2011).

hydration. Indeed, ongoing cement hydration is constricting the pore solution and, at the same time, the hydrate's surface is growing (Chapter 8; Marchon and Flatt, 2016a), which also causes the interfacial area of the solid−liquid interface to increase.

Two main phenomena have to be considered for the interpretation of Figure 13.8. First, in a cementitious material (i.e., charged surfaces and strong aqueous electrolyte), nonionic surfactants associate onto surfaces at the critical aggregation concentration (CAC). Second, at higher surfactant concentration, the surfactant molecules start to self-associate into micelles (CMC).

The results in Figure 13.8 show that at the lowest SRA dosages, all the SRA remains in the liquid phase. Data follow the dash-dotted line ($y = x$). In this regime, SRAs do not adsorb onto solid surfaces and are fully available for reducing the liquid−vapor interface. At about 50 g/L, data depart from the $y = x$ line. This corresponds to the CAC. From this point on, not all added SRAs contribute to reducing the surface tension. It should be noted that the CAC is substantially lower than the CMC, which was determined to be about 160 g/L in synthetic cement pore solution (solid line).

Also, the amount of SRA lost in surface aggregation is limited by the supplied amount of SRA and not by the specific surface of the system. This explains why results do not depend on the hydration time. However, the presence of SRAs on surfaces can modify hydration kinetics (Eberhardt, 2011) as for any other chemical admixture (Chapter 12; Marchon and Flatt, 2016b). Additionally, the distribution of SRA between liquid and interfaces may be affected by processes of competitive adsorption (Chapter 10; Marchon et al., 2016) for which molecular structure directly impacts the affinity for these surfaces (Marchon et al., 2013).

At higher concentrations than those used in Figure 13.8, the solution concentration should eventually reach the CMC. Beyond that point, the admixture concentration in solution should once again increase proportionally to the dosage and be parallel to the $y = x$ line (dash-dotted). While the micelles would not contribute to reducing surface tension, they would act as buffers to maintain a low surface tension as the liquid−vapor interfacial increases in the course of drying. In principle, the same would hold for surfactants aggregated on solid surfaces. However, this would only be the case if they are not entrapped in the growing microstructure. In fact, leaching experiments by Eberhardt (2011) show that only part of the surfactants can be extracted, strongly indicating that part of the surfactants are irreversibly bound to solid surfaces and not available to reduce surface tensions.

In summary, the most important information from Figure 13.8 is that a substantial amount of the admixture is associated with solid surfaces. This can substantially reduce the efficiency of SRAs and may be worsened if they are enclosed by the evolving hydrates microstructure so that surfactant molecules are not able to migrate to the liquid−air interface in the course of drying. This possibility is supported by the results of leaching experiments conducted by Eberhardt (2011), revealing that about 40% of the admixture cannot be extracted.

13.5 Conclusions

In summary, these results show that the Helmholtz free energy made available by drying is used in two processes: deformation and creation of interfacial area. SRAs increase the energy fraction used in the creation of interfacial area by reducing the surface tension of the liquid−vapor interface. It directly follows that less energy is available for deformation and shrinkage is reduced. A limiting factor in this mechanism is that as drying proceeds, the liquid−vapor interfacial area increases. The surfactant concentration decreases in that interface and the surface tension change is lost. This can be partly countered by increasing the surfactant dosage, which explains why SRA dosages are generally high compared to other admixtures. However, as drying proceeds, the interfacial area becomes much too large and incremental shrinkage below about 50% RH is unaffected by SRAs.

From these perspectives, the main difference between the capillary pressure theory and the disjoining pressure one is the role played by the change in interfacial areas. While both identify an important role of the change in surface energy, only the disjoining pressure provides insight into the role of the changing interfacial area during the course of drying and the cap that this puts on the ultimate efficiency of SRAs.

Finally, we note that adsorption onto solid surfaces is a limiting factor for surfactants. It can completely prevent some surface-active products from acting as SRAs if they preferably adsorb at solid−liquid interfaces. It can also reduce the efficiency of some SRAs by preventing a portion of the added admixtures from contributing to a reduction in surface tension.

References

Aïtcin, P.C., 2016. Water and its role on concrete performance. In: Aïtcin, P.-C., Flatt, R.J. (Eds.), Science and Technology of Concrete Admixtures. Elsevier (Chapter 5), pp. 75−86.

Badmann, R., Stockhausen, N., Setzer, M.J., 1981. The statistical thickness and the chemical potential of adsorbed water films. Journal of Colloid and Interface Science 82 (2), 534−542.

Bangham, D.H., Fakhoury, N., Mohamed, A.F., 1932. The swelling of charcoal. Part II. Some factors controlling the expansion caused by water, benzene and pyridine vapours. Proceedings of the Royal Society of London. Series A, Containing Papers of a Mathematical and Physical Character 138 (834), 162−183.

Bangham, D.H., 1934. The swelling of charcoal. Part III. Experiments with the lower alcohols. Proceedings of the Royal Society of London. Series A, Mathematical and Physical Sciences 147 (860), 152−175.

Bangham, D.H., Fakhoury, N., 1930. The swelling of charcoal. Part I. Preliminary experiments with water vapour, carbon dioxide, ammonia, and sulphur dioxide. Proceedings of the Royal Society of London. Series A, Containing Papers of a Mathematical and Physical Character 130 (812), 81−89.

Bangham, D.H., 1937. The Gibbs adsorption equation and adsorption on solids. Transactions of the Faraday Society 33, 805−811.

Beltzung, F., Wittmann, F.H., 2005. Role of disjoining pressure in cement based materials. Cement and Concrete Research 35 (12), 2364−2370.

Bentz, D.P., Garboczi, E.J., Quenard, D.A., 1998. Modelling drying shrinkage in reconstructed porous materials: application to porous Vycor Glass. Modelling and Simulation in Materials Science and Engineering 6 (3), 211−236.

Bentz, D.P., Geiker, M.R., et al., 2001. Shrinkage-reducing admixtures and early-age desiccation in cement pastes and mortars. Cement and Concrete Research 31 (7), 1075−1085.
Coussy, O., Dangla, P., Lassabatère, T., Baroghel-Bouny, V., 2004. The equivalent pore pressure and the swelling and shrinkage of cement-based materials. Materials and Structures 37 (1), 15−20.
Coussy, O., Eymard, R., Lassabatere, T., 1998. Constitutive modeling of unsaturated drying deformable materials. Journal of Engineering Mechanics 124 (6), 658−667.
Coussy, O., 2004a. Unsaturated Thermoporoelasticity. In: Poromechanics, pp. 151−187. http://dx.doi.org/10.1002/0470092718.ch6.
Coussy, O., 2004b. Poroviscoelasticity. In: Poromechanics, pp. 261−277. http://dx.doi.org/10.1002/0470092718.ch9.
Duckheim, C., 2008. Hygrische Eigenschaften des Zementsteins. In: Mitteilungen Aus Dem Institut Für Bauphysik Und Materialwissenschaft, vol. Heft 13. Universität Duisburg-Essen: Cuvillier Verlag Goettingen.
Eberhardt, A.B., 2011. On the Mechanisms of Shrinkage Reducing Admixtures in Self Consolidating Mortars and Concretes. Shaker Verlag GmbH, Aachen, ISBN 978-3-8440-0027-6.
Engstrand, J., 1997. Shrinkage reducing admixture for cementious composition. ConChem Journal - Verlag für Chemische Industrie H.Ziolkowsky GmbH 5 (4), 149−151.
Ferraris, C.F., Wittmann, F.H., 1987. Shrinkage mechanisms of hardened cement paste. Cement and Concrete Research 17 (3), 453−464.
Gagné, R., 2016. Shrinkage-reducing admixtures. In: Aïtcin, P.-C., Flatt, R.J. (Eds.), Science and Technology of Concrete Admixtures, Elsevier (Chapter 23), pp. 457−470.
Gelardi, G., Flatt, R.J., 2016. Working mechanisms of water reducers and superplasticizers. In: Aïtcin, P.-C., Flatt, R.J. (Eds.), Science and Technology of Concrete Admixtures, Elsevier (Chapter 11), pp. 257−278.
Gelardi, G., Mantellato, S., Marchon, D., Palacios, M., Eberhardt., A.B., Flatt, R.J., 2016. Chemistry of chemical admixtures. In: Aïtcin, P.-C., Flatt, R.J. (Eds.), Science and Technology of Concrete Admixtures, Elsevier (Chapter 9), pp. 149−218.
Grabbe, A., Horn, R.G., 1993. Double-layer and hydration forces measured between silica sheets subjected to various surface treatments. Journal of Colloid and Interface Science 157 (2), 375−383. http://dx.doi.org/10.1006/jcis.1993.1199.
Granger, L., Torrenti, J.-M., Acker, P., 1997. Thoughts about drying shrinkage: scale effects and modelling. Materials and Structures 30 (2), 96−105.
Hansen, W., 1987. Drying shrinkage mechanisms in Portland cement paste. Journal of the American Ceramic Society 70 (5), 323−328. http://dx.doi.org/10.1111/j.1151-2916.1987.tb05002.x.
Holt, E., 1999. Reducing early-age concrete shrinkage with the use of shrinkage reducing admixtures Nordic Concrete Research Meeting, Reykjavik, IS.
Holt, E., 2000. Methods of reducing early-age shrinkage. In: Shrinkage, RILEM, Paris.
Holt, E., Leivo, M., 2004. Cracking risks associated with early age shrinkage. Cement and Concrete Composites 26 (5), 521−530.
Horn, R.G., 1990. Surface forces and their action in ceramic materials. Journal of the American Ceramic Society 73 (5), 1117−1135.
Hua, C., Acker, P., Ehrlacher, A., 1995. Analyses and models of the autogenous shrinkage of hardening cement paste: 1. Modeling at macroscopic scale. Cement and Concrete Research 25 (7), 1457−1468.
Leemann, A., Nygaard, P., et al., 2014. Impact of admixtures on the plastic shrinkage cracking of self-compacting concrete. Cement and Concrete Composites 46, 1−7.
Lura, P., 2003. Autogenous Deformation and Internal Curing of Concrete. Technical University Delft, Delft.
Lura, P., Jensen, O.M., van Breugel, K., 2003. Autogenous shrinkage in high-performance cement paste: an evaluation of basic mechanisms. Cement and Concrete Research 33 (2), 223−232.

Lura, P., Pease, B., et al., 2007. Influence of shrinkage-reducing admixtures on development of plastic shrinkage cracks. Aci Materials Journal 104 (2), 187−194.
Mackenzie, J.K., 1950. The elastic constants of a solid containing spherical holes. Proceedings of the Physical Society. Section B 63 (1), 2.
Mantellato, S., Eberhardt, A.B., Flatt, R.J., 2016. In: Aïtcin, P.-C., Flatt, R.J. (Eds.), Formulation of commercial products. Elsevier (Chapter 15), pp. 343−350.
Marchon, D., Flatt, R.J., 2016a. Mechanisms of cement hydration. In: Aïtcin, P.-C., Flatt, R.J. (Eds.), Science and Technology of Concrete Admixtures. Elsevier (Chapter 8), pp. 129−146.
Marchon, D., Flatt, R.J., 2016b. Impact of chemical admixtures on cement hydration. In: Aïtcin, P.-C., Flatt, R.J. (Eds.), Science and Technology of Concrete Admixtures. Elsevier (Chapter 12), pp. 279−304.
Marchon, D., Sulser, U., Eberhardt, A.B., Flatt, R.J., 2013. Molecular design of comb-shaped polycarboxylate dispersants for environmentally friendly concrete. Soft Matter 9 (45), 10719−10728. http://dx.doi.org/10.1039/C3SM51030A.
Marchon, D., Mantellato, S., Eberhardt, A.B., Flatt, R.J., 2016. Adsorption of chemical admixtures. In: Aïtcin, P.-C., Flatt, R.J. (Eds.), Science and Technology of Concrete Admixtures. Elsevier (Chapter 10), pp. 219−256.
Mora-Ruacho, J., Gettu, R., et al., 2009. Influence of shrinkage-reducing admixtures on the reduction of plastic shrinkage cracking in concrete. Cement and Concrete Research 39 (3), 141−146.
Mora, I., Aguado, A., et al., 2003. The influence of shrinkage reducing admixtures on plastic shrinkage. Materiales De Construccion 53 (271-72), 71−80.
Nielsen, L.F., 1973. Rheologische eigenschaften für isotrope linear-viskoelastische komposi-tmaterialien. Cement and Concrete Research 3 (6), 751−766.
Oliveira, M.J., Ribeiro, A.B., et al., 2015. Curing effect in the shrinkage of a lower strength self-compacting concrete. Construction and Building Materials 93, 1206−1215.
Powers, T., 1968. The thermodynamics of volume change and creep. Materials and Structures 1 (6), 487−507.
Saliba, J., Rozière, E., et al., 2011. Influence of shrinkage-reducing admixtures on plastic and long-term shrinkage. Cement and Concrete Composites 33 (2), 209−217.
Sant, G., Scrivener, P.L.K., Weiss, J., 2010. An overview of the mechanism of shrinkage reducing admixtures in mitigating volume changes in fresh and hardened cementitious systems at early ages. International RILEM Conference on Use of Superabsorbent Polymers and Other New Additives in Concrete, RILEM Publications SARL.
Scherer, G.W., 2015. Drying, shrinkage, and cracking of cementitious materials. Journal of Transport in Porous Media, 1−21. http://dx.doi.org/10.1007/s11242-015-0518-5.
Scherer, G.W., 1990. Theory of drying. Journal of the American Ceramic Society 73 (1), 3−14. http://dx.doi.org/10.1111/j.1151-2916.1990.tb05082.x.
Setzer, M., 1973. In: Modified Method to Calculate Pore Size Distributions from Water Vapour Adsorption Data. Academia, Prague.
Setzer, M., 1991. Interaction of water with hardened cement paste. In: Mindess, S. (Ed.), Ceramic Transactions, vol. 16. American Ceramic Society, Westerville, pp. 415−439.
Setzer, M., Wittmann, F., 1974. Surface energy and mechanical behaviour of hardened cement paste. Applied Physics A: Materials Science & Processing 3 (5), 403−409.
Setzer, M.J., Duckheim, C., 2006. In: Bissonnette, B., Gagné, R., Jolin, M., Paradis, F., Marchand, J. (Eds.), The Solid-Liquid Gel-System of Hardened Cement Paste, 16. RILEM Publications SARL. http://dx.doi.org/10.1617/2351580028.
Wittmann, F.H., 1973. Interaction of hardened cement paste and water. Journal of the American Ceramic Society 56 (8), 409−415. http://dx.doi.org/10.1111/j.1151-2916.1973.tb12711.x.

Corrosion inhibitors for reinforced concrete

14

B. Elsener [1,2], *U. Angst* [1,3]
[1]ETH Zurich, Institute for Building Materials, Zurich, Switzerland; [2]University of Cagliari, Italy; [3]Swiss Society for Corrosion Protection, Zurich, Switzerland

14.1 Introduction

A chapter on corrosion inhibitors in a book on concrete admixtures needs three introductory remarks. First, whereas concrete admixtures presented in the other chapters are added in order to improve properties of fresh or hardened concrete, corrosion inhibitors are added to prolong the service life of reinforced concrete, primarily acting at the steel surface. These substances should not be harmful to concrete. Second, the book focuses on concrete admixtures; thus, the inhibitors are added to the fresh concrete with the mixing water and are present at the steel surface from the beginning. Transport properties will play a minor role and all the inhibitors applied from the concrete surface years or decades after hardening will not be treated here but referred to literature (Elsener, 2001, 2007; Söylev and Richardson, 2008; Bolzoni et al., 2014). Third, only substances that show a chemical or electrochemical interaction with the steel surface will be, by definition, treated as corrosion inhibitors for steel in concrete. This is in contrast to the development of more and more multicomponent blends that are marketed as "corrosion inhibitors" with different and multiple mechanisms of action (e.g., "pore blockers").

The service life of a structure (Figure 14.1), since its introduction by Tuuti (1982), has been subdivided into an initiation phase and a propagation phase. Prevention of corrosion is mainly achieved in the design phase by specifying high-quality concrete and adequate cover. Corrosion inhibitors as admixtures can thus be, in principle, an additional means of prevention by acting in two ways: prolonging the initiation time and reducing the corrosion rate in the propagation phase. As most of the design codes (conservatively) assume the time of depassivation to be the end of service life, most of the research on corrosion inhibitors has focused on the delay of corrosion onset.

In this chapter, we briefly present the main corrosion mechanisms of steel in concrete, focusing on chloride-induced pitting corrosion, as this is generally the main deterioration mechanism in infrastructure construction. Then, the available literature on mixed-in corrosion inhibitors is summarized, starting with the "State of the Art Report on Corrosion Inhibitors" published by the European Federation of Corrosion (Elsener, 2001). We put special emphasis on long-term and especially field studies with corrosion inhibitors. Last but not the least, the use of corrosion inhibitors as a preventative

Science and Technology of Concrete Admixtures. http://dx.doi.org/10.1016/B978-0-08-100693-1.00014-X
Copyright © 2016 Elsevier Ltd. All rights reserved.

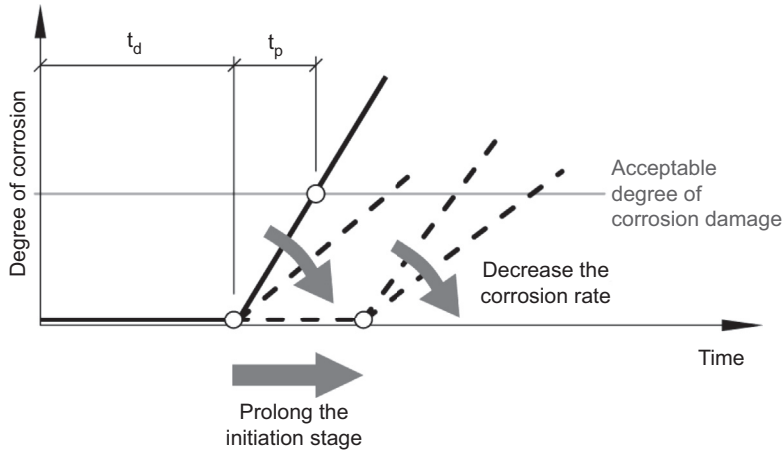


Figure 14.1 Schematic illustration of service life and the possible effect of corrosion inhibitors (t_d = time to depassivation, t_p = time from corrosion propagation to the end of the service life).

technique for reinforced concrete structures is critically discussed. Other methods to improve the durability of reinforced concrete structures are presented in Chapter 24 of this book (Aitcin, 2016).

14.2 Corrosion mechanisms of reinforcing steel in concrete

In the highly alkaline pore solution of concrete (pH of between 12.5 and 13.8, depending on the type of cement used) formed during the hydration of cement, a very thin oxide film (the passive film) protects reinforcing steel from further dissolution. This passive film remains stable as long as the pore water composition remains constant; its thickness and composition slightly change with the pH of the pore solution (Elsener, 2000; Bertolini et al., 2013). When, during the initiation phase, a sufficient amount of chloride ions (from deicing salts or from seawater) has penetrated through the concrete cover and reached the reinforcement or when the pH of the pore solution has dropped to low values due to carbonation, the protective film is destroyed and the reinforcing steel is depassivated (time t_d, Figure 14.1). Depassivated steel in concrete presents a corrosion risk, but significant metal dissolution (corrosion in the form of rust formation, loss in cross-section, etc.) is only possible in the presence of oxygen and water (humidity). The time of corrosion propagation, t_p, is given by the admissible degree of damage (loss in cross-section, spalling) and by the corrosion rate. The initiation phase and propagation phase are governed by different factors and are treated separately.

14.2.1 Initiation phase

During the initiation phase, aggressive substances (chlorides, CO_2) that can depassivate the steel penetrate from the surface into the bulk of the concrete. The initiation

phase ends at time t_d when the steel has been depassivated (Figure 14.1). The duration of the initiation phase depends on the concrete cover depth, the penetration rate of the aggressive agents, and the concentration of the aggressive substances necessary to depassivate the steel. The influence of concrete cover is obvious and all new design codes define cover depths according to the expected environment class (fib, 2013, p. 9). The rate of penetration of aggressive substances depends on the quality of the concrete cover (porosity, permeability) and on the microclimatic conditions (wetting, drying) at the concrete surface.

Prolongation of the initiation phase can be achieved through additional preventive measures:

- Reduce the penetration rate of depassivating agents (e.g., chlorides) by adding reactive binders to the cement (e.g., blast furnace slag, fly ash, silica fume) that diminish porosity of the hydrated cement matrix or by producing low permeability cover concrete.
- Increase the tolerable concentration of depassivating agents by using more corrosion-resistant materials for the reinforcement such as epoxy-coated steels, stainless steels, or nonmetallic materials, by applying electrochemical protection (cathodic prevention) or by using protective admixtures (corrosion inhibitors).

14.2.1.1 Depassivation due to chloride ions

Chloride ions can penetrate into hardened concrete via different transport mechanisms: diffusion of ions into water-saturated concrete (e.g., in submerged marine structures), capillary suction into dry or partially dry concrete (rapid transport of chloride ions with water due to convection), or ion migration (under an electric field). Diffusion of chloride ions takes place in water-saturated (submerged) concrete. It has been known for a long time that chloride ingress is more restricted in cement paste and concrete with a low water−cement ratio (w/c) (Page et al., 1981). Moreover, concretes with reactive binders (fly ash, blast furnace slag, silica fume) may have effective chloride diffusion coefficients nearly one order of magnitude lower than for ordinary Portland cement Browne (1980). Studies by Rasheeduzzafar and Mukarram, 1987 on the time to corrosion initiation show that sulfate-resistant (low C_3A) cement with low binding capacity for chlorides accelerates the initiation of corrosion.

For the depassivation of steel, only the free chlorides in the pore solution of concrete are directly relevant. Chloride ions penetrating into hardened concrete can be bound physically and chemically in the pore system of concrete. Thus, only a fraction of the total (acid-soluble) chloride content is free. The amount of bound chlorides (related to the mass of concrete) depends on the chloride content, the cement type and content, the porosity and pore size distribution, and the pH of the pore solution. The hydroxide concentration (i.e., the pH of the pore solution) has a significant effect on chloride binding because the hydroxides compete with chloride ions for the binding sites (Tritthardt, 1989; Tang and Nilsson, 1993). With a chloride-sensitive sensor element for use in cement paste and mortar, the free chloride concentration in the pore solution can be measured nondestructively (Angst et al., 2010; Elsener et al., 2003).

Electrochemically, the condition for depassivation of the steel due to the action of chlorides is $E_{corr} > E_L$; depassivation and subsequent pitting corrosion occurs when the pitting potential E_L becomes lower than the corrosion potential, E_{corr}, of the reinforcement (Elsener, 2000; Bertolini et al., 2013). In practice, the corrosion potential of the (passive) steel will have a more or less constant value, depending on the pH and on the oxygen content of the pore solution. To reach the conditions for depassivation, the pitting potential E_L has to decrease. This occurs when the chloride concentration at the rebar surface increases. Laboratory experiments have confirmed that the time required to reach depassivation is not a constant but is distributed around a mean value (Breit, 1998; Zimmermann et al., 2000; Fankel, 1998).

In civil engineering practice, a so-called "critical chloride content" for pitting corrosion is often reported. The value 0.4% chlorides per weight of cement frequently cited is based on results of experiments by Richartz (1996) on chloride binding. A review of Angst et al. (2009) on chloride threshold values shows a large scatter in the literature results. A universal "critical chloride content" for pitting corrosion cannot exist, among other reasons, because every critical chloride concentration is associated to a certain corrosion potential: both in laboratory samples and in structures, the pH of the pore solution, concrete humidity, and thus the corrosion potential are expected to vary significantly.

14.2.1.2 Depassivation due to carbonation

The pH of the concrete can change by ingress of acids from the environment, mainly CO_2 from the air and acid rain. Carbonation leads to neutralization of the alkaline pore solution of concrete and requires both CO_2 and water in order to occur. As soon as the pH at the reinforcement is near neutrality, the steel becomes depassivated (ACI, 1996). The time to depassivation of reinforcing steel depends on the total amount of alkaline hydration products present and on the availability of CO_2 and water. The total amount of CO_2 necessary to neutralize the concrete to a certain depth is related to the amount of alkaline cement hydration products in the concrete. In concretes with higher cement contents and with cement types that do not consume $Ca(OH)_2$, such as through pozzolanic reactions, the carbonation front penetrates the concrete more slowly (Hobbs, 1994).

The rate of carbonation also depends on the permeability of concrete to CO_2. The environmental conditions determine the moisture content of the concrete in the cover zone and, in turn, the moisture content determines the degree of saturation of the pores and hence their permeability to gases such as CO_2. Experiments have shown that the carbonation rate is highest at around 60−70% relative humidity (RH) (Wierig, 1984). Under such constant microclimatic conditions, the penetration rate of the carbonation front may be approximated by a square root of time law, both in controlled laboratory environments (20 °C and 65% RH) and in natural exposure conditions sheltered from rain. Under cyclic wetting and drying exposure conditions, typically small carbonation depths are found. This is due to the time hysteresis of wetting (rapid water uptake in pores due to capillary suction) and drying (relatively slow emptying of pores by evaporation), which strongly limits the time of partial saturation during which the carbonation front can

penetrate the concrete (Bakker, 1988). Good quality and dense concrete (low w/c) that is frequently wetted will be less prone to carbonation. Laboratory tests under constant and relatively dry climatic conditions (70% RH) represent a worst-case scenario.

Finally, for the chemical reaction of CO_2 with the alkalis in the concrete (NaOH, KOH, $Ca(OH)_2$), liquid water is needed. Thus, in very dry conditions (RH $<$ 50%), CO_2 can diffuse rapidly into the concrete because a substantial fraction of the pores are not water-filled. Nevertheless, no significant carbonation takes place because of the lack of water.

14.2.2 Propagation phase

Once the steel is depassivated from either chlorides or carbonation, corrosion and the corresponding loss of steel cross-section can occur in the presence of oxygen and humidity. The corrosion rate determines the time until the end of the service life of a structure is reached (Figure 14.1). However, this rate can vary considerably depending on temperature, humidity, and concrete resistivity, among others (Andrade et al., 1996; Zimmermann et al., 1997)

14.2.2.1 Chloride-induced corrosion

A characteristic feature of chloride-induced corrosion of reinforcement steel in concrete (pitting corrosion) is the development of macro-cells (Figure 14.2). Macro-cells describe the coexistence of spatially separated passive and active areas on the same rebar that form short-circuited galvanic elements, with the active area acting as an anode and the passive surface as a cathode. The iron ions dissolved at the anodic site (in the pit) are hydrolyzed; as a consequence, the pH in the pit decreases. This creates a local acidic environment that enhances the solubility of iron ions. At the cathode,

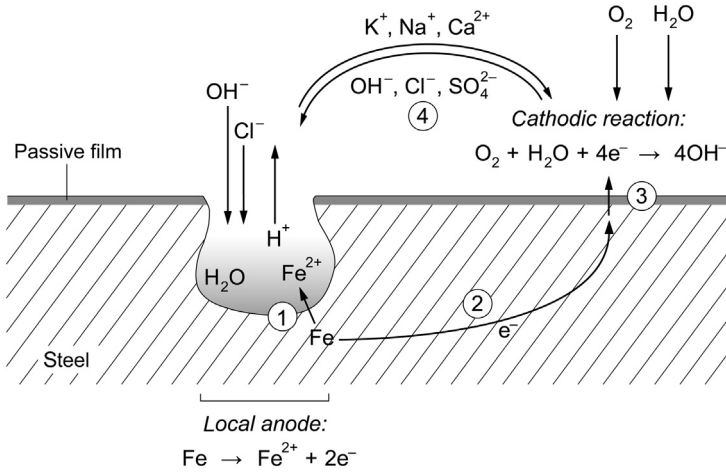


Figure 14.2 Chloride induced corrosion leading to an active-passive macro-cell.

on the other hand, hydroxide ions are produced, which increase the pH and stabilize the passive film.

The corrosion rate (iron dissolution rate in the pit) empirically depends on the electrical resistivity of the concrete, thus on temperature, conductivity of the pore solution, and porosity of the concrete (Hornbostel et al., 2013). Depending on exposure conditions, huge variations in the concrete resistivity, humidity, and the instantaneous corrosion rate have been observed on laboratory samples exposed to weathering and on bridge structures. The propagation rate of corrosion schematically shown in Figure 14.1 is an average value.

14.3 Corrosion inhibitors for steel in concrete

As outlined above, the service life of a structure can be achieved by prolonging the initiation period. Concrete admixtures acting at the steel surface (corrosion inhibitors) can be used as such preventive measures. Corrosion inhibitors are chemical compounds that, when added in adequate (preferably small) amounts to the concrete mixing water, can delay the onset or prevent corrosion of the reinforcement. These admixtures should not adversely affect the concrete properties (e.g., compressive strength), but they may also affect the microstructure of the cement paste. For reinforced concrete, corrosion inhibitors have been studied since 1960, mainly in relation to chloride-induced corrosion. Several summaries of information on steel corrosion inhibitors in concrete and a state-of-the-art report by the European Federation of Corrosion (Elsener, 2000) has been published. In this section, an update on this information is given.

14.3.1 Mechanism

The long experience and positive track record with chemicals operating as corrosion inhibitors (e.g., in the oil, gas, or petroleum industry) is commonly taken as an example for the successful use of corrosion inhibitors, transferring this success also to applications on reinforced concrete. This is a priori not correct because the *mechanisms of inhibitor action* are different:

- In applications for the oil and gas industry (and most others), the steel to be protected is uniformly corroding in slightly acidic or neutral media. Thus, the inhibitors have to protect the bare metal surface, for example, as adsorption inhibitors acting specifically on the anodic or the cathodic partial reaction of the corrosion process or as film forming inhibitors blocking the surface more or less completely (Trabanelli, 1986; Nürnberger, 1996). Usually, a reduction in the corrosion rate by 95−99% can be achieved with a very small inhibitor concentration (on the order of 10^{-3}−10^{-2} mol/L).
- Steel in uncarbonated concrete, on the other hand, is in a highly alkaline environment, where the high concentration of hydroxyl ions acts as a passivation-promoting inhibitor; indeed, steel in concrete is passive, thus protected by a thin oxy-hydroxide layer. This passive layer can be destroyed by the action of chloride ions (see previous section). This is the starting point for any mechanistic action of inhibitors in concrete.

Inhibitors for chloride-induced pitting corrosion are by far less studied than inhibitors for uniform corrosion (DeBerry, 1993). Inhibitors for pitting corrosion can act by enhancing passivity, by film forming prior to the ingress of chlorides, by buffering the pH in the local pit environment, by competitive surface adsorption processes between the inhibitor and chloride ions, or by competitive migration of inhibitor and chloride ions into the pit, thereby inhibiting stable pit growth.

14.3.2 Laboratory studies on admixed corrosion inhibitors

Numerous chemical substances have been suggested as corrosion inhibitors, but only a small group has been investigated in detail. In the 1970 and 1980s, the focus was primarily on anodic inhibitors, especially calcium nitrite, sodium nitrite, stannous chloride, sodium benzoate, and some other sodium and potassium salts (e.g., chromates) (Griffin, 1975; Berke, 1989). Later, organic compounds and mixtures were studied for their inhibitive action (Laamanen and Byfors, 1996; Nmai et al., 1992). Among the many substances tested as possible inhibitors for steel in concrete, only calcium nitrite (marketed by Grace Construction Products (DCI or DCI-S), Euclid Chemical Company (Armatect, Eucon CIA/BCN), and BASF (Rheocrete CNI)), organic inhibitor blends and organic inhibitors based on emulsified esters, alcohols, and amines are discussed here (e.g., marketed by Sika (Ferrogard 901), Cortec (MCI 2000), and BASF (Rheocrete 222+)).

Monofluorophosphate (MFP) cannot be used as a preventive admixed corrosion inhibitor due to its reaction with the fresh concrete, which removes the active substance from the concrete pore solution and strongly retards concrete setting; MFP may thus only be used when applied from the concrete surface.

Note that most of these commercial inhibitors available under different trade names are blends of essentially unknown composition that even might have been or will be changed without notice. Thus, the mechanistic action can be multiple and difficult to identify, even in laboratory studies.

14.3.2.1 Calcium nitrite

Various nitrite inhibitors—including sodium, potassium, and calcium nitrite—have been extensively studied. The first literature reference regarding use as an inhibitor in concrete dates back to the late 1950s (Moskwin and Alekseyeev, 1958). Sodium or potassium nitrites were found to cause moderate to severe loss in concrete compressive strength and to potentially enhance the risk of alkali−aggregate reaction (AAR). Calcium nitrite, on the other hand, increases the compressive strength of concrete and no susceptibility to AAR has been reported (Berke and Rosenberg, 2004). Nevertheless, calcium nitrite acts as an accelerator of cement hydration and thus normally requires the addition of a water reducer and retarder in the concrete mix. Calcium nitrite has been used in parking, marine, and highway structures and has a long and generally positive record, primarily in the USA, Japan, and the Middle East (Gaidis and Rosenberg, 1987; El-Jazairi and Berke, 1990; Page et al., 2000).

Mechanism

Nitrite acts as a passivating inhibitor due to its oxidizing properties, which stabilize the passive film (Page et al., 2000; Elsener, 2000) according to the following reactions:

$$2Fe^{2+} + 2OH^- + 2NO_2{}^- \rightarrow 2NO + Fe_2O_3 + H_2O$$

$$Fe^{2+} + OH^- + NO_2{}^- \rightarrow NO + \gamma FeOOH$$

At a corroding location, nitrite competes with chlorides to react with the released ferrous ions. Because the reactions displayed above can take place more rapidly than migration of dissolved, hydrated ferrous ions—which are maintained soluble thanks to complexation with chlorides—nitrite can stabilize the passive film even in the presence of chlorides. This shows that nitrite is consumed when it acts as corrosion inhibitor and nitrites have to be present in sufficient concentration with respect to chloride ions.

Increasing dosages of $Ca(NO_2)_2$ were found to delay the time to depassivation of rebars in concrete exposed to seawater (Figure 14.3), but even a high dosage of 4% of $Ca(NO_2)_2$ could not prevent corrosion initiation in these severe conditions (Hartt and Rosenberg, 1989). Note that this research clearly demonstrates that the time to corrosion initiation greatly varies due to the stochastic nature of pitting corrosion; results on the efficiency of inhibitors should thus be treated statistically.

Investigations using different experimental techniques in solutions, mortar, and concrete revealed a critical inhibitor (nitrite) to chloride concentration ratio of about 0.6 (with some variation from 0.5 to 1) in order to prevent the onset of corrosion. This implies (1) that there were relatively high nitrite concentrations in the pore water of concrete, and (2) that calcium nitrite dosages should be related to the level of

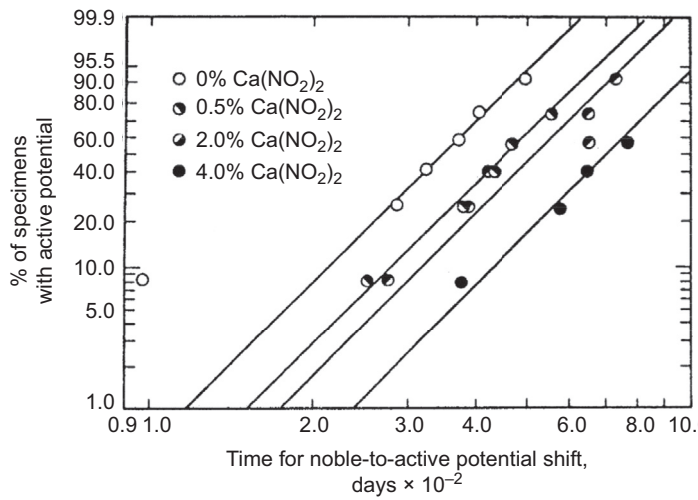


Figure 14.3 Effect of $Ca(NO_2)_2$ concentration on time to corrosion initiation (Hartt and Rosenberg, 1989).

chloride concentration expected during the design life of a structure in order to achieve effective corrosion protection. Too low concentrations of nitrites in poor-quality concrete may increase the corrosion risk, as has been found in laboratory studies on cracked reinforcing beams (Nürnberger, 1996). In contrast to these findings, results on macro-cell corrosion tests on cracked beams showed that $Ca(NO_2)_2$ additions significantly improved corrosion resistance of the embedded steel at cracks (Berke et al., 1993), even at low inhibitor dosage. Due to environmental regulations and concerns about a possible increase of the corrosion rate as a result of insufficient inhibitor concentrations, nitrites have found few applications in Europe.

Long-term efficiency

Leaching out of nitrites from concrete has been a concern in the literature. Nürnberger and Beul (1991), for instance, found that with admixed chlorides and nitrites, both ions were leached out at nearly the same rate. Data from outdoor exposure for 2 years (Tomosawa et al., 1990) or from 7-year-old bridge decks, on the other hand, showed that nearly all nitrites were preserved in the concrete. Leaching of nitrites can be avoided by specifying dense concrete (low w/c ratio, supplementary cementitious materials) and by ensuring concrete cover depths as specified by national and international standards for moderate to severe chloride exposures conditions.

Another long-term concern may be the efficiency of calcium nitrite in inhibiting chloride-induced corrosion over longer time spans. As mentioned above, the inhibitor competes with chloride ions and thus has to be present in a certain concentration with respect to the chloride ions. However, calcium nitrite is consumed in the reactions that stabilize the passive film, which means that the inhibitor concentration decreases upon its action and may after a certain time reach a concentration that is too low to ensure a further corrosion-inhibiting action.

In summary, relatively high nitrite concentrations (depending on the expected maximum chloride concentration at the steel surface) have to be admixed to concrete in order to delay corrosion initiation in chloride exposure environments. In the form of calcium nitrite, the inhibitor does not negatively affect the concrete compressive strength or promote AAR. When used in high-quality concrete and with proper concrete covers (to avoid leaching), calcium nitrite has a long and proven track record in the United States, Japan, and the Middle East. In European countries, on the other hand, it has not been applied frequently.

14.3.2.2 Alkanolamines and amines

Pure compounds

A number of alkanolamines and amines and their salts with organic and inorganic acids have been suggested as corrosion inhibitors for steel in concrete (Mäder, 1994 and literature cited). These substances are in principle vapor phase inhibitors (VPI) or volatile corrosion inhibitors (VCI). Typical compounds are diethanolamine, dimethylpropanolamine, monoethanolamine, and dimethylethanolamine. When admixed to concrete, they do not alter the compressive strength and time of stetting by more than 20% (European patent, 1987; Heren and Oelmez, 1996).

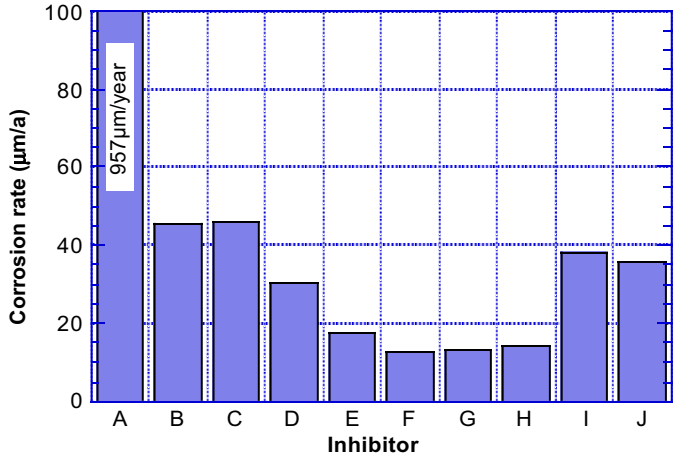


Figure 14.4 Corrosion rate (µm/year) of steel in concrete with different inhibitors mixed in (European patent, 1987). A: Control, B: Dimethylaminoethoxyethanol, D: N,N,N′-trimethyl (hydroxyethyl)-1,3-propane diamine, E: N,N,N′-trimethyl (hydroxypropyl)1,3-propane diamine, F: Methyldiethanolamine, G: Triethanolamine, H: Monoethanolamine, I: Dimethylethanolamine, J: Dicyclohexylamine.

Figure 14.4 shows the corrosion rates in a solution obtained in laboratory experiments where different hydroxyalkylamines or their mixtures were admixed to reinforced concrete samples. In comparison with the control sample (A), all substances were able to reduce the corrosion rate. Another laboratory study using mild steel in solutions of $NaHCO_3$ by mono- and dimethylamines and mono-ethylenamine showed a marked increase of the pitting potential above an inhibitor concentration of 0.1 mol/L (Abd El Halem and Killa, 1980). The inhibitor concentrations needed to inhibit pitting corrosion increased with increasing chloride concentration and lower pH in the solution.

Screening tests on about 80 organic compounds (mainly amines, amino-alcohols, and carboxylates) were performed in order to identify the best inhibiting substances (Ormellese et al., 2009). The nine most effective substances contain in their formula an aminic or carboxylic group, or both. These two functional groups are considered responsible for the adsorption on the passive film and their protective action against chloride-induced corrosion (Bolzoni et al., 2014).

Proprietary blends

Several proprietary blends from different producers (e.g., Sika (Ferrogard 901), Cortec (MCI 2000), or BASF (Rheocrete 222+)) are based on alkanolamines and amines and their salts with organic and inorganic acids. These inhibitors are occasionally termed AMA. The major difficulty with the independent evaluation of these organic corrosion inhibitors is their unknown or at least uncertain composition. One product, for example, is described as colorless to pale liquid with an ammoniacal odor, pH 11−12, a density of 0.88 g/cm^3, and vapor pressure of 4 mmHg (20 °C) containing

1.5% of non-volatile products (Cortec, product sheet) with no further information on composition. This is not near enough information to make sure that the client gets the product that has the effect documented in the test reports.

A comparative test of different organic amines (Phanasgaonkar et al., 1997) used simulated concrete pore water solutions with 1.2% (by weight) chlorides to test both the situation of admixed inhibitor and remedial work. At a concentration of 1% (by weight), the commercial inhibitor Cortec MCI 2000 showed very good corrosion inhibition, while pure dimethylethanolamine was found to be practically ineffective.

Research work at ETH Zurich (Elsener et al., 1999, 2000) investigating a commercial migrating corrosion inhibitor blend (MCI 2000) as an admixed inhibitor has shown that the critical molar concentration ratio of Cl^-/MCI 2000 determined in solutions of saturated $Ca(OH)_2$ is ~ 1, thus very high. The efficiency of the inhibitor to prevent or delay chloride-induced corrosion in mortar samples (lollipop specimens, w/c = 0.5) for different admixed inhibitor contents is shown in Figure 14.6. The time to corrosion initiation increased in the presence of the inhibitor: while the first sample of the series with the highest inhibitor concentration started to corrode after 90 days, this was the case after 50 days without an inhibitor. After corrosion initiation, however, no significant reduction in the corrosion rate was found.

Early results of tests with the proprietary inhibitor Sika Ferrogard 901 were summarized by Laamanen and Byfors (1996): electrochemical measurements in solution demonstrated that the inhibitor blend is effective when present prior to the addition of chlorides, and that a higher inhibitor concentration shows a more pronounced effect. The inhibitor blend was also tested as admixture in mortar and concrete samples that were exposed to seawater and spray with sodium chloride. After 1 year, corrosion had started in specimens with w/c = 0.6. The chloride threshold values were without exception higher for the inhibitor containing samples (4–6% Cl^- by weight of cement)

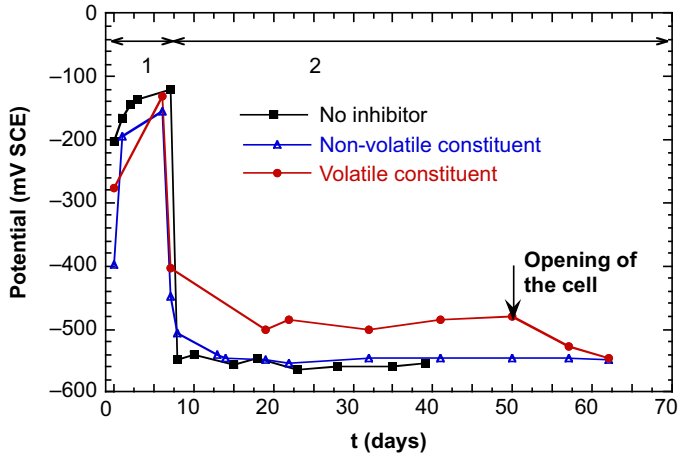


Figure 14.5 Corrosion potentials of rebar samples in solutions containing the two components of the inhibitor: ⑤, no inhibitor; o, volatile constituent; Δ, nonvolatile constituent (Elsener et al., 1999).

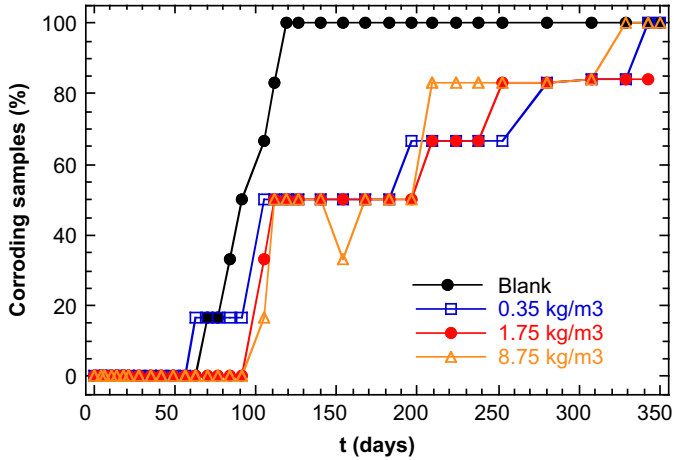


Figure 14.6 Percentage of corroding rebars in mortar versus time of cyclic chloride treatment (Elsener et al., 1999).

compared to the control samples (1−3% Cl^-). At a lower w/c ratio of 0.45, the specimens containing 3% Ferrogard 901 did not start to corrode after 15 months of testing. Studies of Cigna et al. (1997, 2007) reported a delay of corrosion initiation by a factor of two (minimum) to four (maximum) for this proprietary inhibitor blend.

A comparative study on the effectiveness of four commercial inhibitors for use in cement-based materials was performed in mortar samples exposed to cyclic chloride ponding (Figure 14.7(a)). All inhibitors tested according to manufacturer dosage could delay the onset of corrosion, but a significant delay was found only for calcium nitrite with 30 L/m^3 concrete (CN30). The reduction in corrosion rate after initiation of corrosion was moderate, however (Figure 14.7(b)) (Trépanier et al., 2001). These results were

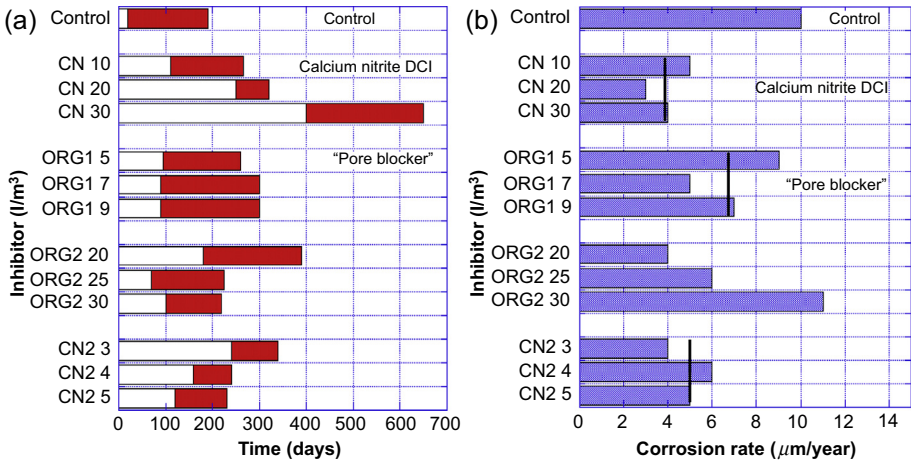


Figure 14.7 Effect of different inhibitors on the initiation of corrosion in mortar (a) and the corrosion rate after initiation (b). Mortar lollipops, w/c = 0.5, at 20 days curing, partially immersed in 3.5% NaCl (steel surface 62.7 cm^2) (Trépanier et al., 2001).

essentially confirmed by Ormellese et al. (2006) in a study of four commercial inhibitors, showing that the time to corrosion initiation were prolonged by adding inhibitors, but the results showed a huge scatter. No significant effect was found regarding the corrosion rate.

Another proprietary inhibitor blend comprising an oil/water emulsion—wherein the oil phase comprises an unsaturated fatty acid ester of an aliphatic carboxylic acid with a mono-, di-, or trihydric alcohol and the water phase comprises a saturated fatty acid, an amphoteric compound, a glycol, and a soap (Bobrowski et al., 1993)—delayed the onset of corrosion. Its main action is to reduce ingress of water and chlorides into the concrete as a pore blocker (Nmai and McDonald, 1999).

14.3.3 Mechanistic action of the organic inhibitor blends

As already indicated, the main difficulty with the independent evaluation of organic "corrosion inhibitors" are their complex, essentially unknown composition. Most of the published work has been undertaken with commercially available blends; their composition might vary over time without notice.

Research work at ETH Zurich revealed that the inhibitor blend Cortec MCI 2000 consisted of two main fractions: a volatile amine, mainly dimethylethanolamine (about 95%), and a nonvolatile part ($\sim$5%) (Elsener et al., 1999, 2000). Electrochemical measurements in alkaline solutions showed that both components of the inhibitor are needed to prevent initiation of corrosion (Figure 14.5). If the volatile or the nonvolatile component were present alone, they had no beneficial effect as a corrosion inhibitor. Electrochemical impedance spectroscopy (EIS) measurements performed with steel in saturated $Ca(OH)_2$ solutions containing 10% of the inhibitor blend MCI 2000 clearly revealed a second time constant at high frequencies, which implies film formation on the passive steel surface in the presence of the inhibitor (Elsener et al., 2000). The use of modern surface analysis techniques (X-ray photoelectron spectroscopy (XPS), Time-of-Flight Secondary Ion Mass Spectroscopy (ToF-SIMS)) has revealed that an organic layer formed on the steel surface in alkaline solutions in the presence of the inhibitor blend (Rossi et al., 1997), which confirms the electrochemical results of Elsener et al. (2000). However, when applied to inhibitor blends of unknown composition, such interpretations remain somewhat speculative.

Summarizing these laboratory studies, several pure organic substances and commercial inhibitor blends can delay the onset of corrosion for chloride-induced corrosion on passive steel, both in alkaline solutions and in mortar or concrete. The time to corrosion in the presence of the studied inhibitors increased by a factor of approximately 1.5−3. However, due to the stochastic nature of localized corrosion, the time to corrosion onset varies greatly—both in the absence and in the presence of inhibiting substances (see Figures 14.3 and 14.6). All investigations—independent of the type of inhibitor—seem to indicate that a critical molar ratio inhibitor/chloride of about 0.5−1 has to be exceeded for the inhibitor to have an effect. This implies that relatively high inhibitor concentrations have to be present in the pore water of concrete in order to act against chlorides penetrating from the concrete surface. To limit chloride ingress and thus the need for excessively high inhibitor concentrations, and also to avoid leaching of the inhibiting substances, the use of admixed inhibitors is thus only recommended in combination with high-quality (dense) concrete.

14.4 Critical evaluation of corrosion inhibitors

Assuming that, for a given substance, a corrosion inhibiting effect is apparent in laboratory experiments, there remain several critical points and open questions for an application on reinforced concrete structures:

- How to test corrosion inhibiting substances reliably in the laboratory in order to obtain practice-related results?
- How to ensure that the inhibitor is present at the reinforcing steel in sufficiently high concentrations with respect to the aggressive (chloride) ions also over a long period of time?
- How to quantify the effect of the inhibitor on corrosion of steel in concrete in comparison to inhibitor-free concrete?

14.4.1 Testing corrosion inhibitors

Newly developed corrosion inhibitors for steel in concrete have to be tested in the laboratory before they can be safely applied in practice. Laboratory tests may include both screening tests in solutions and in mortar and concrete. Accelerated tests should preferably be used in order to allow rapid evaluation of the performance of the inhibiting substance and to define the necessary dosage. The challenge, however, remains to extrapolate these laboratory results to long-term and field performance. The gap between these two situations can only be closed by providing mechanistic understanding of the inhibiting action. This chapter discusses a few selected test methods that can be used to study the performance of inhibitors for steel in concrete.

A *macro-cell* type of test was standardized by the American Society for Testing and Materials as ASTM G109-02 "Standard Test Method for Determining the Effects of Chemical Admixtures on the Corrosion of Embedded Steel Reinforcement in Concrete Exposed to Chloride Environments." The test involves a concrete beam ($28 \times 15 \times 11$ cm) with three embedded reinforcing steel bars—one on the top part of the beam and two at the bottom part. The beams are subjected to cycles of ponding with 3% NaCl solution on the top of the beam during 2 weeks, followed by a dry period of 2 weeks. The macro-cell current between the top bar (anode) and the two bottom bars (cathodes), as well as the open circuit potential of the bars, are measured (reference electrode located in the ponding solution). The end criterion of the test is when the average macro-cell current of the inhibitor-free control specimens exceeds 10 μA (the 95% limit of test duration is approximately 6 months). For the evaluation, the current integrated over time of control and test specimens are calculated and the rebars are examined visually. One disadvantage of this test is its long duration.

Frequently, *electrochemical techniques* are applied to test inhibitors in a wide variety of different experimental test setups. The simplest test, half-cell potential measurements, can be used reliably to determine the time-to-initiation of corrosion (Figure 14.1) by a drop in the corrosion potential of the rebar tested. The statistical distribution of the initiation time has to be taken into account (Figures 14.3 and 14.6). Alternatively or complementary, corrosion rate measurements (using the polarization resistance technique) are possible in the laboratory and suitable in principle, also on

large specimens or in the field. It is strongly recommended to perform visual examination of steel bars at the end of testing for evaluating the corrosion pit area and depth.

In summary, the effect of delaying corrosion initiation by admixed inhibitors can usually be clearly established (if present), but its applicability to long-term field conditions is questionable. A reduction of corrosion rate after initiation is more difficult to quantify and transfer the results to field conditions.

14.4.2 Concentration dependence

The available literature indicates a concentration-dependent effect of inhibitors, in the sense that a critical ratio inhibitor−chloride ratio has to be exceeded (see above). For new structures, the inhibitor dosage thus has to be specified with respect to the expected chloride concentration for the design life of the structure. To check if the inhibitor dosage is really present at the reinforcement is difficult due to the lack of analytical methods to measure the inhibitor concentration (Page, 2005). Regarding the long-term efficiency, it has to be taken into account that inhibitors may be leached out from the concrete, that volatile components may evaporate, or that the inhibiting substance is consumed during its action.

14.4.3 Measurement and control of inhibitor action

One of the main difficulties in evaluating the performance of inhibitors in real structures or in field trials is assessment of the inhibitor action on rebar corrosion "on site". The interpretation of half-cell potential measurements may be difficult due to time-dependent changes in the concrete humidity and resistivity or due to the presence of alternative redox couples introduced by the inhibiting substance. Furthermore, a reduction in corrosion rate due to an inhibitor is not always reflected directly in the half-cell potential.

Results of corrosion rate measurements on site depend on many factors, such as the type of device used or daily and seasonal changes of temperature and concrete humidity. This time variability makes it difficult to evaluate the efficiency of an inhibitor over time. Macro-cell current measurements between isolated anodes and the surrounding cathode (e.g., embedded probes such as "ladders" or macro-cell elements) may give the most indicative results.

14.5 Concluding remarks

This chapter presents the state-of-the-art concerning corrosion-inhibiting admixtures for concrete. It is based on an earlier literature review (Elsener, 2001) and includes updates (Elsener, 2011). The state of the field is similar to 10−15 years ago and can be summarized as follows:

- There is a general agreement that mixed-in corrosion inhibitors can strongly delay the onset of chloride-induced corrosion (by a factor of 2−3 in time), given a sufficiently high dosage. This was apparent from both laboratory and field studies.

- Concerning corrosion propagation, there are no results clearly demonstrating that corrosion inhibitors can reduce the corrosion rate.
- Conclusive long-term field results that confirm short-term laboratory results are mostly missing, particularly for organic corrosion inhibitors.
- It appears that the concrete quality (w/c ratio, supplementary cementitious materials, curing, execution, etc.) have a more pronounced influence on corrosion performance than the presence or absence of corrosion inhibitors. Obviously, the most durable structures can be achieved by combining high-quality concrete with corrosion inhibitors.
- Engineers and contractors working in the area of concrete maintenance should be aware of the fact that the composition of proprietary corrosion inhibitors are marketed under different trade names and may change in composition with time and geographic region.

References

Abd El Halem, S.M., Killa, H.M., 1980. Inhibition of pitting corrosion of mild steel by organic amines. In: Proc. 5th European Symposium on Corrosion Inhibitors, Università degli Studi di Ferrara, pp. 725−740.

ACI Committe 222, 1996. Corrosion of Metals in Concrete. American Concrete Institute, Detroit, USA.

Aitcin, P.-C., 2016. Corrosion inhibition. In: Aitcin, J.P., Flatt, R. (Eds.), Science and Technology of Concrete Chemical Admixtures (Chapter 24), pp. 471−480.

Andrade, C., Sarria, J., Alonso, C., 1996. Statistical study on simultaneous monitoring of rebar corrosion rate and internal RH in concrete structures exposed to the atmosphere. In: Page, C.L., Bamforth, P., Figg, J.W. (Eds.), Corrosion of Reinforcement in Concrete Construction. SCI, pp. 233−242.

Angst, U., Elsener, B., Larsen, C.K., Vennesland, Ø., 2010. Potentiometric determination of the chloride ion activity in cement based materials. Journal of Applied Electrochemistry 40, 564−573.

Angst, U., Elsener, B., Larsen, C., Vennesland, O., 2009. Critical chloride content in reinforced concrete−a review. Cement and Concrete Research 39 (2009), 1122−1138.

Bakker, R.F., 1988. Initiation period. In: Schiessl, P. (Ed.), Corrosion of Steel in Concrete, RILEM Report. Chapman and Hall, pp. 22−42.

Berke, N.S., 1989. Corrosion Inhibitors in Concrete. Corrosion 89, New Orleans. Paper 445.

Berke, N.S., Dallaire, M.P., Hicks, M.C., Ropes, R.J., 1993. Corrosion of steel in cracked concrete. Corrosion NACE 49, 934−943.

Berke, N.S., Rosenberg, A.M., 2004. Calcium nitrite corrosion inhibitor in concrete. In: Vazques, E. (Ed.), Admixtures for Concrete: Improvement of Properties. CRC press, pp. 282−299.

Bertolini, L., Elsener, B., Redaelli, E., Polder, R., Pedeferri, P., 2013. Corrosion of Steel in Concrete−Prevention, Diagnosis, Repair, second ed. WILEY VCH.

Bobrowski,G.S., Bury, M.A., Farrington, S.A., Nmai, C.K., 1993. Admixtures for Inhibiting Corrosion of Steel in Concrete, United States Patent, Patent No. 5.262.089.

Bolzoni, F., Brenna, A., Fumagalli, G., Goidanich, S., Lazzari, L., Ormellese, M., Pedeferri, M.P., 2014. Experiences on corrosion inhibitors for reinforced concrete. International Journal of Corrosion and Scale Inhibition 3, 254−278.

Breit, W., 1998. Critical chloride content−investigations of steel in alkaline chloride solutions. Materials and Corrosion 49 (1998), 539−550.

Browne, R.D., 1980. Mechanisms of corrosion of steel in concrete in relation to design, inspection and repair of offshore and coastal structures. In: Malhotra, V.M. (Ed.), Performance of Concrete in Marine Environment. ACI Publication SP-65, pp. 169–204.

Cigna, R., Mercalli, A., Peroni, G., Grisoni, L., Mäder, U., 1997. Influence of corrosion inhibitors containing aminoalcohols on the prolongation of service life of RC structures. In: Int. Conf. on Corrosion and Rehabilitation of RC Structures, Orlando USA (on CD).

Cigna, R., Mercalli, A., Grisoni, L., Mäder, U., 2007. Effectiveness of mixed in organic inhibitors on extending the service life of reinforced concrete structures. In: Raupach, M., Elsener, B., Polder, R., Mietz, J. (Eds.), EFC publication 38, pp. 203–210.

Cortec Company, Product Information Sheet. http://www.cortecvci.com/Publications/PDS/MCI-2000.pdf (last access 09.09.15).

DeBerry, D.W., 1993. Organic inhibitors for pitting corrosion. In: Raman, A., Labine, P. (Eds.), Review on Corrosion Inhibitor Science and Technology. NACE, Houston.

El-Jazairi, B., Berke, N., 1990. In: Page, C.L. (Ed.), Corrosion of Reinforcement in Concrete Construction. Elsevier Applied Science, London, p. 571.

Elsener, B., Büchler, M., Stalder, F., Böhni, H., 1999. A migrating corrosion inhibitor blend for reinforced concrete, Part I: prevention of corrosion. Corrosion 55, 1155–1163.

Elsener, B., 2000. Corrosion of steel in concrete. In: Corrosion and Environmental Degradation. Materials Science and Technology Series, vol. 2. John Wiley, p. 389–436.

Elsener, B., Büchler, M., Böhni, H., 2000. Organic corrosion inhibitors for steel in concrete. In: Mietz, J., Polder, R., Elsener, B. (Eds.), Corrosion of Reinforcement in Concrete–Corrosion Mechanism and Corrosion Protection. IOM Communication, London, pp. 61–71.

Elsener, B., 2001. Corrosion Inhibitors for Steel in Concrete–State of the Art Report. EFC Publication 35, Maney Publishing.

Elsener, B., Zimmermann, L., Böhni, H., 2003. Non-destructive determination of the free chloride content in cement based materials. Materials and Corrosion 54, 440–446.

Elsener, B., 2007. In: Raupach, M., Elsener, B., Polder, R., Mietz, J. (Eds.), Corrosion Inhibitors for Reinforced Concrete–an EFC State of the Art Report. EFC publication 38, pp. 170–184.

Elsener, B., 2011. Corrosion Inhibitors–An Update on On-going Discussion, 3, Länder Korrosianstagung "Möglichkeiten des Korrosionsschutzes in Beton" 5/6. Mai. Wien GfKorr Frankfurt am Main, pp. 30–41.

European Patent Application, 1987. No. 8630438.2, Publication No. 0 209 978, published 28.01.87 Bulletin 87/5.

fib, 2013. Model Code for Concrete Structures 2010 (MC2010). International Federation for Structural Concrete.

Frankel, G.S., 1998. Journal of Electrochemical Society 145, 2186–2198.

Gaidis, J.M., Rosenberg, A.M., 1987. Cement, Concrete and Aggregates 9, 30.

Griffin, D.F., 1975. Corrosion inhibitors for reinforced concrete. In: Corrosion of Metals in Concrete, ACI SP-49. American Concrete Institute, p. 95.

Hartt,W.H., Rosenberg, A.M., 1989. American Concrete Institute, Detroit, SP 65-33, pp. 609–622.

Heren, Z., Oelmez, H., 1996. Cement and Concrete Research 26, 701–705.

Hobbs, D.W., 1994. Carbonation of concrete containing PFA. Magazine Concrete Research 46, 35–38.

Hornbostel, K., Larsen Claus, K., Geiker Mette, R., 2013. Relationship between concrete resistivity and corrosion rate–a literature review. Cement and Concrete Composites 39, 60–72.

Laamanen, P.H., Byfors, K., 1996. Corrosion inhibitors in concrete–alkanolamine based inhibitors. In: Nordic Concrete Research No. 19, 2/1996, Nordic Concrete Research Oslo.

Mäder, U., 1994. In: Swamy, N. (Ed.), A New Class of Corrosion Inhibitors, Corrosion and Corrosion Protection of Steel in Concrete, vol. II. Sheffield University Press, p. 851.
Moskwin, V.M., Alekseyeev, S.M., 1958. Beton i Zhelezobeton 2, 21.
Nmai, C.K., Farrington, S.A., Bobrowski, G.S., 1992. Concrete International, American Concrete Institute 14, 45.
Nmai, C.K., McDonald, D., 1999. Long term effectiveness of corrosion inhibiting admixture and implications for the design of durable reinforced concrete structures: a laboratory investigation. In: RILEM Int. Symp. on the Role of Admixtures in High Performance Concrete.
Nürnberger, U., Beul, W., 1991. Materials and Corrosion 42, 537–546.
Nürnberger, U., 1996. Corrosion inhibitors for steel in concrete. Otto Graf Journal 7, 128.
Ormellese, M., Berra, M., Bolzoni, F., Pastore, T., 2006. Corrosion inhibitors for chloride induced corrosion in reinforced concrete structures. Cement and Concrete Research 36, 536–547.
Ormellese, M., Lazzari, L., Goidanich, S., Fumagalli, G., Brenna, A., 2009. Corrosion Science 51, 2959.
Page, C.L., Short, H.R., El-Tarra, A., 1981. Diffusion of chloride ions in hardened cement paste. Cement and Concrete Research 11 (1981), 395–406.
Page, C.L., Ngala, V.T., Page, M.M., 2000. Corrosion inhibitors in concrete repair systems. Magazine of Concrete Research 52 (2000), 25–37.
Page, M.M., 2005. Journal of Separation Science 28 (2005), 471–476.
Phanasgaonkar, A., Cherry, B., Forsyth, M., 1997. Corrosion inhibition properties of organic amines in a simulated Concrete environment. In: Proc. Int. Conference "Understanding Corrosion Mechanisms of Metals in Concrete–A Key to Improving Infrastructure Durability", Massachusetts Institute of Technology, MIT (Cambridge, USA) section 6.
Rasheeduzzafar, F.D., Mukarram, K., 1987. Influence of cement composition and content on the corrosion behaviour of reinforcing steel in concrete. In: Malhotra, V.M. (Ed.), Concrete Durability. ACI SP-100, Detroit, pp. 1477–1502.
Richartz, W., 1996. Die Bindung von Chlorid bei der Zementerhärtung. Zement-Kalk-Gips 10, 447–456.
Rossi, A., Elsener, B., Textor, M., Spencer, N.D., 1997. Combined XPS and ToF-SIMS analyses in the study of inhibitor function—organic films on iron. Analusis 25 (5), M30.
Söylev, T.A., Richardson, M.G., 2008. Corrosion inhibitors for steel in concrete: state of the art report. Construction and Building Materials 22, 609–622.
Tang, L., Nilsson, L.O., 1993. Chloride binding capacity and binding isotherms of OPC pastes and mortars. Cement and Concrete Research 23, 347–353.
Tomosawa, F., Masuda, Y., Fukushi, I., Takakura, M., Hori, T., 1990. Experimental study on the effectiveness of corrosion inhibitor in reinforced concrete. In: Proc. Int. RILEM Symp. Admixture for Concrete Improvement and Properties (1990), pp. 382–391.
Trabanelli, G., 1986. Corrosion inhibitors. In: Mansfeld, F. (Ed.), Corrosion Mechanisms. Marcel Dekker, N.Y (Chapter 3).
Trépanier, S.M., Hope, B.B., Hansson, C.M., 2001. Corrosion inhibitors in concrete. Part III: effect on time to chloride induced corrosion initiation and subsequent corrosion rate of steel in mortar. Cement and Concrete Research 31, 713–718.
Tritthart, J., 1989. Chloride binding in cement: the influence of the hydroxide concentration in the pore solution of hardened cement paste on chloride binding. Cement and Concrete Research 19, 683–691.
Tuutti, K., 1982. Corrosion of Steel in Concrete. Swedish Cement and Concrete Research Institute, Stockholm.
Wierig, H.J., 1984. Long-term studies on the carbonation of concrete under normal outdoor exposure. In: RILEM Seminar Hannover.

Zimmermann, L., Schiegg, Y., Elsener, B., Böhni, H., 1997. Electrochemical techniques for monitoring the conditions of concrete bridge structures, repair of concrete structures. Svolvaer Norway. In: Blankvoll, A. (Ed.), Norwegian Road Research Laboratory (1997), pp. 213−222.

Zimmermann, L., Elsener, B., Böhni, H., 2000. Critical Factors for the Initiation of Rebar Corrosion, Corrosion of Reinforcement in Concrete: Corrosion Mechanisms and Corrosion Protection. EFC Publication No. 31, The Institute of Materials, London, pp. 25−33.

Formulation of commercial products

15

S. Mantellato[1], A.B. Eberhardt[2], R.J. Flatt[1]
[1]Institute for Building Materials, ETH Zürich, Zürich, Switzerland; [2]Sika Technology AG, Zürich, Switzerland

15.1 Introduction

Commercial chemical admixtures are classified according to their main action in concrete, as listed in EN 206-1 (ASTM C494, 2013). Most admixtures are usually supplied as low-density aqueous solutions in a range of concentrations by mass between 15% and 40%. Additionally, they can also be present in powder, such as in ready-mix mortars.

Many factors need to be considered when selecting a chemical admixture, the main one being its final application. For instance, in ready-mix concretes, the main requirement is a good slump retention until the concrete is placed. The time span can go from a few to several hours. In some circumstances, such as traffic jams or long distances from the concrete plants to the job sites, the workability should be maintained for a long time. On the other hand, precast concretes require a high water reduction, whereas the slump retention is important only in the first 30 min after mixing. Moreover, a fast hardening process is necessary in precast concretes to increase the number of deforming cycles during the working hours. This aspect is also becoming important in ready-mix applications to speed up construction processes. Readers more interested in the chemical nature of these admixtures may consult the overview proposed by Gelardi et al. (2016).

15.2 Performance targets

Unfortunately, one single pure superplasticizer can most often not efficiently satisfy all of the above-mentioned requirements at the same time. Therefore, commercial concrete admixtures are often multicomponent products appropriately formulated to adapt to the performance needs of different users. Combining different types of superplasticizers and also other admixtures in a single formulation with reliable performance is not a trivial task. The presence of one compound can affect the performance of the others, for example, due to their competitive adsorption on cement (Plank and Winter, 2008; Plank et al., 2010; Bey et al., 2014; Marchon et al., 2016; Marchon et al., 2013). Moreover, the combination of different chemicals can lead to instability of the formulation and sometimes phase segregation.

Most of the conventional components and combinations of them, mainly accelerators and retarders, were developed and patented between 1980s and 1990s, and they are still in use in commercial formulations nowadays (Ramachandran, 1996). At that time, the water

Science and Technology of Concrete Admixtures. http://dx.doi.org/10.1016/B978-0-08-100693-1.00015-1
Copyright © 2016 Elsevier Ltd. All rights reserved.

reduction was obtained by using polynaphtalene sulfonate (PNS) and polymelamine sulfonate (PMS) based-plasticizers.

The innovative turning point occurred at the beginning of 2000s with the introduction to the market of superplasticizers based on polycarboxylate ether polymers (PCEs), together with the intensive use of blended cements and more extreme construction processes. These factors involved new problems related to the formulation stability and compatibility with new materials, promoting research and development toward more robust and advanced commercial products.

15.2.1 Slump retention

A typical commercial admixture may consist of polymers having high water reduction capability in combination with other ones showing good slump retention. For example, the workability of high-range water reducers, such as PNS and PMS, can be enhanced by blending such superplasticizers with lignosulfonates, with the additional advantage of having a low-cost final formulation (Chang et al., 1995).

Other solutions include blends of pure PCEs. In these blends, the slump-keeper polymers can be either copolymers having a high grafting degree (low amount of charges on the backbone) or acrylic-based PCEs, of which the side chains can undergo hydrolysis in alkaline pore solutions (Mäder et al., 2004).

15.2.2 Environmental conditions

The environmental conditions in which the concrete is used play an important role in the choice of the admixtures. In summer or in countries with a hot climate, cement hydration is accelerated and the workability is rapidly lost, affecting the truck discharge, the pumpability, the final casting, and the surface finish. In these circumstances, retarders must be added to the concrete to slow down the hydration process. On the other hand, in cold environments, both setting and hardening can be delayed, and the addition of accelerators is advisable to keep the construction process at a reasonable speed. In winter or in cold countries, concretes should also be resistant to freeze/thaw cycles.

15.2.3 Setting and hardening control

Commercial admixtures may be formulated with various accelerators and retarders either to adapt for climate conditions or accommodate for the retarding effect of one or more components. The use of such compounds allows also gaining the desired setting and/or hardening time. Accelerators and retarders may include inorganic or organic salts or acid-based compounds with a discussing of their working mechanisms given by Marchon and Flatt (2016).

As accelerators, nitrate, nitrite, formate, thiosulfate, and thiocyanate salts are preferred in formulations for precast concretes, whereas triisopropanolamine (TIPA) and triethanolamine (TEA) are more common for ready-mix applications (Ramachandran, 1996). The use of chloride salts is progressively decreasing because they can induce corrosion of steel reinforcements. A new generation of accelerators based on C-S-H seed suspensions has been introduced in recent years (Nicoleau et al., 2013).

In superplasticizer formulations, lignosulfonate salts and carbohydrates (e.g., sucrose and glucose) as well as hydroxylated carboxylic acids and salts (e.g., sodium gluconate, citric and tartaric acids) are commonly used as set retarders (Ramachandran, 1996). Phosphonates (ATMP, HEDP, etc.) are preferred in specific applications where a very strong retardation is required.

In shotcrete, alkali-free admixtures, such as aluminum salts (as hydroxy, sulfate formate, etc.), silicate salts, or amorphous aluminum oxides are generally used as set accelerators. Products based on aluminum sulfate most often also contain an organic or inorganic acid that stabilizes high concentration solutions against precipitation before use (increase of the shelf-life) (Lootens et al., 2008).

15.2.4 Defoamers

Some concrete admixtures, containing PCEs and viscosity modifying admixtures (VMAs), both alone and in combination, have the tendency to produce large air bubbles in concrete that may be persistent even after vibration, mainly in viscous concrete mixes (ACI Materials Journal, 2002; Łaźniewska-Piekarczyk, 2013). Unlike the air produced by air-entraining agents, the amount and the quality of the entrapped air are not controlled, which leads to reduced strength without any benefit for freezing resistance (Dolch, 1996; Nkinamubanzi et al., 2016). To avoid this, defoamers or antifoam agents—such as tributylphosphate (TBP), dibutylphthalate, silicones, esters or carbonic acids, and ethylene oxide/propylene oxide (EO/PO)-based copolymers (Lorenz et al., 2010; Darwin et al., 2000)—are used. They show good effectiveness in concrete at low dosages and are added to formulations in liquid or emulsion form (Shendy et al., 2003; Shendy et al., 2005).

The defoamer should in principle maintain a low air content over mixing time (no spiraling effect) and show good stability. However, part of the defoamer may segregate upward and separate over long storage, leading to an inhomogeneous composition of the admixture. The high hydrophobicity of most of the used defoamers (except the water-soluble TBP) is the reason for the destabilization of aqueous formulations. Therefore, the choice of the adequate defoamer mainly depends on its compatibility with the type, polarity, and concentration of the used superplasticizers and other components, as well as the dilution of the final product.

15.2.5 Co-surfactants and hydrotropic compounds

For all cases of admixtures containing hydrophobic compounds, such as water-insoluble defoamers in formulated superplasticizers or nonionic surfactants in shrinkage-reducing admixtures (SRA), the solubilization capacity of the aqueous solution can be increased through the addition of co-surfactants (Rosen, 2004) or hydrotropic substances (Lunkenheimer et al., 2004). Co-surfactants serve as a solvent to increase molecular solubility, whereas hydrotropic substances impact the water structure (water structure breaker), thus promoting the formation of micelles or microemulsions.

The solubilizing agents are added in admixtures to solubilize water-insoluble compounds in aqueous solutions. Therefore, they prevent the phase separation of hydrophobic compounds during transport and storage so that the admixture can

be exactly dosed without prior agitation or remixing, guaranteeing a homogeneous distribution in concrete.

In particular, the presence of electrolytes in the aqueous phase of fresh concrete significantly decreases the solubility for hydrophobic compounds. Therefore, formulated admixtures may contain additional amounts of co-surfactants and/or hydrotropic compounds to mitigate the loss of hydrophobic compounds through phase separation, self-aggregation, or surface aggregation (Alexandridis and Holzwarth, 1997; Bauduin et al., 2009; Kabalnov et al., 1995; Leontidis, 2002; Morini et al., 2005; Partyka et al., 1984; Tadros, 2006).

For some shrinkage-reducing admixtures (Eberhardt and Flatt, 2016), glycols are used as water structure breakers to solubilize nonionic surfactants in formulation and to decrease self-aggregation of the nonionic surfactant in concrete (Eberhardt, 2011). In the case of superplasticizers, stable combinations of polymeric dispersants and water-insoluble defoamers are based on the addition of co-surfactants that provide sufficient solubilization (Lorenz et al., 2010) or allow the formation of microemulsions (Darwin et al., 2000; Shendy et al., 2003; Shendy et al., 2005).

15.2.6 Biocides

Another aspect to consider is the stability of aqueous solutions of organic admixtures toward microbial attack, both during transport and storage. The contamination and spoilage could lead, in the worst cases, to phase separation of the components and production of gases or unpleasant odors in the storage tanks. Therefore, biocides are added in formulations at dosages far below 1%. Formaldehyde- and isothiazolone-based derivatives and combinations of both as well as Bronopol and glutaraldehyde solutions are very common biocides for concrete additives. Biocides should have low toxicity, good biodegradability, and often be Volatile Organic Carbon (VOC)-free compounds.

15.3 Cost issues

Pure synthetic PCEs are more expensive than older-generation superplasticizers and the extensive use of such products is not always economically convenient. Therefore, the use of PCEs to produce blends can represent a way to reduce the cost of such formulations. However, the use of PCEs in blends is limited. Indeed, blends of PNS and PCE polymers were found to exhibit negative synergy with regard to slump and are not stable in formulations with most of the used proportions (Coppola et al., 1997). However, the drastic increase of viscosity observed with this blend might be beneficial for specific applications in shotcrete (Pickelmann and Plank, 2012). Also, PMS−PCE polymer blends showed intermediate performance regardless of the type of cement and the cost/benefit ratio was not favorable (Coppola et al., 1997). In contrast, PCE polymers can be conveniently used with lignosulfonates showing comparable initial fluidity and slump retention to the pure PCE polymer (Coppola et al., 1997; GonÇalves and Bettencourt-Ribeiro, 2000).

Besides the main active ingredient, the superplasticizer, or blends of them, cost-effective compounds are also often added to formulations to adjust the performance of the final product to the users' demands.

15.4 Conclusions

Advanced technologies are required to achieve high performance in terms of fluidity, strength, and durability, and each concrete mix must be optimized with respect to them. However, not all properties respond in the same way by varying the type or dosage of a particular admixture.

This is where the art of formulation comes into play. By the experienced and balanced combination of a limited number of compounds, a large portfolio of products is offered to cover a much broader range of performances. However, the complexity of cementitious systems, in particular blended ones, makes the efficiency of formulations more demanding. As a consequence, more knowledge-based design of concrete formulations having both a reduced environmental impact and a reliable performance need to be found.

This can be seen as an exciting challenge in which the basic science dealing with cement−admixture interactions can be integrated to obtain rapid outcomes in admixture formulations.

Acknowledgments

Support for Sara Mantellato was provided by the SNF project (n. 140615) titled "Mastering flow loss of cementitious systems."

References

Air-void stability in self-consolidating concrete. ACI Materials Journal 99 (4), 2002. http://dx.doi.org/10.14359/12224.

Alexandridis, P., Holzwarth, J.F., 1997. Differential scanning calorimetry investigation of the effect of salts on aqueous solution properties of an amphiphilic block copolymer (Poloxamer). Langmuir 13 (23), 6074−6082. http://dx.doi.org/10.1021/la9703712.

ASTM C494, 2013. Specification for chemical admixtures for concrete. ASTM International. http://enterprise.astm.org/filtrexx40.cgi?+REDLINE_PAGES/C494C494M.htm#_ga=1.237524416.1533275664.1378974238.

Bauduin, P., Wattebled, L., Touraud, D., Kunz, W., 2009. Hofmeister ion effects on the phase diagrams of water-propylene glycol propyl ethers. Zeitschrift Für Physikalische Chemie/International Journal of Research in Physical Chemistry and Chemical Physics 218 (6/2004), 631−641. http://dx.doi.org/10.1524/zpch.218.6.631.33453.

Bey, H.B., Hot, J., Baumann, R., Roussel, N., 2014. Consequences of competitive adsorption between polymers on the rheological behaviour of cement pastes. Cement and Concrete Composites 54, 17−20. http://dx.doi.org/10.1016/j.cemconcomp.2014.05.002.

Chang, D.Y., Chan, S.Y.N., Zhao, R.P., 1995. The combined admixture of calcium lignosulphonate and sulphonated naphthalene formaldehyde condensates. Construction and Building Materials 9 (4), 205–209. http://dx.doi.org/10.1016/0950-0618(95)00011-4.

Coppola, L., Erali, E., Troli, R., Collepardi, M. (Eds.), 1997. Blending of Acrylic Superplasticizer with Napthalene, Melmine or Lignosulfonate-Based Polymers In: Proceedings 5th CANMET/ACI International Conference on Superplasticizers and Other Chemical Admixtures in Concrete (V.M. Malhotra), Rome, Italy, pp. 203–224.

Darwin, D.C., Taylor, R.T., Jeknavorian, A.A., Shen, D.F., 2000. Emulsified Comb Polymer and Defoaming Agent Composition and Method of Making Same. Patent: US6139623 A.

Dolch, W.L., 1996. 8-Air-Entraining admixtures. In: Ramachandran, V.S. (Ed.), Concrete Admixtures Handbook, second ed. William Andrew Publishing, Park Ridge, NJ, pp. 518–557. http://www.sciencedirect.com/science/article/pii/B978081551373550012X.

Eberhardt, A.B., 2011. On the Mechanisms of Shrinkage Reducing Admixtures in Self Consolidating Mortars and Concretes. Bauhaus University, Weimar.

Eberhardt, A.B., Flatt, R.J., 2016. Working mechanisms of shrinkage-reducing admixtures. In: Aïtcin, P.-C., Flatt, R.J. (Eds.), Science and Technology of Concrete Admixtures, Elsevier (Chapter 13), pp. 305–320.

Gelardi, G., Mantellato, S., Marchon, D., Palacios, M., Eberhardt, A.B., Flatt, R.J., 2016. Chemistry of chemical admixtures. In: Aïtcin, P.-C., Flatt, R.J. (Eds.), Science and Technology of Concrete Admixtures, (Chapter 9), pp. 149–218.

GonÇalves, A., Bettencourt-Ribeiro, A., 2000. Comparative study of influence of superplasticizers and superplasticizer/plasticizer blends on slump-loss. In: Proceedings of the 6th CANMET/ACI International Conference on Superplasticizers and Other Chemical Admixtures in Concrete, Nice, ACI, SP-195, pp. 321–333.

Kabalnov, A., Olsson, U., Wennerstroem, H., 1995. Salt effects on nonionic microemulsions are driven by adsorption/depletion at the surfactant monolayer. The Journal of Physical Chemistry 99 (16), 6220–6230. http://dx.doi.org/10.1021/j100016a068.

Łaźniewska-Piekarczyk, B., April 2013. The influence of admixtures type on the air-voids parameters of non-air-entrained and air-entrained high performance SCC. Construction and Building Materials 41, 109–124. http://dx.doi.org/10.1016/j.conbuildmat.2012.11.086.

Leontidis, E., 2002. Hofmeister anion effects on surfactant self-assembly and the formation of mesoporous solids. Current Opinion in Colloid and Interface Science 7 (1–2), 81–91. http://dx.doi.org/10.1016/S1359-0294(02)00010-9.

Lootens, D., Lindlar, B., Flatt, R.J., 2008. In: Sun, W., VanBreugel, K., Miao, C., Ye, G., Chen, H. (Eds.), Some Peculiar Chemistry Aspects of Shotcrete Accelerators, vol. 61. R I L E M Publications, Bagneux.

Lorenz, K., Yaguchi, M., Sugiyama, T., Albrecht, G., 2010. Defoaming Agent for Cementitious Compositions. Patent: US7662882 B2.

Lunkenheimer, K., Schrodle, S., Kunz, W., 2004. Dowanol DPnB in water as an example of a solvo-surfactant system: adsorption and foam properties. In: Cabuil, V., Levitz, P., Treiner, C. (Eds.), Trends in Colloid and Interface Science XVII, 126. Springer-Verlag Berlin, Berlin, pp. 14–20.

Mäder, U., Schober, I., Wombacher, F., Ludirdja, D., 2004. Polycarboxylate polymers and blends in different cements. Cement, Concrete, and Aggregates 26 (2), 1–5. http://dx.doi.org/10.1520/CCA12314.

Marchon, D., Flatt, R.J., 2016. Impact of chemical admixtures on cement hydration. In: Aïtcin, P.-C., Flatt, R.J. (Eds.), Science and Technology of Concrete Admixtures, Elsevier (Chapter 12), pp. 279–304.

Marchon, D., Mantellato, S., Eberhardt, A.B., Flatt, R.J., 2016. Adsorption of chemical admixtures. In: Aïtcin, P.-C., Flatt, R.J. (Eds.), Science and Technology of Concrete Admixtures (Chapter 10), pp. 219–256.

Marchon, D., Sulser, U., Eberhardt, A.B., Flatt, R.J., 2013. Molecular design of comb-shaped polycarboxylate dispersants for environmentally friendly concrete, Soft Matter. http://dx.doi.org/10.1039/C3SM51030A.

Morini, M.A., Messina, P.V., Schulz, P.C., 2005. The interaction of electrolytes with non-ionic surfactant micelles. Colloid and Polymer Science 283 (11), 1206–1218. http://dx.doi.org/10.1007/s00396-005-1312-7.

Nicoleau, L., Gädt, T., Chitu, L., Maier, G., Paris, O., 2013. Oriented aggregation of calcium silicate hydrate platelets by the use of comb-like copolymers. Soft Matter 9 (19), 4864–4874. http://dx.doi.org/10.1039/C3SM00022B.

Nkinamubanzi, P.-C., Mantellato, S., Flatt, R.J., 2016. Superplasticizers in practice. In: Aïtcin, P.-C., Flatt, R.J. (Eds.), Science and Technology of Concrete Admixture (Chapter 16), pp. 353–378.

Partyka, S., Zaini, S., Lindheimer, M., Brun, B., 1984. The adsorption of non-ionic surfactants on a silica gel. Colloids and Surfaces 12, 255–270. http://dx.doi.org/10.1016/0166-6622(84)80104-3.

Pickelmann, J., Plank, J., 2012. A mechanistic study explaining the synergistic viscosity increase obtained from polyethylene oxide (PEO) and B-naphthalene sulfonate (BNS) in shotcrete. Cement and Concrete Research 42 (11), 1409–1416. http://dx.doi.org/10.1016/j.cemconres.2012.08.003.

Plank, J., Lummer, N.R., Dugonjić-Bilić, F., 2010. Competitive adsorption between an AMPS®-based fluid loss polymer and Welan gum biopolymer in oil well cement. Journal of Applied Polymer Science 116 (5), 2913–2919. http://dx.doi.org/10.1002/app.31865.

Plank, J., Winter, C.H., 2008. Competitive adsorption between superplasticizer and retarder molecules on mineral binder surface. Cement and Concrete Research 38 (5), 599–605. http://dx.doi.org/10.1016/j.cemconres.2007.12.003.

Ramachandran, V.S., 1996. 17-Admixture formulations. In: Ramachandran, V.S. (Ed.), Concrete Admixtures Handbook, second ed. William Andrew Publishing, Park Ridge, NJ, pp. 1045–1076. http://www.sciencedirect.com/science/article/pii/B9780815513735500210.

Rosen, M.J., 2004. Surfactants and Interfacial Phenomena. John Wiley & Sons.

Shendy, S., Bury, J.R., Luciano, J.J., Vickers Jr., T.M., 2003. Solubilized Defoamers for Cementitious Compositions. Patent: US6569924 B2.

Shendy, S.M., Bury, J.R., Vickers Jr., T.M., Ong, F., 2005. Mixture of Cements, Water Insoluble Antifoam Agent and Amine Solubilizer. Patent: US6875801 B2.

Tadros, T.F., 2006. Applied Surfactants: Principles and Applications. John Wiley & Sons.

Superplasticizers in practice

16

P.-C. Nkinamubanzi[1], *S. Mantellato*[2], *R.J. Flatt*[2]
[1]National Research Council Canada, Ottawa, ON, Canada; [2]Institute for Building Materials, ETH Zürich, Zurich, Switzerland

16.1 Introduction

Superplasticizers are used to increase the fluidity of concrete without adding excess water. These molecules physically separate the cement particles by opposing their attractive forces with steric and/or electrostatic forces, as explained in Chapter 11 (Gelardi and Flatt, 2016). As a result, the concrete is easier to place. The concrete workability can be maintained for a long period of time (1−2 hours or more), which is beneficial to many processes, including transport, pouring, pumping, compaction, and casting.

These benefits are so important and numerous that superplasticizers have become key ingredients of modern concretes. For example, they can be used to enhance workability without altering the water-to-binder (w/b) ratio that controls concrete durability and strength (see Chapter 11; Gelardi and Flatt, 2016). They can also be used to decrease the w/b ratio of concrete without compromising workability (Aïtcin, 1998; Dodson, 1990). This can be used to compensate for the lack of initial strength when mineral admixtures that do not react as quickly with water replace part of the cement (Bilodeau and Malhotra, 2000; Saric-Coric, 2001).

An important consequence of the above is that superplasticizers can be used to reduce the environmental impact of concrete construction by reducing the cement content per cubic meter of concrete (see Preface). Several other environmental benefits include the reduction of water consumption, the reduction of the amount of concrete needed to achieve a defined load bearing capacity, and the increase of concrete service life by enhancing durability (Flatt et al., 2012).

Modern concrete can contain several chemical admixtures, and it is essential for concrete producers to ensure that the concrete mixture will meet all the requirements in the fresh and hardened states. Situations of incompatibilities between different admixtures and/or between admixtures and cements should be prevented. In such cases, unexpected behavior can arise, occasionally forcing the producer to discard specific concrete batches. This makes it difficult to guarantee a constant quality over time and the "robustness" of the concrete mixture is compromised.

Fortunately, the interactions between cement and chemical admixtures are becoming better understood, so it is possible to pay more attention to the compatibility and robustness of such combinations. To properly address these issues, a brief overview of the practical benefits coming from the use of the most common superplasticizers is presented. Then, the basic impact of admixtures on rheology is detailed, combining ideally expected behaviors with the effect of cement−superplasticizer incompatibilities.

Science and Technology of Concrete Admixtures. http://dx.doi.org/10.1016/B978-0-08-100693-1.00016-3
Copyright © 2016 Elsevier Ltd. All rights reserved.

16.2 Application perspective on superplasticizers and their use

16.2.1 Main types of superplasticizers

In Chapter 9, we presented an extensive overview of the chemistry of chemical admixtures, in particular on superplasticizers (Chapter 9, Gelardi et al., 2016) Here, the most used superplasticizers are listed in terms of increased water-reduction capability:

- Lignosulfonates (LS), with a limited water-reduction ability of about 10%, are currently used mainly in formulations to enhance the workability retention in ready-mix applications.
- Sulfonated naphthalene formaldehyde condensates (PNS), also known as polynaphthalene sulfonates (PNS), have a weak interaction with clay minerals. They have a water reduction ability up to 30%.
- Polymelamine sulfonate (PMS) and sulfonated melamine formaldehyde condensate (PMS) demonstrate a possible decrease of the water content in concrete up to more than 20−30%.
- Synthetic polymers, such as polycarboxylates and acrylic copolymers (PCEs), have versatile chemical structures and can achieve up to 40% water reduction, but generally they have a low tolerance to clay minerals.

16.2.2 Practical benefits of dispersion by superplasticizers

The different ways to use high-range water-reducing admixtures, shown in Figure 16.1, result in either a reduced yield stress at constant solid content or water content or in an increase of the solid content (or decrease of the water-to-cement [w/c] ratio) at constant yield stress (Ramachandran et al., 1998). A variety of applications can be achieved by decreasing the w/c and at the same time increasing the slump of the concrete (Aïtcin, 1998; Saric-Coric, 2001), such as in the case of self-consolidating concretes, needing high initial slump and high strength of the hardened concrete.

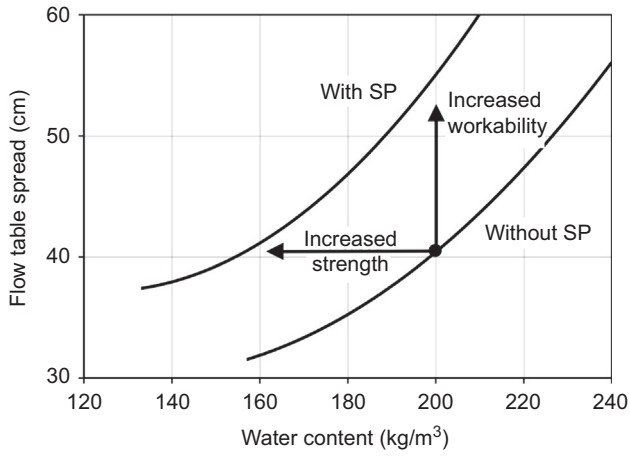


Figure 16.1 Different ways to use high-range water-reducing admixtures. Reproduced with permission from Ramachadran et al. (1998).

Among these practical benefits, the use of admixtures is becoming more important in providing sustainable quality concrete mixtures by using supplementary cementitious materials and more advanced engineering technologies, such as high performance, self-compacting, underwater, fiber-reinforced, high-volume fly ash, high-volume slag, and reactive powder concretes.

16.2.3 Rheological tests for superplasticizers in cementitious systems

Several attempts have been made to determine with a limited number of tests which combinations of cement and superplasticizer may be incompatible. However, these efforts partially failed because of the large variety of performance measured with different water reducers. In addition, cements cannot be fully mastered using constrained standard norms and the direct testing case-by-case under the appropriate operative conditions remains the only solution.

It is worth mentioning that an attempt was made to extend the standards of water reducers to the case of superplasticizers, only to realize that it does not always work. Additionally, some standards organizations decided to use a particular cement as a reference, or a composite cement made of a blend of three common cements used in a particular location. However, these approaches only specifically inform about the specific cement or blend being used, and their results are not predictive of the behavior of the broader range of cements used in practice. Consequently, there is no other way than testing cement/superplasticizer combinations directly.

Because concrete tests are demanding in terms of materials, energy, time, and space, researchers have developed simplified testing procedures on grouts and mortars that are much easier and quicker to perform (Roussel, 2012). Recent developments in rheology have established the fundamental links between many of these tests and basic rheological properties (Roussel, 2012). The most widely used tests are the mini-slump, flow spread, and the Marsh cone test. These tests are usually performed during the 90 min after mixing to evaluate how the rheological properties change in the timeframe when concrete is placed in practice. The first two relate directly to yield stress and the third is mainly controlled by plastic viscosity if the yield stress is low enough (Roussel, 2012).

Surprisingly, a good correlation between Marsh cone tests and mini-slump tests has been found using PNSs. Indeed, results have suggested that plastic viscosity also depends on superplasticizer adsorption, but to a lower extent than yield stress (Hot et al., 2014). This may explain the correlation between both test results. In particular, it may support the idea that Marsh cone tests may also be effective in determining saturation points of superplasticizers. These are the dosages leading to full surface coverage and above which little or no further effect is found (Figure 16.2).

These simplified tests are usually performed on paste rather than concrete. Therefore, it is worth briefly mentioning that the main differences between the rheology of these materials come from the presence of coarse aggregates and sands in the concrete matrix. The paste between these aggregates is subject to high shear forces (and shear energy), which is why, if prepared alone, it must be intensely mixed to

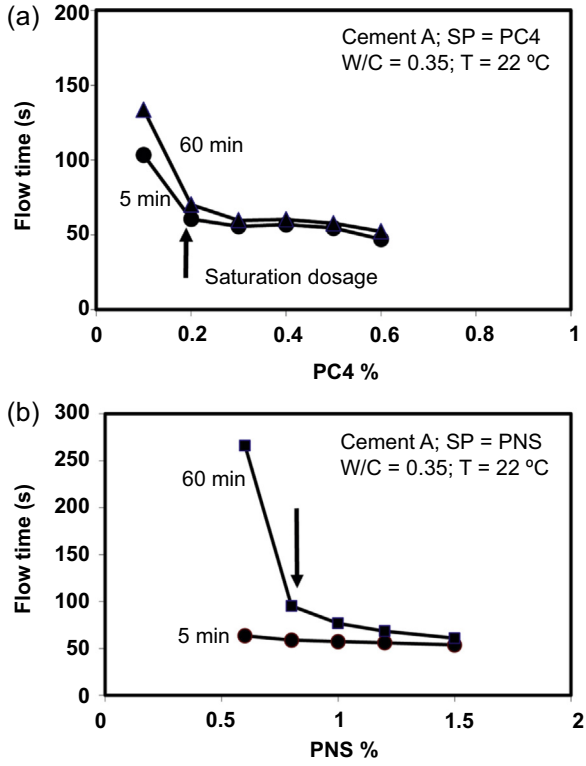


Figure 16.2 Saturation dosages with cement A (Marsh Cone): (a) a case with PC4 illustrating a well-defined saturation point and stable behavior over time, and (b) a case with PNS illustrating a case of rapid flow loss, as discussed in Section 16.4.5.1.
Reproduced with permission from Nkinamubanzi and Aïtcin (2004).

experience similar shearing conditions as in concrete. This issue is of even greater importance in mixes containing chemical admixtures.

Secondly, the mortar matrix in concrete must maintain the aggregates in suspension, and, in turn, the paste in the mortar must sustain the sand grains. If these conditions are not fulfilled, segregation of aggregates and/or sand will occur.

Besides the mixing energy and segregation issues, the composition of aggregates can play a key role. Indeed, the presence of swelling clays has a very negative effect on the fluidity of concretes containing PCE superplasticizers, as explained in Chapter 10 (Marchon et al., 2016) and in Jeknavorian et al., 2003; Ng and Plank, 2012.

It is often observed in concrete that the actual dosage of water reducer used in paste or mortar is overestimated causing, in the worst cases, excessive bleeding, segregation, and retardation (Nkinamubanzi and Aïtcin, 1999, 2004; Aïtcin et al., 2001). This might discourage one from using such scaled-down tests to study the performance of superplasticized systems. However, experienced operators can easily overcome this inconvenience by adjusting dosages in concrete depending on the required performances,

starting from the useful and fast results obtained from those tests. For example, with PNSs, it is found that the saturation point exceeds by 20−25% the actual dosage that has to be used in concrete in order to avoid segregation.

The use of the flow test in pastes to optimize the superplasticizer dosage represents a relatively effective method because one would target the specific yield stress needed to sustain aggregates of the size to be used in concrete following the relation given in Roussel (2006a). This approach also offers a relatively effective way to formulate concrete mix designs.

16.3 Impact of superplasticizers on rheology

It is widely understood and accepted that the main effect of superplasticizers is to reduce the yield stress. This has very important consequences as the yield stress can be defined as the limit stress below which the material stops flowing. It is therefore the property that controls the casting process (Roussel, 2007). Indeed, a theoretical correlation has been established between yield stress and the shape of the concrete at stoppage measured by slump tests (Saak et al., 2004; Roussel, 2006b; Murata, 1984) or mini-cone spread tests (Roussel et al., 2005; Zimmermann et al., 2009; Pierre et al., 2013).

Whether superplasticizers also affect rheological properties other than yield stress is a subject that has been debated for many years. Results that shed new light on this question are summarized in the next section.

16.3.1 Yield stress

In this section, we summarize the main effect of superplasticizers on yield stress. This results from the modification of interparticle forces induced by admixtures, a subject dealt with in more detail in Chapter 11 (Gelardi and Flatt, 2016).

Yield stress decreases with increasing superplasticizer dosage. Once the surface coverage is completed, the interparticle distance can be estimated based on twice the coiled size of the side chains of PCEs (Flatt et al., 2009). This approximation is valid as long as the van der Waals forces are not large enough to cause substantial compression of the adsorbed polymers (see Chapter 11; Gelardi and Flatt, 2016). For a common side chain molar mass of 1000 g/mol, this interparticle distance is in the range of 5 nm. The relationship between yield stress, the polymer structure, and dosage has been confirmed by consolidation experiments (Kjeldsen et al., 2006). Such results are particularly good at high surface coverages. At low surface coverage, the situation is more complex and also of greater practical relevance. A reliable prediction of the performances at low surface coverage, therefore, remains an important and challenging subject.

As a practical consideration, this means that at a very low w/c ratio, PCE polymers with long side chains and high carboxylic to ester (C/E) ratio can counteract more efficiently the attractive forces than polymers with low C/E ratio and short side chains (Winnefeld et al., 2007). The effect of superplasticizers on the rheological properties

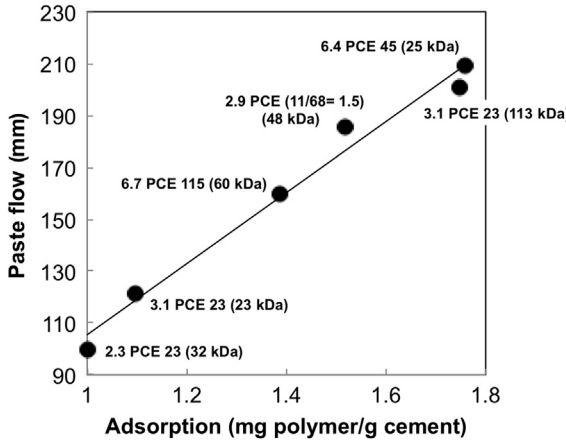


Figure 16.3 Correlation between adsorbed polymer and flow of cement pastes prepared with different PCE polymers having a polymethacrylic-based backbone. *(Adapted from Schober and Flatt (2006).)* Polymer notation indicates the C/E ratio as the first number, the side chain length expressed by the number of PEO monomeric units as the second number, and the molecular weight (Mw) in brackets. The characteristic data of the polymers were obtained combining the data reported in Schober and Flatt (2006) and Houst et al. (2008).

of cementitious materials is strongly linked to the amount of polymer adsorbed onto the surface of cement particles (Schober and Flatt, 2006; Winnefeld et al., 2006) (Figure 16.3).

It is worth keeping in mind, however, that this simple relationship can be altered by the incompatibility of superplasticizers with cements, observed in the case of sulfate competition (Yamada et al., 2001) and formation of organo-aluminate phases (Fernon, 1994; Giraudeau et al., 2009). Further details are given in Chapter 10 (Marchon et al., 2016).

When the polymer dosage decreases below the saturation dosage, the surface is only partially covered by the polymer and particles tend to stick together in those areas where the polymer is not adsorbed. On the contrary, the plateau at a high dosage corresponds to a complete surface coverage, where particles are well dispersed and the yield stress reaches a minimum value (Kjeldsen et al., 2006). Expressions needed to calculate the interparticle forces in conditions of complete and incomplete surface coverage are presented in Chapter 11 (Gelardi and Flatt, 2016).

Saturation and critical dosages can be derived by adsorption isotherms as well as by using flow spread measurements (Yamada et al., 2000), which are related to yield stress. Regarding the saturation dosage, earlier works have proposed to also obtain those by Marsh cone test. However, for low yield stress fluids, this test provides information mainly on the plastic viscosity (Roussel and Le Roy, 2005). Therefore, the Marsh cone cannot reliably be used to detect differences between well-dispersed pastes, although it detects differences for poorly fluid ones.

The identification of critical dosage is not as trivial as for the saturation dosage because it is extremely dependent on the experimental conditions. In a spread flow

test, flow initiation occurs if the yield stress of the paste is lower than the gravitational load on the sample, which depends on the sample height (Roussel and Coussot, 2005; Pierre et al., 2013). Hence, for each and every different mold height, a different critical yield stress should be obtained. Moreover, for specific cementitious systems, this mold-specific limiting yield stress will be reached by the right combination between volume fraction and interparticle forces. The result should therefore also strongly depend on w/c. Provided such limitations are recognized and understood, the critical dosage may nevertheless be a useful comparison criteria between superplasticizers.

16.3.2 Plastic viscosity

In practical cases, mainly with very low w/c ratios, concretes can have very low yield stresses if enough superplasticizers are added, but are nevertheless defined as sticky. This stickiness is most probably related either to plastic viscosity or to shear thickening. In both cases, the excess of energy needed to increase the shear rate above the yield stress increases with the packing fraction of solids as, for example, when w/c is decreased.

A shear thinning behavior in superplasticized systems is generally reported in the literature (Struble and Sun, 1995; Asaga and Roy, 1980; Björnström and Chandra, 2003; Papo and Piani, 2004) and results from the yield stress. Above the yield stress, a linear dependence of shear stress on shear rate is often observed, which is why the Bingham model is often used. As explained in Chapter 7, the slope of this linear regime is referred to as the plastic viscosity (Yahia et al., 2016). However, the range over which the linear regime can be assumed is still under debate.

An answer to this question can be found in the work of Hot et al. (Hot et al., 2014) who introduced the concept of residual viscosity. This isolates the hydrodynamic contribution from the yield stress by defining the residual viscosity as $(\mu_{app} - \tau_0/\dot{\gamma})$. In the limit of the Bingham model, the residual viscosity was confirmed to be independent of shear rate. However, beyond a critical shear rate, the residual viscosity increases, revealing the onset of shear thickening discussed in the next section.

In terms of plastic viscosity, the approach of Hot et al. (2014) offers a less ambiguous determination of the shear rate range over which this parameter may be calculated. Using this procedure and testing different polymers at different dosages, they found that viscous dissipation decreases with increasing polymer adsorption. This implies that the dependence of plastic viscosity is also affected by superplasticizers, although much less than yield stress. This occurs mainly because of the ability of superplasticizers to keep particles apart. An additional effect of the nonadsorbed superplasticizer cannot be excluded but appears to be less important.

16.3.3 Shear thickening

The occurrence of shear thickening (increase of apparent viscosity at high shear rates) becomes relevant as the solids volume fraction increases. The shear thickening behavior of suspensions was related to a change in the lubrication regimes between particles as shear is increased (Fernandez et al., 2013). The approach proposed

involved determining the jamming volume fraction in the Bagnold regime. In particular, experiments involving centrifugal consolidation were suggested as adequate means to determine this important parameter.

In an associated systematic study of the effect of polymethacrylate-based PCEs, it was found that anchoring of PCEs on particle surfaces was the most important factor in increasing the jamming volume fraction and, therefore, in resisting the transition to shear thickening (Fernandez, 2014). In particular, a high density of ionic groups or strong calcium complexing ability came out to be essential features, suggesting that polymers may detach from the surface under high shear forces if adsorption energy is not high enough. This aspect should be carefully taken into account when designing superplasticizers for mixes that may be subject to shear thickening (Fernandez, 2014).

16.3.4 The importance of mixing protocol

Cementitious materials are thixotropic fluids that additionally undergo irreversible structural breakdown under shear and are modified by ongoing reactions. This means that their rheological behavior is time and shear history dependent. Consequently, mixing protocols strongly influence concrete fluidity. As explained in Section 16.2.3, particular care must be taken when scaling down rheological characterization from concrete to paste.

As explained in Chapter 10, the addition time of chemical admixtures is a very important factor in rheology of cementitious systems (Marchon et al., 2016): if they are added at the beginning with the mixing water, the hydrating aluminate phase can sequestrate them from the solution either by forming an organo-mineral phases (Flatt and Houst, 2001; Plank et al., 2006; Giraudeau et al., 2009) or by adsorption on ettringite, of which the specific surface can be increased in presence of admixtures (Dalas et al., 2012). Consequently, a part of the polymer is not available for dispersing the cement and the fluidity is reduced, although the polymer seems to be adsorbed more extensively. Hence, the sequestration of polymers is more pronounced in cements having high content of aluminates (Schober and Mäder, 2003). This effect might to some extent be attenuated with a delayed polymer addition (Uchikawa et al., 1995; Aiad, 2003).

16.3.5 Fluidity retention

Fresh concrete is well known to lose its workability over time. The extent to which this happens depends, among several factors, on the type and dosage of the admixture and the mixing procedure. It was demonstrated that nonadsorbed polymer fraction in solution can impact the fluidity over time (Vickers et al., 2005). This might be explained by assuming either the reserve of polymer in solution can interact with new created surfaces over time or preferential interaction of polymers with aluminates hydrating faster than silicates in the first hours of hydration. In both cases, high surface coverages—and therefore fluidity—are maintained longer (Figure 16.4).

In terms of molecular structure, in practice, polymers having a lower amount of charges on the backbone (lower initial adsorption) and short side chains should be

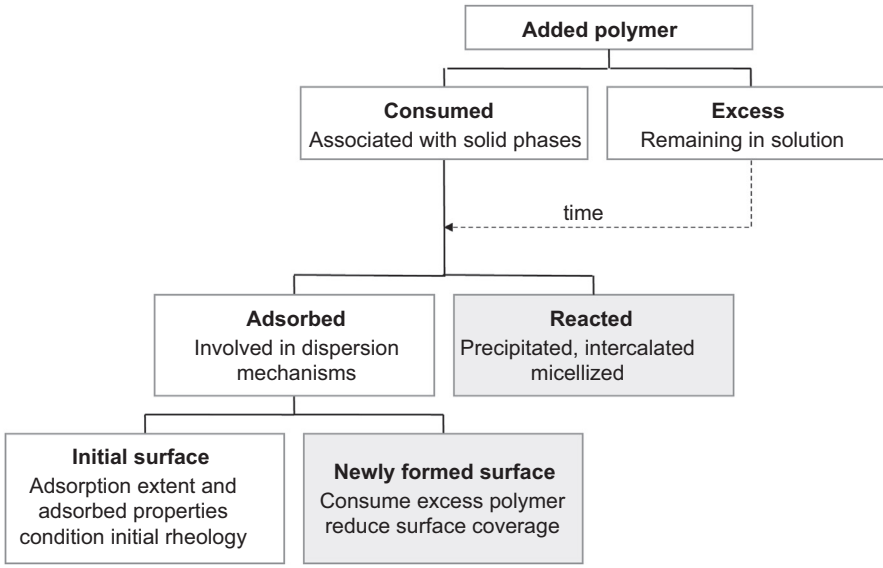


Figure 16.4 Schematic presentation differentiating the polymer that is usually identified as adsorbed (consumed) and the polymer that is actually effective in the dispersion mechanisms. Reproduced from Flatt (2004) with permission.

preferred if extended workability time is desired (Vickers et al., 2005; Yamada et al., 2000). This would more likely be the case in ready-mix applications. In precast applications, where workability retention requirements are of minor interest, more ionic polymers are generally preferred.

A better workability retention can also be obtained by a delayed addition because the polymer is not extensively adsorbed initially and its depletion takes longer (Aiad, 2003). This may also impact the initial fluidity that in many cases would be increased. Higher levels of dispersion may be reached and possible segregation may occur. As a result, in most cases, the superplasticizer dosage should be reduced. This, in turn, would reduce the workability time, so that the final benefits are not obvious.

In an earlier section, we mentioned that the mixing process affects the initial fluidity of concrete. This is also true for its evolution in time. For example, Vickers et al. (2005) found out that the consumption of the polymer is much higher in concretes than in cement pastes mixed at 700 rpm at the same conditions of w/c ratio, mixing time, and polymer dosage. This is attributed to the fact that high energy applied on the cement paste in concrete might form particles with higher surface area on which polymers are adsorbed. The origin of these additional surfaces may result from a more efficient solution exchange on particle surfaces through higher shear, leading to more extensive formation of etch pits and globally faster hydration kinetics (Juilland et al., 2010, 2012).

The important macroscopic observation remains, however: a faster slump loss is generally observed when high shear rates are applied during initial mixing. Ultimately,

these effects most likely result from different rates of specific surface generation through hydration reactions and their modification by shear and/or chemical admixtures, something covered in Chapters 10 and 12 (Marchon et al., 2016; Marchon and Flatt, 2016b).

16.3.6 Delayed fluidification

In concretes, an increase of the fluidity over time, called overfluidification, can be measured. Regnaud et al. (2006) demonstrated that a higher mixing energy and prolonged mixing produce a lower overfluidification. In this study, delayed fluidification resulted from the competition between sulfates and PCEs.

This effect is more pronounced with PCEs having a lower affinity for the surface. In fact, they cannot adsorb extensively because of the high initial sulfate concentration. Consequently, a higher PCE dosage is needed to reach the aimed reference fluidity. As aluminate hydration progresses and consumes sulfates, PCEs from the solution are adsorbed onto the cement particles, increasing dispersion and fluidity.

This study also showed that overfluidification is promoted in the presence of hemihydrate, because it strongly increases the initial sulfate concentration in solution. Sulfates, with the calcium ions dissolved, react and form ettringite, causing a stronger time evolution in sulfate concentration than with the alkali sulfates.

Delayed fluidification can also be observed with acrylic backbones because they rapidly lose their side chains through hydrolysis at high pH (Gelardi et al., 2016, Chapter 9). Their charges increase over time, as well as their dispersion efficiency (at least as long as enough side chains remain on the polymer).

Therefore, delayed fluidification is a property that can be beneficial or detrimental. In many cases, an increased dispersion over time may be undesirable because unexpected bleeding or segregation may occur during transportation—or even worse—after placing. In turn, delayed fluidification is beneficial for extending the workability time, in particular by combining different types of polymers in formulated products (see Chapter 15, Mantellato et al., 2016).

16.4 Unexpected or undesired behaviors

16.4.1 General considerations

Now that the technological and economical potential of superplasticizers has been realized, it has been possible to see unprecedented research efforts devoted to deeply understand interaction mechanisms responsible for incompatibilities and slump loss problems. However, unexpected behaviors using superplasticizers are not restricted to workability loss. Indeed, superplasticizers may detrimentally impact the effect of other chemical admixtures, like in the case of air-entrainers (see Section 16.4.6). This involves a competitive adsorption at liquid−vapor interfaces, unlike water reducers and superplasticizers working at solid−liquid interfaces.

As summarized in the previous sections, the effectiveness of superplasticizers depends on the amount of adsorbed molecules (surface coverage) and on the conformation in their adsorbed state. Any factor affecting them may perturb the performance in concrete. In particular, various processes can reduce the amount of superplasticizers available per unit surface of fine particles in suspension. These are discussed in detail in Chapter 10 (Marchon et al., 2016) and can be summarized as follows:

- *Competitive adsorption*. Preferential adsorption of a compound that prevents the superplasticizer from adsorbing (e.g., sulfates, hydroxyls, and retarders). This depends on the relative affinity of the competing compounds for surfaces as well as on their relative concentrations.
- *Increased specific surface area*. Modification of the surface on which admixtures adsorb, by the interaction with hydration products, having higher specific surface area than anhydrous phases.
- *Formation of organo-aluminate phases*. Sequestration of admixtures in the internal layers of AFm phase.
- *Adsorption onto clay minerals*. This process is of particular concern for PCE superplasticizers, because of the strong affinity of their PEG-based side chains for clay minerals, mainly smectites.

These incompatibilities are intimately related to cement composition and variations thereof. We therefore dedicate another subsection to this question. On this basis, we propose a discussion of the processes controlling performance change.

16.4.2 Inadequacy of standard tests to identify incompatibilities

At first glance, it could be thought that all cements that satisfy the same standard requirements should behave in the same way when tested with the same superplasticizer. Among the documented cases, it can be stated that the use of superplasticizers in concrete having a low w/c ratio enhances possible problems.

Unfortunately, the workability tests used to qualify cements are done on mortars without admixture under standard conditions, implying the use of a high w/c ratio of 0.50 (ASTM C109). The rheology of such a mortar is essentially controlled by water. Under these conditions, even moderate shear forces are sufficient to break down agglomerates and initiate the flow. This results from a lower number of fine particles per unit volume, which, in turn, is controlled by the selected w/c, as explained in Chapter 7 (Yahia et al., 2016).

This also implies that this standard test makes it almost impossible to see problems associated with the use of a superplasticizer. This is why superplasticizers must be generally tested for each particular cement in the actual conditions of use, generally at much lower water contents. Typically, more particle−particle contacts per unit volume of paste are present and their cohesiveness must be reduced for the material to flow under the same conditions as before. Therefore, at low w/c and with superplasticizers, it is the effective surface coverage of cement particles by superplasticizers that controls workability (see Section 16.3.1 and Chapter 11 (Gelardi and Flatt, 2016))—something that standard mortar tests are not designed to evaluate.

Finally, in a system without admixture, the flow evolution in time depends on the formation rate of the first hydration products. On the contrary, in superplasticized

systems, these reactions can have a much greater efficiency because the surface coverage of cement grains by superplasticizers can be reduced.

16.4.3 Robustness of cement/superplasticizer combinations in concrete

A concrete mixture is considered to have a robust behavior when a little variation in the composition of one of the ingredients of the mixture does not lead to a big variation of the properties of the concrete (Figure 16.5).

Tests done with different combinations of cements and superplasticizers showed that a good compatibility and a well-optimized concrete mixture do not necessarily mean a robust mixture. Indeed, a little variation in the dosage of the admixture could lead to detrimental side effects such as segregation, excessive set retardation, or excess air content in concrete.

In the so-called incompatible cement/superplasticizer combinations, it is always possible to find a very narrow range of the superplasticizer dosage necessary to achieve good performance in fresh concrete. However, a very slight deviation from the *ideal* dosage might result in either a rapid slump loss, unacceptable bleeding/segregation, excessive set retardation, or excess air content in concrete. Such behavior is usually referred to a nonrobust combination or process (Nkinamubanzi and Aïtcin, 2004).

Of course, any industry is looking for robust combinations or systems, and would reject very efficient but nonrobust combinations to the profit of less efficient ones that are much more robust. However, for cost reasons, one would also like to use a highly effective product of which only a small amount must be used. This high efficiency at low dosage, however, goes against the principle of robustness, as the response to dosage slope increases. As a general rule, modern industries always

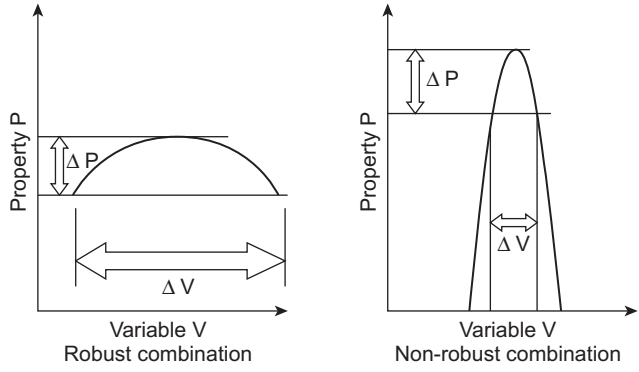


Figure 16.5 Robustness of an industrial process. In the case of the effectiveness of cement/superplasticizer combinations, the variable V typically represents either the superplasticizer dosage, the grading of the aggregates or the sand humidity, while the property P represents either, the concrete's slump, setting time, or initial strength.
Reproduced with permission from Aïtcin et al. (2001) and Nkinamubanzi and Aïticn (2004).

make compromises between efficiency and robustness: the first is often linked to cost–benefit issues, the latter for obtaining constant performances.

16.4.4 Role of cement composition

As observed from the example in the previous paragraph, the cement composition and physico-chemical properties influence the compatibility between cement and superplasticizer. Among these, C_3A content, fineness, the nature of the calcium sulfate ($CaSO_4$) used to control the aluminate phase reactions, as well as the soluble alkalis content are considered the most relevant factors in controlling the rheological properties of cementitious systems.

16.4.4.1 Soluble alkalis and their relation with aluminates

Soluble alkalis, mostly based on Na and K sulfates, dissolve almost immediately, providing sulfates ions to the aqueous phase. These negatively charged species compete with the superplasticizers (also negatively charged) for incorporation in aluminate hydrates (Yoshioka et al., 2002; Giraudeau et al., 2009; Yamada et al., 2001) and/or adsorption at the surface of hydrated and/or anhydrous phases (Yamada et al., 2001).

In cements with low alkali contents, the aspect of incorporation (or specific surface modification) appears to dominate. Indeed, such cements strongly adsorb the superplasticizer in a few minutes, leaving too low amounts of admixture in solution to maintain the fluidity over time (see Section 16.3.5).

These interpretations are supported by the fact that the amount of PNS adsorbed on the cement grains decreases quasi-linearly when the alkali and alkaline sulfate contents increase in the cement grouts (Figure 16.6).

However, additions of small amounts of sodium sulfate can improve the slump retention for low-alkali cements, because of the reduced consumption of

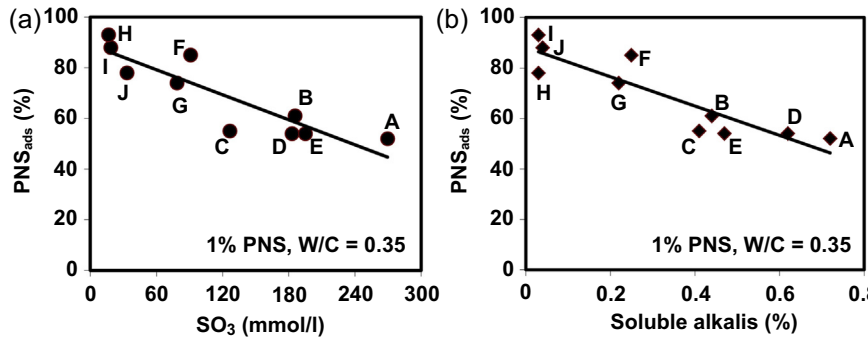


Figure 16.6 Adsorption of PNS as a function of the soluble alkalis and sulfates of the cements (PNS in pore solution measured 5 min after mixing).
Reproduced with permission from Nkinamubanzi and Aïtcin (2004).

superplasticizers in organo-mineral phases and/or limited increase in specific surface area (Aïtcin et al., 2001; Kim et al., 2000; Flatt and Houst, 2001; Giraudeau et al., 2009).

Based on the above result, a reduction in the degree of adsorption would improve workability (retention), which might be viewed as a contradiction to basic dispersion mechanisms. It has been proposed that, in this case, sulfates reduce the scavenging of superplasticizers by aluminate phases, leaving a large amount available for dispersion (Flatt and Houst, 2001). This should be related to the reactivity of C_3A and the availability of the sulfate carriers as well as the alkali content.

The contents in C_3A and soluble sulfates, as well as the fineness of the cements, are key parameters to be considered because they play an important role in the very early stage of hydration reactions, affecting the interactions between cement and admixtures (Jiang et al., 1999; Kim, 2000; Tagnit-Hamou et al., 1992; Flatt and Houst, 2001). Some authors (Nkinamubanzi et al., 2002) have reported that the ratio of the C_3A content and its soluble sulfate (SO_3 sol.), expressed as soluble SO_3/C_3A, is a key parameter that governs the compatibility and the robustness of the cement–superplasticizer combinations (Figure 16.7).

Similar conclusions have recently been obtained in a study also involving PCEs (Habbaba et al., 2014). The authors adjusted dosages for cement pastes to exhibit the same initial flow and evaluated the flow changes induced by both direct and delayed addition. They suggested that flow increase observed in the case of the delayed addition is justified by the fact that a certain amount of superplasticizer has been

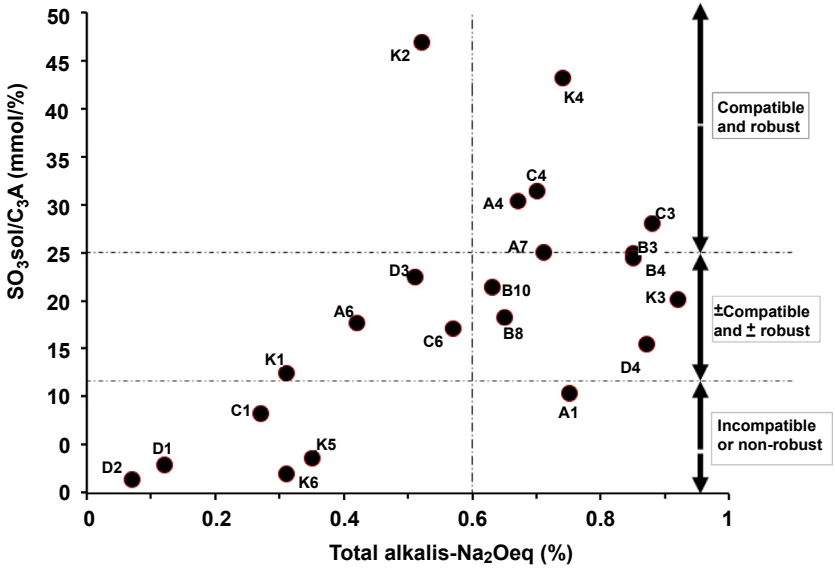


Figure 16.7 Compatibility and robustness of cements as a function of their Na_2O_{eq} content and their SO_3 sol/C_3A.
Reproduced with permission from Nkinamubanzi et al. (2002).

mobilized during the initial formation of aluminate hydrates. Conversely, in case of similar flow, the superplasticizer remains available. In their selection of cements, this occurred if the molar ratio of soluble sulfate to C_3A is larger than about 2. On this basis, these authors similarly concluded that the amount of soluble sulfates determines the amount of polymers that are "scavenged" during the initial hydration of C_3A.

This result is interesting and useful. However, it is not clear if the molar ratio of two has a chemical meaning and if it can be generalized. Indeed, during the initial contact of water and cement, a large portion of the alkali sulfates is solubilized, but only a small fraction of the C_3A reacts. This brings us to the question of the initial reactivity of mineral phases in cement and their exposure to water, presented in the next section.

16.4.4.2 Surface mineralogy

The interaction between cement and superplasticizer is a surface phenomenon. The surface mineralogy of cement particles conditions the nature and density of the electrical charges, being the interstitial phase enriched in positive sites and the silicate phases in negative sites. In past years, relatively little attention has been cast on this aspect. In this section, some concepts are schematically presented to illustrate the possible impact of changes in surface composition of cement grains.

For this, we return to the five hypothetical cement particles presented in Chapter 3 (Figure 3.7; Aïtcin, 2016a). They all have the same interstitial phase/silicate phase ratio. However, their surfaces exposed to water and superplasticizers are very different (C_3S for G1, C_3A and C_4AF for G2, C_3S and a small amount of interstitial phase for G3, etc.). This has a strong effect on initial reactivity (rate of formation of new surfaces), but also on the affinity that superplasticizers can have for these surfaces. Consequently, the performance of these admixtures can be expected to be very different between these different cases.

These examples are extreme and differences between cements will be lower. However, they illustrate how surface rather than bulk mineralogy can influence superplasticizer−cement interactions in the initial stages of cement hydration. Therefore, the fundamental question is whether the surface mineralogical composition is or is not the same as the bulk one. This would be expected if during grinding, cracks do not substantially deflect at grain boundaries. Recent numerical modeling results of this process do not indicate that such deflections are important (Carmona et al., 2015; Mishra et al., 2015). Therefore, bulk composition probably represents a relatively good first approximation for surface composition.

16.4.5 Role of superplasticizers

16.4.5.1 PNS and PMS

Nowadays, the quality of PNS and PMS for use in concrete technology is well mastered. A good commercial PNS polymer has a sulfonation degree around 90%, with more than 85% of these groups in the β-position. Crosslinking can also be well under control in order to maintain the maximum of flexibility of the polymer chains (Piotte, 1993; Nkinamubanzi, 1993; Jolicoeur et al., 1994; Spiratos et al., 2003).

Beyond these process parameters, the only real leverage on these superplasticizers is their molecular mass, in the range of 32−75 kD in the case of PNS (Spiratos et al., 2003). This only leaves a narrow range of variations, so that incompatibilities with cement should come mainly from the cement. More specifically, as mentioned above, soluble alkali and C_3A content play an important role.

Results in Figure 16.2(a) show that, beyond the saturation dosage, the risk of bleeding and segregation increases rapidly and drastically for nonrobust combinations. Moreover, the extra superplasticizer added beyond that saturation dosage results in a strong retardation. On the contrary, a high initial fluidity can be achieved with a quite low superplasticizer dosage, 0.6−0.8% for a PNS, and this fluidity is easily maintained up to 2 h at 20 °C using different cement/superplasticizer combinations (Figure 16.2(b)). The sensitivity of PNSs to cement composition follows the principles described in Section 16.4.4.

16.4.5.2 Different sensitivity of PCEs

Polycarboxylate comb-copolymers allow a much larger flexibility in molecular design (Gelardi et al., 2016, Chapter 9). From this perspective, it is important to insist on the fact that there is not one PCE but a family of PCEs that may have quite different behaviors. Specifically, their susceptibility to incompatibilities with cement relates to their molecular structure.

To illustrate this point, let us consider cements with a high (enough) alkali content so that they are not sensitive to scavenging. In these cases, variations in the alkali content affect the extent of competitive adsorption. Specifically, an increase of the alkali sulfates reduces both adsorption and flow (Yamada et al., 2001). However, the susceptibility of superplasticizers to this depends on their affinity for the surface, which can be related to molecular structure (Marchon et al., 2016, Chapter 10).

Concerning cement with low alkali content, the work of Habbaba et al. (2014) (see Section 16.4.4.1) illustrates that there are differences among the polymers, but it does not determine how these variations relate to molecular structure. In what follows, we propose to examine the flow increase due to the shift from direct to delayed addition.

For PCEs, flow spread diameters vary linearly with the amount of adsorbed polymer (Figure 16.3). Hence, the consequent flow increase is expected to be proportional to the amount of polymer scavenged during the initial aluminate reaction. As shown in Figure 16.8, there is a clear trend with respect to the polymer side chain length: longer side chains lead to less PCE consumption and decreased fluidity, as explained in Habbaba et al. (2014). Furthermore, this trend is qualitatively the same whether the cement with the lowest (almost zero) alkali content or the average of those with a soluble alkali-to-C_3A ratio lower than 2 are considered (the other not being relevant for the present discussion).

A priori, it can be assumed that the polymer consumption relates to the affinity of the polymer for a surface. From this perspective, we propose the use of the adsorption equilibrium constant scaling law presented by Marchon et al. (2013) and explained in Chapter 10 (Marchon and Flatt, 2016a). Moreover, because adsorption energy is probably the driving force of excess polymer consumption, polymers with higher adsorption energy must be more effectively mobilized by the forming aluminate hydrates.

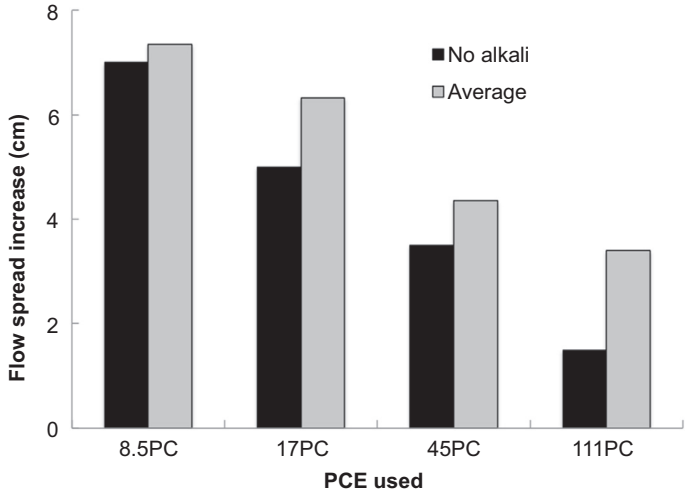


Figure 16.8 Illustration of the flow increase obtained in Habbaba et al. (2014). Values shown here are for the close-to-zero alkali cement as well as the average over the five cements for which the soluble alkali-to-C_3A ratio is <2. The number in front of the polymer label indicates the number of groups EO units in the side chains.

Therefore, we plot data versus the natural log of this equilibrium constant, which relates to adsorption energy. As shown in Figure 16.9, we obtain a linear relation with a very high correlation coefficient. The fact that it passes through the origin is probably coincidental because there are unknown numerical constants whose variation would shift the curve up or down. Nevertheless, in the context of this section, this

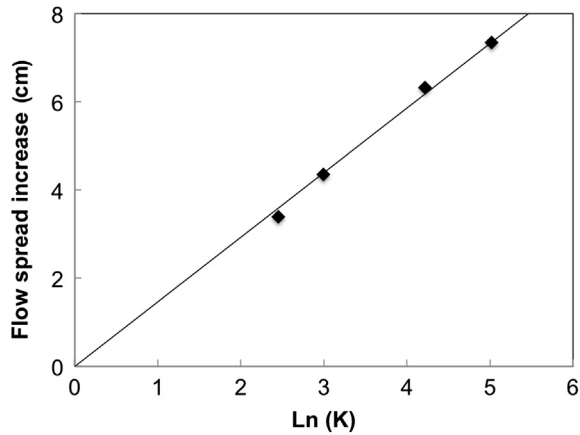


Figure 16.9 Dependence on the flow increase (assume proportional to the amount of scavenged polymer) with respect to the natural logarithm of the adsorption equilibrium constant calculated from molecular structure (Marchon et al., 2013). For this, we use the C/E value of 6 common to all the polymers and the molar mass information given in Plank et al. (2010).

result at least suggests the possibility to develop molecular structure-based arguments to account for the scavenging of PCEs during the hydration of aluminate phases.

In general terms, it is important to emphasize that well-designed PCEs are more effective than PNS at equivalent surface coverage. This results from a thicker polymeric layer with PCEs and, consequently, more effective steric hindrance, as explained in Chapter 11 (Gelardi and Flatt, 2016). Therefore, lower dosages of PCEs are needed to obtain the same or better workability (provided the PCEs adsorb enough). Consequently, because less PCEs are available in the pore solution, their ability to moderate initial reactivity of C_3A may be reduced. This is, of course, an ultrasimplified statement because dosage, molecular structure, and formulation play very important roles. However, it has the advantage of helping us to remember that a decrease of admixture dosages can a priori make the fluidity retention more difficult even if the initial flow is preserved.

16.4.6 Interaction with other admixtures

Modern concrete very often contains two or more chemical admixtures in order to improve its fresh and/or its hardened properties. Besides admixture−cement interactions examined in the previous sections, it is also important to master possible problems due to admixture−admixture interactions and incompatibilities.

The air content stability of the fresh concrete and the quality of the air voids system of the hardened material necessary to achieve the frost resistance of concrete in the presence (or not) of deicing salt is the most frequent problem. In this case, a competitive adsorption at liquid−vapor interfaces is involved, unlike water reducer and superplasticizers working at solid−liquid interfaces.

Most of the water reducing admixtures may affect the air-entraining capability of both air-entraining cement and air-entraining admixtures (AEAs) (Rixom and Malivaganam, 1999). Lignosulfonates entrain air to various degrees ranging from 2% to 6%, although higher amounts have been reported. Bedard and Mailvaganam (2005) reported that concretes in which lignin-based water reducers (WRA) and AEAs were combined showed a substantially higher air content than those concretes in which AEA was added alone. However, the specific surface of the air bubbles in fresh concretes with WRA was substantially reduced. Furthermore, the delayed addition of WRAs was further detrimental to the stability of the air-void system.

As explained in Chapter 6, the addition of superplasticizers, which to some extent can be also considered as surfactants, can modify the relationship between the air content and the spacing factor (Aïtcin, 2016b) and sometimes significantly destabilize the air-void system (Rixom and Mailvaganam, 1999). Details of the mechanism of air entrainment in concrete are discussed in Chapters 10 and 15 (Marchon et al., 2016; Mantellato et al., 2016). Concretes with high-range water reducers can have larger entrained air voids and higher void-spacing factors than normal air-entrained concrete (Baalbaki and Aïtcin, 1994; Plante et al., 1989; Nkinamubanzi et al., 1997). This would generally indicate a reduced resistance to freezing and thawing. However, laboratory tests have shown that concretes with a moderate slump using high-range water reducers have good freeze−thaw durability, even with slightly higher void-spacing factors (Rixom and Mailvaganam, 1999).

The effect of naphthalene- and melamine-based superplasticizers on the air entrainment in high-performance concrete has been extensively studied. It has been demonstrated that a higher amount of air-entraining admixture was needed to entrain an adequate air voids systems in high-performance concrete when these families of high-range water reducers were used (Lessard et al., 1993; Pigeon et al., 1991; Baabaki and Aïtcin, 1994). Laboratory and field tests have shown that high-performance concretes with an adequate air content in the fresh state and a required air-voids system in the hardened concrete can be achieved with these types of high-range water reducers (Aïtcin and Lessard, 1994; Rixom and Mailvaganam, 1999).

Polycarboxylate-based superplasticizers are well known to cause significant air-entraining issues (Macdonald, 2009; Eickschen and Müller, 2013). This is one of the most problematic issues in the North American market. In practice, it might happen that the air-void parameters measured on the hardened concrete are not met despite the total air content of the fresh concrete complied with the requirements. The combination of a proper defoaming agent with polycarboxylates admixtures in formulation solves mostly this problem (Xuan et al., 2003; Chapter 15, Mantellato et al., 2016). However, some presently used defoaming agents have been reported to produce unacceptable results in the field (Kuo, 2010). In past years in North America, cases of concrete mixtures rejection on the job site due to air content fluctuation caused by the use of inadequate combinations of PCEs and defoamers are not negligible. In North America, when the air-voids system properties (spacing factor) are critical, PNS-based admixtures may be preferred.

16.5 Conclusions

Superplasticizers are essential components of modern concrete, allowing the production of highly durable structures with reduced environmental impact. Their working mechanisms rely on their molecular structures and physical−chemical interactions taking place between them and the surface of cement particles. Unfortunately, standard workability tests in cement norms are not adequate for testing these interactions, so combinations of cement and superplasticizers must be tested on a case-by-case basis. In some situations, it is difficult or impossible to find a robust combination giving the desired workability and workability retention without excessive retardation. Such situations are described as cement−superplasticizer incompatibilities.

Such situations represent a major concern in practice. However, they are relatively poorly documented in the literature. This is probably due to the fact that incompatibilities can have several origins and manifest themselves in various ways. It is also something that typically emanates from practical situations in which empirical quick-fix solutions are rapidly sought through changes of mix design. In most cases, this approach may be effective in the short term, but it can lead to situations in which small changes in the composition of one or the other mix components (amounts, nature, or purity) will sooner or later lead once again to inadequate concrete quality, as it has been shown for nonrobust combinations.

This chapter has attempted to better define the origin of these incompatibilities, highlighting the role of soluble alkali, C_3A, and specific surfaces. It is hoped that the mechanistic insight provided along with recommended testing approaches will help users to better control the quality of admixed concrete.

Acknowledgments

Support for Sara Mantellato was provided by the SNF project (n. 140615) titled "Mastering flow loss of cementitious systems." Support for the work done at Sherbrooke University by P.-C. Nkinamubanzi and P.-C. Aïtcin "Projet 98-06 Compatibilité ciment/Adjuvant Phase II", was provided by the French ATILH (Association Technique de l'Industrie des Liants Hydrauliques).

References

Aiad, I., 2003. Influence of time addition of superplasticizers on the rheological properties of fresh cement pastes. Cement and Concrete Research 33 (8), 1229−1234. http://dx.doi.org/10.1016/S0008-8846(03)00037-1.

Aïtcin, P.-C., Lessard, M., October 1, 1994. Canadian experience with air entrained high-performance concrete. Concrete International 16 (10), 35−38.

Aïtcin, P.-C., 1998. High-Performance Concrete. E&FN SPON, London, 591 p.

Aïtcin, P.-C., 2016a. Portland cement. In: Aïtcin, P.-C., Flatt, R.J. (Eds.), Science and Technology of Concrete Admixtures. Elsevier, (Chapter 3), pp. 27−52.

Aïtcin, P.-C., 2016b. Entrained air in concrete: Rheology and freezing resistance. In: Aïtcin, P.-C., Flatt, R.J. (Eds.), Science and Technology of Concrete Admixtures. Elsevier, (Chapter 6), pp. 87−96.

Aïtcin, P.-C., Jiang, S., Kim, B.-G., Nkinamubanzi, P.-C., Petrov, N., July−August 2001. Cement/superplasticizer interaction. The case of polysulfonates. Bulletin des Laboratoires des ponts et chaussées 233, 89−99. RÉF. 4373.

Asaga, K., Roy, D.M., 1980. Rheological properties of cement mixes: IV. Effects of superplasticizers on viscosity and yield stress. Cement and Concrete Research 10 (1980), 287−295. http://dx.doi.org/10.1016/0008-8846(80)90085-X.

ASTM C109 Compressive Strength of Hydraulic Cement Mortars, Copyright © 2014 ASTM International, West Conshohocken, PA, USA, All rights reserved, www.astm.org.

Baalbaki, M., Aitcin, P.C., 1994. Cement superplasticizer/air entraining agent compatibility. In: 4th Int. CANMET/ACIConf. On Superplasticizers and Other Chemical Admixtures, Montreal, Que., Canada, pp. 47−62.

Bedard, C., Mailvaganam, N.P., 2005. The use of chemical admixtures in concrete: Part II: admixture-admixture compatibility and practical problems. ASCE Journal of Performance of Constructed Facilities 263−266.

Bilodeau, A., Malhotra, V.M., January−February 2000. High-volume fly ash concrete systems: concrete solution for sustainable development. ACI Material Journal Vol. 97, No.1.

Björnström, J., Chandra, S., 2003. Effect of superplasticizers on the rheological properties of cements. Materials and Structures 36, 685−692. http://dx.doi.org/10.1007/BF02479503.

Carmona, H.A., Guimaraes, A.V., Andrade, J.S., Nikolakopoulos, I., Wittel, F.K., Herrmann, H.J., 2015. Fragmentation processes in two-phase materials. Physical Review E, Statistical, Nonlinear, and Soft Matter Physics 91 (1), 012402 (012407 pp.).

Dalas, F., Pourchet, S., Nonat, A., Rinaldi, D., Mosquet, M., Korb, J.-P., 2012. Surface area measurement of C3A/CaSO4/H2O/Superplasticizers system. In: Proceedings 10th CANMET/ACI International Conference on Superplasticizers and Other Chemical Admixtures in Concrete, Prague, ACI, SP-288, pp. 103−117.

Dodson, V.H., 1990. Concrete Admixtures. Van Nostrand Reinhold, Technology & Engineering, 211 p.

Eickschen, E., Müller, C., 2013. Interactions of air-entraining agents and plasticizers in concrete. Cement International 2, 88−101.

Fernandez, N., 2014. From Tribology to Rheology Impact of Interparticle Friction in the Shear Thickening of Non-brownian Suspensions. ETH Zürich, Zürich.

Fernandez, N., Mani, R., Rinaldi, D., Kadau, K., Mosquet, M., Lombois-Burger, H., Cayer-Barrioz, J., Herrmann, H.J., Spencer, N., Isa, L., 2013. Microscopic mechanism for shear thickening of non-brownian suspensions. Physical Review Letters 111 (10), 108301. http://dx.doi.org/10.1103/PhysRevLett.111.108301.

Fernon, V., 1994. Caractérisation des produits d'interaction adjuvants/hydrates du ciment. Journées techniques adjuvants, Technodes, Guerville, France, 14 pp.

Flatt, R.J., 2004. Towards a prediction of superplasticized concrete rheology. Materials and Structures 37 (269), 289−300.

Flatt, R.J., Houst, Y.F., 2001. A simplified view on chemical effects perturbing the action of superplasticizers. Cement and Concrete Research 31 (8), 1169−1176. http://dx.doi.org/10.1016/S0008-8846(01)00534-8.

Flatt, R.J., Roussel, N., Cheeseman, C.R., 2012. Concrete: an eco material that needs to be improved. Journal of the European Ceramic Society 32 (11), 2787−2798. http://dx.doi.org/10.1016/j.jeurceramsoc.2011.11.012.

Flatt, R.J., Schober, I., Raphael, E., Plassard, C., Lesniewska, E., 2009. Conformation of adsorbed comb copolymer dispersants. Langmuir 25 (2), 845−855. http://dx.doi.org/10.1021/la801410e.

Gelardi, G., Flatt, R.J., 2016. Working mechanisms of water reducers and superplasticizers. In: Aïtcin, P.-C., Flatt, R.J. (Eds.), Science and Technology of Concrete Admixtures. Elsevier, (Chapter 11), pp. 257−278.

Gelardi, G., Mantellato, S., Marchon, D., Palacios, M., Eberhardt, A.B., Flatt, R.J., 2016. Chemistry of chemical admixtures. In: Aïtcin, P.-C., Flatt, R.J. (Eds.), Science and Technology of Concrete Admixtures. Elsevier, (Chapter 9), pp. 149−218.

Giraudeau, C.-, D'Espinose De Lacaillerie, J.-B., Souguir, Z., Nonat, A., Flatt, R.J., 2009. Surface and intercalation chemistry of polycarboxylate copolymers in cementitious systems. Journal of the American Ceramic Society 92 (11), 2471−2488. http://dx.doi.org/10.1111/j.1551-2916.2009.03413.x.

Habbaba, A., Dai, Z., Plank, J., 2014. Formation of organo-mineral phases at early addition of superplasticizers: the role of alkali sulfates and C3A content. Cement and Concrete Research 59 (May), 112−117. http://dx.doi.org/10.1016/j.cemconres.2014.02.007.

Hot, J., Bessaies-Bey, H., Brumaud, C., Duc, M., Castella, C., Roussel, N., September 2014. Adsorbing polymers and viscosity of cement pastes. Cement and Concrete Research 63, 12−19. http://dx.doi.org/10.1016/j.cemconres.2014.04.005.

Houst, Y.F., Bowen, P., Perche, F., Kauppi, A., Borget, P., Galmiche, L., Le Meins, J.-F., et al., 2008. Design and function of novel superplasticizers for more durable high performance concrete (superplast project). Cement and Concrete Research 38 (10), 1197−1209. http://dx.doi.org/10.1016/j.cemconres.2008.04.007.

Jeknavorian, A.A., Jardine, L.A., Koyata, H., Folliard, K.J., 2003. Interaction of superplasticizers with clay-bearing aggregates. In: Proceedings of the 7th Canmet/ACI Int. Conf. Superplasticizers and Other Chemical Admixtures in Concrete, SP-216. ACI, Berlin, pp. 1293–1316.

Jiang, S., Kim, B.-G., Aïtcin, P.-C., 1999. Importance of adequate soluble alkali content to ensure cement/superplasticizer compatibility. Cement and Concrete Research 29 (1), 71–78.

Jolicoeur, C., Nkinamubanzi, P.-C., Simard, M.A., Piotte, M., 1994. Progress in understanding the functional properties of superplasticizers in fresh concrete. In: Malhotra, V.M. (Ed.), Proceedings of the 4th CANMET/ACI International Conference on Superplasticizers and Other Chemical Admixtures in Concrete, Montreal, pp. 63–87. ACI SP-148.

Juilland, P., Gallucci, E., Flatt, R.J., Scrivener, K., 2010. Dissolution theory applied to the induction period in alite hydration. Cement and Concrete Research 40 (6), 831–844. http://dx.doi.org/10.1016/j.cemconres.2010.01.012.

Juilland, P., Kumar, A., Gallucci, E., Flatt, R.J., Scrivener, K.L., 2012. Effect of mixing on the early hydration of alite and OPC systems. Cement and Concrete Research 42 (9), 1175–1188. http://dx.doi.org/10.1016/j.cemconres.2011.06.011.

Kim, B.-G., 2000. Compatibility between Cement and Superplasticizers in High-performance Concrete: Influence of Alkali Content in Cement and the Molecular Weight of PNS on the Properties of Cement Pastes and Concrete. Ph.D. Thesis. Université de Sherbrooke.

Kim, B.-G., Jiang, S., Aïtcin, P.-C., 2000. Slump improvement of alkalies in PNS superplasticized cement pastes. Materials and Structures 33 (230), 363–639.

Kjeldsen, A.M., Flatt, R.J., Bergström, L., 2006. Relating the molecular structure of comb-type superplasticizers to the compression rheology of MgO suspensions. Cement and Concrete Research 36 (7), 1231–1239. http://dx.doi.org/10.1016/j.cemconres.2006.03.019.

Kuo, L.L., 2010. Defoamers for hydratable cementitious compositions. U.S. Patent 8,187,376 filed August 24, 2010, and issued April 26, 2012.

Lessard, M., Gendreau, M., Gagné, R., 1993. Statistical analysis of the production of a 75 MPa air-entrained concrete. In: 3rd International Symposium on High Performance Concrete, Lillehammer, Norway, June, ISBN 82-91 341-00-1, pp. 793–800.

MacDonald, K., 2009. Polycarboxylate Ether and Slabs, Understanding How They Work in Floor Construction, Concrete Construction.

Mantellato, S., Eberhardt, A.B., Flatt, R.J., 2016. Formulation of commercial products. In: Aïtcin, P.-C., Flatt, R.J. (Eds.), Science and Technology of Concrete Admixtures. Elsevier, (Chapter 15), pp. 343–350.

Marchon, D., Flatt, R.J., 2016a. Mechanisms of cement hydration. In: Aïtcin, P.-C., Flatt, R.J. (Eds.), Science and Technology of Concrete Admixtures. Elsevier, (Chapter 8), pp. 129–146.

Marchon, D., Flatt, R.J., 2016b. Impact of chemical admixtures on cement hydration. In: Aïtcin, P.-C., Flatt, R.J. (Eds.), Science and Technology of Concrete Admixtures. Elsevier, (Chapter 12), pp. 279–304.

Marchon, D., Sulser, U., Eberhardt, A.B., Flatt, R.J., 2013. Molecular design of comb-shaped polycarboxylate dispersants for environmentally friendly concrete. Soft Matter 9 (45), 10719–10728. http://dx.doi.org/10.1039/C3SM51030A.

Marchon, D., Mantellato, S., Eberhardt, A.B., Flatt, R.J., 2016. Adsorption of chemical admixtures. In: Aïtcin, P.-C., Flatt, R.J. (Eds.), Science and Technology of Concrete Admixtures Elsevier, (Chapter 10), pp. 219–256.

Mishra, R.K., Geissbuhler, D., Carmona, H.A., Wittel, F.K., Sawley, M.L., Weibel, M., Gallucci, E., Herrmann, H.J., Heinz, H., Flatt, R.J., 2015. En route to multimodel scheme for clinker comminution with chemical grinding aids. Advances in Applied Ceramics.

Murata, J., 1984. Flow and deformation of fresh concrete. Matériaux et Construct. 17 (2), 117–129. http://dx.doi.org/10.1007/BF02473663.

Ng, S., Plank, J., 2012. Interaction mechanisms between Na montmorillonite Clay and MPEG-based polycarboxylate superplasticizers. Cement and Concrete Research 42 (6), 847–854. http://dx.doi.org/10.1016/j.cemconres.2012.03.005.

Nkinamubanzi, P.-C., 1993. Influence des dispersants polymériques (superplastifiants) sur les suspensions concentres et les pâtes de ciment. Ph.D. thesis, No. 853. Université de Sherbrooke, 180 p.

Nkinamubanzi, P.-C., Aïtcin, P.-C., 1999. Compatibilité Ciment-adjuvant projet 98–06, ATILH II.

Nkinamubanzi, P.-C., Aïtcin, P.-C., 2004. Cement and superplasticizer combinations: compatibility and robustness. Cement and Concrete Aggregates 26 (2), 1–8.

Nkinamubanzi, P.-C., Baalbaki, M., Aïtcin, P.-C., 1997. Comparison of the performance of four superplasticizers on high-performance concrete. In: Malhotra, V.M. (Ed.), Proceedings of the Fifth CANMET/ACI International Conference on Superplasticizers and Other Chemical Admixtures in Concrete, Supplementary Papers, Rome, 1997, pp. 199–206.

Nkinamubanzi, P.-C., Kim, B.G., Aïtcin, P.-C., February 2002. Some Key Cement Factors that Control the Compatibility between Naphthalene-based Superplasticizers and Ordinary Portland Cements. L'Industria Italiana Del Cemento, pp. 192–202.

Papo, A., Piani, L., 2004. Effect of various superplasticizers on the rheological properties of Portland cement pastes. Cement and Concrete Research 34, 2097–2101. http://dx.doi.org/10.1016/j.cemconres.2004.03.017.

Pierre, A., Lanos, C., Estellé, P., 2013. Extension of spread-slump formulae for yield stress evaluation. Applied Rheology 23 (6), 63849.

Pigeon, M., Gagné, R., Aïtcin, P.-C., Banthia, N., 1991. Freezing and thawing tests of high-strength concretes. Cement and Concrete Research 21 (5), 844–852.

Piotte, M., 1993. Caractérisation du poly(naphtalènesulfonate): influence de son contre-ion et de sa masse molaire sur son interaction avec le ciment. Thèse (Ph.D.). Université de Sherbrooke.

Plank, J., Keller, H., Andres, P.R., Dai, Z., 2006. Novel organo-mineral phases obtained by intercalation of Maleic anhydride–allyl ether copolymers into layered calcium aluminum hydrates. Inorganica Chimica Acta 359 (15), 4901–4908. Protagonist in Chemistry: Wolfgang Herrmann. http://dx.doi.org/10.1016/j.ica.2006.08.038.

Plank, J., Zhimin, D., Keller, H., Hössle, F.v., Seidl, W., 2010. Fundamental mechanisms for polycarboxylate intercalation into C3A hydrate phases and the role of sulfate present in cement. Cement and Concrete Research 40 (1), 45–57. http://dx.doi.org/10.1016/j.cemconres.2009.08.013.

Plante, P., Pigeon, M., Foy, C., 1989. The influence of water reducers on the production and stability of the 28 air-void system in the concrete. Cement and Concrete Research 19, 621–633.

Ramachandran, V.S., Malhotra, V.M., Jolicoeur, C., Spiratos, N., 1998. Superplasticizers: Properties and Applications in Concrete, CANMET. Minister of Public Works and Government Services, Canada.

Regnaud, L., Nonat, A., Pourchet, S., Pellerin, B., Maitrasse, P., Perez, J.-P., Georges, S., 2006. Changes in cement paste and mortar fluidity after mixing induced by PCP: a parametric study. In: Proceedings of the 8th CANMET/ACI International Conference on Superplasticizers and Other Chemical Admixtures in Concrete, Sorrento, October 20–23, 2006, pp. 389–408. http://hal.archives-ouvertes.fr/hal-00453070.

Rixom, R., Mailvaganam, N., 1999. Chemical Admixtures for Concrete. E & FN Spon, London.

Roussel, N., 2006a. A theoretical frame to study stability of fresh concrete. Materials and Structures 39 (1), 81–91. http://dx.doi.org/10.1617/s11527-005-9036-1.

Roussel, N., 2006b. Correlation between yield stress and slump: comparison between numerical simulations and concrete rheometers results. Materials and Structures 39 (4), 501–509. http://dx.doi.org/10.1617/s11527-005-9035-2.

Roussel, N., 2012. 4-From industrial testing to rheological parameters for concrete. In: Roussel, N. (Ed.), Understanding the Rheology of Concrete. Woodhead Publishing Series in Civil and Structural Engineering. Woodhead Publishing, pp. 83–95. http://www.sciencedirect.com/science/article/pii/B9780857090287500042.

Roussel, N., Le Roy, R., 2005. The Marsh cone: a test or a rheological apparatus?. Cement and Concrete Research 35, 823–830.

Roussel, N., Coussot, P., 2005. Fifty-cent Rheometer' for yield stress measurements: from slump to spreading flow. Journal of Rheology (1978-Present) 49 (3), 705–718. http://dx.doi.org/10.1122/1.1879041.

Roussel, N., Stefani, C., Leroy, R., 2005. From mini-cone test to Abrams cone test: measurement of cement-based materials yield stress using slump tests. Cement and Concrete Research 35 (5), 817–822. http://dx.doi.org/10.1016/j.cemconres.2004.07.032.

Roussel, N., 2007. Rheology of fresh concrete: from measurements to predictions of casting processes. Materials and Structures 40 (10), 1001–1012. http://dx.doi.org/10.1617/s11527-007-9313-2.

Saak, A.W., Jennings, H.M., Shah, S.P., 2004. A generalized approach for the determination of yield stress by slump and slump flow. Cement and Concrete Research 34 (3), 363–371. http://dx.doi.org/10.1016/j.cemconres.2003.08.005.

Saric-Coric, M., 2001. Interactions superplastifiant-laitier dans les ciments au laitier: propriétés du béton. Ph.D. Thesis. Université de Sherbrooke, 582 p.

Schober, I., Flatt, R.J., 2006. Optimizing polycaboxylate polymers. In: Proceedings 8th CANMET/ACI International Conference on Superplasticizers and Other Chemical Admixtures in Concrete, Sorrento, ACI, SP-239, pp. 169–184.

Schober, I., Mäder, U., 2003. Compatibility of polycarboxylate superplasticizers with cements and cementitious blends. In: Proceedings 7th CANMET/ACI International Conference on Superplasticizers and Other Chemical Admixtures in Concrete, Berlin, ACI, SP-217, pp. 453–468.

Spiratos, N., Pagé, M., Mailvaganam, N.P., Malhotra, V.M., Jolicoeur, C., 2003. Superplasticizers for Concrete: Fundamentals, Technology and Practice. Supplementary Cementing Materials for Sustainable Development, Ottawa, Canada.

Struble, L., Sun, G.-K., 1995. Viscosity of Portland cement paste as a function of concentration. Advanced Cement Based Materials 2, 62–69. http://dx.doi.org/10.1016/1065-7355(95)90026-8.

Tagnit-Hamou, Baalbaki, M., Aïtcin, P.C., 1992. Calcium sulfate optimization in low water/cement ratio concretes for rheological purposes. In: 9th International Congress on the Chemistry of Cement, New Delhi, India, vol. 5, pp. 21–25.

Uchikawa, H., Sawaki, D., Hanehara, S., 1995. Influence of kind and added timing of organic admixture on the composition, structure and property of fresh cement paste. Cement and Concrete Research 25 (2), 353–364. http://dx.doi.org/10.1016/0008-8846(95)00021-6.

Vickers Jr., T.M., Farrington, S.A., Bury, J.R., Brower, L.E., 2005. Influence of dispersant structure and mixing speed on concrete slump retention. Cement and Concrete Research 35 (10), 1882–1890. http://dx.doi.org/10.1016/j.cemconres.2005.04.013.

Winnefeld, F., Becker, S., Pakusch, J., Götz, T., 2006. Polymer structure/concrete property relations of HRWR. In: Proceedings 8th CANMET/ACI International Conference on Superplasticizers and Other Chemical Admixtures in Concrete, Sorrento, ACI, Supplementary Papers, pp. 159−177.

Winnefeld, F., Becker, S., Pakusch, J., Götz, T., 2007. Effects of the molecular architecture of comb-shaped superplasticizers on their performance in cementitious systems. Cement and Concrete Composites 29 (4), 251−262. http://dx.doi.org/10.1016/j.cemconcomp.2006.12.006.

Xuan, Z., Ho-Wah, J. and Jeknavorian, A.A., 2003. Defoamer for water reducer admixture. U.S. Patent 6,858,661 filed October 15, 2003, and issued April 26, 2005.

Yamada, K., Ogawa, S., Hanehara, S., 2001. Controlling of the adsorption and dispersing force of polycarboxylate-type superplasticizer by sulfate ion concentration in aqueous phase. Cement and Concrete Research 31 (3), 375−383. http://dx.doi.org/10.1016/S0008-8846(00)00503-2.

Yamada, K., Takahashi, T., Hanehara, S., Matsuhisa, M., 2000. Effects of the chemical structure on the properties of polycarboxylate-type superplasticizer. Cement and Concrete Research 30 (2), 197−207. http://dx.doi.org/10.1016/S0008-8846(99)00230-6.

Yoshioka, K., Tazawa, E., Kawai, K., Enohata, T., 2002. Adsorption characteristics of superplasticizers on cement component minerals. Cement and Concrete Research 32, 1507−1513.

Yahia, A., Mantellato, S., Flatt, R.J., 2016. Concrete rheology: A basis for understanding chemical admixtures. In: Aïtcin, P.-C., Flatt, R.J. (Eds.), Science and Technology of Concrete Admixtures. Elsevier, (Chapter 7), pp. 97−128.

Zimmermann, J., Hampel, C., Kurz, C., Frunz, L., Flatt, R.J., 2009. Effect of polymer structure on the sulfate-polycarboxylate competition. In: Holland, T.C., Gupta, P.R., Malhotra, V.M. (Eds.), Procedure of the 9th ACI Interntational Conference on Superplasticizers and Other Chemical Admixtures in Concrete. American Concrete Institute, Detroit, SP-262-12, pp. 165−176.

Air entraining agents

17

R. Gagné
University of Sherbrooke, Sherbrooke, QC, Canada

17.1 Introduction

Concrete always contains a (more or less important) volume of air bubbles. These bubbles are formed during the mixing of concrete. In the absence of an air entraining agents (AEA) or a contaminant that entrains air, the total volume of air entrapped in concrete is usually between 1% and 3%. In order to increase the amount of air present in the concrete, it is necessary to introduce an AEA in the concrete (see Chapter 6; Aïtcin, 2016b).

Generally speaking, the entrainment of a small amount of tiny bubbles improves some other properties of the fresh and hardened concrete (see Chapter 6; Aïtcin, 2016a). In Nordic areas, the use of entrained air is recommended in concrete exposed to freezing and thawing cycles, depending on the presence of deicing salts.

17.2 Mechanisms of air entrainment

The shear paddles of a mixer create vortexes that trap air bubbles in the paste and the mortar. In the absence of an AEA, the air bubbles that are trapped in the paste or in the mortar are not stable and coalesce to form coarser bubbles. These coarse bubbles are submitted to a buoyancy upthrust so that they are eliminated at the top surface of the concrete. Later, the vibration will also facilitate the elimination of the last coarse air bubbles still trapped in the fresh concrete so that the final volume of entrapped air in concrete is quite small, usually less than 3%. These **entrapped air bubbles** have diameters of 0.3−5 mm, close to that of **sand grains**. These bubbles cannot efficiently protect concrete against an attack of freezing and thawing cycles (Pigeon and Pleau, 1995).

During concrete mixing, the introduction of an AEA favors the formation of numerous finer air bubbles that are very stable and do not coalesce. These **intentionally entrained** tiny air bubbles have usually a diameter of 5−100 μm, like **cement particles**. When formulating a concrete mix, it is possible to control the volume of entrained air and the structure of the bubble network through the selection and the dosage of an appropriate AEA.

As seen in Chapters 6 and 9, AEAs are organic molecules having various chemical compositions that are acting as surfactants (Aïtcin, 2016b; Gelardi et al., 2016). These molecules have usually a hydrophilic termination bound to a hydrophobic

Science and Technology of Concrete Admixtures. http://dx.doi.org/10.1016/B978-0-08-100693-1.00017-5
Copyright © 2016 Elsevier Ltd. All rights reserved.

chain, as described in Chapter 9 (Gelardi et al., 2016). The hydrophobic and hydrophilic ends of the AEA are adsorbed at the air−water or cement−water interfaces (see Chapter 10; Marchon et al., 2016). This adsorption decreases strongly the air−-water superficial tension. The higher the concentration of the surfactant, the greater the decrease of the surface tension of the solution, so that the AEA favors the stabilization of small bubbles because of this decrease of the superficial tension at the air−water interface.

Two principal mechanisms are proposed to explain the stabilizing function of the AEA (Kreijger, 1967). The first one implies the hydrophilic termination of the air-entraining molecules that can be fixed on the positive sites existing at the surface of cement particles. The air bubbles are maintained at a certain distance from each other and are fixed on a solid surface of the suspension.

The second mechanism involves the capacity of certain types of molecules to produce an insoluble hydrophobic precipitate that forms a membrane at the water−air interface so that the air bubbles are coated with a sufficiently thick and strong solid film to generate a steric effect that favors the dispersion of the air bubbles and avoids their coalescence (Mielenz et al., 1958).

17.3 Principal characteristics of a bubble network

The principal characteristics of an air bubble network are as follows:

- The total volume of the entrained air
- The average volumic surface of this system
- The spacing of the air bubbles in the network

The total volume of the air bubbles is usually expressed as a percentage of the total volume of a concrete. In a non-air-entrained concrete, usually this volume is smaller than 3%. In an air-entrained concrete, the total volume of air may vary between 4% and 10% according to the specifications.

Two standard testing methods exist to measure the total volume of air in fresh concrete. For normal weight concretes made with relatively dense aggregates, the ASTM C231/231M test method (*Air content of freshly mixed concrete by the pressure method*) is based on the change in volume of concrete with a change in pressure. It uses a portable apparatus (air meter) with a basic operational design employing the principle of Boyle's law (ASTM, 2010). For lightweight concrete or concretes made with highly porous aggregates, the ASTM C173/C173M test method (*Air content of freshly mixed concrete by the volumetric method*) measures the air contained in the mortar fraction of the concrete, but it is not affected by air that may be present inside porous aggregate particles. It uses a portable apparatus (air meter) to measure the volume change after the addition of water and isopropyl alcohol to dispel air void and foam (ASTM, 2012a). Using these test methods to measure the total volume of air does not provide any indication of the dimension and spacing of air bubbles.

The spacing of the air bubbles is a very important parameter that influences the degree of protection of a concrete facing freezing and thawing cycles. This spacing is characterized by what is called the spacing factor ($\overline{L}$). In fact, the spacing factor characterizes the average spacing of the air bubbles as measured when observing bubbles sections appearing on a polished concrete surface under an optical microscope (ASTM C457/C457M, 2012b; Chapter 6; Aïtcin, 2016b). The calculation of $\overline{L}$ takes into account the total volume of the bubbles and their dimensions. For a uniform air-bubble network composed of an average-size air bubble, $\overline{L}$ is the half-distance between two adjacent air bubbles (Figure 17.1). The spacing factor of a non-air-entrained conventional concrete is usually greater than 700 μm, while a concrete well protected by a satisfactory network of entrained air has a spacing factor that varies from 100 to 200 μm.

The average volumic surface of a bubble network (α) corresponds to the ratio of the surface and the volume of an average dimension air bubble (expressed in mm^{-1}). The average volumic surface is obtained when calculating the spacing factor using the ASTM C457/457M standard procedure. When the average dimension of the air bubbles decreases, the volumic surface increases. The volumic surface of a satisfactory bubble network obtained using an appropriate dosage of an AEA is usually greater than 25 mm^{-1} (Pigeon and Pleau, 1995). Figure 17.2 shows that the fulfillment of this requirement results usually in the production of a spacing factor lower than 200 μm (Saucier et al., 1991).

17.4 Production of a bubble network

To optimize the composition of an air-entrained concrete, it is necessary to select and find the dosage of the AEA that will produce a network of air bubbles, of which the total volume and spacing factor are within the specifications. It is also necessary to

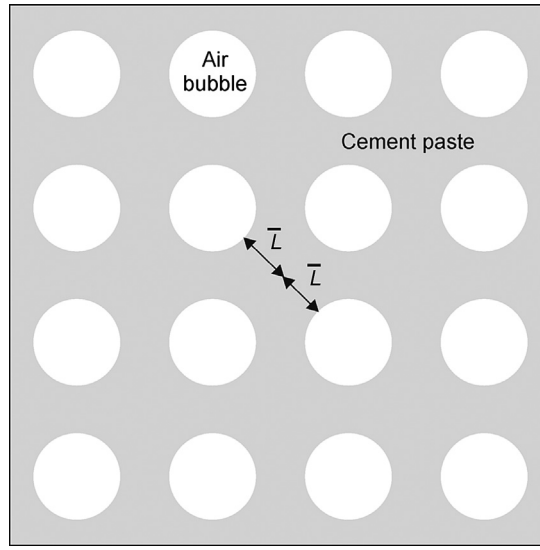


Figure 17.1 Schematic representation of the spacing factor of air bubbles ($\overline{L}$). Courtesy of Prof. Richard Gagné.

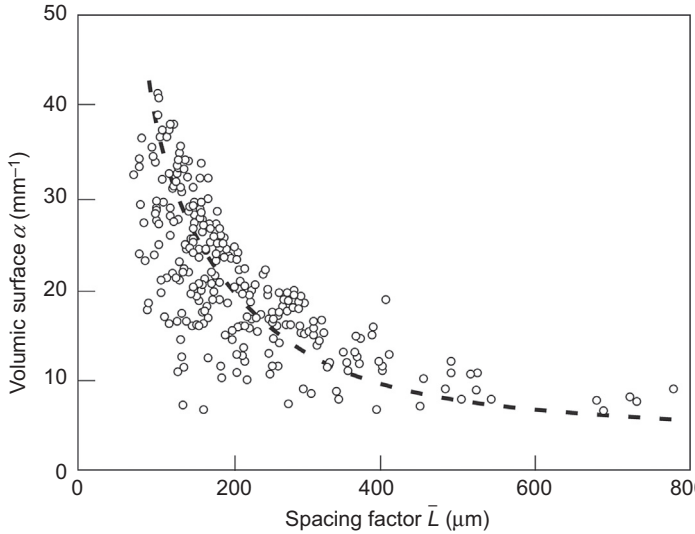


Figure 17.2 Typical relationship between the volumic surface (α) and the spacing factor ($\overline{L}$) of an air-bubble network in concrete (Saucier et al., 1991).

check the stability of the network of air bubbles in order to be sure that it will not be modified during transportation, pumping, and placing.

The process of formulating an air-entrained concrete is not always easy and necessitates very often an iterative approach. It is not possible for admixtures companies to propose precise dosages of their proprietary product, permitting them to immediately obtain the bubble network corresponding to the specifications. This is mainly due to the wide diversity of commercial AEA and the high number of mixture designs and placing parameters influencing the production of the bubble network. The process of selecting the AEA optimal dosage must start with the values found in the technical sheets of the AEA, starting with the lowest value, then the average value, and finally the highest value (the artillery technic for fixing the firing parameters). Then, it is easy to make an interpolation.

The selection of the optimum dosage depends on the materials used to make concrete (cement, supplementary cementitious materials; aggregates particularly sand and other admixtures) of the water−cement ratio (w/c) or water−binder ratio (w/b), the mixing method, the type of mixer, and the conditions of placing (temperature, vibration, etc.).

First, trial batches are made in the laboratory to find a dosage as close as possible to the final dosage before doing field trial batches with the mixing system used and ambient conditions. Of course, the increase of the AEA dosage results in an increase, not necessarily linear, of the volume of entrained air. It must be mentioned that the increase of the volume of air often results in an increase of the workability of concrete and a decrease of its compressive strength. Therefore, in some cases, it will be necessary to decrease the w/c or w/b or adjust the water dosage to satisfy at the same time the

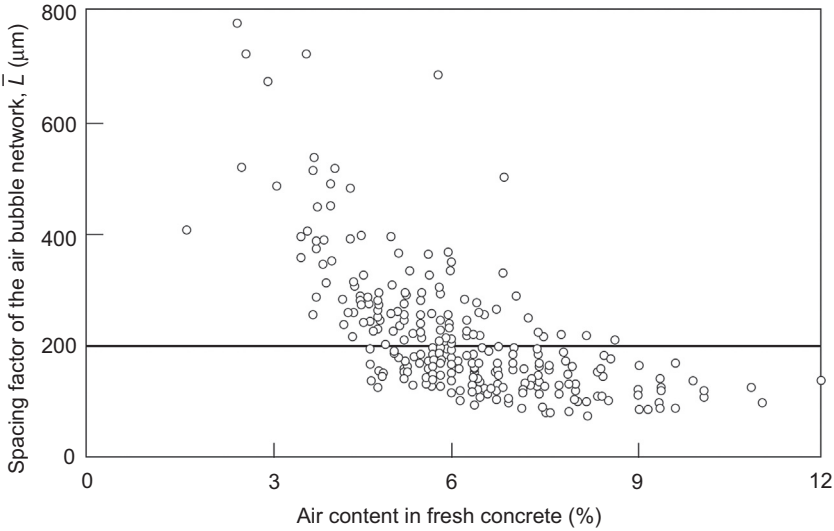


Figure 17.3 Relationship between the total air content and the spacing factor of the air bubble network (Saucier et al., 1991).

requirements on workability and strength. However, the production of the total volume of entrained air within the specification does not guarantee that the spacing factor of this network of air bubbles is satisfactory. However, usually commercial AEAs provide a satisfactory spacing factor for a good protection against the action of freezing and thawing cycles. ASTM procedures C233/C233M and C260/260M cover the test methods and the standard specifications for air-entraining admixtures for concrete (ASTM 2011, 2010b).

The volume of entrained air necessary to obtain a spacing factor of 200 μm is variable and depends on the type of AEA, the type of concrete, and the mixing equipment to produce it. Figure 17.3 presents experimental data showing the relationship between the spacing factor and the total volume of air (Saucier et al., 1991). The same total volume of air may correspond to different spacing factors. For a total volume of air, the smaller the average dimension of the air bubbles, the smaller the spacing factor (bubbles are closer to each other). The average dimension of the air bubbles varies greatly depending on the type and dosage of the AEA and, of course, of the mixing equipment. The data of Figure 17.3 show that the usual range of specified total volume of air (4−8%) gives spacing factors varying between 100 and 400 μm.

17.4.1 Influence of formulation parameters

17.4.1.1 Cement

In the technical data of commercial AEAs, the dosage of the AEA is usually expressed as a function of the mass of cement (mL of AEA/kg of cement). When the cement dosage of 1 m^3 of concrete increases, the volume of paste increases so

it is necessary to stabilize more air bubbles to protect it against freezing and thawing or to improve concrete rheology. Therefore, when expressing the AEA dosage as a function of the mass of cement, it is easier to determine the quantity of AEA required to achieve the desired air volume. Moreover, the efficient use of an AEA is directly linked to the dosage of water in concrete. The air entrainment is less efficient when the water dosage is high; therefore, it is necessary to have a higher amount of AEA. Concretes having a high cement dosage have usually a high water dosage. Therefore, again, when expressing the AEA dosage as a function of the mass of cement, it is easier to optimize the AEA dosage as a function of the water dosage of the concrete.

The finer the cement is, the higher is the AEA dosage necessary to produce a certain volume of air. For the same amount of cement, a higher fineness increases the amount of AEA absorbed on solid surfaces (see Chapter 10; Marchon et al., 2016). Consequently, less AEA remains in solution for producing and stabilizing the air bubbles (Du and Folliard, 2005).

The alkali content of a cement may also influence the production and stability of a network of air bubbles. An increase of the alkali content of a cement from 0.6% to 1.25% $Na_2O_{eq.}$ has resulted in a 0.5% increase of the total volume air for concretes with and without entrained air (Samoui et al., 2005). A cement rich in alkalis increases the stability of the bubble network (Plante et al., 1989).

17.4.1.2 Consistence and superplasticizer

The consistence and rheological properties of a concrete may have a great influence on the production of the network of air bubbles. The air bubbles are produced by the action of the vortexes created by the paddles of the mixer. If the concrete is too fluid, the vortexes are formed easily, but the paste and the mortar cannot stabilize sufficiently the air bubbles. These bubbles rapidly migrate to the surface of concrete under buoyancy upthrust so that they are lost very rapidly after their formation during mixing, transportation, and placing (vibration). On the contrary, when the viscosity of concrete increases, it is more difficult to shear concrete during mixing so that it is necessary to generate more energy to create the vortexes responsible for the formation of the air bubbles, but the network obtained is usually very stable due to the great viscosity of the paste that limit the mobility of the air bubbles. Experience shows that it is possible to produce a satisfactory network of air bubbles in viscous concrete using a higher dosage of AEA. In practice, it is observed that for a certain amount of AEA, the volume of entrained air increases when the slump passes, for example, from 75 to 150 mm. When the slump exceeds 150 mm, the volume of entrained air may decrease due to the increasing instability of the big bubbles that are moving upward to the surface of the concrete (Dodson, 1990).

A variation in the w/c could influence concrete consistency and consequently the entrainment of air. For example, a decrease of w/c results in an increase of the yield stress and the viscosity of the paste. According to Du and Foliard (2005), an increase of the yield stress and the viscosity of the paste generates “energy barriers” that prevent the formation of air bubbles. Moreover, it is possible to define a relationship between the yield stress of the paste and the size of the largest stable inclusion having a different density than the paste (Roussel, 2006).

Superplasticizers may increase or decrease the volume of entrained air according to their dosage, their chemical nature, and the slump of concrete. These variations depend on two essential mechanisms:

- The modification of the consistency of the cement paste
- The possibility of a chemical interaction with the AEA

According to the mechanism described in the previous paragraphs, the addition of a superplasticizer usually facilitates the production of a network of air-entrained bubbles by decreasing the yield stress and the viscosity of the paste (Du and Folliard, 2005). It is necessary to avoid an overdosage of superplasticizer because a too low yield stress of the paste can create an instability of the air bubble system (air loss during transportation and placing).

The chemical nature of the superplasticizer can influence the mechanism of production and the stability of the air-entrained bubble network (see also Chapter 16; Nkinamubanzi et al., 2016). Polynaphtalene-based superplasticizers have usually very few chemical interactions with commercial AEA. For example, for a given polynaphtalene-based superplasticizer, the relationship between the AEA dosage and the volume of entrained air is rather linear. Therefore, it is easy to optimize the dosage of the AEA in order to obtain the total volume of air required.

As a consequence of their chemical nature, the polycarboxylate-based superplasticizers present usually have secondary effects: they entrain some air. In order to fight this air entrainment, commercial polycarboxylate formulations often contains a certain amount of defoamer to limit the production of an excessive volume of air. Moreover, presently, the chemical composition of polycarboxylate-based superplasticizers is quite variable; therefore, the possibility of an interaction with the AEA is more frequent and difficult to predict. When polycarboxylate-based superplasticizers contain some defoamer, it is usually necessary to use a higher dosage of AEA to counteract the action of this defoamer.

The relationships between the dosage of a PCE superplasticizer and the AEA dosage and the total volume of air are not linear. For example, low AEA dosages produce very little air; however, as soon as a critical dosage of the AEA is reached, the volume of air increases rapidly. It has been observed that a particular polycarboxylate-based superplasticizer had increased drastically the total volume of air over 10% during the transportation of the concrete from the plant to the field (Gagné et al., 2004).

When combining the use of a polycarboxylate-based superplasticizer and an AEA, a more or less great proportion of the total volume of entrained air may be produced by the action of the superplasticizer and not by the AEA. The bubbles produced by the superplasticizer are usually coarser than those produced by the AEA (Pigeon et al., 1989; Plante et al., 1989). The coarse air bubbles entrained by the superplasticizer do not protect concrete against the action of freezing and thawing cycles because they do not decrease the spacing factor. In the case of some cement/AEA combinations, the spacing factor may pass from less than 200 μm before the introduction of the superplasticizer to close to 400 μm after the addition of the superplasticizer (Plante et al., 1989).

From a practical point of view, producing a satisfactory bubble network giving good protection against freezing and thawing cycles requires that the network of air bubbles is entrained principally by the AEA and not by the secondary function of the superplasticizer. The specific nature of the interactions controlling this means that general relations between superplasticizer and AEA cannot be given in the same way as for the role of cement types. Being aware of the possible problem is part of finding an adequate solution.

17.4.1.3 Supplementary cementitious materials

The size and reactivity of the particles of supplementary cementitious materials influence greatly the production of a bubble network as well as the AEA dosage.

Silica fume, when used at a 5−10% dosage of the mass of cement, has very few effects on the production of the network of air bubbles (Pigeon et al., 1989). In some cases, silica fume may decrease the volumic surface (smaller bubbles) and increase slightly the volume of entrained air. This increase of the volume of air is noticed only when a superplasticizer is used to compensate for the greater water demand of the mix (Pigeon et al., 1989).

The use of fly ash usually decreases the efficiency of AEA. Zhang (1996) has shown that a concrete containing a certain amount of fly ash necessitates higher dosages of AEA, in some cases up to 5 times the dosage used in a concrete containing only Portland cement. Several physicochemical characteristics of the fly ash are responsible for that increase of the AEA dosage. From a physical point of view, it is sometimes the specific surface area of the fly ash that is greater than that of the volume of cement it replaces in the mix. Fly ash has a specific gravity significantly lower than that of Portland cement; a given mass of cement is replaced by a higher volume of fly ash and consequently by a material has a higher external surface so that a higher amount of AEA can be absorbed at the surface of the fine particles. Moreover, some fly ash particles can be hollow (see Chapter 5; Aïtcin, 2016a) or porous so that the absorption of the AEA is increased. From a chemical point of view, fly ash may also contain some highly absorptive unburned carbon particles that are partially neutralizing the effect of AEA, particularly when that carbon is present as a very thin layer of soot covering the fly ash particles (Du and Folliard, 2005). The absorptive properties of the carbon present in the fly ash depend on the size of the particles, their surface chemistry, and the shape of the reactive sites (Du and Folliard, 2005).

In spite of these interferences, most of the time it is possible to produce an efficient network of air bubbles having the required spacing factor that respects the other design requirements to provide to concrete an efficient protection against freezing and thawing cycles (Bouzoubaa et al., 2003; Langley and Leaman, 1998; Zhang, 1996).

Blast furnace slags decrease the efficiency of AEA. For a given volume of entrained air, it is necessary to increase the AEA dosage as the slag dosage increases. Saric-Coric and Aïtcin (2003) have shown that in concretes containing 50−80% slag, it was necessary to multiply the AEA dosage by a factor of 2−4. According to these authors, the increase of the slag dosage resulted in a very low production of Ca^{2+} ions. These ions that are forming insoluble salts with the hydrophilic ends of the AEA play a key role in the stabilization of the bubble network.

17.4.1.4 Aggregates

The shape and the texture of aggregate particles, their grain size distribution, and the maximum size of the coarse aggregates may decrease the volume of entrained air (Du and Folliard, 2005). For a constant cement and AEA dosage, the volume of entrained air increases when increasing the dosage of the fine aggregate. Sand particles having a diameter between 160 and 630 μm favor the entrainment of air and, on the contrary, an increase of the proportion of particles having a diameter smaller than 160 μm decreases significantly the volume of air entrained (Du and Folliard, 2005). Some aggregates contaminated by oil or organic matters may generate large variations in the entrained air.

17.4.1.5 Admixtures

AEA can present some physicochemical interactions with some other admixtures used in the concrete formulation (water reducer, superplasticizer, retarder, accelerator, etc.). These interactions can be generally associated with the presence of inorganic electrolytes or polar organic molecules (Du and Folliard, 2005).

The great variety and complexity of the molecules contained in commercial admixtures do not permit the formulation of general recommendations that could eliminate rapidly incompatible combinations. However, certain technical data sheets clearly indicate incompatibilities between certain types of admixtures. In the absence of such recommendations, there is no other solution than to check the compatibility between trial mixes and commercial admixtures.

17.4.1.6 Fibers

During mixing, the presence of fibers reduces the formation of vortexes in which air bubbles are generated so that the efficiency of the AEA is greatly reduced. In many cases, it is necessary to increase by 50% the AEA dosage to compensate for the loss of efficiency of the mixer to form vortexes. The negative influence of the fibers on the entrainment of air increases with the length, rigidity, and dosage of the fibers. Whenever possible, it is better to start to build a correct air bubble network in the concrete before adding the fibers. Gagné et al. (2008) have shown that it is possible to produce a bubble network of good quality having a spacing factor lower than 200 μm in a concrete containing 0.5% by volume of hooked steel fibers or 0.5% of synthetic structural fibers 60 mm long.

17.4.2 Influence of the mixing procedure parameters

17.4.2.1 Type of mixer

The type of mixer influences the air-entraining mechanism as well as the distribution of the air bubbles in the paste and the mortar (fractioning and coalescence). The mixing parameters (e.g., sequence of addition of the materials, duration, speed, torque, shearing) influence the generation of the bubble network (Du and Folliard, 2005).

The volume of concrete in the mixer has also its importance: a too low or too high amount of concrete in the mixer affects the degree of shearing of the mix and the formation of vortexes.

The wear of the paddle as well as its cleanliness may result in a significant decrease of the entrainment of air bubbles and their dispersion so that it is sometimes necessary to increase the mixing time to entrain the required volume of air.

17.4.2.2 Temperature

The increase of concrete temperature results in a decrease of the volume of entrained air. In winter, AEAs can lose some of their efficiency when hot water is used to heat concrete; in such a case, it is better to start to introduce the hot water and later the AEA when the water has increased the temperature of the concrete. Otherwise, it will be necessary to increase the AEA dosage and the spacing factor will have a tendency to decrease. On the contrary, if the AEA dosage is decreased in order to take into account the drop of concrete temperature, the spacing factor will increase. Relatively complex physicochemical mechanisms have been proposed to try to explain the decrease of AEA efficiency when concrete temperature increases (Du and Folliard, 2005).

17.5 Stability of the network of entrained bubbles

The stability of the network of air bubbles is a very important parameter. The agitation of the concrete during its transportation, the addition of admixtures in the field, the pumping, and vibration may result in the disappearance of some air bubbles at the surface of the fresh concrete and on the coalescence of the small bubbles to form coarser air bubbles. This loss of air and the formation of coarse bubbles increase the spacing factor. From a practical point of view, it is important that the characteristics of the bubble network—total volume and spacing factor—remain stable from the beginning of the mixing to the end of placing.

17.5.1 Influence of the transportation of the fresh concrete

The agitation of the fresh concrete during its transportation may favor the fusion of small bubbles to form coarser bubbles and also their elimination. This modification of the bubble network changes some of its characteristics, particularly its spacing factor, but usually the composition of commercial AEA is adjusted to produce and stabilize the bubble network during normal operations of transportation and placing.

Saucier et al. (1990) have measured the evolution of the characteristics of the air-entrained bubble network in concrete between the end of the mixing at the ready-mix plant and its placing in the field. The characteristics of the network of the air bubbles were measured on hardened concrete samples taken after 15, 25, 70, and 90 min after the first contact between the cement and the water. These concretes were produced in central mixer or directly in a ready-mix truck (dry batch). Two types of AEA, two types of superplasticizers, and three different cements were studied. In the

absence of superplasticizer, the two AEAs under study produced a stable network during transportation and placing. The addition of a superplasticizer at the plant had sometimes destabilized the bubble network, resulting in an increase or decrease of the volume of the entrained air and of the spacing factor. The less stable networks were obtained with the lowest dosage of AEA.

17.5.2 Influence of vibration and pumping

The volume of entrained air decreases when the duration of the internal vibration increases. The air loss is more important in concretes having a high slump and a high volume of entrained air. However, a well-controlled vibration usually results in a relatively small loss of air. In that case, the loss of air corresponds to the loss of coarse bubbles, which is good from a mechanical point of view. This loss of coarse bubbles has very little influence on the value of the spacing factor, which is good for freeze−thaw durability.

The influence of the placing technique on the bubble network has been studied during the construction of a slab on ground on a concrete containing initially 8% of entrained air at the exit of the mixing truck (Hover and Phares, 1996). Four methods of placing were considered:

- Direct pouring from the truck
- Pumping (two configurations)
- Pouring with a bin
- Pouring with a conveyer

In all the cases, a vibrating screed was used to finish the surface.

Globally, the measured characteristics of the bubble network of the fresh and hardened concrete indicated that the method of placing had very little effect on the volume of air. The pumping with a configuration resulting in a free fall of the concrete in the final vertical section of the pump line generated an air loss between 0.5% and 2% (percentage point). The use of a flexible end forming a half-loop at the end of the vertical conduct of the pump resulted in a smaller air loss. The use of a bin generated an air loss between 0.5% and 1%. The loss of air associated with the use of a conveyer was between 1% and 1.5%. The finishing of the surface with the vibrating screed generated a loss of air of 0.5%. In spite of these air losses, in all the cases, the air bubble network had a spacing factor under 200 μm.

The pumping configuration using tubes laying horizontally on the soil has very little effect on the volume of air and on the spacing factor (Lessard et al., 1996). A configuration including a vertical final part giving a free fall of the concrete generates very limited air losses on the order of 1%, but the spacing factor may increase drastically, passing from 180 to 300 μm (Lessard et al., 1996). The use of a constriction at the end of the last vertical part of the pumping line avoids the free fall of concrete in the pumping line so that the spacing factor does not decrease too much. The increase of the spacing factor measured in vertical sections results essentially from the coalescence of the air bubbles, the impact forces generated during the decompression, and the free fall of the concrete in the vertical section from the pumping tube.

17.6 Conclusion

Entrained air modifies the rheology of concrete and its durability to freezing and thawing cycles. The air-entrained bubble network is characterized by the total volume of entrained air expressed as a percentage of the volume of concrete, the diameter of the bubbles (in μm or mm), the spacing factor that represents the average half-distance between two adjacent air bubbles (in μm), and the average volumic surface (mm^{-1}). The spacing factor is only important when concrete has to be freeze−thaw resistant.

Air bubbles are entrained by the AEA in the form of very tiny spherical bubbles having a diameter varying from 1 to 100 μm—a diameter similar to that of cement particles. On the contrary, the coarse entrapped air bubbles rather have a diameter varying from 0.5 to 5 mm, a diameter similar to that of sand particles.

Many factors such as the parameters of formulation, the cement type and fineness, the consistency, the superplasticizer dosage, the presence of supplementary cementitious materials, the use of other types of admixtures, the use of fibers, the mixing and transportation techniques, as well as concrete temperature influence the characteristics of the air-entrained network. It is also important to check that the air-entrained bubble network remains stable during transportation, placing, pumping, and finishing.

Despite the complexity of the action of all these factors, usually it is not difficult to fix the formulation of a mix by trial and error and produce a network of entrained air bubbles that satisfies the design requirements.

References

Aïtcin, P.-C., 2016a. Water and its role on concrete performance. In: Aïtcin, P.-C., Flatt, R.J. (Eds.), Science and Technology of Concrete Admixtures. Elsevier (Chapter 5), pp. 75−86.

Aïtcin, P.-C., 2016b. Entrained air in concrete: Rheology and freezing resistance. In: Aïtcin, P.-C., Flatt, R.J. (Eds.), Science and Technology of Concrete Admixtures. Elsevier (Chapter 6), pp. 87−96.

ASTM Standard C231/C231M-10, 2010. Standard Test Method for Air Content of Freshly Mixed Concrete by the Pressure Method. ASTM International, West Conshohocken, PA.

ASTM Standard C260/C260M-10, 2010b. Standard Specification for Air-Entraining Admixtures for Concrete. ASTM International, West Conshohocken, PA.

ASTM Standard C233/C233M-10, 2011. Standard Test Method for Air-Entraining Admixtures for Concrete. ASTM International, West Conshohocken, PA.

ASTM Standard C173/C173M-12, 2012a. Standard Test Method for Air Content of Freshly Mixed Concrete by the Volumetric Method. ASTM International, West Conshohocken, PA.

ASTM Standard C457/C457M-12, 2012b. Standard Test Method for Microscopical Determination of Parameters of the Air-void System in Hardened Concrete. ASTM International, West Conshohocken, PA.

Bouzoubaa, N., Fournier, B., Bilodeau, A., 2003. De-icing salt scaling resistance of concrete incorporating supplementary cementing materials. In: Proceedings of the Sixth Canmet/ACI Conference on Durability of Concrete, Supplementary Papers, Thessaloniki, pp. 791−821.

Dodson, V.H., 1990. Concrete Admixtures. Van Nostrand Reinhold, New York, 208 pp.

Du, L., Folliard, K.J., 2005. Mechanisms of air entrainment in concrete. Cement and Concrete Research 35, 1463−1471.

Gagné, R., Bissonnette, B., Lauture, F., Morin, R., Morency, M., 2004. Reinforced concrete bridge deck repair using a thin adhering overlay: results from the Cosmos bridge experimental repair. In: International RILEM TC 193-RLS Workshop on Bonded Concrete Overlays, June, Stockholm, 16 pp.

Gagné, R., Bissonnette, B., Morin, R., Thibault, M., 2008. Innovative concrete overlays for bridge-deck rehabilitation in Montréal. In: 2nd International Conference on Concrete Repair, Rehabilitation and Retrofitting, Cape Town, 24−26 November, 6 pp.

Gelardi, G., Mantellato, S., Marchon, D., Palacios, M., Eberhardt, A.B., Flatt, R.J., 2016. Chemistry of chemical admixtures. In: Aïtcin, P.-C., Flatt, R.J. (Eds.), Science and Technology of Concrete Admixtures. Elsevier (Chapter 9), pp. 149−218.

Hover, K.C., Phares, R.J., September 1996. Impact of concrete placing method on air content, air-void system parameters, and freeze-thaw durability. Transportation Research Record 1532, 1−8.

Kreijger, P.C., 1967. Action of A-E agents and water-reducing agents and the difference between them. In: Rilem-abem International Symposium on Admixtures for Mortar and Concrete, Bruxelles, 30 August−1 September, Topic II, pp. 33−37.

Langley, W.S., Leaman, G.H., 1998. Practical Uses for High-volume Fly Ash Concrete Utilizing a Low Calcium Fly Ash, vol. 1. American Concrete Institute, ACI Special Publication SP-178, pp. 545−574.

Lessard, M., Baalbalki, M., Aïtcin, P.-C., September 1996. Effect of pumping on air characteristics of conventional concrete. Transportation Research Record 1532, 9−14.

Marchon, D., Mantellato, S., Eberhardt, A.B., Flatt, R.J., 2016. Adsorption of chemical admixtures. In: Aïtcin, P.-C., Flatt, R.J. (Eds.), Science and Technology of Concrete Admixtures. Elsevier (Chapter 10), pp. 219−256.

Mielenz, R.C., Wolkodoff, J.S., Backstrom, H.L., Flack, H.L., 1958. Origin, evolution, and effects of the air void system in concrete : part 1. entrained air in unhardened concrete. Journal of the American Concrete Institute 30 (1), 95−121.

Nkinamubanzi, P.-C., Mantellato, S., Flatt, R.J., 2016. Superplasticizers in practice. In: Aïtcin, P.-C., Flatt, R.J. (Eds.), Science and Technology of Concrete Admixtures. Elsevier (Chapter 16), pp. 353−378.

Pigeon, M., Plante, P., Plante, M., 1989. Air void stability - part I: influence of silica fume and other parameters. ACI Materials Journal 86 (5), 482−490.

Pigeon, M., Pleau, R., 1995. Durability of Concrete in Cold Climates, Modern Concrete Technology 4. E & FN SPON, London, 244 pp.

Plante, P., Pigeon, M., Saucier, F., 1989. Air void stability - part II: influence of superplasticizer and cements. ACI Materials Journal 86 (6), 581−587.

Roussel, N., 2006. A theoretical frame to study stability of fresh concrete. Materials 797 and Structures 39, 75−83.

Saric-Coric, M., Aïtcin, P.-C., 2003. Bétons à haute performance à base de ciments composés contenant du laitier et de la fumée de silice. Revue Canadienne de Génie Civil 30 (2), 414−428.

Saucier, F., Pigeon, M., Plante, M., 1990. Field tests of superplasticized concretes. ACI Materials Journal 87 (1), 3−11.

Saucier, F., Pigeon, M., Cameron, M., 1991. Air-void stability - part V: temperature, general analysis, and performance index. ACI Materials Journal 88 (1), 25−36.

Smaoui, N., Bérubé, M.A., Fournier, B., Bissonnette, B., Durand, B., 2005. Effects of alkali addition on the mechanical properties and durability of concrete. Cement and Concrete Research 35 (2), 203−212.

Zhang, D.S., 1996. Air entrainment in fresh concrete with PFA. Cement and Concrete Composite 18 (6), 905−920.

Retarders

18

P.-C. Aïtcin
Université de Sherbrooke, QC, Canada

18.1 Introduction

It may be necessary to delay the initial setting time of concrete for various reasons, such as the following:

- In summer when the concrete temperature is high, causing the concrete loses its slump too rapidly if its setting time is not delayed
- When concrete delivery takes more than 1.5 h
- When cold joints have to be avoided in massive concrete construction
- When concrete is slipformed at a very slow rate

It is possible to delay concrete setting time using two different approaches: one physical, the other chemical:

- Concrete can be cooled using ice or liquid nitrogen. Using this "physical approach," the initial setting time of concrete can be delayed by a few hours at maximum.
- A chemical retarder can be introduced into the concrete during its mixing. In this case, concrete setting can be delayed almost at will, up to 24 h or more if necessary, without any negative effects on its final strength and durability.

Usually, the second approach is the most popular one because it is simple to implement, easy, and not very expensive. However, the control of the initial setting by a chemical retarder is not so easy due to the numerous factors that are simultaneously affecting this delay, such as the precision of the dosage system of the concrete plan and the temperature of all the ingredients used to make the concrete.

All admixture companies offer different types of retarders, quite often combined with a water reducer or a superplasticizer. Personally, the author of this chapter prefers to use separately a water reducer and/or a superplasticizer, and to adjust the retarder dosage to fine-tune the specific dosage of each of these basic admixtures. Using this approach, it is possible to obtain the desired effect on the retardation of the setting time, taking into account the initial temperature of the different ingredients of concrete, the ambient temperature, the length of the delivery time, etc.

During the construction of the Hibernia offshore platform in Newfoundland, setting had to be delayed for 24 h to provide enough time for the placing crew to place a lift of concrete in the very congested area all around the platform base, which had a diameter of 100 m. In such a case, it was necessary to adjust the amount of retarder to take into account the effect of the ambient temperature because, in a slipforming operation, it is very important that the concrete has the right consistency and strength when proceeding with the lifting of the forms. Some days, when the ambient temperature was

Science and Technology of Concrete Admixtures. http://dx.doi.org/10.1016/B978-0-08-100693-1.00018-7
Copyright © 2016 Elsevier Ltd. All rights reserved.

changing very rapidly, it was necessary to adjust the retarder dosage several times. If in one place the concrete had not set enough, it would collapse during the lifting; however, if it hardened too much, it would stick to the forms and tear the freshly deformed surface.

18.2 Cooling concrete to retard its setting

The hydration reaction—or rather, the hydration reactions of the different hydraulic phases of a Portland cement—are all exothermic so that they are self-activated according to an Arrhenius' type of law (Baron and Sauterey, 1982):

$$K = \mathrm{A}\ \mathrm{e}^{-\frac{E_a}{RT}}$$

where K is the specific hydrating rate, A is a constant, E_a is the activation energy, R is the gas constant, and T is the temperature expressed in degrees Kelvin. From this, the following practical relationship can be deduced:

$$\frac{t_1}{t_2} = \exp\frac{E}{R}\left(\frac{1}{T_1} - \frac{1}{T_2}\right)$$

where t_1 and t_2 represent the hydration time at temperatures T_1 and T_2.

Therefore, by cooling concrete, it is possible to retard its setting. From a practical point of view, it is quite easy and not very costly to decrease the concrete temperature. It is only necessary to replace a part of the mixing water with an equivalent weight of ice or to use liquid nitrogen when the replacement of the mixing water is not enough to decrease the concrete temperature to a targeted value.

Portable ice-making machines that produce ice flakes are commonly rented in Canada to decrease concrete temperature in summer. However, when the concrete must contain a certain amount of entrained air, a minimum of water has to be used to allow the entrainment of the specified air content. It happens that the decrease of the initial temperature of the concrete when replacing most mixing water by ice may still not be enough to produce a concrete whose temperature falls within the recommended range of temperature prescribed in the specifications. In such a case, it is necessary to use liquid nitrogen, as was done during the summertime construction of the CN Tower in downtown Toronto (Bickley, 2012) (Figure 18.1).

It is easy to calculate the effect of the substitution of a mass M_i of ice on the temperature of a fresh concrete using the following formula (Mindess et al., 2003):

$$T = \frac{0.22(T_a M_a + T_c M_c) + T_w M_w + T_{wa} M_{wa} - 80 M_i}{0.22(M_a + M_c) + M_w + M_{ma} + M_i}$$

where T is the temperature in degrees Celsius of the fresh concrete; T_a, T_c, T_w, and T_{wa} are the temperatures in degrees Celsius of the aggregates, cement, added mixing water,



Figure 18.1 Cooling concrete with liquid nitrogen.
Courtesy of John A. Bickley.

and free moisture on aggregates, respectively (generally $T_a = T_{wa}$); M_a, M_c, M_w, and M_{wa} are the mass in kilograms of the aggregates, cement, free moisture on aggregates, and mixing water, respectively; and M_i is the mass of ice.

What is more difficult to calculate is the retardation of the setting corresponding to a certain quantity of ice. From a practical point of view, the best way to find it is to make three batches containing, for example, 25, 50, and 100 kg of ice and to measure the effect of these substitutions on the setting time. The substitution of some of the mixing water by an equivalent mass of ice is also commonly used in mass concreting to limit the maximum temperature of the concrete and the risk of thermal cracking.

When substituting ice to water, it is always necessary to keep a minimum of liquid water in the mix to ensure a uniform mixing.

18.3 The use of retarders

When it is necessary to retard the setting of concrete for several hours, a retarder must be used.

18.3.1 Different chemicals used to retard concrete setting

It has been found that the following chemicals retard concrete setting:

- Some salts of lignosufonic acid known as lignosulfonates (the sodium salt, in particular); these retarders act also as dispersants
- Some salts of carboxylic acid that also act as dispersants
- Sugar or sugar derivatives that act only as retarders
- Certain inorganic salts

During the 1950s, some inorganic salts were used in the concrete industry, such as zinc oxide (Z_nO), sodium metaborate ($Na_2B_2O_7$), sodium tetraborate ($Na_2B_4O_7$),

tin sulfate ($SnSO_4$), lead acetate ($Pb(C_2H_3O_2)_2$), and calcium phosphate (CaP_2O_3). However, this practice is not used today; currently, concrete producers prefer to use liquid organic retarders that can be automatically introduced into the mixer through the water line.

However, it is important to know about the effect of these chemicals on concrete setting time because some of these chemicals can contaminate some of the concrete ingredients and create setting problems (see Section 18.6.1). The mechanism of the retardation of cement setting by these different chemicals can be explained in different ways depending on the chemical nature of the retarders. Fluorides and phosphates isolate the anhydrous cement particles from the interstitial solution by forming insoluble salts (Young, 1976). Zinc oxide retards C_3S hydration without affecting C_3A hydration like lead.

18.3.2 Different retarders standardized in North America

ASTM recognizes three types of retarders, identified as of Types B, D, and G. In fact, only retarders of Type B are true retarders; retarders of Type D and G are also dispersants. Type D retarders are water reducers that retard cement setting, while Type G are superplasticizers that also contain some retarder. In this chapter, only Type B retarders will be discussed. More precisely, the discussion will be confined to retarders based on sugar.

18.3.3 Sugar as a retarder

Even though sugar is used to retard cement hydration according to Ramachandran (1995), the retarding effects of sugars are not perfectly understood, despite the progress realized in recent years (see Chapter 12). We are not still able to explain clearly why some sugars are very efficient retarders and other are not (Marchon and Flatt, 2016b). All of the explanations found in the literature deal with absorption, precipitation, complexion, and nucleation phenomena. An overview on these phenomena is given in Chapter 10 (Marchon et al., 2016), while basic information on the chemistry and cement chemistry is respectively covered in Chapters 9 and 8 (Gelardi et al., 2016; Marchon and Flatt, 2016a).

It appears that sucrose is the best retarder. Glucose, maltose, and lactose have moderate retarding effects, while other sugars like trehalose have no retarding effects at all. The most accepted explanation for the retarding effect of sugars is that sugars and their derivatives essentially retard the hydration of the C_3S by retarding the precipitation of $Ca(OH)_2$.

We do know that sucrose is a very efficient retarder. It is very simple to dose it to obtain a targeted retardation. We also know how to use it. The unanswered questions are *why* and *how* sucrose retards cement hydration. These issues are discussed in Chapter 12 (Marchon and Flatt, 2016b).

Sugar may be used in combination with temperature to retard cement hydration, as seen in Figure 18.2, which represents the combined effect of the temperature of a concrete temperature and its dosage of retarder on its setting time.

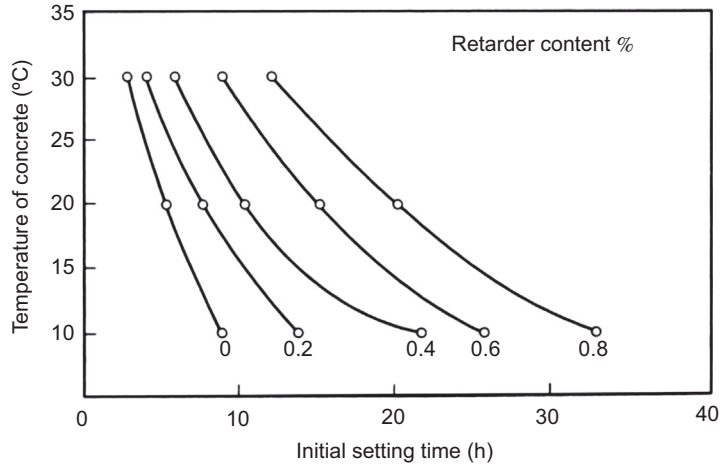


Figure 18.2 Combined effect of the temperature and the dosage of a retarder on the setting time. From Neville (2011), Massaza and Testolin (1980).

Sugars also favor the dissolution of calcium ions in the interstitial water so that the precipitation of portlandite is delayed. It is well recognized that it is the precipitation of portlandite that results in the rapid formation of C−S−H from C_3S.

However, most authors are convinced that sugars also affect C_3A hydration. Thus, the retardation of the C_3S can be altered because some of the C_3A absorbs a part of the retarder, which will then not be available later to retard the hydration of the C_3S. This is of some importance when deciding the timing of the introduction of the retarder during the mixing.

18.3.4 Dosage

The technical data provided by admixture companies suggest dosages that can usually vary by a factor of two. These values are always given in terms of the mass of active solids related to the mass of cement. In fact, from a practical point of view, the effect of a certain mass of active solids is influenced by the following factors, among others:

- The composition of the cement to be retarded
- Concrete initial temperature
- Ambient temperature
- Desired duration of the retardation
- The duration of the concrete delivery

In Section 18.2, the influence of initial temperature of concrete and ambient temperature is discussed because hydration reaction obeys an Arrhenius type of law. Therefore, some experimental work must be carried out for the fine-tuning of the dosage of retarder. This experimental work should be done on an experimental concrete having about the same initial temperature as that expected in the site.

During this experimental work, it is always wise to proceed with different dosages covering the dosages recommended by the manufacturer. The first dosage should be selected in the lower part of the suggested dosage, the second one in the middle, and the third one in the higher part. It is always good to select the three dosages as far as possible from each other, in order to be sure that the desired retardation of the experimental concrete can be obtained. It is always safer to make an interpolation rather than an extrapolation. It is the most rapid way to obtain the correct dosage of retarder to provide the right time of retardation looked for.

When a retarder is used simultaneously with a superplasticizer (rather than using a Type G retarder, where the proportions of retarder and superplasticizer have been fixed by the admixture manufacturer), it is always better to do a factorial design experiment (see Appendix A2) to find the right amount of retarder for that particular application.

18.4 Addition time

Most of the technical data sheets provided by admixture companies suggest retarder dosages based on their experience in the local market they are serving; very few of these technical data sheets suggest an optimum timing for the introduction of the retarder during mixing. The time at which the admixture is added can be as important as the absolute value of the dosage. In most batching plants, the admixtures are all introduced almost at the same time in the water line. However, for complex placing situations such as slow slipforming, where relatively high dosages of retarders have to be used, it is better to delay as long as possible the introduction of the retarder. This provides the maximum time for the sulfate ions provided by the calcium sulfate added during the grinding to neutralize the maximum amount of C_3A contained in the cement. In this way, a minimum amount of retarder will react with the C_3A and most of the active solids will remain in the mix to control the setting of the C_3S. This also applies when high performance concretes (HPCs) having a low w/c or w/b have to be retarded.

18.5 Some case history of undue retardations

18.5.1 Cracking of prefabricated slabs just after the removal of the forms

Because some prefabricated slabs were to be exposed to very harsh environmental conditions, the use of galvanized reinforcing bars was specified. Just after ordering the reinforcing bars, the precaster was informed that the project was delayed for several months. When the galvanized reinforcing bars were delivered, they were stored in the outside storage yard without any special protection. When the precast slabs were finally cast 6 months later, the reinforcing bars were covered with a white film of zinc oxide (known as white rust), to which nobody pay any attention.

After the removal of the forms of the first series of slabs, during their transportation to the storage yard, all of the slabs showed severe cracking, in spite of the fact that the

surface concrete was quite hard and the tested specimens had the expected compressive strength permitting them to be manipulated without any problem. The following day, production was stopped in order to find the reason for this unusual severe cracking. The cracking problem was finally linked to the zinc oxide layer present on the surface of the reinforcing bars, which acted as a strong retarder for the concrete in contact with the reinforcing bars. Owing to the retarding action of the zinc oxide, the reinforcing bars were separated from the hardened concrete by a layer of unhydrated concrete, so the slabs behaved almost as unreinforced slabs. To solve this cracking problem, it was only necessary to brush the reinforcing bars to remove the zinc oxide cover before using them.

18.5.2 A particularly hard-working aggregate trucker

Some years ago, one Tuesday morning in mid-November, the quality control (QC) manager of a large concrete ready-mix producer in Montréal received several phone calls indicating that the concrete delivered on Monday morning had not started to harden. Quickly, the QC manager realized that all the suspect concretes had been delivered roughly between 10 a.m. and noon. The concrete delivered on Monday morning before 10 a.m. and that delivered in the afternoon were fine. He could not blame it on the cement, because all of the concrete had been batched using the same cement delivery. On Wednesday morning, all of the suspect concretes had hardened, but one engineer in charge of the construction of some bowling lanes demanded that the bowling lanes be demolished. This was not so easy because the concrete was already quite hard when the demolition started.

During the rest of the week, the production of concrete was absolutely normal.

The following Tuesday morning, the same problem occurred. All of the customers facing the problem were told that, for some unknown reason, the concrete produced in the ready-mix plant between about 10 a.m. and noon was exhibiting a strong retardation and that, in spite of an exhaustive checking of the fabrication of the concrete, the reason for this retardation was unknown.

This phenomenon happened for 4 weeks in a row in November and then stopped quite miraculously.

During the company Christmas party, discussions about that strange phenomenon were rampant among the employees of the concrete plant. During a discussion between the QC manager and the yardman, the yardman told the QC manager that since the hiring of a new independent truck driver to transport the aggregates, there were no longer any problems related to aggregate deliveries. The aggregates were always delivered on time and the truck driver was always ready to do overtime. The yardman added also that this truck driver was a very hard-working person and that, during his weekends in November, he had been transporting the waste from a nearby sugar plant.

The QC manger suddenly realized what happened on the Tuesday mornings in November. Because the truck driver had not washed the bin of his truck after transporting the sugar wastes, the first load of sand delivered on Monday morning was contaminated by the sugar left in his bin. As this sand started to be used around 10 a.m. after the sand delivered on Friday, the contaminated sand unduly retarded the concrete

produced between 10 a.m. and noon. When the second delivery of sand started to be used in the afternoon, the retardation problem no longer occurred because the bin of the truck had been cleaned by the first load of sand. The truck driver was therefore told to wash the bin of his truck after transporting a material other than the sand for the concrete plant, which he did very scrupulously. The following November, on weekends, the truck driver continued to clean the sugar plant, but without any undue consequences on the hardening of the concrete, because every Sunday evening he cleaned the bin of his truck.

Note that on the first Tuesday morning that this problem happened, the QC manager took some specimens of the concrete of the bowling lanes to test them at 28 days. He was happy to send the excellent results to the engineer who had demanded the demolition of the concrete lanes.

18.5.3 An accidental overdosage of retarder

Hydro Quebéc, the hydropower company of Quebec, was doing some repair work on a dam located a 5-h drive from the closest ready-mix plant. As this repair work involved only about 30 m^3 of concrete, it was decided to use this ready-mix plant rather than transporting a small portable batching plant to the site. Of course, the concrete produced in the ready-mix plant had to be retarded in order to be sure that after a 5-h drive it still had a slump between 100 and 150 mm, but also that the concrete would be hard enough the next day for the removal of the forms. The contract included a $10,000 fine for each day of lost electricity production if the repair work was delayed.

Owing to some delays while carrying out certain preliminary work, the concrete deliveries were scheduled only 4 days before the critical day when the fine would begin to apply. The owner of the small ready-mix plant decided that he would be in charge of the operation, and that he would personally add by hand the retarder in each of the six ready-mix trucks. He prepared six doses of retarders in six plastic pails that were placed on the floor of the concrete plant.

During the batching of the third load of concrete, the owner of the batching plant received an urgent phone call that obliged him to stay in his office for about 15 min. The operator of the plant, believing that his boss had not added the retarder, put a pail of retarder in the truck.

At the end of the day, when the sixth load of concrete had to be delivered, the boss realized that the last pail of retarder was missing, so he concluded that one truck had received a double dosage of retarder. As he had personally added the retarder to trucks 1, 2, 3, 4, and 5, he asked his batcher if he had added some retarder to a particular truck load. The answer was, "Yes, when you had a long phone call during the loading of the third truck."

Therefore, the third load of concrete that was already placed in the forms had received a double dosage of retarder. The next morning, as expected, the concrete from the first, second, fourth, fifth, and sixth loads had hardened, but a hole made in the forms at the level of the third load of concrete showed that this concrete had not yet started to harden. The solution to avoid the $10,000 fine was to rapidly build a small heated shelter so that 24 h before the critical date, the forms could be removed.

The heating of the concrete was sufficient to counteract the retarding action of the overdosage of retarder.

18.5.4 Slipforming the gravity base of an offshore platform

During a cold, sunny, but windy period of 3 days, the QC manager in charge of the production of the concrete for the construction of a gravity base faced a serious problem. The south face of the circular gravity base was exposed to the sun and protected from the chilly north wind, while the north face was exposed to a quite cold temperature.

This temperature difference created problems when the forms had to be lifted. If the lifting was carried out when the concrete of the north face was hard enough, on the south face the concrete would be too hard and stick to the form, so that during the lifting the surface concrete would be torn quite deeply. If the slipping of the form was done when the concrete of the south face was hard enough, on the north face the concrete would be too weak and collapse because it had not enough time to set.

This difficult situation lasted for 3 days before normal winter conditions prevailed again and no longer disturbed the slipforming operation. That problem did not occur on the inside face of the base because it was not exposed to the same thermal situation as the external surface. The torn surface had to be repaired at a very high cost (Figure 18.3).

To prevent this type of problem, it is only necessary to isolate the concrete placed between the slip-forms with 50 mm of Styrofoam so that the external temperature no longer influences the hardening conditions of the concrete placed between the forms (Lachemi and Elimov, 2007). Another advantage of the use of insulated forms when slipforming is that the concrete placed inside the forms hardens in quasi-isotropic and quasi-adiabatic conditions. Insulated slip forms have been used successfully during the construction of three large liquefied gas reservoirs of 180,000 m^3 in St. John, New Brunswick, Canada.



Figure 18.3 External surface of an offshore platform due to the fact that the slipforming occurred too late.

18.6 Conclusion

By using chemical retarders, it is possible—but not always easy—to retard concrete setting for almost as long as necessary. The most common retarders are sugar based. The dosage of the retarder has to be adjusted to take into account the necessary time of retardation, the reactivity and fineness of the cement, the actual temperature of the concrete produced, and the ambient temperature. In each specific case, the retarder dosage should be fine-tuned by preparing two-to-three trial batches, or using a factorial design plan in the most complicated cases. The cooling of concrete with ice and/or liquid nitrogen can also be used to somewhat delay concrete setting or to control the temperature of concrete in summer.

References

Baron, J., Sauterey, R., 1982. Le Béton Hydraulique. Presses De L'école Nationale Des Ponts et Chaussées, Paris.

Bickley, J.A., 2012. The CN Tower—a 1970's adventure in concrete technology. In: ACI Spring Convention 2012, Address at the Student Lunch Meeting, Toronto, Canada, p. 20.

Gelardi, G., Mantellato, S., Marchon, D., Palacios, M., Eberhardt, A.B., Flatt, R.J., 2016. Chemistry of chemical admixtures. In: Aïtcin, P.-C., Flatt, R.J. (Eds.), Science and Technology of Concrete Admixtures. Elsevier (Chapter 9), pp. 149−218.

Lachemi, M., Elimov, R., 2007. Numerical modeling of slipforming operation. Computer and Concrete 4 (1), 33−47.

Marchon, D., Flatt, R.J., 2016a. Mechanisms of cement hydration. In: Aïtcin, P.-C., Flatt, R.J. (Eds.), Science and Technology of Concrete Admixtures. Elsevier (Chapter 8), pp. 129−146.

Marchon, D., Flatt, R.J., 2016b. Impact of chemical admixtures on cement hydration. In: Aïtcin, P.-C., Flatt, R.J. (Eds.), Science and Technology of Concrete Admixtures. Elsevier (Chapter 12), pp. 279−304.

Marchon, D., Mantellato, S., Eberhardt, A.B., Flatt, R.J., 2016. Adsorption of chemical admixtures. In: Aïtcin, P.-C., Flatt, R.J. (Eds.), Science and Technology of Concrete Admixtures. Elsevier (Chapter 10), pp. 219−256.

Massaza, F., Testolin, M., 1980. Latest development in the use of admixtures for cement and concrete, Il Cemento 77 (2), 73−146.

Mindess, S., Darwin, D., Young, J.F., 2003. Concrete. Prentice Hall, Englewood Cliffs, N.J., USA.

Neville, A.M., 2011. Concrete Properties. Prentice Hall, Harlow, England, 846 pp.

Ramachandran, V.S., 1995. Concrete Admixtures Handbook, second ed. Noyes Publications, Park Ridge, N.J., USA. pp. 102−108.

Young, F., 1976. Reaction Mechanisms of Organic Admixtures with Hydrating Cement Compounds, Transportation Research Record No. 564. Transportation Research Board, Washington DC, USA, pp. 1−9.

Accelerators

19

P.-C. Aïtcin
Université de Sherbrooke, QC, Canada

19.1 Introduction

Sometimes, it is necessary to accelerate the hardening of concrete, such as in the case of urgent repair work, or to accelerate the production rate in a precast concrete plant to be able to remove the forms earlier. The theoretical solution is quite simple: as seen in Chapter 1, from a physical point of view the only thing to do is to decrease the average distance between cement particles in the cement paste (Aïtcin, 2016a). In fact, as the system is flocculated, what this really means is that the number of contacts between grains in the paste must be reduced. From a chemical point of view, it is necessary to increase the hydration rate of the C_3S, which is essentially responsible for the production of C−S−H, the "glue" of cement paste. Both answers can be implemented at the same time. The physical answer improves the long-term strength and durability of concrete.

However, it is important to point out that chemical acceleration of the hydration of C_3S can have negative secondary effects: in many cases it can, but does not always, result in a loss of long-term strength and durability. Therefore, before deciding to chemically accelerate C_3S hydration, it is appropriate to see if this acceleration of the hardening of concrete may not be obtained by a reduction of the water−cement ratio (w/c) or water−binder (w/b), which will also improve the long-term properties of concrete. More specifically, changes in w/c and w/b have little effect on the rate of chemical reactions. However, the time needed to reach a given strength is reduced if less water is used. In this sense, a change in w/c or w/b is not a true acceleration, but it is nevertheless effective with respect to the requirement from practice, which is to reach the given properties at a specified time. As an alternative, different chemical products have been found to increase, in a matter of few hours, the early strength of concrete. These products are known as accelerators of hardening or, more simply, accelerators.

19.2 Different means to accelerate concrete hardening

19.2.1 The use of high-strength cement

To increase concrete early strength at a specified time, the use of high-strength and/or high early-strength cement has to be considered first. Usually, this cement is richer in C_3S and C_3A, which is ground finer than for normal Portland cement. Of course, when using such cement, it is necessary to increase the water and/or superplasticizer dosages

Science and Technology of Concrete Admixtures. http://dx.doi.org/10.1016/B978-0-08-100693-1.00019-9
Copyright © 2016 Elsevier Ltd. All rights reserved.

to obtain the same initial workability. Usually, the rate of the slump loss is greater when using this cement, and concrete temperature increases more rapidly because of the accelerated hydration of the C_3S. This increase of temperature has two effects:

- Positively, it increases the initial strength more rapidly due to the autoactivation of the hydration of the C_3S, which obeys an exponential Arrhenius type of law.
- Negatively, it creates large thermal gradients within concrete elements. This can result in cracking problems when the temperature of concrete decreases down to ambient temperature after the removal of the forms.

19.2.2 Decreasing w/c or w/b

Decreasing the w/c or w/b with an appropriate dosage of superplasticizer results in an increased number of bonds created by the C−S−H in the percolating particle network of the paste (Chapter 1; Aïtcin, 2016a). It was seen that when the w/c or w/b is decreased, the cement particles are getting closer on average to each other so that the hydrates formed at their surface have to grow on a shorter distance before intermixing with the hydrates grown on adjacent cement particles; thus, strong early bonds are created rapidly. The alternative view considers that particles are not regularly distributed in space and separated from each other but rather flocculated and form a three-dimensional percolated particle network. In this case, the previously discussed effect of decreasing w/c or w/b is to increase the number of connections in this network and therefore also to increase the strength. It is an analogous case to the yield stress model, YODEL (Flatt and Bowen, 2006), presented in Chapter 7 (Yahia et al., 2016). Both explanations account for the effect of the w/c or w/b effect but use a different microstructural representation of the paste.

During the construction of the Passerelle de Sherbrooke (see Chapter 25; Aïtcin, in this volume-b), a 55 MPa compressive strength was obtained at 24 h, in spite of the fact that the cement used was a cement developing a very low heat of hydration due to its very low content of C_3S and C_3A. This high early strength was obtained because of the very low w/b (0.26) used to make this concrete. To reach such a closeness of the cement particles, it was necessary to use as much as 19 kg of active solids of a polynaphtalene superplasticizer corresponding to a dosage of 35 L/m^3. However, the use of such a high dosage of superplasticizer succeeded in neutralizing the very early hydration of the C_3S and C_3A. The initial setting time was only retarded by a few hours.

19.2.3 Heating of concrete

If the first two options do not adequately accelerate the short-term strength gains looked for, concrete may be heated. Because hydration reactions obey an exponential Arrhenius type of law, an increase of the initial temperature results in an acceleration of cement hydration, more quickly liberating its heat of hydration. Most often, the associated increase of the C_3S hydration results in a rapid slump loss and a long-term loss of strength. Usually, the increase of the initial temperature of concrete

during its batching is obtained by heating mixing water. Using the following formula, it is possible to calculate the final temperature of concrete:

$$T = \frac{0.22(T_a M_a + T_c M_c) + T_w M_w + T_{wa} M_{wa}}{0.22(M_a + M_c) + M_w + M_{wa}}$$

where T is the temperature of the fresh concrete in degrees Celsius; T_a, T_c, T_w, and T_{wa} are the temperature of the aggregates, cement, added mixing water, and free moisture on aggregates, respectively, in degrees Celsius (generally, $T_a = T_{wa}$); and M_a, M_c, M_w, and M_{wa} are the mass of the aggregates, cement, free moisture on aggregates, and mixing water, respectively, in kilograms.

In precast plants, it is easy to implement the external heating of the precast elements. In such a case, a metallic formwork is particularly advantageous because it favors heat transfer, but large thermal gradients are created because fresh concrete is not a very good heat conductor. In these situations, it is the superficial part of the heated concrete element that become hotter than its inside part. This is not too problematic because this external layer is in compression.

19.2.4 Insulated forms

When considering the heating of concrete to increase its early strength, it is too often forgotten that the use of insulated forms is beneficial because it takes advantage of the heat of hydration to increase concrete temperature. For sustainability, it is a very good solution. Because self-compacting concretes are commonly used in precast plants, it is no longer necessary to vibrate intensively concrete (and the forms) so that the addition of a fragile insulating material over the forms is not such a big problem. This option can be combined with the three previous ones.

19.2.5 Use of an accelerator

It is only when all of these options to increase concrete's early compressive strength are not sufficient to reach the targeted initial compressive strength on time that the use of a chemical accelerator can be considered, if permitted by local construction codes.

Several chemical products are known to accelerate to a certain degree concrete initial strength, but up to now none of them have been found to be as efficient as calcium chloride ($CaCl_2$)—which has, unfortunately, a great negative secondary effect on the durability of the reinforcing bars. However, an interesting alternative consisting of the use of suspensions of dispersed C−S−H particles has appeared as an effective alternative, as explained in Chapter 8 (Marchon and Flatt, 2016a).

19.3 Different types of accelerators

The American Concrete Institute (ACI) *Manual of Concrete Practice* (Committee 212) for the use of admixtures in concrete recognizes four types of accelerators:

- Some inorganic salts such as chlorides, bromides, fluorides, carbonates, thiocyanates, nitrites, thiosulfates, silicates, aluminates, and alkaline hydroxides

- Some soluble organic compounds such as triethanolamine (TEA), calcium formate, calcium acetate, calcium propionate, and calcium butyrate
- Setting accelerators such as sodium silicate, sodium aluminate, aluminum chloride, sodium fluoride, and calcium chloride
- Various solid accelerators such as calcium aluminate, silicate, finely divided magnesium carbonate, and calcium carbonate

These accelerators can be used without any problem in conjunction with water reducers and superplasticizers.

However, despite this impressive long list of chemicals that can be used to accelerate concrete hardening, it must be admitted that none of them beat calcium chloride when concrete initial compressive strength has to be rapidly increased.

19.4 Calcium chloride as an accelerator

In this chapter on accelerators, we present only in detail the use of calcium chloride because it is the most efficient and the most used in practice and it is not very expensive. Moreover, its action on concrete has been abundantly studied. However, it will be seen that its operational mode is not entirely understood and that there still exist some controversies among researchers (Ramachandran, 1995) to explain its mode of action. It must also be pointed out that its negative effects on the durability of the reinforcing bars are attenuated in low w/c or w/b concrete, which are particularly impervious due to the great compactness of their microstructure.

According to Ramachandran (1995), calcium chloride has been used in concrete since 1873 and a patent was taken in 1885. Between 1960 and 1990, large research efforts were done in order to better understand its mode of action. Cook, cited by Ramachandran (1995), found 240 references on the use of calcium chloride that were published between 1960 and 1986. Even in 1981, Ramachandran published a book entitled *Calcium Chloride in Concrete Science and Technology*. However, despite all of these research efforts, Ramachandran (1995) admitted:

> *"Many aspects of the action of calcium chloride are controversial, ambiguous and incompletely understood. In spite of, the above, to this day, enormous interest is being shown on various aspects of calcium chloride because it is not only economical to use but also is the most efficient of all accelerators".*

When researchers working for admixture companies are asked why so little research is being done to better understand the accelerating role played by calcium chloride, the same answer is always given: calcium chloride works well but we do not make money selling it. When the author tells them that if the mode of action of calcium chloride was better understood, it could be possible to find chemicals that could accelerate C_3S hydration without presenting the negative secondary effect of calcium chloride on reinforcing steel, the answer is always also: the use of calcium chloride is not a priority for our company. Economic reality overcomes scientific knowledge in private companies. To date, all the research done on a trial-and-error mode has shown that there is not a more efficient accelerator than calcium chloride.

19.4.1 Mode of action

Although calcium chloride has been used for a long time, it is surprising to see how its mode of action is not perfectly understood. Everybody agrees on the fact that if early strength is increased, it is because C_3S hydration is accelerated; however, the actual mechanism that accelerates C_3S hydration is not well understood.

Several researchers studied the acceleration mechanism of calcium chloride on pure C_3S, C_3A, C_2S, and C_4AF phases and in each case proposed a mechanism of action. However, experience shows that the hydration of the three other phases is also accelerated. In his literature review on calcium chloride acceleration, Ramachandran (1995) gives not less than 12 reasons that could explain the accelerating effect of calcium chloride. While we do not believe in several of these options based on more recent research on cement hydration, we feel that it is useful to reproduce the list of reasons that Ramachandran cited. This gives an overview of the possible interpretations. Those formulated reasons were that calcium chloride does the following:

1. Combines with C_3A and C_4AF so that the setting is accelerated because these compounds create active sites that favor C_3S hydration
2. Increases the hydration of C_3A and C_4AF and consequently that of the C_3S
3. Reacts with the hydrated lime (portlandite) produced by the hydration of the C_3S and forms $3CaO \cdot CaCl_2 \cdot 12H_2O$
4. Could form hydration nuclei having a low C/S ratio (Calcium/Silica ratio) on the initial porous C−S−H
5. Forms a special type of ettringite
6. Favors the formation of a complex salt containing chloride ions on C_3S that activates C_3S hydration
7. Acts as a catalyst of C_3A hydration but does not act directly on one of the four principal hydraulic phases of Portland cement
8. C_4AH_{13} forms rather than C_3 AH_6 when C_3A is hydrated in the presence of $CaCl_2$
9. The coagulation of the hydrosilicates could be responsible for the acceleration
10. Could decrease the pH of the interstitial solution and would increase the dissolution rate of the hydrated lime
11. All of the cement phases are getting faster in solution in the presence of calcium chloride
12. Following the diffusion of Cl^- ions in the hydrates that are formed initially, OH^- ions are diffusing faster and accelerate the precipitation of calcium hydroxide and consequently, the dissolution of the silicates

Based on more recent research in cement hydration covered in Chapters 8 and 12, we must emphasize that hydration is a coupled chemical process in which it is difficult to distinguish causes and consequences (Marchon and Flatt, 2016a,b). The main factors related to calcium chloride are, however, in our opinion dealing both with nucleation and dissolution kinetics.

19.4.2 Mode of addition

Calcium chloride is commercially available under three different forms: two solid forms and one liquid. Calcium chloride can be bought in the form of flakes containing 77−80% of calcium chloride or granules containing 94% of calcium chloride. In its

liquid form, it contains from 30% to 42% of calcium chloride per liter of solution, usually sold as 30% solution.

From a practical point of view, the ACI *Manual of Concrete Practice* (Committee 212) recommends the introduction of liquid calcium chloride in the water line in order to avoid direct contact between cement and calcium chloride that could cause a flash set. When flakes or granules of calcium chloride are introduced directly in the mixer, these flakes and granules have not always enough time to dissolve during the mixing of concrete. Undissolved calcium chloride may generate undesirable dark spots on concrete surface.

19.4.3 Rules concerning the use of calcium chloride

In some countries, the use of calcium chloride is prohibited; in other countries, it is permitted without any restrictions (Russia); in still others, it is permitted with restrictions and its dosage is limited to a critical dosage. For example, in Canada, it is possible to use up to 2% of calcium chloride in nonreinforced concrete. Kosmatka et al. (2011) stated that calcium chloride should be used with caution in the following cases:

- Vapor-cured concretes
- When two different metals are embedded in concrete
- For concrete slabs supported by permanent galvanized steel forms in the production of colored architectural concrete

On the contrary, the use of calcium chloride is absolutely prohibited in the following cases:

- Concrete for parking structures
- Prestressed beams
- Concrete elements containing pieces of aluminum
- Concrete made with potentially reactive aggregates
- Concrete containing aggregates potentially reactive to soils or water containing sulfates
- In floors that are receiving metallic hardeners that could react with alkalies (USA)
- In mass concrete
- In hot weather
- In nuclear power plants (In this case, specifications even forbid the use of sodium naphthalene sulfonate superplasticizer because the soda used to neutralize the sulfonic acid can contain some Cl^- ions remaining from its fabrication from sea water. In such a case, it is mandatory to use a calcium salt of polynaphthalene sulfonate obtained by the neutralization of the sulfonic acid by lime. The same situation should hold for other types of superplasticizers.)

19.5 Shotcrete accelerators

Accelerators for shotcrete represent a very separate class of products that have very specific requirements. In this section, we give a brief overview on their role, composition, and working mechanisms.

In tunneling and mining, the most widely spread use of concrete is wet spraying. In this situation, fluid concrete is pumped to a nozzle, where it is accelerated and intermixed with an airflow containing a liquid accelerator (Blümel and Lutsch, 1981). The material is projected at a very high speed, about 30–40 m/s (Tidona, 2004). The shotcrete must adhere to the surface it is projected onto. It must therefore change from a fluid to a sticky material in a matter of about 50–60 ms (Lootens et al., 2008). After that, it must continue to develop strength to be able to build up a respectable layer of sprayed concrete, typically 200–400 mm in a period of about 1 h (Eberhardt et al., 2009). More importantly, its strength must continue to increase to secure material, typically over a period of couple of hours (Eberhardt et al., 2009). This is particularly important in cases of water infiltrations that can build up important hydrostatic pressure behind the sprayed concrete. In this respect, the use of fibers is also very important in shotcrete, even more for overhead applications.

From a chemical point of view, shotcrete accelerators may be divided into two main classes: silicates and aluminum salts. Silicates were the first products to be used. They have a lower performance than aluminum-based products, not allowing as thick layers to be built up. However, they are very cost-effective and remain highly used in some parts of the world (e.g., China). The products based on aluminum salts are themselves divided into two classes: alkali and alkali-free products. Concerning the alkali products, these are basic salts of aluminum. They are highly effective to obtain fast early strength gain, although the long-term strength is lower (Paglia, 2000). However, alkali shotcrete accelerators present a major health and safety issue as they can be the cause of severe burns when they contact skin. The most serious cases are if they get in contact with eyes, as they can cause blindness.

Alkali-free accelerators are acidic solutions of aluminum salts. They have largely been marketed because they do not entrain the same health and safety issues as their alkali counterparts. They also do not exhibit a reduction of the long-term strength (Paglia, 2000). Chemically, these products are based on highly concentrated aluminum sulfate solutions that are stabilized against precipitation by including various mineral and/or organic acids (Lootens et al., 2008).

The initial action of shotcrete accelerators has been shown to result in the fast precipitation of ettringite (Paglia, 2000; Xu and Stark, 2005; Lootens et al., 2008). This causes a fast flocculation of the system, but it does not have much of an effect on the hydration of alite (Paglia, 2000; Xu and Stark, 2005). To reach the desired setting time, the accelerator must include a high aluminum concentration. In fact, in many cases, this leads to concentrations in excess of various aluminum salts, so that precipitates may form over time, which is clearly undesirable (limited shelf life). To stabilize the admixture, various acids are added. However, as already noted, some of these acids may compromise the intermediate or even long-term strength development (Lootens et al., 2008; Eberhardt et al., 2009). This effect is linked to the nature of the anion in the acid, which can strongly alter alite hydration. As a consequence, the stability of sprayed concrete can be compromised, and this is an issue that is given very serious consideration in the industry.

Finally, it is important to point out that the introduction of a shotcrete accelerator can perturb the cement reactivity by modifying the aluminate–silicate–sulfate balance

(Juilland, 2009). The importance of this balance has been explained in Chapter 8 and the possibility for admixtures to perturb it is discussed in more detail in Chapter 12 (Marchon and Flatt, 2016a,b). Juilland (2009) demonstrated that these same principles can specifically influence the setting and hardening behavior of shotcrete systems.

19.6 Conclusions

There exist different means to accelerate concrete hardening and initial strength, such as the use of high-strength cement, cement with low w/c or w/b ratios, heat, or insulated forms. If any of these options cannot provide an initial strength that is high enough, then it is necessary to use calcium chloride if the local codes permit it. It is important to check in what cases its use is permitted and what is the maximum dosage permitted. Despite its potentially negative secondary effects, calcium chloride remains the most efficient and cheapest accelerator used in the concrete industry.

Accelerators for shotcrete are completely different products based on silicates or aluminum salts. Some commercial products may contain alkalis, which make their handling dangerous. Usually, their use results in a reduction of the long-term compressive strength.

References

Aïtcin, P.-C., 2016a. The importance of the water−cement and water−binder ratios. In: Aïtcin, P.-C., Flatt, R.J. (Eds.), Science and Technology of Concrete Admixtures. Elsevier (Chapter 1), pp. 3−14.

Aïtcin, P.-C., 2016b. Curing compounds. In: Aïtcin, P.-C., Flatt, R.J. (Eds.), Science and Technology of Concrete Admixtures. Elsevier (Chapter 25), pp. 483−488.

Blümel, O.W., Lutsch, H., 1981. Spritzbeton. Springer Verlag.

Eberhardt, A.B., Lindlar, B., Stenger, C., Flatt, R.J., 2009. On the Retardation Caused by Some Stabilizers in Alkali Free Accelerators. Ibausil.

Flatt, R.J., Bowen, P., 2006. Yodel: a yield stress model for suspensions. Journal of the American Ceramic Society 89 (4), 1244−1256.

Juilland, P., 2009. Early Hydration of Cementitious Systems (Ph.D. thesis) EPFL, no. 4554.

Kosmatka, S.H., Kerkoff, B., Panarese, W.C., McLeod, N.F., McGrath, R.J., 2011. Design and Control of Concrete Mixtures, (EB 101), eighth ed. Cement Association of Canada, Ottawa, Canada. 411pp.

Lootens, D., Flatt, R.J., Lindlar, B., 2008. Some peculiar chemistry aspects of shotcrete accelerators. In: Sun, W., van Breugel, K., Miao, C.Ye G., Chen, H. (Eds.), Proceedings of the First International Conference On Microstructure Related Durability of Cementitious Composites. RILEM Publications S.A.R.L, pp. 1255−1261.

Marchon, D., Flatt, R.J., 2016a. Mechanisms of cement hydration. In: Aïtcin, P.-C., Flatt, R.J. (Eds.), Science and Technology of Concrete Admixtures. Elsevier (Chapter 8), pp. 129−146.

Marchon, D., Flatt, R.J., 2016b. Impact of chemical admixtures on cement hydration. In: Aïtcin, P.-C., Flatt, R.J. (Eds.), Science and Technology of Concrete Admixtures. Elsevier (Chapter 12), pp. 279−304.

Paglia, 2000. The Influence of Calcium Sufo-aluminate as Accelerating Component within Cementitious Systems (Ph.D. thesis) n°13852, ETHZ.

Ramachandran, V.S., 1981. Calcium Chloride in Concrete, Science and Technology. Applied Science Publisher Ltd, London, U.K.

Ramachandran, V.S., 1995. Concrete Admixtures Handbook, second ed. Noyes Publications, Park Ridge, NJ, USA. 102−108.

Tidona, B., 2004. Bericht der Düsenentwicklung in der Spritzbeton-Verfahrenstechnik (FH-Winterthur, Diploma thesis, 2004).

Xu, Q., Stark, J., 2005. Early hydration of ordinary Portland cement with an alkaline accelerator. Advances in Cement Research 19 (1), 1−8.

Yahia, A., Mantellato, S., Flatt, R.J., 2016. Concrete rheology: A basis for understanding chemical admixtures. In: Aïtcin, P.-C., Flatt, R.J. (Eds.), Science and Technology of Concrete Admixtures. Elsevier (Chapter 7), pp. 97−128.

Working mechanism of viscosity-modifying admixtures

20

M. Palacios, R.J. Flatt
Institute for Building Materials, ETH Zürich, Zurich, Switzerland

20.1 Introduction

Viscosity-modifying admixtures (VMAs) are essential to control the stability and cohesion of concrete with very specific rheological requirements, such as self-compacting concrete, underwater concrete, or shotcrete. In self-compacting concrete, high amounts of fine powder materials such as fly ash, silica fume, or limestone have been normally used to prevent segregation and bleeding. However, these fine powders are not always locally available and/or might have a variable composition. For this reason, the use of VMAs has progressively increased in recent years to provide more robust mix designs. In addition, some VMAs, such as cellulose and guar gum derivatives, have water retention properties and they are mainly used in rendering mortars. They reduce the adsorption of water into a porous substrate, increasing cement hydration and mechanical strength of the mortar.

As explained in Chapter 9 (Gelardi et al., 2016), there is a high variability of VMAs. Inorganic VMAs such as colloidal silica are frequently used; however, in this chapter, we mainly focus on polymeric VMAs because they allow a greater deal of structural variations. Polymeric VMAs enhance the stability of the mix by increasing one or several rheological parameters at the same time, such as plastic viscosity, yield stress, shear thinning behavior, and thixotropy. Their mode of action depends on their physico-chemical properties, dosage, and the presence of other admixtures in the mix.

A comprehensive review of the effects of VMAs on the rheological properties of cementitious systems has recently been given elsewhere (Khayat and Mikanovic, 2012). Here, we will focus mainly on the working mechanism of these admixtures, their compatibility when they are used in the presence of superplasticizers, and their effect on the hydration of cement.

20.2 Performance of VMAs

20.2.1 Mechanisms of action of VMAs

VMAs increase the stability of cementitious systems due to a combination of different physico-chemical phenomena that depend on the nature of the VMA and its concentration (Khayat and Mikanovic, 2012). Polymeric VMAs are highly hydrophilic and have high capacity to bind water molecules, increasing their effective volume in

Science and Technology of Concrete Admixtures. http://dx.doi.org/10.1016/B978-0-08-100693-1.00020-5
Copyright © 2016 Elsevier Ltd. All rights reserved.

solution. This leads to an increase of the dynamic viscosity of the interstitial solution and to an increase of the macroscopic viscosity of the cement suspension (Brumaud, 2011; Brumaud et al., 2013).

In addition, depending on the nature and concentration of the polymer, the following mechanisms can occur (see Figure 20.1):

- *Bridging flocculation* involves the adsorption of a chain of a high-molecular-weight polymer onto two or more cement particles, physically holding them together (Fellows and Doherty, 2005). This mechanism involves an increase of the yield stress of cement suspensions.
- *Polymer–polymer association*. Associative polymers contain segments distributed along the chain that have a tendency to interact with each other. As a consequence, intramolecular and intermolecular associations between the polymer chains can develop, producing a three-dimensional network and an increase of the viscosity of the interstitial solution (Chassenieux et al., 2011).
- *Entanglement*. At high concentrations, the chains of VMA polymers can entangle and increase the apparent viscosity of the interstitial solution and cement suspension (Khayat and Mikanovic, 2012).
- *Depletion flocculation* occurs because nonadsorbed polymers are depleted from a "volume exclusion shell" around larger particles. The difference of polymer concentration in bulk solution with respect to the depleted zone leads to an increase of the osmotic pressure in the system, which causes its flocculation. This mechanism does not modify plastic viscosity of suspensions, but it leads to an increase of the yield stress (Palacios et al., 2012).

20.2.2 Impact of VMAs on the rheology of cementitious systems

A common feature of all polymeric VMAs is that they increase the apparent viscosity of the aqueous solution, being higher the increase with the dosage of polymer.

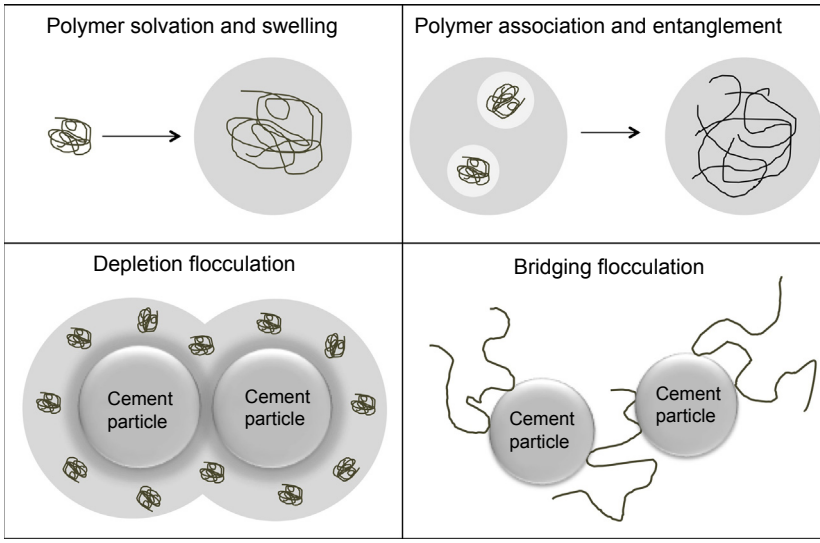


Figure 20.1 Sketch of the different mechanisms of action of polymeric VMAs.

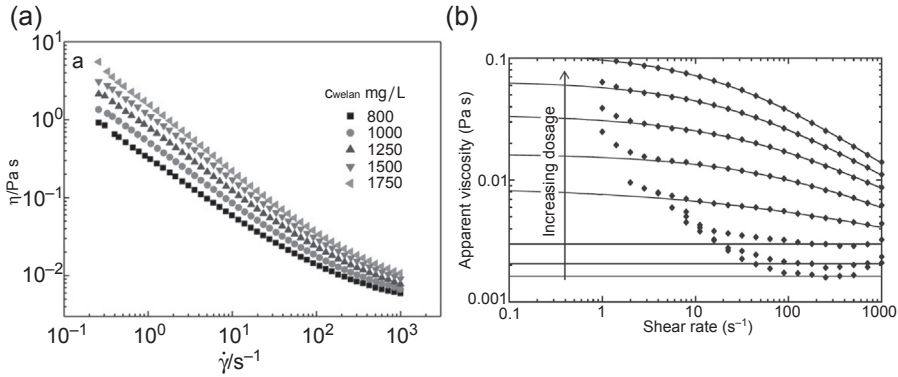


Figure 20.2 Examples of shear thinning behavior induced by (a) welan gum on aqueous solutions and (b) hydroxypropylguar on mortar pore solution.
Reproduced from Xu et al. (2013) and Poinot et al. (2013), respectively, with permission.

As shown in Figure 20.2, aqueous systems (as cement pore solutions) containing VMAs have a shear-thinning behavior where apparent viscosity decreases with shear rate. At low shear rates, disruption of polymer entanglements is balanced by the formation of new interactions and no effect on the viscosity is observed. At higher shear rates, the disentanglement of polymers predominates and chains align in the direction of the flow, consequently decreasing the apparent viscosity with the shear rate. This shear thinning behavior is observed not only in aqueous solutions but also in cementitious systems containing VMAs. This is highly desirable in concrete production, as VMAs increase the stability of the concrete once it is placed and enhance fluidity during mixing and pumping operations.

There are very few studies on the rheology of cementitious systems containing VMAs as the only admixture, and most of them deal with water retention agents. Brumaud (2011) showed that cellulose derivatives increase the viscosity of cement pastes.

Regarding the impact of water retention agents on the yield stress, contradictory results have been found in the literature. Some authors confirm that cellulose derivative (CE) admixtures slightly decrease the yield stress (Patural et al., 2011; Hossain and Lachemi, 2006). Patural et al. (2012) explained this decrease in base of the steric hindrance induced by the CE adsorbed onto cement particles. On the contrary, Brumaud (2011) observed an increase of the yield stress of cement pastes due to bridging flocculation prompted by the adsorbed admixture (see Figure 20.3). The difference obtained in the literature might come from the different structure and molecular weight of the CE polymers used. For example, Brumaud used CE with higher molecular weight than Patural et al.

20.2.3 *Performance of VMAs in the presence of superplasticizers*

In applications such as self-compacting concrete, it is essential to accomplish opposing rheological requirements, in particular high fluidity during casting and high viscosity

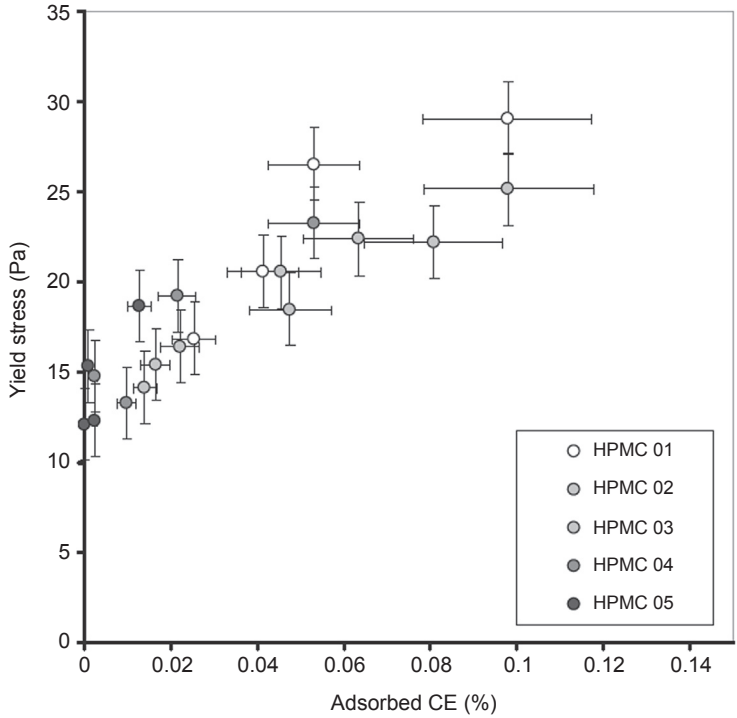


Figure 20.3 Yield stress of cement pastes with a w/c = 0.4 as a function of HPMC adsorption. Reproduced from Brumaud et al. (2014) with permission.

at rest to avoid segregation. For that reason, a combination of superplasticizers and VMAs is widely used. Chemistry and mechanism of action of both types of admixtures are different and problems of incompatibility might appear in practice. For example, adsorbing VMAs might compete with superplasticizers to absorb onto cement particles, reducing their dispersing properties.

20.2.3.1 Impact of VMAs on the rheological properties in the presence of superplasticizers

As observed in Figure 20.4, for a fixed dosage of superplasticizer, the addition of VMAs increases the plastic viscosity and/or yield stress. In practice, this increase of yield stress is normally corrected by the addition of extra water or more superplasticizer. In the cases illustrated in Figure 20.4(a), the CE shows a much more marked increase of plastic viscosity than yield stress. This observed effect might come from a specific combination of cellulose with a superplasticizer, but it is not necessarily a general behavior. In contrast, the other polymers show similar relative increases in both plastic viscosity and yield stress, as can be seen in Figure 20.4(b).

Welan gum and diutan gum are VMAs commonly used in combination with superplasticizers. Shear-thinning behavior is more pronounced in the presence of diutan

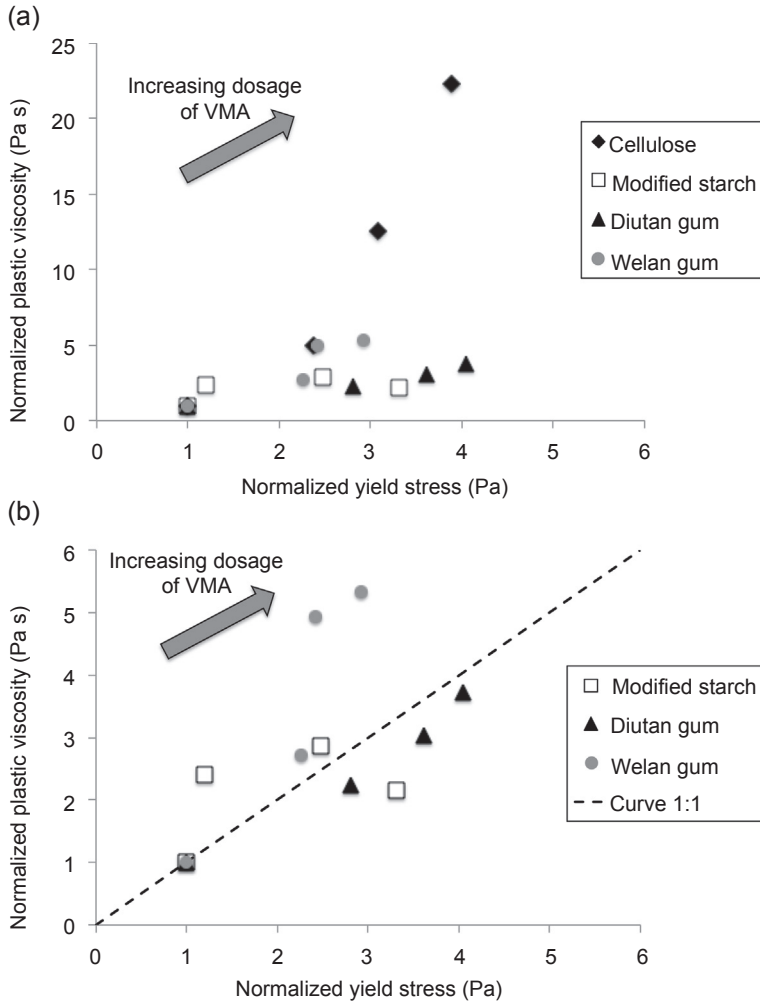


Figure 20.4 (a) Effect of type and concentration of VMAs on the rheological parameters of concrete-equivalent mortar of Self-compacting concrete (SCC) consistency. Dosage of superplasticizer was kept constant. (b) Image shown in detail.
Adapted from Khayat and Mikanovic (2012).

gum than welan gum because of its higher molecular weight (Sonebi, 2006). As shown in Figure 20.4(b), both gums and modified starch increase 2−5 times the plastic viscosity and yield stress of cement mortars with respect to those without VMA (Khayat and Mikanovic, 2012). This contrasts with the previously mentioned behavior of the cellulose derivative admixtures that mainly control the stability of the cementitious systems by significantly increasing the plastic viscosity. It should, however, be emphasized that these differences are illustrated on systems containing specific superplasticizers. Therefore, these observations should be taken as illustrations of possible

differences between combinations of a superplasticizer and a VMA rather than a general rule.

As explained before, polymeric VMAs physically adsorb large amounts of water by hydrogen bonds, increasing their effective volume and consequently the viscosity of the interstitial fluid of cementitious systems (Brumaud, 2011; Brumaud et al., 2013; Oosawa and Asakura, 1954). Apart from this specific effect on the continuous phase, the increase of yield stress observed in presence of welan gum and diutan gum could be explained by a combination of two mechanisms. On one hand, both gums have an anionic character and can also adsorb onto cement particles (see Figure 20.5 or Plank et al., 2010). For basic information on factors governing polymer adsorption as well as more specifically the role of molecular structure of PCEs on their adsorption, readers are referred to Chapter 10 (Marchon et al., 2013, 2016).

In the presence of a PCE superplasticizer, a competition between welan gum and superplasticizer to adsorb onto cement particles may occur as both polymers have a similar affinity for cement surface in the range of dosage of polymers normally used in concrete (see Figure 20.5). In this situation, yield stress would increase because of bridging flocculation. However, if not all the welan gum polymer is adsorbed, this polymer still remains in solution and could contribute to the increase of the yield stress by the depletion flocculation mechanism explained at the beginning of this chapter. However, first-order calculations of the depletion flocculation force do not seem large enough to explain the magnitude of yield stress change. More careful calculations would be needed. Furthermore, the competitity adsorption between PCE superplasticizer and a cellulose-based VMA has been probed by Bessaies-Bey et al. (2015) by using a combination of two techniques, total organic carbon (TOC) analyzer and dynamic light scattering (DLS).

In the case of modified starch VMAs, several studies have concluded that they significantly increase the yield stress. Again, this increase could be explained by a combination of both bridging and depletion flocculation. However, the effect of modified starch on the plastic viscosity is not clear. While Palacios et al. (2012) concluded that this VMA does not increase significantly the plastic viscosity of cement pastes, Figure 20.4(b) shows that starch-modified VMAs triple this rheological parameter.

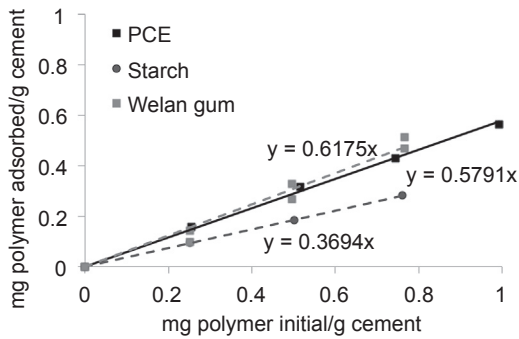


Figure 20.5 Adsorption of PCE superplasticizer and starch-modified and welan gum VMAs in the range of concentrations normally used in concrete.
Reproduced from the American Concrete Institute (Palacios et al., 2012) with permission.

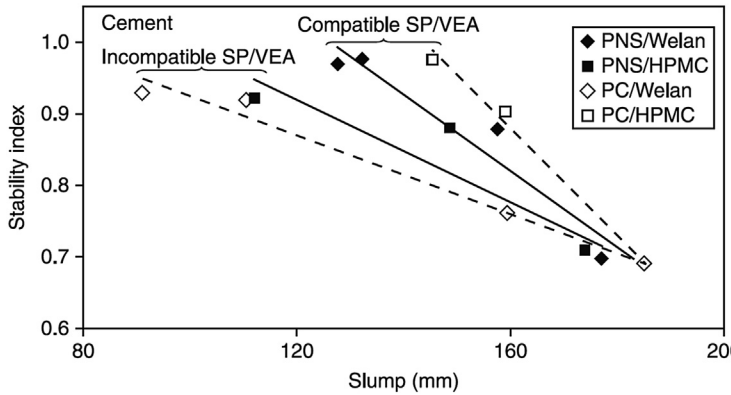


Figure 20.6 Stability of cement pastes as a function of spread flow (w/c = 0.65 and constant dosage of superplasticizer).
Reproduced from Khayat and Mikanovic (2012) with permission.

20.2.3.2 Compatibility of polymeric VMAs with superplasticizers

Kawai and Okada (1989) confirmed that cellulose-derivative VMAs are compatible with melamine-based and PCE superplasticizers. On the contrary, Figure 20.6 suggests certain incompatibilities of these VMAs with naphtalene-based superplasticizers (PNS) as the addition of cellulose derivatives decreases the slump flow (increases the yield stress) without much improvement in the stability of the mix (Khayat and Mikanovic, 2012). For the same reason, Figure 20.6 also reveals that PCEs and welan gum are incompatible while welan gum seems to be compatible with naphtalene- and melamine-based superplasticizers (Khayat and Mikanovic, 2012).

20.3 Working mechanisms of water retention agents

In building materials, cellulose ether (CE) and hydroxypropylguar (HPG)-derived polymers are normally used to improve the ability of a render or plaster to retain its constitutive water. In particular, they reduce the water loss due to capillary absorption into the porous substrate, onto which an overlay material is applied. This makes it possible for cement to hydrate and for adhesive and mechanical properties to develop (Brumaud et al., 2013; Marliere et al., 2012).

The working mechanism of both types of polymers has been proven to be similar. Firstly, CE and HPG admixtures increase the viscosity of cement pore solution. Brumaud et al. (2013) measured the influence of different CEs on the viscosity of distilled water and synthetic cement pore solutions. They confirmed that hydroxyethoxy methoxy cellulose (HEMC) and hydroxypropoxy methoxy cellulose (HPMC) increase the viscosity of these solutions; this increase depends on the molar mass, nature of the ether(s), and its dosage. However, as shown in Figure 20.7, at dosages lower than 1%, the viscosity increase does not depend on the molecular parameters, such as degree of substitution (DS) or mass substitution (MS). Only at very high

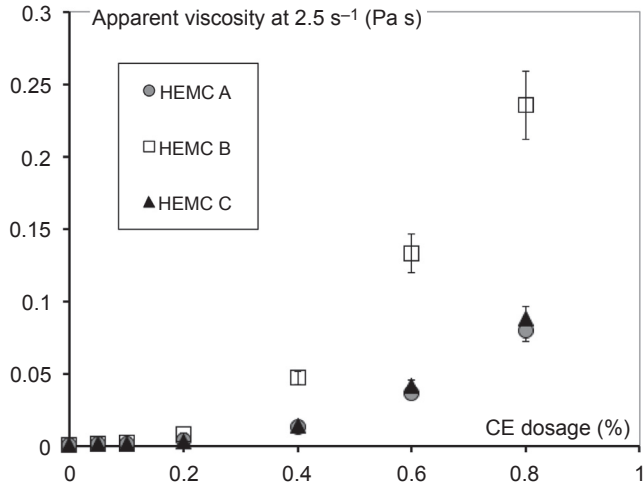


Figure 20.7 Apparent viscosity at 2.5 s^{-1} for various dosages of hydroxyethoxy methoxy cellulose (HEMC) in distilled water. HEMC B has a molar mass that is 2.5 times higher than the molar mass of HEMCs A and C. HEMCs A and C have an equivalent mass substitution (MS) and a different degree of substitution (DS) whereas HEMCs A and B have a different MS and similar DS.
Reproduced from Brumaud et al. (2013) with permission.

CE dosages (higher than 1%) is there a slight dependency on these molecular parameters and viscosity of the aqueous solution.

Water retention of cementitious systems increases with the molecular weight and dosage of CE admixtures. Several studies (Brumaud et al., 2013; Bülichen et al., 2012) have confirmed that the mechanism controlling the water retention of CE polymers depends on the concentration used. Below a critical concentration corresponding to the overlap of the polymer coils, water retention of mortars is dictated by the increase of the viscosity of the interstitial solution, no matter the polymer structural parameters (Brumaud et al., 2013). Most of the studies conclude that the increase of the viscosity induced by CE admixtures may reduce the mobility of the interstitial solution and increase water retention.

In contrast, Patural et al. (2012) showed by nuclear magnetic resonance dispersion measurements that the surface diffusion coefficient of water is not modified by the presence of CE, despite the high increase of the solution viscosity induced by these polymers. However, CEs transiently increase the fraction of mobile water molecules present at the solid hydrate surfaces.

At dosages above the critical concentration, the associative nature of the CE molecules mainly governs their water retention ability. There are two reasons for this. The first is that CEs form aggregates in solution, increasing the viscosity of the interstitial fluid. The second is that these polymer aggregates are a few micrometers in size (see Figure 20.8), so that they may jam and/or plug the porosity of the fresh paste or mortar (Sonebi, 2006; Patural et al., 2011; Brumaud et al., 2013). In addition, Jenni et al. (2003, 2006) found that methyl hydroxyethyl cellulose (MHEC) is transported through

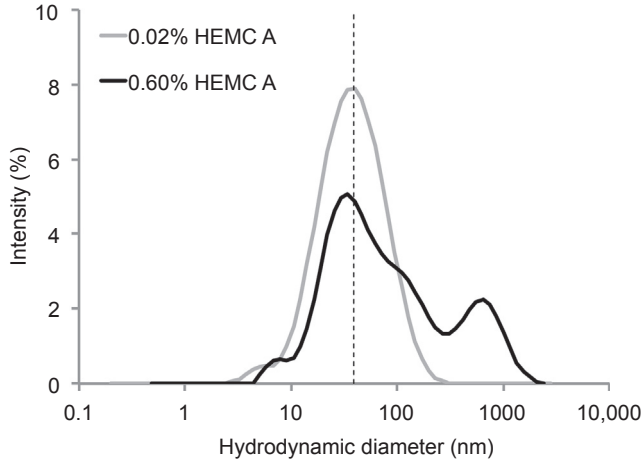


Figure 20.8 Hydrodynamic diameter of HEMC in aqueous solution below and above the overlapping concentration.
Reproduced from Brumaud et al. (2013) with permission.

the capillary pores of mortars and accumulated at the interface between the layer in contact with the substrate and the substrate surface, reducing the porosity.

Similar results as those presented above for CE have been obtained by Poinot et al. (2014) for HPG. They confirmed that water retention of cement mortars depends on HPG concentration. They also found that at concentrations higher than the overlapping concentration, a high increase of the water retention is induced due to the formation of polymer aggregates. However, at dosages below the critical concentration, almost no effect of HPG on water retention is observed. This last result contrasts with the case of CE polymers (see Figure 20.9) (Poinot et al., 2014). The reasons for this are not clear but may be to be found in the lower intrinsic viscosity of the selected polymers.

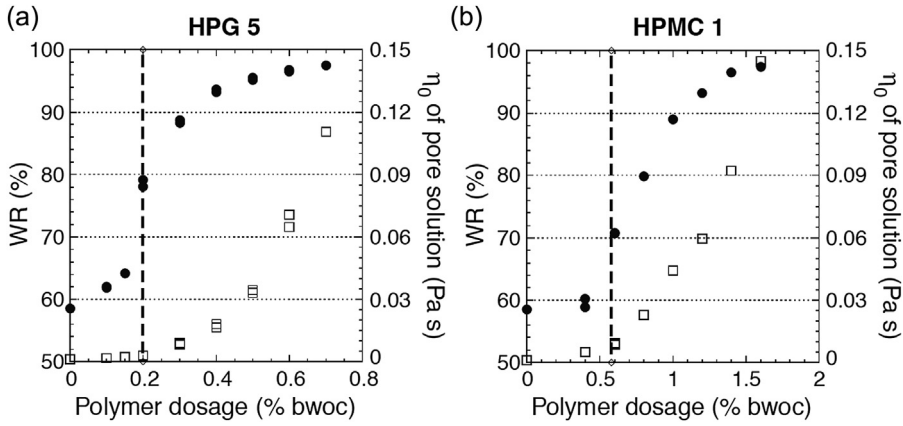


Figure 20.9 Effect of polymer agglomerates formation on water retention for (a) hydroxypropylguar (HPG) and (b) hydroxypropoxy methoxy cellulose (HPMC).
Reproduced from Poinot et al. (2014) with permission.

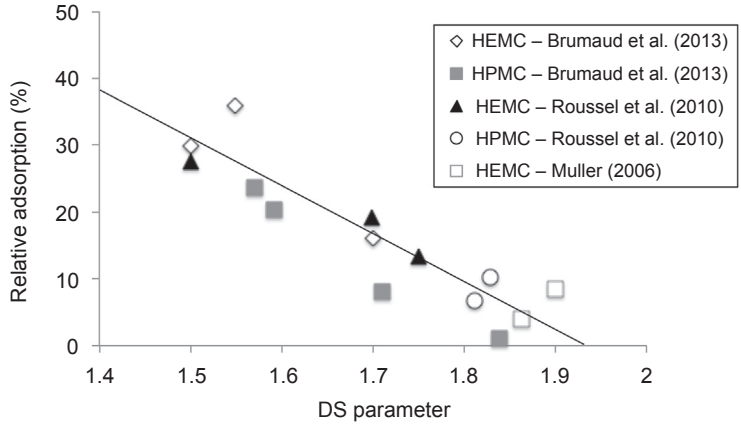


Figure 20.10 Relative adsorption of CE as a function of DS for a CE dosage of 0.2% (Roussel et al., 2010; Muller, 2006; Brumaud et al. (2013)).
Reproduced from Brumaud et al. (2013) with permission.

In cement pastes containing CE polymers, Brumaud (2011) determined that the viscosity of the interstitial solution was lower than expected from the dosage used. This difference was explained by a partial adsorption of these polymers onto the surface of cement particles, causing a decrease of polymer concentration in the pore solution and therefore also of the viscosity. Other authors have also confirmed that CE polymers can adsorb on cement particles (Bülichen et al., 2012; Khayat and Mikanovic, 2012; Brumaud et al., 2013) and that the extent of this depends on DS, as shown in Figure 20.10.

However, because CEs are nonionic polymers, the origin of this adsorption is unclear. According to Bülichen et al. (2012), the adsorbed polymer may not correspond to the cellulose derivative but to byproducts present in commercial MHEC that are able to adsorb onto cement particles. In any case, authors agree that the water retention properties of CE are not related to CE adsorption onto cement particles.

At this point, it is worth mentioning that adsorption measurements of CEs are not easy to perform by the depletion method without introducing artifacts, specifically at dosages above the critical concentration where CE aggregates could be trapped within the porosity of the cement pastes (Brumaud et al., 2013; Bülichen et al., 2012).

20.4 Influence of polymeric VMAs on hydration of cement

Most of the studies on the impact of VMAs on cement hydration have been done using cellulose derivatives or hydroxypropylguar retention agents. They were done by conductivity measurements on highly diluted systems and isotherm calorimetry using lower water−cement (w/c) ratios. In this section, we propose only a brief review of some findings of the literature concerning these specific cases. More detailed information on cement hydration mechanisms and how chemical admixtures can affect them can be found in Chapters 8 and 12, respectively (Marchon and Flatt, 2016a,b).

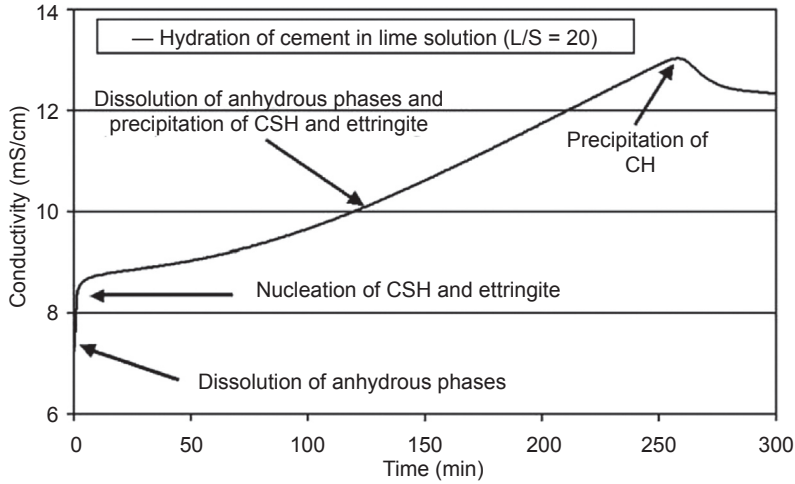


Figure 20.11 Example of a conductivity curve of cement hydration (liquid−solid ratio = 20). Reproduced from Pourchez et al. (2006) with permission.

Figure 20.11 shows the typical conductivity curve of cement reaction where the initial precipitation of portlandite involves a drop of the electrical conductivity (Comparet, 2004; Pourchez et al., 2010). In the presence of CE and HPG, a delay in the time of portlandite precipitation is observed, indicating a delay of C_3S hydration that is higher with the dosage of polymer (see Figure 20.12) (Pourchez et al., 2010).

Pourchez et al. (2010) analyzed the concentration of silicate and calcium as dissolution of C_3S progressed in highly diluted systems. They found that CE polymers had almost no influence on the dissolution of pure C_3S. These authors measured the concentration of calcium and silicates over time and calculated the amount of initial C−S−H nuclei based on the decrease of silicate concentration during the hydration of C_3S where the calcium concentration is constant. This was calculated according to Eqn (20.1) based on the works of Garrault and Nonat (2001) and Pourchez (2006):

$$\text{C−S−H initial nuclei} = \frac{\Delta\left[{H_2SiO_4}^{2-}\right]}{\frac{1}{3}\left(\frac{C}{S}\right) - 1} \tag{20.1}$$

where C/S is the calcium-to-silicon ratio of the C−S−H.

As shown in Figure 20.13, the amount of initial C−S−H nuclei decreases in the presence of CE polymers.

Additionally, Figure 20.12(a) shows that CEs have very limited impact on the rate of C−S−H growth, as the slopes in the stage of hydration are relatively similar to the reference. On the contrary, HPGs (see Figure 20.12) decrease the slope of the curve, indicating that they mainly slow down the growth of hydrate phases rather than their nucleation (Poinot et al., 2013). For both polymers, these authors have proposed that the adsorption onto C−S−H and portlandite is the main reason for the induced delay. They also indicated that the increase of the viscosity of the aqueous media, and possible decrease of water migration, does not play any role on the slowing down of the hydration induced by CEs and HPGs.

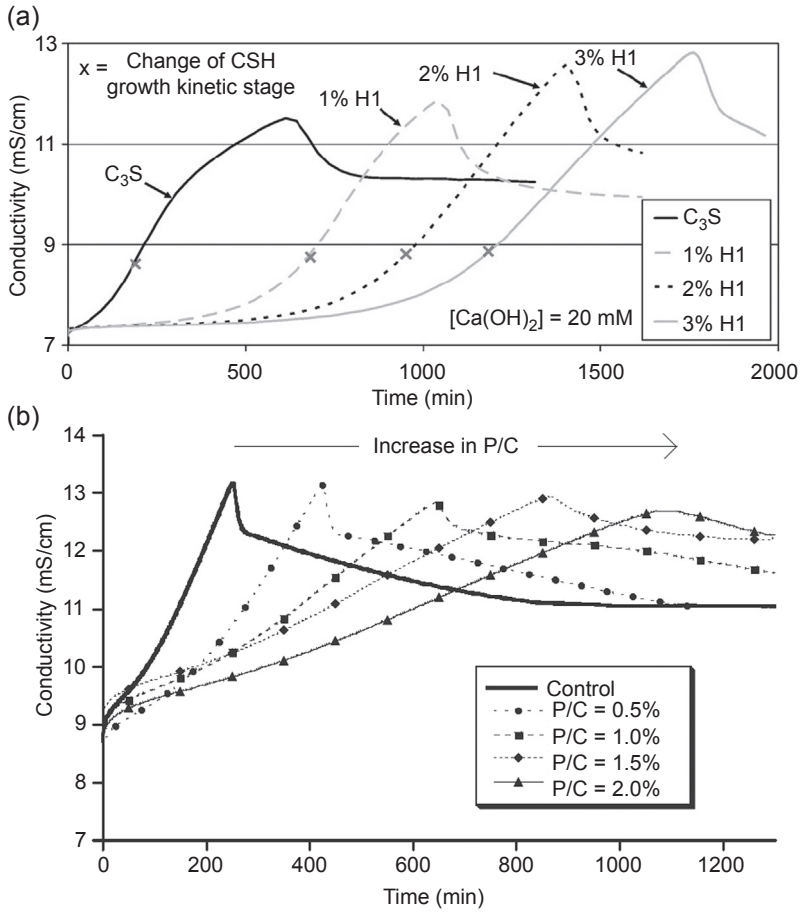


Figure 20.12 Conductometric curves of C_3S hydration in the presence of (a) cellulose derivatives and (b) hydroxypropylguars.
Reproduced from Pourchez et al. (2010) and Poinot et al. (2013), respectively, with permission.

The effect of other VMAs on the hydration of cement still remains unclear. Leemann and Winnefeld (2007) showed that in mixes containing both PCE-based superplasticizer and VMAs, the presence of polymeric VMAs does not significantly modify cement hydration (see Figure 20.14). On the contrary, Khayat and Yahia (1997) observed a clear delay of the setting time of cement grouts containing a naphtalene-based superplasticizer and a welan gum VMA.

Finally, we can note that the addition of inorganic VMAs, such as microsilica or nanosilica slurries, accelerates cement hydration as they introduce additional nucleation and/or growth surfaces that can consume ions released by the dissolving anhydrous phases (Leemann and Winnefeld, 2007). From this point of view, when retardation is an issue, such compounds may be valid alternatives, provided they are effective enough in modifying the other more essential properties.

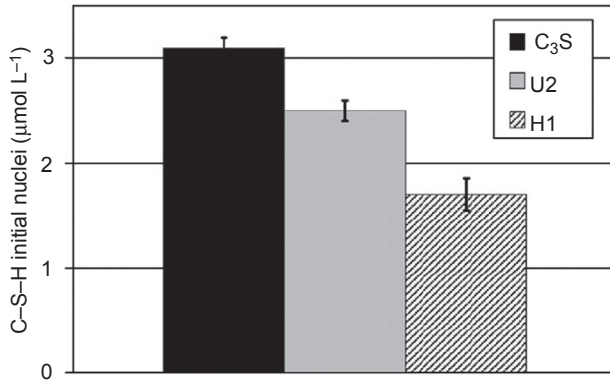


Figure 20.13 The impact of CE on the amount of initial nuclei of C−S−H after 30 min of C_3S hydration (liquid/solid = 100, polymer/solid = 2%, $Ca(OH)_2$ = 20 mM).
Reproduced from Pourchez et al. (2010) with permission.

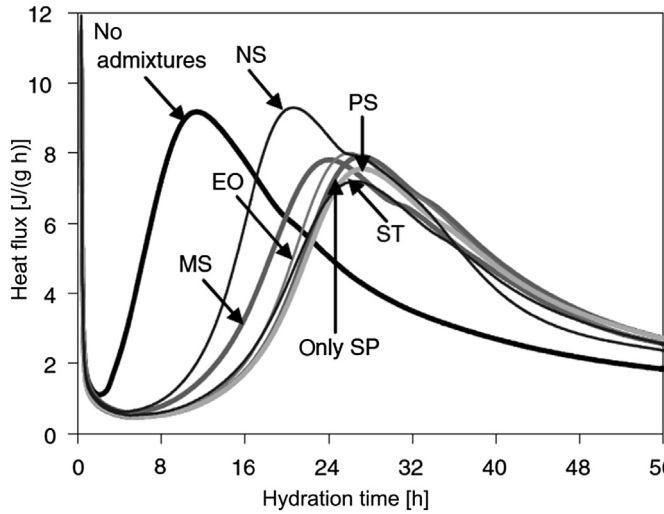


Figure 20.14 Isothermal heat flow curve of cement pastes with w/c = 0.4% and 1% of superplasticizer (SP) and different VMAs (ST, starch derivative; PS, natural polysaccharide; MS, microsilica; NS, nanosilica; EO, ethylene oxide derivative).
Reproduced from Leemann and Winnefeld (2007) with permission.

20.5 Use of VMAs in SCC formulation

In recent years, SCC application has progressively increased. Table 20.1 shows the concrete mix design of three SCCs containing different types of VMAs used in Canada. The three concretes had a compressive strength of 35 MPa at 28 days (Table 20.2).

SSC1 was used in the Fermont in Quebec Province to build a special tank. The high density of steel reinforcement (see Figure 20.15) required the use of an SCC. This SCC

Table 20.1 Composition of SCC

Nomenclature	Sand (kg)	Aggregates (kg)	Water (L)	Cement (kg)	Fly ash (kg)	Water/binder	Superplasticizer (L)	VMA (L)	Water reducer (L)	Retarder (L)
SCC1	794	885 (5−14 mm)	168	378[a]	42	0.40	5.0[c]	1.0[e]	0.80	–
SCC2	762	793 (2.5−10 mm)	179	460[b]	–	0.40	4.0[d]	3.0[f]	–	–
SCC3	810	889 (2.5−10 mm)	153	400[a]	–	0.40	3.5[d]	1.0[e]	0.75	1.0

[a]Cement containing 7−7.5% of silica fume.
[b]Ternary cement containing 20% of fly ash and 5% of silica fume.
[c]PNS.
[d]PCE.
[e]Biopolymer.
[f]Welan gum-based.

Table 20.2 Fresh and hardened properties of SCC

Nomenclature	Spread (mm)	Air content (%)	Compressive strength at 28 days (MPa)
SCC1	650 ± 50	6–8	35
SCC2	675 ± 50	6–8	35
SCC3	625 ± 50	6–8	35



Figure 20.15 Construction of Fermont tank in Quebec using SSC1.

was prepared using a mix of several chemical admixtures, a PNS superplasticizer, a water-reducing admixture, and a biopolymer-based VMA.

SCC2 was used to build a retaining wall at Les Escoumins in Quebec Province (see Figure 20.16). In this case, the use of the SCC allows observation of the defects of the



Figure 20.16 Retaining wall at Les Escoumins in Quebec.

formwork. Highly fluid and stable SCC was obtained by using a PCE superplasticizer in combination with a welan gum-based VMA.

Finally, SCC3 was used in Parc Forillon in Quebec Province. Again, a mix of different chemical admixtures was required to obtain the suitable fresh properties of the concrete. Specifically, a PCE superplasticizer, a water reducer, a retarder, and a biopolymer based VMA were used.

20.6 Conclusions

Modern concrete, such as self-compacting concrete, underwater concrete, or shotcrete require very specific rheological properties. The addition of VMAs allows a reduction of the amount of fine powder materials in concrete at the same time that its stability, cohesion, and robustness are substantially increased. The understanding of the working mechanism of VMAs promotes the design of robust concrete mixes that can provide the best fresh and hardened state properties.

This chapter focuses on polymeric VMAs as they allow a higher variability of structural variations. The mechanism of action of these admixtures and their impact on the rheological properties depends on the nature of the VMA and the presence of other admixtures in the mix. In general, water retention admixtures delay cement hydration while the influence of other VMAs on cement hydration depends on its chemical composition.

In practice, problems of incompatibility between specific combinations of VMAs and superplasticizers must be avoided. These could lead to a quick loss of fluidity without much improvement in the stability of concrete. An understanding of the mechanism of action of the different types of polymers may decrease the risk of having such problems on site.

Acknowledgments

The authors would like to thank Prof. Pierre-Claude Aïtcin for providing the SCC formulations in Section 20.5.

References

Bessaies-Bey, H., Baumann, R., Schimtz, M., Radler, M., Roussel, N., 2015. Polymers and cement particles: competitive adsorption and its macroscopic rheological consequences. Cement and Concrete Research 75, 98−106.

Brumaud, C., 2011. Origines microscopiques des consequences rhéologiques de l'ajout d'éthers de cellulose dans une suspension cimentaire. l'Universite Paris-Est, Paris.

Brumaud, C., Bessaies-Bey, H., Mohler, C., Baumann, R., Schmitz, M., Radler, M., Roussel, N., 2013. Cellulose ethers and water retention. Cement and Concrete Research 53, 176−184. http://dx.doi.org/10.1016/j.cemconres.2013.06.010.

Brumaud, C., Baumann, R., Schmitz, M., Radler, M., Roussel, N., 2014. Cellulose ethers and yield stress of cement pastes. Cement and Concrete Research 55, 14–21. http://dx.doi.org/10.1016/j.cemconres.2013.06.013.

Bülichen, D., Kainz, J., Plank, J., 2012. Working mechanism of methyl hydroxyethyl cellulose (MHEC) as water retention agent. Cement and Concrete Research 42, 953–959. http://dx.doi.org/10.1016/j.cemconres.2012.03.016.

Chassenieux, C., Nicolai, T., Benyahia, L., 2011. Rheology of associative polymer solutions. Current Opinion in Colloid & Interface Science 16, 18–26. http://dx.doi.org/10.1016/j.cocis.2010.07.007.

Comparet, C., 2004. Etude des interactions entre les phases modèles représentatives d'un ciment Portland et des superplastifiants du béton. Université de Bourgogne, France.

Fellows, C.M., Doherty, W.O.S., 2005. Insights into bridging flocculation. Macromolecular Symposia 231, 1–10. http://dx.doi.org/10.1002/masy.200590012.

Garrault, S., Nonat, A., 2001. Hydrated layer formation on tricalcium and dicalcium silicate surfaces: experimental study and numerical simulations. Langmuir 17, 8131–8138. http://dx.doi.org/10.1021/la011201z.

Gelardi, G., Mantellato, S., Marchon, D., Palacios, M., Eberhardt, A.B., Flatt, R.J., 2016. Chemistry of chemical admixtures. In: Science and Technology of Concrete Admixtures. Elsevier (Chapter 9), pp. 149–218.

Hossain, K.M.A., Lachemi, M., 2006. Performance of volcanic ash and pumice based blended cement concrete in mixed sulfate environment. Cement and Concrete Research 36, 1123–1133. http://dx.doi.org/10.1016/j.cemconres.2006.03.010.

Jenni, A., Herwegh, M., Zurbriggen, R., Aberle, T., Holzer, L., 2003. Quantitative microstructure analysis of polymer-modified mortars. Journal of Microscopy 212, 186–196. http://dx.doi.org/10.1046/j.1365-2818.2003.01230.x.

Jenni, A., Zurbriggen, R., Holzer, L., Herwegh, M., 2006. Changes in microstructures and physical properties of polymer-modified mortars during wet storage. Cement and Concrete Research 36, 79–90. http://dx.doi.org/10.1016/j.cemconres.2005.06.001.

Kawai, T., Okada, T., 1989. Effect of superplasticizer and viscosity increasing admixture on properties of lightweight aggregate concrete. In: Presented at the Third International Conference, Detroit, pp. 583–604.

Khayat, K.H., Mikanovic, N., 2012. Viscosity-enhancing admixtures and the rheology of cement. In: Understanding the Rheology of Concrete. Cambridge, Woodhead, pp. 209–228.

Khayat, K.H., Yahia, A., 1997. Effect of welan gum-high-range water reducer combinations on rheology of cement grout. ACI Materials Journal 94, 365–374.

Leemann, A., Winnefeld, F., 2007. The effect of viscosity modifying agents on mortar and concrete. Cement and Concrete Composites 29, 341–349. http://dx.doi.org/10.1016/j.cemconcomp.2007.01.004.

Marchon, D., Flatt, R.J., 2016a. Mechanisms of cement hydration. In: Science and Technology of Concrete Admixtures. Elsevier (Chapter 8), pp. 129–146.

Marchon, D., Flatt, R.J., 2016b. Impact of chemical admixtures on cement hydration. In: Science and Technology of Concrete Admixtures. Elsevier (Chapter 12), pp. 279–304.

Marchon, D., Sulser, U., Eberhardt, A.B., Flatt, R.J., 2013. Molecular design of comb-shaped polycarboxylate dispersants for environmentally friendly concrete. Soft Matter 9 (45), 10719–10728. http://dx.doi.org/10.1039/C3SM51030A.

Marchon, D., Mantellato, S., Eberhardt, A.B., Flatt, R.J., 2016. Adsorption of chemical admixtures. In: Aïtcin, P.-C., Flatt, R.J. (Eds.), Science and Technology of Concrete Admixtures. Elsevier (Chapter 10), pp. 219–256.

Marliere, C., Mabrouk, E., Lamblet, M., Coussot, P., 2012. How water retention in porous media with cellulose ethers works. Cement and Concrete Research 42, 1501−1512. http://dx.doi.org/10.1016/j.cemconres.2012.08.010.

Muller, I., 2006. Influence of Cellulose Ethers on the Kinetics of Early Portland Cement Hydration. University of Karlsruhe.

Oosawa, F., Asakura, S., 1954. Surface tension of high-polymer solutions. Journal of Chemical Physics 22, 1255. http://dx.doi.org/10.1063/1.1740346.

Palacios, M., Flatt, R.J., Puertas, F., Sanchez-Herencia, A., 2012. Compatibility between polycarboxylate and viscosity-modifying admixtures in cement pastes. In: Presented at the 10th International Conference on Superplasticizers and Other Chemical Admixtures in Concrete, Prague.

Patural, L., Korb, J.-P., Govin, A., Grosseau, P., Ruot, B., Devès, O., 2012. Nuclear magnetic relaxation dispersion investigations of water retention mechanism by cellulose ethers in mortars. Cement and Concrete Research 42, 1371−1378. http://dx.doi.org/10.1016/j.cemconres.2012.06.002.

Patural, L., Marchal, P., Govin, A., Grosseau, P., Ruot, B., Devès, O., 2011. Cellulose ethers influence on water retention and consistency in cement-based mortars. Cement and Concrete Research 41, 46−55. http://dx.doi.org/10.1016/j.cemconres.2010.09.004.

Plank, J., Lummer, N.R., Dugonjić-Bilić, F., 2010. Competitive adsorption between an AMPS®-based fluid loss polymer and welan gum biopolymer in oil well cement. Journal of Applied Polymer Science 116, 2913−2919. http://dx.doi.org/10.1002/app.31865.

Poinot, T., Govin, A., Grosseau, P., 2014. Importance of coil-overlapping for the effectiveness of hydroxypropylguars as water retention agent in cement-based mortars. Cement and Concrete Research 56, 61−68. http://dx.doi.org/10.1016/j.cemconres.2013.11.005.

Poinot, T., Govin, A., Grosseau, P., 2013. Impact of hydroxypropylguars on the early age hydration of Portland cement. Cement and Concrete Research 44, 69−76. http://dx.doi.org/10.1016/j.cemconres.2012.10.010.

Pourchez, J., 2006. Aspects physico-chimiques de l'interaction des éthers de cellulose avec la matrice cimentaire. Ecole Nationale des Mines de Saint-Etienne.

Pourchez, J., Grosseau, P., Ruot, B., 2010. Changes in C_3S hydration in the presence of cellulose ethers. Cement and Concrete Research 40, 179−188. http://dx.doi.org/10.1016/j.cemconres.2009.10.008.

Pourchez, J., Peschard, A., Grosseau, P., Guyonnet, R., Guilhot, B., Vallée, F., 2006. HPMC and HEMC influence on cement hydration. Cement and Concrete Research 36, 288−294. http://dx.doi.org/10.1016/j.cemconres.2005.08.003.

Roussel, N., Lemaître, A., Flatt, R.J., Coussot, P., 2010. Steady state flow of cement suspensions: a micromechanical state of the art. Cement and Concrete Research 40, 77−84. http://dx.doi.org/10.1016/j.cemconres.2009.08.026.

Sonebi, M., 2006. Rheological properties of grouts with viscosity modifying agents as diutan gum and welan gum incorporating pulverised fly ash. Cement and Concrete Research 36, 1609−1618. http://dx.doi.org/10.1016/j.cemconres.2006.05.016.

Xu, L., Xu, G., Liu, T., Chen, Y., Gong, H., 2013. The comparison of rheological properties of aqueous welan gum and xanthan gum solutions. Carbohydrate Polymers 92, 516−522. http://dx.doi.org/10.1016/j.carbpol.2012.09.082.

Antifreezing admixtures

21

P.-C. Aïtcin
Université de Sherbrooke, QC, Canada

21.1 Introduction

Despite the fact that antifreeze admixtures are currently used in Russia, Finland, Poland and China for placing concrete without any special protection under temperature as low as −15 °C, antifreeze admixtures are not used in Canada, Alaska and the northern parts of the United States, or elsewhere in Europe (besides Finland and Poland). Presently in Finland, it is possible to buy on the market prepacked sacks of concrete and mortars in which an appropriate dosage of calcium nitrite has been included. These prepacked mixtures can be used under temperatures as low as −10 °C without any special protection against such a very low temperature. Very little English literature can be found on the subject except one comprehensive article written by Ratinov and Rozenberg in Ramachandran's book on concrete admixtures (Ramachandran, 1995).

The basic idea of using an antifreeze admixture is very simple: it consists of incorporating in the mixer a soluble salt that lowers the freezing temperature of water. Lowering the freezing temperature of water by adding a soluble salt is a well-known phenomenon. Fahrenheit used it when he selected the origin of his temperature scale: The temperature 0 °F corresponds to the minimum temperature at which a saturated solution of calcium chloride freezes. Seawater freezes around −1.8 °C according to its salinity.

21.2 Winter concreting in North America

When facing the first low temperature at the beginning of winter season, Canadian concrete producers start to heat the mixing water in order to increase the temperature of the fresh concrete. As the temperature continues to decrease, they start heating the coarse aggregates and the sand with steam.

In the field, when night temperature is decreasing close to 0 °C, contractors protect the freshly poured concrete with insulating blankets. When it freezes harder, they build temporary polyethylene heated shelters to protect concrete against freezing. Of course, there is a price associated to the application of all these measures: on average, they charge 25% more for winter concreting.

When the ambient temperature is lower than −10 °C in Canada, concrete is delivered only for inside applications. At −15 °C, ready-mix plants stop producing concrete until the ambient temperature goes up. Currently, antifreeze admixtures are not used at all in Canada.

Science and Technology of Concrete Admixtures. http://dx.doi.org/10.1016/B978-0-08-100693-1.00021-7
Copyright © 2016 Elsevier Ltd. All rights reserved.

21.3 Antifreeze admixtures

According to Ratinov and Rosenberg, nitrites, nitrates, calcium chloride, sodium chloride, ammonia, etc. have been used as antifreeze admixtures in Russia (Ramachandran, 1995). Usually, a combination of some of these chemicals is used. In practice, the most popular formulations are the ones based on nitrites. In China and Finland, a mixture of sodium nitrite ($NaNO_2$) and sodium sulphate ($Na_2 SO_4$) is used, as well as a mixture of sodium nitrate and calcium nitrite, $Ca(NO_2)_2$. Pedro Hernandez (1989), during his master's thesis, used essentially calcium nitrite as an antifreeze admixture.

As calcium nitrite is currently available in North America to provide an additional protection against the corrosion of reinforcing bars, the use of calcium nitrite as an antifreeze admixture should become an interesting alternative for winter concreting. Of course, the dosage of calcium nitrite that has to be added as an antifreeze admixture is much higher than the one used as a corrosion inhibitor. A saturated solution of $Ca(NO_2)_2$ freezes at a temperature of about $-20\ ^\circ C$.

21.4 The construction of high-voltage power lines in the Canadian North

The anchors of the power lines erected in the Canadian North could benefit from this technology. In the Canadian North, high-voltage power lines are erected in winter because it is very easy to transport on the snow all the materials needed to erect the lines as well as the personnel. The frozen rivers and lakes are no longer obstacles for the progression of the construction of the lines. The only negative point is that the rock in which the anchors have to be fixed is totally or partially frozen, depending on the latitude at which the power line is located. In both cases, it is necessary to heat the rock around the anchorage hole in order to create an unfrozen zone around it before injecting the grout that will fix the anchor. In fact, the rock has to be unfrozen deep enough so that when the heating stops there is enough time for the grout to harden and get enough strength before the rock comes back to its initial frozen temperature.

The use of an antifreeze admixture could avoid such a long and complicated process. In order to prove the feasibility of such an alternative, experimental anchors were cast in Nanisivik in the extreme north of Baffin Island.

21.5 The use of calcium nitrite in Nanisivik

Nanisivik is a village located in the extreme north of Baffin Island at the 73 parallel where Nanisivik Mines exploits a zinc mine (Figure 21.1). An airport is connected to Ottawa twice a week and a harbour facility exists to ship the extracted zinc ore.

To study the feasibility of using grouts containing calcium nitrite as an antifreeze admixture, it was possible to take advantage of all of the facilities of the mining



Figure 21.1 Location of Nanisivik in Baffin Island.

company (food and dwelling, drills, transportation, etc.) and establish a temporary small laboratory inside a garage.

Two series of experiments were done: the first one in a cap of rock close to the plant as seen in Figure 21.2 and a second one in a gallery of the mine where the rock and the air were all year round at −12 °C (Figure 21.3).

At 300 mm below its surface, the temperature of the rock was −12 °C for the 12 anchors tested. The ambient temperature was −15 °C when the grouting was done.

The grouts were prepared in a garage using water at 10 °C and transported to the site immediately to be poured in the anchor holes. They contained some aluminium powder in order to create a small expansion of the volume of the grout to improve the bonding of the grout with the anchor and the rock. Only the first 300 mm of the anchors were grouted and thermocouples installed at the bottom of the anchor to monitor the temperature of the grout (Figures 21.4 and 21.5). The composition of the grout is shown in Table 21.1.



Figure 21.2 The selected rock cap for the testing outside the mine.



Figure 21.3 Grouting the anchors in the mine gallery.

Dosages are given in proportion of the cement mass. In the case of the superplasticizer and the calcium nitrite, the dosage corresponds to that of their solid content.

On the cap of rock, the anchors were pull out after 14 days. In the frozen gallery of the mine, the anchored bars were supposed to be pulled out 1 year later. A small rectangular base was built around each anchor to support the base of the hollow jack used to pull out the anchors (Figure 21.5).



Figure 21.4 Installation of the 12 anchors.

Table 21.1 Composition of the grout

High early strength cement (O)	1
Water (W)	0.44
Silica fume (FS)	0.10
Aluminium powder	0.7×10^{-4}
Superplasticizer	0.03
Sodium nitrite (N)	0.12
N/(N + E) ratio	0.21
W/(C + FS) ratio	0.40



Figure 21.5 The small rectangular base built around each anchor to support the base of the hollow jack used to pull out the anchors. The temperature of each grout was monitored by a thermocouple.

The results obtained on the cap of rock were compared to those obtained in an unfrozen rock in Sherbrooke; they were excellent (Benmokrane et al., 1987). However, in the case of the anchors grouted in the frozen gallery, after a year at −12 °C it was impossible to pull them out because by error the grouted length was too long; the load that had to be developed to extract them was well over the capacity of the jack. It was necessary to cut the anchors with acetylene torches and seal the anchoring hole with a grout to avoid any accident in the gallery.

21.6 Conclusion

This experience of the Université de Sherbrooke in the Canadian Arctic has shown the great potential of using antifreeze admixture in concrete or grouts, as is currently done in Finland, Russia and China. The use of this technology could result in important savings when erecting power lines. Antifreeze admixtures can also be used to increase the length of the concrete season in the Canadian North by adding 2 months to the usual concreting season. Concreting could start 1 month earlier and stop 1 month later, which would be a great advantage in the short concreting seasons of the north.

References

Benmokrane, B., Aïtcin, P.C., Ballivy, G., 1987. Injection d'ancrages à base de ciment Portland dans l'Arctique, Revue Canadienne de Génie Civil 14 (5), 690−693.

Hernandez, P., 1989. Master Degree Thesis No 556, Université de Sherbrooke.

Ramachandran, V.S., 1995. Concrete Admixtures Handbook, second ed. Noyes Publications, Park Ridge, NJ, USA, pp. 740−799.

Expansive agents

22

R. Gagné
University of Sherbrooke, QC, Canada

22.1 Introduction

Expansive agents are admixtures sold as powders that are added to concrete. In the early stage of hardening, they produce a controlled internal reaction so that the apparent volume of concrete increases. A concrete containing an expansive agent is also known as shrinkage compensated concrete (ACI, 2011). This type of concrete is used in constructions where it is absolutely necessary to decrease as much as possible the cracking of concrete related to drying and/or autogenous shrinkage. The main practical application of expansive agents deals with the construction of concrete slabs on ground, large walls, and concrete repairs (ACI, 2011; Collepardi et al., 2005, 2008; Gagné et al., 2008).

The internal expansion occurs typically during the first 7 days following the batching of concrete; usually, it is not greater than 0.1% after 7 days of curing (Bissonnette et al., 2008). Although the resulting expansion is not very large, it decreases significantly the risk of cracking in the case of restrained shrinkage.

Internal expansion can be produced using different types of expansive agents that produce expansive hydrates when they react with water. It must be emphasized that most of these reactions lead to products that occupy less volume than the reactants. However, as for cement hydration, the volume of solids increases. The expansion is understood to result from conditions causing the hydrates to grow under supersaturated conditions. Crystallization pressure is therefore the underlying process explaining this expansion (Scherer, 1999). In particular, the process of dissolution of an anhydrous phase coupled with the precipitation of a hydrate can generate important expansive forces by crystallization pressure (Flatt, 2002; Flatt et al., 2014). The kinetics and intensity of this internal expansion depend on different parameters, particularly:

- The chemical nature of the expansive agent
- The dosage of the expansive agent
- The type and duration of water curing
- The cement dosage

22.2 Principle

An expansive agent is used during the early hardening of concrete to produce a volumetric expansion that, according to different chemical mechanisms, mitigates totally or partially the volumetric contraction induced by the different forms of shrinkage.

Science and Technology of Concrete Admixtures. http://dx.doi.org/10.1016/B978-0-08-100693-1.00022-9
Copyright © 2016 Elsevier Ltd. All rights reserved.

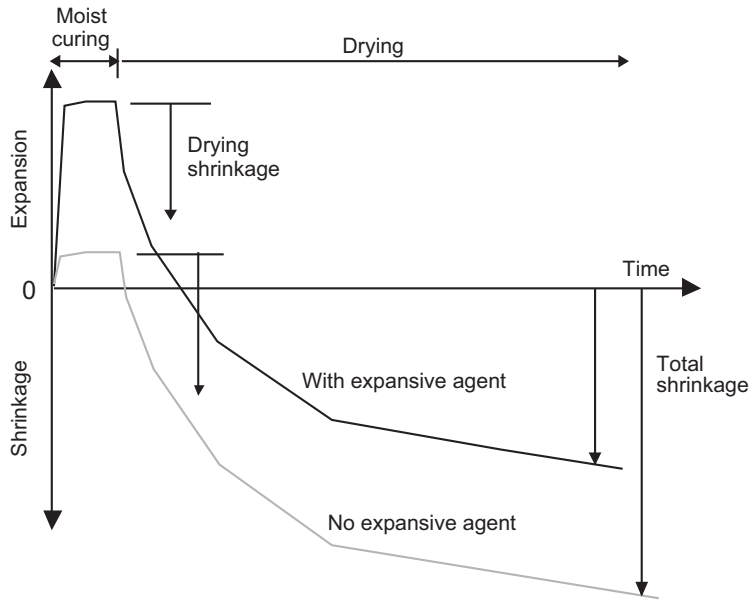


Figure 22.1 Schematic representation of the swelling and the drying shrinkage of two concretes, one containing an expansive agent and another that does not contain an expansive agent.

Figure 22.1 presents the free shrinkage of two concretes containing or not an expansive agent. It is shown in Figure 22.1 that when concrete does not contain any expansive agent, it presents a small expansion when it starts to be water cured. The reason for this expansion is not clear, but most likely results from an expansive reaction, such as hydration of the free lime present in any clinker.

Immediately after the end of the water curing, concrete drying generates a loss of water that is responsible of the drying shrinkage of concrete, as shown in Chapter 6 (Aïtcin, 2016). At the beginning, this shrinkage progresses rapidly, but in the long term it stabilizes. The kinetics and final extent of drying shrinkage depend on several parameters, such as concrete composition, environmental conditions, and the geometry of the concrete elements.

A concrete containing an expansive agent presents an initial swelling larger than that of a similar concrete that does not contain any expansive agent. This expansion occurs during the water curing of concrete. According to the type of the expansive agent, the maximal expansion in obtained between the second and the seventh day of water curing. Then, drying shrinkage starts as soon as the water curing is finished. Usually, the kinetics and extent of drying shrinkage are not influenced by the type of expansive agent used (Collepardi et al., 2005; Bissonnette et al., 2014). This can be seen in Figure 22.1 in that the dimensional change after curing is similar in both cases.

However, in situations of restrained shrinkage discussed below, what matters most is the total shrinkage, which is defined as the dimensional change between the initial

condition and the final one. In that case, as also illustrated in Figure 22.1, the expansive agent reduces the total shrinkage.

When volumetric variations (swelling as well as shrinkage) are not restrained, concrete is not subjected to any stress (Bissonnette et al., 2014). On the contrary, when these volumetric variations are restrained, the development of drying shrinkage generates internal tensile stresses that may result in the cracking of concrete. For example, in the case of a concrete slab on the ground, drying shrinkage is partially restrained by the friction of the slab with the soil. A too-large drying shrinkage may result in the cracking of the slab. A similar cracking can also develop in the case of a thin concrete overlay used to repair a damaged concrete. It is the bonding between the overlay and the concrete sub-base that is responsible for this cracking. Finally, in the case of large concrete elements, the core of the concrete can exert self-restraint of its exterior. In all of these cases, in order to reduce the risk of cracking, it is necessary to reduce the effect of drying shrinkage. An expansive agent may be used to reduce this risk, but it is not the only way to reduce it, as it will be shown in Chapter 23 (Gagné, 2016).

Figure 22.2 represents the stress variations in a concrete sample submitted to restrained volumetric variations. In the case of the concrete that does not contain any expansive agent, restrained drying shrinkage results in tensile stresses when shrinkage is progressing. Cracking occurs when the tensile stress developed by the restrained shrinkage becomes greater than concrete tensile strength (Bissonnette et al., 2014).

In the case of concrete that contains an expansive agent, concrete expansion is also restrained, so that it generates an internal compressive stress during water curing (chemical prestressing). When drying shrinkage starts to develop at the end of the curing period, the internal compression is relaxed. Finally, in the long term, the final tensile stress is smaller than in the previous case and may eliminate or at least decrease significantly the risk of cracking (Figure 22.2). However, it should be noted that, in the

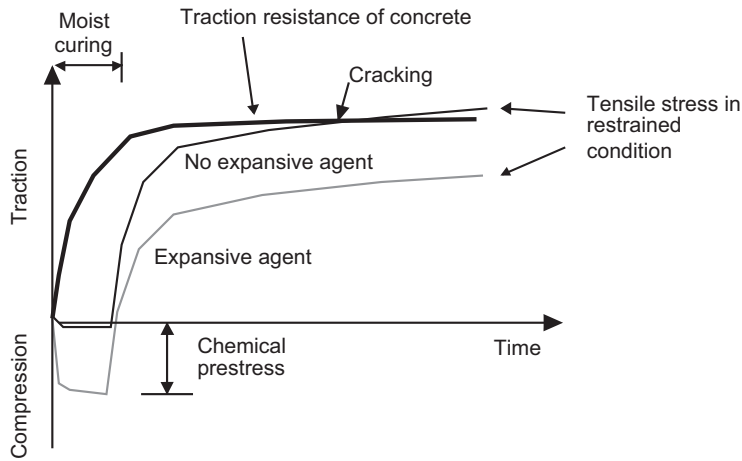


Figure 22.2 Schematic representation of the development of stresses in concrete with or without an expansive agent when volumetric variations are restrained.

case of self-restraint, the benefit of the expansive agent would not be present as the concrete core would also expand. However, the situation of a large element only subject to self-restraint is probably relatively rare.

22.3 Expansion mechanisms

Different types of expansive agents are used to produce this initial expansion. The two most important ones are one containing a calcium sulphoaluminate and the other granules of dead-burn lime (CaO). The American Concrete Institute (ACI) Committee 233 proposed a classification of the expansion mechanisms that is a function of the chemical nature of the minerals that are responsible for the formation of these expansive hydrates (ACI, 2011). For example, an expansive agent of Type K (calcium sulphoaluminate) results in the formation of ettringite. Expansive agents of Type G are based on dead-burn lime; they result in the formation of hydrated lime (portlandite) (ACI, 2011).

22.3.1 Expansion due to the formation of ettringite

In this case, the expansive agent is essentially composed of a mixture of calcium sulphoaluminate (C_4A_3S) and dead-burn lime (CaO) that results in the rapid formation of ettringite during water curing (Ish-Shalom and Bentur, 1974; Bentur and Ish-Shalom, 1974). This kind of expansion is also used in Type K cements in the United States. This type of agent of expansion is formulated so that the final expansion stops when the reactive product is fully hydrated and has produced an expansion almost equal to the anticipated drying shrinkage. A Type K component agent, sold in the form of a powder, is directly added to concrete during its batching. In this approach, the expansive agent is diluted in some Portland cement that should be subtracted from the cement dosage. Replacement rates of 10−16% of Portland cement are used in order to compensate for drying shrinkage in a concrete repair (Bissonnette et al., 2014). This dilution of the expansive agent in Portland cement avoids dosage errors for the very small quantities of expansive agents that have to be used.

In order to occur, the expansion reaction necessitates the use of a large quantity of water during the initial days. In optimal conditions, 7 days of water curing are enough to provide the maximal expansion, which is reached after 4−7 days as seen in Figure 22.3 (Bissonnette et al., 2014). External temperature plays a very important role in the final expansion; at a temperature lower than 5 °C, the expansion mechanism is slowed down and does not reach the anticipated expansion at 20 °C.

The use of a sulphoaluminate-based expansive agent can result in a rapid decrease of concrete workability because of the initial important water consumption (Phillips et al., 1997). When the loss in workability is too large, it is useful to use a superplasticizer in order to maintain an adequate workability that will result in an easy placing of concrete. For a given water−cement ratio (w/c), concretes containing an expansive sulphoaluminate-based expansive agent are developing a compressive strength equal to or even slightly higher than that of a regular concrete (Phillips et al., 1997).

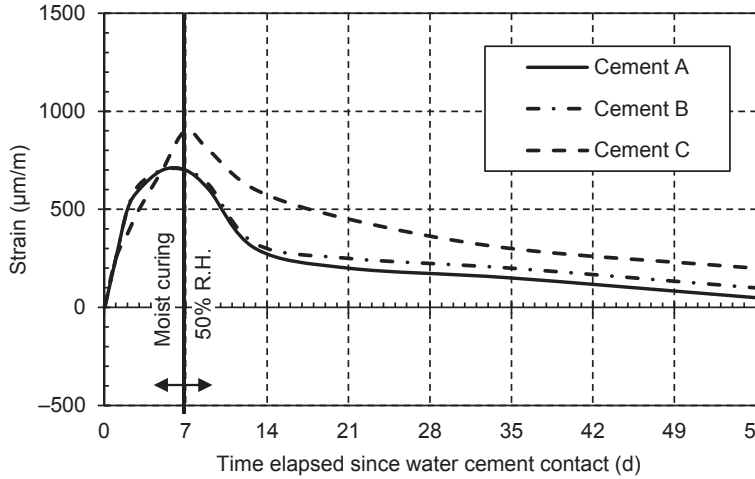


Figure 22.3 Free expansion of a concrete containing a Type K component expansive agent (w/b = 0.38; Type K component dosage = 10%) (Bissonnette et al., 2014).

Some interactions between the expansive agent and certain admixtures have been reported in the literature, particularly in the case of air-entraining agents. However, numerous field projects in which superplasticizers and air-entraining agents have been used simultaneously show that it is possible to find the right dosage of these two admixtures to obtain a concrete meeting the most stringent specifications (Phillips et al., 1997).

22.3.2 Expansion due to the formation of portlandite

Portlandite formation is also another way to produce a rapid expansion in the cement paste. The expansive agent contains granules of dead-burn lime (CaO) that produce crystals of portlandite ($Ca(OH)_2$) when they enter in contact with water. Commercial products are added directly in the mixer; usually, they are diluted in Portland cement. These expansive agents are of Type G according to the previously mentioned ACI 223 Committee report (ACI, 2011).

The expansion observed is quite rapid and reaches its maximum within 48 h (Figure 22.4) (Bissonnette et al., 2014). The formation of portlandite crystals necessitates some water, so an efficient water curing must be put in place in order to achieve the expected expansion. The curves observed in Figure 22.4 show that the expansion is quite rapid and occurs essentially during the first 24 h. Therefore, it is very important that concrete setting is not too much delayed by ambient temperature or by the admixtures used in the mix because otherwise most of the expansion may occur in the plastic states of concrete and will be lost.

Usually, commercial products are used at a dosage of 3−10% of the cement mass. They can be used in replacement or in addition to the mass of concrete. When they are used in addition, they must replace an equivalent volume of sand. Calcium

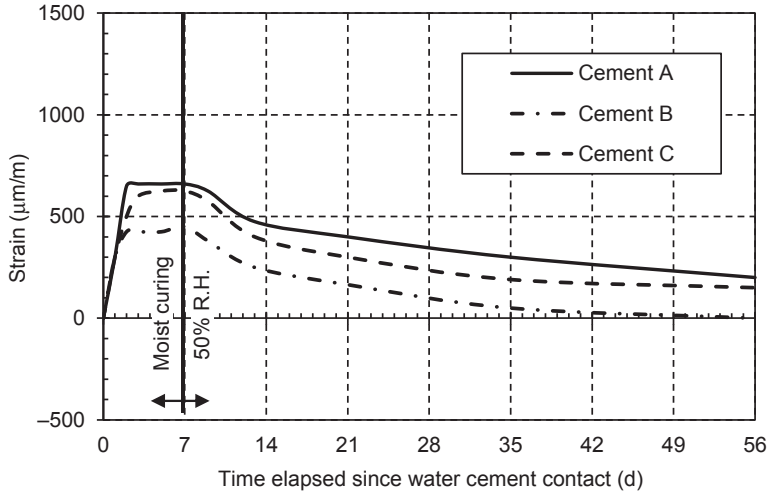


Figure 22.4 Free expansion of a concrete containing a calcium oxide-based expansive agent (w/b = 0.38; expansive agent dosage = 3%) (Bissonnette et al., 2014).

oxide-based expansive agents do not influence significantly concrete rheology and admixture dosage. When they are used in addition to the mass of cement, they can result in a slight increase of compressive strength.

22.4 Measurement of free and restrained expansion

The expansion induced by expansive agents can be measured in free or restrained conditions. Free expansion characterizes the expansion of a concrete specimen that is not confined by the side of the mold or by any reinforcing bar. Restrained expansion is measured on a sample presenting a very light reinforcement equal to 0.3%, according to ASTM C878 Standard Test Method (ACI, 2010).

22.4.1 Free expansion

The measurement of free expansion is used to characterize the expansion that can be obtained with an expansive agent. It is used to find the appropriate dosage of the expansion agent. Expansion is measured on concrete prisms comporting metallic inserts. These prisms can be of the same size as the ones recommended by ASTM C157 Standard (ASTM, 2014).

When expansion is measured, it is very important to demold concrete specimens as soon as possible in order to avoid the development of some restriction on the faces of the mold. The first length reading must be taken as soon as possible in order to detect all of the initial expansion. In the case of a CaO-based expansive agent, the first expansion may occur as soon as 6−8 h after the first contact of the cement with water.

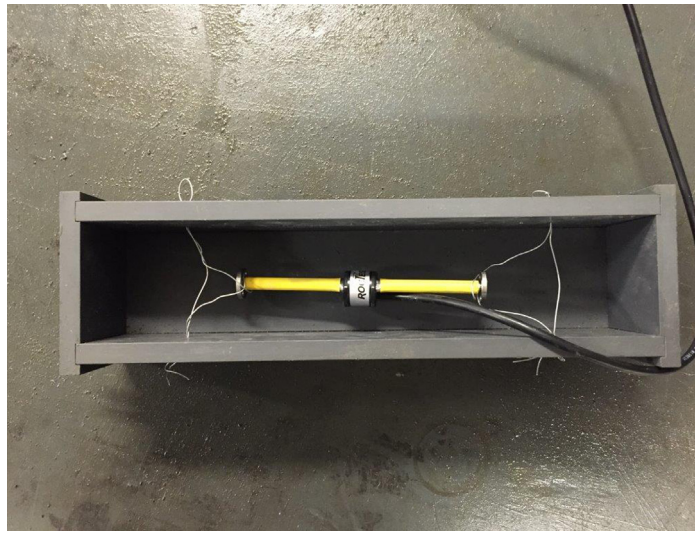


Figure 22.5 Molds and vibrating wire gages (Aïssi et al., 2014).

Vibrating wire gages can be used to measure the expansion. They are placed at the center of the specimens, as seen in Figure 22.5 (Aïssi et al., 2014). In this case also, if a measure of the free expansions has to be taken, it is important to demold the specimens as soon as possible. Vibrating wire gages are connected to an acquisition data system that measure continuously the expansion as well as the temperature at the center of the specimen. One disadvantage of this method is that vibrating wire gages are expensive and cannot be recuperated after their use. Figure 22.6 presents typical curves obtained with vibrating wire gages.

22.4.2 Restrained expansion

Restrained expansion is measured according to ASTM C878 Standard Test Method (ASTM, 2014). This experimental measurement tries to reproduce the expansion of a concrete that is partially restrained by a reinforcing bar. Concrete prisms are made using the same type of mold as the one prescribed in ASTM Standard Test Method C157 (Figure 22.7). However, before casting of the prism, two plates are placed at both ends of the mold. These two plates are joined together by a steel treaded rod having a diameter of 4.8 mm (Figure 22.8). This configuration simulates a reinforcing equal to 0.3%. It is similar to that used to control the cracking due to thermal shrinkage of slabs on ground.

The specimens are demolded 6 h after the first water−cement contact in order to take the first length measurement before the start of the internal expansion reaction. Specimens are then water cured for 7 days. During this period of time, measures are taken in a sequence defined by the standard. Figure 22.8 presents the expansion obtained when performing such a test.

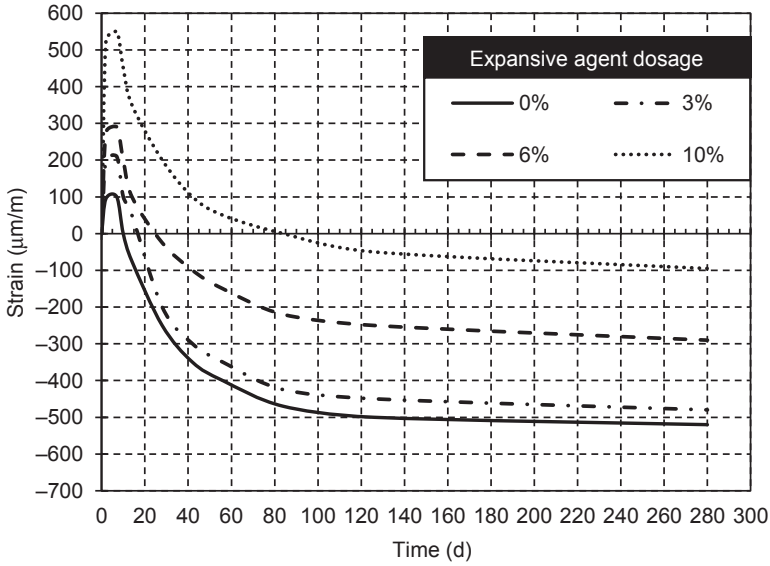


Figure 22.6 Free expansion measured using vibrating wire gages for a concrete containing a calcium-based expansive agent (w/c = 0.72) (Aïssi et al., 2014).

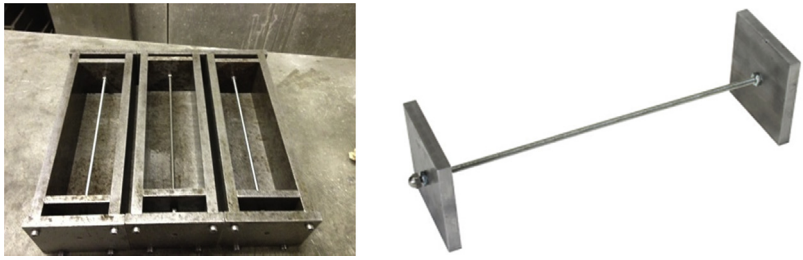


Figure 22.7 Typical molds used to measure the restrained expansion according to ASTM C878 standard procedure (Aïssi et al., 2014).

22.5 Factors affecting the expansion

22.5.1 Expansive agent dosage

The expansion obtained is a function of the dosage of the expansive agent. This dosage is usually given as a massic percentage of the expansive agent to the mass of binder. Figure 22.6 presents the free expansion of a 25 MPa concrete as a function of a CaO-based expansive agent. Of course, the higher the dosage, the larger the expansion. For this concrete, a 10% dosage resulted in an expansion greater than 500 µm/m after 2 days of curing under 100% relative humidity. The expansion is

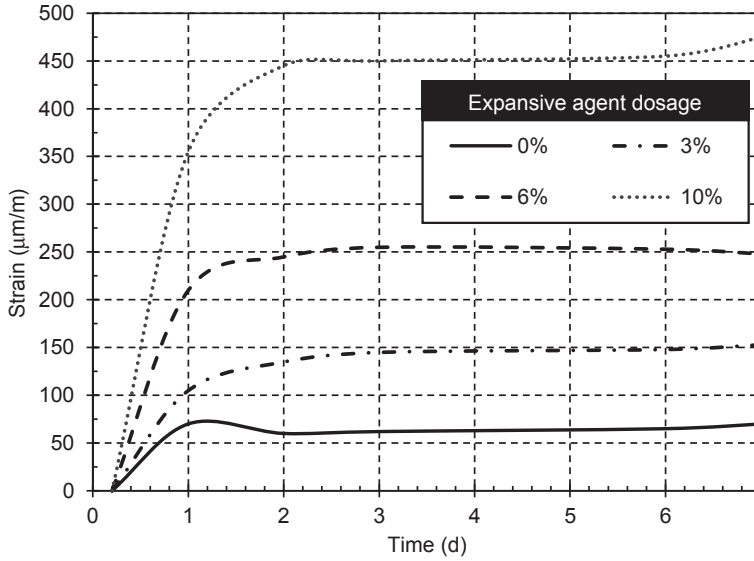


Figure 22.8 Typical restrained expansion curves obtained using ASTM C878 standard procedure for a concrete with a calcium-based expansive agent (w/c = 0.72) (Aïssi et al., 2014).

not only a function of the dosage of the expansive agent, it is also function of the binder dosage. For a fixed dosage of the expansive agent, the expansion is greater in a concrete containing 400 kg/m^3 of binder than in a concrete containing only 275 kg/m^3 of binder.

22.5.2 Curing conditions

Curing conditions influence drastically the final expansion because water is absolutely necessary to obtain an expansion. Therefore, in order to fully develop the potential of expansion, it is important to provide curing conditions that provide sufficient water curing. Figure 22.9 presents the restrained expansion of two concretes having a water–binder ratio (w/b) equal to 0.38 containing, respectively, 16% of a calcium sulphoaluminate-based expansive agent (a) and 8% of a calcium-oxide based expansive agent (b) (Bissonnette et al., 2014). A first series of concrete was cured at 100% relative humidity (RH) during 7 days and later on at 50% RH. A second series of concrete was cured in air after the demolding just 6 h after their casting. The influence of the curing on expansive reactions clearly appears for the two types of expansive agents. For the calcium sulphoaluminate-based expansive agent, the absence of water curing (curing in air) did not produce practically any expansion. For the calcium-based expansive agent, the absence of water curing produced an expansion, but it was only equal to 30% of the expansion obtained under water curing.

Collepardi et al. (2005) studied the influence of curing conditions on the restrained expansion of a concrete having a w/c of 0.42 containing 9% of a

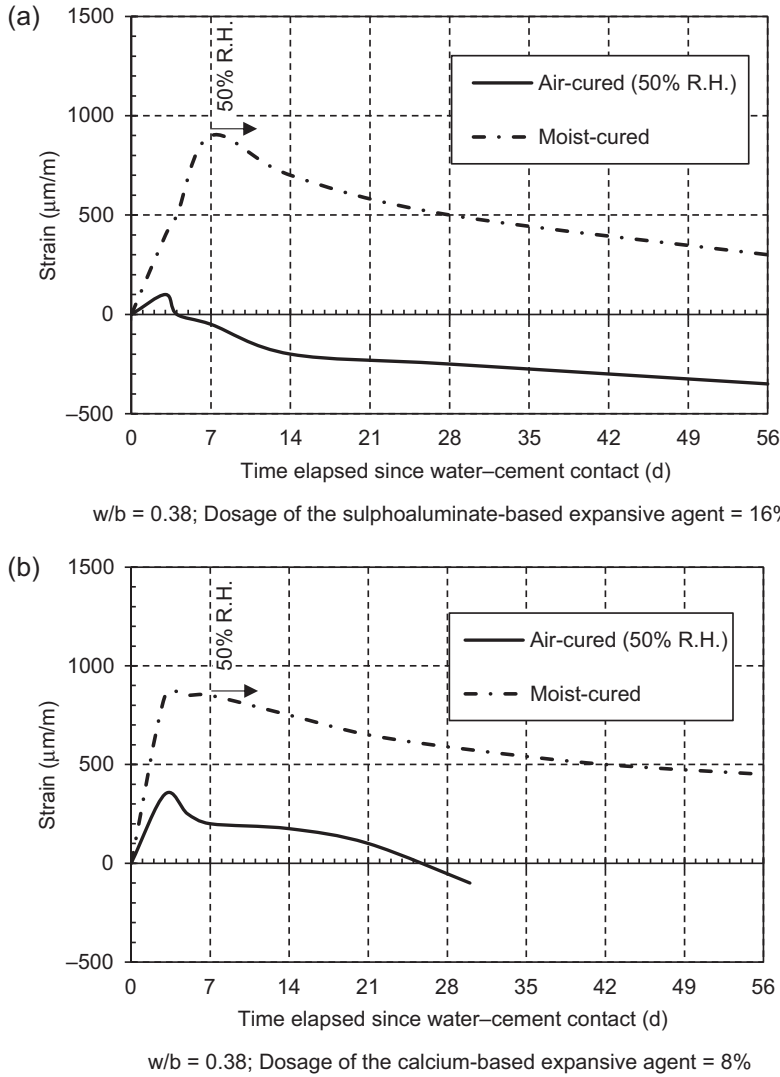


Figure 22.9 Effect of the curing conditions on the restrained expansion of a concrete made with a sulphoaluminate-based expansive agent (a) and a calcium-based expansive agent (b) (Bissonnette et al., 2014).

calcium-based expansive agent. Two curing conditions were studied—one corresponding to a curing under water during 36 h and a second curing regime where samples were wrapped in a polyethylene film. The results show that water curing produced the larger expansion, whereas sealed curing produced an expansion corresponding roughly to only 60% of the expansion obtained with water curing (Collepardi et al., 2005).

22.5.3 Temperature

Curing temperature has a great influence on the kinetics of the expansion and on the final expansion of a concrete (Bissonnette et al., 2014). Figure 22.10 presents the influence of curing temperature on the free expansion of two series of concrete having a w/b of 0.38 that contained 16% of calcium sulphoaluminate-based expansive agent

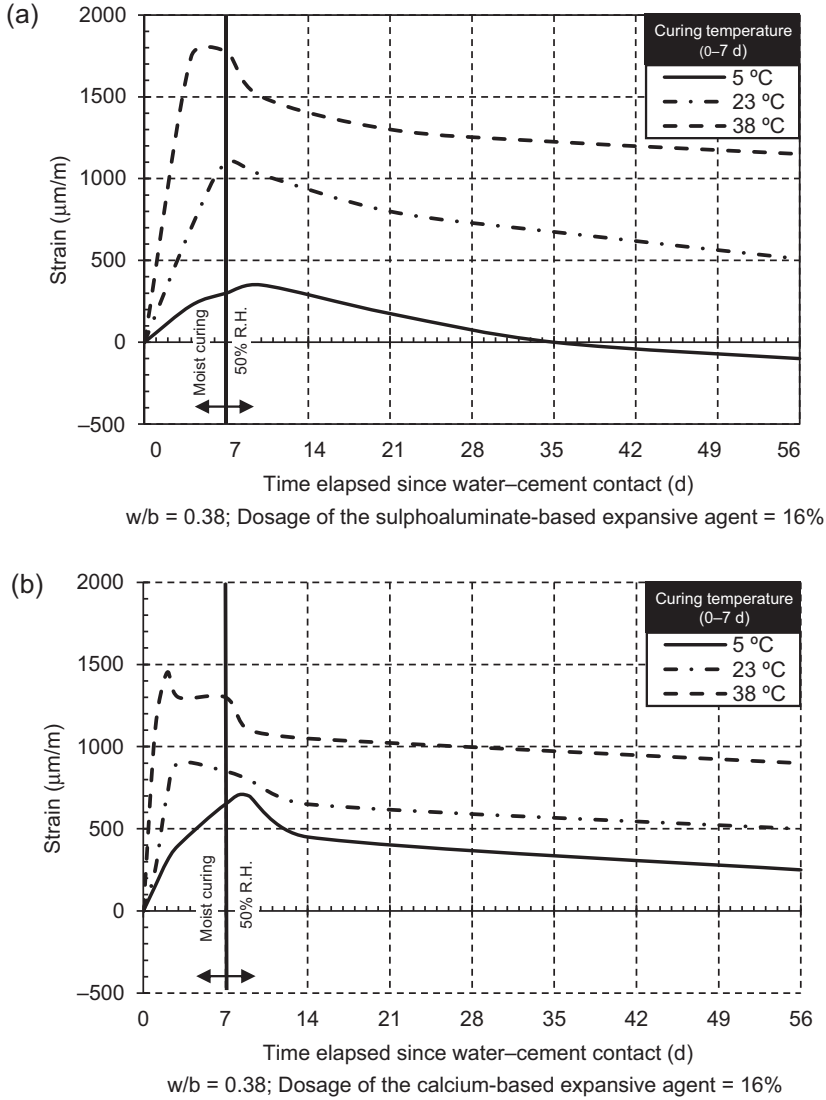


Figure 22.10 Effect of the curing temperature on the restrained expansion of a concrete made with a sulphoaluminate-based expansive agent (a) and a calcium-based expansive agent (b) (Bissonnette et al., 2014).

and 16% of a calcium-based expansive agent. Concrete samples were submitted to 7 days of water curing at 5, 23, and 38 °C. For the two types of expansive agents, an increase of the curing temperature resulted in an increase of the initial kinetics of the expansion. The maximum expansion was greatly influenced by temperature. For the concretes containing the calcium sulphoaluminate-based expansive agent, a cold temperature (5 °C) resulted in a decrease of 60% of the expansion obtained at 23 °C; the curing at 38 °C resulted in an expansion that is 50% greater than the expansion measured at 23 °C. The expansion obtained with the calcium oxide-based expansive agent was less influenced by the temperature. A curing temperature of 5 °C resulted in a decrease of 20% of the expansion compared with 23 °C curing, while curing at 38 °C results in an increase of 30% of the expansion. An important question to examine is whether the reactions take place but just do not develop substantial pressures, or whether they are delayed and may occur at a later stage. Such situations would lead to crystallization pressure developing in a hardened material, which is a damaging process known, for example, in delayed ettringite formation (Taylor et al., 2001; Flatt and Scherer, 2008).

22.5.4 Test method: restrained versus free expansion

The expansion measured in the laboratory is function of the test method used. The expansion can be measured as a free expansion or as a restrained expansion. As previously mentioned, free expansion can be measured using vibrating wires, while restrained expansion is usually measured according to ASTM C878 Testing Method. For a given concrete, free expansion is, of course, greater than restrained expansion. Figure 22.11 presents the results obtained with a 25 MPa concrete having binder dosage of 270 kg/m^3 and a w/c of 0.72 (Aïssi et al., 2014). This concrete was produced

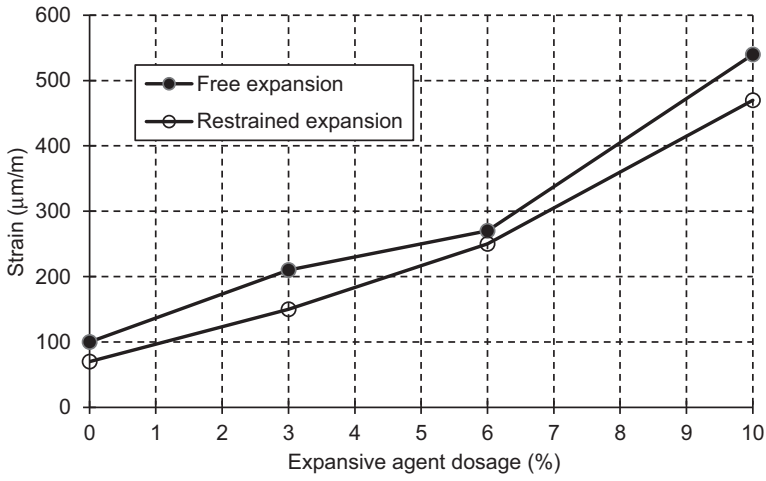


Figure 22.11 Free and restrained expansion of a 25 MPa concrete containing a calcium-based expansive agent (Aïssi et al., 2014).

using a dosage of CaO-based expansive agent of 0%, 3%, 6%, and 10%. The free expansion at 7 days of the reference concrete was 100 μm/m. The restrained expansion of the reference concrete is slightly smaller because of the restriction imposed by the two end-plates and the treaded rod.

Globally, the results presented in Figure 22.11 show that free expansion and restrained expansion grow approximately linearly as a function of the dosage of the expansive agent. The gap between the two values obtained does not vary very much with the dosage of the expansive agent. On an average, restrained expansion is approximately 35 μm/m smaller than free expansion.

22.6 Field applications of concretes containing expansive agents

Concretes containing expansive agents are mostly used to build bridge decks and slabs on ground (Phillips et al., 1997; Richardson et al., 2014). Expansive agents can also be used for concrete repairs and thin bonded concrete overlays (Gagné et al., 2008). These concrete elements are usually submitted to restrained shrinkage. In bridge decks, the restriction of the shrinkage is essentially due to the bonding of the deck on the principal and secondary beams that support them. For slabs on ground, it is the friction on the soil that presents the main cause of shrinkage. In the case of concrete repairs and thin bonded overlays, restrained shrinkage results from the bonding on the substrate concrete. For all of these structures, the absence of shrinkage cracks is very important for long-term durability.

22.6.1 Bridge decks

The Ohio Turnpike Commission had a good experience using concrete containing a calcium sulphoaluminate-based expansive agent (Type K cement) for bridge deck construction (Phillips et al., 1997). This approach is justified by the importance of limiting shrinkage cracking in order to increase the long-term durability of bridge decks.

Typically, air-entrained concretes containing a calcium sulphoaluminate-based expansive agent having a 28-day compressive strength of 30 MPa are prescribed. The Type K cement dosage is around 425 kg/m^3 and the w/c is between 0.34 and 0.45. Three projects used concrete containing 7% entrained air having a slump between 100 and 175 mm (Phillips et al., 1997). The field experience obtained from these experimental projects shows that it was possible to produce, pump, and place these concretes. Their cracking behavior due to restrained shrinkage was significantly better than that of an ordinary concrete. The authors mentioned also that the calcium sulphoaluminate-based expansive agent had the tendency to shorten the period of time available for placing. Therefore, it is very important to place concrete very rapidly using a pump. They also insist on the importance of providing a good curing in order to develop the expansion due to the use of calcium sulphoaluminate-based expansive agent.

22.6.2 Slabs on ground

It is possible to build large slabs on the ground that do not present any joints using a concrete containing an expansive agent. Collepardi et al. (2008) reported the construction of an 800 m^2-slab on the ground without any joint using a 30 MPa (w/c = 0.62) containing 285 kg/m^3 of cement and 25 kg/m^3 of a CaO-based expansive agent. The 230 mm-slump concrete was placed using a pump; the surface was finished with a rotating trowel and then protected from evaporation by a plastic film (Collepardi et al., 2008).

22.6.3 Bonded concrete overlays

Expansive agents can be used to decrease or eliminate the cracking of thin bonded concrete overlays used to repair reinforced concrete bridge decks. Gagné et al. (2008) have published a study showing the construction and monitoring of several thin bonded concrete overlays on concrete bridge decks in the Montreal area (Gagné et al., 2008). Among the nine types of thin bonded overlays tested, four contained an expansive agent. Three of them contained 6% of CaO-based expansive agent and the last one a calcium sulphoaluminate-based expansive agent (Type K cement). The three overlays containing the CaO-based expansive agent were produced using cement dosages between 375 and 426 kg/m^3. The corresponding w/c were between 0.37 and 0.44. In all cases, the expansive dosage was 24 kg/m^3. These concretes contained 7−8% air and were reinforced with hooked metallic fibers (40 kg/m^3) in order to limit the shrinkage crack opening if it had to occur. The 28-day compressive strength of the three concretes was between 36 and 41 MPa and the slump between 130 and 180 mm. The concrete overlay with a calcium sulphoaluminate-based expansive agent contained 376 kg/m^3 of Type K cement with a w/c = 0.40. The concrete contained 8% of entrained air and 38 kg/m^3 of hooked fibers. This concrete had a 28-day compressive strength of 43 MPa and a slump of 160 mm.

All these thin bonded overlays had a thickness between 75 and 125 mm. They were placed with a vibrating screed on the repaired concrete that was conditioned in a saturated surface dry state. Concrete surface was prepared using a heavy scarifier. Just after the placing, the concrete overlay was covered with a water-saturated nonwoven geotextile for 7 days. All these repairs have been monitored for 2.5 years since their construction. Among the nine types of repairs studied, those that did not contain any expansive agent developed more or less severe restrained shrinkage cracking. The most important cracking appeared on the repair done with an high performance concrete (HPC) having a 28-day compressive strength of 79 MPa (Gagné et al., 2008). The four repairs containing an expansive agent were not cracked at all after 2.5 years. These results confirm that during curing internal expansion was able to eliminate the cracking due to the restrained drying shrinkage (Gagné et al., 2008).

22.7 Conclusion

Expansive agents are used to decrease concrete shrinkage. Two types of expansive materials are presently used—one based on calcium sulphoaluminate and another based on dead-burn lime. Some commercial formulations are a combination of these two

expansive materials. As the dosage of these expansive agents is usually quite small, they are diluted in a certain quantity of Portland cement in order to mitigate the effect of an error of dosage. When using an expansive agent, it is very important to properly water cure concrete in order to be sure to provide the expansive agent with the necessary water to obtain the desired expansion. The expansion obtained depends essentially of the dosage of the expansive agent but also of the temperature and the efficiency of the water curing.

The use of expansive agents is very simple and very efficient, provided that good water curing is applied on concrete and the temperature is not too cold.

References

ACI, 2010. Guide to Design of Slabs-on-Ground. ACI Committee 360R-10. American Concrete Institute, Farmington Hills, USA.

ACI, 2011. Standard Practice for the Use of Shrinkage-Compensating Concrete. ACI Committee 223−98. American Concrete Institute, Farmington Hills, USA.

Aïssi, M., Gagné, R., Bastien, J., 2014. Étude de l'influence d'un agent d'expansion interne et d'un agent réducteur de retrait sur les variations volumiques libres et restreintes d'un béton. In: Séminaire progrès dans le domaine du béton, ACI − Section du Québec et de l'Est de l'Ontario, Québec, 2−3 décembre, 16 p.

Aïtcin, P.-C., 2016. Entrained air in concrete: Rheology and freezing resistance. In: Aïtcin, P.-C., Flatt, R.J. (Eds.), Science and Technology of Concrete Admixtures. Elsevier (Chapter 6), pp. 87−96.

ASTM Standard C157/C157M, 2014. Standard Test Method for Length Change of Hardened Hydraulic-Cement Mortar and Concrete. ASTM International, West Conshohocken, PA.

ASTM Standard C878/C878M, 2014. Standard Test Method for Restrained Expansion of Shrinkage-Compensating Concrete. ASTM International, West Conshohocken, PA.

Bentur, A., Ish-Shalom, M., 1974. Properties of type K expansive cement of pure components − II proposed mechanism of ettringite formation and expansion in unrestrained paste of pure expansive component. Cement and Concrete Research 4, 709−721.

Bissonnette, B., Perez, F., Blais, S., Gagné, R., 2008. Évaluation des bétons à retrait compensé pour les travaux de réparation. Canadian Journal of Civil Engineering 35 (7), 716−726.

Bissonnette, B., Jolin, M., Gagné, R., Certain, P.-V., Perez, F., 2014. Evaluation of the Robustness of Shrinkage-Compensating Concrete Repair Concretes Prepared with Expansive Components. ACI C223 Special Publication, 17 p.

Collepardi, M., Borsoi, A., Collepardi, S., Ogoumah Olagot, J.J., Troli, R., 2005. Effects of shrinkage reducing admixture in shrinkage compensating concrete under non-wet curing conditions. Cement and Concrete Composites 27, 704−708.

Collepardi, M., Troli, R., Bressan, M., Liberatore, F., Sforza, G., 2008. Crack-free concrete for outside industrial floors in the absence of wet curing and contraction joints. Cement and Concrete Composites 30, 887−891.

Flatt, R.J., 2002. Salt damage in porous materials: how high supersaturations are generated. Journal of Crystal Growth 242, 435−454.

Flatt, R.J., Caruso, F., Aguilar Sanchez, A.M., Scherer, G.W., 2014. Chemomechanics of salt damage in stone. Nature Communications 5 (4823), 1−5.

Flatt, R.J., Scherer, G.W., 2008. Thermodynamics of crystallization stresses in DEF. Cement and Concrete Research 38, 325−336.

Gagné, R., 2016. Shrinkage-reducing admixtures. In: Aïtcin, P.-C., Flatt, R.J. (Eds.), Science and Technology of Concrete Admixtures. Elsevier (Chapter 23), pp. 457−470.

Gagné, R., Bissonnette, B., Morin, R., Thibault, M., 2008. Innovative concrete overlays for bridge-deck rehabilitation in Montréal. In: 2nd International Conference on Concrete Repair, Rehabilitation and Retrofitting, Cape Town, 24−26 November, 6 p.

Ish-Shalom, M., Bentur, A., 1974. Properties of type K expansive cement of pure components − I Hydration of unrestrained paste of expansive component − Results. Cement and Concrete Research 4, 519−532.

Phillips, M.V., Ramey, G.E., Pittman, D.W., 1997. Bridge deck construction using type K cement. Journal of Bridge Engineering 2, 176−182.

Richardson, D., Tung, Y., Tobias, D., Hindi, R., 2014. An experimental study of bridge deck cracking using type K-cement. Construction and Building Materials 52, 366−374.

Scherer, G.W., 1999. Crystalisation in pores, Cement and concrete research 29, 1347−1358.

Taylor, H.F.W., Famy, C., Scrivener, K.L., 2001. Delayed ettringite formation. Cement and Concrete Research 31, 683−693.

Shrinkage-reducing admixtures

23

R. Gagné
University of Sherbrooke, QC, Canada

23.1 Introduction

On the first application of high-performance concrete having a water–cement ratio (w/c) or water–binder ratio (w/b) less than 0.40, early severe cracking can be observed when the concrete is placed without any special water curing. Therefore, it is not possible to ignore the rapid development of autogenous shrinkage that develops as soon as Portland cement starts to hydrate in the absence of an external source of water. Before the use of low w/c or w/b concrete, autogenous shrinkage was negligible when using concretes having a w/c or w/b greater than 0.50.

The lower the w/c or w/b is below this 0.40 critical value, the faster and the greater is the development of autogenous shrinkage. The higher the w/c or w/b is above this critical value, the more negligible is the autogenous shrinkage because the excess water in the capillary system plays the role of an external source of water. However, later, the higher the w/c or w/b is, the greater the drying shrinkage will be.

In Chapter 5, it was shown that coarse or fine saturated lightweight aggregates can be used for internal curing because saturated lightweight particles act as a small reservoir of water that are well dispersed within the mass of concrete (Aïtcin, 2016). By capillary suction, the very fine pores generated by the chemical contraction drain the water contained in the larger pores of the lightweight aggregates. Consequently, menisci appear inside the lightweight aggregates as they are emptied from the water they contained, which does not create autogenous shrinkage in the cement paste. Of course, in practice, this water transfer does not work perfectly, particularly in cement pastes having very low w/c or w/b.

Moreover, it is not always easy to find suitable lightweight aggregates for implementing an internal curing. Therefore, shrinkage-reducing admixtures (SRAs) have become an interesting alternative to fight the consequences of autogenous shrinkage, especially when their use is combined with careful external water curing. In Chapters 10 and 13, we have seen that SRAs are surfactants that reduce the superficial tension of the air–water interface in the dehydrating pore system, as well as the angle of contact of these menisci with the walls of the pore system, so that the tensile stresses developed by this apparent drying phenomenon and autogenous shrinkage are decreased significantly (Marchon et al., 2016; Eberhardt and Flatt, 2016).

To mitigate the effects of autogenous shrinkage, it is also possible to use an expansive agent in order to create an increase of the apparent volume of the cement paste equal to the reduction of the apparent volume that should have been created by the

Science and Technology of Concrete Admixtures. http://dx.doi.org/10.1016/B978-0-08-100693-1.00023-0
Copyright © 2016 Elsevier Ltd. All rights reserved.

free development of autogenous shrinkage (see Chapter 22; Gagné, 2016). It is also possible to combine these two techniques, especially in the case of repair works, as will be seen in the last section of this chapter. As explained in Chapter 13, SRAs can also be used to decrease the effect of drying shrinkage of a concrete having a w/c or w/b greater than 0.40 (Eberhardt and Flatt, 2016).

23.2 Principal molecules used as shrinkage-reducing admixtures

SRAs contain various surfactants, as seen in Chapter 9 (Gelardi et al., 2016). These compounds include the following:

- Monoalcohols having a OH^- function group (hydroxyl)
- Glycols: these alcohols present two hydroxyl functional groups attached to two adjacent carbon atoms
- Polyoxyalkylene glycol alkyl esthers: the cyclic alkyl radical constitutes the hydrophobic tail of the surfactant, whereas the hydrophilic head is the hydrated oxyalkylene chain
- Polymeric surfactants
- Amino alcohols

As each admixture company keeps secret the composition of its SRA, it is not recommended to switch from one commercial product to another without having done some preliminary laboratory work.

23.3 Typical dosages

To produce a significant reduction of autogenous shrinkage of low w/c or w/b concretes and drying shrinkage of high w/c or w/b concretes, it is necessary to use high dosages of SRAs. The dosage is usually expressed as a percentage of the cement mass (from 1% to 2%) or in l/m^3 of concrete for each commercial formulation. Table 23.1 gives some typical values used to mitigate autogenous shrinkage of ordinary and high-performance concrete with or without air-entraining agents (AEA) in Montreal, Canada.

Table 23.1 Typical SRA dosages for air-entrained and non-air-entrained ordinary and high-performance concretes

	Non-air-entrained concrete		Air-entrained concrete	
Compressive strength (MPa)	30	60	30	60
Cement dosage (kg/m^3)	300	400	360	450
SRA dosage (l/m^3)	6	3	3.6	4.5

Courtesy of Prof. Richard Gagné.

For example, when using an HPC, the City of Montreal specifies a dosage of 6−8 l/m^3 of SRA. The cost of the SRA that is added to each cubic meter of concrete is negligible when compared to the direct cost of potential repair work, as well as the social costs associated with the disturbance of traffic, if the apparent surface of an HPC structure severely cracks due to the uncontrolled development of a severe autogenous shrinkage.

23.4 Laboratory studies on the use of shrinkage-reducing admixtures

23.4.1 Autogenous shrinkage

23.4.1.1 Mortars

Different SRAs have been tested in air-entrained mortar having a w/c of 0.47. The cement dosage was 595 kg/m^3 (Apaya, 2011). Autogenous shrinkage was measured using vibrating wires cast in the mortar specimens (75 × 75 × 350 mm^3). The specimens were kept sealed 24 h in their molds. Immediately after demolding, the specimens were sealed in two self-adhering aluminum foils, which corresponded to a curing condition in the absence of an external source of water. Autogenous shrinkage was monitored for 14 days.

The curves in Figure 23.1 show the development of autogenous shrinkage for the reference mortar and for five mortars containing different commercial SRAs used

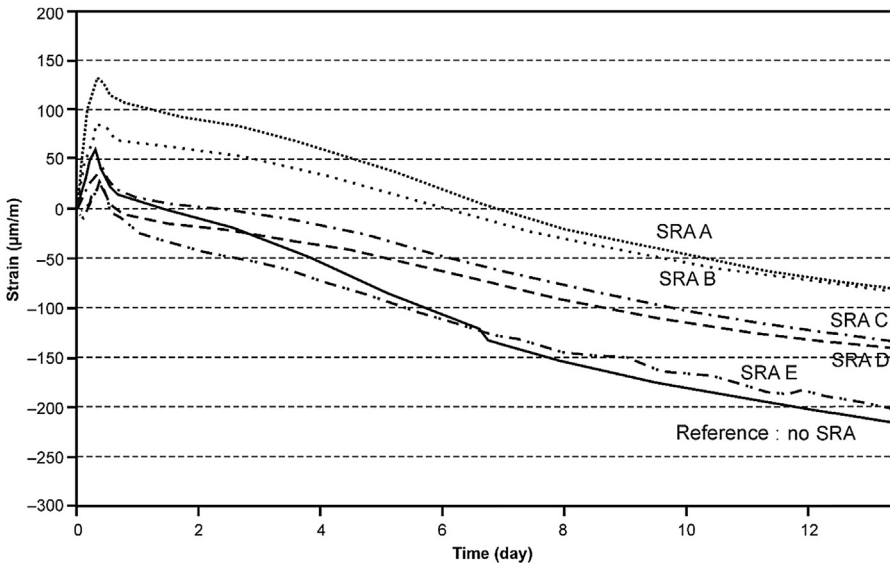


Figure 23.1 Autogenous shrinkage of a reference mortar (no SRA) and of five mortars containing commercial SRAs (A, B, C, D, and E) (Apaya, 2011).
Courtesy of Prof. Richard Gagné.

with the recommended dosage by the admixture companies. All SRAs produced a more or less important decrease of the autogenous shrinkage. SRA A and SRA B were the most efficient because their use resulted in an initial expansion greater than for the three others SRAs (75 and 140 μm/m), which annihilated a part of the autogenous shrinkage developed later. Sant et al. (2011) suggested that this expansion would result from the modification of the mechanism and kinetic of the precipitation of portlandite. SRAs B, C, and D produced a lower initial expansion, but the 14-day autogenous shrinkage decreased. On the contrary, SRA E had practically no effect on the development of autogenous shrinkage.

23.4.1.2 Self-compacting concrete

Figure 23.2 presents the development of the autogenous shrinkage of air-entrained SCC specimens made with a commercial SRA at the dosage recommended by the admixture company (Apaya, 2011). The concrete has a w/c of 0.47 and a cement dosage of 420 kg/m^3. Autogenous shrinkage was measured during 14 days (sealed specimens) with a vibrating wire gage cast in the specimen and compared to the autogenous shrinkage measured on a reference specimen. In this case, the addition of the SRA resulted in very significant decrease of the autogenous shrinkage. This decrease resulted from the initial expansion observed during the first 24 h and from the reduction of the slope of the curve later.

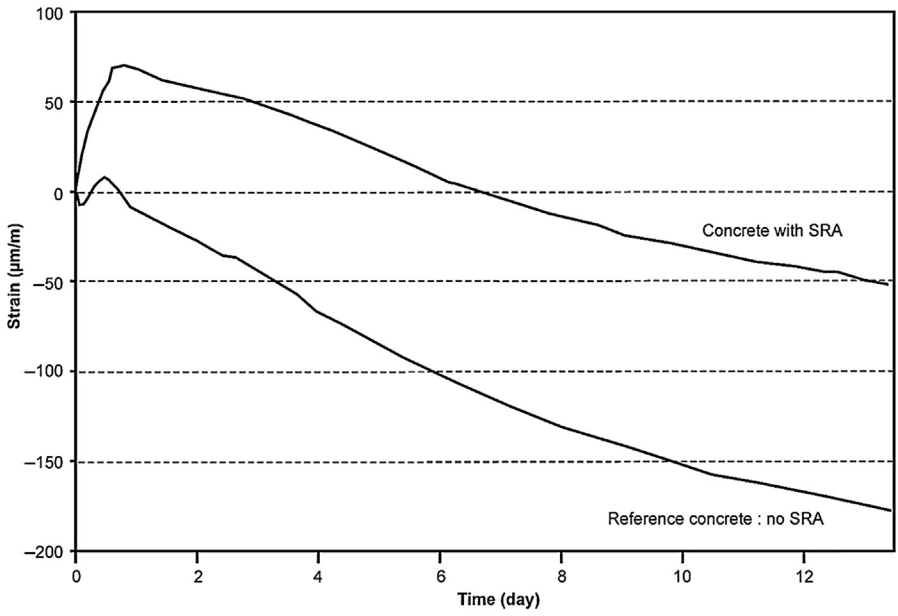


Figure 23.2 Effect of an SRA on the autogenous shrinkage of a self-compacting air-entrained concrete (Apaya, 2011).
Courtesy of Prof. Richard Gagné.

23.4.2 Drying shrinkage

23.4.2.1 Mortar

Figure 23.3 represents the development of the drying shrinkage, measured with a vibrating wire gage, of mortars having a w/c equal to 0.47 (Apaya, 2011). The origin of the curves corresponds to the end of a 14-day sealed curing. All mortars were air entrained and the same five commercial SRAs were used according to the manufacturer's recommended dosage. A reference mortar was also tested. The drying shrinkage that was measured after 300 days was quite high (800−1300 μm/m) because the specimens were made with a mortar that was particularly rich in cement (595 kg/m^3). These curves show that all of the commercial SRAs decreased the drying shrinkage after almost a year of curing at 23 °C and 50% relative humidity (RH). The less efficient SRA (SRA E) decreased the drying shrinkage by 6% while the most efficient decreased it by 33% (SRA B).

23.4.2.2 Self-compacting concrete

Figure 23.4 presents the influence of different commercial SRAs on the development of drying shrinkage of an SCC (w/b = 0.47) having a cement dosage of 420 kg/m^3 that was dried for 6 months at 23 °C and 50% RH (Apaya, 2011). After 6 months, the drying shrinkage of the concrete containing the SRA is 17% lower than the one of the reference concrete.

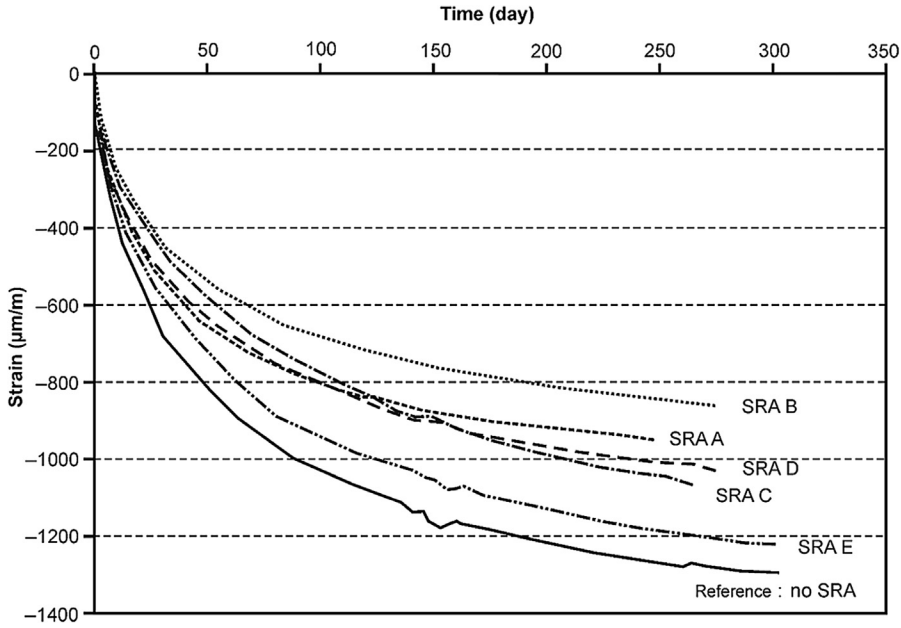


Figure 23.3 Drying shrinkage of a reference mortar (no SRA) and of five mortars containing commercial SRAs (A, B, C, D, and E) (Apaya, 2011).
Courtesy of Prof. Richard Gagné.

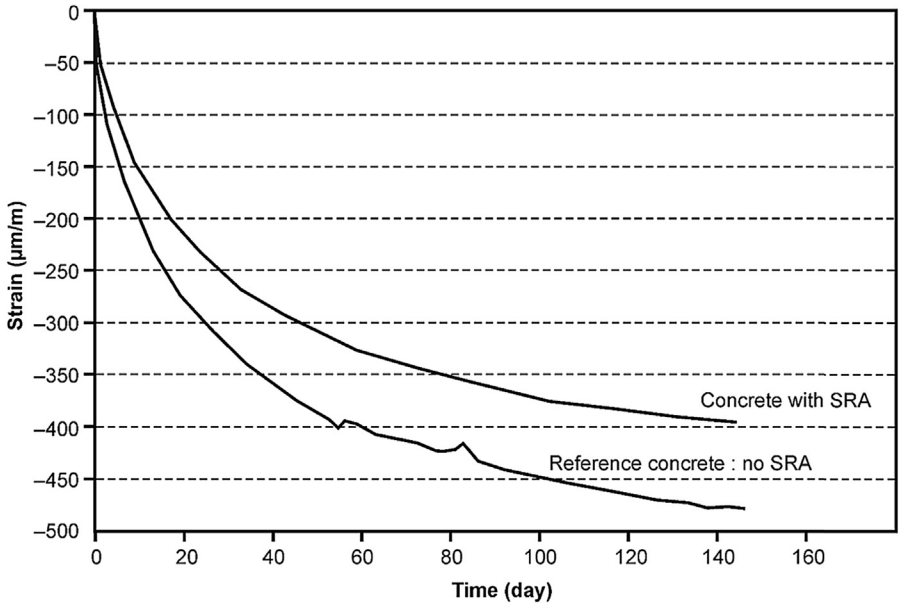


Figure 23.4 Effect of an SRA on the drying shrinkage of a self-compacting air-entrained concrete (Apaya, 2011).
Courtesy of Prof. Richard Gagné.

23.4.3 Combination of an SRA and of an expansion agent to decrease to total shrinkage

For this case, the role of the SRA is to decrease drying shrinkage and the role of the expansive agent is to provide an initial expansion that compensates for the development of the early autogenous shrinkage. Figure 23.5 presents the deformations of three concretes having a compressive strength of 25 MPa and a w/c equal to 0.72. These three concretes were cured for 7 days at 100% RH and later for almost 240 days at 50% RH.

The reference concrete did not contain any expansive agent or any SRA; its total shrinkage was 380 µm/m after 270 days of drying. The use of 2% of SRA (relative to the mass of cement) resulted in a slight increase of the initial expansion during the 7 days of water curing and in a 30% lower drying shrinkage.

A type G expanding agent (lime-based expansive agent) was used at a dosage of 10% of the mass of the cement in combination with an SRA in order to annihilate the final shrinkage. During the moist curing period, the expansive agent produced an expansion that compensated for a great part of the final drying shrinkage. After this initial expansion, it was the SRA that decreased the intensity of the drying shrinkage, as seen in Figure 23.5. During the first 91 days ($7 > d > 98$), the slopes of the shrinkage curves are quite similar. They are less steep than the curve related to the reference concrete.

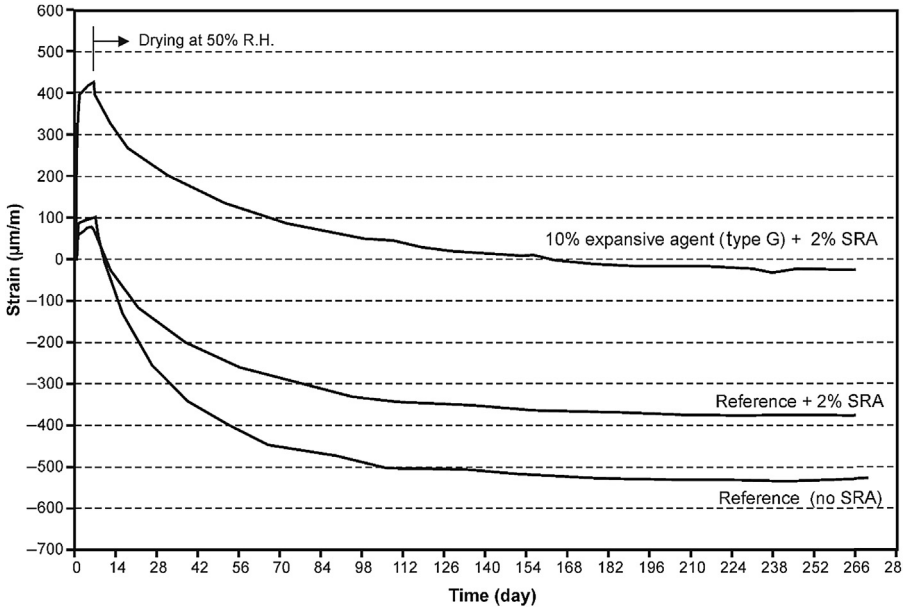


Figure 23.5 Effect of an expansive agent (type G) and an SRA on the initial expansion and drying shrinkage of a 25 MPa concrete (Aïssi, 2015).
Courtesy of Prof. Richard Gagné.

23.4.4 Effect of SRAs on air entrainment

Commercial SRAs, being surfactants, may strongly influence air entrainment. Therefore, from a practical point of view, it is important to check the compatibility of the SRA−AEA combination when an SRA has to be used in an air-entrained concrete. It is important to read carefully the technical data sheet of the SRA because some admixtures companies are specifying different commercial SRAs for air-entrained and non-air-entrained concrete. Moreover, in these technical data sheets, the use of a specific AEA that is compatible with the SRA is usually recommended.

Figure 23.6 presents the dosage of a number of AEAs used to entrain 12−15% of air in mortar samples (Apaya, 2011). For the reference mortar, the AEA dosage was 30 mL/100 kg of binder in order to reach the target. SRA A and SRA E were found to have no effect on the dosage of the air-entraining admixture. For these two SRAs, a dosage 30 mL/100 kg of binder provided an air content of 12−15%, similar to that of the reference concrete. For SRAs B, C, and D, it was necessary to increase significantly the amount of AEA in order to obtain the same amount of air. For example, in the case of SRA B, it was necessary to use a dosage of 500 mL/kg of binder, which is 15 times the dosage used for the reference mortar. Despite this very high dosage of AEA, the initial air content was only 8%, which was 50% short of the 12% lower target.

The SRA−AEA interaction seems to be associated with the hydrophile−lipophile balance (HLB) of the surfactant used as SRA. The molecules having a high HLB (>7)

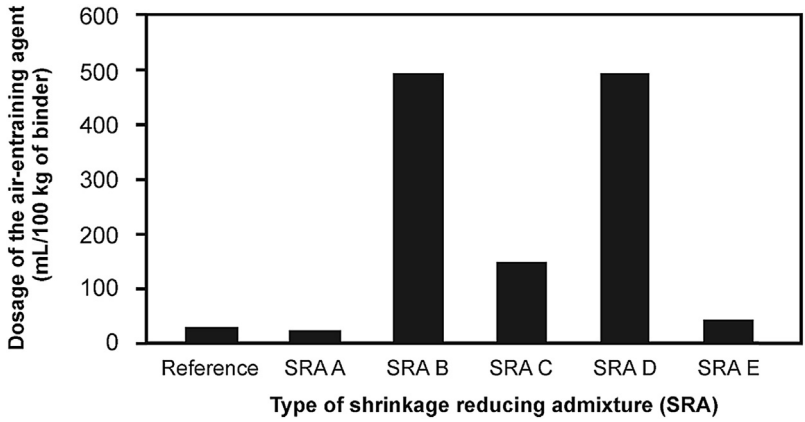


Figure 23.6 Effect of the type of SRA on the air-entraining agent dosage required to produce 12−15% air in mortar samples (Apaya, 2011).
Courtesy of Prof. Richard Gagné.

generally have less of an effect on the air entrainment than the molecules having an HLB less than 7, which can react strongly with the air entrainment process (Apaya, 2011).

SRA may influence the stability of the bubble network. Figure 23.7 presents the variation of the air volume for air-entrained mortars having a w/c = 0.47 that has been monitored between 10 and 70 min after the first cement−water contact. For the SRAs E, C, and D, the air loss was respectively 6%, 5%, and 3%. The use of the SRAs A and B did not result in any air loss between 10 and 70 min. These data show that it is difficult to predict the effect of an SRA on the stability of an air bubble network produced with a specific AEA. When deciding to use an SRA in an air-entrained concrete, it is therefore recommended to use an SRA and an AEA

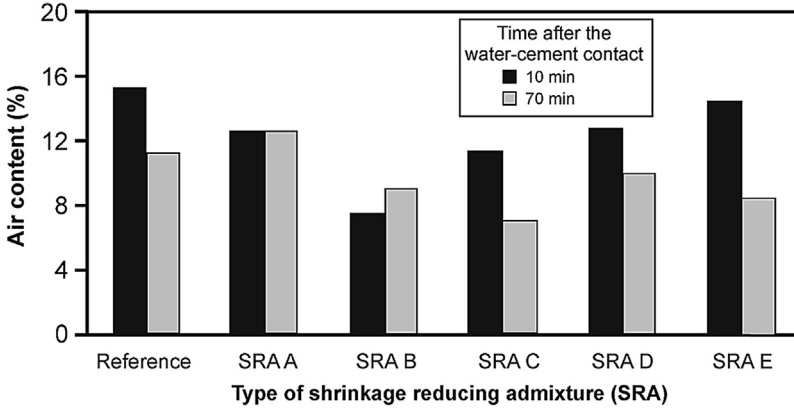


Figure 23.7 Effect of the type of SRA on the air content at 10 and 70 min after the water−cement contact (Apaya, 2011).
Courtesy of Prof. Richard Gagné.

from the same company and to make some laboratory trial batches before doing some convenience batches in the field.

23.4.5 Resistance to freezing and thawing

To obtain a good durability to freezing and thawing for a concrete containing SRA, it is necessary to fulfill the same formulation and placing requirements as the requirements for concrete that do not contain an SRA (Pigeon and Pleau, 1995):

- Select a w/b adapted to the severity of the conditions of exposition.
- Use an AEA that will produce a bubble network with a spacing factor less than 250 μm.
- Use good-quality aggregates.
- Use placing techniques (transportation, pumping, vibration, etc.) that do not destabilize the bubble network.
- Use a curing method that provides good durability characteristics.

The possible interaction between the SRA and AEA is the principal point to be checked when formulating a concrete containing an SRA that will be exposed to freezing and thawing cycles in the presence of or not of deicing salts. It is very important to select an SRA−AEA combination that is compatible and to optimize the AEA dosage in order to produce a stable bubble network having a spacing factor less than 250 μm. Field experience has shown that the freezing and thawing durability of concrete is excellent when this last requirement and the previous ones are satisfied.

Apaya (2011) studied the freezing and thawing durability of two SCC concretes, one without SRA and the other with 1% SRA (relative to the mass of binder). The cement used contained 30% slag and the w/b was 0.42. The two concretes also contained a viscosity modifier (0.07% of the mass of mixing water). The reference concrete and the SRA concrete contained, respectively, 9% and 7% of entrained air (the spacing factor was not measured). The AEA dosage was 60 mL/100 kg of binder for the reference concrete and 20 mL/100 kg of binder for the concrete containing the SRA. The durability of these two concretes was evaluated using the two following standardized procedures: the resistance to internal cracking was measured with Procedure A of ASTM C666 Standard (ASTM, 2015) and the salt-scaling resistance was measured according to ASTM C672 (ASTM, 2012). The result of the testing has shown that these two concretes successfully passed ASTM C666 with an internal increase in length that was less than 200 μm/m after 300 cycles of freezing and thawing. The durability factor of these two concretes after 300 cycles of freezing and thawing was greater than 90%. The scaling resistance of these two concretes was very good because the mass of scaled-off particles was less than 0.2 kg/m^2 after 50 cycles of freezing and thawing (Apaya, 2011).

The durability of concretes containing an SRA has been studied in the laboratory and in the field by Gagné et al. (2008). Two concretes containing an SRA were used for thin bonded overlays repairs on bridge decks in the Montreal area in Canada. These bridge decks are severely exposed to deicing salts and to frequent freezing and thawing cycles.

The first concrete had a w/b of 0.40 and contained 2% SRA. This concrete also contained 4.0 kg/m^3 of synthetic structural fibers. A very high total volume of entrained air was obtained (18%) due to a strong interaction between the polycarboxylate superplasticizer and the AEA. During the transportation of the concrete, the total air volume passed from 9% at the ready-mix plant to 18% at the construction site. Due to this very high air content, the spacing factor was very low (50 μm). All concretes were cured under water-saturated geotextile pads for 7 days.

Accelerated freezing and thawing and salt-scaling tests were done in the laboratory on specimens taken in the field during construction. These tests showed that the concrete had a very good resistance to internal cracking after 300 cycles of freezing and thawing, with a durability factor of 102%. The scaling resistance in the presence of deicing salts was excellent; the mass of scaled-off particles after 50 cycles was only 0.07 kg/m^2—a value that is well under the maximum limit of 0.5% kg/m^2 specified in Quebec standards. After 13 years of exposure, no significant scaling was observed on this concrete overlay.

A second air-entrained fiber-reinforced concrete containing an SRA was used in a thin bonded concrete overlay on another bridge in Montreal, Canada (Gagné et al., 2008). This repair was severely exposed to freezing and thawing cycles in the presence of deicing salts. The cement used was a binder containing 8% silica fume. The concrete had a w/b ratio of 0.39; its SRA dosage was 2% of the mass of the binder. The AEA produced a total volume of air of 9% and a spacing factor of 140 μm. To optimize the freezing and thawing durability, the resurfacing was cured for 7 days under saturated geotextile pads.

ASTM C666 and ASTM C672 tests were done on specimen taken in the field. The durability factor after 300 cycles was 100% and the mass of scaled-off particles was 0.07 kg/m^2 (Gagné et al., 2008). After 10 years of exposure, no significant scaling is observed on this concrete overlay.

23.5 Field applications

Gagné et al. (2008) performed a field test program to evaluate the efficiency of an SRA in decreasing the cracking due to restrained shrinkage on thin bonded concrete overlays. The testing program consisted of monitoring the cracking in the service of six types of thin overlays used to repair the surface of bridge decks in the Montreal area in Canada. The thickness of these thin overlays was between 75 and 125 mm. This type of repair is very prone to cracking because autogenous and drying shrinkage are strongly restrained by the adhesion on the underlying concrete surface. It is very important to minimize the cracking of these repairs in order to protect concrete against the penetration of chloride ions.

Six types of fiber-reinforced air-entrained concretes were used for this repair program. Two concretes contained an SRA dosage equal to 2% of the mass of cement. The main mix design characteristics of these two SRA concrete have been presented

in the previous section (Gagné et al., 2008). Four other concretes without SRA were also tested:

- A high-performance concrete (79 MPa) reinforced with 40 kg/m^3 of steel fibers
- A normal-strength concrete (35 MPa) reinforced with 5.2 kg/m^3 of structural synthetic fibers
- A 35 MPa concrete reinforced with 40 kg/m^3 of steel fibers and containing 6% of a type G expansive agent
- A 35 MPa concrete reinforced with 40 kg/m^3 of steel fibers made with a type K cement.

The monitoring of the cracking in service was done during a period of 100−135 weeks after the repair of the bridge deck. Figure 23.8 represents the evolution of the cracking as a function of time. The cracking is expressed in linear meters of cracks per square meter of surface. The overlay made with the high-performance concrete developed the highest crack density. The overlay made with the 35 MPa concrete reinforced with fibers was slightly less cracked. After 6 months of service, the crack density of the two overlays containing fibers and SRA was two times less than the crack density of the normal-strength concrete without SRA and three times less than the crack density of the high-performance concrete. The two overlays containing fibers and an expansion agent did not present any cracks.

Globally, this series of field tests has shown that the use of an SRA (2% of the mass of cement) significantly decreases the cracking of the thin bonded concrete overlays. Usually, this type of repair is very susceptible to cracking due to the high surface/volume ratio and the strong shrinkage restriction from the bonding of the overlay to the underlying concrete. For this type of application where the risk of cracking is very

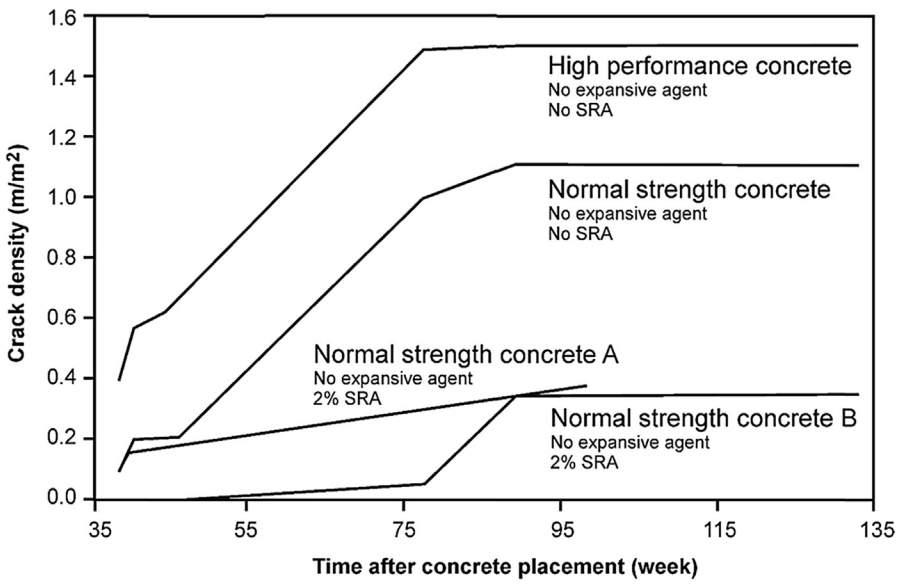


Figure 23.8 Evolution of the crack density in thin concrete overlays made with and without shrinkage reducing admixtures (SRAs) (Gagne et al., 2008).
Courtesy of Prof. Richard Gagné.

high, the use of an SRA did not result in the total elimination of cracking but decreased it significantly. Only the use of an expansive agent eliminated cracking of the thin bonded overlay.

23.6 Conclusion

The use of shrinkage-reducing admixtures represents a simple and efficient way to fight the following:

- The early cracking of concrete having a w/c or w/b smaller than 0.40 due to the early development of autogenous shrinkage
- The long-term cracking of concretes submitted to severe drying shrinkage for concrete having a w/b or w/c greater than 0.40.

SRAs can be used alone or in combination with expansive agents. Their dosages are much higher than the dosage of the other chemical admixtures used in concrete, with the exception of the superplasticizer dosages in HPC having a very low w/c (on the order of 0.30−0.35).

References

Aïssi, M., 2015. Étude de l'influence d'un agent d'expansion interne et d'un agent réducteur de retrait sur les variations volumiques libres et restreintes d'un béton (Master's thesis dissertation). University of Sherbrooke, Civil Engineering Department, Canada, 122 p.

Aïtcin, P.-C., 2016. Water and its role on concrete performance. In: Aïtcin, P.-C., Flatt, R.J. (Eds.), Science and Technology of Concrete Admixtures. Elsevier (Chapter 5), pp. 75−86.

Apaya, I., 2011. Retrait endogène et de séchage des BAP à air entraîné contenant divers composés organiques comme anti-retrait (Master's thesis dissertation). University of Sherbrooke, Civil Engineering Department, Canada, 122 p.

ASTM Standard C666/C666M, 2015. Standard Test Method for Resistance of Concrete to Rapid Freezing and Thawing. ASTM International, West Conshohocken, PA.

ASTM Standard C672/C272M, 2012. Standard Test Method for Scaling Resistance of Concrete Surfaces Exposed to Deicing Chemicals. ASTM International, West Conshohocken, PA.

Eberhardt, A.B., Flatt, R.J., 2016. Working mechanisms of shrinkage reducing admixtures. In: Aïtcin, P.-C., Flatt, R.J. (Eds.), Science and Technology of Concrete Admixtures. Elsevier (Chapter 13), pp. 305−320.

Gagné, R., 2016. Expansive agents. In: Aïtcin, P.-C., Flatt, R.J. (Eds.), Science and Technology of Concrete Admixtures. Elsevier (Chapter 22), pp. 441−456.

Gagné, R., Bissonnette, B., Morin, R., Thibault, M., 2008. Innovative concrete overlays for bridge-deck rehabilitation in Montréal. In: 2nd International Conference on Concrete Repair, Rehabilitation and Retrofitting, Cape Town, 24−26 November, 6 p.

Gelardi, G., Mantellato, S., Marchon, D., Palacios, M., Eberhardt, A.B., Flatt, R.J., 2016. Chemistry of chemical admixtures. In: Aïtcin, P.-C., Flatt, R.J. (Eds.), Science and Technology of Concrete Admixtures. Elsevier (Chapter 9), pp. 149−218.

Marchon, D., Mantellato, S., Eberhardt, A.B., Flatt, R.J., 2016. Adsorption of chemical admixtures. In: Aïtcin, P.-C., Flatt, R.J. (Eds.), Science and Technology of Concrete Admixtures. Elsevier (Chapter 10), pp. 219−256.

Pigeon, M., Pleau, R., 1995. Durability of Concrete in Cold Climates. In: Modern Concrete Technology, vol. 4. E. & F.N. Spon, London, 244 p.

Sant, G., Lothenbach, B., Julliand, P., Le Saout, G., Weiss, J., Scrivener, K., 2011. The origin of early age expansion induced in cementitious materials containing shrinkage reducing admixtures. Cement and Concrete Research 41 (3), 218−229.

Corrosion inhibition

24

P.-C. Aïtcin
Université de Sherbrooke, QC, Canada

24.1 Introduction

It is still not known how to make concrete absolutely impervious to chloride ions, as it is found when testing concrete according to AASHTO T-277 (test for rapid determination of the chloride permeability of concrete) or its ASTM equivalent C 1202 (test method for electrical indication of concrete ability to resist chloride penetration). Gagné et al. (1993) demonstrated that the water−cement ratio (w/c) and the concrete cover were the two most important factors commanding the apparition of a first crack following the corrosion of reinforcing steel by chloride ions. Lévy (1992) showed that the 60 MPa concrete used to build the Joigny Bridge in France was offering a far better protection against carbonation than a regular 40 MPa concrete.

As has been pointed out in Chapter 14 on the mechanisms of the corrosion process of reinforcing steel, the most efficient way to retard the progression of aggressive agents within concrete is to protect the first rank of reinforcing steel with an adequate cover of **well-cured** low w/c concrete (Elsener and Angst, 2016). The addition of corrosion inhibitors in the concrete provides only an additional safety factor that will delay the initiation time and thereafter significantly lower the corrosion rate.

The steel reinforcing bars that are used to reinforce concrete do not rust as long as the pH of the interstitial solution in the capillary porosity remains greater than 11. Usually in concrete, the pH of the interstitial solution stays between 12 and 12.5 as a consequence of the solubility of the portlandite crystals ($Ca(OH)_2$) that are formed during C_3S and C_2S hydration. In such a high pH solution, the steel surface remains covered by a passive film of ferrous oxide (FeO), which blocks the oxidation of the steel rebar. However, as soon as the pH of the interstitial solution becomes lower than 11, this protective film is torn; in the presence of oxygen, the steel starts to corrode and is transformed into rust.

This transformation of steel into rust results in a large volume increase, which creates internal forces that are strong enough to spall the concrete cover over the reinforcing bars. After the spalling of its concrete cover, the reinforcing bar is in direct contact with oxygen and water, so its corrosion develops rapidly and can cause the disappearance of the reinforcing bar if no immediate action is taken to stop this destructive process.

Two exterior factors can result in a decrease of the pH of the interstitial solution below this critical value of 11:

- The carbonation of the hydrated lime present in concrete due to the penetration of CO_2 in concrete
- The penetration of chloride ions

Science and Technology of Concrete Admixtures. http://dx.doi.org/10.1016/B978-0-08-100693-1.00024-2
Copyright © 2016 Elsevier Ltd. All rights reserved.

When the microstructure of concrete is very dense, it does not favor the movement of the different ionic species present in the interstitial water. Therefore, the use of a concrete having a low w/c or water−binder ratio (w/b) is a good **preventive** measure against the corrosion of reinforcing steel. However, when using such a concrete, it is necessary to be sure that the concrete cover is not cracked. This can be achieved by good external water curing of the exposed surface of concrete.

24.2 The effect of chloride ions on reinforcing steel bars

When chloride ions reach reinforcing steel bars, they decrease the pH of the interstitial solution in contact with the reinforcing bars so that the passive film of iron oxide that was covering the reinforcing bar is destroyed. The rebar start its corrosion process. The amount of chloride ions needed to stop the protection is a function of the initial pH of the interstitial solution. It is not necessary for this concentration to be very high to annihilate the protection provided by the initial passive film of iron oxide. This explains the severe damage caused by the use of deicing salts on bridge decks and on multilevel parking garages in the northern part of the United States and Canada, as shown in Figure 24.1(b).

When chloride ions start to penetrate in concrete submitted to freezing and thawing cycles, they not only corrode reinforcing steel bars but they also attack the hydrated cement paste. To protect concrete as much as possible against the destructive action of chloride ions, Canadian standards recommend the use of low w/c air-entrained

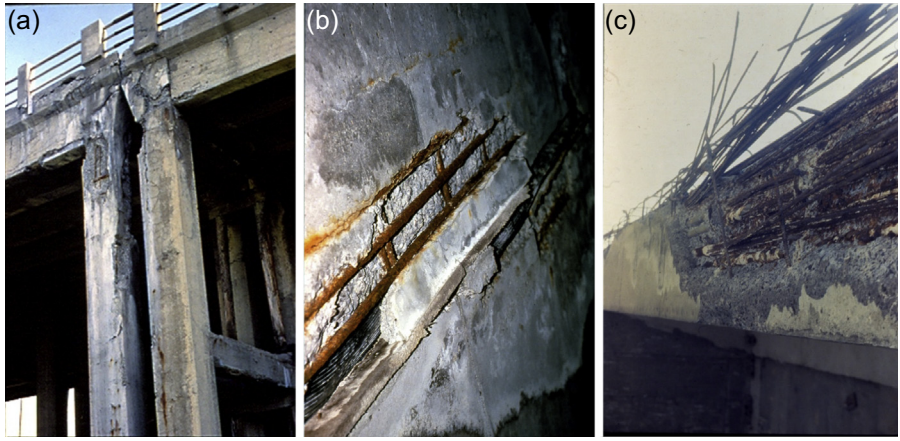


Figure 24.1 Example of chloride ion attacks on reinforced concrete and prestressed beams. (a) Attack of concrete due to a bad drainage of deicing salts running from the upper deck. (b) Corrosion of reinforcing steel in an indoor parking garage due to the progression of chloride ions dripping from the parked cars through the parking slab. (c) Attack of chloride ions on a prestressed beam.
Courtesy of Gilbert Haddad.

concrete having a spacing factor less than 240 μm. However, even with a low w/c and a low spacing factor, Canadian experience shows that it is always safer to place a protective impervious membrane on bridge decks or internal parking garage floors to be sure that chloride ions will not penetrate in concrete. In the case of concrete surfaces exposed to deicing salt that do not present any risk of wear, a thin hydrophobic layer of acrylic coating can be placed on concrete surfaces that need to be protected against the penetration of chloride ions.

In the case of prestressed and posttensioned concrete, the effects of chloride ions can be catastrophic. The corrosion of the cables is accelerated because they are under tension. Therefore, the use of calcium chloride is banned in prestressed and posttensioned concretes.

In nuclear power plants, some specifications even forbid the use of **sodium salt** of polynaphtalene sulfonates. The soda that is used to neutralize the sulfonic acid is usually obtained from seawater, so it may contain traces of chloride ions. In this case, the use of the **calcium salt** of the polysulfonate naphthalene is specified. This calcium polysulfonate salt is obtained by neutralizing the sulfonic acid with lime. It takes more time to neutralize the sulfonic acid and to produce this calcium salt because the neutralization proceeds at a lower rate than when using soda; in addition, a final filtration step has to be added after the neutralization to eliminate the uncombined lime. As a result, the calcium salt is more expensive but safer from a chloride ion point of view.

24.3 Increasing the protection of steel reinforcement against corrosion

Because it is not possible to totally eliminate the corrosion of steel reinforcing bars, it is only possible to increase the level of protection against corrosion. Three different techniques can be used:

- The use of a low w/c concrete
- A cathodic protection for the reinforcing bars
- The introduction of corrosion inhibitors in concrete during its batching

24.3.1 The use of low w/c or w/b concrete to decrease the risk of corrosion

The implementation of all these strategies works better when the microstructure of the concrete is very dense and does not favor the movement of the different ionic species present in the interstitial water. Therefore, the use of a high-performance concrete having a low w/c or w/b is a good **preventive** measure against the corrosion of reinforcing steel. However, when using a high-performance concrete, it is necessary to be sure that the concrete cover over the reinforcing bars is not cracked. This can be achieved by good external water curing of the exposed surface of concrete.

24.3.2 Cathodic protection

Corrosion of reinforcing bars can be avoided by cathodic protection under the form of an external sacrificial anode of zinc or cadmium or by an impressed current system. When using cathodic protection, the surface of the reinforcing steel behaves as a cathode when the electrochemical process starts to work so that it does not corrode. It is the metal of the sacrificial anode that is corroding. Therefore, it is only necessary to check the rate of corrosion of the sacrificial anode and to renew it regularly, which is in principle very easy because this anode is outside the protected concrete.

Theoretically, this type of protection is very attractive and foolproof. However, in practice, the results obtained in the field are not so good. To provide good protection against corrosion, it is necessary to multiply the cells of cathodic protection, check regularly if they are operating properly, and change the sacrificial anode when needed. If this monitoring is not done regularly, perhaps due to turnover of the personnel who were involved in the initial installation of the cathodic protection, corrosion resumes when the anode is not renewed. Therefore, field results may be quite often deceptive.

24.3.3 Corrosion inhibitors

To retard the risk of corrosion of reinforcing steel, additional protection can be provided through the introduction of a corrosion inhibitor in concrete during its batching. The limited dosage of corrosion inhibitors that are usually used in practice retards the beginning of the corrosion process. The protective action of the corrosion inhibitor should stop when it has fixed the maximum amount of oxygen it could fix during its oxidation. When the corrosion inhibitor is totally oxidized, steel corrosion should resume.

The expression *corrosion inhibitor* groups two types of admixtures:

- Some chemical products that are added to concrete during mixing to obtain an additional protection to the natural protection provided by the natural alkalinity of the hydrated cement paste
- Some chemical products that are applied on a concrete surface that needs some protection because the reinforcing steel of this concrete started to corrode

Only commercial admixtures having a well-defined chemical composition for which "serious" research has been done are presented in this chapter (Berke and Weil, 1992; Justnes, 2006, 2010; Cusson et al., 2008; Elsener, 2011; Østnor and Justnes, 2011).

Elsener (2011) provided the following words of caution concerning the use of some commercial products that are supposed to fix the problem of corrosion: "Engineers and contractors working in the area of concrete maintenance should be aware of the fact that the composition of proprietary corrosion inhibitors in repair systems marketed under different trade names may change with time and geographic region."

In this chapter, most of our attention is devoted to calcium nitrite, which is presently the most widely corrosion inhibitor used in practice.

24.3.3.1 Calcium nitrite

When some oxygen ions penetrate concrete, calcium nitrite reacts with oxygen to be transformed into calcium nitrate. However, when all the calcium nitrite added during the mixing has been transformed into calcium nitrate, oxygen ions resume their attack on the reinforcing steel. Therefore, the addition of some calcium nitrite in concrete provides only additional protection against corrosion of reinforcing steel, not perpetual protection. However, this additional protection is very interesting in the case of low w/c concretes, which already offer strong resistance to the penetration of oxygen within concrete. For example, the City of Montreal systematically adds some calcium nitrite to the high-performance concretes that are used to build downtown-area infrastructures when repair works are complicated, very expensive, and create traffic jams.

Of course, higher dosages provide longer-term additional protection, but there is always a financial limit for this additional protection. For example, since 1992, the City of Montréal has added 12 L/m^3 of calcium nitrite to all the high-performance concretes used in the downtown area to provide additional protection to the reinforcing bars and to prolong the passivation of steel. In the case of shotcrete repairs, the dosage of calcium nitrite is increased to 20 L/m^3. At this dosage, calcium nitrite also acts as a setting and hardening accelerator.

In the case of repair works where a layer of about 100 mm of new concrete has to be applied to replace an altered concrete, a migrating anti-corrosion admixture (monofluorophosphate of sodium) is applied on the surface of concrete before applying the new concrete containing the calcium nitrite. This so-called migrating agent penetrates into the concrete and provides additional protection to the subjacent reinforcing bars.

24.4 Mitigating steel corrosion

24.4.1 Epoxy-coated reinforcing bars

An epoxy coating can be placed on reinforcing steel in order to provide to steel definitive protection against corrosion because concrete will never be in contact with an interstitial solution having a low pH. It could be a foolproof solution if the epoxy can be glued very tightly with steel, which is not the case. Epoxy-coated steel is not a very efficient composite material because epoxy cannot be glued very strongly to steel and concrete does not glue very well to epoxy. As the handling of epoxy-coated bars in the field can be sometimes quite rough, the epoxy-coating can spall so that later the corrosion process starts in this unprotected particular spot. In Figure 24.2, the results of a quite rough handling of epoxy-coated rebar can be seen. In that particular case, the extra cost of the epoxy-coated rebars was a waste of money due to the total lack of control in the field.

24.4.2 Stainless steel reinforcing bars

Some engineers believe that the use of stainless steel bars is the solution to avoid the corrosion of reinforcing bars. However, as one of my professors of materials would



Figure 24.2 Example of the consequence of a very rough handling of epoxy-coated rebars. Courtesy of Daniel Vézina.

start his lecture on stainless steel, "Stainless steel is steel that is stainless in name only." This very expensive solution to avoid the problem of corrosion of the reinforcing steel may not always be a foolproof solution. If a metallic insert is placed near a piece of stainless steel with a different electrochemical potential, a corrosion cell is created. In order to avoid the multiplication of such galvanic cells, all metallic inserts have to be made using the same grade of stainless steel. In practice, there are many reasons to place metallic inserts in hardened concrete and many people who ignore or forget this basic knowledge about corrosion.

24.4.3 Galvanized reinforcing steel

Some architects may specify the use of galvanized reinforcing bars in order to avoid the apparition of rust stains, particularly on architectural panels. In such a case, the zinc coating acts as a sacrificial anode that protects the steel of the reinforcing rebar from corrosion. This protection lasts as long as the zinc coating. Two types of galvanization processes can be used to protect steel rebars: the hot and the cold process. The hot process is more efficient in protecting reinforcing rebars, but of course it is also more expensive.

When galvanized rebars are used, it is very important to check that the rebars are not covered with a thin white film, called "white rust." This white rust is a thin film of zinc oxide, which is a very strong retarder of concrete hydration (read the case study on the consequences of such a situation in Section 18.6.1).

24.5 Eliminating steel corrosion

Because it is very difficult to be sure that reinforcing bars will not corrode despite all of the protective techniques that can be implemented, the only way to eliminate definitively the problem of reinforcing bar corrosion is to eliminate them and to replace

them with glass fiber reinforcing bars polymer (GFRP). Of course, these reinforcing bars are more expensive than regular steel reinforcing bars, but they eliminate the problem of corrosion.

Presently in North America, almost one bridge per day is built using GFRP (Mohamed and Benmokrane, 2012). The first structure using this new type of reinforcing bars was built in 2007 (Benmokrane et al., 2007) and is still in very good conditions. GFRP can also be used in special structures exposed to chloride ion penetration (Mohamed and Benmokrane, 2014). Examples of the use of GFRP are shown in Figures 24.3–24.5.



Figure 24.3 The use of glass fiber reinforced bars in a bridge deck.
Courtesy of Daniel Vézina and Brahim Benmokrane.



Figure 24.4 The use of glass fiber reinforced bars in an internal parking garage.
Courtesy of Brahim Benmokrane.



Figure 24.5 The use of glass fiber reinforced bars in a continuously reinforced pavement. Courtesy of Brahim Benmokrane.

24.6 Conclusion

As long as the pH of the interstitial solution inside concrete remains greater than 11, reinforcing steel bars are protected against corrosion by a thin film of passive ferrous oxide. Just after the placing of concrete, such a high pH value is maintained due to the presence of 20−30% of soluble hydrated lime crystals (portlandite) liberated by the hydration of C_3S and C_2S. However, as soon as this pH decreases below 11 due to the carbonation of these portlandite crystals, the passive film of ferrous oxide is torn and the reinforcing steel bar starts to rust. Chloride ions can also destroy this passive film.

The decrease of the pH of the interstitial solution is a concern because presently supplementary cementitious materials (SCM) are blended with Portland cement clinker in order to lower the carbon footprint of cement. When these SCM start to react, they transform some hydrated lime into secondary C−S−H, decreasing the amount of hydrated lime that can go into solution in the interstitial solution to maintain its pH over 11.

The use of low w/b concretes reduces significantly the penetration of carbon dioxide, oxygen, and chloride ions within concrete. The microstructure of these concretes is so dense that their permeability is very low. However, when the use of a low w/c or w/b concrete does not minimize the risk of corrosion of the reinforcing bars enough, a corrosion inhibitor can be added during the mixing of concrete. Usually, calcium nitrite is used. This calcium nitrite is transformed into calcium nitrate by the oxygen ions that are penetrating into concrete. However, when all the calcium nitrite has been transformed into calcium nitrate, steel reinforcing bars are no longer protected against corrosion.

Cathodic protection is sometimes used to protect reinforcing steel from rusting. However, according to the author's field experience, the results obtained from this method of protection against corrosion are not as good as they should be.

The best way to be sure that reinforcing bars placed in a concrete will not rust is to use fiber glass reinforcing bars.

References

Benmokrane, B., El-Salakawy, E., El-Gamal, S.E., Sylvain, G., September/October 2007. Construction and testing of Canada's first concrete bridge deck totally reinforced with glass FRP bars: Val-Alain bridge on HW 20 east. ASCE, Journal of Bridge Engineering 12 (5), 632−645.

Berke, N.S., Weil, T.G., 1992. World-Wide Review of Corrosion Inhibitors in Concrete, Advance in Concrete Technology. ACI SP. CANMET, Ottawa, pp. 899−924.

Cusson, D., Qian, S., Chagnon, N., Baldock, B., January 2008. Corrosion inhibiting systems for durable concrete bridges. Five-years field performance evaluation. Journal of Materials in Civil Engineering, ASCE 20, 20−28.

Elsener, B., 2011. Corrosion inhibitors − uan update on on-going discussion. In: 3 Länder Korrosionstagung "Möglichkeiten des Korrosionsschutzes in Beton" 5./6. Mai Wien GfKorr Frankfurt am Main, pp. 30−41.

Elsener, B., Angst, U., 2016. Corrosion inhibitors for reinforced concrete. In: Aïtcin, P.-C., Flatt, R.J. (Eds.), Science and Technology of Concrete Admixtures. Elsevier (Chapter 14), pp. 321−340.

Gagné, R., Aïtcin, P.-C., Lamothe, P., 1993. Chloride ion permeability of different concretes. In: The Proceedings of the Conference on Durability of Building Materials and Components, E and FN Spon Editor, Omya, Japan, vol. 2, pp. 117−130.

Justnes, H., 2006. Corrosion Inhibitors for Reinforced Concrete. ACI SP234-4, pp. 53−70.

Justnes, H., 2010. Calcium nitrate as multifunctional concrete admixture. Alite Inform − International Analytical Review on Concrete, Cement and Dry Admixtures. ISSN: 0010-5317 16 (4−5), 38−45.

Lévy, c., 1992. Accelerated carbonation: comparison between the Joigny Bridge high performance concrete and ordinary concrete in High Performance Concrete edited by Yves Malier, E and FN Spon, London, pp. 305−311.

Mohamed, H., Benmokrane, B., 2012. Recent Field Applications of FRP Composite Reinforcing Bars in Civil Engineering Infrastructures. In: Proceedings of the 6th International Conference on Composites in Civil, Offshore and Mining Infrastructures (ACUN-6), Melbourne, Australia, November 14−16, 6 pp.

Mohamed, H.M., Benmokrane, B., 2014. Design and performance of reinforced concrete water chlorination tank totally reinforced with GFRP bars. ASCE Journal of Composites for Construction 18 (1), 05013001-1−0501301-11.

Østnor, T.A., Justnes, H., 2011. Anodic corrosion inhibitors against chloride induced corrosion of concrete rebars. Advances in Applied Ceramics 110 (3), 131−136.

Curing compounds

25

P.-C. Aïtcin
Université de Sherbrooke, QC, Canada

25.1 Introduction

This chapter is one of the shortest of this book—this does not mean that it is unimportant. In fact, now that concretes having water−cement ratios (w/c) lower than 0.42 are increasingly being used, it is necessary to specify field curing practices according to concrete w/c.

In the past, the usual practice was to cover the concrete surface with an impervious curing membrane as soon as it was finished in order to prevent the water contained in concrete from evaporating. The rapid application of this impervious membrane eliminates the development of plastic shrinkage when the concrete surface is exposed to dry air and/or windy conditions, as well as the development of drying shrinkage as long as the membrane remains intact. Moreover, when concrete is made with a blended cement, this impervious membrane keeps inside the concrete all of the water needed to hydrate the cementitious materials contained in the blended cement, which are reacting more slowly than the Portland cement.

25.2 Curing concrete according to its w/c

In Chapters 1 and 5 (Aïtcin, 2016a,b), it was seen that concretes having a w/c greater than 0.42 develop very limited autogenous shrinkage (the higher the w/c, the lower their autogenous shrinkage). However, that is not the case for concretes having w/c lower than 0.42 (the lower the w/c, the more rapid and more intense the development of autogenous shrinkage). Autogenous shrinkage is a consequence of the apparition of menisci in the pore system of a hydrating cement paste due to its volumetric contraction (chemical contraction). The very fine pores created by this chemical contraction are draining the water contained in coarse capillaries so that menisci are appearing in the porous system. As the size in which these menisci are created decreases, the resulting tensile stresses increase so that the apparent volume of concrete may decrease significantly, creating what is called its *autogenous shrinkage*.

Therefore, from a theoretical point of view, it is easy to get rid of autogenous shrinkage. It is only necessary to provide some external water to the cement paste to refill the porosity created by its chemical contraction. If the hydrating cement paste does not contain any menisci, it does not shrink.

Science and Technology of Concrete Admixtures. http://dx.doi.org/10.1016/B978-0-08-100693-1.00025-4
Copyright © 2016 Elsevier Ltd. All rights reserved.

To provide external water to the cement paste, it has been seen that two techniques can be used:

- Curing concrete with an **external** source of water (external to concrete)
- Curing concrete with an **internal** source of water (internal to concrete)

In the latter case, the source of water is internal for concrete but external for the cement paste. For example, saturated lightweight aggregates can be used to replace a certain volume of aggregates so that the water contained in these aggregates can be drained by the very fine pores created by chemical contraction rather than the water present in the fine capillaries of the cement paste. Therefore, if no menisci are appearing within the hydrated cement paste, it does not shrink. Some menisci may be formed in large capillaries before the drainage of the water contained in the saturated lightweight aggregates starts, but they generate very weak tensile stresses that do not result in a significant contraction of the concrete's apparent volume.

Let us analyze these two solutions. Experience shows that when using an external source of water to cure low w/c concretes, external water does not penetrate more than about 50 mm inside concrete because these concretes are quite impervious. However, it is important to point out that this external water curing limited to concrete cover (that is, covering the first rank of reinforcing steel) reinforces the hydration of the cement paste in this very important part of concrete from a durability point of view.

As far as internal curing is concerned, theoretically, it should not be necessary to provide any external water curing when an internal curing is provided to concrete. However, the author recommends that, whenever possible, it is good to provide external water curing to reinforce concrete cover. It is a belt and suspender solution, but in matter of durability it is a very safe and not too costly solution.

Therefore, it is very important that designers specify concrete curing according to the w/c of concrete they are using.

25.3 Specifying the curing of a concrete with a w/c greater than the critical value of 0.42

Curing membranes must be specified to cure concrete having a w/c greater than 0.42 made with either Portland cement or blended cement. When concrete is cast in dry and moderately windy conditions, usually the bleeding water that covers the finished concrete surface protects the concrete from plastic shrinkage long enough to have time to apply a curing membrane at a dosage (L/m^2) recommended by admixture companies. It is only when air is particularly dry and/or particularly windy that fogging is recommended before applying curing membranes.

Admixture companies are selling two types of curing compounds: one pigmented and the other transparent. Whenever possible, it is better to apply a pigmented curing membrane in order to see the surface of concrete that has been effectively protected.

Curing compounds are essentially paraffin emulsions. When the water that supports the curing compound evaporates, paraffin particles coalesce to form an impervious

film that will prevent water contained in concrete from evaporating. In exceptional cases in floor applications, if the floor has to be painted, or if it will receive a topping, acrylic resins are used as curing nmembranes.

ASTM Standard Test methods C 309 ("Standard Specification for Liquid Membrane-Forming Compounds for Curing Concrete") and C 1315 ("Standard Specification for Liquid Membrane-Forming Compounds Having Special Properties for Curing and Sealing Concrete") may be used to evaluate the impermeability of curing membranes. This consists of measuring the weight loss of a concrete specimen that has been covered with a curing compound and placed in a dry atmosphere having a relative humidity of 50% and a temperature of 21 °C.

When a curing membrane has been applied on a concrete surface, it is useless to water cure it directly because this external water will not penetrate within concrete due to the presence of this impervious membrane.

25.4 Specifying the curing of concretes having a w/c lower than the critical value of 0.42

As previously said, in order to avoid as much as possible the rapid development of autogenous shrinkage that may result in a severe early cracking of concrete surface, it is very important to provide some curing water to the cement paste in the form of **external** or **internal** curing.

25.4.1 External curing

In this case, it is important to avoid spraying the concrete surface with a curing compound. Because low w/c concrete presents little or no bleeding water in order to avoid the development of plastic shrinkage, it is essential to apply as soon as possible an **evaporation retarder** on concrete surface. Evaporation retarders are emulsified fatty alcohols like n-hexadecanol (also known as cetylalcohol) that cover the concrete surface with a monomolecular film that prevents concrete water from evaporating. Admixture companies provide a dosage range (L/m^2) that gives adequate protection to the concrete surface.

Later, when the concrete surface is hard enough to support direct water curing without any risk of damaging its surface (usually after 24 h), this monomolecular film of evaporation retarder is washed away by the first water applied to the concrete surface. In North America, evaporation retarders are also currently used in summer to decrease water evaporation from domestic and public swimming pools.

Water curing can be pursued by using two layers of saturated geotextile weighing more than 300 g/m^2 rather than burlaps. It is easier to manipulate two soaked thin layers than a thicker layer of geotextile. Burlaps do not store as much water and they have to be resaturated quite often when facing dry and windy conditions. After 7 days of direct water curing, a curing membrane may be applied, especially when blended cement has been used.

Here we provide a **note of caution**: The water used to cure concrete must not be too cold because it can cause a thermal shock at the surface of the concrete that will result in the cracking of the concrete surface. This applies especially when a concrete bridge is built in the bush and the contractor uses river water to cure its concrete. If this water is very cold, it has to be heated to a temperature close to that of the concrete it is supposed to cure.

25.4.2 Internal curing

If, for example, some saturated lightweight aggregates have been introduced in concrete during its mixing to provide enough extra water to cement paste in order to avoid its autogenous shrinkage, a curing compound can be applied directly on the concrete surface to avoid the development of plastic and autogenous shrinkage. However, despite the fact that theoretically there is no need to provide concrete with external water curing, like in the previous case, the author prefers to apply an evaporation retarder first, then an external curing for 3 days in order to reinforce concrete cover, and then finally a curing membrane to prevent drying shrinkage.

25.4.3 Curing concrete columns

Many people are convinced that it is not necessary to water-cure concrete columns. The author has never seen any cracked concrete columns but he prefers to water cure columns for at least 3 days to reinforce concrete cover and increase the durability of this crucial part of the column.

25.5 Enforcing adequate curing practices in the field

To enforce such curing practices in the field, it is necessary to do the following:

- Write clear specifications telling contractors what to do, when to do it, and how to do it.
- Pay contractors separately for each item so that curing concrete becomes a profitable activity.
- Continue to pay inspectors to check that contractors are doing what they were asked to do and paid to do.

25.6 Conclusion

Curing is a very important activity to improve a concrete structure's lifecycle because cracked concrete is only impervious in between cracks. Now that low w/c concretes are increasingly being used to build more sustainable structures, it is important to cure concrete according to its w/c.

High w/c concretes (w/c > 0.42) have to be covered as soon as possible with a curing membrane because they are not subjected to significant autogenous shrinkage.

In addition, they contain enough water to hydrate all the cement particles and the supplementary cementitious materials they contain.

Low w/c concretes (w/c < 0.42) must receive some water curing in order to avoid the development of autogenous shrinkage, which can result in an early cracking of their surface. This water curing can be **internal** in the form of saturated lightweight aggregates or it can be **external** by direct application of an external source of water. In the latter case, as soon as the concrete surface is finished, an **evaporation retarder** has to be applied on the concrete surface to avoid the development of plastic shrinkage. Sometimes in very dry and windy conditions, it is absolutely necessary to do the finishing under fogging (Figure 5.3). Then, direct water curing has to be started as soon as the concrete surface is hard enough. It is important to realize that this external water curing will be effective only on the first 50 mm of concrete surface. However, improving the impermeability of concrete cover is very important from a durability point of view.

To enforce an adequate water curing for low w/c concretes, it is only necessary to **pay contractors specifically** to do it and **inspectors** to check that they do it correctly.

References

Aïtcin, P.-C., 2016a. The importance of the water−cement and water−binder ratios. In: Aïtcin, P.-C., Flatt, R.J. (Eds.), Science and Technology of Concrete Admixtures. Elsevier (Chapter 1), pp. 3−14.

Aïtcin, P.-C., 2016b. Water and its role on concrete performance. In: Aïtcin, P.-C., Flatt, R.J. (Eds.), Science and Technology of Concrete Admixtures. Elsevier (Chapter 5), pp. 75−86.

Self-consolidating concrete

26

A. Yahia, P.-C. Aïtcin
Université de Sherbrooke, QC, Canada

26.1 Introduction

According to an ACI 237 Committee report (2007), self-consolidating concrete (SCC) is highly flowable, non-segregating concrete that can spread into place, fill the formwork and encapsulate the reinforcement without any mechanical consolidation. In the literature, this class of concrete has been also designated as self-levelling, self-compacting or self-placing. This chapter uses the expression 'self-consolidating' recommended by the ACI 237 Committee.

This type of concrete was developed at the beginning of the 1980s in Japan (Tanaka et al., 1993; Hayakawa et al., 1995; Miura et al., 1998; Okamura and Ozawa, 1994, 1995) to decrease the labour cost associated with concrete pouring and improve the surface quality of concrete. The extra cost incurred in the production of SCC was compensated by the savings on concrete placement due to the very costly Japanese workforce. The use of SCC soon spread rapidly all over the world (Khayat and Feys, 2010).

In North America SCC is currently used in pre-cast plants to eliminate the need for mechanical consolidation and the noise nuisance associated with pouring ordinary concrete. Precast concrete can also manifest surface defects, such as honeycombing, which incur additional labour costs in performing surface repairs (Yahia et al., 2011). Moreover, the use of SCC removes the need for vibration to ensure proper consolidation, and can thus result in savings in equipment purchase and maintenance (ACI 237, 2007), extend the life of steel forms and improve construction productivity. SCC has become an attractive solution in pre-cast concrete and construction, and its use is starting to develop in the ready-mix industry because some contractors have realized its numerous advantages. Indeed, the use of SCC enables the casting of concrete that develops the desired mechanical properties independent of the skill of the vibrating crew (ACI 237, 2007). Also, the noiseless aspect of SCC allows flexibility in working time in cities where some noise restrictions exist after 5 pm.

As a background to the rest of the chapter, we emphasize that SCC must have adequate rheological properties, mainly a low enough yield stress. This plays an important role in form filling (Roussel, 2012) and represents a necessary but not sufficient criterion: the passing ability of aggregates in a specific reinforcement must also be taken into account. Recent developments have for example shown that statistical models can be quite effective at defining proper aggregate size distributions (Roussel et al., 2009). Provided the proper aggregate sizes and volume fractions are chosen, numerical modelling (or analytical solutions for simple flow fields) can predict form

Science and Technology of Concrete Admixtures. http://dx.doi.org/10.1016/B978-0-08-100693-1.00026-6
Copyright © 2016 Elsevier Ltd. All rights reserved.

filling based on rheological parameters such as yield stress (Thrane, 2012). In what follows we give an overview on formulation issues using these underlying principles. However, the discussion adheres closely applied mix design criteria and guidelines to give a more direct link to practice.

26.2 SCC formulation

Three functional requirements are generally needed for the material to be considered as self-consolidating, namely: filling ability, passing ability and resistance to segregation (ACI 237, 2007). The SCC mix proportions must be tailored to ensure a mortar matrix with appropriate yield stress to improve deformability while maintaining adequate viscosity to ensure adequate segregation resistance, hence good passing ability and proper placing. Superplasticizers impart fluidity, while viscosity-modifying admixtures (VMAs) may be used to enhance the stability of SCC against segregation. Overviews on the chemical structures and working mechanisms of these admixtures are given in Chapters 9, 11, 16 and 20 (Gelardi et al., 2016; Gelardi and Flatt, 2016; Nkinamubanzi et al., 2016; Palacios and Flatt, 2016).

In order to design a functional SCC with required properties, including passing ability, filling capacity and good segregation (static and dynamic) resistance, it is necessary to modify concrete formulation. A first set of measures concerns the sand and aggregates, as explained in Chapter 7 (Yahia et al., 2016). These are to:

- Reduce the size of the coarse aggregate to a maximum value of 14 mm, or even 10 mm for very congested areas.
- Reduce the usual proportion of 60% of coarse aggregates and 40% of sand used in conventional concrete to a 50−50% proportion, or even lower in cases when the reinforcing steel is very congested. In some cases it is necessary to lower the proportion of coarse aggregate to 40% and the maximum size of the aggregate to 10 mm.

The second set of measures concerns the formulation of the paste. More details of this are discussed in Chapter 7 on rheology (Yahia et al., 2016). Here we only emphasize the most significant aspects in the pragmatic formulation of effective SCC mixes. The most significant of these modifications concerns the amount of fine material that has to be used to make a stable SCC with good passing ability and filling capacity. This is greatly enhanced by a larger spacing of the sand and coarse aggregate particles when the paste volume is increased (Roussel et al., 2009). However, this paste must have adequate properties, so its proportions must also be changed. The main target of this step is to optimize the grain-size distribution, thus ensuring greater packing density. In one approach to this target, the volume of powder is increased to reduce the free water and improve cohesiveness of the mixture, thus increasing the stability of the SCC. Powders include cement, fly ash, ground-granulated blast-furnace slag, limestone fines, silica fume, material crushed to finer than 0.125 mm (No. 100 sieve) and other non-cementitious fillers (ACI 237, 2007). In a second approach, a VMA can be used to increase the viscosity of SCC when using lower powder contents. The use of VMAs can also improve robustness,

i.e. increase the ability of the mixture to tolerate variations in batching water (more information on VMAs is provided in Chapter 18).

Of course, it is possible to combine these two approaches and develop SCC where intermediate dosages of filler and VMA are used. The choice of a particular option depends on the availability and relative cost of the fine materials and the VMA, as well as on the facilities available at the batching plant and the robustness of the SCC composition that is required.

Three basic mixture-proportioning approaches for developing SCC mixtures have been used:

- high powder content and high range water reducer admixture (HRWRA)
- low powder content, HRWRA and VMA
- moderate powder content, HRWRA and VMA dose (stability can be controlled by blending aggregates, lowering water content or using a VMA) (ACI 237, 2007).

The first approach is mainly based on increasing the powder content (powder type). The second approach decreases powder content and incorporates a moderate dosage of VMAs, while the third approach consists of incorporating a high dosage of VMA. The first and second approaches were mainly employed initially in Japan and Asia, while the third was used in North America. Tables 26.1–26.3 show mix designs of various SCC mixtures used in Japan, Europe and North America.

26.3 Quality control

Several tests methods have been proposed to evaluate the filling and passing capacity of SCC.

Table 26.1 Typical SCC mixtures used in Japan (Ouchi et al., 2003)

Constituents (kg/m^3)	J-powder type	J-combined type	VMA type
Water	175	165	165
Cement	530[a]	298	220
Fly ash	70	206	–
Ground blast-furnace slag	–	–	220
Binder	**600**	**504**	**440**
Sand	750	700	870
Coarse aggregate	790	870	825
VMA	No	Yes (low)	Yes (moderate)
Slump flow	Dosage of HRWR is adjusted to achieve the targeted slump flow		

[a]Low-heat cement is used.

Table 26.2 Typical SCC mixtures used in Europe (Ouchi et al., 2003)

Constituents (kg/m^3)	E-powder type	E-combined type	E-VMA type
Water	190	192	200
Cement	280	330	310
Limestone	265	–	–
Fly ash	–	–	190
Ground blast-furnace slag	–	200	–
Binder	**525**	**530**	**500**
Sand	865	870	700
Coarse aggregate	750	750	750
VMA	No	No	Yes (moderate to high dosage)
Slump flow	Dosage of HRWR is adjusted to achieve the targeted slump flow value		

Table 26.3 Typical SCC mixtures used in North America (Ouchi et al., 2003)

Constituents (kg/m^3)	E-powder type	E-combined type	E-VMA type
Water	174	180	154
Cement	408	357	416
Limestone	–	119	–
Fly ash	45	–	–
Ground blast-furnace slag	–	–	–
Binder	**525**	**476**	**416**
Sand	1052	936	1015
Coarse aggregate	616	684	892
VMA	No	No	Yes (moderate)
Slump flow	Dosage of HRWR is adjusted to achieve the targeted slump flow value		

1. Japan Society of Civil Engineers: Concrete Library 93, High-fluidity Concrete Construction Guideline, 1999.
2. Bernabeu and Laborde, SCC Production System for Civil Engineering, Final Report of Task 8.3, Brite EuRam Contract No. BRPR-CT96-0366.
3. Precast, Prestressed Concrete Institute, Interim Guidelines for the Use of Self-Consolidating Concrete in Precast, Prestressed Concrete Institute Member Plants, TR-6-03.

- ASTM C 1611C and 1611M slump flow measurement of SCC.
  This is performed like a conventional slump test, but instead of measuring the vertical collapse of the concrete cone when the steel cone is removed, the average horizontal spread of the SCC is measured (Figure 26.1). Usually this spread is measured in two directions at 90° from each other. The value measured relates directly to yield stress (Roussel, 2012).



Figure 26.1 Slump flow measurement.

Passing ability is measured using a J-ring consisting of reinforcing bars that fit around the base of a standard ASTM C 143/C slump cone (Figure 26.2). The slump cone is filled with the SCC and lifted, as when performing a flow test. The final spread of the concrete is then compared to that obtained in the regular flow test described previously. This test helps to identify possible blocking issues due to the relation between aggregate size and rebar spacing. Provided this is not an issue, the test result also relates to yield stress.

- An L-box test can also be used to measure the passing ability of SCC (Figure 26.3). An 'L'-shaped container is divided into two parts, a vertical one and a horizontal one, separated by a sliding door. An obstacle of three reinforcing bars can be positioned in the horizontal part. The height of the SCC left in the vertical section is compared to the height of the SCC at the end of the horizontal box. In a similar way to the J-ring, this identifies possible issues of blocking due to inadequate aggregate size distribution. In the absence of this problem, the test result once again relates to yield stress (Nguyen et al., 2006). However, the resolution is not very good because the horizontal part is too short. For a strict yield stress measurement it is therefore preferable to use only a longer horizontal channel, the Laboratoire Central des Ponts et Chaussées in France (LCPC) box (Roussel, 2007).
- SCC stability is measured by filling a column 610 mm long and 200 mm in diameter (Figure 26.4). The SCC is left sitting for 15 min after pouring, then the SCC column is divided into four parts that are removed individually. Each part is washed in a No. 4 sieve (4.75 mm) and the retained aggregate is weighed.

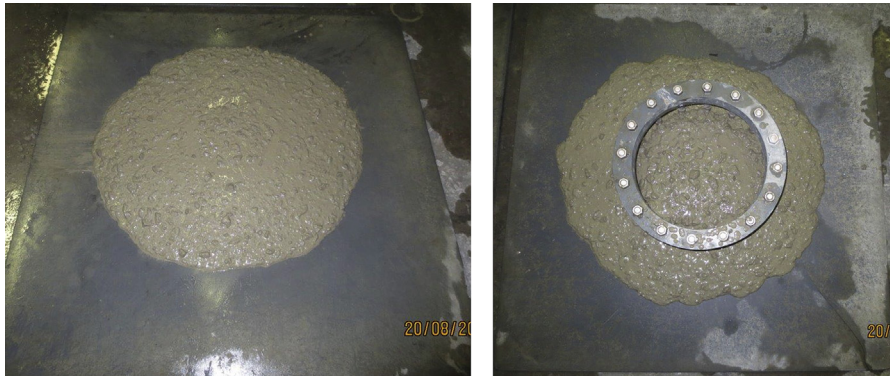


Figure 26.2 Measuring passing ability with a J-ring.

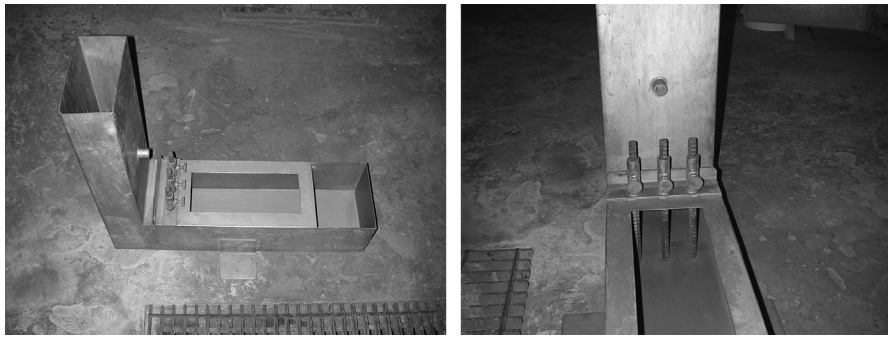


Figure 26.3 Measuring passing ability with an L-box.



Figure 26.4 Measuring SCC static stability.

Usually, when designing the formulation of SCC by trial mixes, the first objective is to obtain the right flow. When the targeted flow has been obtained, other tests are performed to fine-tune the final SCC composition.

Typically, industrial SCCs have w/b between 0.38 and 0.42.

26.4 Fresh properties

26.4.1 Plastic shrinkage

SCCs are prone to develop some plastic shrinkage cracking because they exhibit little or no surface bleeding. Therefore SCC should be protected in that respect in the same way as low w/c or w/b conventional concrete, as explained in Chapters 5 and 23 (Aïtcin, 2016; Gagné, 2016).

26.4.2 Pumping

One great advantage of SCC is its ability to be pumped. In Dubai the pre- and post-tensioned floors of the more recent high-rise buildings have been built with pumped SCC (Clarke, 2014). In Mumbai, Samsung is pumping SCC to cast the floors of an 80-storey building (the Worli project). When pumping SCC, pumping pressures are significantly reduced and air content remains stable. Even when the pump line has a diameter larger than 75 mm, usually it is not necessary to prime the line with a slurry.

26.5 Hardened properties

SCC hardened properties are measured in North America according to ASTM standard test methods. It is found that they are essentially functions of the w/b, as for conventional concrete. However, the elastic modulus of SCC is 10−15 % lower than that of conventional concrete with the same w/b because the coarse aggregate content of SCC is lower than that of conventional concrete.

SCC is prone to present more creep in compression than conventional concrete due to its high amount of paste.

SCC resistance to freezing and thawing cycles in the presence or absence of deicing salts has been found to depend, as with conventional concrete, on the value of the spacing factor of the entrained air bubbles.

26.6 Case studies

26.6.1 Senboku LNG Terminal II in Osaka, Japan

Osaka Gas Company is importing liquefied natural gas (LNG) from Indonesia, Malaysia, Brunei and Australia to supply city gas in Osaka and the six prefectures

of Kinki region. In the beginning LNG was stored in steel tanks in Terminal I, commissioned in October 1971, and Terminal II, commissioned in 1977. These steel tanks were surrounded by a concrete wall delimiting a quite large safety perimeter equipped with water-curtain facilities and high-expansion foaming equipment in case of a spill. With steadily increaing consumption of city gas over the years, new steel tanks were built to match demand; and at the end of the 1990s Osaka Gas built a larger 40 MPa concrete tank that could store 1.3 times more LNG than the first steel tanks used in the terminal (seen in the background in Figure 26.5).

The construction of the concrete tank was so successful that Osaka Gas ordered a second one after the commissioning of the first. But as gas consumption was still increasing and the space available for the construction of new concrete tanks was shrinking, Osaka Gas built a larger concrete storage tank using post-tensioned SCC with a compressive strength of 60 MPa; it is able to store 1.3 times more LNG than the previous 40 MPa concrete tanks and 2.0 times more than the initial steel tanks (Figure 26.6).

Of course, the cost of a 60 MPa SCC was much higher than the cost of a conventional 40 MPa concrete, but the use of 60 MPa SCC presented several significant competitive advantages.

- It multiplied the storage capacity of each concrete tank by a factor of 1.3 when compared to a storage tank built with a 40 MPa conventional concrete.
- It decreased the thickness of the concrete wall from 1100 mm (in the case of a wall built with a 40 MPa concrete) down to 800 mm, so the volume of concrete needed to build the storage tank was reduced from 13,000 to 9500 m^3 – a reduction of 27%. As the consequence the number of piles to support the whole storage tank could be reduced from 1353 to 1293 – a reduction of 4.4%.



Figure 26.5 Construction of post-tensioned concrete LNG storage tank with a 60 MPa SCC in Senboku Terminal II in Osaka.
With Courtesy of Osaka Gas CO., LTD.

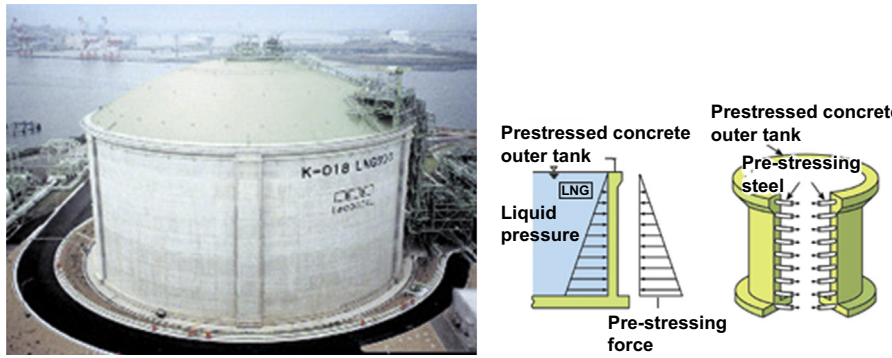


Figure 26.6 Finished 60 MPa post-tensioned concrete tank. With Courtesy of Osaka Gas CO., LTD.

- It decreased the construction time by a factor of 1.5 because 4.4-m-high concrete lifts of SCC could be cast at a time since it was not necessary to vibrate the concrete to ensure good pouring.
- It eliminated the need for a huge and expensive crew of temporary workers to pour concrete because the SCC did not need to be vibrated.

For the construction of this first storage tank with 60 MPa SCC, five to seven nearby ready-mix concrete plants operated non-stop for five hours to provide continuous deliveries of 1000 m^3 of SCC to the site. This very short delivery time eliminated overtime expenses for the regular crews.

The flowability of each truckload was checked before it was poured into the six concrete pumps used to place concrete all over the perimeter of the tank through a system of steel pipes. Concrete was emitted from the pipes every 5 m, so its top surface was almost horizontal.

This solution was so successful that a second post-tensioned concrete storage tank was built using a 60 MPa SCC.

26.6.2 Construction of the reaction walls of the structural laboratory at the Université de Sherbrooke

To increase the facilities of the first structural concrete laboratory at the Université de Sherbrooke to test dynamic responses of large structural sections, it was necessary to build a large, heavily reinforced concrete reaction wall involving the pouring of 260 m^3 of concrete.

As more than 2000 students, professors, technicians and secretaries worked in the faculty from 8 am to almost midnight (for the students), it was out of the question to build this strong wall during working hours with conventional concrete that has to be vibrated, due to the noise nuisance associated with the vibration of so large a volume of concrete. Thus casting a conventional concrete was limited to Sunday from 8 am to 10 pm, which was a very costly solution for building the three sections of the strong wall. The delivery of 40 loads of SCC from a local ready-mix producer solved the noise problem: the three pours were done silently during daily working hours without any complaints (Figure 26.7).



Figure 26.7 Two of the strong walls in the Department of Civil Engineering at the Université of Sherbrooke.

When it was necessary to build a second strong wall in a new addition to the structural laboratory, the same solution was adopted.

26.7 Selling SCC to contractors

A friend of the authors working in the marketing department of a large ready-mix company developed the following strategy to promote the use of SCC to contractors.

- Never try to sell SCC for the first time to a contractor on Monday morning; the answer will always be 'Thank you, the concrete is a too expensive.'
- Wait until a Friday afternoon, when the contractor has been obliged to delay a large concrete pour until 4 pm, meaning that his placing crew will have to work hard until 7−8 pm. It is the perfect time to propose the use of SCC to the field engineer and foreman, and this will allow them to leave the site before 6 pm (a Friday evening with an important soccer, rugby, hockey, football, basketball or baseball game makes the sale easier).

The same friend told the authors that after having successfully sold a large pour of SCC one Friday afternoon to a project, the next Monday morning the foreman noticed his crew was working quite slowly. He asked one of the workers: 'Why are you working so slowly this morning?' The answer was: 'As you know, late this afternoon we will have to place another large pour of concrete, so we need to keep our energy to do it; but if you order an SCC instead of conventional concrete, instead of leaving the site at 7−8 pm we (and you too) will leave at 5 pm.' The concrete order was changed for SCC, and the workers resume working very hard to leave earlier.

26.8 Conclusion

The development of SCC is one of the latest achievements that has significantly improved concrete's competitiveness as a structural material, because it significantly reduces the cost of pouring concrete. As SCCs are easily pumpable, their use is gaining acceptance in casting the floors of high-rise buildings, because a limited number of cranes can be used to lift all the other materials needed for finishing the floors. Presently the combined use of high performance concrete (HPC) and SCC is displacing steel in the construction of high-rise buildings (Aïtcin and Wilson, 2015).

In pre-cast plants SCCs are currently used because they facilitate and accelerate the pouring of concrete by eliminating the need to vibrate it. Moreover, they decrease the noise level in the plant and prolong the life of the moulds because they are no longer subjected to intense vibration.

Finally, the noiseless aspect of pouring SCC is a great advantage when concrete has to be cast in a building during working hours or in cities where there are noise restrictions after 5 pm.

The formulation of SCC is flexible enough to accommodate different local conditions concerning the availability of its ingredients. In some places rather large amounts of fine materials can be used, while in others the viscosity of the SCC can be adjusted using a VMA. In some locations a combination of fine materials and VMA will be used to adjust SCC viscosity.

The overall cost balance of using SCC must be considered in a global sense and factored in during planning. Strictly looking at material costs will never favour SCC, but will always miss the net global advantages. Using SCC requires tighter quality control, but knowledge and practical experience are now available to handle this properly. There are great opportunities to seize for those who can understand the overall benefit of SCC and properly implement its use.

References

Aïtcin, P.-C., 2016. Water and its role on concrete performance. In: Aïtcin, P.-C., Flatt, R.J. (Eds.), Science and Technology of Concrete Admixtures. Elsevier (Chapter 5), pp. 75–86.

ACI 237R-07, 2007. Emerging Technology Series. Self-Consolidating Concrete Reported by ACI Committee 237.

Aïtcin, P.-C., Wilson, W., 2015. The Sky's the Limit, vol. 37. Concrete International. No 1, pp. 53–58.

Clark, G., 2014. Challenges for concrete in tall buildings. Structural Concrete 15 (4), 448–453 (Accepted and published online).

Gagné, R., 2016. Shrinkage-reducing admixtures. In: Aïtcin, P.-C., Flatt, R.J. (Eds.), Science and Technology of Concrete Admixtures. Elsevier (Chapter 23), pp. 457–470.

Gelardi, G., Flatt, R.J., 2016. Working mechanisms of water reducers and superplasticizers. In: Aïtcin, P.-C., Flatt, R.J. (Eds.), Science and Technology of Concrete Admixtures. Elsevier (Chapter 11), pp. 257–278.

Gelardi, G., Mantellato, S., Marchon, D., Palacios, M., Eberhardt, A.B., Flatt, R.J., 2016. Chemistry of chemical admixtures. In: Aïtcin, P.-C., Flatt, R.J. (Eds.), Science and Technology of Concrete Admixtures. Elsevier (Chapter 9), pp. 149–218.

Hayakawa, M., Matsuoka, Y., Yokota, K., 1995. Application of super workable concrete in the construction of 70-story building in Japan. Advances in Concrete Technology, ACI SP-154 381−397.

Khayat, K.H., Feys, D. (Eds.), 2010. Design, Production and Placement of Self-Consolidating Concrete. RILEM Book Series. Springer, London, UK.

Miura, N., Takeda, N., Chikamatsu, R., Sogo, S., 1998. Application of super workable concrete to reinforced concrete structures with difficult construction conditions. High Performance Concrete in Severe Environment, ACI SP-140 163−186.

Nguyen, T.L.H., Roussel, N., Coussot, P., 2006. Correlation between L-box test and rheological parameters of a homogeneous yield stress fluid. Cement and Concrete Research 36 (10), 1789−1796. http://dx.doi.org/10.1016/j.cemconres.2006.05.001.

Nkinamubanzi, P.-C., Mantellato, S., Flatt, R.J., 2016. Superplasticizers in practice. In: Aïtcin, P.-C., Flatt, R.J. (Eds.), Science and Technology of Concrete Admixtures. Elsevier (Chapter 16), pp. 353−378.

Okamura, H., Osawa, K., 1994. Self-compacting Concrete in Japan ACI International Workshop on High Performance Concrete ACI SP-159, pp. 31−44.

Okamura, H., Osawa, K., 1995. Mix Design for Self-compacting Concrete, 26. Concrete Library of JSCE, pp.107−120.

Ouchi, M., Nakamura, S.-A., Osterberg, T., Hallberg, S.-E., Lwin, M., 2003. Applications of self-compacting concrete in Japan, Europe and the United States. In: 5th Internatinnal Symposium, ISHPC? Tokyo-Odaiba, pp. 1−18.

Palacios, M., Flatt, R.J., 2016. Working mechanism of viscosity-modifying admixtures. In: Aïtcin, P.-C., Flatt, R.J. (Eds.), Science and Technology of Concrete Admixtures. Elsevier (Chapter 20), pp 415−432.

Roussel, N., 2007. The LCPC box: a cheap and simple technique for yield stress measurements of SCC. Materials and Structures 40 (9), 889−896. http://dx.doi.org/10.1617/s11527-007-9230-4.

Roussel, N., 2012. From industrial testing to rheological parameters for concrete. In: Roussel, N. (Ed.), Understanding the Rheology of Concrete, Woodhead Publishing Series in Civil and Structural Engineering. Woodhead Publishing, pp. 83−95 (Chapter 4). http://www.sciencedirect.com/science/article/pii/B9780857090287500042.

Roussel, N., Nguyen, T.L.H., Yazoghli, O., Coussot, P., 2009. Passing ability of fresh concrete: a probabilistic approach. Cement and Concrete Research 39 (3), 227−232. http://dx.doi.org/10.1016/j.cemconres.2008.11.009.

Tanaka, K., Sato, K., Wanatabe, S., Suenaga, K., 1993. Development and utilization of high performance concrete for the construction of the Akashi Kaikyo Bridge. High Performance Concrete in Severe Environment, ACI SP-140 26−31.

Thrane, L.N., 2012. Modelling the flow of self-compacting concrete. In: Roussel, N. (Ed.), Understanding the Rheology of Concrete, Woodhead Publishing Series in Civil and Structural Engineering. Woodhead Publishing, pp. 259−285 (Chapter 10). http://www.sciencedirect.com/science/article/pii/B9780857090287500108.

Yahia, A., Khayat, A.Y., Bizien, G., 2011. Use of self-consolidating concrete to cast large concrete pipes. Canadian Journal of Civil Engineering 38, 1112−1121.

Yahia, A., Mantellato, S., Flatt, R.J., 2016. Concrete rheology: A basis for understanding chemical admixtures. In: Aïtcin, P.-C., Flatt, R.J. (Eds.), Science and Technology of Concrete Admixtures. Elsevier (Chapter 7), pp. 97−128.

Ultra high strength concrete

27

P.-C. Aïtcin
Université de Sherbrooke, QC, Canada

27.1 Introduction

Ultra high strength concrete (UHSC) is one of the most spectacular developments of recent years in the area of Portland cement-based materials. Initially this new type of concrete, developed by Pierre Richard, the former scientific director of the French Bouygues Company, was known as reactive powder concrete (RPC) (Richard and Cheyrezy, 1994). The UHSC formulation is the fruit of Richard's personal reflections after research carried out for the French Army to increase the compactness of the granular solid fuel used in military rockets. After completing this research project his basic idea was to apply to concrete the same principles used when optimizing the packing of solid fuels for rockets. Despite the fact that RPC did not contain any coarse aggregate (the average size of its coarsest particle is 200 μm), Richard called this material **concrete**, when from a grain-size distribution point of view he should have called it a mortar. Why?

In fact, when very fine steel fibres are added in such a mortar to improve its strength and toughness, these fibres act like reinforcing bars in ordinary reinforced concrete, considering the 100-times scale factor between the coarsest particles of the aggregate and the reinforcing bars of a standard concrete (Table 27.1).

Thus from a mechanical point of view, this **fibre-reinforced mortar** works at a micro-scale like reinforced **concrete**. Richard also used the word **reactive** because most of the powders introduced into the mix had more or less reacted by the end of the hydration process. Finally, the French acronym for reactive powder concrete, *béton de poudre réactive* (BPR) could be read as **B**éton **P**ierre **R**ichard.

Richard developed RPC to overcome the inherent weakness of most **h**igh-**p**erformance **c**oncretes (HPCs) when they reach a compressive strength of about 150 MPa. At such a strength level, even the strongest aggregates used to make concrete fail when concrete specimens are tested in compression. Attempts to reduce the maximum diameter and increase the intrinsic strength of the coarse aggregates have proven to be successful, but often very expensive, and even in the best cases it

Table 27.1 Scale factor between an armed concrete and an RPC

	Aggregate	Reinforcement	
	∅ max (mm)	∅ (mm)	Length (mm)
RPC	0.2	0.2	12
Concrete	20	20	1200

Science and Technology of Concrete Admixtures. http://dx.doi.org/10.1016/B978-0-08-100693-1.00027-8
Copyright © 2016 Elsevier Ltd. All rights reserved.

is very difficult to obtain a compressive strength in excess of 180 MPa (Bache, 1981). So why not remove the coarse aggregate to make a much stronger material because of its very low w/b ratio − a material in which the coarsest particles are not in contact with each other to avoid stress concentrations at the points of contact? This was Richard's basic idea when he developed RPC.

27.2 Ultra high strength concrete concept

UHSC results from the application of the following principles:

1. An increase of the homogeneity of the material due to the elimination of the coarse aggregates.
2. An increase of matrix compactness by optimizing the grain-size distribution of all the powers used.
3. Elimination of the transition zone between coarse aggregates and the cement paste.
4. A limitation on the volume of sand to prevent sand particles from contacting each other in the hardened cement paste.
5. An improvement of the mechanical properties of the hydrated cement paste through a special heat treatment that produces a refinement of the microstructure of the UHSC.
6. The elimination of entrapped air bubbles and the porosity created by chemical shrinkage by compressing UHSC during its hardening when possible.
7. The elimination of the first autogenous shrinkage by compressing the UHSC at about 80% of its one-day compressive strength to eliminate porosity-created chemical contraction.

In the following, we review very briefly how these principles can be put into practice.

27.2.1 Increasing the homogeneity of UHSC

The elimination of the coarse aggregate and its substitution by sand particles results in a decrease in the size of the micro-cracks of mechanical, thermal or chemical origin which are linked in an ordinary concrete to the presence of coarse aggregates that can be considered as rigid inclusions in a homogeneous matrix. This reduction in the size of the micro-cracks results in an improvement in compressive and tensile strengths.

It is, however, important to adjust the amount of sand to prevent sand particles, which act as rigid inclusions in the matrix, from coming into contact with each other. Each sand grain must behave like an individual inclusion, and not as part of a densely packed aggregate skeleton. Hence when shrinkage develops, the matrix is free to contract as much as necessary because it is no longer restrained by the aggregate skeleton.

The increase of the packing density of the cementitious matrix by using powders with complementary grain-size distributions and ultrafine silica fume particles eliminates the occurrence of a transition zone between the sand particles and the paste (Figure 27.1). As a consequence, the stress transfer between the paste and the sand particles is improved.

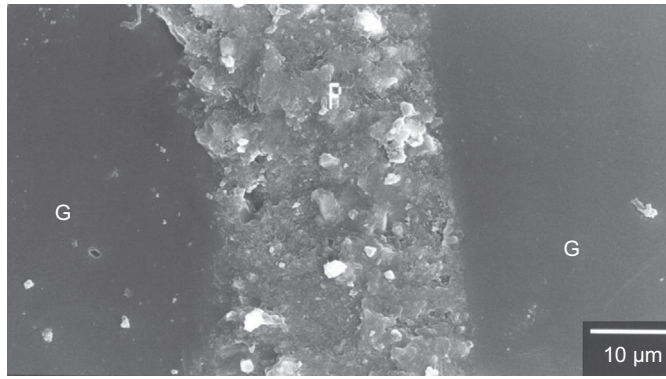


Figure 27.1 Microstructure of an RPC. One can notice:

- the granular loosening, with the two cement grains (G) being clearly separated by a quite large band of hydrated paste (P);
- the absence of a transition zone between aggregates and hydrated cement paste;
- the extreme compactness of the hydrated cement paste.

Courtesy of Arezki Tagnit-Hamou (Aïtcin, 2008).

27.2.2 Increasing the packing density

The optimization of the packing density of the cementitious matrix minimizes the interparticle voids and the amount of mixing water.

Table 27.2 gives the composition of a typical UHSC similar to that used to construct the Sherbrooke pedestrian bikeway bridge.

As previously mentioned, when possible UHSC compactness can be increased by pressing fresh UHSC, which results in the elimination of some of its mixing water, most of the entrapped air bubbles and even a large part of the chemical shrinkage occurring during the early hardening of the cement paste.

Table 27.2 Typical composition of an RPC

Materials	kg/m^3
Cement	705
Silica fume	230
Crushed quartz	210
Sand	1010
Superplasticizer	17
Steel fibres	140
Water	185
Water/binder	0.27

27.2.3 Improving the microstructure by thermal treatment

UHSC is usually heated to 70−90 °C in a water bath or by steam curing for two days to obtain the maximum strength from all the powders it contains. However, this water curing must be done **after two days of curing at ambient temperature** in order for the initial hydration to develop sufficiently. Such a heat curing results in an acceleration of the pozzolanic reaction between silica fume and the lime liberated by cement hydration. This special curing results in a significant increase of compressive strength.

27.2.4 Improving the ductility of UHSC

When they are not reinforced with very thin steel fibres, UHSC matrices exhibit a purely elastic behaviour until they fail in a brittle mode. UHSC ductility can be improved by the addition of steel fibres, but not just any kind of steel fibres. The fibres must have a diameter/length ratio in accordance with the scale effect discussed previously in order for the UHSC to act as a reinforced concrete. As seen in Figure 27.2, a 140 kg/m^3 dosage (1.8% by volume) of 12-mm long fibres provides a pseudo-ductile behaviour.

Figure 27.3 is a photograph taken with a SEM showing the fracture surface of a piece of fibre-reinforced UHSC.

UHSC can also be confined in a steel tube, which results in a significant increase in its compressive strength and ductility. A maximum compressive strength of 375 MP, associated with a strain greater than 1%, was achieved with a UHSC similar to that used during the construction of the Sherbrooke pedestrian bikeway when it was confined in stainless-steel tube with a diameter of 150 mm and a thickness of 2 mm, as shown in Figure 27.4.

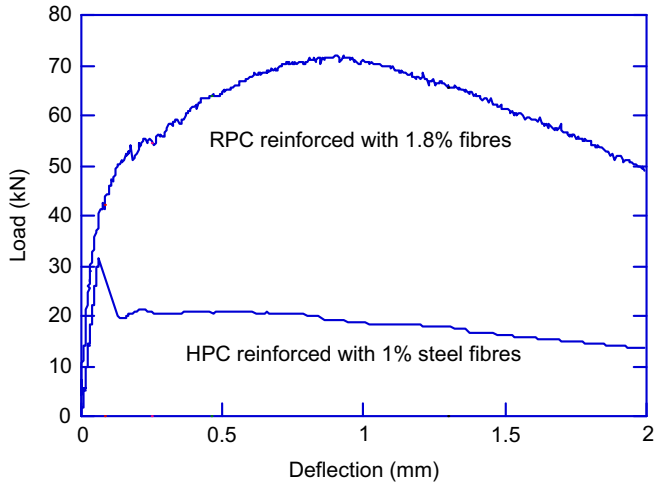


Figure 27.2 Pseudo-ductile behaviour of a fibre-reinforced UHSC.

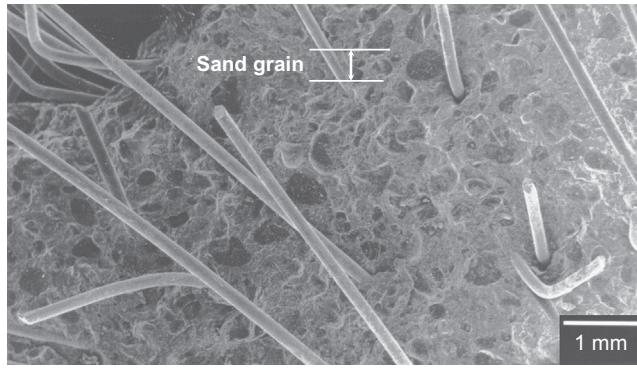


Figure 27.3 Fractured surface of steel-fibre-reinforced UHSC.

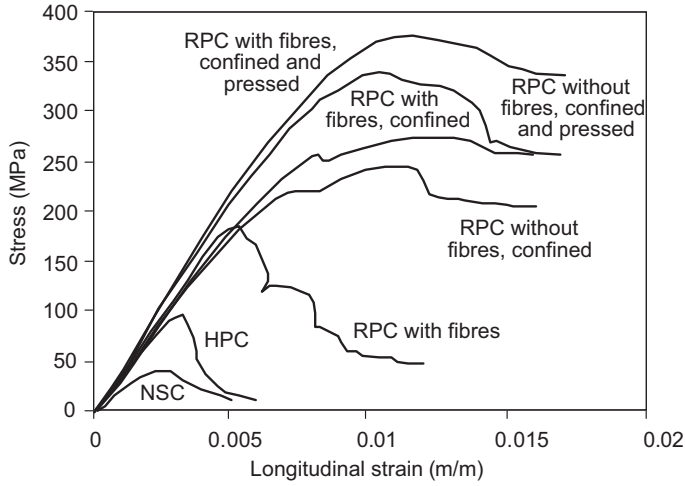


Figure 27.4 Compressive stress−strain curves for different RPCs fabricated at the Université de Sherbrooke.

27.2.5 Improving the packing density of different powders

Finally the various powders used in the preparation of UHSC must have a grain size distribution that produces a mix having a very high dry density. The proper proportions can be obtained by trial and error using a factorial design plan or by using an adequate packing model (de Larrard and Sedran, 1994).

27.2.6 Reinforcing the cement paste matrix with hard inclusions

A recent and very interesting development happened when, using some very fine glass powder, Professor Tagnit-Hamou and his research team were able to improve both the rheology and the mechanical properties of hardened UHPC. In their UHPC the glass

particles act as very hard and rigid inclusions that strengthen the cement paste. This technology, currently used in metallurgy, is called 'strength hardening' (Tagnit-Hamou et al., 2015).

27.3 How to make a UHSC

From a practical point of view, it is not complicated to make UHSC when the basic principle guiding the selection of the right Portland cement is known. All the tests done to find the best Portland cement to make RPC by Coppola (1996) and Aïtcin (1998) showed that the best choice to make UHSC is a cement with the lowest C_3A content possible (5% maximum if possible) and not too high C_3S (50% maximum). Moreover, this cement must have a low specific surface area of about 350 m^2/kg.

By limiting both the amount and the fineness of the two most reactive phases of Portland cement, it is possible to produce UHSC that will not be too viscous and will maintain a good rheology long enough to be poured without any difficulty. Factors affecting the rheology of concrete, apart from superplasticizers, are covered in Chapter 7 (Yahia et al., 2016). Table 27.3 gives the principal characteristics of the cement used to build the Sherbrooke pedestrian bikeway: a Type 20 M Canadian cement with a very low hydration heat, used in mass concrete when building hydroelectric dams. Oil-well cements have characteristics quite close to such a cement, and can also be used to produce UHSC.

27.3.1 Why such cement characteristics?

The most important thing when producing UHSC is not obtaining a high strength but rather keeping good control of its rheology for long enough to pour it easily. Currently, the production of a cement which is ideal for UHSC is not favoured by cement producers, because when such cement is used in high w/c concretes (w/c greater than 0.50) it does not provide high early strength. Moreover, it is more difficult to produce such cement than regular Portland cement because it contains a too-fluid interstitial phase. Cement producers prefer to produce fine cements rich in C_3A and C_3S, the two most reactive phases of clinker, because with such cements it is possible to obtain a high early strength with a relatively high w/c ratio. **But high C_3A and C_3S contents and a high specific surface area have disastrous consequences on the rheology of low w/c concretes, and in particular UHSC**.

Table 27.3 Principal characteristics of the cement used to build the Passerelle de Sherbrooke

C_3S	C_2S	C_3A	C_4AF	Alkali equivalent	L.O.I.	Specific surface area
45%	37%	0%	15%	0.3%	1.2%	340 m^2/kg

When making UHSC it is unnecessary to have high amounts of C_3A and C_3S contents to get a high early strength, because, as shown in Chapter 1, in UHSC strength is a consequence of the very short distance between cementitious particles and not the reactivity of the C_3A and C_3S (Aïtcin, 2016). With the cement used to build the Sherbrooke pedestrian bikeway, which had very low C_3A and C_3S contents, a compressive strength of 55 MPa was obtained in 24 h because of the very low w/c used.

27.3.2 Selection of the superplasticizer

The second most important consideration is careful selection of the right superplasticizer: it must provide a good rheology long enough to pour the UHSC, **entrap as little air as possible** and not retard UHSC hardening excessively. For the Sherbrooke pedestrian bikeway, a sodium salt of a polynaphthalene sulphonate was used; others have successfully used polyacrylate superplasticizers.

Those who are not ready to invest money and time in this long process should instead buy a commercial UHSC, sold under different trade names.

For basic information on the chemistry of superplasticizers, their working mechanisms, use in practice and impact on hydration, readers are referred to Chapters 9, 11, 16 and 12, respectively (Gelardi et al., 2016; Gelardi and Flatt, 2016; Nkinamubanzi et al., 2016; Marchon and Flatt, 2016).

27.4 Construction of the Sherbrooke pedestrian bikeway

27.4.1 Design

This 60 m-long UHSC structure was built from six pre-cast post-tensioned elements. It was erected almost like a steel structure (Aïtcin et al., 1998).

The structure is a pre-stressed open-web-space truss that does not contain any passive reinforcement (reinforcing bars). The main tensile stresses are counterbalanced by post-tensioning, while some secondary tensile stresses are resisted directly by steel fibres.

The cross-section is composed of two 380 × 320 mm bottom chords and a 30-mm thick upper deck containing transverse stiffening ribs. The total height of the truss is 3.0 m and its overall width is 3.3 m (Figure 27.5)

Truss diagonals are made of UHSC confined in thin stainless tubes joined to the top and bottom chords through two greased and sheathed anchored mono-strands. Special anchorages were designed by VSL Company of Switzerland, as shown in Figure 27.6. These anchors did not need any bearing plates or local zone spirals since the anchor heads were directly in contact with the RPC, which was able to withstand the high compressive strength developed by the anchorage. Construction details have been previously published (Bonneau et al., 1996).

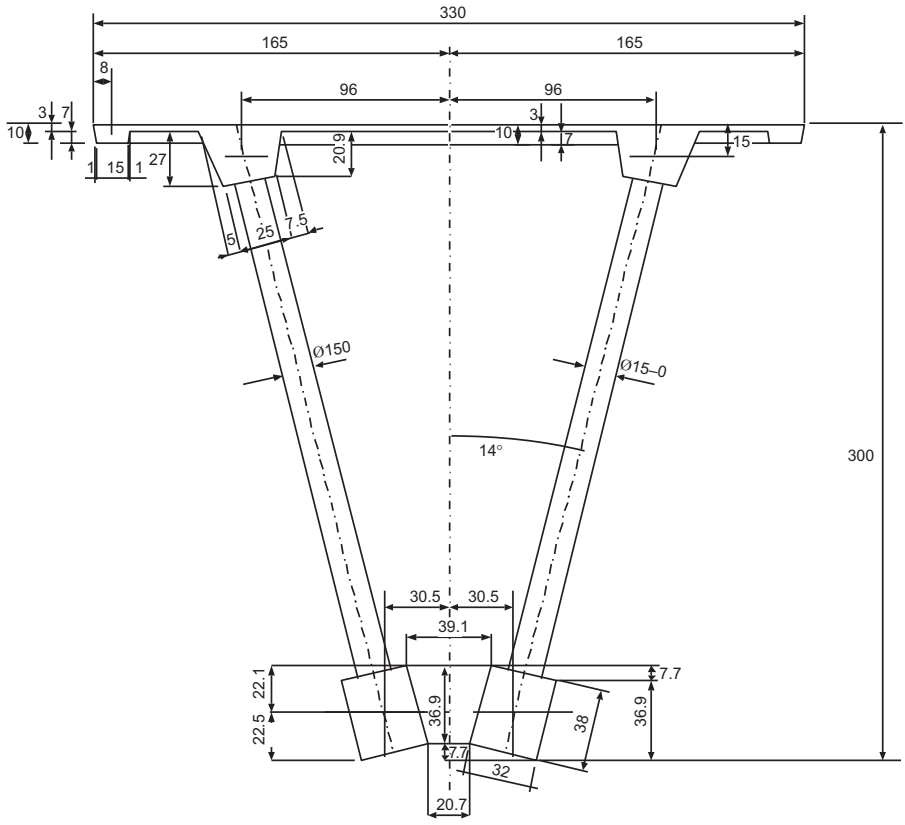


Figure 27.5 Transversal section of the superstructure (units: cm).

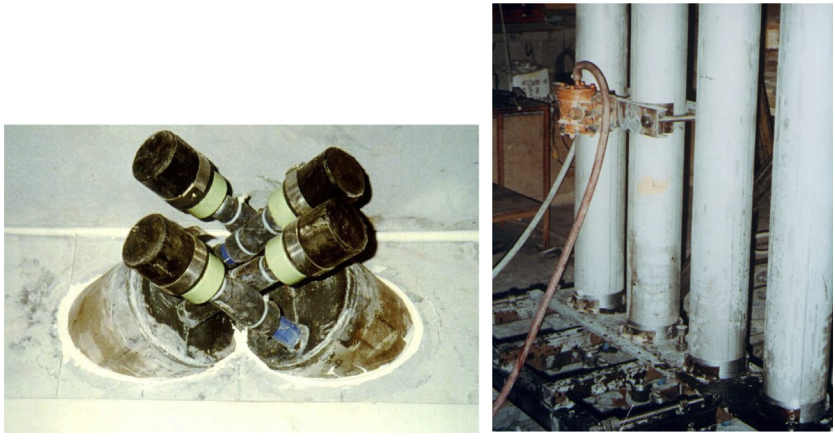


Figure 27.6 Fabrication of the diagonals.

27.4.2 Construction

27.4.2.1 Phase I: fabrication of the confined post-tensioned diagonals

The 150-mm stainless steel tubes containing two post-tensioning cables were filled with fibre-reinforced UHSC (Figure 27.6).

The UHSC was compressed (5 MPa) for 24 h to eliminate most of the entrapped air bubbles, extract uncombined mixing water and compensate for some of the initial chemical contraction. The level of the UHSC in the tubes went down by 100 mm during compression.

Two days after their casting, the diagonals were cured for two days at 90 °C. The external water vapour did not penetrate the UHSC very deeply except at both ends.

27.4.2.2 Phase II: construction of the deck and the lower beam

Each of the six pre-cast elements was cast using usual pre-casting techniques. Each of the pre-cast elements was used to cast the next element (match cast) to get a perfect joint (Figure 27.7).

27.4.2.3 Phase III: curing

As in the case of the diagonals, the 90 °C curing started 48 h after the casting of the UHSC. Polyethylene sheets were used to wrap each pre-cast element and create an enclosure in which steam could be introduced to cure the UHSC (Figure 27.8). This 90 °C curing lasted for two days.

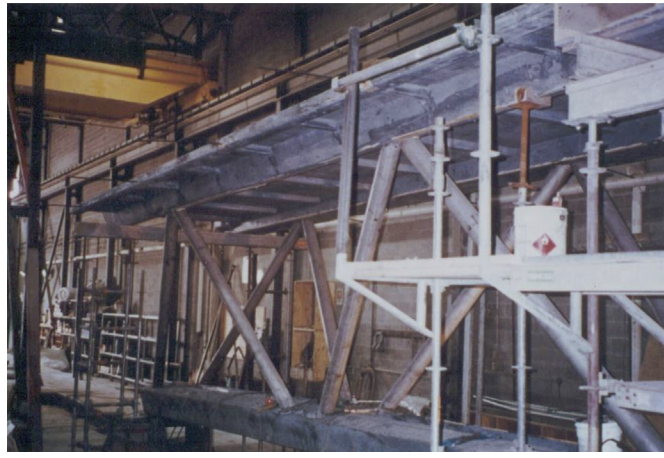


Figure 27.7 Construction of a prefabricated element in the pre-cast plant.

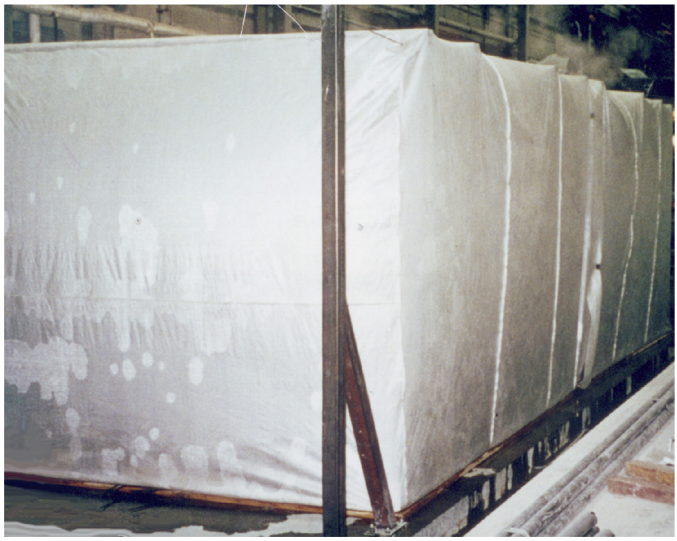


Figure 27.8 Curing of a pre-cast element.

27.4.2.4 Phase IV: transportation to the site

The six pre-cast elements were transported by trucks to the site without any particular problem. Each of the four central elements was 10 m long and weighed 18 tonnes. The two end elements weighed 24 tonnes each (Figure 27.9).

27.4.2.5 Phase V: assembling the prefabricated elements

The assembly of the prefabricated elements was carried out on a stone bed that was temporarily built in the middle of the Magog River. The bridge was assembled in two parts. The joints did not receive any special treatment (UHSC against UHSC), as can be seen in Figures 27.10 and 27.11.



Figure 27.9 Transportation of the prefabricated elements.



Figure 27.10 Assembling the northern part of the bridge.

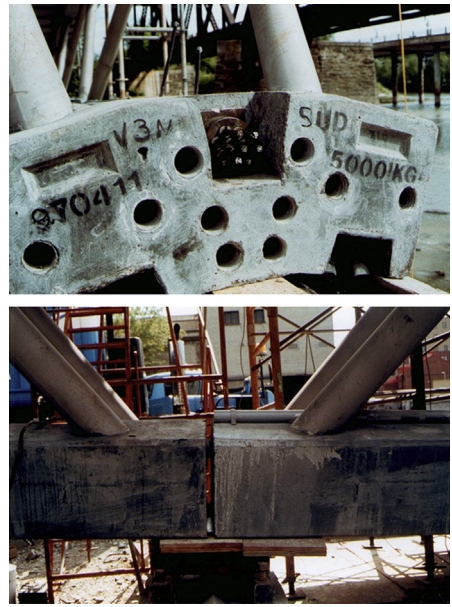


Figure 27.11 Assembling two prefabricated elements (dry joint).

27.4.2.6 Phase VI: post-tensioning

The two halves of the bridge were post-tensioned before lifting the whole platform on to the two piles, as shown in Figure 27.12.

The assembled Passerelle is presented in Figure 27.13.



Figure 27.12 Assembling the two halves of the bridge.



Figure 27.13 The completed Passerelle.

27.5 Testing the structural behaviour of the structure

One year after its construction, the Sherbrooke pedestrian bikeway was tested statically and dynamically to monitor its structural behaviour.

The static loading was done using barrels that were progressively filled with water. The values of the actual deflection were compared to the calculated ones, and were in very close agreement with the theoretical values calculated by Pierre Richard.

The longitudinal, transversal and torsional resonant frequencies were measured and compared to the theoretical values calculated by Richard. In this case, too, the actual values were very close to the calculated ones, as can be seen in Table 27.4. The dynamic behaviour was tested again 10 years later, and the resonance frequencies measured were almost the same as those measured in 1998.

27.6 Long-term behaviour

As indicated by the monitoring of the natural resonant frequencies and a close visual inspection, it can be said that the Sherbrooke pedestrian bikeway is ageing very well (Aïtcin et al., 2014).

The pedestrian bikeway is now illuminated every night as part of the architectural patrimony of the city of Sherbrooke (Figure 27.14).

27.7 Some recent applications of UHSC

UHSCs have been used in Japan to build the taxiways of a new landing strip in an extension of Haneda Airport in Tokyo, and in France to build two spectacular structures: the Museum of Mediterranean Civilizations (MUCEM) in Marseille and the Louis Vuitton Foundation building in Paris. In these last two prestigious buildings the architectural potential of UHSC has been exploited to build very light concrete panels.

Table 27.4 Resonance frequencies calculated and measured on the Passerelle

Modes		Frequency (Hz)			Damping (%)	
		Calculated	1998	2010	1998	2010
Flexural	1st	2.17	2.2	2.3	1.2 ± 0.2	1.1 ± 0.9
	2nd	7.33	7.5	7.5	0.3 ± 0.1	0.6 ± 0.1
	3rd	12.84	12.9	13.0	0.2 ± 0.002	0.4 ± 0.1
	4th	17.8	–	18.1	–	0.3 ± 0.2
Torsional	1st	4.14	4.2	4.3	0.7 ± 0.2	1.0 ± 0.5



Figure 27.14 The Passerelle at night.

27.7.1 The extension of Haneda Airport in Tokyo

To increase the landing capacity of Haneda Airport in Tokyo, a new landing strip has been built in the Bay of Tokyo, as shown in Figures 27.15–27.21.

The landing strip itself was built using pre-cast conventional pre-tensioned 30 MPa reinforced concrete, while the taxiway was built with pre-cast pre-tensioned slabs made of UHSC. All the pre-cast concrete slabs were built in two adjacent pre-cast plants that produced almost exactly the same surface of slabs.



Figure 27.15 The additional landing strip built at Haneda Airport in the Bay of Tokyo.



Figure 27.16 The reinforcing system of the conventional slabs.



Figure 27.17 Installed slabs made of conventional concrete.

All the conventional concrete and USHC slabs had the same length (7.875 m) and the same width (3.75 m).

The conventional concrete slabs had a thickness of 320 mm and weighed 23.5 tonnes each. The UHSC slabs had a maximum thickness of 270 mm at the level of the transverse stiffening ribs and a minimum thickness of 75 mm in between ribs; they weighed only 10.3 tonnes each.



Figure 27.18 The moulds used to build the UHSC slabs.



Figure 27.19 Installation of the pre-tensioned reinforcing system.

During the project it was necessary to hire 140 workers to produce 24 slabs of conventional concrete per day, but only 100 workers in the UHSC plant were employed to produce 21 slabs per day. The difference in the number of workers involved in this particular project compensated largely for the extra cost of the UHSC in comparison to the cost of the 30 MPa concrete.



Figure 27.20 The filling of the moulds with UHSC.



Figure 27.21 The UHSC slabs stocked in the plant yard.

27.7.2 The MUCEM in Marseille

UHSC is not simply a Portland cement-based material that is stronger than ordinary or high-performance concrete: it can be used as an architectural material to conceive very light structural or architectural elements. It was used during the construction of the

MUCEM in Marseille in France to build an outside façade panel looking like concrete lace (Figure 27.22).

27.7.3 Louis Vuitton Foundation building in Paris

The Louis Vuitton Foundation building in Paris, designed by Frank Gehry, is a very spectacular building using white panels of UHSC.

It is clad with almost 19,000 different pieces of white Ductal (Figure 27.23). All the pieces have a uniform thickness of 27 mm and a maximum weight of 30 kg, and are

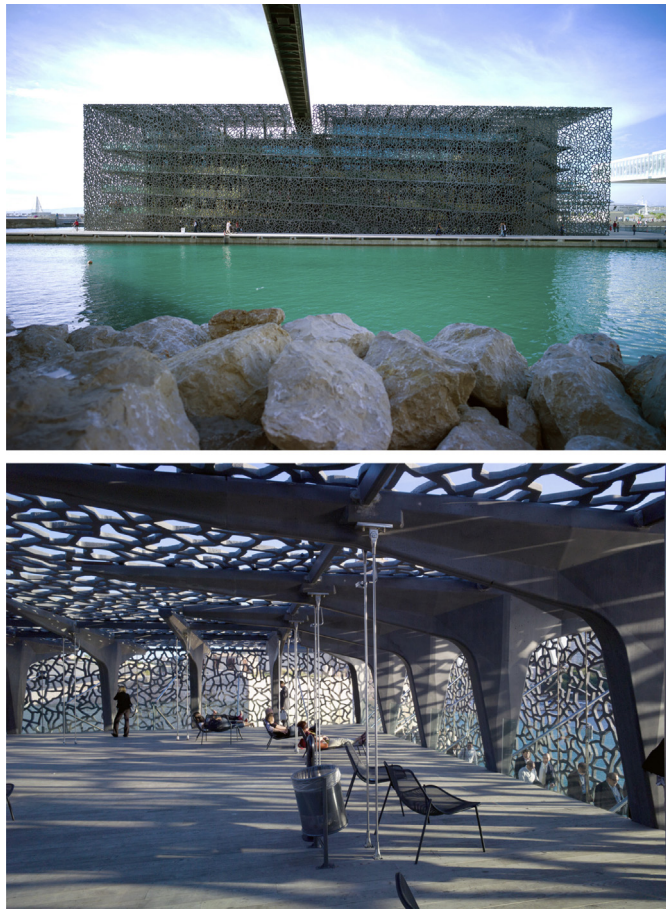


Figure 27.22 External and internal views of MUCEM.
Courtesy of Patrick Paultre.



Figure 27.23 Louis Vuitton Foundation building.
Courtesy of Louis Vuitton Foundation, © Iwan Baan (2014).



Figure 27.24 Partial view of Louis Vuitton Foundation building.
Courtesy of Louis Vuitton Foundation, © Iwan Baan (2014).

placed by hand. Each piece was cast under vacuum in a silicone mould placed in a polystyrene template. Metallic inserts were placed in the mould to fix the pieces on the supporting structure. All the pieces of Ductal were painted in white to give them a perfectly white, mineral, smooth finish (Figures 27.24 and 27.25).



Figure 27.25 Exterior cladding reflecting the branches of a tree.
Courtesy of Louis Vuitton Foundation.

27.8 Conclusion

UHSC is the last spectacular development in the domain of Portland cement-based materials. It was developed by Pierre Richard, the former scientific director of the French building company Bouygues. By eliminating the coarse aggregate, improving the packing density of different powders with specific grain-size distributions and using water or steam curing at 90 °C, it is possible to increase the compressive strength of UHSC to over 200 MPa when using mineral powders, 270 MPa when using glass powder (Soliman et al., 2014) and 800 MPa when using iron powders. When 1−2% of very

thin and long fibres are introduced in such a matrix it behaves like a pseudo-ductile material, working at a microstructural level like reinforced concrete, which explains why this material (which from its grain-size distribution is a mortar) is called a concrete.

This material has been increasingly used to build various impressive light structures, like the cyclo-pedestrian footbridge in Sherbrooke, the extension of Haneda Airport in Tokyo and two recent architectural buildings in France: the MUCEM in Marseille and The Iceberg, the Louis Vuitton Foundation building in Paris.

References

Aïtcin, P.-C., 1998. High Performance Concrete. E and FN Spon, London.

Aïtcin, P.-C., 2008. Binders for durable and sustainable concrete, ISBN 978-0-415-38588-6.

Aïtcin, P.-C., 2016. The importance of the water−cement and water−binder ratios. In: Aïtcin, P.-C., Flatt, R.J. (Eds.), Science and Technology of Concrete Admixtures. Elsevier (Chapter 1), pp. 3−14.

Aïtcin, P.-C., Lachemi, M., Adeline, R., Richard, P., 1998. The Sherbrooke reactive powder concrete footbridge. Journal of the International Association for Bridge and Structure Engineering 8 (2), 140−147.

Aïtcin, P.-C., Lachemi, M., Paultre, P., 2014. The first UHSC structure, 15 years later. In: All Russian Conference, Tome 7, pp. 2−22.

Bache, H.H., 1981. Densified cement ultra-fine particle-based materials. In: Second International Conference on Superplasticizers in Concrete, Ottawa, Canada.

Bonneau, O., Poulin, C., Dugat, J., Richard, P., Aïtcin, P.C., 1996. Reactive powder concrete from theory to practice. Concrete International 18 (4), 47−49.

Coppola, L., Troli, R., Cerruli, T., Collepardi, M., 1996. The influence of materials and performance of reactive powder concrete. High Performance Concrete and Performance of Concrete Structures, Florianopolis, Brazil, 502−513.

Gelardi, G., Flatt, R.J., 2016. Working mechanisms of water reducers and superplasticizers. In: Aïtcin, P.-C., Flatt, R.J. (Eds.), Science and Technology of Concrete Admixtures. Elsevier (Chapter 11), pp. 257−278.

Gelardi, G., Mantellato, S., Marchon, D., Palacios, M., Eberhardt, A.B., Flatt, R.J., 2016. Chemistry of chemical admixtures. In: Aïtcin, P.-C., Flatt, R.J. (Eds.), Science and Technology of Concrete Admixtures. Elsevier (Chapter 9), pp. 149−218.

de Larrard, F., Sedran, T., 1994. Optimization of ultra-high-performance concrete by the use of a packing model. Cement and Concrete Research 24 (6), 997−1009.

Marchon, D., Flatt, R.J., 2016. Mechanisms of cement hydration. In: Aïtcin, P.-C., Flatt, R.J. (Eds.), Science and Technology of Concrete Admixtures. Elsevier (Chapter 8), pp. 129−146.

Nkinamubanzi, P.-C., Mantellato, S., Flatt, R.J., 2016. Superplasticizers in practice. In: Aïtcin, P.-C., Flatt, R.J. (Eds.), Science and Technology of Concrete Admixtures. Elsevier (Chapter 16), pp. 353−378.

Richard, P., Cheyrezy, M., 1994. Reactive powder concrete with high ductility and 200−800 MPa compressive strength. ACI SP-144 507−508.

Soliman, N., Tagnit-Hamou, A., Aïtcin, P.-C., 2014. A new generation of ultra-high performance glass concrete. In: Third All-Russian Conference on Concrete and Reinforced Concrete, Moscow, May 12−16, pp. 218−227.

Tagnit-Hamou, A., Soliman, N., Omran, A.F., Moussa, M.t., Gauvreau, N., Provencher, F., 2015. Novel ultra-high performance glass concrete. Concrete International 37 (3), 41−47.

Yahia, A., Mantellato, S., Flatt, R.J., 2016. Concrete rheology: A basis for understanding chemical admixtures. In: Aïtcin, P.-C., Flatt, R.J. (Eds.), Science and Technology of Concrete Admixtures. Elsevier (Chapter 7), pp. 97−128.

Conclusions and outlook on the future of concrete admixtures

28

R.J. Flatt
Institute for Building Materials, ETH Zürich, Zürich, Switzerland

28.1 Chemical admixtures are to concrete, what spices are to cooking

Chemical admixtures and spices are *almost magical products*, which, when added in small amounts and in the right proportions, can radically change essential properties of the *mix*. This analogy can be extended in many ways, as illustrated in the following:

Interfaces. The reason for the stunning effect that these products have at such low dosages comes from the fact that they act at interfaces. This concerns taste buds and olfactory receptors for spices. For chemical admixtures, this results in most cases from adsorption at the solid−liquid or the liquid−vapor interfaces (see Chapter 10; Marchon et al., 2016).

Essential compounds. Spices and chemical admixtures should be considered as an *integral part of the overall recipe* (see Chapter 1; Aïtcin, 2016). They must be planned for, although some final adjustments (type and dosage) may be carried out in the last stages of mixing.

Dosage. Added in too-small amounts, both chemical admixtures and spices will go unnoticed. Added in too-large amounts, they may cause various undesired reactions. In concrete technology, *dosage should not be governed by cultural preferences but fixed by performance targets*.

Power. The more powerful these substances are, the less one needs but the easier it becomes to overdose them. In concrete technology, this is related to the issue of robustness (see Chapter 16; Nkinamubanzi et al., 2016).

Saturation. Above a certain dosage, increased dosages go relatively unnoticed (saturation point in concrete technology). Some products (e.g., Polynaphtalene Sulfonate or PNS) perform well close to their saturation point. Others (e.g., Polycarboxylate ethers or PCEs, depending on their specific structure) are rather used below their saturation point. In such cases, the notion of surface coverage is very important in quantifying their performance (see Chapter 11; Gelardi and Flatt, 2016).

Blends. Spices as well as chemical admixtures may be blended before use and supplied as such. In concrete technology, the analogue of *spice blends* would be referred to as a *formulated product* (see Chapter 15; Mantellato et al., 2016). Formulated products make life easier, but they cannot be used for everything everywhere.

Secrecy. In a very similar way to great chefs, most admixture companies tend to try and keep the composition of their recipes (formulated products) secret. This does not, however, prevent people from learning to cook with books and practical experience. In this book, rather than providing a compilation of recipes, we tried to provide readers with insights that will help them *become great and independent chefs—or at least enlightened consumers*.

Science and Technology of Concrete Admixtures. http://dx.doi.org/10.1016/B978-0-08-100693-1.00028-X
Copyright © 2016 Elsevier Ltd. All rights reserved.

Cost. Although their unit price is high, the low dosages of spices and chemical admixtures imply that their cost is only (in general) a *second-order component of the total price of the mix*.

Supply limitations. We live in a world of limited resources; despite this, we must find out how to provide access to decent food and housing to the increasingly large world population. This has to be done in the most effective way possible. However, even if spices can play an important role in improving food taste in this endeavor, we believe that the importance and impact of chemical admixtures is even greater because of their *direct benefit to sustainability*.

28.2 Of good and bad concrete

Inspired by Adam Neville's preface in *Properties of Concrete* (Neville, 1996), we can state that 'the ingredients of good concrete are very simple: water, cement, sand, aggregates, mineral additions, and chemical admixtures. However, the ingredients of bad concrete are essentially the same. The difference lies in the know-how and the understanding'.

In this book, we aimed to provide a comprehensive text concerning the use and working mechanisms of chemical admixtures for concrete. We emphasized how chemical admixtures can be used to enhance the quality and durability of concrete, while also reducing the overall environmental footprint of the construction sector (see Chapter 1; Aïtcin, 2016). Such objectives are very clear societal macro-trends and convincing clear indicators that the importance of using chemical admixtures will continue to grow.

We also tried to indicate possible problematic situations, such as cemen—superplasticizer incompatibilities. In such cases, we tried to focus on defining the underlying reasons to provide the understanding needed for effective problem solving.

28.3 Environmental challenges

The issue of limited resources presents the greatest challenge that we have to deal with in the twenty-first century. Construction consumes up to 40% of natural resources, and sustainable construction therefore represents a major societal objective (Aïtcin and Mindess, 2011). As explained in Chapter 1, producing good and durable concrete with reduced clinker contents can significantly contribute to this objective.

However, the quantitative targets that must be reached are extremely demanding. This means that concrete performance must be pushed to its limits, so that the number and dosage of *spices* used must be increased. Mastering such situations represents a major research endeavor, requiring control of the interactions between chemical admixtures, to which we have to add the handling of an increased variety of locally sourced materials with a larger compositional variety than in the past.

This is where the *Science of chemical admixtures* comes into play, representing an area of research that can make major contributions to sustainable construction. It develops the understanding that valuably complements the know-how of *enlightened formulators and practitioners*.

28.4 The science of chemical admixtures

So what do we need to know? Well, first we must recognize that chemical admixtures are so effective because they act at interfaces. As summarized by Flatt et al. (2012) and shown in Figure 28.1, these mostly include the solid−liquid (e.g., superplasticizers, retarders) and liquid−air (e.g., air-entraining admixtures, shrinkage reducers) interfaces, but also the solid−air interfaces (e.g., grinding aids).

Understanding these processes that occur at interfaces, the competition between admixtures and their interactions with the various materials found in concrete represents a fascinating puzzle with tremendous practical implications. These are very complex multicomponent heterogeneous reactive chemical systems. However, this must not scare us. In the words of Stephen Hawking, "… The next (21st) century will be the century of complexity." or those of Gerd Binnig, winner of the Nobel Prize in Physics (1986), who also advised: "The topic of complexity poses the greatest problem (challenge) that there is today."

Therefore, the complexity of our systems should not be a barrier or an embarrassment, but rather a source of stimulation and pride. Indeed, the mastering of this complexity represents a fantastic scientific objective, with tremendous excitement for research and application. However, we must also not forget the wise words of Albert Einstein, who stated: "Any fool can make things bigger, more complex, and more violent. It takes a touch of genius—and a lot of courage—to move in the opposite direction."

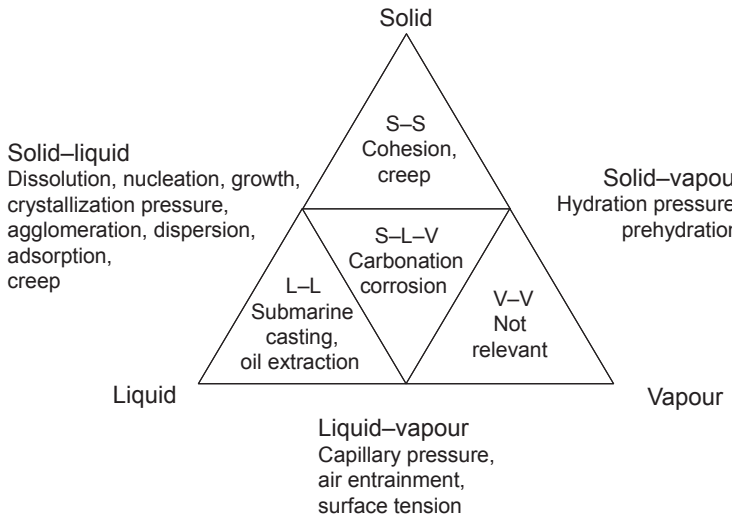


Figure 28.1 Illustration of the role played by different interfaces in the system. S−S = solid−solid, L−L = liquid−liquid, V−V = vapor−vapor, S−L−V = solid−liquid−vapor.
Reproduced from Flatt et al. (2012) with permission.

We hope that the *Science and technology of concrete admixtures* will move things in the right direction and contribute to helping us meet the tremendous challenges of this century.

References

Aïtcin, P.-C., 2016. The importance of the water−cement and water−binder ratios. In: Aïtcin, P.-C., Flatt, R.J. (Eds.), Science and Technology of Concrete Admixtures, Elsevier (Chapter 1), pp. 3−14.

Aïtcin, P.-C., Mindess, S., 2011. Sustainability of Concrete. Spon Press (Taylor and Francis), London, UK, 301p.

Flatt, R.J., Roussel, N., Cheeseman, C.R., 2012. Concrete: an eco material that needs to be improved. Journal of the European Ceramic Society 32 (11), 2787−2798. http://dx.doi.org/10.1016/j.jeurceramsoc.2011.11.012.

Gelardi, G., Flatt, R.J., 2016. Working mechanisms of water reducers and superplasticizers. In: Aïtcin, P.-C., Flatt, R.J. (Eds.), Science and Technology of Concrete Admixtures, Elsevier (Chapter 11), pp. 257−278.

Mantellato, S., Eberhardt, A.B., Flatt, R.J., 2016. Formulation of commercial products. In: Aïtcin, P.-C., Flatt, R.J. (Eds.), Elsevier (Chapter 15), pp. 343−350.

Marchon, D., Mantellato, S., Eberhardt, A.B., Flatt, R.J., 2016. Adsorption of chemical admixtures. In: Aïtcin, P.-C., Flatt, R.J. (Eds.), Science and Technology of Concrete Admixtures, Elsevier (Chapter 10), pp. 219−256.

Neville, A.M., 1996. Properties of Concrete. Wiley.

Nkinamubanzi, P.-C., Mantellato, S., Flatt, R.J., 2016. Superplasticizers in practice. In: Aïtcin, P.-C., Flatt, R.J. (Eds.), Science and Technology of Concrete Admixtures, Elsevier (Chapter 16), pp. 353−378.

Appendix 1: Useful formulae and some applications

P.-C. Aïtcin

Université de Sherbrooke, QC, Canada

A1.1 The 'hidden' water in concrete

When making concrete either in the laboratory or in the field, the most difficult thing is to keep tight control of the amount of water actually used when making the mix. It is always easy to weigh a certain amount of cement or aggregates, and to read the number of litres of water passing through a meter. When using a superplasticizer it is not so difficult to calculate the amount of water brought into the mix by the superplasticizer, as will be shown later. What is definitely much more difficult is to keep a tight and constant control of the precise amount of water brought into the mix by the aggregates, especially by the sand, because the water content of the aggregates, and especially that of the sand, can vary considerably. The water content, w_{tot}, of an aggregate is defined as the amount of evaporable water divided by the dry mass of the aggregate, and is expressed as a percentage. To measure it, it is only necessary to place a certain amount of wet sand in an oven at 105 °C and weigh it when it has a constant mass. The use of a microwave oven can reduce the duration of the drying.

Depending on the level of control exercised over the water content of the aggregate, and more particularly of the fine aggregate, a better or poorer quality concrete can be produced. For example, a variation of 1% in the water content of the approximately 800 kg of sand that is used to produce 1 m^3 of concrete corresponds to a variation of 8 L of water in the mix. If this variation occurs in a high-performance concrete (HPC) mix that contains 150 L of water and 455 kg of cement per cubic metre, which corresponds to a water/cement ratio of 0.33, the w/c ratio could range from 0.31 to 0.35, which represents a non-negligible difference in terms of slump, compressive strength and permeability. It is therefore very important to be able to control the precise amount of water contained in the aggregates, and thus it is essential to define a reference state for the aggregates.

A1.2 Saturated surface dry state for aggregates

By convention in North America this reference state is called the saturated surface dry (SSD) state. It is defined in ASTM C127 Standards for the Coarse Aggregate and ASTM C128 Standards for the Fine Aggregate. These two standard test methods describe in detail how to measure the SSD state. Very briefly, for coarse aggregate

the SSD state is obtained by soaking the aggregate in water for 24 h and then drying it in an oven to constant mass. A coarse aggregate in the SSD state is shown schematically in Figure A1.1. A represents a superficial pore, B a pore entirely filled with water, c a partially saturated pore, D a closed pore that do not communicate with the surface of the particle and e an inaccessible pore.

For fine aggregate, by convention the SSD state is obtained when a small, truncated sand cone no longer holds together owing to the capillary forces between the wet sand particles. Figure A1.2 illustrates the determination of the SSD state for sand.

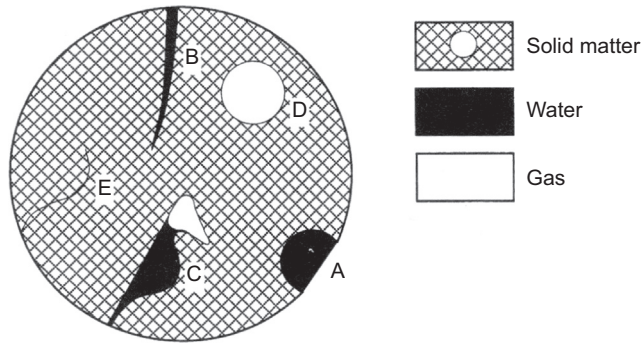


Figure A1.1 Schematic representation of an aggregate particle in the SSD state. Aïtcin (1998).

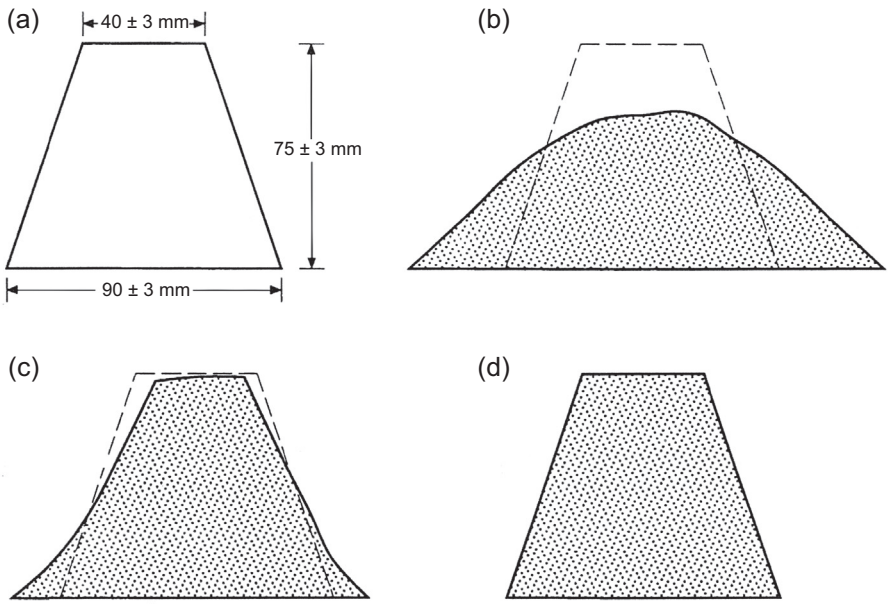


Figure A1.2 Determination of the SSD state for sand: (a) standardized mini-cone used; (b) sand with a water content below its SSD state; (c) sand in an SSD state; (d) sand with a water content above its SSD state. Aïtcin (1998).

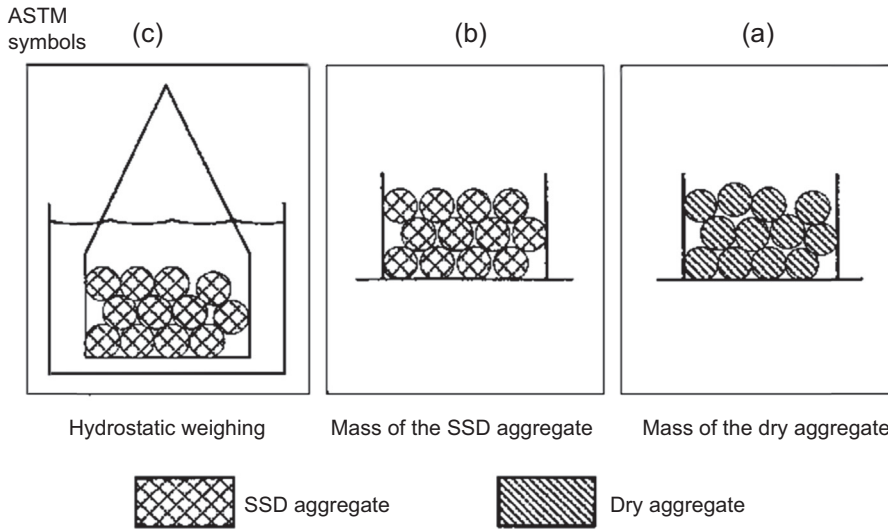


Figure A1.3 Schematic representation of the measurement of the absorption and SSD specific gravity of a coarse aggregate. Aïtcin (1998).

The determination of the absorption of a coarse aggregate and its SSD specific gravity are represented schematically in Figure A1.3.

In both cases, the amount of water absorbed in the aggregate when it is in the SSD state, w_{abs}, corresponds to the aggregate absorption. This absorption is expressed as a percentage of the mass of the dry aggregate.

In North America, concrete compositions are always expressed with the coarse and fine aggregates in their SSD states.

A1.3 Moisture content and water content

The SSD state of an aggregate is very important when calculating or expressing the composition of a particular concrete, because it establishes a clear differentiation between the two types of water typically found in an aggregate. The water absorbed within the aggregate does not contribute either to the slump of the concrete or to its strength because it does not participate in cement hydration. When the water content of the aggregate is lower than in its SSD state, the aggregate will absorb some water from the mix, which increases the rate of slump loss of concrete. On the other hand, when the water content of an aggregate is higher than its SSD state, the aggregate will bring water into the mix (as shown in Figure A1.4) if no special correction is made and thus increase the water/binder ratio and increase the slump. Thus the amount of mixing water has to be modified to keep the w/b ratio and the slump constant.

The difference between the total water content w_{tot} and w_{abs}, is called the moisture content of the aggregate and is denoted by w_h. The moisture content of an aggregate

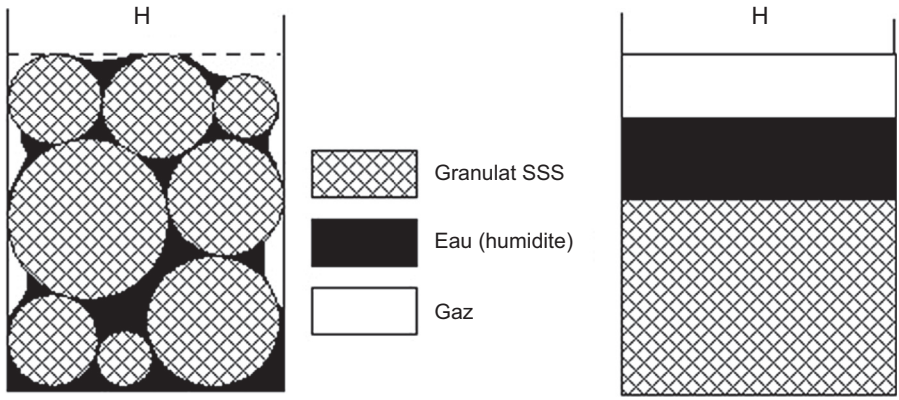


Figure A1.4 Schematic representation of a wet coarse aggregate. Aïtcin (1998).

can be negative if the total water content is lower than the water absorption, w_{abs}, if an aggregate having an absorption of 0.8% is absolutely dry, $w_{tot} = 0$, so consequently $w_h = -0.8\%$ and 8 L of water could be absorbed by the coarse aggregate in the fresh concrete after mixing. This amount of water will undoubtedly have a significant effect on the rate at which this particular concrete will lose its slump during transportation if no water content adjustment is made, because the absorption of these 8 L of water is not instantaneous.

On the other hand, when the same coarse aggregate has a total water content of 1.8% after a rain shower, $w_h = 1.0\%$ and the 10 L of extra water brought to the mix by the coarse aggregate drastically increases the amount of mixing water. If no correction of the mix is made, this can have a detrimental effect on the slump, compressive strength and permeability.

Therefore, in this book the following definitions will be used. The total water content of an aggregate is defined as:

$$w_{tot} = \frac{\text{Mass of the wet aggregate} - \text{mass of the dry aggregate}}{\text{Mass of the dry aggregate}} \times 100 \qquad \text{(A1.1)}$$

With the ASTM conventions shown in Figures A1.3 and A1.4:

$$w_{tot} = \frac{H - A}{A} \times 100 \qquad \text{(A1.2)}$$

The absorption of an aggregate, w_{abs}, will correspond to:

$$w_{tot} = \frac{\text{Mass of the SSD aggregate} - \text{mass of the dry aggregate}}{\text{Mass of the dry aggregate}} \times 100 \qquad \text{(A1.3)}$$

Or with the ASTM conventions shown in Figure A1.4:

$$w_{abs} = \frac{B - A}{A} \times 100 \tag{A1.4}$$

A1.4 Specific gravity

The specific gravity of an aggregate in the SSD state is called the SSD specific gravity. Figure A1.3 illustrates schematically how to measure the SSD specific gravity of either coarse or fine aggregate.

The SSD specific gravity of an aggregate is equal to:

$$G_{SSD} = \frac{B}{B - C} \tag{A1.5}$$

The SSD specific gravity expresses how much denser than water a SSD aggregate is. The application of Archimedes' principle shows that G_{SSD} is the specific gravity that has to be used to calculate exactly the volume occupied by the aggregates in the concrete mix (Aïtcin, 1971).

For Portland cement or any supplementary cementitious material, the specific gravity, G_c, is equal to the mass of the dry material divided by its dried density. The ASTM C188 standard test method explains how to measure this value practically:

$$G_c = \frac{A}{A - C} \tag{A1.6}$$

A1.5 Supplementary cementitious material content

It is convenient to express the amount of supplementary cementitious material and/or filler used when making an HPC as a percentage of the cement mass, or even to express individually the content of the different supplementary cementitious materials used in such concrete. However, the expression 'supplementary cementitious material content' can have two different meanings depending on whether the supplementary material is incorporated at the concrete plant or was already incorporated at a cement concrete plant separately from Portland cement: in this case the term 'content' is only related to the mass of Portland cement that is used to make the concrete. When the supplementary cementitious material is added at the cement plant its content is related to the mass of the blended cement and not only to the cement content.

The following examples illustrate the differences between these two definitions of the expression 'supplementary cementitious material' and/or filler content.

A1.5.1 Case 1

An HPC is made in a concrete plant using 400 kg of Portland cement, 100 kg of fly ash and 40 kg of silica fume that are added separately in the mixer. What is the supplementary cementitious material content of this concrete?

The fly ash content is $(100/400) \times 100 = 25\%$, and the silica fume content is $(40/400) \times 100 = 10\%$.

A1.5.2 Case 2

An HPC is made using 400 kg of blended cement containing 7.5% silica fume. What is the actual amount of cement introduced in the mixer?

In this blended cement, Portland cement represents only 92.5% of the blend, therefore the actual Portland cement used to make this concrete is

$$400 \times 0.925 = 370 \text{ kg}$$

As both definitions of the expression 'supplementary cementitious material content' are in use and have their own merits, they will both be used in this book. The reader should remember that this expression has a different meaning when the supplementary cementitious material and/or filler is added at the cement plant to produce a blended cement and when it is added at the concrete plant on top of the amount of cement.

A1.6 Superplasticizer dosage

The dosage of a superplasticizer can be expressed in different ways. It can be given in litres of commercial solution per cubic metre of concrete — this is the best way to express it at the batching plant. However, it is not the best way to express it in scientific papers or in a book because not all commercial superplasticizers have the same solids content and specific gravity. When making an HPC, it would be a serious mistake to use the same liquid dosage of superplasticizer with a superplasticizer that has a different specific gravity and solids content. For example, melamine superplasticizers can be found as liquid solutions having a solids content of 22%, 33% or 40%. Thus it is always better to give the superplasticizer dosage as the amount of solids it contains expressed as a percentage of the mass of cement. This way of expressing the dosage is important when comparing the costs of different commercial superplasticizers. (In fact, it is actually the amount of active solids that should be taken into account and not the total amount of solids, because not all the solids in a superplasticizer are active dispersing molecules, and commercial superplasticizers always contain some residual sulphate. However, for the sake of simplicity this last distinction is not made in this book.)

To move from a dosage expressed in litres per cubic metre to a dosage expressed in solids, it is necessary to know the value of the specific gravity of the liquid superplasticizer and its solids content.

A1.6.1 Specific gravity of the superplasticizer

According to Figure A1.5, the specific gravity of the superplasticizer is:

$$G_{sup} = \frac{M_{liq}}{V_{liq}} \tag{A1.7}$$

if M_{liq} is measured in grams and V_{liq} in cubic centimetres.

A1.6.2 Solids content

According to Figure A1.5, the solids content, s, of the superplasticizer is:

$$s = \frac{M_{liq}}{V_{liq}} \times 100 \tag{A1.8}$$

Therefore the total solids content M_{sol} contained in a certain volume of superplasticizer having a specific gravity equal to G_{sup} and a total solids content equal to s is:

$$M_{sol} = \frac{s \times M_{liq}}{100} = \frac{s \times G_{sup} \times V_{liq}}{100} \tag{A1.9}$$

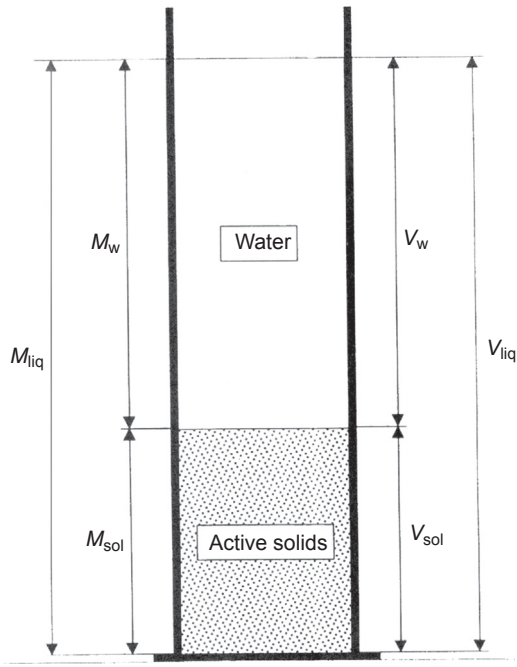


Figure A1.5 Schematic representation of a superplasticizer. Aïtcin, 1998.

For example, 6 L of a melamine superplasticizer with a specific gravity of 1.10 and a total solids content of 22% contain $0.22 \times 1.1 \times 6 = 1.45$ kg of solids, while 6 L of a naphthalene superplasticizer with a specific gravity of 1.21 and a total solids content of 42% contain $0.42 \times 1.21 \times 6 = 3.05$ kg of solids.

A1.6.3 Mass of water contained in a certain volume of superplasticizer

When adding a liquid superplasticizer to a concrete mixture, it is necessary to take into account the amount of water added to the concrete in order to be able to calculate the exact w/b ratio. This is done in the following way. From Figure A1.5:

$$M_{liq} = M_w + M_{sol} \quad \text{or} \quad M_w = M_{liq} - M_{sol}$$

From Eqn (A1.8):

$$M_{liq} = \frac{M_{sol} \times 100}{s}$$

Then:

$$M_w = \frac{M_{sol} \times 100}{s} - M_{sol}$$

This can be written as:

$$M_w = M_{sol}\left(\frac{100}{s} - 1\right) \quad \text{or} \quad M_w = M_{sol}\left(\frac{100 - s}{s}\right) \tag{A1.10}$$

Replacing M_{sol} by its value in Eqn (A1.9):

$$M_w = \frac{V_{liq} \times s \times G_{sup}}{100} \times \frac{100 - s}{s}$$

Finally:

$$M_w = V_{liq} \times G_{sup} \times \frac{100 - s}{s} \tag{A1.11}$$

When using proper units (g and cm^3, and/or kg and L), M_w and V_w are expressed by the same number, so:

$$V_w = V_{liq} \times G_{sup} \times \frac{100 - s}{s} \tag{A1.12}$$

As a sample calculation, 8.25 L of naphthalene superplasticizer with a specific gravity of 1.21 and a solids content of 40% have been used in a concrete in order to obtain the desired slump. What is the volume of water V_w that is added to the concrete when using a solution of a commercial superplasticizer? According to Eqn (A1.12), the amount of water is:

$$V_w = 8.25 \times 1.21 \times \frac{100 - 40}{100} = 6.0 \text{ L/m}^3$$

A1.6.4 Other useful formulae

If $d\%$ is the dosage of the solids of a superplasticizer suggested by the manufacturer to obtain a desirable slump in a concrete containing a mass C of cementitious material, the volume of liquid superplasticizer V_{liq} having a specific gravity G_{sup} and a solids content s can be calculated as follows:

$$M_{sol} = C \times \frac{d}{100} \tag{A1.13}$$

But from Eqn (A1.9):

$$M_{sol} = \frac{s \times M_{liq}}{100} \tag{A1.14}$$

Therefore:

$$\frac{s \times M_{liq}}{100} = C \times \frac{d}{100} \tag{A1.15}$$

Replacing M_{liq} by its value deduced from Eqn (A1.8):

$$\frac{s \times G_{sup} \times V_{liq}}{100} = C \times \frac{d}{100}$$

$$V_{liq} = \frac{C \times d}{s \times G_{sup}} \tag{A1.16}$$

A1.6.5 Mass of solid particles and volume needed

If C it the total mass of the cementitious materials used in a particular mix and $d\%$ is the suggested dosage of solid particles, then the mass M_{sol} of solids needed is:

$$M_{sol} = C \times \frac{d}{100} \tag{A1.17}$$

The volume of liquid superplasticizer needed to have M_{sol} of solid particles is calculated as follows.

Replacing M_{liq} in Eqn (A1.7) by its value found from Eqn (A1.8):

$$V_{liq} = \frac{M_{liq}}{G_{sup}} \quad \text{and} \quad M_{liq} = \frac{M_{sol} \times 100}{s}$$

Then:

$$V_{liq} = \frac{M_{sol} \times 100}{s \times G_{sup}} \tag{A1.18}$$

A1.6.6 Volume of solid particles contained in V_{liq}

From Figure A1.5:

$$V_{sol} = V_{liq} - V_w$$

Replacing V_w by its value given by Eqn (A1.7):

$$V_{sol} = V_{liq} - V_{liq} \times G_{sup} \times \frac{100 - s}{100} \tag{A1.19}$$

$$V_{sol} = V_{liq}\left(1 - G_{sup} \times \frac{100 - s}{100}\right) \tag{A1.20}$$

A1.7 Sample calculation

A1.7.1 Example 1: Expressing a dosage in L/m³ as a percentage of solids content

An HPC containing 450 kg of cement per cubic metre of concrete has been made using 7.5 L of naphthalene superplasticizer with a specific gravity of 1.21 and a solids content of 41%. What is the superplasticizer dosage, expressed as the percentage of its solids content, to the mass of cement?

The mass of 7.5 L of superplasticizer is:

$$7.5 \times 1.21 = 9.075 \text{ kg}$$

The solids content in this mass of superplasticizer is:

$$9.075 \times \frac{41}{100} = 3.72 \text{ kg}$$

The superplasticizer dosage of the mass of cement is:

$$\frac{3.72}{450} \times 100 = 0.8\%$$

A1.7.2 Example 2: Moving from a dosage expressed as a percentage of solids to a dosage expressed in L/m^3

In a scientific paper, it is stated that a 1.1% superplasticizer dosage was used in a 0.35 w/c ratio HPC containing 425 kg of Portland cement per cubic metre of concrete. A melamine superplasticizer with a specific gravity of 1.15 and a 33% solids content was used to produce the mix. What is the amount of commercial solution that was used?

The amount of superplasticizer solids is:

$$\frac{425 \times 1.1}{100} = 4.675 \text{ kg}$$

This amount of solids is contained in 4.675/0.33 = 14.17 kg of liquid melamine, which represents 14.17/1.15 = 12.31 of commercial solution.

A1.8 The absolute volume method

A1.8.1 Introduction

When a satisfactory trial batch has been obtained in the laboratory it is necessary to calculate its proportions for 1 m^3 of concrete, the usual formulation of concrete composition. This composition is always presented for aggregates in SSD conditions. For batching purposes it is only necessary to adjust the weight of sand and coarse aggregate to take into account their actual water content.

It is necessary to calculate precisely the volume of the concrete made in this trial batch. Some relevant characteristics of the aggregates and admixtures will be needed first to calculate the w/c ratio of the batch and its absolute volume. Knowing the absolute volume of each of the concrete ingredients (the aggregates being in an SSD state), it is easy to calculate their weight to make 1 m^3 of concrete.

The organogram of this method is presented in Figure A1.6.

Let us apply this method to three particular trial batches.

A1.8.2 Trial batches

In the following three batches the same cement with a specific gravity of 3.14 is used. For the first two trial batches the coarse aggregate is a limestone with an SSD specific gravity of 2.70 and an absorption of 1%, and the sand is a granitic sand with a specific gravity of 2.65 and an absorption of 1.5%. For the last trial batch the coarse aggregate has a specific gravity of 2.75 and an absorption of 1%, and the sand a specific gravity of 2.65 and an absorption of 1%.

A1.8.2.1 First trial batch

The first trial batch is a non-air-entrained concrete without any admixture; its entrapped air content is 2%. The coarse aggregate is in an SSD state, while the sand has a total water content of 4%.

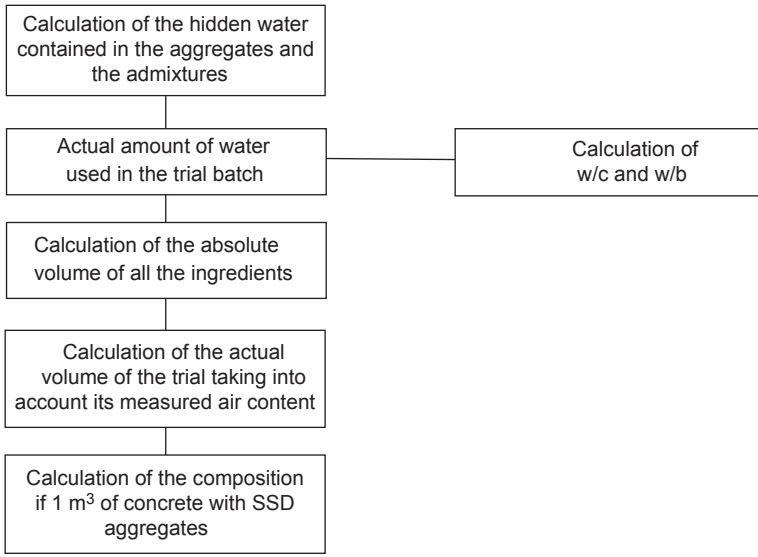


Figure A1.6 Organogram of the absolute volume method to calculate the proportions of 1 m^3 of concrete (SSD aggregates) from the proportions of a trial batch.

The composition of the trial batch is given in Table A1.1.

Let us calculate the amount of water hidden in the sand. The amount of free water contained in the sand is $h = w_{tot} -$ abs that is $h = 4 - 1.5 = 2.5\%$.

The amount of wet sand used is 85 kg, thus the mass of the SSD sand can be calculated using the formula $M_{SSD} = M_h/(1 + h)$. In this case this gives 85/1.025, which is 82.93 kg, and the amount of free water the sand contains is equal to $85 - 82.93 = 2.07$ kg.

The total amount of water in the mixer is therefore $14 + 2.07 = 16.07$ L.

The w/c ratio of the concrete is $16.07/35 = 0.46$.

The absolute volume of the cement is $35/3.14 = 11.15$ L.

The absolute volume of the SSD coarse aggregate is $105/2.70 = 38.89$ L.

The absolute volume of the SSD sand is $82.93/2.65 = 31.29$ L.

Therefore the volume of the solids ingredients and the water used in this trial batch is as shown in Table A1.2.

Table A1.1 Composition of the first trial batch

Water	Cement	Aggregate		Entrapped
		Coarse	Sand	Air
14 L	35 kg	105 kg	85 kg	2%

Table A1.2 Volumetric composition of the first trial batch in litres

Water	Cement	Aggregate		Total
		Coarse	Fine	
16.07	11.15	38.89	31.29	97.4 L

Table A1.3 Composition of 1 m^3 of the first trial batch of concrete

Aggregate SSD	Water	Cement	Aggregate		Entrapped air
			Coarse	Fine	
Trial batch	16.07	35	105	82.9	2%
1 m^{3*}	162	352	1060	830	2%

m^3 = cubic meter

In fact this volume represents 98% of the volume of the trial batch because the amount of entrapped air is 2%.

To have the composition of 1 m^3 of this concrete it is necessary to multiply each of the quantities given in Table A1.2 by 98/97.4 that is 10.06.

The composition of the concrete is therefore as shown in Table A1.3.

These values have been rounded to the closest 1 L for the water, 1 kg for the cement and 10 kg for the aggregate to take into account the precision of the balances used in a batching plant.

The unit weight of the concrete is $162 + 352 + 1060 + 830 = 2404$ kg/m^3.

A1.8.2.2 Second trial batch

The second trial batch is an air-entrained concrete containing a water reducer and made using the weights of materials shown in Table A1.4.

Let us suppose that this time the coarse aggregate is dry, $w_{tot} = 0\%$. The sand has a total water content of 4%, and the solid content of the water reducer is 20% and its specific gravity is 1.1.

Let us calculate the amounts of hidden water in the aggregate and the admixture.

As the coarse aggregate is dry it will absorb some water during its mixing, $M_{SSD} = M_h/(1 + \text{abs})$.

The mass of the SSD coarse aggregate when it has absorbed some batching water is 106.05 kg.

Table A1.4 Composition of the second trial batch

Water	Cement	Aggregate		Total air content	Water reducer
		Coarse	Sand		
14 L	35 kg	105 kg	80 kg	6%	0.1 L

Table A1.5 Absolute volume of the solid ingredients and water of the second trial batch in litres

Water	Cement	Aggregate		Water reducer	Total
		Coarse	Fine		
14.90	11.15	39.28	29.45	0.1	94.78 L

The coarse aggregate will absorb 1.05 L of water.

The M_{SSD} of the wet sand is $M_{SSD} = M_h/(1 + h)$, which is $80/1.025 = 78.05$ kg. It will bring 1.95 kg of water to the mix.

The volume of water contained in the water reducer is calculated as follows. The mass of the water reducer is $0.1 \times 1.1 = 0.11$ kg. The amount of solids is $0.11 \times 0.2 = 0.021$ kg. Therefore the amount of water brought by the water reducer is $0.11 - 0.021 = 0.09$ L, which is negligible in comparison to the water 'hidden' within the aggregates.

The amount of water used when making the trial batch is $14 - 1.05 + 1.95 = 14.90$ L.

The w/c ratio of this entrained-air concrete is therefore $14.9/35 = 0.43$.

The absolute volume of the cement is $35/3.14 = 11.15$ L.

The absolute volume of the SSD coarse aggregate is $106.05/2.70 = 39.28$ L.

The absolute volume of the SSD sand is $78.05/2.65 = 29.45$ L.

The absolute volume of the solid ingredients and water used to make this trial batch are shown in Table A1.5.

In fact this volume represents only 94% of the volume of the batch, since its air content is 6%.

Therefore the absolute volume of the trial batch was $94.78/(1 - 0.06) = 100.83$ L. To make 1 m^3 (1000 L) it will be necessary to multiply the masses of the different ingredients by 1.0083.

The composition of the trial batch (SSD aggregates) is shown in Table A1.6.

To obtain the composition of 1 m^3 of this concrete (SSD aggregates) it is necessary to multiply the proportions of the trial batch was by 1000/100.83, which is 9.918.

Thus, the composition of the concrete is as shown in Table A1.7.

The unit weight of the concrete was therefore $149 + 347 + 1050 + 770 = 2316$ kg/m^3.

Table A1.6 Composition of the second trial batch (SSD aggregates)

Water	Cement	Aggregate		Water reducer	Air
		Coarse	Fine		
15	35	106.05	78.05	0.1	6%
L	kg			L	%

Table A1.7 Composition of the second concrete

Water	Cement	Aggregate SSD		Air content	Volume of water reducer
		Coarse	Fine		
149	347	1050	770	6	1
L	kg			%	L

A1.8.2.3 Third trial batch

The third trial batch was done to fine-tune the composition of an HPC in which a blended cement containing 10% of a class F fly ash with a specific gravity of 2.50 was used. To obtain the right consistency in the HPC, 0.91 L of a polynaphthalene sulfonate (PNS) superplasticizer was used. This PNS had a specific gravity of 1.21 and a solids content of 42%. The aggregates used to make this batch had the characteristics shown in Table A1.8.

The entrapped air content of the concrete was 1.5%.

The composition of this third trial batch is given in Table A1.9.

As the coarse aggregate was dry it absorbed a certain volume of the mixing water to reach its SSD state. The SSD mass of the coarse aggregate is calculated as follows:

$$100 \text{ kg } (1 + (1/100)) = 101.01 \text{ kg}$$

Therefore the coarse aggregate will absorb 1.01 L of water.

As the sand had a total water content of 3.9, its humidity was $h = 3.9 - 1.0 = 2.9\%$.

Table A1.8 Characteristics of the aggregates used in the third trial batch

Aggregate	G_{SSD}	w_{abs} in %	w_{tot} in %
Coarse	2.75	1.0	0
Fine	2.65	1.0	3.9

Table A1.9 Composition of the third trial batch

Water	Cement	Fly ash	Aggregate		Superplasticizer	Air content
			Coarse	Fine		
12	45	5	100	70	0.9	1.5
L	kg				L	%

The SSD mass of the sand is $70/(1 + 2.9/100) = 68.03$ kg therefore the sand was containing 1.97 L.

The amount of water contained in the superplasticizer was equal to:

$$V_{\text{liq}} = 0.9 \times 1.21 \times (100 - 42/100) = 0.63 \text{ L}$$

The amount of water was $12 - 1.01 + 1.97 + 0.63 = 13.59$ L.

The w/c of the concrete was therefore $13.59/45 = 0.30$ and its w/b ratio $13.59/50 = 0.27$.

The volume of the cement used was $45/3.14 = 14.33$ L.

The volume of fly ash used was $5/2.5 = 2.00$ L.

The volume of SSD coarse aggregate was $101.01/2.75 = 36.73$ L.

The volume of SSD sand was $68.03/2.65 = 25.67$ L.

The volume of the solids contained in the superplasticizer was $V_{\text{sol}} = 0.9(1 - 1.21(1 - 42/100))$, which is equal to 0.27 L.

The sum of these volumes is:

$$13.59 + 14.33 + 2.0 + 36.73 + 25.67 + 0.27 = 92.59 \text{ L}$$

Taking into account the 1.5% of entrapped air the actual volume of the trial batch was:

$$92.59/(1 - 1.5/100) = 94 \text{ L}$$

To have the proportions for 1 m^3 of this concrete it is necessary to multiply the proportions of the trial batch by $100/94 = 10.64$.

The composition of the trial batch was as shown in Table A1.10.

The composition of 1 m^3 of this concrete (SSD aggregates) is shown in Table A1.11.

Table A1.10 Composition of the third trial batch

Water	Cement	Fly ash	Aggregate		Superplasticizer	Air content
			Coarse	Fine		
13.59	45	5	101.01	68.03	0.9	1.5
L	kg				L	%

Table A1.11 Composition of the third concrete

Water	Cement	Fly ash	Aggregate		Superplasticizer	Air content
			Coarse	Fine		
145	480	53	1075	725	9.6	1.5
L	kg				L	%

Table A1.12 Suggested amount of coarse aggregate

Irregular	Cubic	Rounded	
1000 kg	1050 kg	1100 kg	kg/m^3

Table A1.13 Suggested amount of mixing water excluding the water contained in the superplasticizer

Non-air-entrained Air-entrained	165 150	L

These values are typical to High Performance Concrete

A1.8.3 Simplified method to calculate the composition of 1 m^3 of concrete with a given w/c or w/b ratio

The amount of coarse SSD aggregate can be selected according to its shape, as given in Table A1.12.

The amount of mixing water to be used excluding the water of the superplasticizer is given in Table A1.13.

The starting dosage of superplasticizer is given in Table A1.14. When making the trial batch it will be adjusted to obtain the desired initial slump.

The mass of the cement to be used is calculated from the w/c or w/b ratio because we have fixed the amount of water. The only unknown mass is the mass of the sand. It is calculated according to the absolute volume method.

$$\text{vol. of the sand} = 1\ \text{m}^3 - \text{vol. of the water} - \text{vol. of the cement} - \text{vol. of the coarse aggregate} - \text{vol. of the superplasticizer}$$

A1.8.3.1 Sample calculation

Let us calculate the composition of an air-entrained concrete with a w/c ratio equal to 0.35 made with Portland cement with a specific gravity equal to 3.14. The coarse aggregate is cubic and has an SSD specific gravity of 2.70, and the sand has an SSD specific gravity of 2.65. A polynaphthalene-based superplasticizer is used.

In Table A1.12 the suggested dosage of the coarse aggregate is 1050 kg/m^3.

As this concrete will be air-entrained the amount of mixing water will be 150 L, as shown in Table A1.13.

Table A1.14 Suggested dosage of superplasticizer

Polynaphthalene Polymelamine Polycarboxylate ether (PCE)	0.8% 0.4%	Of the mass of cementitious materials

Table A1.15 Proportion of the trial batch

Water	Cement	Fly ash	Aggregate SSD		Superplasticizer	Air content
			Coarse	Fine		
150	429	0	1050	680	6.75	6
L	kg				L	%

The amount of cement is obtained from the targeted w/c. It is in this case 150/0.35 = 429 kg.

The volume of active solids of the superplasticizer will be 429 × 0.8/100 = 3.43 kg.

The volume of the liquid superplasticizer will be:

$$V_{liq} = \text{Mass of solids} \times 100/1.21 \times 42 \text{ that is } 343/1.21 \times 42 = 6.75 \text{ L}$$

Calculation of the volume of the sand is done as follows.

Absolute volume of the water: 150 L.

Absolute volume of the cement: 429/3.14 = 136.62 L.

Absolute volume of the coarse aggregate: 1050/2.70 = 388.89 L.

Absolute volume of the superplasticizer: 6.75 L.

Absolute volume of air: 60 L.

Total volume of the ingredients except the sand + the amount of water will be:

$$150 + 136.62 + 388.89 + 6.75 + 60 = 744.62 \text{ L}$$

The volume of the SSD sand is therefore equal to 1000 − 744.62 = 255.38 L.

The mass of the SSD sand is 255.38 × 2.65 = 677 kg, rounded to 680 kg.

The proportions of this trial batch are shown in Table A1.15.

As mentioned earlier, the amount of superplasticizer will have to be adjusted to obtain the targeted slump.

References

Aïtcin, P.-C., 1971. Density and porosity measurements of solids. ASTM Journal of Materials 6 (2), 282−294.

Aïtcin, P.C., 1998. High Performance Concrete. E and FN SPON.

Appendix 2: Experimental statistical design

A. Yahia, P.-C. Aïtcin

Université de Sherbrooke, QC, Canada

A2.1 Introduction

The objective of an experiment is to obtain an answer to one or several questions. For example, what is the minimal dosage of superplasticizer (SP) that gives a maximum slump in order to minimize the placing costs without impairing the compressive strength of a concrete? This dosage is a function of different parameters, such as the characteristics of the cement, the type of SP, the composition of the concrete and its water/cement (w/c), etc.

But in addition to this first question, it could be also interesting to obtain an answer to the following points.

- What is the effect of a modification of the characteristics of the cement or a variation of the w/c on the optimal dosage of SP, to evaluate the robustness of this dosage?
- Is the initial slump kept long enough to give time to place this concrete easily?
- What is the optimal formulation of the concrete if its performance and robustness have to be maximized and its cost minimized?

The answer to this complex optimization process has to take into account the w/c, the type and dosage of SP, the type and the dosage of the cement, the type and dosage of the supplementary cementitious material and the interactions between these factors. Some factors can have antagonist effects – for example, when designing the composition of a self-consolidating concrete (SCC), the SP increases the slump flow (i.e. reduces the yield stress) while the viscosity modifier admixture reduces the slump flow (i.e. increases the yield stress) and increases the viscosity. The optimization of the composition of an SCC is therefore a complex exercise because a great number of factors have to be controlled, as well as their interactions. When trying to find this optimal composition by a trial-and-error method it is necessary to do a great number of tests, because in this method only one parameter at a time is varied, while all the others stay at a fixed level.

Let us take a very simple example of optimization. Let us suppose that we want to study the influence of SP dosage on the fluidity of a cement paste by measuring its flow when doing a mini-cone test. For this experimental programme the selected w/c values are 0.35 and 0.40 and the SP dosages are 0.2%, 0.4%, 0.6%, 0.8%, 1.0%, 1.2%, 1.4% and 1.6%. Figure A2.1 presents the experimental conditions of the 16 tests that have to be done (eight dosages for two different w/c ratios of 0.35 and 0.40).

Figure A2.2 shows the experimental values obtained.

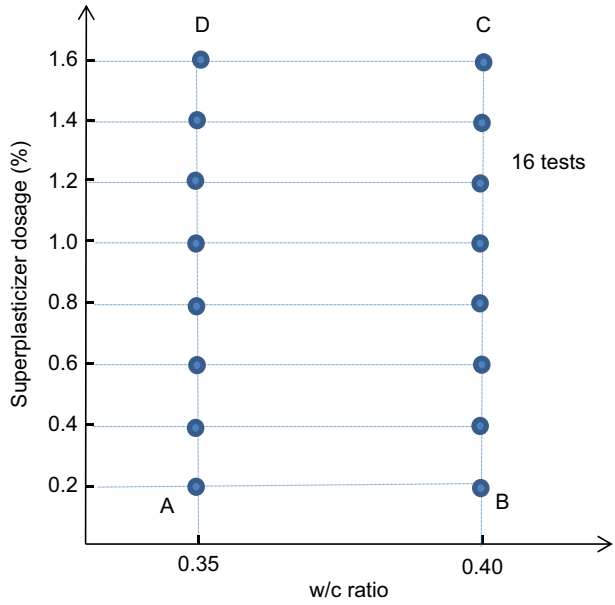


Figure A2.1 Representation of experimental conditions on the study of flow as a function of SP dosage.

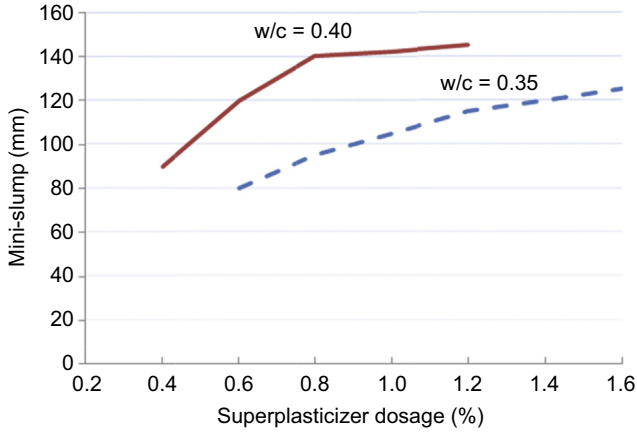


Figure A2.2 Variation of the initial flow of a cement paste as a function of its SP dosage (Yahia and Khayat, 2001).

It is seen that the 0.2% dosage was too low to obtain any flow for both w/c, even for w/c of 0.35. It was necessary to reach a dosage of 0.6% to get a measurable flow. Moreover, it is seen that for w/c of 0.40 the two dosages of 1.4% and 1.6% were too high to obtain a stable grout. Finally, the maximum flow is obtained for an optimal dosage of SP equal to 0.8% for w/c of 0.40 and 1.6% for w/c of 0.35.

But it is not known how this optimal dosage varies between these two values of the w/c or outside this range. To obtain an answer to this new question, it is necessary to do additional tests. If the flow of another w/c of 0.40 has to be studied, eight new values of the dosage of superplasticizer have to be added. This represents a total of 24 tests, as shown in Figure A2.3. In this figure, points A, B, C and D represent the limits of the new experimental domain, in which the experimental value (the response) gives the variation of the flow as a function of the SP dosage for each value of the w/c.

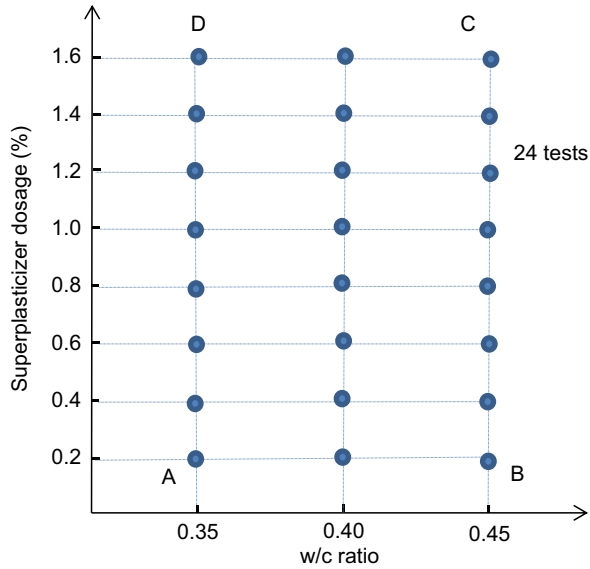


Figure A2.3 Experimental determination of the influence of SP dosage on the flow of three cement pastes with different w/c.

In spite of the fact that this experimental approach is based on a large number of tests, it does not give any answer to some other specific questions. For example, what happens if some other parameters that have been kept fixed in this study vary, and what are the new responses? Moreover, this approach does not give any idea of the interactions of the different factors that are under study.

In contrast, a statistical design method considers the variation of several factors at the same time. This method is particularly interesting because it decreases considerably the number of tests while ensuring results that are as good as or even better than in the approach presented in Figures A2.1 and A2.2 (Box et al., 1978; Montgomery, 2005; Sado and Sado, 1991; Yahia and Khayat, 2001; Khayat et al., 1999).

A2.2 Terminology

A2.2.1 Notions of factor, level of a factor and response

A **factor** is a parameter that influences the property studied, producing the **response**. This factor can influence more or less significantly the response. For example, some

significant factors currently studied when determining the optimal composition of a concrete mix are the w/c, the SP dosage, the cement type and its dosage, etc. A statistical design can be used to identify simultaneously the factors that influence the response, their level of influence and the interactions of these factors.

Two types of factors can be studied: quantitative and qualitative. A quantitative factor is measurable, while a qualitative factor is not measurable. For example, the w/c is a quantitative factor, while the type of cement or SP is a qualitative factor. The method used to analyse and interpret the responses given by these two types of factors is different when using a statistical design.

The value given to a factor in an experimental design is called its **level**. To use a statistical design, it is necessary to study at least two different levels: a minimum and a maximum (**two-level factorial plan**).

A2.2.2 Dimensionless coded values

The use of **dimensionless coded values** simplifies considerably the presentation and analysis of a statistical design method comprising two levels. Turning **absolute values** into coded values is done by changing the origin of the coordinate system and the unit on each axis. The coded values are obtained by using the following equation:

$$\text{Coded value} = \frac{\text{absolute value} - \text{value at the center}}{\frac{1}{2}(\max - \min)} \tag{A2.1}$$

As can be seen in Figure A2.4, to obtain the coded values, a value of $\mathbf{-1}$ is given to the lower level of dosage of SP and a value of $\mathbf{+1}$ to a higher level of SP dosage. For example, the middle of the intervals $\mathbf{(-1, +1)}$, that is the new origin of the coordinates, has the **absolute values of 0.425 and 0.8%**.

The new system of coordinates that will be used is presented in Figure A2.5.

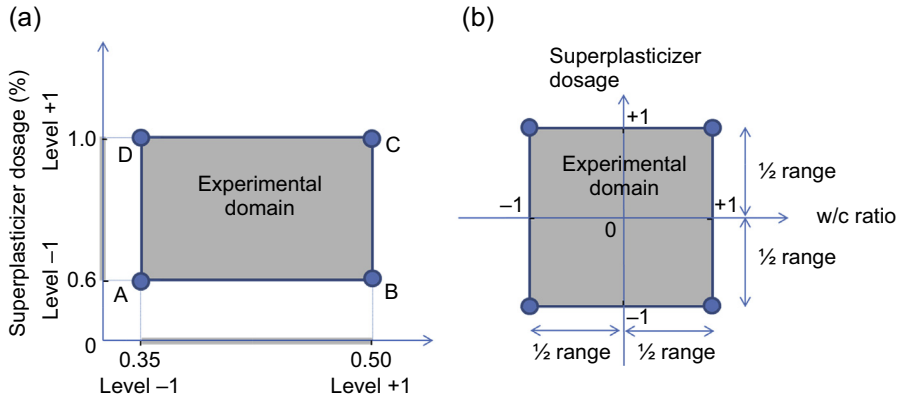


Figure A2.4 Moving from absolute values to coded values.

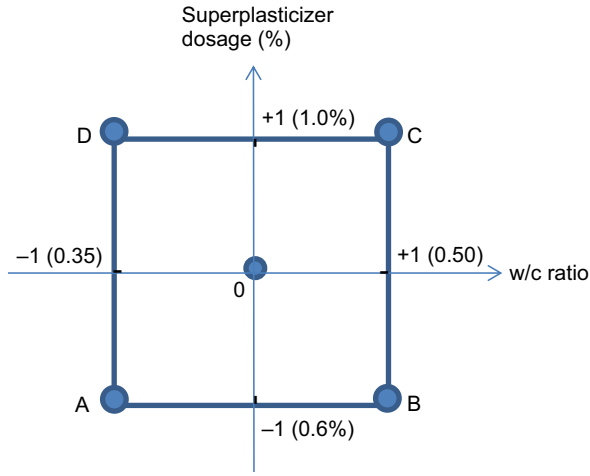


Figure A2.5 Coordinate system using coded values.

The **range** represents half the difference between the **lower level** (minimum) and the **higher level** (maximum) for each factor, as shown in Figure A2.4(b). The value of the coded value can be rewritten as follows:

$$\text{Coded value} = \frac{\text{absolute value} - \text{value at the center}}{\frac{1}{2}(\max - \min)}$$

$$= \frac{\text{absolute value} - \text{value at the center}}{\text{Range}}$$

In Table A2.1 it is possible to find the expression of the coordinates of the points A, B, C and D in the two systems.

The −1 and +1 coded values for the different factors are introduced to study the different factors with a constant amplitude of 2.0 (Box, 1978; Montgomery, 2005; Sado and Sado, 1991) whatever the magnitude of the absolute variations of the two factors under study and their nature. This mode of presentation simplifies the

Table A2.1 Coordinates of points A, B, C, D presented in Figures A2.4 and A2.5

	Absolute coordinates		Coded coordinates	
	w/c	SP (%)	w/c	SP (%)
A	0.35	0.6	−1	−1
B	0.50	0.6	+1	−1
C	0.50	1.0	+1	+1
D	0.35	1.0	−1	+1

calculation and permits a comparison of the effect of each factor and their interactions. All statistical design softwares are based on the analysis of coded values.

A2.2.3 Experimental domain

A2.2.3.1 Definition

An experimental domain can be represented in a space having a dimension equal to k, with k being the number of factors under study. In the case of two dimensions this domain is limited by the higher and lower values of each studied factor Figure A2.6:

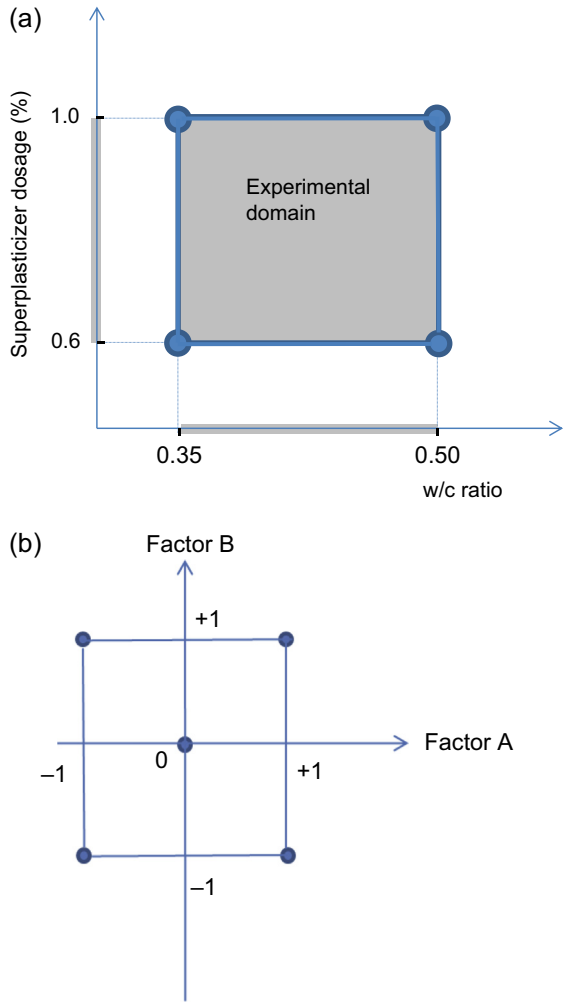


Figure A2.6 Definition of a two-dimensional experimental domain: (a) absolute values, (b) coded values.

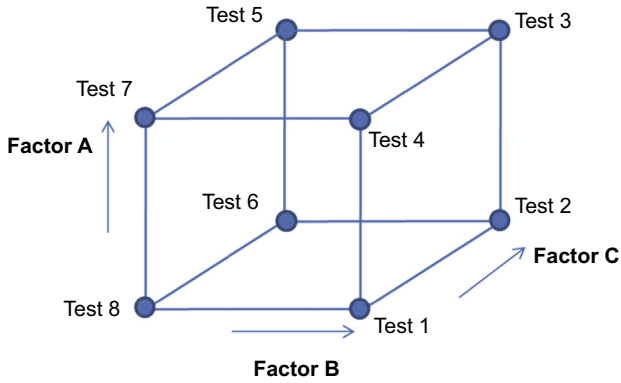


Figure A2.7 Definition of a three-dimensional experimental domain.

An experimental domain can also be defined in three dimensions, as shown in Figure A2.7.

Here we will only consider two-dimensional models.

A2.2.3.2 Selection of the experimental domain

The selection of points in the experimental domain has a direct relationship with the number of experiments to be done and the precision of the effects and their interaction. This is the most important decision when performing a statistical design, because two apparently contradictory objectives are achieved at the same time: minimizing the number of experiments and maximizing the precision obtained with the experimental values and the model. Therefore the limits of the experimental domain have to be selected so that the effects of parameters are obtained with the maximum precision possible.

A2.2.4 Application 1

A concrete producer decides to use a two-level statistical design to study the effect of the w/c and cement dosage on the rheological and mechanical properties of a concrete. The two levels of the w/c are 0.35 and 0.45, and those of the cement contents are 320 and 400 kg/m^3.

- What is the range of these two factors?
- What are the coded value of these two factors?
- What are the coded values of a concrete with a w/c of 0.38 and a cement dosage of 370 kg/m^3?

The answers are as follows.

1. The range of the factor w/c $= \frac{1}{2}(0.45 - 0.35) = 0.05$.

The range of the factor cement content $= \frac{1}{2}(400 - 320) = 40$ kg/m^3.

2. The coded values corresponding to these two factors can be calculated as follows:

$$\text{Coded value of w/c of } 0.35 = \frac{0.35 - 0.40}{\frac{1}{2}(0.45 - 0.35)} = -1$$

$$\text{Coded value of w/c of } 0.45 = \frac{0.45 - 0.40}{\frac{1}{2}(0.45 - 0.35)} = +1$$

$$\text{Coded value of cement content of } 320\ \text{kg/m}^3 = \frac{320 - 360}{\frac{1}{2}(400 - 320)} = -1$$

$$\text{Coded value of cement content of } 400\ \text{kg/m}^3 = \frac{400 - 360}{\frac{1}{2}(400 - 320)} = +1$$

3. The coded values of a concrete mixture made with a w/c of 0.38 and a cement content of 370 kg/m^3 can be calculated as follows:

$$\text{Coded value of w/c of } 0.38 = \frac{0.38 - 0.40}{\frac{1}{2}(0.45 - 0.35)} = -0.40$$

$$\text{Coded value of cement content of } 370\ \text{kg/m}^3 = \frac{370 - 360}{\frac{1}{2}(400 - 320)} = +0.25$$

A2.3 Mathematical treatment of a statistical design

A2.3.1 Expression of a response as a function of the factors and their interaction

Using a presentation based on coded values, all the statistical designs are treated mathematically in the same manner whatever are the factors and responses under study and their absolute values. All the commercial soft wares of statistical design are based on the analysis of coded values.

The response to a given **factor** is usually written as **Y**.

Each response is the result of one or several experiments. When it is the result of several experiments it is necessary to represent it by its average value. One must therefore know the experimental error for each of these responses. This value can be estimated from the standard deviation of the measured responses. Knowing this error it is also necessary to evaluate if the effect of the factor is significant or not.

The effect of a **factor** on a **response** is obtained by comparing the value of the response when the factor changes from its lower level (−1), $\mathbf{Y_1}$ to its high level (+1), $\mathbf{Y_2}$. The effect of a factor on a response can be positive, negative or neutral.

In a mathematical model describing the variation of the response as a function of the factor, the effect of a factor appears as a **coefficient of influence $\mathbf{a_i}$.** For example, when studying the slump of a concrete as a function of its **w/c** and the dosage of SP, the response *Y* can be written in the case of a linear model as:

$$\text{Slump} = a_0 + a_1 \cdot \text{w/c} + a_2 \cdot \text{SP} + a_{12} \cdot \text{w/c} * \text{SP} + E \tag{A2.2}$$

In this model coefficient $\mathbf{a_1}$ represents the influence of the **w/c**, coefficient $\mathbf{a_2}$ the effect of the **SP dosage**, $\mathbf{a_{12}}$ represents the interaction of the **two factors** and **E** the error associated with this linear model. The error indicates the validity of the model. In this particular case it is obvious that coefficients $\mathbf{a_1}$ and $\mathbf{a_2}$ are positive, because if the w/c and the SP dosage increase the slump increases.

A2.3.2 Interaction

Two factors interact if the effect of one factor depends on the level of the other. When studying the efficiency of an SP in a concrete, it is found that there is an interaction between the w/c and the SP dosage. The interaction is strong in the case of low w/c but not as strong in the case of high w/c.

A2.3.3 Validation of the model

A model has to reproduce the experimental results as precisely as possible. It is therefore necessary to validate it or reject it by making a series of experiments within the domain under study. This validation is done by reproducing the same experiment at the centre of the experimental domain several times. The centre of the experimental domain is the best place to detect any discrepancies in the linearity of the responses (Box et al., 1978). In a coded system this point corresponds to level 0 for each factor. Therefore for a response the value given by the model is equal to coefficient $\mathbf{a_0}$. It is thus only necessary to compare $\mathbf{a_0}$ with the experimental values obtained at the centre of the experimental domain. A close correspondence between these two values indicates that the model is valid.

If a linear model is not valid it will be necessary to use a non-linear model that takes into account all the quadratic effects possible. A non-linear model can be written as follows:

$$\begin{aligned}\text{Slump} = {} & a_0 + a_1 \cdot \text{w/c} + a_2 \cdot \text{SP} + a_{11} \cdot \text{w/c} * \text{w/c} + a_{22} \cdot \text{SP} * \text{SP} \\ & + a_{12} \cdot \text{w/c} * \text{SP} + E\end{aligned} \tag{A2.3}$$

The existence of a quadratic effect means that the effect of a factor on the response depends on its own level (Box et al., 1978; Montgomery, 2005; Sado and Sado, 1991). Coefficients $\mathbf{a_{13}}$, $\mathbf{a_{22}}$ and $\mathbf{a_{33}}$ traduce second-order interactions of between factors SP and w/c.

A2.3.4 Case of a first-order interaction

Let us suppose that one test has been done at the four points limiting the experimental domain in Figure A2.8 and coded values are shown in Table A2.2.

Let us say that the slump depends on the value of the w/c, the SP dosage and their interaction. We will also consider that our model introduces an error *E*.

$$\text{Slump} = a_0 + a_1 \cdot \text{w/c} + a_2 \cdot \text{SP} + a_{12} \cdot \text{w/c} * \text{SP} + E \tag{A2.4}$$

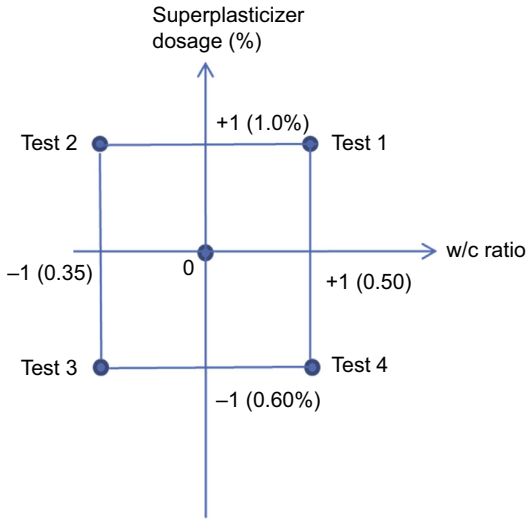


Figure A2.8 Performed tests.

Table A2.2 Experimental coded values

	SP (%)	w/c	SP × w/c	Response (Y)
Test 1	+1	+1	+1	Y_1
Test 2	−1	+1	−1	Y_2
Test 3	−1	−1	+1	Y_3
Test 4	+1	−1	−1	Y_4

Each response Y_i can be expressed as follows:

$$Y_1 = a_0 + a_1 \cdot (+1) + a_2 \cdot (+1) + a_{12} \cdot (+1) = a_0 + a_1 + a_2 + a_{12}$$
$$Y_2 = a_0 + a_1 \cdot (-1) + a_2 \cdot (+1) + a_{12} \cdot (-1) = a_0 - a_1 + a_2 - a_{12}$$
$$Y_3 = a_0 + a_1 \cdot (-1) + a_2 \cdot (-1) + a_{12} \cdot (+1) = a_0 - a_1 - a_2 + a_{12}$$
$$Y_4 = a_0 + a_1 \cdot (+1) + a_2 \cdot (-1) + a_{12} \cdot (-1) = a_0 + a_1 - a_2 - a_{12}$$

To calculate the effects (i.e. the coefficients $\mathbf{a_i}$) of these two factors, it is necessary to solve a system of four linear equations. The matrix of effects (A), the response column (Y) and the vector of coefficients ($\mathbf{a_i}$) is defined as follows:

$$A = \begin{bmatrix} 1 & 1 & 1 & 1 \\ 1 & -1 & 1 & -1 \\ 1 & -1 & -1 & 1 \\ 1 & 1 & -1 & -1 \end{bmatrix}, \quad Y = \begin{bmatrix} Y_1 \\ Y_2 \\ Y_3 \\ Y_4 \end{bmatrix}, \quad \text{and } a = \begin{bmatrix} a_0 \\ a_1 \\ a_2 \\ a_3 \end{bmatrix}$$

$$\begin{bmatrix} 1 & 1 & 1 & 1 \\ 1 & -1 & -1 & 1 \\ 1 & 1 & -1 & -1 \\ 1 & -1 & 1 & -1 \end{bmatrix} \begin{bmatrix} 1 & 1 & 1 & 1 \\ 1 & -1 & 1 & -1 \\ 1 & -1 & -1 & 1 \\ 1 & 1 & -1 & -1 \end{bmatrix} = 4 \begin{bmatrix} 1 & 0 & 0 & 0 \\ 0 & 1 & 0 & 0 \\ 0 & 0 & 1 & 0 \\ 0 & 0 & 0 & 1 \end{bmatrix} = 4I$$

where, $I = \begin{bmatrix} 1 & 0 & 0 & 0 \\ 0 & 1 & 0 & 0 \\ 0 & 0 & 1 & 0 \\ 0 & 0 & 0 & 1 \end{bmatrix}$ is the identity matrix.

A2.3.5 Criterion of optimality

The criterion of optimality is based on the minimal Cauchy-Schwartz standard deviation for N experiments. According to Hadamard (Box et al., 1978), this criterion is met if the transposed matrix of matrix A satisfies the following equation:

$$A^{\mathrm{T}}A = N\,\mathbf{I}$$

where A^{T} is the transposed matrix of matrix A, N is the number of experiments and I is the identity matrix.

In the case of two factors with two levels it is easy to verify that:

$$\begin{bmatrix} 1 & 1 & 1 & 1 \\ 1 & -1 & -1 & 1 \\ 1 & 1 & -1 & -1 \\ 1 & -1 & 1 & -1 \end{bmatrix} \begin{bmatrix} 1 & 1 & 1 & 1 \\ 1 & -1 & 1 & -1 \\ 1 & -1 & -1 & 1 \\ 1 & 1 & -1 & -1 \end{bmatrix} = 4 \begin{bmatrix} 1 & 0 & 0 & 0 \\ 0 & 1 & 0 & 0 \\ 0 & 0 & 1 & 0 \\ 0 & 0 & 0 & 1 \end{bmatrix} = 4\,\mathbf{I}$$

Different commercial softwares are available to solve the system of equations corresponding to the experimental plan, draw iso-response curves and provide the degree of validity of the mathematical models in the experimental domain. In the following application, a statistical approach consisting in a linear model is illustrated (application 2). Statistical models have been used by Khayat et al., 1995; Nehdi et al., 1997; Yahia, 1997 for example.

A2.3.6 Application 2

A2.3.6.1 Influence of the w/c and water dosage on the SP dosage of an HPC

A two-level factorial design was carried out to evaluate the influence of w/c and water dosage (W) and their second-order interactions on SP dosage to achieve a given slump

Table A2.3 Coded and absolute values of the modelled factors

Coded values			
Variables	−1	0	+1
w/c	0.25	0.28	0.31
Water content (l/m^3)	130	140	150

and compressive strength at various ages of a high-performance concrete (HPC). This example was reported in Rougeron and Aïtcin (1994). The effect of each factor is evaluated at three different levels corresponding to coded values of −1, 0 and +1. The corresponding absolute values of the modelled factors are summarized in Table A2.3. In the case of two independent variables, a two-level factorial design consists of four ($N_f = 2^2 = 4$) factorial points, and three replicate points at the centre of the experimental domain to estimate the degree of experimental error for the modelled responses and evaluate the linearity assumptions.

The derived statistical models are valid for HPC mixtures with proportions of w/c of 0.22 (−1) to 0.31 (+1) and water content of 130 (−1) to 150 l/m^3 (+1). The central point was a mixture where variables were equal to the middle-level value corresponding to w/c of 0.28 and water content of 140 l/m^3. The modelled responses are SP dosages to achieve a slump of 200 ± 20 mm. Compressive strength at 1 ,7 and 28 days of age were measured in each case.

The modelled experimental region consisted of coded values ranging between −1.0 and +1.0. The coded and absolute values of the modelled variables (PV/IPV, w/c and WRA) are summarized in Table A2.3.

The mixture proportions and test results used to model the linear effect of w/c and water content on properties of HPC mixtures are summarized in Table A2.4.

A2.3.6.2 Results and discussion

Table A2.5 summarizes the test results for mixtures used to establish statistical models describing the effect of independent variables w/c and water content on SP dosage and the mechanical properties of HPC mixtures.

The derived models for SP dosage, compressive strength at 1, 7, and 28 days are given in Table A2.6. These equations were determined based on a multi-regression analysis.

The above models are established using coded values of independent variables calculated using Eqn (A2.1). A negative estimate of a given parameter indicates that the response decreases when the value of that parameter increases. The majority of derived estimates were obtained with 90% confidence interval.

A quantitative evaluation of the accuracy of the derived models is investigated on three mixtures located at the centre of the experimental domain to compare the measured responses to those estimated using the established models. The experimental responses measured at the centre of the domain for SP, compressive strengths after 1, 7, and 28 days, is 13 L/m^3, 36.2, 64.2 and 86.5 MPa, respectively. The corresponding

Table A2.4 **Mixture proportioning and test results of the investigated HPC mixtures**

Mixture proportions								
				Cement	Sand	Aggregate		
Mix	Coded value w/c-w	w/c	Water (l/m^3)	(kg/m^3)			SP (l/m^3)	Slump (mm)
1	−1 −1	0.25	130	520	710	1100	25	210
2	−1 +1	0.25	150	600	630	1100	19	200
3	+1 −1	0.31	130	420	798	1100	12	200
4	+1 +1	0.31	150	485	720	1100	10	180
5	0 0	0.28	140	500	720	1100	13	200
6	0 0	0.28	140	500	720	1100	13	200
7	0 0	0.28	140	500	720	1100	13	200

Table A2.5 Test results for HPC mixtures used to establish statistical models

Mixture proportions				Compressive strength (MPa)		
Mix	Coded value w/c − w	w/c	Water (l/m^3)	1 day	7 days	28 days
1	−1 −1	0.25	130	41.5	66.8	80.0
2	−1 +1	0.25	150	45.0	61.2	80.8
3	+1 −1	0.31	130	33.7	54.5	69.6
4	+1 +1	0.31	150	36.5	66.5	69.0
5	0 0	0.28	140	36.2	64.2	86.5
6	0 0	0.28	140	36.2	64.2	86.5
7	0 0	0.28	140	36.2	64.2	86.5

Table A2.6 Derived statistical models

Properties		Statistical model	R^2
SP dosage (l/m^3)		15.0 − 5.5 w/c − 2.0 water + 1.0 w/c × water	0.870
Compressive strength (MPa)	1 day	38.0 − 4.1 w/c + 1.6 water	0.862
	7 days	61.8 − 1.8 w/c + 1.6 water (w/c) + 4.4 w/c × water	0.978
	28 days	74.6 − 5.6 w/c	0.994

predicted values are 15.0 l/m^3 for SP demand and 38.0, 61.8 and 74.6 MPa for compressive strength after 1, 7, and 28 days, respectively. The established models predict the SP demand with an error of approximately 15%, and compressive strength after 1, 7, and 28 days with errors of 5%, 4% and 16%, respectively. These models can therefore predict the modelled responses with a reasonable error ranging between 4% and 16%. The models can be extended to include the quadratic effect and improve their accuracy. In this case, a composite design should be carried out, including extra mixtures to extend the experimental domain.

A2.3.6.3 Exploitation of the model

The established models can be used to visualize the effect of modelled parameters, facilitate HPC mixture design and strike a trade-off among mixture parameters to achieve the targeted properties of HPC.

For example, Figures A2.9 and A2.10 give the iso-response curves for the SP dosage and the 1-day compressive strength as a function of the w/c and water dosage.

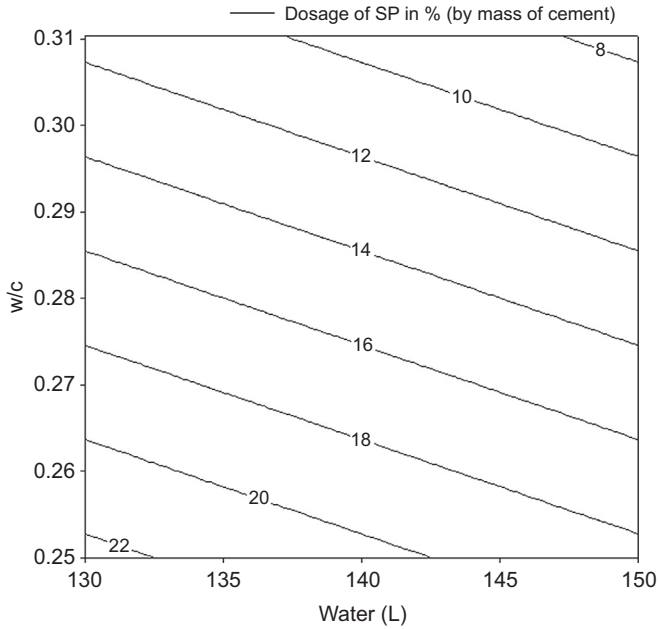


Figure A2.9 Iso-response of SP dosage with w/c and water content. Rougeron and Aïtcin (1994).

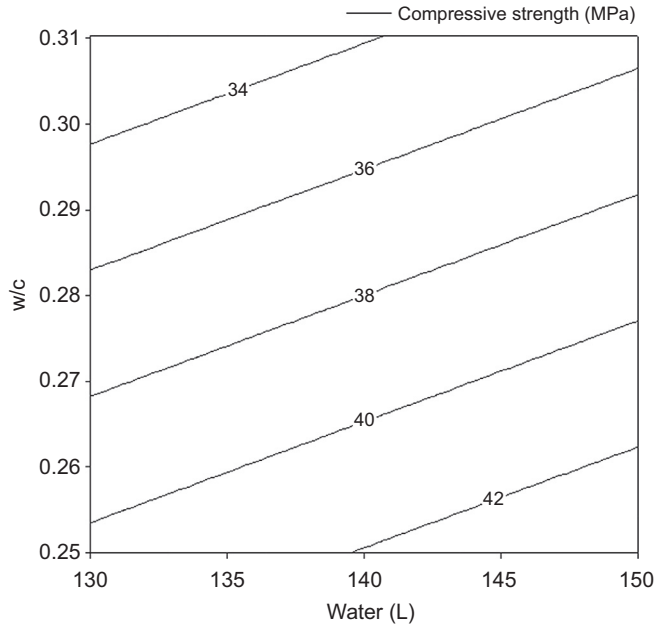


Figure A2.10 Iso-response of 1 day compressive strength with w/c and water content.

It is seen for example that a 40 MPa compressive strength concrete can be obtained with a w/c of 0.22 and a water dosage of 130 l/m^3, or with a w/c of 0.273 and a water dosage of 150 l/m^3. According to Figure A2.10, in the first case the SP dosage is about 22 l/m^3 while in the second case it is about 15 l/m^3. This second mix is more economical than the first one.

A2.4 Conclusion

Statistical design is a powerful tool when studying the interaction of Portland cement and admixtures in Portland-cement-based materials. It can be used to establish the trade-off between significant factors and achieve targeted properties for a given set of constraints while minimizing the number of trial batches. Furthermore, using this approach a mathematical model describing the main influence and second-order interaction of various parameters on a given property can be established. However, a critical step when using a statistical design is the selection of the experimental domain to be studied, and it is part of the art of the researcher to define it properly. The different softwares presently available on the market are not complicated to use after a familiarization period.

References

Box, E.P., Hunter, W.G., Hunter, J.S., 1978. Statistics for Experimenters: An Introduction to Design, Data Analysis, and Model Building. In: Wiley Series in Probability and Mathematical.

Khayat, K.H., Sonebi, M., Yahia, A., Skaggs, B.C., 1995. Statistical models to predict flowability, washout resistance, and strength of underwater concrete. In: RILEM International Conference on Production Methods and Workability of Concrete, Glasgow, pp. 463–481.

Khayat, K.H., Yahia, A., Sonebi, M., 1999. Application of statistical models for proportioning underwater concrete. ACI Materials Journal 96 (6), 634–640.

Montgomery, D.C., 2005. Design and Analysis of Experiments, sixth ed. John Wiley & Sons.

Nehdi, M., Mindess, S., Aïtcin, P.-C., 1997. Statistical modelling of the microfiller effect on the rheology of composite cement pastes. Advances in Cement Research 9 (33), 37–46.

Rougeron, P., Aitcin, P.-C., December 1994. Optimization of the composition of a high-performance concrete. Cement Concrete and Aggregate, CCAGPD 16 (2), 115–124.

Sado, G., Sado, M.C., 1991. Experimental Design: From Experience to Quality Assurance (Available in French), second ed. AFNOR. 265 pp.

Yahia, A., 1997. Rheology and Performance of Cement-based Materials for Underwater Structures Repair (Available in French). Ph.D. dissertation. Université de Sherbrooke, 213 pp.

Yahia, A., Khayat, K.H., 2001. Experiment design to evaluate interaction of high-range water-reducer and anti-washout admixtures in high-performance cement grout. Cement and Concrete Research Journal 31 (5), 749–757.

Appendix 3: Statistical evaluation of concrete quality*

P.-C. Aïtcin

Université de Sherbrooke, QC, Canada

A3.1 Introduction

In spite of all the attention paid to controlling the variability of the materials used to make concrete, weighing or metering these materials in sophisticated automated installations and testing the concrete according to precise and stringent standards, concrete remains a material made and tested by humans, and whose properties are affected by ambient temperature over which we have no control. Therefore concrete is variable. Thus we must still ask various questions.

- How variable is it?
- How is it possible to reduce this variability?
- How can we be sure that this variability does not affect the safety of the structure?

These aspects of concrete require some statistical treatment. It is the objective of this appendix to present some basic and practical notions that are commonly used when establishing statistical control over any concrete production (Valles, 1972; Day, 1995; Schrader, 2007). This subject is often not well covered in concrete courses.

A3.2 Normal frequency curve

A3.2.1 Variability of concrete properties

When measuring any particular characteristic of concrete, the numerical value obtained at the end of the control process depends on a large number of factors that are independent of each other and whose variation is limited.

In such a case statisticians tell us that the numerical values obtained obey a normal frequency distribution law, also called a 'normal law' or 'Laplace-Gauss law', whose graphical representation is the well-known bell-shaped curve (Figure A3.1).

In spite of the fact that the normal frequency curve implies an infinite number of values, it is very useful to know its properties when dealing with the numerical values of a limited number of tests carried out on a selected number of specimens among a finite population corresponding to the number of the concrete deliveries that have been tested. Consequently, it is useful to look at this general law and apply some of its properties to the statistical control of concrete production.

* Aïtcin, P.C., Mindess S., Sustainability of Concrete, ISBN 978-0-415-57196-8, SPON PRESS.

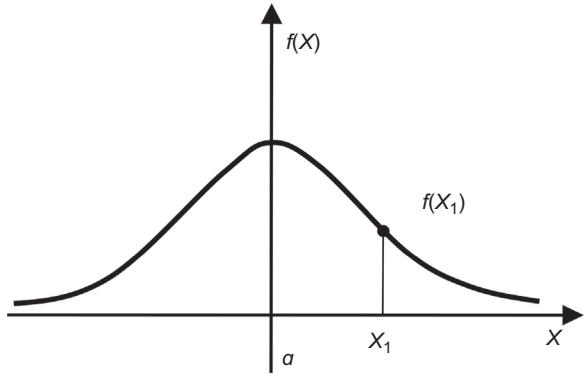


Figure A3.1 Normal frequency distribution curve: the y axis is placed at the average value, a, and $f(x_1)$ represents the number of samples with the value x_1.

A3.2.2 Mathematical expression of the normal frequency curve

The probability density $f(x)$ for each value X of a characteristic is:

$$f(x) = \frac{1}{\sigma\sqrt{2\pi}} \cdot e^{\frac{-(x-a)^2}{2\sigma^2}} \tag{A3.1}$$

where 'a' represents the average value, σ^2 represents the variance and σ represents the standard deviation. Usually, instead of using X, it is better to use the reduced centre value:

$$x = \frac{X - a}{\sigma}$$

In this case, the origin of the abscissa is the average value, a, and the values are measured with units equal to the standard deviation. Equation (A3.1) then becomes:

$$f(x) = \frac{1}{\sqrt{2\pi}} \cdot e^{\frac{-x^2}{2}} \tag{A3.2}$$

Equation (A3.2) gives the bell-shaped curve that is represented in Figure A3.2.

A3.2.3 Some properties of the normal frequency curve

A normal frequency curve corresponding to an infinite number of values is entirely defined when we know the average value, a, and the standard deviation, s. The average value gives the position of the axis of symmetry of the normal frequency curve on the O-x axis, and the standard deviation gives the general shape of the curve: the smaller the standard deviation, the sharper the curve. In fact, the standard deviation represents the abscissa of the two inflection points on the bell-shaped curve and at the same time the radius of curvature at the top of the curve, as shown in Figure A3.2.

Figure A3.3 shows two normal frequency curves with the same average value but different standard deviations. In the case of the normal frequency curve (I)

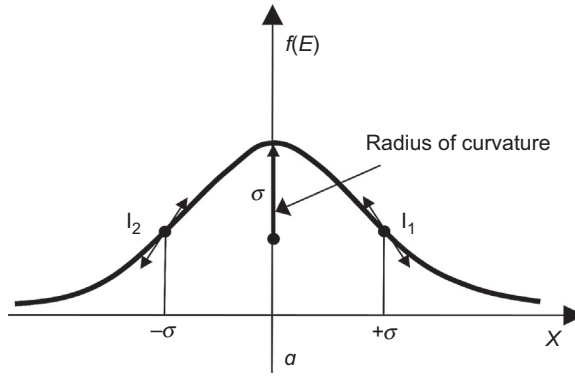


Figure A3.2 Some properties of the bell-shaped curve I_1 and I_2 are the inflection points.

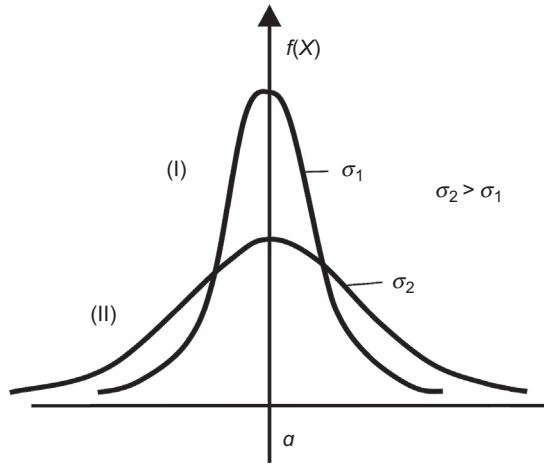


Figure A3.3 Comparison of two bell-shaped curves with the same average value but different standard deviation.

corresponding to the lower standard deviation, most of the x values are close to the average value. In the case of the normal frequency curve (II), the values of x are spread over a greater distance from the average value.

A3.2.4 Areas under the normal frequency curve

As seen in Figure A3.4, the area under the curve lying between:

- σ and $-\sigma$ is equal to 68.2% of the total area beneath the bell-shaped curve
- 2σ and -2σ is equal to 95.2%
- 3σ and -3σ is equal to 99%.

In Figure A3.5 the area under the curve to the left of x_1 represents the number of values lower than x_1. Tables giving the area to the left of x_1 are available: they give the probability of having a value of $f(x)$ lower than x_1.

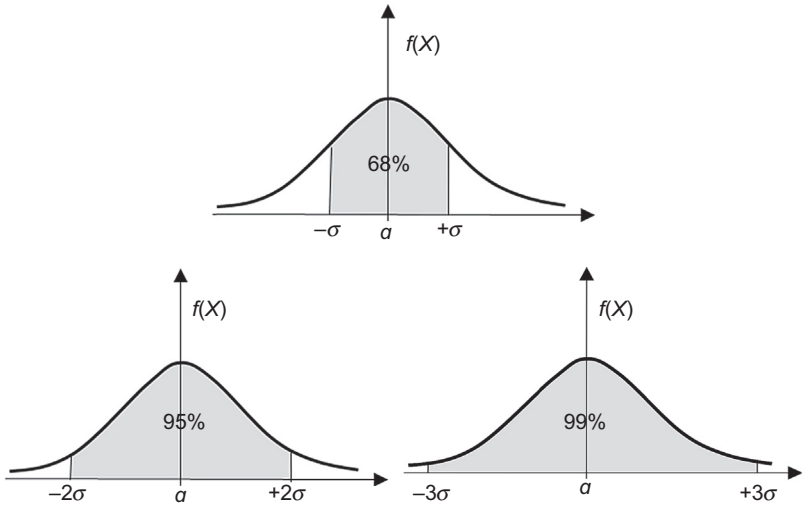


Figure A3.4 Areas under the normal frequency curve for specific values of σ.

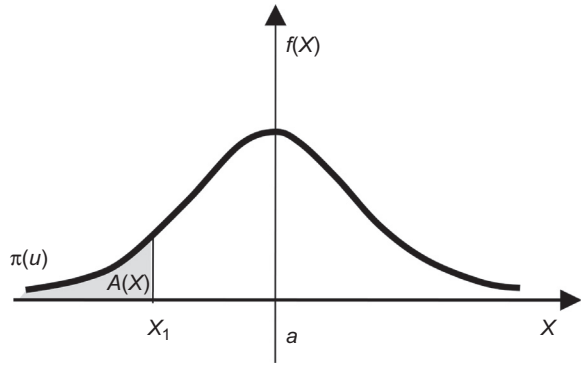


Figure A3.5 When compared to the total area under the bell-shaped curve, the area $A(x)$ at the left of x_1 represents the percentage of the values with a value smaller than x_1.

A3.2.5 Coefficient of variation

The coefficient of variation, V, expressed as a percentage, is frequently used to characterize the shape of a distribution curve. It is calculated as follows:

$$V = \frac{\sigma}{A} \times 100\% \tag{A3.3}$$

A3.3 Controlling the quality of concrete production

Generally, concrete quality is tested by measuring the compressive strength of two or three specimens. When controlling concrete production, it is not practical to measure the compressive strength of each truckload; control is instead carried out on a limited number of loads, chosen using a random number table. To carry out a useful statistical analysis, it is necessary to have at least 30 individual results. However, before doing any calculations on values obtained when carrying out this control, it is important to check that this set of results has a distribution approaching that of a normal distribution curve.

A3.3.1 Histogram

The numerical values are separated in different classes, the number of tests falling within each class is counted and a histogram is drawn (Figure A3.6). When preparing the histogram, it is important to select carefully the value of the unit cell in which the numerical values are classified. When testing concrete strength, it is usually convenient to use a unit cell corresponding to 2 MPa. Usually, when characterizing concrete compressive strength, the histograms obtained have a shape that looks roughly like a normal distribution curve, as seen in Figure A3.6, but there are some cases in which the shape can be quite different, as seen in Figure A3.7.

In the two cases presented in Figure A3.7, it is not sensible to calculate an average value and a standard deviation because the sets of values obtained cannot be fitted with normal distribution curves. In fact, the curve fitting the histogram in Figure A3.7(a) corresponds to a mixture of two populations with average values of a_1 and a_2. Each of these populations can be fitted by two separate normal distribution curves, as shown in Figure A3.8. Figure A3.7(b) shows a truncated bell-shape curve where the lowest values have been systematically eliminated.

Only when it has been verified that the set of values can be fitted with a normal distribution curve can average and standard deviation values be calculated, and the result compared to the values appearing in Table A3.1.

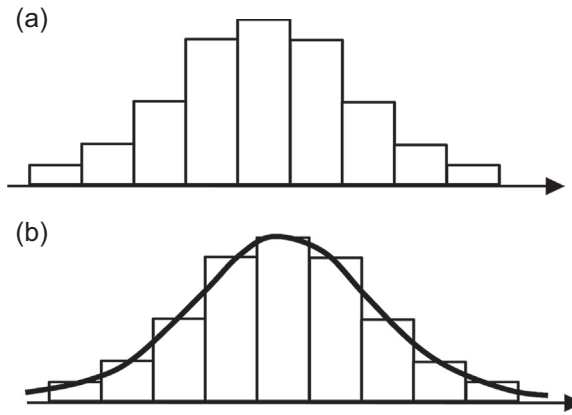


Figure A3.6 Histograms: (a) histogram (b) histogram with a fitted distribution curve.

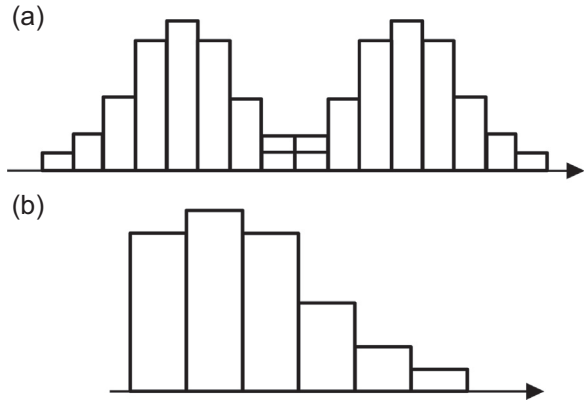


Figure A3.7 Examples of histograms that cannot be fitted by a bell-shaped curve: (a) a mix of two sets of values each obeying a normal distribution curve (b) a skewed distribution showing that low values have been eliminated.

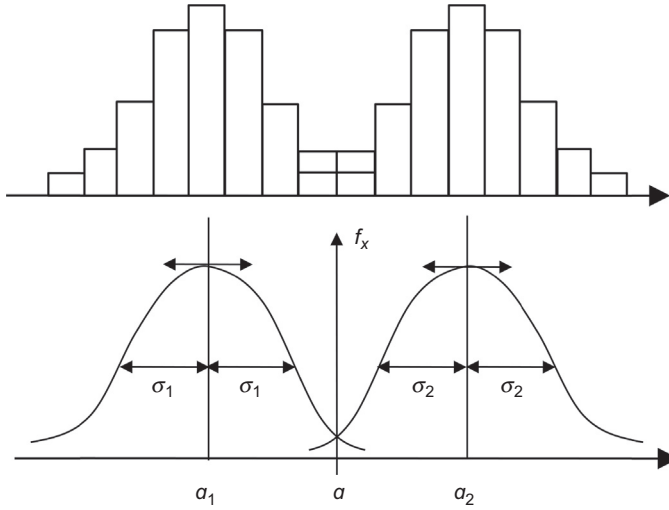


Figure A3.8 Decomposition of Figure A3.7(a) into two mixed populations.

A3.3.2 Within-test variation

When comparing the two individual values obtained from the tested specimens representing a particular load of concrete of the same age, it is possible to extend the statistical analysis. In a perfect world, these values should be identical because they are obtained from a unique concrete. However, the non-homogeneity of the concrete

Table A3.1 Factors for computing within-test standard deviation*

Number of specimens	d_2	$1/d_2$
2	1.128	0.8865
3	1.693	0.5907
4	2.059	0.4857
5	2.326	0.4299
6	2.534	0.3946
7	2.704	0.3698
8	2.847	0.3512
9	2.970	0.3367
10	3.078	0.3249

* Table B2, ASTM Manual on Quality Control of Materials, ASTM (2002).

load, the variation in the individual sampling process, and the transportation and curing of the specimens usually make the individual values different. It is possible to treat the difference between a pair of specimens as a set of statistical data, and calculate in each case the range in which these different individual values fall. From this new set of data, it is possible to calculate the within-test standard deviation:

$$\sigma_1 = \frac{1}{d_2} \times \overline{R} \tag{A3.4}$$

where σ_1 is the within-test standard deviation, d_2 is a constant depending on the number of specimens averaged to calculate a test value (given by ACI 214 Table 3.4.1, reproduced in Table 14.1) and R is the average range within groups of companion cylinders. One can also calculate the within-test coefficient of variation:

$$V_1 = \frac{\sigma_1}{\overline{x}} \times 100 \tag{A3.5}$$

where V_1 is the within-test coefficient of variation and x is the average value. The σ_1 and V_1 values can be used as an indication of the quality of testing. If σ_2 is the batch-to-batch coefficient of variation, the overall standard deviation 's' and the within-test standard deviation σ_1 are linked by the relationship:

$$\sigma = \sigma_1^2 + \sigma_2^2 \tag{A3.6}$$

A3.3.3 Sample calculation

The 28-day compressive strengths of concrete for a particular construction project have been determined 35 times on sets of two specimens. The results obtained are

Table A3.2 **Experimental results**

	1	**2**	**3**	**4**	**5**	**6**	**7**	**8**	**9**	**10**
1	58.5	64.9	65.0	60.1	64.7	65.0	63.8	64.7	64.7	61.1
2	58.2	64.8	65.3	60.5	65.9	65.4	66.6	65.5	64.2	61.9
	11	**12**	**13**	**14**	**15**	**16**	**17**	**18**	**19**	**20**
1	62.7	68.2	64.6	66.7	63.9	67.2	67.6	68.7	59.3	59.5
2	59.8	69.8	65.2	67.9	64.1	67.2	67.4	67.8	59.7	59.8
	21	**22**	**23**	**24**	**25**	**26**	**27**	**28**	**29**	**30**
1	55.9	61.3	60.6	63.6	63.3	62.7	63.5	63.0	62.2	63.7
2	56.4	66.0	60.5	63.6	63.5	62.5	63.5	63.4	62.7	63.9
	31	**32**	**33**	**34**	**35**					
1	66.4	56.9	63.2	65.4	62.9					
2	66.9	57.1	63.4	65.1	63.5					

shown in Table A3.2. The calculations are carried out up to two digits after the decimal point.

- Draw the frequency distribution of the average values using a 2 MPa unit cell.
- Does the population of the average values correspond to a normal distribution curve?
- How do the average compressive strength, standard deviation and coefficient of variation vary as the test programme goes on?
- Using Table A3.2, how can you assess the quality control of this production of concrete?
- What are the average range and the within-test standard deviation and coefficient of variation?

How can you assess the control of the testing?

A3.3.4 Discussion of results

The results shown in Tables A3.3−A3.5 can be obtained easily, for instance by using an Excel program.

Figure A3.9 shows the variation of the strength measured as the average of the two individual specimens of each set. It shows that despite all the care taken when producing this concrete, the results obtained in the field present a certain variability. This variability depends not only on the variability of the concrete but also on the variability of the testing.

Figure A3.10 shows that the frequency distribution of the strengths has (approximately) the characteristic bell-shape of the normal distribution law. **Thus it is legitimate to calculate the standard deviation and coefficient of variation of the test results**.

Figures A3.11−A3.13 show the variations of the average strength, standard deviation and coefficient of variation respectively. It can be seen that after sample 21 these values are quite stable. (ACI 214 recommends at least 30 samples to obtain an average value of statistical validity.)

With a standard deviation and a coefficient of variation of 3.8 MPa and 4.5%, respectively, according to Table A3.6 the production and its control may be classified as 'good'.

Figure A3.14 represents the variation of the range and Figure A3.15 the within-test standard deviation.

Figures A3.16 and A3.17 represent the within-test standard variation and coefficient of variation. Here, too, it is seen that with 35 samples, stable values are obtained.

A3.4 Specifying concrete compressive strength

Concrete must be specified on a statistical basis. It is not realistic or sensible to write a specification such as 'the concrete must *always* have a compressive strength greater than *X* MPa' because it is statistically impossible to produce such a concrete. A specification must always identify clearly how many times it is allowable for the value obtained to be lower than *X*. It might be 10% of the time, 5% or 1% of the time, depending on the degree of severity selected by the specifier. In any case, the specifier

Table A3.3 Average values and range

	1	**2**	**3**	**4**	**5**	**6**	**7**	**8**	**9**	**10**
$\overline{X}$	58.35	64.85	65.15	60.30	65.30	65.20	62.90	65.10	64.45	61.5
R	0.3	0.1	0.3	0.4	1.2	0.4	0.6	0.8	0.5	0.8
	11	**12**	**13**	**14**	**15**	**16**	**17**	**18**	**19**	**20**
$\overline{X}$	61.25	69.00	64.90	67.30	64.00	67.20	67.50	68.00	59.50	59.65
R	2.9	1.6	0.6	1.2	0.2	0.0	0.2	0.4	0.4	0.3
	21	**22**	**23**	**24**	**25**	**26**	**27**	**28**	**29**	**30**
$\overline{X}$	56.15	63.65	60.70	63.60	63.40	62.60	63.50	63.20	62.45	63.80
R	0.5	4.7	0.2	0.0	0.2	0.2	0.0	0.4	0.5	0.2
	31	**32**	**33**	**34**	**35**					
$\overline{X}$	66.85	57.00	63.30	65.25	63.20					
R	0.5	0.2	0.2	0.3	0.6					

Table A3.4 Average strength, cumulative average, standard deviation and coefficient of variation

#	Average value (MPa)	Average (MPa)	Standard deviation σ (Mpa)	Coefficient of variation V (%)
1	58.35	–	–	–
2	64.85	61.60	3.25	5.3
3	65.15	62.78	2.84	4.5
4	60.30	62.16	2.56	4.1
5	65.30	62.79	2.55	4.1
6	65.20	63.19	2.45	3.9
7	62.90	63.15	2.24	3.5
8	65.10	63.39	2.17	3.4
9	64.45	63.51	2.06	3.2
10	61.50	63.31	2.03	3.2
11	61.25	63.12	2.02	3.2
12	69.00	63.61	2.52	4.0
13	64.90	63.71	2.43	3.8
14	67.30	63.97	2.51	3.9
15	64.00	63.97	2.42	3.8
16	67.20	64.17	2.47	3.8
17	67.50	64.37	2.51	3.9
18	68.00	64.57	2.58	4.0
19	59.50	64.30	2.75	4.3
20	59.65	64.07	2.86	4.5
21	56.15	63.69	3.26	5.1
22	63.65	63.69	3.18	5.0
23	60.70	63.56	3.17	5.0
24	63.60	63.56	3.10	3.9
25	63.40	63.56	3.03	4.8
26	62.60	63.52	2.98	4.7
27	63.50	63.52	2.92	4.6
28	63.20	63.51	2.86	4.5
29	62.45	63.47	2.82	4.4

Continued

Table A3.4 Continued

#	Average value (MPa)	Average (MPa)	Standard deviation σ (Mpa)	Coefficient of variation V (%)
30	63.80	63.48	2.77	4.4
31	66.65	63.58	2.78	4.4
32	57.00	63.38	2.97	4.7
33	63.30	63.38	2.92	4.6
34	65.25	63.43	2.89	4.6
35	63.20	63.42	2.85	4.5

Table A3.5 Within-test variation

Within-test variations				
#	Range (MPa)	Average range (MPa)	Standard deviation σ (MPa)	Coefficient of variation V (%)
1	0.30	–	–	–
2	0.10	0.20	0.18	0.27
3	0.30	0.23	0.21	0.32
4	0.40	0.28	0.24	0.40
5	1.20	0.46	0.41	0.62
6	0.40	0.45	0.40	0.61
7	0.60	0.47	0.42	0.66
8	0.80	0.51	0.45	0.70
9	0.50	0.51	0.45	0.70
10	0.80	0.54	0.48	0.78
11	2.90	0.75	0.67	1.09
12	1.60	0.83	0.73	1.06
13	0.60	0.81	0.72	1.10
14	1.20	0.84	0.74	1.10
15	0.20	0.79	0.70	1.10
16	0.00	0.74	0.66	0.98
17	0.20	0.71	0.63	0.93
18	0.40	0.69	0.62	0.91

Table A3.5 Continued

Within-test variations				
#	Range (MPa)	Average range (MPa)	Standard deviation σ (MPa)	Coefficient of variation V (%)
19	0.40	0.68	0.60	1.01
20	0.30	0.66	0.59	0.98
21	0.50	0.65	0.58	1.03
22	4.70	0.84	0.74	1.16
23	0.20	0.81	0.72	1.18
24	0.00	0.78	0.69	1.08
25	0.20	0.75	0.67	1.05
26	0.20	0.73	0.65	1.03
27	0.00	0.70	0.62	0.98
28	0.40	0.69	0.61	0.97
29	0.50	0.69	0.61	0.97
30	0.20	0.67	0.59	0.93
31	0.50	0.66	0.59	0.88
32	0.20	0.65	0.58	1.01
33	0.20	0.64	0.56	0.89
34	0.30	0.63	0.56	0.85
35	0.60	0.63	0.55	0.88

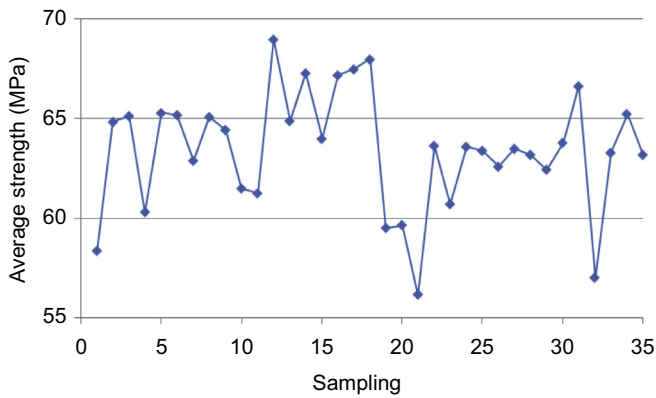


Figure A3.9 Average strength of the samples.

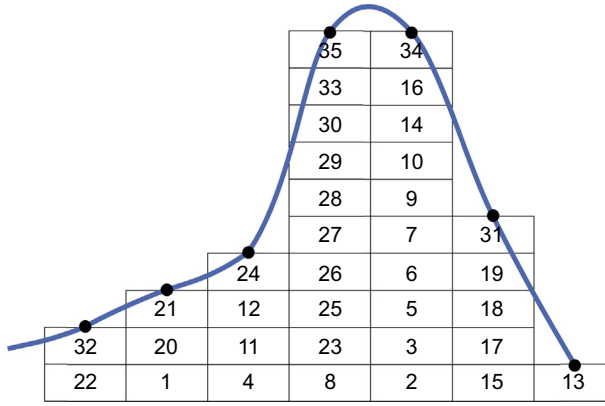


Figure A3.10 Histogram of compressive strengths.

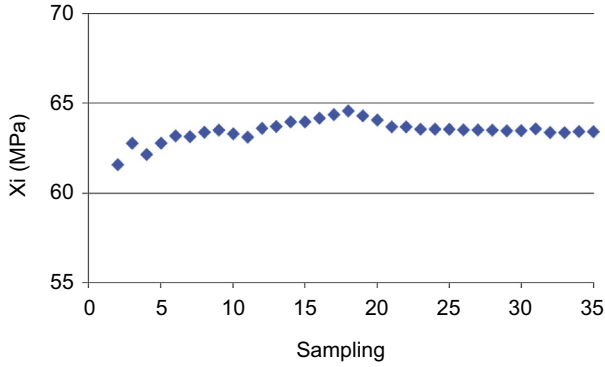


Figure A3.11 Variation of the average strength.

must accept that a limited number of test specimens might be lower than the value of X selected for the design.

The second very important point that must be specified is the number of samples that will be tested. Again, it is not practical to test all the batches to calculate the true average strength and standard deviation. Only a limited number of batches will be tested, but how many?

ACI 214 suggests that to make a 'satisfactory' statistical analysis it is necessary to have at least 30 samples, so that the average value and standard deviation calculated from this limited number of samples are representative of the actual average and standard deviation of the whole production. Statisticians tell us that the population of the average values calculated from a limited number of samples obeying a normal

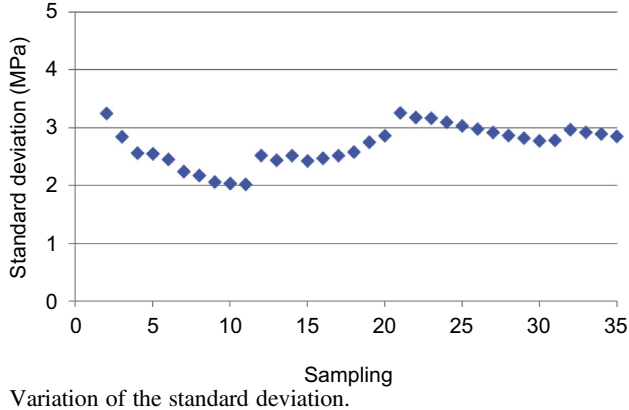


Figure A3.12 Variation of the standard deviation.

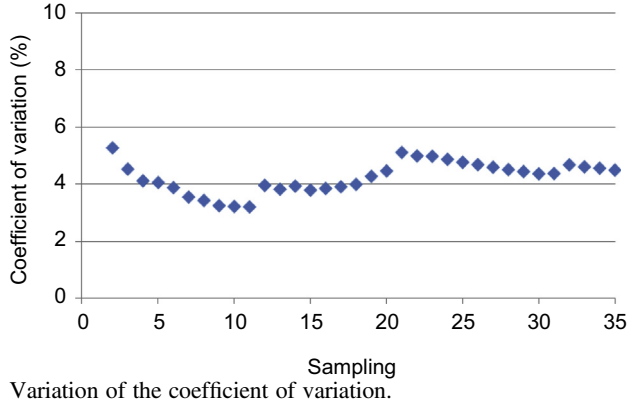


Figure A3.13 Variation of the coefficient of variation.

distribution generates normal distribution curves. Thus the smaller the standard deviation of the actual population, the greater the chance that the average value and standard deviation estimated from a limited number of samples will be closer to the actual average value and standard deviation of the entire population.

A3.5 Limitations of a statistical analysis

It is important to realize that a statistical analysis of concrete production can result in an incorrect evaluation of its conformity to the specification because a statistical analysis

Table A3.6 Standard deviation and coefficient of variation according to ACI 214

Overall variation					
	Standard variation for different control standards (MPa)				
Class of operation	**Excellent**	**Very good**	**Good**	**Fair**	**Poor**
General construction	Below 2.8	2.8−3.4	3.4−4.1	4.1−4.8	Above 4.8
Laboratory and batching	Below 1.4	1.4−1.7	1.7−2.1	2.1−2.4	Above 2.4
	Within-test variation				
Class of operation	**Coefficient of variation for different control standards (%)**				
Field control testing	Below 3.0	3.0−4.0	4.0−5.0	5.0−6.0	Above 6.0
Laboratory trial batches	Below 2.0	2.0−3.0	3.0−4.0	4.0−5.0	Above 5.0

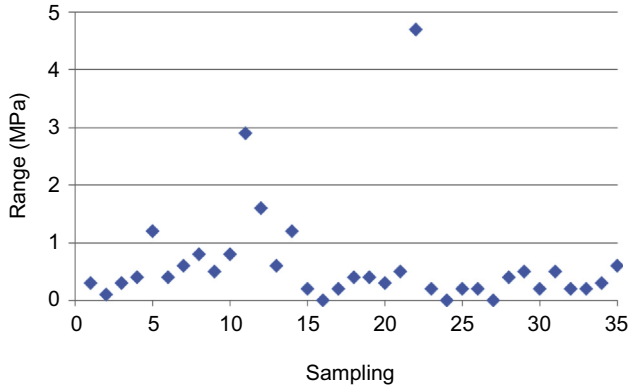


Figure A3.14 Variation of range.

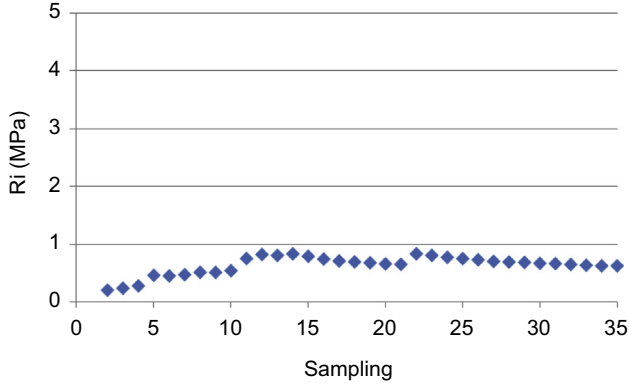


Figure A3.15 Variation of average range.

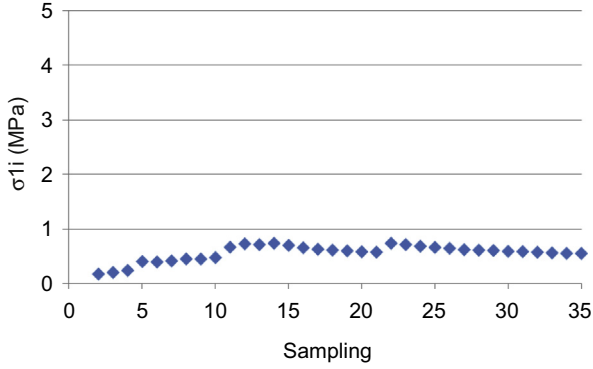


Figure A3.16 Within-test standard deviation.

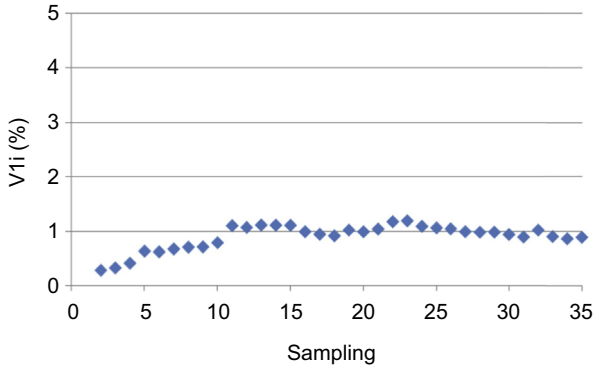


Figure A3.17 Within-test coefficient of variation.

is carried out on a limited number of samples and not on all batches. The use of a random number table to select the loads that are checked does not limit that risk. Without entering into the field of combinatory analysis, it is possible that the selected sampling benefits either the producer or the consumer. Let us examine two very simple hypothetical (but likely) cases.

The construction of a particular structure requires the use of 100 loads of concrete. The specification permits the delivery of a maximum of five loads of concrete with a compressive strength lower than the design strength. The statistical analysis of this production is based on the results obtained on 30 samples selected using a random number table.

A3.5.1 The case of a good but unlucky concrete producer

The concrete producer is a good one that has adjusted the average strength of its production, taking into account its usual standard deviation, to produce a concrete that statistically meets the specification. But when the selection of the 30 tested loads is made the producer is particularly unlucky, because the five defective loads have all been selected. As a result, it is judged on 25 satisfactory loads and five defective ones. Its production will be evaluated as not meeting the specification, despite the fact that in reality this is not true.

A3.5.2 The case of a bad but lucky concrete producer

The concrete producer is a bad one. It has produced a concrete that does not meet the specification but he is very lucky: none of the bad loads has been selected for sampling. This producer will be evaluated as meeting the specification although in reality this is not the case.

A3.5.3 The risk to the producer and the risk to the consumer

The acceptance or rejection of concrete for a particular project based on a statistical analysis inevitably includes the risk of rejecting concrete matching the specification or accepting concrete that does not match the specification. In a perfect world, it would be fair that the risks of accepting bad production or refusing good production are equal. However, according to Chung (1978), the present standards favour the producer rather than the consumer, and he proposed a new acceptance criterion to share both risks better. To date (2014), nothing has been done to change this situation!

A3.6 Conclusion

Despite all the attention given to controlling the variability of the materials used to make concrete, any concrete displays a certain degree of variability because it is made from variable raw materials processed by human beings in more or less sophisticated plants, it is delivered under variable temperature conditions and it is tested by human beings. As with any man-made material, concrete must be specified on a statistical basis. It must be admitted that, in spite of all the care taken to produce, process, deliver and test low w/c ratio concrete, a limited number of samples can fail the design criteria selected by the designer.

Using statistical analysis, it is possible to produce a concrete that matches the design characteristics selected by the designer. Of course, the average value that will have to be obtained by the producer will increase with the severity of the design criteria and the standard deviation of the concrete plant.

When making a statistical analysis of the ranges of numerical values obtained on the different samples taken from the same concrete sample, it is possible to evaluate the quality of control by calculating the within-test variation. Consequently, the variability of concrete can be split between the variation due to its production and the variation due to its sampling and testing. It is, however, important to emphasize that when evaluating concrete production on a statistical basis, there is always a risk that good production is rejected or bad production is accepted.

Concrete is a complex material that is variable. It is important to make all necessary efforts to reduce this variability in order to build more durable and sustainable structures. Statistical analysis can help us to achieve this.

References

ACI Standard 214 R-02, re. Recommended Practice for Evaluation of Strength Test Results of Concrete. ACI Manual of Concrete Practice, Part II, pp. 1−20.

ASTM Manual series MNL 7A, 2002. Manual on Presentation of Data and Control Chart Analysis, seventh ed. ASTM International. 100 Barr Harbor Drive, West Conshohocken, PA 19428.

Chung, H., 1978. How good is good enough − a dilemma in acceptance testing of Concrete. ACI Journal 75 (8), 374−380.

Day, K.W., 1995. Concrete Mix Design, Quality Control and Specification. E and FN SPON, London, p. 350.

Schrader, E., 2007. Statistical acceptance criteria for strength of mass concrete. Concrete International 29 (6), 57−61.

Valles, M., 1972. Eléments d'Analyse Statistique − Application au Contrôle de la Qualité dans l'Industrie du Béton. Monographie No. 4. published by CERIB, Paris, 64 p.

Index

Note: Page numbers followed by "f" and "t" indicate figures and tables, respectively.

A
Absolute volume
  contraction, 16−18
  method, 541−548
Absorptivity, influence of entrained air, 90
Acceleration
  chemically induced, 405
  decreasing w/c or w/b, 406
  heating, 406−407
  high strength cement, 405−406
  insulated forms, 407
  physically induced, 405
  use of accelerator, 407
Acceleration period, 133−134, 136−138, 279−280
  in alite hydration, 140
  in cement hydration, 137−138
  effect
    of available surface, 135
    of C-S-H nuclei, 135
    of retarders, 290
  nucleation and growth hypothesis, 136
  onset, 133−134
Accelerators, 279, 405, 407
  calcium chloride, 408−410
  different types, 407−408
  in formulation, 343−344
  inorganic salts, 407
  negative effects, 408
  for shotcrete, 410−412
  soluble organic compounds, 408
Acceptance standards, 44
Ackermanite, 59
Acrylate monomers, 289
  hydrolysis of side chains, 288−289
    chemistry, 289−290
  impact on adsorption, 289
  methacrylate monomers, 289
  role of carboxylate functions, 289
Acrylic resins as curing membranes, 484−485
Active solids, 536, 548
Admixture(s)
  absorption, 61−62
  dosage impact on hydration, 282
  effect on rheology, 77
  modification of cement hydration, 129
Adsorbed conformation, 159
Adsorbed layer thickness, 262, 267−268, 273
  effect on interparticle forces, 272
  of polycarboxylate ethers, 268, 270, 272−275
  of polynaphtalene sulphonates, 269
Adsorption
  competition. *See* Competitive adsorption
  conformation, 220
    role of monomers size, 227−228
    role of structural parameters, 227−228
  critical dosage, 221
  effect of
    charge density, 228
    dosage, 220
    molecular structure, 226
    polydispersity, 224−225
  energy, 222−223, 226
  equilibrium constant, 222, 224, 234
    derivation of KA, 229
  equilibrium with solution, 242
    effect of admixture dosage, 219
    effect of admixture type, 219
    effect of surface, 219
  of lignosulfonates
    effect of molecular mass, 227
    effect of polydispersity, 224
  measurement, experimental issues, 220, 241

Adsorption (*Continued*)
of PCEs, 287–289
effect of molecular mass, 227
effect of polydispersity, 224
of polymers, general principles, 226
raffinose, 295–296
rate, 229
reversibility, 232–233
role of entropy, 222, 226
saturation dosage, 220
of SNFC, effect of molecular mass, 227
solution depletion method, 219–220
sucrose, 295–296
superplasticizers, effect of molecular mass, 227
of surfactants
conformation, 230
4 regimes, 231
liquid-vapor interface, 239
solid-liquid interface, 230
of vinyl copolymers, effect of molecular mass, 227
Adsorption isotherm, 219, 221
equilibrium plateau, 242
importance of equilibrium, 226
of lignosulfonates, 224
linear regime, 221–222, 224
effect of polydispersity, 224
equilibrium constant K, 222
measurement limitations, 226
models, 222
Langmuir, 222
of PCEs, 224
plateau, 222–223
role of competitive adsorption, 233
AEAs. *See* Air entraining admixtures
Affinity for surface
impact on saturation dosage, 220, 222
AFm
formation, 129, 138–139
effect of superplasticizers, 288–289
phases, 129–130
Aft. *See* Ettringite
Aggregates effect on rheology, 109
Aggressive agents, 20, 23
Aggressive ions, 76
Air bubbles
diameter, 87–88
distribution, 87
improvement of rheology, 87
influence
on mechanical properties, 87
of slump, 87
of vibration, 87
of viscosity, 87
shape, 87
total volume, 87–88
Air content effect on concrete theology, 116
Air entraining admixture, 219, 239
adsorption
liquid-vapor interface, 239
solid-liquid interface, 230
Air entraining admixtures, 182–197. *See also* Surfactants
classification, 183
compatibility, 154, 192, 195–196
raw materials, 183
Air entraining agent, 87, 379
factors influencing dosage, 382–383
influence of silica fume, 386
interaction with superplasticizer, 384–386
optimum dosage, 382
PCE influence, 385
Air entraining dosage
critical dosage, 385
effect
of fly ash, 386
of silica fume, 386
of slag, 386
as function
of cement mass, 383–384
of water dosage, 382–384
influence
of aggregates, 387
of alkali content, 384
of cement, 383–384
of concrete consistency, 384–386
of fineness of cement, 384
of mixing method, 382, 387–388
of other admixture, 387
of sand, 382, 387
of superplasticizer, 384–386
of type of mixer, 387–388
of w/c and w/b, 382–383

Air entrainment
  effect
    on viscosity, 384–385
    on yield stress, 384–385
  mechanism, 379–380
Aliphatic sugars impact on hydration, 290, 292–293
Alite, 30, 132
  composition impurities, 132
Alite hydration, 131–138
  acceleration period, 133–134, 136–138
  impact of aluminum ions
    adsorption on silicates, 140
    C-A-S-H formation, 140
  effect of C-S-H seeding, 137–138
  dissolution rate, 133–134
    function of saturation degree, 133–134
  induction period, 133, 135–136
    role of CH precipitation, 138–139
  initial deceleration, 132–133
    etch pits formation, 133
    metastable C-S-H, 133
    protective membrane, 133
    role of dislocations, 133
    saturation degree, 133–134
    step retreating, 133
  initial dissolution, 132–135
  main hydration peak, slope, 135
  main stages, 130
  products of hydration, 138–139
  silicate concentration, 135
  slow dissolution step hypothesis, 133–134
Alkali content influence on entrained air, 384
Alkali equivalent, 33
Alkali sulphates, 32–33, 49
Alkali/aggregate reaction, 83, 90–91
Alkanolamines, 329–333
Aluminate(s), 57–58
  phase, 38
  reactivity
    effect of time of addition, 58
    experimental issues, 243
    specific surface, 243
Alumino-silicate, 65–66
Aluminum salts, 411
  as accelerators, 411
  alkali free, 411
  with alkalis, 411
Amines, 329–333
  volatile amine, 333
Aminic group in corrosion inhibitors, 330
Amorphous state, 54
Angle of contact, 457
Anhydrite, 30–31, 48–49, 129
Antagonist effects, 549
Antifoam agents. *See* Defoamers
Antifreezing admixture, 433–434
  ammonia, 434
  calcium chloride, 434
  nitrate, 434
  nitrite, 434
  sodium chloride, 434
Apparent viscosity, 121–122
Apparent volume contraction, 15, 17–18
Aqueous phase. *See* Pore solution
Architectural panels, 476
  use of galvanized reinforcing rebars, 476
Artificial pozzolan, 61, 66
ASTM C 457–98 Standard, 91
ASTM C 666 Standard, 91–92
Atomic force microscopy, measurement of interparticle forces, 271f
Attractive forces, 257, 268, 273. *See also* Van der Waals forces
  depletion forces, 268
  influence on yield stress, 107
  ion correlation forces, 259
Autogenous shrinkage, 17–18, 20–23, 44–45, 79, 81–82, 457, 459–460, 483, 486
  origin, 17–18, 20
  use of SRA, 459
Average strength, 575t–576t, 577f
  specifying, 573
  variation, 578f
Average value, 566, 566f, 574t

B

Backbone of PCEs, impact on adsorption, 227
Ball mill, 30–31, 49
Belite, 30
  nests, 31
Bell shaped curve, 565–566, 567f
  area under, 568f
BET, 237
  experimental issues, 247

Betaines, 193
Bidentate complexes
  PCEs, 281–282
  sugars, 296
Bingham material, 101–103
Biocides in formulation, 346
Blaine fineness, 36
Blast furnace slag. *See* Slag
Bleeding, 76–77, 109
  correlation with yield stress, 109
  how to reduce it, 109
  influence of entrained air, 89
  effect of VMA, 109
Blended cements, 6–7, 9, 11, 48, 68, 70–72, 483
  binary, 70
  containing filler, 3–4, 9–11
  entrained air, 93–94
  initial strength, 7–8
  long term strength, 9
  quaternary, 70
  supplementary cementitious material, 3–4, 6–9
  ternary, 70
Bogue composition, 34t–35t, 36
Bonded overlays, 453–454
Bridge decks, 453, 466
  effect of deicing salts, 472
  expansive agents, 453
  use of expansion agent, 457–458
Brownian motion, 104, 106, 263–264
  influence on rheology, 106
Bubble network
  effect of AEA dosage, 379
  influence
    of mix time design, 382
    of placing parameter, 382
  iterative approach, 382
  principal characteristic, 380–381
  production, 381–388
  stability, 381–382, 384, 388–389
Buff cement, 28
Burning zone, 28, 30–31, 33, 36
By-products, 53

C

C-A-S-H, 140
C-S-H, 39–40, 53, 65–66
  formation, 129, 132–133, 135–138
    admixtures complexation, 281
    effect of carboxylates, 284–285
    role of nuclei, 135
  morphology
    aggregation of nanoparticles, 136
    fibrillar morphology, 137
    inner product, 137
    outer product, 137
    sheets of silicate chains, 136
  secondary, 8, 43
  seeding, 290
    effect on alite hydration, 137–138
    effect on microstructure, 137–138
  structure, 136
    jennite, 136
    tobermorite, 136
C/E ratio. *See* Grafting density of PCEs
C_2S, 28, 30–31, 39, 59, 65–66
  simplified notation, 28
C_3A, 3, 6, 30, 36–38, 49
  C_4AF balance, 40
  content in UHSC, 508–509, 508t
  cubic, 30
  grey cement, 36
  hydration, 38–39
  monoclinic, 30, 46
  orthorhombic form, 30, 46
  polymorphic form, 45–46
  simplified notation, 28
C_3A hydration, 130–131
  dissolution effect of PCEs, 287
  influence of sulfates source and content, 131
    dissolution, 131
    main stages, 130
    sulfate depletion point, 130
    with sulfates, 130
    without sulfates, 130
  initial deceleration, 130
    adsorption of sulfates, 130
    protective membrane, 133
  organomineral phases, 285
  specific surface effect of superplasticizers, 285
C_3S, 3, 6, 28, 31, 36, 39
  content in UHSC, 508–509, 508t
  hydration, 38
  simplified notation, 28

C_3S hydration
acceleration, 408
dissolution effect
of latexes, 282
of PCEs, 282
retardation, complexation, 282
C_4AF, 28, 36
C_3A balance, 36
grey cement, 36
white cement, 36
CAC. *See* Critical aggregation concentration
$CaCO_3$. *See* Calcium carbonate
Calcined bauxite, 12
Calcined clay, 65–66
Calcium aluminate hydrates formation, 130
Calcium carbonate
formation effect of PCEs, 283–284
in gypsum, 49
Calcium chloride, 407
as accelerator, 408–410
banning in precast concrete, 473
banning in prestressed concrete, 473
mode of action, 409
mode of addition, 409–410
rules governing its use, 410
Calcium concentration
effect of
complexation, 283–284
latexes, 282
sugars, 296
Calcium hydroxide. *See* Portlandite
Calcium nitrite, 327, 433–434, 475
accelerator, 327
concentration, 328f
delay of depassivation, 328
dosage, 434
efficiency, 328
inhibitor of corrosion, 328
leaching, 329
long-term efficiency, 329
mechanism of action, 328–329
use in Europe, 328–329
use in Nanisivik, 434–438
use Japan, 327
Calcium silicate hydrate. *See* C-S-H
Calcium sulfate. *See* Calcium sulphate
Calcium sulphate, 30–31, 38, 48–49
different forms, 129
influence of final grinding, 129
synthetic, 49
Calcium sulphoaluminate, 38, 444, 449, 451–454
CaO content, 33
Capillary pores, 17–18
desaturation, 80
network, 8, 11
size, 11
Capillary porosity effect of seeding, 137–138
Capillary pressure
calculation of, 310
limits of application, 307
shrinkage reduction, 307
Capillary suction, 323, 457
Capillary system, 46–47
Capillary water, 17–20, 22, 76, 83
Carbon footprint, 3, 6–7, 43, 47–48
Carbonates, 57–58
Carbonation, 471
effect on corrosion of reinforcing rebars, 471
shrinkage, 22
Carbonation front, 324–325
influence of pH, 324
Carboxylate functions
impact on
C-S-H nucleation, 282
complexation, 282
dissolution, 282
Casein, 153–154
structure, 153f
Cathodic protection influence on steel corrosion, 474
Cellobiose, 292f
Cement
minimum interparticle distance, 263–264
phase composition, 129, 138
Cement fineness, 3, 6, 10
impact on hydration, 279
Cement hydration, 138–139
alite hydration, 131–138
impact of aluminum ions, 139
C_3A hydration, 130–131
effect of fineness, 279
influence on plastic viscosity, 110

Cement hydration (*Continued*)
main stages, 130
mechanism affecting, 279, 284
modification by admixtures, 129
products of hydration, 138−139
retardation, different hypotheses, 281
role
of ettringite precipitation, 138−140
of sulfates, 131
silicate-aluminate-sulfate balance, 139−140
sulfate depletion point, 139
Cement kiln, 46
Cement particles, 4, 6−7, 9, 11−12
average distance, 4
minimum distance, 4−6
Cement paste, chloride ion attack, 472−473
Centrifugation, experimental issues, 244
CH. *See* Portlandite
Charge density
impact on adsorption, 228
of PCEs
impact on adsorption, 282
impact on yield stress, 288−289
Chelation. *See* complexation
Chemical composition
Bogue composition, 36
natural pozzolan, 66−67
of Portland cement, 33−36
slag, 58
of supplementary cementitious materials, 53
Chemical contraction, 16−19, 22, 79, 81−82
Chloride ions, 471
attack on cement paste, 472−473
bound, 323
corrosion of steel, 322
effect on corrosion, 472f, 473
free, 323
influence
of cement type, 323
of pore size distribution, 323
of porosity, 323
penetration, 472−473
pore, 323
Chloride pitting corrosion, 324
Citrates, competitive adsorption, 233
Class F fly ash, 61, 66f
Clay
fabrication of Portland cement, 27
influence on plastic viscosity, 116
Clay minerals
impact on specific surface, 238
kaolinite, 238
mica, 238
montmorillonite, 238
muscovite, 238
PCEs adsorption, 238
Clinker, 27−28, 48, 53, 68
addition of calcium sulphate, 38
alite, 30
beige, 28
belite, 30
colour, 33
commercial, 46
interstitial phase, 31
types, 48
Type I/II, 48
Type V, 48
white, 28
Closed system, 17−21, 44−45
CMC. *See* Critical micellation concentration; Critical Micelle Concentration
Co-surfactants, 239
Coal, 60−62
Coalescence of air bubbles, 93, 380
Coarse aggregate
properties, 497
in SCC, 492−493
Coarse sand, 89
Coded values, 552−554, 552f, 554f, 560t
Coefficient of variation, 568, 573, 575t−576t, 579f
Cohesion, 415
Cohesiveness of SCC, 492−493
Coke, 57−58
Colloidal forces, 104
influence on rheology, 104
Columns, 486
Commercial admixtures, 279
formulations, 343
Compactness of UHSC, 503
Compatibility, SRA-AEA, 463−465

Competitive adsorption, 219, 224, 233, 241, 363, 370
citrates, 233
hydroxides, 233–234
impact on adsorption isotherm, 233
nitrates, 233
polymeric admixtures, 233
sulfate ions, 233
Complexation, 281
during C-S-H nucleation, 282
during C_3S hydration, 282
with calcium ions, 281–282
impact
on calcium concentration, 282
on supersaturation, 281
by PCEs, 281–282
crown ethers, 281–282
mono-/bidentate ligand, 281–282
by phosphonates, 282
role
of carboxylate functions, 281–282
of side chains, 283–284
stability, 282, 293–296
by sugars, 282, 292–293
raffinose, 295–296
sucrose, 295–296
Compressive strength, 3, 8–9, 11–12
control, 3
influence of lightweight aggregate, 82
of UHSC, 503–504
Concentration dependence, 335
Concrete
commercial admixtures for
precast, 343–344
ready-mix, 343–344
shotcrete, 346
consistency influence of entrained air, 384–386
cover, 23, 322–323, 471
how to protect it, 484
preventive measures against corrosion, 326
curing, 77, 80
dimensional variation, 75–76
durability, 76–77
fresh properties, 75
hardened properties, 75
as multi scale material, 97
overlay, 454
production quality control, 569–573
repair, 441, 444, 453
rheology, 76–77
skin, 77
sustainability, 76–77, 82
Concrete rheology
casting, 97
of cement type, 113
change with time, 110
of chemical admixture, 113
of chemical composition, 113
of crushed aggregates, 113
effect
of aggregates, 110
of air content, 116
of fly ash, 114
of mortar/aggregates ratio, 112–113
of paste/aggregates ratio, 112–113
of processing energy, 110
of shear rate, 116
of solid concentration, 110–111
of excess paste/mortar, 112f
influence of rheology
on finishing, 97
on handling, 97
on hardening, 97
of mixing, 97
intensity, 110
of paste composition, 113–116
on pumping, 97
relation between slump and yield stress, 108f
of rolled aggregates, 113
of supplementary cementitious material, 113
of temperature, 113
on transportation, 97
of water, 113
Concreting season, lengthening, 438
Confidence interval, 560
Confined UHSC, 506
Conformation
adsorption, surfactants, 230
change impact on entropy, 222, 226
of PCEs
in solution, 227–228
when adsorbed, 227–228
of superplasticizers onto surfaces, 266, 268

Consumption
by hydrates precipitation, 219–220, 234
ineffective adsorption, 234
by intercalation, 219–220
organo-mineral phases, 234
role of specific surface, 237
Contact angle, 503–504
Corrosion
effect
of carbonation, 471
of chloride ion penetration, 472–473
of microstructure, 472
mechanism, 322–326
preventive measures, 472
propagation, 322f
rate, 325–326
influence of concrete resistivity, 325
influence of humidity, 325
influence of temperature, 325
Corrosion inhibitor, 321, 326, 434, 471, 474
addition, 474
application, 474
calcium nitrite, 475
critical evaluation, 334–335
diethanolamine, 329
dimethylethanolamine, 333
dimethylpropanolamine, 329
laboratory studies, 327–333
mechanism of action, 322–326
monoethanolamine, 329
in oil and gas industry, 326
testing, 334–335
Coverage degree, 220, 226
impact on
adsorption equilibrium, 233
loss of fluidity, 221
effect of surface changes, 237
Crack density, 467, 467f
Crack propagation, 90
Cracking of prefab slabs, 400
initial setting
chemical approach, 395
delay it, 395
physical approach, 395
Creep of SCC, 497
Cristobalite, 64, 66–67
Critical aggregation concentration, 231, 317
Critical chloride content, 324
Critical dosage, 221
determination by rheological tests, 358–359
Critical micellation concentration, 231, 239–241
Critical Micelle Concentration, 313
Critical ratio inhibitor/cement, 335
Critical shear rate, 106
Crushed aggregates, influence on rheology, 113
Crystal lattice, 54
Crystalline state, 54–55
Crystallization pressure, 441, 451–452
Crystallized particles, 61–62
in fly ash, 61–62
CSA 231 Standard, 92
Cube strength, 10, 46
Curing, 483
columns, 486
concrete, 77, 80
according to w/c, 77, 483–484
importance, 471
practice specifying, 483–484
Curing conditions, influence on expansion, 449–450
Curing membrane, 23, 80–81, 483
acrylic resins, 484–485
paraffin emulsions, 484–485
pigmented, 484
transparent, 484

D

Dead burn lime, 444
appropriate dosage, 446
dosage, 448–449, 450f, 452–453
formation of portlandite, 445–446
increase in concrete strength, 445–446
influence on concrete rheology, 445–446
Debye length, 259, 270
of cement pore solution, 266
effect of electrolyte concentration, 259
Deceleration period
in alite hydration, 138
in cement hydration, 138–139
coverage of particles, 138
impingement degree, 138
Defoamers, 279
in formulation, 345
use in PCE formulation, 385

Deformation energy, 309
  calculation of, 309
  dependence on
    disjoining pressure, 309
    relative humidity, 310
    shrinkage reduction, 309
Degree of thixotropy, 117
Degree of vitrification, 59
Deicing salts
  attack on concrete, 472–473
  drainage, 472
  effect on bridge decks, 472, 472f
Delayed ettringite formation (DEF), 47
Delayed fluidification
  effect of mixing protocol, 362
  effect of sulfates concentration, 362
Delayed polymer addition
  fluidity retention, 360–362
  mixing protocol, 360
Depassivated steel, 322, 324
Depassivation, 323–325
Depletion flocculation, 416, 416f, 420
Desorption, 219, 232–233
  effect of
    admixture concentration, 219, 233
    ionic composition, 219
  isotherms modelling, 311–312
  rate, 229
Diameter, silica fume, 62–64
Diatomaceous earth, 67, 68f, 71f
Dicalcium silicate. *See* C_2S
Diethanolamine as corrosion inhibitor, 329
Different types of shrinkage, 22
  autogenous shrinkage, 17–18, 20–23
  drying shrinkage, 22–23
  plastic shrinkage, 22–23
Diffuse layer. *See* Goüy-Chapman double layer model
Diffusion of chloride ions, 323
Dilution
  of expansive agents, 444
  of Portland cement, 8
Dimethylethanolamine, 329
Dimethylpropanolamine as corrosion inhibitor, 329
Disjoining pressure
  deformation energy, 309
  dependence on relative humidity, 306
  liquid film, 308
  surface forces, 308
Dispersion
  forces. *See* Van der Waals forces
  importance of adsorption, 219
  surface coverage, 241
Dissolution
  in alite hydration, 132–135
  in C_3A hydration, 130
  effect
    of adsorbed admixtures, 282
    of latexes, 282
    of PCEs, 282
    of retarders, 279–280, 290
  influence of
    crystal orientation, 134–135
    density of defects, 134–135
    fracture surface, 134–135
    particle size distribution, 134–135
    specific surface area, 134–135
  process, 78
Dissolution-precipitation process, 42, 129
Distance between cement particles, 4, 4f
  average, 4
  minimum, 4–6
Diutan gum, 418–420
Divalent ions, 270
  effect on
    interparticle forces, 266
    stability of AEAs, 182–183
  ion correlation forces, 259
DLVO theory
  definition, 262–266
  effect of electrolyte concentration, 260f
Dormant period, 39, 49
Dosage of admixture, impact on fluidity, 219
Dosage of superplasticizer
  active solids, 536
  l/m^3, 540
  solids, 537–538
Drying shrinkage, 22–23, 79–80, 197–198, 442, 483
  elimination, 83
  influence
    of concrete composition, 442
    of environmental conditions, 442
    of geometry, 442
  in mortar, 461
  use of SRA, 458

Ductibility of UHSC, 506
Durability, 3–4, 10–12, 87
  influence of compressive strength, 88–89
  influence of w/c, 88–89
  factor, 465–466

E
Effect of entrained air
  on deicing salt, 379
  on freeze-thaw resistance, 389
  properties
    of fresh concrete, 380, 388–389
    of hardened concrete, 388–389
Effect of shear paddles on air content, 379
Effect of vibration on air content, 380
Effective water, 75
Elastic behavior, 103
Elastic modulus
  influence of lightweight aggregate, 82
  of SCC, 497
Electric arc furnace, 62, 63f
Electrical conductivity, 78, 78f
Electrochemical impedance spectroscopy (EIS), 333
Electrolyte concentration, 260f
  effect on
    Debye length, 259, 270
    Hamaker constant, 258
    interparticle forces, 257
Electrostatic force, 258–262
  effect of adsorbed layer thickness, 262, 268
  in DLVO theory, 262
  electrostatic potential, 261–262
    definition, 260f
    effect of Debye length, 259
    surface potential, 259, 261
  Goüy-Chapman double layer model, 258
Eliminating steel corrosion, 476–477
Entrained air, 87–88
  in blended cement, 93–94
  concrete, 465–466
  dissipation of energy, 88, 90
  effect
    on bubbles, 380
    of carbon content, 94
    of fibers, 387
    of mixer type, 387–388
    of mixing procedure, 387–388
    of placing, 389
    of soot, 93–94
    of temperature, 388
    of unburned carbon, 93–94
    of vibration, 384, 388–389
    on workability, 382–383
  fluidification of cement paste, 88
  free volume, 88
  freezing and thawing, 88
  influence
    on absorptivity, 90
    on bleeding, 89
    of fly ash, 93–94
    of formulation parameter, 383–387
    on internal bleeding, 89
    on permeability, 90
    on segregation, 89
    on transition zone, 89–91
  rheology, 87–88
  size of air bubbles, 381
  volume of paste, 88
  of wear of paddles, 384
Entrapped air, 87–88, 379
  in UHSC, 504–505, 511
Entropy
  conformation changes, 222, 226
  role in adsorption effect of molecular structure, 222, 226
Epoxy coated rebar, 475, 476f
Etch pits, 133
Ettringite, 38, 40, 41f, 46–49
  dehydration, BET measurement, 247
  delayed, 47
  expansive, 45
  formation, 129–130, 138–139
    change of saturation degree, 287
    effect of admixtures, 287
    effect of superplasticizers, 286–287
  influence of supersaturation degree, 130
  morphology, 130–131
    effect of superplasticizers, 237–238
    modified by PCEs, 287
    role on specific surface, 237–238
  secondary, 46–47
  in shotcrete, 411
  stability, 130
  trapped in air bubble, 90
  unit cell, 49, 50f

Evaporation of water, 22
drying shrinkage, 22
plastic shrinkage, 22
Evaporation retarder, 23, 80−81, 485
Excess paste/mortar approach, 112f
impact of granular classes, 112−113
influence on rheology, 112
thickness, 112−113
Excluded volume interaction effect of dosage, 222
Expansion
factors affecting expansion, 448−453
influence
of cold temperature, 451−452
of curing conditions, 449−450
of temperature, 451−452
mechanism, 444−446
Expansion agent, 457−458
Type G, 462
Expansive agents, 441
different types, 441
dosage influence on expansion, 448−449
ettringite formation, 444−445
field applications, 453−454
formulation, 444
type G, 444−445
type K, 444, 453
Expansive chemicals, 45
Experimental domain, 554
2D experimental domain, 554f
3D experimental domain, 555f
definition, 554−555
selection, 555
Experimental error, 556, 559−560
Experimental issues
adsorption measurement, 241
aluminates reactivity, 243
BET, 247
centrifugation, 244
filters, 244
GPC, 245−246
HPLC, 245−246
ionic composition, 242
light scattering, 246
mixing energy, 243
pore solution extraction, 244
pore solution stabilization, 244
pressure filtration, 244
solid content, 242
specific surface, 243, 247
suspensions preparation, 242
time of addition, 243
TOC, 244
ultracentrifugation, 244−245
UV/Vis spectrometry, 245
zeta potential, 247
Exterior factors causing corrosion, 471
External curing, 81, 485−486
External source of water, 81−82
influence on shrinkage, 81−82
External temperature, 444
influence on expansion reaction, 444
External water, 19−20, 23, 483−484, 486
curing, 457

F

False set, 38
Ferrosilicon, 62
Fibers effect on entrained air, 387
Fibrillar morphology in C-S-H formation, 137
Filler, 3−4, 6−7, 11, 67−68
in blended cement, 9−11
ground glass, 69−70
limestone, 68
silica, 68
use in SCC, 492−493
Filling ability, 492
Filters, experimental issues, 244
Fineness, 31, 36−37, 46, 48, 53
clinker, 68
slag, 60
Flash set, 38, 130
Flocculation, 11−12
Flow behaviour types, 97−98, 102−103
Flow curve, 100−101, 102f, 121−122
Flow retention, 289−290
Fluidity, 353
effect of admixture dosage, 219−220
effect of aluminates content, 360
in presence of polycarboxylate ethers, 360
loss effect of polymer in solution, 221
effect of sulfates content, 362, 365
in presence of polycarboxylate ethers, 371

Fluidity (*Continued*)
in presence of polymelamine sulfonate, 354, 367−368
in presence of polynapthalene sulfonate, 354, 367−368
effect of surface mineralogy, 367
Fluxing agent, 58
Fly ash, 60−62, 230
Class C, 61, 66f
Class F, 61, 66f
crystallized, 62
effect on entrained air, 93−94
freezing and thawing, 88
sulfocalcic, 61
effect of unburned carbon, 386
effect on AEA dosage, 386
use in SCC, 492−493
Fogging, 81f
Formulated product, 279
composition, 279
impact on hydration, 279
Fractured surface of UHSC, 507f
Free energy
adsorbate-surface-solvent interactions, 222
surfactants adsorption, 239
Free lime, 33, 441−442
Free shrinkage, 441−442
measurement, 446−447
Freezing
temperature of water, 433
sea water, 433
and thawing, 47, 47f
Friction forces, 99
influence on rheology, 103
Friedel's salt formation, 129
Fuel influence on production cost, 27
Full hydration, 16−20, 23

G

Galvamic elements, short-circuited, 325−326
Galvanized reinforcing rebars, 476
Gehlenite, 59
Gel water, 16, 19−21
Geotextile, 466
saturated, 466
use to cure concrete, 466
GFRP. *See* Glass fiber reinforcing polymer rebars
Gibbs-Duhem equation
surfactants adsorption, 240
Glass fiber reinforcing polymer rebars, 476−477
Glucose, 279−280, 295
impact on hydration, 279−280, 281f
as retarder, 398
Goüy-Chapman double layer model
definition, 258
GPC, experimental issues, 245−246
Grafting density of PCEs
impact on adsorption, 227, 288−289
Grain size distribution
fly ash, 61−62
optimization in SCC, 492−493
of powders in UHSC, 503−504, 507
Gravity forces, 103
influence on rheology, 103
Grinding, 36−38
of Portland cement influence on sulfates, 129
Ground glass, 69−70
use in UHSC, 69
high voltage power line anchors, 435
Gypsum, 30−31, 38, 48−49
content, 3, 68
dehydration, BET measurement, 247

H

Hamaker constant, 105
of cement, 264
definition, 257−258
effect of electrolyte concentration, 258
Haneda airport extension, 515−518, 516f
Hard inclusions, 69
strengthening effect, 20−21
Hardening, 129, 136
Heat of hydration, 15
Heat recovery system, 63f, 64
Heat release, 39f, 44
of Portland cement, effect of retarders, 286−287
Heat treatment of UHSC, 504
Heated shelters, 433
Heating
of aggregates, 433
concrete to accelerate hardening, 406−407

Helmholtz free energy
components
deformation energy, 309−310
total, 310
dependence on relative humidity, 310
Hemicarboaluminate formation, 129
Hemihydrate, 30−31, 38, 48−49, 131
Herschel-Bulkley model, 103−104
Hidden water, 75, 531
High furnace, 57f
High range water reducer adsorption, 219
High rise buildings use of SCC, 497
High strength cement to accelerate hardening, 405−406
High voltage power line, 434
High volume fly ash concrete, 9
High volume slag concrete, 9
Histogram, 569, 569f
skewed distribution, 570f
HLB. *See* Surfactants
Homogenization hall, 28
Honeycomb, 491
HPLC, experimental issues, 245−246
Hump, 55, 64
Hydrated lime, 39, 43
influence on mechanical properties, 43
Hydrated lime, 53
Hydration
autogenous shrinkage, 44−45
C_3A, 46
C_3S, 38
of cement, 424
C-S-H, 425, 427f
C3S, 425, 426f−427f
microsilica, 426, 427f
nanosilica, 426, 427f
heat release, 39f, 44
of four principal phases, 39
Portland cement, 39−42
influence on concrete rheology, 110
physical consequence, 75−76
of Portland cement
under water, 18−19
w/b = 0,36, 19
w/c = 0,30, 20−22
w/c = 0,42, 17−19
w/c = 0,60, 19−20
side effects, 44−45
thermodynamic consequence, 76
volumetric consequence, 76
volumetric contraction, 44
Hydrocalumite
composite with PCEs, 236−237
formation, 129, 131
Hydrodynamic forces, 104
influence on rheology, 106
Hydrogarnet formation, 130
Hydrolysis of side chains in PCEs, 289
Hydrophilic surface
adsorption of surfactants, 230
effect of counter ions, 231
effect of hydrophobic tail, 231
effect of surfacial charges, 231
Hydrophilic termination, 379−380
Hydrophobic surface, adsorption of surfactants, 230
Hydrophobic termination, 379−380
Hydrotropes, 239
Hydroxides, competitive adsorption with PCEs, 234
Hypothetical cement particles, 37

I

Ice
ice-making machine, 396
setting delay, 395−396
Illites, 66
Impingement degree, 138
Impurities, 57−58, 60
Incompatibility
admixture/admixture, 353
cement/admixture, 364
Increase of slump, influence on air entrainment, 384
Individual inclusion, 504
Induction period, 279−280
in alite hydration, 133, 135−136
in cement hydration, 138−139
effect of retarders, 279−280
Inertial forces, 104
influence on rheology, 104
Influence of commercial admixtures, 344
Influence of supplementary cementitious material on corrosion, 329

Influence of w/c
autogenous shrinkage, 22
on superplasticizer dosage, 559–560
Influence on compressive strength
basalt, 12
calcined bauxite, 12
granite, 12
porphyry, 12
trap rock, 12
Inhibitor action
control, 335
measurement, 335
Initial expansion, 444, 446
Initial rheology, 38, 46
Initial strength, 7–8, 11
Initial swelling, 442
Initiation phase, 322–325
duration, 322–323
Inner product, 137–138
Insulated form to accelerate hardening, 407
Insulating blankets, 433
Interaction, 556–559
Intercalation, consumption of admixtures, 219–220
Interfaces
air-water, 379–380
cement-water, 379–380
Internal bleeding, 89
Internal curing, 22–23, 83–84, 457
saturated lightweight aggregates, 485–486
Internal expansion, 441
influence
of chemical nature of expansive agent, 441
of dosage of expansive agent, 441
of duration of water curing, 441
of type of expansive agent, 442
intensity, 441
Internal source of water, 82–83
influence on shrinkage, 82
Internal water, 484
Interparticle forces, 257, 264
atomic force microscopy, 271f
calculation with Hamaker software, 264, 273
effect of
charge plane position, 265–266
divalent ions, 270
electrolyte concentration, 258, 260f
Zeta potential, 269, 269f
Interstitial phase, 28, 30f, 31, 37, 40, 46
Interstitial solution, pH, 471–472
Intrinsic strength of coarse aggregate, 503–504
Ion migration, 323
Ionic plans, 54
Ionic species solubility, 76
Ionic strength. *See* Electrolyte concentration
Iron oxide, pellets, 57–58
Iron powder, 12
Iso-responses, 562, 563f

J
J-ring test, 494–495, 495f
Jennite-like structure, C-S-H formation, 136
Jensen and Hansen model, 16–17, 19

K
KA, adsorption equilibrium constant derivation, 230
Kaolinite, 65–66
impact on adsorption, 238
Krieger-Dougherty model, 110–111

L
L box test, 495
Laboratory studies on inhibitors, 327–333
Lactose, 292f
Lactose as retarder, 398
Langmuir adsorption isotherm, 222, 227, 242
Laplace law, 80
Laplace-Gauss law, 565
Latex impact on C_3S dissolution, 282
LCPC box testing SCC, 495
Le Chatelier experiment, 15–16, 16f
Leaching, 43, 76
SRA, 317
Light scattering
experimental issues, 246
Lignite, 60–61
Lignosulfonate(s), 150–153, 287
adsorption
effect of molecular mass, 227
effect of polydispersity, 224
characterization, 152

effect on cement hydration, 152, 154
in formulation, 346
production, 153
structure, 152f
Lignosulphonates. *See* Lignosulfonate(s)
Limestone
fabrication of Portland cement, 27
filler use in SCC, 492–493
Liquefied natural gas (LNG), 497–498
Liquid crystals self-association of surfactants, 219
Liquid nitrogen to delay setting, 395–396
Liquid saturation. *See* Pore saturation
Liquid-vapor interface
creation of interfacial area, 315–317
estimation of interfacial area, 311–313
impact of SRA, 313
SRA concentration, 315–317
Liquid-vapor interface, 219
Liquid-vapor interfacial area. *See* Liquid-vapor interface
Liquid-vapor/air interface, surfactants adsorption, 219, 239
LOI, 33
Long term compressive strength, 8–9, 11, 68
Loss of fluidity, 221
effect of competitive adsorption, 233
effect of coverage degree, 221
effect of polymer in solution, 221
effect of specific surface, 221
Loss of workability, 38
Loss on ignition. *See* LOI
Louis Vuitton's Foundation in Paris, 520–521, 521f
Low alkali cement, 36
Low w/c concrete, 457–458
influence on protection of reinforcing steel, 471, 473

M

Macro-cell, 325–326
testing method, 334
Magnesia, 33
Maltodextrin impact on hydration, 295
Maltose, 292f
as retarder, 398
Manufactured sand, 89
Match casting, 511
Matrix of effects, 558–559
Maximum attractive force, 258, 265, 272–273
effect of
adsorbed layer thickness, 274
superplasticizer adsorption, 268, 270
surface coverage, 273, 274f
yield stress, 257–258, 261–262
Measurement of air content
lightweight concrete, 380
normal density concrete, 380
Mechanical bonds creation, 15
Mechanical properties
influence of air content, 87
influence of portlandite, 39–40
Mechanism of action, 415–418
bridging flocculation, 416, 420
cellulose ether, 421–422
depletion flocculation, 416
entanglement, 416
hydroxypropylguar derivatives, 421–422, 423f
polymer-polymer association, 416
Melilite, 59
Menisci, 17–18, 20, 22, 76, 80–82, 457
formation, 483–484
Metakaolin, 65–66, 65f, 71f
Method of placing
conveyer, 389
influence on entrained air, 389
use of constriction, 389
Mica impact on adsorption, 238
Micelles
Critical Micelle Concentration, 317
formation, 239
self-association of surfactants, 219
surface tension, 313
Micro cracks in UHSC, 504
reduction of size, 504
Microstructure
effect of C-S-H seeding, 137–138
of cement paste, 3
effect on corrosion, 472–473
Migrating agent, 475
Mineral composition of cement impact on hydration, 279
Minicone test, 549
Minor oxides, 33

Mitigating steel corrosion
epoxy coated rebar, 475
galvanized reinforcing, 476
GFRP, 476–477
stainless steel, 475–476
Mixer type effect on entrained air, 387–388
Mixing
energy, experimental issues, 243
procedure effect on entrained air, 387–388
protocol
direct polymer addition, 360
impact on delayed fluidification, 362
water, 534
modification of dosage, 534
Mixture design, influence of bubble network, 382
Model(s)
for adsorption isotherm, 222
Langmuir, 222
validation, 557
Modified starch, 418–420
Moisture content, 533–535
Molecular architecture of admixtures
impact on hydration, 279
PCE, 279, 281–282
sugars impact on hydration, 290
Monocarboaluminate formation, 129
Monodentate complexes
PCEs, 281
sugars, 296
Monoethanolamine, 329
Monofluorophosphate(s), 327
corrosion inhibitor, 475
Monomers size role in conformation when adsorbed, 227–228
Monosulfoaluminate formation, 38, 40, 46–47, 129–131
Montmorillonite, 66
impact on adsorption, 238
Morphology of cement particles, 37
MUCEM in Marseille, 519–520
Multicomponent blends of inhibitor, 321
Muscovite impact on adsorption, 238

N

N, structural parameter, 227–228
Na_2O equiv, 33, 36
Nanisivik experiment, 434–438
monitoring, 435
Nano-particles
experimental issues, 244
impact on rheology, 244
Natural pozzolan, 66–67
Newtonian materials, 101–102, 121–122
NF P18-424 Standard, 91
NF P18-425 Standard, 91
Nitrates competitive adsorption, 233
Non porous material, 19
Non-newtonian materials, 121–122
Normal frequency curve, 565–568
area under, 567
reduced centre value, 566
Normal law, 565
Nuclear power plant, 473
banning of sodium salt of PNS, 473
Nucleation and growth process, 136
Nucleation/growth process
effect of retarders, 279–281
on dispersive effect, 283
on favored crystal growth direction, 283
on nuclei, 283
Nuclei
C-S-H effect of carboxylates, 283–284
poisoned by retarders, 283

O

Open porosity, 20
Optimization process, 549
Organic corrosion inhibitors mechanism of action, 330–331
Organo-mineral phases
aluminates phases, 235
stability, 237
formation, 234
effect of addition time, 235
hydrocalumite, 236–237
impact on
adsorption isotherm, 235
dispersion, 235
hydration rate, 235
specific surface, 237
Organomineral phases, 285
Origin of shrinkage, 22
autogenous shrinkage, 17–18, 20–23
drying shrinkage, 22–23
plastic shrinkage, 22–23
Oscillation rheometry, 119

Outer product, 42, 137–138
Overlays, 453–454

P
P, structural parameter, 227–228
Packing density
  improving, 507
    of UHSC, 504
  in SCC, 492–493
Paraffin emulsions as curing compounds, 484–485
Parking garage
  effect of deicing salt, 472
  exterior multilevel, 472
Particle interaction, 105–106
Passive film, 322, 328, 471
  destruction, 472–473
PCEs. *See* Polycarboxylate ethers
Peclet number, 106
PEG
  monomer size, 229
  side chains, 164f, 167–168
Percolation threshold, 104–105
Perlite, 67, 69f
Permeability, 322–323
  influence of entrained air, 88, 90
pH
  of interstitial solution, 43
  of pore solution, 322
Phosphonate(s)
  complexation, 281–282
  terminated PEG brushes, 159–160
Pig iron, 56, 58
Pitting potential, 324
Placing, 89, 92
  parameters influence on bubble network, 382
Plastic shrinkage, 22–23, 79–81, 483–485
Plastic viscosity, 549
  definition, 121–122
  influence
    of clays, 116
    of fly ash, 114
    of silica fume, 114
  relation
    to rheological tests, 360
    to surface coverage, 360
  shear thickening, 359
  shear thinning, 359
PMS, 49
PNS. *See* Polynaphtalene sulfonates
Polyacrylates influence on air content, 93
Polycarboxylate ethers, 161, 268, 270, 279, 281–282
  adsorbed layer thickness, 262, 267–268, 270
  adsorption
    on clay minerals loss of dispersion, 238
    impact on saturation degree, 287
    effect of molecular mass, 227
    effect of polydispersity, 224
    role of molecular structure, 288–289
  in alkaline activated system, 234
  anionic charge density, 162
  backbone impact on adsorption, 227
  characterization, 168
  competitive adsorption
    hydroxides, 234
    sulfate ions, 233
  complexation, 281
    crown ethers, 281–282
    mono-/bidentate ligand, 281–282
  conformation
    in solution, 169–171, 227–228
    when adsorbed, 227–228
      surface occupied, 227–228
  dosage effect on dispersion, 268
  effect of
    adsorbed conformation, 267
    adsorbed layer thickness, 270
    superplasticizer molecular structure, 267–275
  grafting degree effect on interparticle forces, 272
  grafting density impact on adsorption, 227
  hydrolysis, 164
  impact on
    air entrainment, 354, 368, 371
    $CaCO_3$ precipitation, 283–284
    dissolution, 282
    ettringite morphology, 287
    ettringite nucleation, 287
    hydration, 279, 281–282
    nucleation/growth, 282
    sulfate consumption, 287
    sulfate depletion peak, 286
  influence on air entrainment, 385

Polycarboxylate ethers (*Continued*)
molecular design, 279
molecular structure
effect on interparticle forces, 272−275
impact on adsorption, 227
radius of gyration, 169−171, 227−228
retardation role of molecular structure, 288−289
secondary effect, 385
side chain
length effect on interparticle forces, 272
impact on adsorption, 227
steric forces, 266−268, 271
structural parameters, 227−228
synthesis, 167−168
Polydispersity
impact on adsorption, 224
lignosulfonates, 224
PCEs, 225
superplasticizers, 227
Polymelamine, 49, 157−159, 158f, 354, 367−368
Polymethacrylate monomer size, 229
Polynaphtalene sulfonates, 49, 154−157, 473
banning of sodium salt, 473
calcium salt, 473
characterization, 156
impact on air entrainment, 354, 367−368
sodium salt, 473
synthesis, 155f
Polynaphthalene, 49
Polyoxyethylene di-phosphonates. *See* Phosphonate terminated PEG brushes
Polyoxyethylene phosphonates. *See* Phosphonate terminated PEG brushes
Pore saturation
relative humidity, 312f
SRA dosage, 312f
surface tension, 312f
Pore solution
extraction, 241
experimental issues, 244
stabilization, experimental issues, 245
Porosity, 322−323
Portland cement, 3, 6−9, 11−12
chemical composition, 8, 11, 33−36
colour, 33
dilution, 8
fabrication, 48
free lime, 33
hydration, 15, 17−18
insolubles, 33
magnesia, 33
production cost, 27
sulphates, 33
Portlandite, 8, 39−40, 41f, 43
expansive agent, 445−446
formation, 129, 132−134
impact on C-S-H precipitation, 283
effect of raffinose, 296
saturation degree, 297
effect of sucrose, 283, 296
effect of sugars, 291
Power's model, 16
Power's work on hydration, 16−22
Pozzolan, 43, 53
artificial, 61, 66
natural, 66−67
Pozzolanic
material, 43
reaction, 53
in UHSC, 506
Pre-cast plants use of SCC, 491, 501
Precalcinator, 31, 32f
Precast elements banning of calcium chloride, 473
Precipitation of hydrates, consumption of admixtures, 219−220
Preheater, 31
Pressure filtration, experimental issues, 244
Prestressed beams effect of chloride ion, 472f
Preventive measure against corrosion, 323, 472−473
Propagation phase, 321, 325−326
Protection of steel reinforcing, 473
cathodic protection, 474
corrosion inhibitor, 474−475
low w/c concrete, 473
Protective impervious membrane, 472−473
Protective membrane
in alite hydration, 133
in C_3A hydration, 130
Pseudoplastic behaviour, 121−122

Pumping, 89
  influence
    of air entraining agent, 93
    of constriction, 389
    of half end loop, 389
    of spacing factor, 93
    of mixing water, 93
    of other admixture, 93
    of pump, 93
  of SCC, 497
  total air content, 93

Q
Quadratic effects, 557
Qualitative factors, 552
Quality control of SCC, 493–497
Quality of water, 75–76
Quantitative factors, 552
Quartz, 54
Quenching, 55, 64
  of clinker, 28, 31–33

R
Radius of gyration, PCEs, 227–228
Raffinose, 293f
  adsorption, 295–296
  complexation
    deprotonation at high pH, 295–296
    monodentate complexes, 296
  impact on portlandite formation, 296
Range, 574t
  variation of range, 581f
Rate
  of adsorption, 229
  of desorption, 229
  of penetration of aggressive agent, 322–323
Raw meal, 27–28, 31–33, 36
Reaction wall use of SCC, 499–500
Reactive powder concrete, 12. *See also* Ultra high strength concrete (UHSC)
Recycling, 53
Reduced centre value, 566
Reinforcing bars corrosion, 471–472
Relative humidity (RH)
  capillary pressure, 310
  deformation energy, 310
  disjoining pressure, 306, 310
  Helmoltz free energy, 310
  influence on cabonation rate, 324–325
  pore saturation, 312f
  shrinkage reduction, 306, 314
Repair work, 443, 453–454, 457–458
  use of SRA, 459
Residual viscosity, 105–106, 359
Residual yield stress, 107–108
Resistance to freezing and thawing, 465–466
  of SCC, 497
Restrained expansion, 446
  demolding, 447
  measurement, 447
Restrained shrinkage, 441–443, 453
Retardation
  effect of admixtures
    chemical nature, 279
    dosage, 279
    molecular architecture, 279
    time of addition, 279
  effect of cement
    composition, 279
    fineness, 279
  by complexation. *See* Complexation
  complexation of calcium ions
    limitations, 281–282
  disruption of nucleation, 281
  effect
    of ambient temperature, 395–396, 399
    of temperature of ingredients, 395
  field problems, 400–403
  effect of formulated product, 279
  importance of C_3A content, 287
  inhibition of dissolution, 281–282
  inhibition of nucleation/growth, 282
  mechanism, 398
  effect of PCEs, 279, 281–282, 288–289
    backbone, 289
    molecular architecture, 288–289
  perturbation of silicate-aluminate-sulfate balance, 281, 285–287
  role of PCEs molecular architecture, 288–289
  saturation degree, 287
  effect of sugars, 279–280, 290
    glucose, 279–280
    saccharides, 290

Retardation (*Continued*)
sucrose, 31, 291, 295−297
effect of sulfate availability, 279
by superplasticizers, 287−290
Retarder(s), 77, 171−174, 219. *See also* Sugars
addition time, 400
chemistry, 171
combination
with superplasticizer, 395
water-reducer, 395
different chemicals, 397−398
dosage, 399−400
ambient temperature, 399
concrete initial temperature, 399
duration of concrete delivery, 399
duration of retardation, 399
as function of cement, 399
effect of
chemical nature, 279
dosage, 279
molecular architecture, 279
time of addition, 279
in formulation, 343−344
impact on
dissolution, 279−280
growth, 279−280
heat release, 279−280
induction period, 279−280
nucleation, 279−280
silicate-aluminate-sulfate balance, 285−287
slope of acceleration period, 279−280
sulfate depletion peak, 279−280
inorganic salts, 171, 397−398
overdosage, 402−403
sugar, 398−399
use in field, 397−400
Retempering, 77
Reynolds number, 106
Rheological
behavior of paste, 104
properties of SCC, 491−492
Rheology, 415−417
bridging flocculation, 416
definition, 97−101
diutan gum, 418−420
improvement, 88
influence
of dead burn lime, 444−445
of sulphoaluminate, 444−445, 449
modified starch, 418−420
shear thinning behavior, 417f, 418−420
superplasticizer, 418−420
of UHSC, 508−509
welan gum, 418−421
Rheometer, 101, 121−122
Rigid inclusion, 6
Risk
to consumer, 583
of cracking, 443−444
to producer, 583
Robustness, 364−365
Role in suspension stability, 263−264
Rolled aggregates influence on concrete rheology, 113
Rusting, 478

S

Saccharides
impact on C_3S hydration effect of dosage, 291−292
molecular structures, 291−292
Sacrificial anode, 474
Saturated lightweight aggregates, 22, 82, 484, 486
coarse, 82
fine, 82
Saturated surface dry state. *See* SSD state
Saturation degree
effect of
complexation, 281
PCEs adsorption, 287
retarders, 283, 297
sugars, 291
impact
on alite hydration, 133
on ettringite precipitation, 130
Saturation dosage
determination by rheological tests, 356f, 358−359
impact on adsorption, 220
plastic viscosity, 359
shear thickening, 359−360
Scaling resistance, 465−466
SCC. *See* Self-consolidating concrete
Sea water, 75−76, 83−84

Sealant, 23
Secondary C-S-H, 43
Secondary ettringite, 46–47
Secondary ion mass spectroscopy, time of flight, 333
Segregation, 76–77, 109
  influence of entrained air, 89
  influence on aggregate mix, 109
  influence on maximum packing, 109
  influence on permeability, 109
  influence on strength, 109
  influence on yield stress of paste, 109
Self-compacting concrete. *See* Self-consolidating concrete (SCC)
Self-consolidating concrete (SCC), 44, 89, 460, 491
  associated costs, 491
  cohesiveness, 492–493
  creep, 497
  elastic modulus, 497
  field advantages, 497–499
  formulation, 492–493
  hardening properties, 497
  high powder content, 493
  in high rise building, 497
  low powder content, 493
  materials used, 493
  moderate powder content, 493
  noise nuisance, 491, 499
  packing density, 492–493
  passing ability, 491–492, 495
    noise nuisance, 491, 499
    noise restrictions, 501
  plastic shrinkage, 497
  post tensioned, 498, 498f–499f
  proportion of coarse aggregate, 492
  proportioning, 493
  pumping, 497
  quality control, 493–497
  reaction walls, 499–500
  reduction of size of coarse aggregate, 492
  resistance to freezing and thawing, 465–466, 497
  rheological properties, 491–492
  selling SCC, 500
  spacing factor, 497
  static stability, 496f
  statistical model, 491–492
  surface quality, 491
  testing, 493–495, 499
  typical SCC mixtures, 493t–494t
  use in LNG tank, 497–499
  use in precast industry, 491
  use in ready mix industry, 491
  use of SRA, 460
  use of VMA, 492
  viscosity, 492
  yield stress, 492, 495
Self-levelling. *See* Self-consolidating concrete (SCC)
Self-placing. *See* Self-consolidating concrete (SCC)
Selling SCC, 500
Semi-dilute regime effect of dosage, 222
Service life of concrete structure, 321
Set retarders. *See* Retarders
Setting, 129–130
Shale fabrication of Portland cement, 27
Shear laminar flow, 98–99
  stress field, 98–99
Shear rate, 98–100
  critical, 106
  definition, 106
  dimension, 100
Shear stress, 99–100, 121–122
Shear thickening, 103–104
  definition, 121–122
  effect
    on extrusion, 105–106
    on mixing, 105–106
    on pumping, 105–106
  influence of superplasticizer, 105
Shear thinning, 103–104
  definition, 121–122
  plastic viscosity, 359
Sherbrooke pedestrian bikeway, 505
  assembling, 512
  completed passerelle, 514f
  confinement, 511
  construction, 511–513
  curing, 511
  day view, 511
  design, 509
  diagonals, 510f, 511
  long term behavior, 515
  match cast, 511
  natural frequency resonance, 515

Sherbrooke pedestrian bikeway (*Continued*)
night view, 516f
post tensioning, 511
pressing of diagonals, 511
static loading, 515
testing, 515
transportation, 512
Short term compressive strength, 68
Shotcrete acceleration, 410–412
Shotcrete repair, 475
use of calcium nitrate, 475
Shrinkage
apparent volume contraction, 78–79
compensated concrete, 441
different types, 78–79
influence of curing conditions, 78–79
Shrinkage reducing admixture, 219, 457
adsorption
liquid-vapor interface, 239
onto solid surfaces, 317
solid-liquid interface, 230
amino alcohols, 205
classification, 205
compatibility, 196–197, 200
concentration
liquid phase, 317
liquid-vapor interface, 315–317
dosage
effect on surface tension, 313
pore saturation, 312
effect on entrained air, 465–466
and expansion agent, 462
expansive agent, 462
field use, 466–468
glycols, 201–202
alkylene glycols, 201
monoalcohols, 201
polyoxyalkylene glycols, 201
solubility, 201
impact
on interfacial area, 313
on surface tension, 313
laboratory studies, 459–466
leaching, 317
multi-component SRAs, 201, 203
in overlays, 466–467
polymeric surfactants, 203–205
polyoxyalkylene glycol alkyl ethers, 202–203
principal molecules, 458
repairs, 465–467
resistance to freezing and thawing, 465–466
typical dosages, 458–459
use in self-compacting concrete, 460
working mechanism, 197–198
Shrinkage reduction, 197–198, 202–203
impact of relative humidity, 306, 314
theory of
capillary pressure, 307
disjoining pressure, 311
energy balance, 307
Side chains of PCEs, impact on adsorption, 227, 288–289
Significant factor, 551–552
Signification
of w/b, 11
of w/c, 11
Silane, 83
Silica content, 33
Silica fume, 62–64
diameter, 64
effect on entrained air, 386
gray, 64
influence on plastic viscosity, 114
in UHSC, 504
use in SCC, 492–493
white, 59f
Silicate content, 36
Silicate phase, 28, 31
Silicate salts
as accelerator, 407, 411
w/c or w/b decrease to accelerate hardening, 406
Silicate-aluminate-sulfate balance, 139–140, 298
effect of
retarders, 281, 285
superplasticizers, 285
importance of
C_3A content, 287
cement model, 285
sulfate depletion point, 286
Silicates, 57–58, 65–66
Silicon, 62
Size of air bubbles, effect on spacing factor, 381
Skewed distribution, 570f

Slabs on ground, 441, 454
cracking, 447
friction on soil, 453
Slag, 43, 58, 60
cold slag, 59, 59f
degree of disorganization, 59
effect on AEA dosage, 386
hot slag, 59, 59f
reactivity, 59
use in SCC, 492−493
Slow dissolution step hypothesis, 133−134
limitation, 133−134
Slump
loss, 49, 77, 533
relation with yield stress, 108f
retention, 344
test, 108
SNFC, adsorption effect of molecular mass, 227
Solid-liquid interface, 219
adsorption of surfactants, 219
Solid(s)
active, 536
content
adsorption measurement, 242
of superplasticizer, 537−538
gel, 16−21
in superplasticizer, 537−538
Solubility rate of calcium sulphates, 49
Soluble alkalis, 242
Solution depletion method, 219−220, 241
Solvo-surfactants, 239
Soot, 61−62
Spacing factor, 88, 91−92, 381−383, 472−473, 497
Canadian regulation, 91−92
definition, 381
signification, 91
effect of size of air bubbles, 381
Spalling due to corrosion, 471
Specific gravity
coarse aggregate, 533, 533f
of Portland cement, 3−5
Portland cement, 535
SSD, 535
Specific surface, 5, 43
area, 36−37, 226
changes impact on coverage degree, 237
effect of
admixtures, 237
aluminates reactivity, 243
experimental issues, 243, 247
impact on loss of fluidity, 221
role of organo-mineral phases, 237
Specifying curing conditions according to w/c, 484−485
Sprayers, 80
SRA. *See* Shrinkage reducing admixture
SRA-AEA interaction, 463
effect on stability of bubbles, 463−464
SSD state, 75, 531−532
coarse aggregate, 531−532
fine aggregate, 532
schematic representation, 532f
Stability, 415−416, 421f
Stabilization of air bubbles, 87, 92
Stainless steel reinforcement, 475−476
Standard deviation, 556, 559, 566
overall, 570−571
variation, 573, 579f
Static stability of SCC, 496f
Statistical analysis, 569, 578−579
limitation, 579−583
lucky bad producer, 582
risk of consumer, 583
risk of producer, 583
unlucky good producer, 582
Statistical design, 551−552
absolute values, 552, 552f, 554f, 560, 560t
coded value, 552−554, 554f, 560, 560t
confidence interval, 560
criteria of optimality, 559
definition of factor, 551−552, 556−557
experimental
approach, 551
domain, 554−555
error, 556
first order interaction, 557−559
high level, 556
interaction, 556−557
of second order, 557, 559−560
level, 551−553
lower level, 552−553, 556
mathematical treatment, 556−564
matrix of effects, 558−559
non-linear model, 557

Statistical design (*Continued*)
quadratic effects, 557, 560−562
qualitative factor, 552
quantitative factor, 552
range, 551, 553
response, 551−552, 556−557
column, 558−559
vector of coefficient, 558−559
Statistical model, 491−492
Steam curing of UHSC, 506
Steel
fiber in UHSC, 503, 506, 507f
forms life time, 491
Steric hindrance. *See* Steric forces
Stern layer. *See* Goüy-Chapman double layer model
Stickiness, 359
Strength
development role of C-S-H, 137−138
initial, 7−8
long term, 8−9, 11
Rupture of concrete, 12
Strengthening effect
hard inclusions, 20−21
rigid inclusions, 6
Stress
concentration, 503−504
at contact angle, 503−504
transfer, 504
Structural breakdown curves, 117−119, 118f
Structural build up, 119−120
Structural parameters of PCEs
P, N, n, 227−228
role in conformation, 227−228
Substitution rate, 7, 10−11
of Portland cement, 8−9
Sucrose, 283, 292t
adsorption, 295−296
on aluminates, 298
on C_3S, 297−298
on mica, 297
effect of pH, 297−298
on portlandite, 296
complexations
deprotonation at high pH, 295−296
effective retarder, 290
impact on dissolution kinetics, C_3S, 297
impact on dissolution effect of solid to liquid ratio, 297
impact on hydration, 295
with addition of portlandite, 296
impact on portlandite
formation, 296
morphology, 296
nucleation, 283
impact on saturation degree, 297
monodentate complexes, 296
Sugars, 279, 282, 290−291, 293−295
α-methyl glucoside, 292t
aliphatic sugar, 290, 292−293
binding capacity, 295
cellobiose, 292t
chemistry, 171
classification of retarding effect, 291
complexation, 282, 293−295
complexing ability, 173
degradation in alkaline conditions, 298
as delayed accelerators, 290
disaccharides, 173−174
glucose, 279−280, 292t
impact on hydration, 295
stereoisomers, 172
glycosidic bond, 173
impact on hydration, 279
role of molecular structure, 290−291
impact on ions concentration, 291
calcium, 291
impact
on durability, 290
on long-term strength, 290
on pH, 291
on portlandite formation, 296
on saturation degree, 291
lactose, 292t
linear saccharides, 291−292
maltodextrin impact on hydration, 295
maltose, 292t
mono-/bidentate complexes, 296
monosaccharides, 172−173
non-reducing, 291
non-retarding, 291
oligosaccharides, 174
polysaccharides, 174. *See also* Viscosity modifying admixtures
raffinose, 174, 174f, 292t, 295−296
reducing, 291

saccharides, 291–292
seeding effect, 290
stereochemistry, 172–173
sucrose, 173
thehalose, 292t
Sulfate
availability impact on hydration, 279
consumption
effect of PCEs, 286–287
role of surface area, 287
depletion peak, 286
effect of PCEs, 286
effect of retarders, 279–280
depletion point, 130, 138–139
dissolution effect of PCEs adsorption, 286
sensitivity parameter, 233
Sulfate ions
competitive adsorption, 233
with PCEs, 233
Sulfocalcic fly ash, 61
Sulphates in cement, 38
Sulphoaluminate, 40, 444–445
appropriate dosage, 450f
influence on AEA, 444–445
influence on workability, 444–445
interaction with admixture, 444–445
Superabsorbent polymers (SAP), 22, 82
Superficial tension, 379–380, 457
Superplasticizers (SPs), 9, 12, 38, 46, 49, 267, 417–421
adsorption, 267–275
adsorbed layer thickness, 267–268, 270
affinity role of aluminates, 226
conformation, 267, 270
effect on maximum attractive force, 258, 265, 272–273
effect on minimum interparticle distance, 263–264
effect on surface charge, 258
effect on zeta potential, 269, 269f
electrostatic stabilization, 269
electrosteric stabilization, 266, 270
influence on separation distance, 105
effect of molecular mass, 227
reducing attractive forces, 106
reducing degree of flocculation, 105
reducing yield stress, 105
steric forces, 266–268, 271
steric stabilization, 266–268
dosage, 536–540
effect
on spacing factor, 385
on yield stress, 257–258
impact
on aluminate-sulfate interaction, 285
on hydration, 287
on silicate-aluminate-sulfate balance, 285
influence
of fluidity of paste, 549
on entrained air, 385
interaction with AEA, 385
mass
of solids, 539–540
of water, 538–539
perturbing
AFm formation, 285
ettringite formation, 285
polydispersity, 227
reduction of inter particles forces, 111
saturation dosage, 109
schematic representation, 537f
in UHSC, 509
use in SCC, 492
volume needed, 539–540
Supplementary cementitious material, 3–4, 6–9, 7f–8f, 11, 53, 70, 140
content, 535–536
diatomaceous earth, 67, 68f, 71f
hydrothermal vitreous silica, 67
perlite, 67, 69f
rice husk ash, 67, 70f–71f
Surface charge, 258
effect of electrolyte concentration, 260f
effect of superplasticizer adsorption, 268–275
Surface coverage, 241
relation to yield stress, 357
saturation of surface, 220
zeta potential, 247
Surface forces
disjoining pressure, 308
liquid film, 308

Surface tension
  interfacial area, 313
    micelles, 313
  role of surfactants adsorption, 240–241
  impact of SRA dosage, 313
Surfactants
  amphoteric, 193–195
    amine oxides, 193
    betaines, 193
  anionic, 188–192
    adsorption, 189
    carboxylic acid salts, 189–190
      classification, 189
      synthesis, 189
    precipitation, 189
    sulfonic acid salts, 190–191
      alkylbenzenesulphonate, 190
      α-Olefin Sulphonates, 190
      sodium dodecylbenzenesulphonate, 190
    sulfuric acid salts, 191–192
      alcohol ether sulphates, 191
      sodium alkyl sulphates, 191
    taurates, 192
      structure, 191f
  applications, 185t
  cationic
    compatibility, 192
    quaternary ammonium salts, 192
  classification, 172, 175t
  hydrophilic-lipophilic balance, 182–185
  hydrophobic chain, 184, 192f
  non-ionic, 195–197, 200
    compatibility, 195–197
    solubility, 195–196, 198
  structure, 183–184
Surfactants, 219, 458
  adsorption
    conformation, 230
    driving force, 239
    effect of dissolved salts, 230
    effect of molecular structure, 230
    effect of temperature, 230
    4 regimes, 231
    ionic, 230
    liquid-vapor interface, 219
      surface tension, 240–241
    non-ionic, 230, 232
      isotherm, 232
      on cement, 232
      solid-liquid interface, 219
    formation of
      hemi-micelles, 231
      liquid crystals, 219
      micelles, 219, 239
    on liquid-vapour interface, 239
    non-ionic, 239
Suspension
  agglomeration, 263–264
  effect of
    Brownian motion, 263–264
    shear forces, 263–264
    superplasticizers, 257, 267–275
  flocculation, 268
  stability, 257, 263–264
Sustainability, 3, 10–11, 53
Swelling, 16, 22
Swelling clay minerals. *See* Clay minerals
Synthesis, 159f
Synthetic calcium sulphate, 49

T

Temperature
  effect on air entrainment, 388
  influence on expansion, 451–452
  influence on setting time, 395
Tensile forces, 17–18, 20, 76, 80
Ternary diagram, 58
Testing corrosion inhibitor, 334–335
  macro-cell, 334
Tetracalciumferro-aluminate. *See* C_4AF
Tetrahalose as retarder, 398
Thehalose, 292t
Thermal conductivity, 76
Thermal contraction, 22
Thermal shrinkage, 22
Thermal treatment of UHSC, 506
Thixotropy, 106–108
  comparison, 119
  consequence on processing, 116–117
  definition, 121–122
  degree of thixotropy, 117
  equilibrium approach, 117
  experimental method to measure it, 117–120
  function of shear rate, 117
  function of time, 117

hysteresis curves, 117
hysteresis loop, 117
oscillation rheometry, 119
steady state approach, 120
structural breakdown, 107
time dependence, 107
ultrasound spectroscopy, 119
Threo-dihydroxy function, 292–293
Time of addition impact on hydration, 279
Time of depassivation influence of calcium nitrite, 321
Tobermorite-like structure, C-S-H formation, 136
TOC experimental issues, 244
Total shrinkage, 442–443
Total volume of air, 379–380, 383
Toughness of UHSC, 503
Transition zone, 89
in UHSC, 504
Transport properties, 321
Transportation of concrete
stability of bubble network, 388–389
Trapping expansive products, 90–91
Trial and error method, 549
Trial batch to determine AEA optimum dosage, 382–383
Tricalcium aluminate. *See* C_3A
Tricalcium silicate. *See* C_3S
Trisulfoaluminoferrite. *See* Ettringite
2D model, 4, 4f–5f, 6–7, 7f–8f, 10f

U

Ultra high strength concrete (UHSC), 12, 69, 71f, 503
autogenous shrinkage, 504
cement characteristics, 508–509
compactness, 503
compressive strength, 503–504
confined, 511
ductility, 506
entrapped air, 504–505
formulation, 503
grain size distribution, 503
heat treatment, 504
homogeneity, 504
limitation of sand volume, 504
micro cracks, 504
packing density, 505
rheology, 508
steam curing, 506
superplasticizer, 509
toughness, 503
transition zone, 504
Ultracentrifugation experimental issues, 244–245
Ultrafiltration for adjusting molecular mass, 227
Ultrasound spectroscopy, 119
Unburned carbon effect on AEA dosage, 386
Unburned coal in fly ash, 61–62
Unit cell, 4–7, 5f, 8f, 9, 54
Unreacted Portland cement, 20–21
cores, 20–21
UV/Vis spectrometry experimental issues, 245

V

Valence, 54
Van der Waals forces
continuum theory, 259
in DLVO theory, 262
microscopic theory, 257–258
Variation of initial flow, 550f
Vibrating wire, 459
gages, 447, 447f
measurement of free shrinkage, 448f
use for SRA, 461
Vibration influence on entrained air, 389
Vinyl copolymers, 160–161
adsorption effect of molecular mass, 227
Viscosity, 101, 105–106
modifiers, 279
of SCC, 492
Viscosity modifying admixtures, 149, 175
cellulose-ether derivatives, 177, 179f
synthesis, 177
classification, 175t
degree of substitution, 177
diutan gum, 176–177
structure, 176f
guar gum
derivatives, 177–180
structure, 180f
influence
on bleeding, 109
on segregation, 109

Viscosity modifying admixtures (*Continued*)
modified-starch
structure, 181f
synthesis, 180−181
polyethylene oxide
structure, 182f
synthesis, 181−182
stability, 175−177
use in SCC, 492
welan gum, 176−177, 176f
synthesis, 176−177
Vitreous material, 55
Vitreous silica, 53
VMAs. *See* Viscosity modifying admixtures
Volatile corrosion inhibitor (VCI), 329
Volume of entrained air influence of various parameters, 382−383, 389
Volumetric contraction, 22, 44, 81−82, 441−442, 483
Volumetric substitution, 7
Volumic surface, 381, 382f
Vortex effect on air entrainment, 379, 384

W
w/b
how to lower it, 11−12
importance, 11
influence
on compressive strength, 11−12
on size of capillaries, 11
signification, 11
w/c
hidden meaning, 4−6
how to lower it, 11−12
importance, 11
influence
of curing, 483−484
on compressive strength, 12
on freeze thaw resistance, 91
signification, 11
Waste concrete, 89
Waste waters, 84
Water
absorption, 533−534
beneficial action, 76
chemical role, 75
content control, 533−535
curing, 8
according to w/c, 23
low w/c concretes, 23
effect on hydration, 76−77
effective, 75
evaporation influence on shrinkage, 80
external source, 81−82
hidden, 75
influence
on plastic viscosity, 113
on rheology, 77
on shrinkage, 78−83
on workability, 77
on yield stress, 113
insoluble compounds
air entrainers, 219
shrinkage reducing admixtures, 219
surfactants, 219
physical role, 75
quality, 75−76
reducer, 46
adsorption, 219
retention agent, 421
adsorption, 424
interstitial solution, 422
overlapping concentration, 423f
polymer aggregates, 422−423
sea water, 83−84
wetting of cement particles, 77
Water-soluble compounds
high range water reducers, 219
retarders, 219
water reducers, 219
Weakness of HPC, 503−504
Wear of paddles, effect on air entrainment, 384
Welan gum, 418−421
Wet aggregate schematic representation, 534f
Wetting hysteresis, 324−325
White cement, 28, 33, 46
White rust, 400
Winter concreting
in China, 433−434
in Finland, 433−434
lengthening season, 434
in North America, 433
in Poland, 433
in Russia, 433

Within test variation, 570–571, 576t–577t
  standard deviation, 571t, 580t, 581f
  variation, 576t–577t, 580t
Workability, 97
  different types, 97
  influence
    of chemical admixtures, 108
    of entrained air, 89
    of water, 77
  loss, 77
W_{tot} definition, 531, 533–534

X

X-Ray diffractogram, 56f–57f, 64f
  diatomaceous earth, 67, 68f, 71f
  metakaolin, 66
  natural pozzolan, 66–67
  Portland cement, 66–67
  rice husk ash, 66–67, 71f
  silica fume, 62–64
  slag, 70

Y

Yield stress, 101. *See also* Maximum attractive force
  α-methyl glucoside, 292t
  of cement suspension, 257–258
  definition, 121–122
  effect
    of charge density of PCEs, 288–289
    of superplasticizers, 257–258, 261–262
  influence
    of aggregate content, 111
    of distribution, 105
    of fineness of cement, 111
    of particle size, 105
    of slump, 105
    of time, 108
    of volume fraction, 108f
    of w/c, 111
    of water, 110–111
  model, 105
  origin, 104–105
  plastic viscosity, 110
  relation
    to rheological tests, 357–358
    to surface coverage, 357
  of SCC, 491–492

Z

Zeta potential
  definition, 269, 269f
  effect on interparticle forces, 270–272
  experimental issues, 247
  measurement techniques, 270
    acoustophoresis, 261
    of cement suspension, 264, 269
    microelectrophoresis, 261
  effect of superplasticizer adsorption, 268, 270
Zinc oxide effect on retardation, 400–401
Zirconium, 62